Journal of Mathematics

Extremal and Spectral Graph Theory

Lead Guest Editor: M. T. Rahim
Guest Editors: Jinde Cao, Slamin Slamin, Imran Javaid, Muhammad Imran, and Zahid Raza

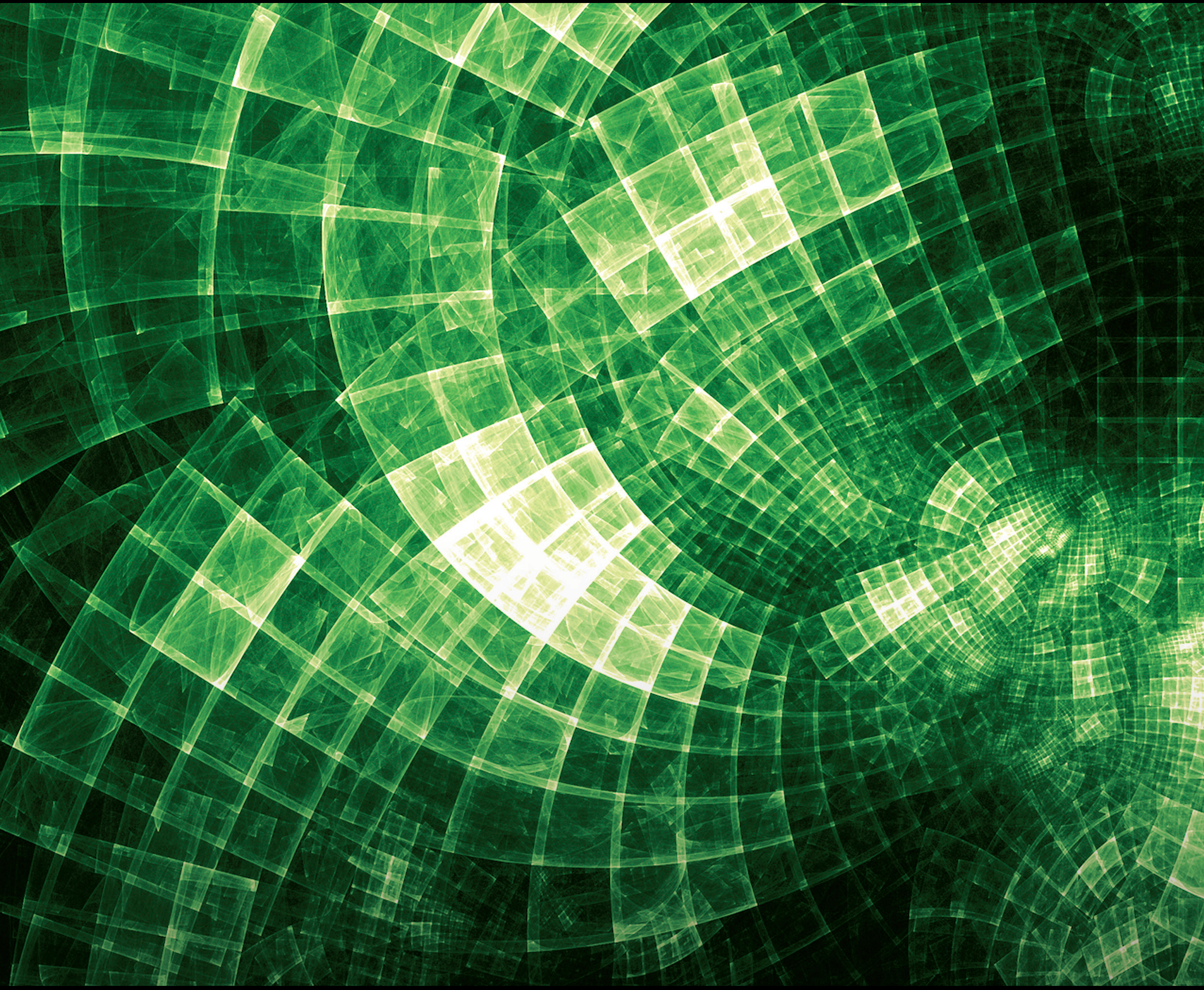

Extremal and Spectral Graph Theory

Journal of Mathematics

Extremal and Spectral Graph Theory

Lead Guest Editor: M. T. Rahim
Guest Editors: Jinde Cao, Slamin Slamin, Imran Javaid, Muhammad Imran, and Zahid Raza

Copyright © 2023 Hindawi Limited. All rights reserved.

This is a special issue published in "Journal of Mathematics." All articles are open access articles distributed under the Creative Commons Attribution License, which permits unrestricted use, distribution, and reproduction in any medium, provided the original work is properly cited.

Chief Editor

Jen-Chih Yao, Taiwan

Algebra

SEÇİL ÇEKEN, Turkey
Faranak Farshadifar, Iran
Marco Fontana, Italy
Genni Fragnelli, Italy
Xian-Ming Gu, China
Elena Guardo, Italy
Li Guo, USA
Shaofang Hong, China
Naihuan Jing, USA
Xiaogang Liu, China
Xuanlong Ma, China
Francisco Javier García Pacheco, Spain
Francesca Tartarone, Italy
Fernando Torres, Brazil
Zafar Ullah, Pakistan
Jiang Zeng, France

Geometry

Tareq Al-shami, Yemen
R.U. Gobithaasan, Malaysia
Erhan Güler, Turkey
Ljubisa Kocinac, Serbia
De-xing Kong, China
Antonio Masiello, Italy
Alfred Peris, Spain
Santi Spadaro, Italy

Logic and Set Theory

Ghous Ali, Pakistan
Kinkar Chandra Das, Republic of Korea
Jun Fan, Hong Kong
Carmelo Antonio Finocchiaro, Italy
Radomír Halaš, Czech Republic
Ali Jaballah, United Arab Emirates
Baoding Liu, China
G. Muhiuddin, Saudi Arabia
Basil K. Papadopoulos, Greece
Musavarah Sarwar, Pakistan
Anton Setzer, United Kingdom
R Sundareswaran, India
Xiangfeng Yang, China

Mathematical Analysis

Ammar Alsinai, India
M.M. Bhatti, China
Der-Chen Chang, USA
Phang Chang, Malaysia
Mengxin Chen, China
Genni Fragnelli, Italy
Willi Freeden, Germany
Yongqiang Fu, China
Ji Gao, USA
A. Ghareeb, Egypt
Victor Ginting, USA
Azhar Hussain, Pakistan
Azhar Hussain, Pakistan
Ömer Kişi, Turkey
Yi Li, USA
Stefan J. Linz, Germany
Ming-Sheng Liu, China
Dengfeng Lu, China
Xing Lü, China
Gaetano Luciano, Italy
Xiangyu Meng, USA
Dimitri Mugnai, Italy
A. M. Nagy, Kuwait
Valeri Obukhovskii, Russia
Humberto Rafeiro, United Arab Emirates
Luigi Rarità, Italy
Hegazy Rezk, Saudi Arabia
Nasser Saad, Canada
Mohammad W. Alomari, Jordan
Guotao Wang, China
Qiang Wu, USA
Çetin YILDIZ, Turkey
Wendong Yang, China
Jun Ye, China
Agacik Zafer, Kuwait

Operations Research

Ada Che, China
Nagarajan DeivanayagamPillai, India
Sheng Du, China
Nan-Jing Huang, China
Chiranjibe Jana, India
Li Jin, United Kingdom
Mehmet Emir Koksal, Turkey
Palanivel M, India

Stanislaw Migorski, Poland
Predrag S. Stanimirović, Serbia
Balendu Bhooshan Upadhyay, India
Ching-Feng Wen, Taiwan
K.F.C. Yiu, Hong Kong
Liwei Zhang, China
Qing Kai Zhao, China

Probability and Statistics

Mario Abundo, Italy
Antonio Di Crescenzo, Italy
Jun Fan, Hong Kong
Jiancheng Jiang, USA
Markos Koutras, Greece
Fawang Liu, Australia
Barbara Martinucci, Italy
Yonghui Sun, China
Niansheng Tang, China
Efthymios G. Tsionas, United Kingdom
Bruce A. Watson, South Africa
Ding-Xuan Zhou, Hong Kong

Contents

Hindawi
Journal of Mathematics
Volume 2023, Article ID 6205632, 5 pages
https://doi.org/10.1155/2023/6205632

Research Article

(Generalized) Incidence and Laplacian-Like Energies

A. Dilek Maden [1] and Mohammad Tariq Rahim [2]

[1] *Department of Mathematics, Faculty of Science, Selçuk University Campus, Konya 42075, Turkey*
[2] *Deparmant of Mathematics, Abbottabad University of Science and Technology, Abbottabad 22010, Pakistan*

Correspondence should be addressed to A. Dilek Maden; aysedilekmaden@selcuk.edu.tr

Received 28 February 2022; Revised 19 May 2023; Accepted 15 July 2023; Published 12 August 2023

Academic Editor: Mohammad W. Alomari

Copyright © 2023 A. Dilek Maden and Mohammad Tariq Rahim. This is an open access article distributed under the Creative Commons Attribution License, which permits unrestricted use, distribution, and reproduction in any medium, provided the original work is properly cited.

In this study, for graph Γ with r connected components (also for connected nonbipartite and connected bipartite graphs) and a real number $\varepsilon(\neq 0, 1)$, we found generalized and improved bounds for the sum of ε-th powers of Laplacian and signless Laplacian eigenvalues of Γ. Consequently, we also generalized and improved results on incidence energy (IE) and Laplacian energy-like invariant (LEL).

1. Introduction

Let Γ denote a finite, simple, and undirected graph of order n. The edge and vertex sets of Γ are denoted by $E(\Gamma) = \{e_1, e_2, \ldots, e_m\}$ and $V(\Gamma) = \{v_1, v_2, \ldots, v_n\}$, respectively. If the vertex v_i is neighbour to v_j, then write $v_i \sim v_j$. The degree of the vertex $v_i \in V(\Gamma)$, symbolized by d_i, is the number of vertices adjacent to v_i.

The adjacency matrix and the degree matrix of graph Γ are denoted by $A(\Gamma)$ and $D(\Gamma)$, respectively. Let $\mu_1(\Gamma) \geq \mu_2(\Gamma) \geq \cdots \geq \mu_n(\Gamma) = 0$ be the eigenvalues of the Laplacian matrix $L(\Gamma)$ of Γ where $L(\Gamma) = D(\Gamma) - A(\Gamma)$ [1, 2]. Let$q_1(\Gamma) \geq q_2(\Gamma) \geq \cdots \geq q_n(\Gamma)$ be the eigenvalues of the signless Laplacian matrix $Q(\Gamma)$ of Γ where $Q(\Gamma) = D(\Gamma) + A(\Gamma)$ [3]. Since the matrices $A(\Gamma)$, $L(\Gamma)$, and $Q(\Gamma)$ are real and symmetric matrices, thus they have real eigenvalues. So, we can write their eigenvalues such that $\lambda_1(\Gamma) \geq \lambda_2(\Gamma) \geq \cdots \geq \lambda_n(\Gamma)$, $\mu_1(\Gamma) \geq \mu_2(\Gamma) \geq \cdots \geq \mu_n(\Gamma)$, and $q_1(\Gamma) \geq q_2(\Gamma) \geq \cdots \geq q_n(\Gamma)$, respectively. $L(\Gamma)$ and $Q(\Gamma)$ are semidefinite matrices, according to the Geršgorin disc theorem. From here, all eigenvalues of Laplacian and signless Laplacian matrices of Γ are non-negative integers. In [3], it has been found that $\mu_i(\Gamma) > 0\,(i = 1, 2, \ldots, n-1)$ for a connected nonbipartite graph Γ. Additionally, Γ is a bipartite graph if and only if $q_n = 0$.

The link between the eigenvalues of a graph and the molecular orbital energy levels of $\pi-$ electrons in conjugated hydrocarbons is the most crucial chemical application of graph theory. The total $\pi-$ electron energy in conjugated hydrocarbons is calculated by the sum of absolute values of the eigenvalues corresponding to the molecular graph Γ which has a maximum of four degree generally for the Hüchkel molecular orbital approximation. The energy of Γ given by Gutman in [4] is as follows:

$$E(\Gamma) = \sum_{i=1}^{n} \left|\lambda_i(\Gamma)\right|. \tag{1}$$

Nowadays, there is a lot of study on graph energy, as can be seen from the recent papers [5].

The square roots of the eigenvalues of the matrix MM^T are known as the singular values of some $n \times m$ matrix M and its transpose M^T. Recently, in [2], Nikiforov introduced and explored the notion of graph energy. He defined the energy $E(\Gamma)$ of a graph to be the sum of singular values of any matrix M. Clearly, $E(\Gamma) = E(A(\Gamma))$.

Assume that $I(\Gamma)$ represents the vertex-edge incidence matrix of the graph Γ. Then, for Γ having vertex set $V(\Gamma)$ and edge set $E(\Gamma)$, the $(i, j)-$ entry of $I(\Gamma)$ is 0 if v_i is not incident with e_j and 1 if v_i is incident with e_j. Jooyandeh et al. [6]

introduced the notion of incidence energy of a graph. Accordingly, the incidence energy IE of Γ is the sum of the singular values of the incidence matrix of Γ. The following expression is given by Gutman et al. [7]:

$$\mathrm{IE} = \mathrm{IE}(\Gamma) = \sum_{i=1}^{n} \sqrt{q_i(\Gamma)}. \tag{2}$$

Some basic information on IE may be seen in [6, 7].

As abovementioned, one can compute the incidence energy of a graph Γ by calculating the eigenvalues of signless Laplacian matrix of Γ. However, the problem is much more complicated for some classes of graphs due to the computational complexity of finding eigenvalues of signless Laplacian matrix. Thus, to compute the invariant for some classes of graphs, it is crucial to find their lower and upper bounds. Zhou [8] found the upper bounds on the incidence energy in terms of the first Zagreb index. Different lower and upper bounds on IE have been studied by various researchers.

In [9], associated to the Laplacian eigenvalues, authors introduced the invariant called the Laplacian energy-like invariant (or Laplacian-like energy) which is defined as follows:

$$\mathrm{LEL} = \mathrm{LEL}(\Gamma) = \sum_{i=1}^{n-1} \sqrt{\mu_i}. \tag{3}$$

Firstly, it was examined in [9] that LEL and Laplacian energy have similar characteristics. It has also been shown that it resembles to graph energy much more closely. For detailed information, see [10].

For a graph Γ of order n and a real number ε not equal to 0 and 1 in [8], the sum of the εth powers of the nonzero Laplacian eigenvalues is defined as follows:

$$\sigma_\varepsilon = \sigma_\varepsilon(\Gamma) = \sum_{i=1}^{n-1} \mu_i^{\varepsilon}. \tag{4}$$

If ε is 0 and 1, then the cases are trivial as $\sigma_0 = n-1$ and $\sigma_1 = 2m$, where m denotes the cardinality of the edge set of Γ. It is clear that $\sigma_{1/2}$ is equal to LEL. We should note that $n\sigma_{-1}$ is also equal to the Kirchhoff index of Γ (for more detail (one can see [11, 12]). Many studies on σ_ε have recently been published in the literature. For details, see [13, 14].

Similar to the definitions of IE, LEL, and σ_ε, Akbari et al. [15] defined the sum of the εth powers of the signless Laplacian eigenvalues of Γ as follows:

$$s_\varepsilon = s_\varepsilon(\Gamma) = \sum_{i=1}^{n} q_i^{\varepsilon}, \tag{5}$$

and they also gave some connections between σ_ε and s_ε. If ε is 0 and 1, then the cases are trivial as $s_0 = n$ and $s_1 = 2m$. Note that $s_{1/2}$ is equal to the incidence energy IE. We observed that Laplacian eigenvalues and signless Laplacian eigenvalues of bipartite graphs are equal [1, 3, 16]. Therefore, for bipartite graphs, σ_ε and s_ε are equal, and hence, LEL is equal to IE [17]. Recently, different properties, as well as different lower and upper bounds of s_ε have been established in [15, 17, 18].

Lemma 1 (see [19]). *Let $a_1, a_2, \ldots, a_n$ be nonnegative numbers. Then,*

$$\begin{aligned} n\left[\frac{1}{n}\sum_{i=1}^{n} a_i - \left(\prod_{i=1}^{n} a_i\right)^{1/n}\right] &\le n\sum_{i=1}^{n} a_i - \left(\sum_{i=1}^{n}\sqrt{a_i}\right)^2 \\ &\le n(n-1)\left[\frac{1}{n}\sum_{i=1}^{n} a_i - \left(\prod_{i=1}^{n} a_i\right)^{1/n}\right]. \end{aligned} \tag{6}$$

The equality among them holds if and only if $a_1 = a_2 = \cdots = a_n$.

We aim to obtain some strong bounds using the efficient inequality technique in Lemma 1 for main results. Also, we give some generalizations for s_ε, σ_ε, indicence energy IE, and the Laplacian energy-like invariant LEL of graphs (with r connected components, connected nonbipartite, and connected bipartite).

The following main lemmas are required for our main results.

Let $t = t(\Gamma)$ denote the number of spanning trees of a graph Γ. Let $\Gamma_1 \times \Gamma_2$ be the Cartesian product of the graphs Γ_1 and Γ_2. We define the following number for a graph Γ.

$$t_1 = t_1(\Gamma) = \frac{2t(\Gamma \times K_2)}{t(\Gamma)}. \tag{7}$$

Lemma 2 (see [20]). *If Γ is a connected bipartite graph with n vertices, then $\prod_{i=1}^{n-1}\mu_i = \prod_{i=1}^{n-1} q_i = nt(\Gamma)$. If Γ is a connected nonbipartite graph with n vertices, then $\prod_{i=1}^{n} q_i = t_1$.*

Lemma 3 (see [21]). *Let Γ be a connected graph with $n \ge 3$ vertices and maximum degree Δ. Then, $\mu_2 = \cdots = \mu_{n-1}$ if and only if $\Gamma \cong K_n$ or $\Gamma \cong K_{1,n-1}$ or $\Gamma \cong K_{\Delta,\Delta}$.*

Lemma 4 (see [21]). *Let Γ be a connected graph of order n. Then, $\mu_1 = \cdots = \mu_{n-1}$ if and only if $\Gamma \cong K_n$.*

Lemma 5 (see [3]). *The spectra of $L(\Gamma)$ and $Q(\Gamma)$ coincide if and only if the graph Γ is bipartite.*

2. Main Results

After above preliminary informations, we are ready to give our main results.

It is well known that if a graph Γ has r connected components, the spectrum of Γ is the union of the spectra of Γ_i, $1 \le i \le r$ (and multiplicities are added). The same also holds for the Laplacian and the signless Laplacian spectrum.

Firstly, we give lower and upper bounds on s_ε and σ_ε for a graph with r connected components.

Theorem 6. *Let Γ be a graph of order n with r connected components such that p of them are connected bipartite. Then,*

$$\begin{gathered}\sqrt{\sigma_{2\varepsilon} + (n-r)(n-r-1)R_{n-r}^{2\varepsilon/(n-r)}} \le \sigma_\varepsilon \le \sqrt{\sigma_{2\varepsilon}(n-r-1) + (n-r)R_{n-r}^{2\varepsilon/(n-r)}},\\ \sqrt{s_{2\varepsilon} + (n-p)(n-p-1)\Delta_{n-p}^{2\varepsilon/(n-p)}} \le s_\varepsilon \le \sqrt{s_{2\varepsilon}(n-p-1) + (n-p)\Delta_{n-p}^{2\varepsilon/(n-p)}},\end{gathered} \tag{8}$$

where $R_{n-r} = \prod_{i=1}^{n-r}\mu_i$ and $\Delta_{n-p} = \prod_{i=1}^{n-p} q_i$. Equalities occur in both bounds if and only if $\mu_1 = \mu_2 = \cdots = \mu_{n-r}$ and $q_1 = q_2 = \cdots = q_{n-p}$, respectively.

Proof. Note that 0 is an eigenvalue of Laplacian matrix with multiplicity r. Taking $a_i = \mu_i^{2\varepsilon}$, replacing n by $n-r$ in Lemma 1, we obtain the following equation:

$$W \le (n-r)\sum_{i=1}^{n-r}\mu_i^{2\varepsilon} - \left(\sum_{i=1}^{n-r}\mu_i^{\varepsilon}\right)^2 \le (n-r)W, \tag{9}$$

where

$$W = (n-r)\left[\frac{1}{n-r}\sum_{i=1}^{n-r}\mu_i^{2\varepsilon} - \left(\prod_{i=1}^{n-r}\mu_i^{2\varepsilon}\right)^{1/(n-r)}\right]. \tag{10}$$

Since $\sum_{i=1}^{n-r}\mu_i^{\varepsilon} = \sigma_\varepsilon$, we have the following equation:

$$W \le (n-r)\sigma_{2\varepsilon} - \sigma_\varepsilon^2 \le (n-r)W. \tag{11}$$

Observe that

$$\begin{aligned}W &= (n-r)\left[\frac{1}{n-r}\sum_{i=1}^{n-r}\mu_i^{2\varepsilon} - \left(\prod_{i=1}^{n-r}\mu_i^{2\varepsilon}\right)^{1/(n-r)}\right]\\ &= (n-r)\left[\frac{1}{n-r}\sigma_{2\varepsilon} - R_{n-r}^{2\varepsilon/(n-r)}\right]\\ &= \sigma_{2\varepsilon} - (n-r)R_{n-r}^{2\varepsilon/(n-r)}.\end{aligned} \tag{12}$$

Hence, we get the result.

From Lemma 1, the equalities hold if and only if $\mu_1 = \mu_2 = \cdots = \mu_{n-r}$.

It is known that 0 is an eigenvalues of signless Laplacian matrix with multiplicity p. For s_ε, the proof is similar, replacing n by $n-p$ and taking $a_i = q_i^{2\varepsilon}$ in Lemma 1.

As a special case, if we take $\varepsilon = 1/2$, we get the bounds for the LEL and IE given as follows: □

Corollary 7. *Let Γ be a graph of order n with r connected components such that p of them are connected bipartite. Then,*

$$\begin{gathered}\sqrt{2m + (n-r)(n-r-1)R_{n-r}^{1/(n-r)}} \le \mathrm{LEL} \le \sqrt{2m(n-r-1) + (n-r)R_{n-r}^{1/(n-r)}},\\ \sqrt{2m + (n-p)(n-p-1)\Delta_{n-p}^{1/(n-p)}} \le IE \le \sqrt{2m(n-p-1) + (n-p)\Delta_{n-p}^{1/(n-p)}},\end{gathered} \tag{13}$$

where $R_{n-r} = \prod_{i=1}^{n-r}\mu_i$ and $\Delta_{n-p} = \prod_{i=1}^{n-p} q_i$. Equalities hold in both bounds if and only if $\mu_1 = \mu_2 = \cdots = \mu_{n-r}$ and $q_1 = q_2 = \cdots = q_{n-p}$, respectively.

Note that, if we take $r = 1$ and $p = 0$ in Theorem 6, we reach the following result.

Corollary 8. *Let Γ be a nonbipartite connected graph of order n. Let t and t_1 be as given in Lemma 2. Then,*

$$\sqrt{\sigma_{2\varepsilon} + (n-1)(n-2)(nt)^{2\varepsilon/(n-1)}} \le \sigma_\varepsilon \le \sqrt{\sigma_{2\varepsilon}(n-2) + (n-1)(nt)^{2\varepsilon/(n-1)}}, \tag{14}$$

and

$$\sqrt{s_{2\varepsilon}+n(n-1)t_1^{2\varepsilon/n}} \leq s_\varepsilon \leq \sqrt{s_{2\varepsilon}(n-1)+nt_1^{2\varepsilon/n}}. \tag{15}$$

Inequalities (14) and (15) hold in both bounds if and only if $\Gamma \cong K_n$ and $q_1 = q_2 = \cdots = q_n$, respectively.

Taking $\varepsilon = 1/2$ in Corollary 7, we have the following corollary.

Corollary 9. *Let Γ be a nonbipartite connected graph of order n and t and t_1 be as given in Lemma 2. Then,*

$$\sqrt{2m+(n-1)(n-2)(nt)^{1/(n-1)}} \leq \mathrm{LEL} \leq \sqrt{2m(n-2)+(n-1)(nt)^{1/(n-1)}}, \tag{16}$$

and

$$\sqrt{2m+n(n-1)t_1^{1/n}} \leq \mathrm{IE} \leq \sqrt{2m(n-1)+nt_1^{1/n}}. \tag{17}$$

Equalities (16) and (17) hold in both bounds if and only if $\Gamma \cong K_n$ and $q_1 = q_2 = \cdots = q_n$, respectively.

Now, we consider the bipartite graph case of the above theorem (Theorem 6). In the next corollary, we actually improved the results which were obtained in [22].

Corollary 10. *Let Γ be a connected bipartite graph with n vertices. Let t be as given in Lemma 2. Then,*

$$\sqrt{s_{2\varepsilon}+(n-1)(n-2)(nt)^{2\varepsilon/(n-1)}} \leq s_\varepsilon = \sigma_\varepsilon \leq \sqrt{s_{2\varepsilon}(n-2)+(n-1)(nt)^{2\varepsilon/(n-1)}}, \tag{18}$$

and

$$\sqrt{2m+(n-1)(n-2)(nt)^{1/(n-1)}} \leq \mathrm{IE} = \mathrm{LEL} \leq \sqrt{2m(n-2)+(n-1)(nt)^{1/(n-1)}}. \tag{19}$$

Equalities (18) and (19) hold in both bounds if and only if $\Gamma \cong K_n$, $\Gamma \cong K_{1,n-1}$, or $\Gamma \cong K_{\Delta,\Delta}$, where Δ is the maximum degree.

As it is well known in graph theory, every tree is bipartite. In addition, for a tree T, $m = n-1$ and $t = 1$. From Corollary 10, we have the following.

Corollary 11. *Let T be a tree of order n. Then,*

$$\begin{aligned} &\sqrt{\sigma_{2\varepsilon}+(n-1)(n-2)n^{2\varepsilon/(n-1)}} \leq s_\varepsilon(T) = \sigma_\varepsilon(T) \leq \sqrt{\sigma_{2\varepsilon}(n-2)+(n-1)n^{2\varepsilon/(n-1)}},\\ &\sqrt{(n-1)\left[2+(n-2)n^{1/(n-1)}\right]} \leq \mathrm{IE}(T) = \mathrm{LEL}(T) \leq \sqrt{(n-1)\left[2(n-2)+n^{1/(n-1)}\right]}. \end{aligned} \tag{20}$$

Equalities hold in both bounds if and only if $T \cong K_{1,n-1}$.

Remark 12. It is pertinent to mention here that in equations (15) and (17), for connected nonbipartite graphs, we recover the same lower bounds as in Theorem 2.6 (i) and Corollary 2.7 (i) in [22] through a different approach. For connected bipartite graphs, it can be seen that lower bounds (18) and (19) are better than lower bounds obtained in Theorem 2.6 (ii) and Corollary 2.7 (ii) in [22], respectively. Moreover, we obtained extra upper bounds for the relevant parameters and generalized them as different forms [22].

3. Accomplishment Remarks

In this paper, we have obtained new results for the graph invariants s_ε and σ_ε of a simple graph Γ with r connected components (connected nonbipartite and connected bipartite), where $\varepsilon(\neq 0,1)$ is a real number. Also, as a result, we generalized and improved the results on incidence energy (IE) and Laplacian energy-like invariant (LEL).

Data Availability

All data and materials used to obtain the results are included within the article.

Conflicts of Interest

The authors declare that they have no conflicts of interest.

References

[1] R. Merris, "Laplacian matrices of graphs: a survey," *Linear Algebra and its Applications*, vol. 197, pp. 143–176, 1994.

[2] V. Nikiforov, "The energy of graphs and matrices," *Journal of Mathematical Analysis and Applications*, vol. 326, no. 2, pp. 1472–1475, 2007.

[3] D. Cvetković, P. Rowlinson, and S. K. Simić, "Signless Laplacians of finite graphs," *Linear Algebra and Its Applications*, vol. 423, no. 1, pp. 155–171, 2007.

[4] I. Gutman, "The energy of a graph," *Graz. Forschungszentrum*, vol. 103, no. 100-105, pp. 1–22, 1978.

[5] J. Rada and A. Tineo, "Upper and lower bounds for the energy of bipartite graphs," *Journal of Mathematical Analysis and Applications*, vol. 289, no. 2, pp. 446–455, 2004.

[6] M. Jooyandeh, D. Kiani, and M. Mirzakhah, "Incidence energy of a graph," *Match Communications in Mathematical*, vol. 62, no. 3, pp. 561–572, 2009.

[7] I. Gutman, D. Kiani, and M. Mirzakhah, "On incidence energy of graphs," *Match Communications in Mathematical*, vol. 62, no. 3, pp. 573–580, 2009.

[8] B. Zhou, "On sum of powers of the Laplacian eigenvalues of graphs," *Linear Algebra and Its Applications*, vol. 429, no. 8-9, pp. 2239–2246, 2008.

[9] J. Liu and B. Liu, "A Laplacian-energy like invariant of a graph," *Match Communications in Mathematical*, vol. 59, pp. 355–372, 2008.

[10] B. Liu, Y. Huang, and Z. You, "A survey on the Laplacian-energy like invariant," *Match Communications in Mathematical*, vol. 66, pp. 713–730, 2011.

[11] D. Bonchev, A. T. Balaban, X. Liu, and D. J. Klein, "Molecular cyclicity and centricity of polycyclic graphs I Cyclicity based on resistance distances or reciprocal distances," *International Journal of Quantum Chemistry*, vol. 50, no. 1, pp. 1–20, 1994.

[12] J. Palacios, "Foster's formulas via probability and the Kirchhoff index," *Methodology and Computing in Applied Probability*, vol. 6, no. 4, pp. 381–387, 2004.

[13] K. Das, K. Xu, and M. Liu, "On sum of powers of the Laplacian eigenvalues of graphs," *Linear Algebra and Its Applications*, vol. 439, no. 11, pp. 3561–3575, 2013.

[14] G. X. Tian, T. Z. Huang, and B. Zhou, "A note on sum of powers of the Laplacian eigenvalues of bipartite graphs," *Linear Algebra and Its Applications*, vol. 430, no. 8-9, pp. 2503–2510, 2009.

[15] S. Akbari, E. Ghorbani, J. H. Koolen, and M. R. Oboudi, "On sum of powers of the Laplacian and signless Laplacian eigenvalues of graphs," *Electronic Journal of Combinatorics*, vol. 17, no. 1, p. R115, 2010.

[16] R. Merris, "A survey of graph Laplacians," *Linear and Multilinear Algebra*, vol. 39, no. 1-2, pp. 19–31, 1995.

[17] S. B. Bozkurt and I. Gutman, "Estimating the incidence energy," *Match Communications in Mathematical*, vol. 70, pp. 143–156, 2013.

[18] M. Liu and B. Liu, "On sum of powers of the signless Laplacian eigenvalues of graphs," *Hacettepe Journal of Mathematics and Statistics*, vol. 41, pp. 2243–2251, 2012.

[19] B. Zhou, I. Gutman, and T. Aleksić, "A note on the Laplacian energy of graphs," *Match Communications in Mathematical*, vol. 60, pp. 441–446, 2008.

[20] D. Cvetković and S. K. Simić, "Towards a spectral theory of graphs based on the signless Laplacian, II," *Linear Algebra and Its Applications*, vol. 432, no. 9, pp. 2257–2272, 2010.

[21] K. Das, "A sharp upper bound for the number of spanning trees of a graph," *Graphs and Combinatorics*, vol. 23, no. 6, pp. 625–632, 2007.

[22] A. D. Maden, "New bounds on the incidence energy, randić energy and randić estrada index," *Match Communications in Mathematical*, vol. 74, pp. 367–387, 2015.

Hindawi
Journal of Mathematics
Volume 2022, Article ID 1618498, 7 pages
https://doi.org/10.1155/2022/1618498

Research Article

Graph Theory Algorithms of Hamiltonian Cycle from Quasi-Spanning Tree and Domination Based on Vizing Conjecture

T. Anuradha,[1] **T. Lakshmi Surekha**,[1] **Praveena Nuthakki**,[1] **Bullarao Domathoti**,[2] **Ganesh Ghorai**,[3] **and Faria Ahmed Shami**[4]

[1]*Department of Information Technology, Velagapudi Ramakrishna Siddhartha Engineering College, Vijayawada, AP, India*
[2]*Department of Computer Science and Engineering, Jawaharlal Nehru Technological University, Ananthapuram 517501, India*
[3]*Department of Applied Mathematics with Oceanology and Computer Programming, Vidyasagar University, Midnapore 721102, India*
[4]*Department of Mathematics, Bangabandhu Sheikh Mujibur Rahman Science and Technology University, Gopalganj, Bangladesh*

Correspondence should be addressed to T. Anuradha; anuradha_it@vrsiddhartha.ac.in, Bullarao Domathoti; bullaraodomathoti@gmail.com, and Faria Ahmed Shami; fariashami@bsmrstu.edu.bd

Received 24 February 2022; Accepted 16 July 2022; Published 25 August 2022

Academic Editor: M. T. Rahim

Copyright © 2022 T. Anuradha et al. This is an open access article distributed under the Creative Commons Attribution License, which permits unrestricted use, distribution, and reproduction in any medium, provided the original work is properly cited.

In this study, from a tree with a quasi-spanning face, the algorithm will route Hamiltonian cycles. Goodey pioneered the idea of holding facing 4 to 6 sides of a graph concurrently. Similarly, in the three connected cubic planar graphs with two-colored faces, the vertex is incident to one blue and two red faces. As a result, all red-colored faces must gain 4 to 6 sides, while all obscure-colored faces must consume 3 to 5 sides. The proposed routing approach reduces the constriction of all vertex colors and the suitable quasi-spanning tree of faces. The presented algorithm demonstrates that the spanning tree parity will determine the arbitrary face based on an even degree. As a result, when the Lemmas 1 and 2 theorems are compared, the greedy routing method of Hamiltonian cycle faces generates valuable output from a quasi-spanning tree. In graph idea, a dominating set for a graph $S = (V, E)$ is a subset D of V. The range of vertices in the smallest dominating set for S is the domination number (S). Vizing's conjecture from 1968 proves that the Cartesian fabricated from graphs domination variety is at least as big as their domination numbers production. Proceeding this work, the Vizing's conjecture states that for each pair of graphs S, L.

1. Introduction

Finite integral multipliers are used in the greedy routing algorithm. For the maximal tree, subgraphs are used, in which subgraph is denoted as S. If the edges are suitably labeled, the two trees are distributed among them. Here the variation of a tree's maximum number is established on the vertices n and it is known as the Cayley. In general, a graph S is drawn from the spanning tree vertices. The spanning tree is evaluated by using a single edge S. To define the system's vertex, a diagonal matrix is introduced. The variation between the adjacency matrix and the incidence matrix is determined by the spanning tree. Thus, the subgraph S contains all the vertices, and the diameter for any single tree graph D is denoted as

$$\operatorname{diam}(T(S)) \le \min\{n-1, m-n+1\}. \quad (1)$$

A spinning graph diameter is determined by one of the two trees, T_1 or T_2, and is denoted as

$$d(T_1, T_2) = n - 1 - |E(T_1) \cap E(T_2)| = \frac{|E(T_1) \Delta E(T_2)|}{2}. \quad (2)$$

The graph tree operation is denoted as $T\colon S \longrightarrow S$. The subsequent matrix is to combine rows and columns. Next to defining the spanning tree estimation, the product value is obtained. Cauchy-Binet present the estimation. This entire calculation is followed by vertices and adjacency calculations. The edges of the cycle are counted by the sign, and an insertion form appears [1]. To classify subgraphs and establish paths from subgraphs, the edge is connected to the spanning tree. The geometric cycle is not equal to the value of the subgraph.

2. Hamiltonian Cycle from Quasi-Spanning Tree of Faces

There is precisely one Hamiltonian cycle along with no cubic graphs, which is a unique Hamiltonian graph because a minimum of three Hamiltonian cycles are there in a Hamiltonian cubic graph. In 1978, Thomason showed that in a graph with the vertices of the odd degree, in an even number of Hamiltonian cycles, all edges are confined, proving Smith's result [2]. Hence, uniquely Hamiltonian graphs unless even degree vertices and especially k regular exclusively. Odd k does not have Hamiltonian graphs. What is even k? Thomason showed that by Lovász local lemma, k-regular exclusively even $k \geq 300$ does not have Hamiltonian graphs [3], by a cautious option of parameters, theirs statements provide 73 rather of 300. That was modified by Haxell, Seamone, and Verstraete to $k \geq 23$. No 4-regular exclusively Hamiltonian graphs existed assumed by Sheehan. The fact of this assumption would indicate that cycles are the only regular exclusively Hamiltonian graphs, as according to Petersen's 2-factor theorem.

According to Thomason's result, an exclusively Hamiltonian graph has a necessity of minimum of two even degree vertices. This connection between the degree of the graph and either or not it is exclusively Hamiltonian increases several ordinary enquiries, such as either there are any exclusively Hamiltonian graphs of degree 3. Swart and Entringer gave a positive answer to that question by relating in closely cubic graphs an infinite family, that is, graphs along precisely two degrees 4 vertices and all of the other cubic vertices. Fleischer lately demonstrated that there are graphs with every vertex having a degree of 4 or 14 that are uniquely Hamiltonian [4].

Jackson and Bondy examined that an individually Hamiltonian graph of order n consumes minimum one-degree vertex maximum $c\log 28n + 3$, which means the minimum degree is smaller than this number, here $c \approx 2.41$. Jamshed and Abbasi modified that to $\log 2n + 2$, here $c \approx 1.71$. Jackson and Bondy were especially attentive to planar exclusively Hamiltonian graphs in their article. A graph necessity has a minimum of two vertices of degree 2 or 3 that are displayed by them and assumed that all planar individually Hamiltonian graphs must have a minimum of two vertices of degree 2.

Proposition 1. *Given S consumes a Hamiltonian cycle through the exterior red face outdoor, all blue face within, and an edge is shared by no two red faces are together within, then the reduced graph H consumes a face's spanning tree through in D does not contain the external face.*

Proof. S consumes a Hamiltonian cycle through the exterior red face external, every blue faces consistent to vertices in within, and an edge is shared by no two red faces are together insides, if and only if the reduced graph H consumes a face's quasi-spanning tree through in D does not contain the external face. □

Theorem 1. *Assume that all red faces have 6 sides or 4 sides, whereas blue faces have 3 or 5 sides, and that blue faces through 3 sides or 5 sides are adjacent to a minimum of one red face along with 4 sides (no conjecture is created for blue faces by 4, 6, 7, 8, 9, . . . sides). The reduced graph H, which is obtained by crumbling blue faces, then has a correct quasi-spanning tree of faces, prove S a Hamiltonian cycle.*

2.1. We Now Prove the Main Result of This Section. Assume that all of S's red faces have 4 sides or 6 sides, whereas the faces of blue are chance. Assume that the reduced graph H contains a triangle T with a minimum one vertex within, and no triangle in T is none a face (i.e., includes minimum a vertex inside), and that no digon within T is not a face (i.e., includes minimum one vertex within). We shall simplify the inside of the triangle T one step at a time while preserving the property that which is no digon inside of T that is not a face but authorizing the presence of triangles inside of T that are not faced, subject to the succeeding conditions. Handle entire sets of parallel edges like a single edge. Assume T_1 and T_2 are different triangles within of T, along T_1 including T_2 and perhaps T_1 like as T, where T_2 is not a face, and so that there is no triangle T_3 differ from T_1 and T_2 like that T_1 includes T_3 and T_3 includes T_2. Then, we assume that T_2 is a child of T_1. We will need that no triangle T_1 consumes three different children T_2, T_2', and T_2'', any steps in explanation of the inside of the triangle T.

The invariant property of T is that no digon within T is not a face, and no triangle within T consumes three different children.

Lemma 1. *Assume T consumes a minimum of two vertices within and fulfills the invariant property, proving that it is feasible to choose a triangle T' that is to say a face within T and crimple T' into an only vertex so that T even gratify the invariant property [4].*

Proof. Assume that triangle T_1 within T includes a minimum of two vertices and that not any triangle within T_1 is not a face. Take $T_1 = v_1v_2v_3$, in T_1, we declare that v_1 consumes a minimum of two different neighbors v_4, v_5. Else, if v_1 consumes no neighbors, so v_1 goes to a triangle within T_1 with an edge v_2v_3 parallel to the side of T_1, which is a contradiction to the hypothesis that has no digon within of T it is nonface, and while v_1 has unique like a neighbor v_4 within of T_1, therefore $v_2v_3v_4$ is a triangle within of T_1 it is not a face, which is also a contradiction to the hypothesis.

Then we can select v_4 and v_5 to v_2, v_4, v_5 are successive neighbors of v_1, and crumble the triangle $v_1v_4v_5$. There will be no digons that are not faced as a result of this because like a digon gets here before the crumpling from a triangle which is not a face within T_1, a contradiction to the hypothesis. Inside T_1, though, triangles that do not face may appear. Similar triangles derived from quadrilaterals $v_1v_4v_6v_7$, $v_1v_5v_8v_9$, and $v_4v_5v_{10}v_{11}$. The quadrilaterals $v_1v_5v_8v_9$ can be one of two types: they can contain v_4 or they cannot contain v_4, but they cannot have diagonal edges v_1v_8 or v_5v_9, because then either a triangle this isn't a face was within the quadrilateral, otherwise crumpling the side $v_1v_5$is does not provide the quadrilateral a triangle which is non a face. Such indicates that all like quadrilaterals including v_4 are couple included in all other, and every such quadrilateral that do not comprise v_4 are pairwise included together [9]. The analogous properties prove that for the quadrilaterals $v_1v_4v_6v_7$, However, there is only one kind of these, namely those that contain v_5. Else, $v_6 = v_2$ and we consume the diagonal edge v_2v_4. The quadrilaterals $v_4v_5v_{10}v_{11}$ contain analogous properties, but they are of a unique kind [10, 11], specifically do not comprise v_1, then they are included in the triangle $T_1 = v_1v_2v_3$. A quadrilateral $v_1v_4v_6v_7$ including v_5 essential also include at all quadrilateral $v_1v_5v_8v_9$ that does not contain v_4 and any quadrilateral $v_4v_5v_{10}v_{11}$ that does not contain v_1, and any quadrilateral $v_4v_5v_{10}v_{11}$ that does not contain v_1 must also contain any quadrilateral $v_1v_5v_8v_9$ that contains v_4 [12]. These assurances that these quadrilaterals do not take a main, next crumpling $v_1v_4v_5$, inside T_1, three triangles are not faces and do not conclude together, therefore conserving the property that three children are not taken by triangles [13-15].

For residual case in crumpling a triangle, here is a triangle T_1 which consumes any one child T_2 or two children T_2 and T_3, here together T_2 and T_3 consume precisely one vertex within. Assume T_2 shares no sides through any T_1 or T_3. We must take the quadrilaterals $v_1v_2v_4v_5$, $v_1v_3v_6v_7$, and $v_2v_3v_8v_9$ once more when writing $T_2 = v_1v_2v_3$. Quadrilaterals $v_1v_2v_4v_5$ including v_3, v_3, $v_1v_3v_6v_7$ including v_2, $v_2v_3v_8v_9$ including v_1, and $v_1v_2v_4'v_5'$ not including v_3 may not exist at the same time. For if $v_6 = v_5$, then $v_1v_5v_7$ is not a face and therefore equals T_1, thus v_1 is a vertex of T_1 and the quadrilateral $v_2v_3v_8v_9$ cannot include v_1; while $v_7 = v_4$, $v_1v_5v_4$ is T_1, and the similar argument applies, and while $v_6 = v_4$, then $v_8 = v_5$ and $v_9 = v_7$, so the triangle $v_5v_4v_7$ is T_1, this is not possible because the quadrilateral $v_1v_2v_4'v_5'$ would be inside the triangle $v_1v_2v_7$, it is called a face. As a result of symmetry, we can assume that after identifying v_1 and v_2, there is either no quadrilateral $v_1v_2v_4v_5$ including v_3, otherwise no quadrilateral $v_1v_2v_4v_5$ not including v_3, which will provide an increase to a fresh triangle which is not a face. Crumpling the triangle $v_1v_2v_0$ identifies v_1 and v_2 and creates unique triangles through pairwise confinement introduce the new vertex $v_1 = v_2$, except the triangle T_3, so conserving the property that three children are not taken by triangles. Assume $T_1 = v_1v_2v_3$ shares a single side by T_1, it is a side v_2v_3, then one of the other two sides is not shared by T_3, say the side v_1v_2, and the quadrilaterals $v_1v_2v_4v_5$ unable to include v_3, thus repeatedly we were able to crumple the triangle $v_1v_2v_0$ by v_0 within T_2, producing unique triangles through pairwise confinement introducing the new vertex $v_1 = v_2$, except the triangle T_3, so conserving the property that no triangle consumes three children. While T_2 and T_3 share aside v_1v_3, then every quadrilateral $v_1v_2v_4v_5$ that includes v_3v_3 also includes T_3 [16]. As a result, crumpling $v_1v_2v_0$ with v_0 inside T_2 provides two families of triangles through pairwise confinements concerning $v_1 = v_2$, one including v_3 and the another includingv_3, conserving the property that three children are not taken by triangles.

The succeeding proposition incorporates Herbert Fleischner's result [17]. □

Proposition 2. *Let us consider blue faces remain random and G's red faces get 4 to 6 sides. The reduced graph H has only one triangle which is in the outer layer and it does not have any faces, other than that the H graph has no triangles. H also incorporated no diagonal direction which is not even considered to face. H has a spanning tree face which is triangles and S is said to be Hamiltonian when H contains odd number vertices.*

Proof. While saving the invariant property, collaborate triangle faces into single vertices and redo Lemma 1. The total of vertices stays odd until the outer face remains by reducing the vertices by two. Eventually, a spanning tree is formed by the collaborated triangle. The main observation that results to this result is as follows: □

Lemma 2. *.In Theorem 1, take S as same. If the graph H has triangle T with only one vertex, there is no other triangle inside T, which is not considered to be a face also as it does not have any digons. To find out the acceptable quasi-spanning tree of faces for the graph H', identifying the appropriate quasi-spanning tree face is reduced. By separating all inside vertices (T) and incident edges, it tends to incorporate the look-alike edge inside T to every edge of T, H' obtained from the reduction graph H.*

Proof. As shown in the previous Lemma, by collapsing the triangle faces repeatedly we can wind up a v in T or else make nothing inside T. In a quasi-spanning tree of faces, choose one of the three triangles which imply v, which corresponds to the one in three diagonal directions for the sides of H' in T. And we might either choose triangle T in H' in a face of quasi-spanning trees. When the time T holds an off vertex and which is inside of T, in this scenario the vertex v which is in the T is obtained, and then when the moment T has an even number of vertices and which is in T, in this case, we reached T which has no vertices.

The parity inside the T is represented by the two cases. Initially, if there is a digon named v_1, v_2 has one endpoint which is in T, and to frame a triangle we need to collaborate v_1v_2, the framed triangle does not have any faces out of the quadrilaterals such as $v_{1,}v_{2,}v_{4,}v_5$, again there are a family of two quadrilaterals, consisting of two triangles as $v_{1,}v_{2,}v_{3,}$ and $v_{1,}v_{2,}v_3'$. Quadrilaterals have $v_{3,}$ and v_3'. The quadrilaterals provide triangles with pairwise boundaries of each family, which assures the property invariant that does not have T_1, which is equivalent to T or them have no children. Theorem allows S as connected cubic bipartite planar graph of three nodes. Let us assume, H' be the subgraph of H and reduced graph S is H,

Here we got the results by removing all the possible edges with successive side by side edges. If the graph has one and two and three connected elements since H' has face's spanning trees, then S contains a Hamiltonian cycle. In the occurrence of a single element for H', all faces among three colors of classes are considered.

We demonstrate vertex v inside of t only when there are no digons of v_1, v_2. Which pertained to one of four triangles that share with side T. After that, an appropriate quasi-spanning tree is built, two triangles v_1, v_2, v_3 and v, v_3, v_4 are included in the suitable spanning tree of faces and it does not share its edge. The collaborated triangles which are to remove v, identify v_1 upon v_2 also identifies v_3 with v_4 and convert 5 vertices to only 2 vertices, also change the number of vertices. Hence the complete proof of Lemma is derived.

We can write $T = v_1, v_2, v_3$ when there are no digons inside T initially. There need to be 2 vertices inside of T is present, if not the single vertex which inside T have a degree and it does not have any digons, assuming that the blue face with 3 sides is needed to be adjacent to one red face with at least 4 sides. This indicates v_1 need to have at least two distinct neighbors inside T, if not the case, v_0 is considered to be only one vertex of T, since there are no such triangles as faces. If we calculate v_1, v_2 and v_2, v_3, then v_1 contains a degree of 4. Similarly, edges v_2, v_3 holds at least a degree of 4. Further, there is no such vertex of T that has degree 3 or 5, as all of the blue faces with 3 to 5 sides are close to one red face with 4 sides, as a result, a vertex is considered to be incident to digon. As per Euler's formula, there must be three vertices of degree 4 in T, on the other hand, there are 6 vertices of degree 4, T is present. Let us assume v_0 which is inside T contains four consecutive neighbors: $v_4 v_5 v_6 v_7$. The quadrilateral share one edge with $T = v_1 v_2 v_3$, as we know T indicates triangle. As v_1, v_3 and v_1, v_2 are getting shared, v_1 has only one adjacent neighbor which is v_0 in T and it has degree 3 and not 4. Let us say v_4, v_7 might be shared with T. In this scenario, make v_0 to an appropriate vertex of quasi and choose the two triangles such as $v_0 v_6 v_7$ and $v_0 v_4 v_5$. Here, recognizing v_4 and v_5 detaching v_0 identifying v_6, v_7 and lessens the total number of vertices by 3. The quadrilaterals v_4, v_5, v_8, v_9 have the edge of v_6, v_7 which produces fresh triangles that contain v_6, v_7, v_{10}, v_{11} of quadrilaterals which also gives new triangles that contain v_4 and v_5 of edges. The quadrilaterals $v_6, v_7, v_{10}', v_{11}'$ have edges $v_{4,} v_5$ which gives triangles that are newly created and those triangles having quadrilaterals of v_4, v_5', v_8' does not have the edge $v_6 \& v_7$. By recognizing v_4, v_5 and v_6, v_7, we tend to attain two families of newly created triangles with every family giving containment which is considered as pairwise that occurs among its triangles.

This gives that the property does not have T_1 triangle and equal to T or else inside of T having three children. Before proceeding to minimize the number of vertices by T, which increases to two till a single vertex is not inside of T and thus finishes off the proof with variation in parity of numbers inside of T. As recently expressed, this decreases the issue of tracking down an appropriate semitraversing the tree of countenances for H to the assignment of erasing the vertices inside H and interfacing equal edges to the sides of T to acquire H'.

Theorem 1 produces Lemma as a digon is considered as the outer face or else a triangle which has vertices inside of it. There is a triangle that has vertices inside and it does not have any triangles or two vertices of diagon inside or else the diagon contains vertices inside and in the same manner it does not have any triangles or diagons vertices inside. By removing the vertices and adding the same parallel edges to the side of T, this T has vertices inside and it does not have any triangle either. It can be clarified as per Lemma 1. The digon v_1, v_2 have a triangle with vertices inside, when a digon v_1, v_2 has vertices inside but it does not have any triangle and it has a v_0 of a single vertex. Among v_0, v_1 and v_0, v_2, either one considered as a digon; only v_0 had the degree. For instance, it happens when v_0, v_1 is a digon. After removing the vertex v_0, we can moreover choose the digon v_0, v_1 otherwise the triangle v_0, v_1, v_2, that represent also not selecting or choosing the digon v_1, v_2 which has developed a face. When the outer face has no vertices in it and that the graph H is simplified. In such a case, what is considered to complete this process is while selecting the face involved all the vertices in the quasi-spanning tree faces of H and hence Theorem 1 is proved.

Coming up next is a rundown of corollary is an uncommon instance of Theorem 1 that sums up Goodey's outcome to diagrams S with just 4 sides or 6 sides. □

Corollary 1. *Assume S be a 3-connected cubic planar bipartite graph, while the S faces are three colored, through all S vertex incident to a face of all color, since two of the three color classes include only that have 4 sides or 6 sides. The reduced graph H, which is acquired by crumpling the class of the third color, thus includes a correct face's quasi-spanning tree, and hence S is a Hamiltonian cycle.*

2.2. NP Complete and Polynomial Problems. The following result is for a face's spanning tree where the majority of the faces are digons.

Theorem 2. *Consider S stay a 3-connected cubic planar bipartite graph. Assume the reduced graph H for S, and H' the subgraph of H found by eliminating each edge with consecutive parallel edges. H' has a face's spanning tree if it includes one or two or three connected components, and S contains a Hamiltonian cycle. In one of the three color classes, all the faces are squares in the case of a single component for H'.*

Proof. We can take H' be a spanning tree that corresponds to a spanning tree of digons in H, while H' is a single linked component.

We can take a f face of H which takes vertices from together components if H' has two connected components. For the two components of H', we assume two spanning trees of digons, starting with this face f, and enhance that digons are unique at the same time show they do not create a cycle including f. The single face f and the added digons desire eventually span H.

Although H' consumes three connected components, it is possible that H has a face f that touches each three, and we can move from f to two components by examining for the two components, the three spanning trees of digons. Otherwise, we consider the first component, which has faces that contact it, as well as the second and third components, which also contain faces that contact it and the third component. We can select a face f contact the first component and second component, and a face f' contact the first component and third component, so that those two faces do not divide each vertex, thus a cut of H has a minimum of four edges because of 3-connectivity and the reality that at all cut consumes an edge's even number. Initial through those two faces from the three spanning trees we can enhance digons for the three components thus far, a face's spanning tree for H is found since they do not form a cycle.

The result for three connected components applies to four connected components as well, but the result is not valid for five connected components.

Following that, we show how to decide in polynomial time that the reduced graph H consumes a face's spanning tree that is digons or triangles. Simply expands of the result, the case of a face's spanning tree where all but a face's constant number are digons or triangles. □

3. Domination in Graphs

Consider $S = (V, E)$ be a graph through the vertex set V and the boundary set E. If each vertex in s is adjacent to the vertex in s, it is a dominant set of S. The domain number of S, mentioned by $\gamma\,(S)$ that is called the minimum cardinality of a dominant set of S.

In the investigated branch of the diagram concept, supremacy in diagrams was used. The superiority of the diagrams was utilized in the examined division of the diagram idea. Blending problems with optimal problems, classical problems, and combinatorial problems is a growing principle. It has several applications in a range of fields, including body sciences, engineering, life sciences and society, and so on. The research interest in the graph concept these days is centered on dominance. This is essentially a list of new parameters that may be improved from basic dominance definitions. The NP completeness of elementary domination problems and investigate the relation to another NP completeness by them and action growth in the domination principle.

When in a graph S every vertex is incident on at least one edge in g, the set of edges g is said to cover S. The edge covering a set of a graph S is said to be an edge covering or a cover subgraph or simply a S cover (e.g., a spanning tree in a linked graph is a cover). The example of a computer network over the relation minimum vertex coverage is shown in Figure 1 [5].

3.1. Applications of Domination in Graph. The graph applications of domination have been applied in a variety of

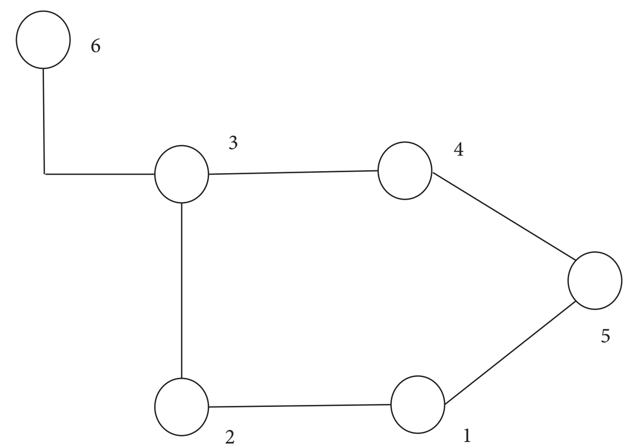

FIGURE 1: The set of vertices $g = \{1,3,4\}$ in S all vertices are cover.

fields. The dominion comes from structural challenges in which there is a constant type of centers (e.g., hearth stations, hospitals) and space must be kept to a minimum. To diminish the number of locations where a surveyor needs to commit to taking peak measurements for a whole area, surveyors use standards of domination.

3.2. Domination Path. A graph containing a dominating path is one where each vertex exterior of P includes a neighbor on P. Let $V\,(S)$ represents the vertex and $E\,(S)$ represents a S graph's edge set. $N_S\,(v)$ represents a vertex's neighborhood v in S and $d_S\,(v)$ denotes its degree. For $D, T \subseteq V\,(S) D$, represented by letting $N_S\,(T) = U_{v\in \mathrm{T}} N_S\,(v) - T$ and letting $N_D\,(T) = N_S\,(T) \cap D$ and $d_D\,(T) = |N_D\,(T)|$. Likewise, $\delta(S)$ represents the minimum vertex degree and $\Delta(S)$ represents the maximum vertex degree.

Theorem 3. *Since $n \geq 2$, each connected n-vertex graph S along $\delta\,(S) > (n - 1/3) - 1$ contains a dominating path and proves the inequality is acute.*

Proof. The sharpness structure is declared for $n \equiv 1 \mathrm{mod} 3$. In general, assume Q_i for $k = 1$ the structure be a clique over $\lfloor (n + 2 - i)/3 \rfloor$ vertices, $i \in \{1, 2, 3\}$. Then the three cliques jointly moreover include $n - 1$ vertices, $\delta(G) = \lfloor n - 1/3 \rfloor - 1$. Now presume that S is a connected graph of n-vertex over $\delta\,(S) \geq (n - 1)/3$ which include no dominating path; find that $n \leq 3t + 3$, here $t = \delta\,(S)$. Assume first that S is 2-connected. Dirac showed that S essential since containing a cycle over at least min $\{n, 2\delta\,(S)\}$ vertices. A path over minimum $n - t$ is a dominating path vertex, so we can connect $t < (n/2)$. Once S is 2-connected, we consume $t \geq 2$, and S contain a cycle C of length minimum $2t$. While $V\,(C)$ dominating path does not have the vertex set, further few vertex u and on C its neighbors are not. Since S is connected, here is the shortest path P_u start at $V\,(C)$ and end at u. Summing to a path P_u along with C at one end and u's alternative neighbor at the other end (existing then $t \geq 2$) gains a path P along minimum $2t + 3$ vertices. While P it is not that a dominating path, therefore $V\,(P)$ neglects its neighborhood and some other vertex, it needs $n \geq 3k + 4$, an inconsistency. Therefore, S must include a cut-vertex v. Every component of $S - v$ has minimum t vertices, so $S - v$ has a maximum of three components. Since $S - v$ has maximum $3t + 2$ vertices, consuming three components along minimum t vertices needs one through precisely t vertices. So, a $S - v$ component shall be a complete graph through all vertices adjacent to v. Further two components take order maximum $k + 2$, therefore a vertex w in like a component H is nonadjacent to maximum one other vertex of H, while w is nonadjacent to v. As a result, S contains a dominating path that include v and in this case two vertices each from the two majors $S - v$ components. In the leftover case, $S - v$ consumes two components, though also contains a cut-vertex w, therefore $S - v - w$ include three closely complete components flexible in a dominating path as shown in the above section. While every component of $S - v$ is 2-connected, since all contain a cycle which is spanning or consumes minimum $2t - 2$ vertices, then removing v depart a minimum degree at least $t - 1$. All component contains at most $2t + 2$ vertices because it includes minimum t vertices. We get a path across v that is dominating and neglects very few vertices. On other hand provides a brief proof of nearly the optimal threshold for 2-connected graphs. Dirac's theorem proves too that suppose $\delta(H) > |V(H)|/2$, therefore H is Hamiltonian-connected, sense that some two vertices are a spanning path's terminus. In a P path start at u and end at v and $R \subseteq V(P)$, consider R^+ represent the instant successors set vertices of R with P, and consider R^- represents the set of instant predecessors. We know that $|R^+| = |R^-| = |R|$ once R includes no terminus of P. □

3.3. Vizing's Conjecture in Domination. The comparison of the dimensions of minimal dominant sets and Vizing conjectures in the S and L graphs, in the Cartesian product graph that is called a dominant set. The proof of the Vizing theorem with the use of some colors, every simple non-oriented graph can be multicolored.

Let $S = [V(S), E(S)]$ be determinate. In vertex subsets, P dominates K though $K \subseteq N[P]$, that is, while each K vertex is in P, otherwise is adjacent to a P vertex. P dominates outwardly K, when K, P are separate and P dominate K. The S domain number is the lowest represented cardinal $\gamma(S)$ dominating $V(S)$. Although D dominates $V(S)$, further, D dominates S and this D is a S's dominant set.

Each closed quarter in S must span any dominant set of S. Hence, the domain number of S is minimum similar to the cardinality of whatever set $X \subseteq V(S)$ consuming the characteristics that for different x_1, x_2 in X, and $N[x_1] \cap N[x_2] = \theta$. So, a set X is known as 2-packing and $\sigma(S)$ is represented the maximum cardinality of a 2-packing in S and is named the 2-packing number of S. The independence number of a vertex in S is the maximum cardinality $\sigma(S)$ of an independent set of vertices in S, and the smallest cardinality of a dominant set that is likewise independent is represented $I(S)$.

Assume S is not a complete graph prove for every vertex pair v_1 and v_2 which are not adjacent to S, it is proved that $\gamma(S) - 1 \leq \gamma(S + v_1v_2) \leq \gamma(S)$. While S has the property that $\gamma(S) - 1 = \gamma(S + v_1v_2)$ for that pair of nonadjacent vertices, since S is critical concerning the domain (or critical for brevity).

The graph S, which has the domain number u. S is known as a separable graph if all of its vertices can be enclosed by all of its subgraphs.

Theorem 4. *Suppose a decomposable graph S' have a spanning subgraph S, so that $\gamma(S) = \gamma(S')$, then L holds for each graph L, $\gamma(S \times L) = \gamma(S)\gamma(L)$*

Proof. Undirected, finite graphs, coherent, and simple are all considered. Specific, let S denote a graph have the edge set $E = E(S)$ and the vertex set $V = V(S)$. $m, n \in V$ are two vertices and its neighbors, otherwise in case $mn \in E$. The m's open neighborhood belongs to V and it is the m's neighbor set, denoted as $N_s(m)$, whereas the closed neighborhood $N_s[m] = N_s(m) \bigcup \{m\}$. The D' s open neighborhood contained in V and it is the set of all neighbors of vertices in D, denoted as $N_s(D)$, whereas the D' s closed neighborhood is $N_s[D] = N_s(D) \bigcup D$. But S is detached from the context, it perhaps represented by $N(D)$ and $N[D]$ or $N_s(D)$ and $N_s[D]$ correspondingly. The space among two vertices $m, n \in V$ is in S the shortest length (m, n) path and is represented by $d_s(m, n)$. In two graphs, the Cartesian products are $S(V_1, E_1)$ and $L(V_2, E_2)$ represented by $S \times L$, is a vertex-set graph $V_1 \times V_2$ and edge set $E(S \times L) = \{((u_1, v_1), (u_2, v_2))\colon v_1 = v_2 \text{and} (u_1, u_2) \in E_1, \text{or} u_1 = u_2 \text{and} (v_1, v_2) \in E_2\}$.

A subset of vertices $D \subseteq V(S)$ is known as a dominant set of half sum, if $N[D] = V(S)$, and every vertex $u \in D$ a vertex $v \in D$ occurs, thus $d(u, v) \leq 2$. When D is a dominant set of half-sums in the induced subgraph $D \cup T$ of S, a vertex set D semidominates a vertex set T. The semitotal dominance number of S, denoted as $\gamma_{t2}(S)$, is known as a minimum half-sum dominating set size of S. A 2-pack is a subset of S vertices T in which each pair of T' s vertices are a minimum of 3 separate. The maximum 2-pack size of S is known as the 2-pack number [6–8]. □

Theorem 5. *To S, L are all isolate-free graphs. Then,*

$$\gamma_{t2}(S \times L) \geq \rho(S)\gamma_{t2}(L). \tag{3}$$

Proof. Let us take $\{v_1, \ldots, v_p(S)\}$ be a max of 2 packages of graph. Consider without restrictions as $\rho(S) = \gamma(S)$. Every vertex in the graph is at least three far from the packing of vertices. The closed adjacent $N_s[v_i]$ are represented as pairwise disjoint and for $i = 1, \rho(S)$. Consider $\{v_1, \ldots, v_p(S)\}$ is said to be a partition of $V(S)$ just like for $1 \leq \rho(S), N_s[V_i]$. Let B be an $\gamma_{t2}(S \times L)S$-set. For $i = 1, \rho(S)$. Let $B_i = B \cap (V_i \times V(L))$. Moreover, consider a minimum set C_i of vertices $S \times L$ that L_i dominate completely and include as several vertices as feasible in L_i. Further $C_i \subseteq v_i \times V(L)$. Next x is not present in L_i when C_i has a vertex, and x is considered to be the uniquely determined vertex that entirely dominates x' for $x' \in L_i$. Since x' contains neighbors that pertain to L_i, vertices in C_i dominate that all neighbors, even now C_i is a semisumerally dominant set once x is changed to x' in C_i. Hence, vertices set that almost fully dominate L_i and have further vertices in L_i, therefore, called C_i, is an inconsistency. Since $C_i \subseteq L_i$ are subsets, and thus C_i is a partial dominance of L in $S \times L$ persuaded by L_i. Then B_i partially dominance $\{v_i\} \times (L)$, $|B_i| \geq |C_i|$. Therefore, $\gamma_{t2}(S \times L) \geq \rho(S) \sum i = 1|C_i| \geq \rho(S) \sum i = 1\gamma_{t2}(S \times L) = \rho(S)\gamma_{t2}(L)$.

The subtotal must be calculated of the domination number and the results of Vizing's type based on it. Separating minimum half dominating sets into partially dominating sets which is considered as completely dominate. $U = \{u_1, \ldots, u_k\}$ is considered to be a minimum of a semidominant set of graphs S, note that it is suitable for each graph. It might be partitioned into two sets of $X\&Y$. Here X represents vertices set of U that are nearer to anyone vertex of U, on the other hand, Y represented as U on X. Take $\{U_1, \ldots, U_k\}$ as the minimum dominating set of vertices for every graph S, also take $X_i\&1 \leq i \leq k$, and $X_i\&Y_i$ represents partitions in allied and free sets considerably. Therefore, it represents U_i, so as a result, $|X_i|$ is considered to be the max extent for $1 \leq i \leq k$, a maximum relayed semitotal dominant set of S. Maximum of allied partition of the graph S is represented as $\{X_i, Y_i\}$. The set X_i denote a maximum related set of S, and the set Y_i a minimum free set of S. Each maximal related partition of $S\{X, Y\}$ assume $x(S) = |X|$ and $y(s) = |Y|$. □

4. Conclusion

Hamiltonian cycle's quasi-spanning tree of faces is executed in this research. In a cubic bipartite planer graph, a polynomial time technique is utilized to reduce the issues in the minimum quasi spanning tree. For another graph-like products and other domination, numerous researchers have conducted Vizing's conjecture. But still, this conjecture is not yet demonstrated. To prove Vizing's conjecture, a graph theory described one or two conjectures which are still considered as wider problems. To separate free graphs, Vizing types are based on the subtotal of domination number and it proved as well. Vizing's conjecture is said to be true when the polynomial time was positive concerning the particularly build ideal. And here Vizing's conjecture is designed by the graph theory as an appropriate pair.

Data Availability

No data were used to support this study.

Disclosure

An earlier version of the manuscript is presented as preprint in [4] in the link https://theory.stanford.edu/~tomas/barnew.pdf.

Conflicts of Interest

The authors declare that there are no conflicts of interest regarding the publication of this article.

Acknowledgments

The authors thank VR Siddhartha Engineering College, Vijayawada, Shree Institute of Technical Education, Tirupati, and Bangabandhu Sheikh Mujibur Rahman Science and Technology University, Gopalganj, Bangladesh.

References

[1] S. Mondal, A. Dey, and T. Pal, "Robust and minimum spanning tree in fuzzy environment," *International Journal of Computing Science and Mathematics*, vol. 1, no. 1, pp. 1–524, 2017.

[2] A. Dey, S. Mondal, and T. Pal, "Robust and minimum spanning tree in fuzzy environment," *International Journal of Computing Science and Mathematics*, vol. 10, no. 5, pp. 513–524, 2019.

[3] A. Dey, R. Pradhan, A. Pal, and T. Pal, "A genetic algorithm for solving fuzzy shortest path problems with interval type-2 fuzzy arc lengths," *Malaysian Journal of Computer Science*, vol. 31, no. 4, pp. 255–270, 2018.

[4] D. Barnette, *Conjecture 5, Recent Progress in Combinatorics*, W. T. Tutte, Ed., p. 343, Academic Press, New York, NY, USA, 1969.

[5] M. A. Henning, "Essential upper bounds on the total domination number," *Discrete Applied Mathematics*, vol. 244, pp. 103–115, 2018.

[6] G. Brinkmann, J. Goedgebeur, and B. D. McKay, "Generation of cubic graphs," *Discrete Mathematics & Theoretical Computer Science*, vol. 13, no. 2, pp. 69–80, 2011.

[7] D. Maji, G. Ghorai, and F. A. Shami, "Some New Upper Bounds for the Y-Index of Graphs," *Journal of Mathematics*, vol. 2022, no. 5, 13 pages, Article ID 4346234, 2022.

[8] D. Maji, G. Ghorai, and Y. U. Gaba, "On the reformulated second Zagreb index of graph operations," *Journal of Chemistry*, vol. 2021, no. 5, 17 pages, Article ID 9289534, 2021.

[9] E. Gaar, A. Wiegele, D. Krenn, and S. Margulies, "An optimization-based sum-of-squares approach to Vizing's conjecture," in *Proceedings of the 2019 on International Symposium on Symbolic and Algebraic Computation*, pp. 155–162, ACM, Beijing, China, July 2019.

[10] R. Davila, T. Kalinowski, and S. Stephen, "A lower bound on the zero forcing number," *Discrete Applied Mathematics*, vol. 250, pp. 363–367, 2018.

[11] R. A. Borzooei and H. Rashmanlou, "Domination in vague graphs and its applications," *Journal of Intelligent and Fuzzy Systems*, vol. 29, no. 5, pp. 1933–1940, 2015.

[12] M. A. Henning and D. F. Rall, "On the total domination number of Cartesian products of graphs," *Graphs and Combinatorics*, vol. 21, no. 1, pp. 63–69, 2005.

[13] B. L. Hartnell and D. F. Rall, "On dominating the Cartesian product of a graph and K_2," *Discussiones Mathematicae Graph Theory*, vol. 24, no. 3, pp. 389–402, 2004.

[14] G. Brinkmann, K. Coolsaet, J. Goedgebeur, and H. M´elot, "House of Graphs: a database of interesting graphs," *Discrete Applied Mathematics*, vol. 161, no. 1-2, pp. 311–314, 2013.

[15] G. Brinkmann and J. Goedgebeur, "Generation of cubic graphs and snarks with large girth," *Journal of Graph Theory*, vol. 86, no. 2, pp. 255–272, 2017.

[16] D. Maji, G. Ghorai, M. K. Mahmood, and M. A. Alam, "On the inverse problem for some topological indices," *Journal of Mathematics*, vol. 2021, no. 1, 8 pages, Article ID 9411696, 2021.

[17] A. Dey, A. Pal, and T. Pal, "Interval type 2 fuzzy set in fuzzy shortest path problem," *Mathematics*, vol. 4, p. 62, 2016.

Hindawi
Journal of Mathematics
Volume 2022, Article ID 7834080, 6 pages
https://doi.org/10.1155/2022/7834080

Research Article

Weighted Graph Irregularity Indices Defined on the Vertex Set of a Graph

Zainab Alsheekhhussain,[1] Tamás Réti,[2] and Akbar Ali[1]

[1]*Department of Mathematics, Faculty of Science, University of Ha'il, Ha'il, Saudi Arabia*
[2]*Óbuda University, Bécsiút, 96/B, H-1034, Budapest, Hungary*

Correspondence should be addressed to Akbar Ali; akbarali.maths@gmail.com

Received 15 February 2022; Revised 28 May 2022; Accepted 6 June 2022; Published 28 June 2022

Academic Editor: M. T. Rahim

Copyright © 2022 Zainab Alsheekhhussain et al. This is an open access article distributed under the Creative Commons Attribution License, which permits unrestricted use, distribution, and reproduction in any medium, provided the original work is properly cited.

Performing comparative tests, some possibilities of constructing novel degree- and distance-based graph irregularity indices are investigated. Evaluating the discrimination ability of different irregularity indices, it is demonstrated (using examples) that in certain cases two newly constructed irregularity indices, namely $IRDE_A$ and $IRDE_B$, are more selective.

1. Introduction

Only connected graphs without loops and parallel edges are considered in this study. For a graph G with n vertices and m edges, $V(G)$ and $E(G)$ denote the sets of vertices and edges, respectively. Let $d(u)$ be the degree of vertex u of G. Let uv be an edge of G connecting the vertices u and v. Let $\Delta = \Delta(G)$ and $\delta = \delta(G)$ be the maximum and the minimum degrees, respectively, of G. In what follows, we use the standard terminology in graph theory; for notations not defined here, we refer the readers to the books [1, 2].

For a connected graph G, the set of numbers n_j of vertices with degree j is denoted by $\{n_j = n_j(G)\colon n_j > 0, 1 \le j \le \Delta\}$. For simplicity, the numbers $n_j(G)$ are called the vertex-parameters of graph G. For two vertices $u, v \in V(G)$, the distance $d(u,v)$ between u and v is the number of edges in a shortest path connecting them.

Two connected graphs G_1 and G_2 are said to be vertex-degree equivalent if they have an identical vertex-degree sequence. Certainly, if G_1 and G_2 are vertex-degree equivalent, then their vertex-parameters sets satisfy the equation $n_j(G_1) = n_j(G_2)$ for every j. A graph is called k-regular if all its vertices have the same degree k. A graph which is not regular is called a nonregular graph. A connected graph G is said to be *bidegreed* if its degree set consists of only two elements, where a degree set of G is the set of all distinct elements of its degree sequence.

2. Preliminary Considerations

A topological index TI of a graph G is any number associated with G (in some way) provided that the equation $TI(G) = TI(G')$ holds for every graph G' isomorphic to G. A lot of existing topological indices are degree- and distance-based ones [3–5]. Graph irregularity indices form a notable subclass of the class of traditional topological indices; where a topological index TI of a (connected) graph G is called a graph irregularity index if $TI(G) \ge 0$, and $TI(G) = 0$ if and only if graph G is a regular graph. Details about the existing graph irregularity indices can be found in [6, 7]. The readers interested in the general concept of irregularity in graphs may consult the book [8].

In several situations, it is crucial to know how much irregular a given graph is; for example, see [9, 10] where irregularity measures are used to predict physicochemical properties of chemical compounds, and see [11–14] for some applications of irregularity measures in network theory.

Most of the existing irregularity indices used in mathematical chemistry are degree-based irregularity indices. There exist irregularity indices which form a particular subset Φ of the set of degree-based irregularity indices; we say that an irregularity index ϕ belongs to the set Φ if for every pair of vertex-degree equivalent graphs G_1 and G_2, the equation $\phi(G_1) = \phi(G_2)$ holds.

The most popular topological indices that are used in defining degree-based irregularity indices, are the first and second Zagreb indices (see for example [15]), denoted by M_1 and M_2, respectively, and the so-called forgotten topological index [15], denoted by F. The first and second Zagreb indices of a graph G are defined as

$$\begin{aligned} M_1(G) &= \sum_{u\in V(G)} d_u^2, \\ M_2(G) &= \sum_{uv\in E(G)} d_u d_v, \end{aligned} \tag{1}$$

and the forgotten topological index is defined as

$$F(G) = \sum_{u\in V(G)} d_u^3. \tag{2}$$

There exist numerous degree-based graph irregularity indices in literature, some of them are listed below.

The variance Var is a degree-based graph irregularity index introduced by Bell [16]. The variance Var of a graph G of order n and size m is defined as

$$Var(G) = \frac{1}{n}\sum_{u\in V(G)}\left(d_u - \frac{2m}{n}\right)^2 = \frac{M_1(G)}{n} - \frac{4m^2}{n^2}. \tag{3}$$

We also consider the following four irregularity indices:

$$IRV(G) = n^2\mathrm{Var}(G) = nM_1(G) - 4m^2, \tag{4}$$

$$IR_1(G) = \sqrt{\frac{M_1(G)}{n}} - \frac{2m}{n}, \tag{5}$$

$$IR_2(G) = \sqrt{\frac{M_2(G)}{m}} - \frac{2m}{n}, \tag{6}$$

$$IR_3(G) = F(G) - \frac{2m}{n}M_1(G). \tag{7}$$

It is remarked here that, except IR_2, all the irregularity indices formulated above belong to the set Φ.

3. Weighted Irregularity Indices Defined on the Vertex Set of a Graph

In this section, we consider irregularity indices defined on the set of vertices of a graph G. The majority of these indices are weighted degree- and distance-based topological indices. Most of them may be considered as extended versions of the Wiener index; for example, see [17]. Let us consider the weighted vertex-based topological index of a graph G formulated as

$$ZW(G) = \frac{1}{2}\sum_{u,v\in V(G)} Z(u,v)W(u,v), \tag{8}$$

where $Z(u,v)$ and $W(u,v)$ are appropriately selected non-negative 2-variable symmetric functions; both of them are defined on the vertex set $V(G)$ of G. For simplicity, we call the function $W(u,v)$ as the weight function of G. By taking

$$Z(u,v) = |d_u - d_v|^p. \tag{9}$$

in Equation (8), we get the following graph irregularity index

$$IRR_p(G) = \frac{1}{2}\sum_{u,v\in V(G)} |d_u - d_v|^p W(u,v), \tag{10}$$

where p is a positive real number. Depending on the choice of the parameter p and the weight function $W(u,v)$, various types of irregularity indices can be deduced. For instance, the choices $p = 1$ and $W(u,v) = 1$ lead to the so-called total irregularity of a graph G defined by

$$Irrt_1(G) = \frac{1}{2}\sum_{u,v\in V(G)} |d_u - d_v|. \tag{11}$$

It was introduced by Abdo et al. in [18]. Also, assuming that $p = 2$ and $W(u,v) = 1$, we have the irregularity index $Irrt_2(G)$, introduced in Ref. [19]:

$$Irrt_2(G) = \frac{1}{2}\sum_{u,v\in V(G)} (d_u - d_v)^2. \tag{12}$$

At this point, the following known proposition [19] concerning $Irrt_2$ needs to be stated.

Proposition 1. *For every graph G with n vertices and m edges, it holds that*

$$\begin{aligned} Irrt_2(G) &= \frac{1}{2}\sum_{u,v\in V(G)} (d_u - d_v)^2 = nM_1(G) - 4m^2 \\ &= n^2\mathrm{Var}(G) = IRV(G). \end{aligned} \tag{13}$$

In Equation (9), by taking $Z(u,v) = (d_u - d_v)^2$ and $W(u,v) = d(u,v)$, we obtain the following irregularity index:

$$IRD(G) = \frac{1}{2}\sum_{u,v\in V(G)} (d_u - d_v)^2 d(u,v). \tag{14}$$

Note that IRD is a weighted degree- and distance-based irregularity index. Although IRD is a new irregularity index which is not known in the literature, but we prove in the next proposition that this irregularity index can be written in the linear combination of the following two topological indices

$$DG(G) = \sum_{u\in V(G)} d_u^2 D_G(u), \tag{15}$$

and

$$\mathrm{Gut}(G) = \frac{1}{2}\sum_{u,v\in V(G)} (d_u d_v) d(u,v), \tag{16}$$

where $D_G(u)$ is identical to the transmission $\mathrm{Tr}(u)$ of the vertex $u \in V(G)$ and $\mathrm{Gut}(G)$ is the so-called Gutman index; for example, see [20].

Proposition 2. *For a (connected) graph G, it holds that*

$$IRD(G) = \frac{1}{2}\sum_{u,v\in V(G)} (d_u - d_v)^2 d(u,v) = DG(G) - 2\mathrm{Gut}(G). \tag{17}$$

Proof. Note that

$$\frac{1}{2}\sum_{u,v\in V(G)} (d_u - d_v)^2 d(u,v) = \frac{1}{2}\sum_{u,v\in V(G)} \left(d_u^2 + d_v^2\right) d(u,v) - 2Gut(G). \tag{18}$$

For the graph G, it holds [21] that

$$\frac{1}{2}\sum_{u,v\in V(G)} (\omega(u) + \omega(v)) d(u,v) = \sum_{u\in V(G)} \omega(u) D_G(u), \tag{19}$$

where $\omega(u)$ is any quantity associated with the vertex u of G. By taking $\omega(u) = d_u^2$ in (19) and using the obtained identity in (18), we get

$$\begin{aligned}\frac{1}{2}\sum_{u,v\in V(G)} (d_u - d_v)^2 d(u,v) &= \sum_{u\in V(G)} d_u^2 D_G(u) - 2\mathrm{Gut}(G) \\ &= DG(G) - 2\mathrm{Gut}(G).\end{aligned} \tag{20}$$

□

Remark 1. From Proposition 2, it follows that the inequality

$$DG(G) \geq 2\mathrm{Gut}(G) \tag{21}$$

holds for every (connected) graph G, with equality if and only if G is regular.

Remark 2. Because IRD is a weighted version of the irregularity index $Irrt_2$, it is expected that its discrimination power is better than that of $Irrt_2$.

Remark 3. Based on identity Equation (20), one can establish another irregularity index IRQ defined by

$$IRQ(G) = \frac{DG(G) - 2\mathrm{Gut}(G)}{2\mathrm{Gut}(G)} = \frac{DG(G)}{2\mathrm{Gut}(G)} - 1. \tag{22}$$

As $\mathrm{Gut}(G) > 1/2$ for every (connected) graph of order at least 3, one has

$$IRQ(G) = \frac{DG(G)}{2\mathrm{Gut}(G)} - 1 < DG(G) - 2\mathrm{Gut}(G) = IRD(G). \tag{23}$$

4. Discriminating Ability of Novel Weighted Irregularity Indices

For comparing the discrimination ability of the irregularity indices IRD and IRQ with the traditional degree-based irregularity indices Var, IR_1, IR_2, and IR_3, we use the 6-vertex graphs G_i $(i = 1, 2, 3, 4)$ depicted in Figure 1. It is remarked here that the graphs shown in Figure 1 belong to the family of connected threshold graphs, and graph G_1 is isomorphic to the connected 6-vertex antiregular graph (for example, see [22, 23]).

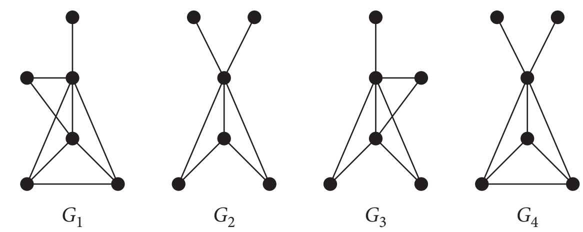

Figure 1: Four 6-vertex nonregular graphs selected for tests.

For the four graphs depicted in Figure 1, computed values of preselected topological indices M_1, M_2, F, and corresponding irregularity indices are summarized in Tables 1 and 2.

Comparing irregularity indices listed in Tables 1 and 2, the following conclusions can be drawn. Among the four tested graphs, the index G_1 achieves the maximum value (that is, 249) of IR_3. The irregularity indices IR_1 and IR_2 are maximum for the graph G_2 (namely, $IR_1(G_2) \approx 0.375$ and $IR_2(G_2) \approx 0.5202$). As it can be seen that $\mathrm{Var}(G_1) \approx 1.667$, while $\mathrm{Var}(G_2) = \mathrm{Var}(G_3) = \mathrm{Var}(G_3) \approx 1.889$ and that all the four graphs have the same value of $Irrt_1$, which is 26. Also, the relation $Irrt_2(G) = n^2\mathrm{Var}(G)$ is confirmed for the considered graphs: $Irrt_2(G_1) = 60$ and $Irrt_2(G_2) = Irrt_2(G_3) = Irrt_2(G_4) = 68$. Moreover, we have $IRD(G_1) = IRD(G_2) = IRD(G_3) = 80$ and $IRD(G_4) = 92$, while the computed values of the irregularity index IRQ are different for all four graphs. From these observations, one can conclude that the degree variance Var, the total irregularity index Irr_1, together with the irregularity indices Irr_2, and IRD have a limited discrimination ability for the considered four graphs.

5. Novel Irregularity Indices Constructed by Using the External Weight Concept

The weight function $W(u,v)$ included in (9) can be considered as an "internal" weight function. Introducing the external weight concept, one can construct novel irregularity indices. By using them, the original sequence of previously determined irregularity values can be appropriately modified for a given set of graphs considered.

By definition, an external weight $EW(G)$ for a graph G is a positive-valued topological index computed as a function of one or more traditional topological indices. By means of an external weight $EW(G)$ a novel irregularity index $IRE(G)$ can be created as defined below:

$$IRE(G) = EW(G) \times IR(G), \tag{24}$$

where $IR(G)$ is an arbitrary irregularity index. By appropriately selected external weights $EW(G)$, one can establish several different versions of irregularity indices $IRE(G)$ satisfying some restrictions or desired expectations. As an

Table 1: Computed topological indices of the four graphs shown in Figure 1.

Graph	m	M_1	M_2	F	Var	IR_1	IR_2	IR_3
G_1	9	64	106	252	5/3	0.266	0.4319	249.0
G_2	7	44	57	170	17/9	0.375	0.5202	167.7
G_3	8	54	79	214	17/9	0.333	0.4758	211.3
G_4	8	54	82	208	17/9	0.333	0.5349	205.3

Table 2: Computed topological indices of the four graphs shown in Figure 1.

Graph	m	$Irrt_1$	$Irrt_2$	DG	Gut	IRD	IRQ
G_1	9	26	60	388	154	80	0.2597
G_2	7	26	68	270	95	80	0.4211
G_3	8	26	68	326	123	80	0.3252
G_4	8	26	68	332	120	92	0.3833

example, consider the three external weights defined for a graph G of order n and size m as follows:

$$EW_A(G) = \frac{m^2}{100n}, \tag{25}$$

$$EW_B(G) = \frac{M_2(G) + F(G)}{n^2}, \tag{26}$$

$$EW_C(G) = \frac{1}{2 \times \mathrm{Gut}(G)}. \tag{27}$$

Using the three external weights listed above, the following irregularity indices of new type are obtained:

$$IRDE_A(G) = EW_A(G) \times IRD(G), \tag{28}$$

$$IRDE_B(G) = EW_B(G) \times IRD(G), \tag{29}$$

$$IRDE_C(G) = EW_C(G) \times IRD(G). \tag{30}$$

For graphs shown in Figure 1, the computed external weights and the corresponding irregularity indices are summarized in Table 3.

Comparing the computed irregularity indices mentioned in Table 3, one can conclude that the graph G_1 has the maximum irregularity indices $IRDE_A(G_1) = 10.8$ and $IRDE_B(G_1) = 795.6$, while the maximum value of the irregularity index $IRDE_C$ is attained by the graph G_2 where $IRDE_C(G_2) = 0.4211$ (it should be emphasized here that the graph G_1 is identical to the 6-vertex connected antiregular graph, and it is usually desired that the connected antiregular graph attains the maximum value of an irregularity index among all connected graphs of a fixed order.)

It is remarked here that the irregularity indices IRQ and $IRDE_C$ are identical to each other because

$$\begin{aligned} IRQ(G) &= \frac{DG(G)}{2\mathrm{Gut}(G)} - 1 = \frac{DG(G) - 2\mathrm{Gut}(G)}{2\mathrm{Gut}(G)} \\ &= EW_C(G) \times IRD(G) = IRDE_C(G). \end{aligned} \tag{31}$$

Table 3: Computed topological indices of the four graphs shown in Figure 1.

Graph	m	EW_A	$IRDE_A$	EW_B	$IRDE_B$	EW_C	$IRDE_C$
G_1	9	0.1350	10.800	9.944	795.6	0.0032	0.2597
G_2	7	0.0817	6.533	6.306	504.4	0.0053	0.4211
G_3	8	0.1067	8.533	8.139	651.1	0.0041	0.3252
G_4	8	0.1067	9.813	8.056	741.1	0.0042	0.3833

6. Additional Considerations

An interesting open problem can be formulated as follows: find a deterministic relationship between the following weighted bond-additive indices (see [24]).

$$BA_p(G) = \sum_{uv\in E(G)} |d_u - d_v|^p W(u,v) \tag{32}$$

and weighted atoms-pair-additive indices

$$IRR_p(G) = \frac{1}{2} \sum_{u,v\in V(G)} |d_u - d_v|^p W(u,v). \tag{33}$$

Depending on the definitions of the above irregularity indices, we observe that there exist graphs for which the mentioned relationship is perfect. As an example, when $p = 1$ and $W(u,v) = d(u,v)$ then for the wheel graph W_n of order n with $n \geq 5$, one has

$$\frac{1}{2} \sum_{u,v\in V(W_n)} |d_u - d_v| d(u,v) = \sum_{uv\in E(W_n)} |d_u - d_v| = AL(W_n), \tag{34}$$

where AL is the Albertson irregularity index [25].

The sigma index $\sigma(G)$ of a graph G is defined (for example, see [26]) as

$$\sum_{uv\in E(G)} (d_u - d_v)^2. \tag{35}$$

This irregularity index is a natural generalization of the Albertson irregularity index. For the wheel graph W_n of order n with $n \geq 5$, the following identity holds:

$$\begin{aligned} IRD(W_n) &= \frac{1}{2} \sum_{u,v\in V(W_n)} (d_u - d_v)^2 d(u,v) \\ &= \sum_{uv\in E(W_n)} (d_u - d_v)^2 = \sigma(W_n). \end{aligned} \tag{36}$$

It is possible to construct a particular graph family for which the concept outlined above can be extended. For two graphs J_1 and J_2 with disjoint vertex sets, $J_1 \cup J_2$ denotes the disjoint union of J_1 and J_2. The join $J_1 + J_2$ of J_1 and J_2 is the graph obtained from $J_1 \cup J_2$ by adding edges between every vertex of J_1 and every vertex of J_2.

Proposition 3. *Define the bidegreed graph H_n of order n as follows:*

$$H = H_0 + \left(\cup_{j\geq 1} H_j\right), \tag{37}$$

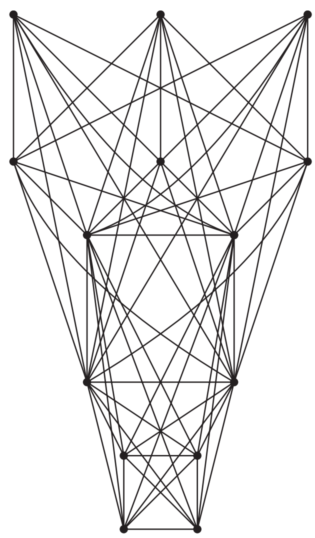

Figure 2: The bidegreed graph H_{14}.

where H_0 is an r-regular graph and each H_j is an $r\prime$-regular graph. It holds that

$$\begin{aligned}\mathrm{BAD}_p(H_n) &= \frac{1}{2}\sum_{u,v\in V(H_n)} \left|d_u - d_v\right|^p d(u,v)\\ &= \sum_{uv\in E(H_n)} \left|d_u - d_v\right|^p = AL_p(H_n),\end{aligned} \tag{38}$$

where AL_pG is a modified version of the generalized Albertson irregularity index (see [27]).

Proof. We note that

$$BAD_p(H_n) = \sum_{uv\in E(H_n)} \left|d_u - d_v\right|^p + \sum_{uv\notin E(H_n)} \left|d_u - d_v\right|^p d(u,v). \tag{39}$$

Observe that $d_x = d_y$ for every pair of nonadjacent vertices $x, y \in V(H_n)$, which implies that

$$\sum_{uv\notin E(H_n)} \left|d_u - d_v\right|^p d(u,v) = 0. \tag{40}$$

and hence Equation (39) yields the desired result.

As an example concerning Proposition 3, consider the bidegreed graph H_{14} of order 14 and size 59 constructed as follows:

$$H_{14} = C_4 + \left(K_{3,3} \cup K_4\right), \tag{41}$$

where C_4 is the (2-regular) cycle graph with 4 vertices, $K_{3,3}$ is the (3-regular) complete bipartite graph of order 6, and K_4 is the (3-regular) complete graph on 4 vertices (see Figure 2. The graph H_{14} contains ten vertices of degree 7 and four vertices of degree 12. Note that if $uv \notin E(H_{14})$, then $u \in V(J)$ and $v \in V(K)$, where $J, K \in \left\{K_{3,3}, K_4\right\}$, and both the vertices u, v have the degree 7 in H_{14}. Thus,

$$\sum_{uv\notin E(H_{14})} \left|d_u - d_v\right|^p d(u,v) = 0 \tag{42}$$

and the desired conclusion holds. □

Data Availability

The data about this study may be requested from the authors.

Conflicts of Interest

The authors declare that they have no conflicts of interest.

References

[1] J. A. Bondy and U. S. R. Murty, *Graph Theory*, Springer, Berlin, Germany, 2008.

[2] G. Chartrand, L. Lesniak, and P. Zhang, *Graphs & Digraphs*, CRC Press, Boca Raton, FL, USA, 2016.

[3] A. Ghalavand and A. R. Ashrafi, “Some inequalities between degree and distance-based topological indices of graphs,” *MATCH Communications in Mathematical and in Computer Chemistry*, vol. 79, pp. 399–406, 2018.

[4] T. Réti and I. Baranyi, “On the irregularity characterization of mean graphs,” *Acta Polytechnica Hungarica*, vol. 18, no. 5, pp. 207–220, 2021.

[5] S. Li and Y. Wu, “On the extreme eccentric distance sum of graphs with some given parameters,” *Discrete Applied Mathematics*, vol. 206, pp. 90–99, 2016.

[6] I. Ž. Milovanović, E. I. Milovanović, V. Ćirić, and N. Jovanović, “On some irregularity measures of graphs,” *Scientific Publications of the State University of Novi Pazar Series A Applied Mathematics Informatics and mechanics*, vol. 8, pp. 21–34, 2016.

[7] J. A. d. Oliveira, C. S. Oliveira, C. Justel, and N. M. M. d. Abreu, “Measures of irregularity of graphs,” *Pesquisa Operacional*, vol. 33, no. 3, pp. 383–398, 2013.

[8] A. Ali, G. Chartrand, and P. Zhang, *Irregularity in Graphs*, Springer, Berlin, Germany, 2021.

[9] I. Gutman, P. Hansen, and H. Mélot, “Variable neighborhood search for extremal graphs. 10. Comparison of irregularity indices for chemical trees,” *Journal of Chemical Information and Modeling*, vol. 45, no. 2, pp. 222–230, 2005.

[10] T. Réti, R. Sharafdini, Á. Drégelyi-Kiss, and H. Haghbin, “Graph irregularity indices used as molecular descriptors in QSPR studies,” *MATCH Communications in Mathematical and in Computer Chemistry*, vol. 79, pp. 509–524, 2018.

[11] T. A. B. Snijders, “The degree variance: an index of graph heterogeneity,” *Social Networks*, vol. 3, pp. 163–174, 1981.

[12] R. Criado, J. Flores, A. García del Amo, and M. Romance, “Centralities of a network and its line graph: an analytical comparison by means of their irregularity,” *International Journal of Computer Mathematics*, vol. 91, no. 2, pp. 304–314, 2014.

[13] E. Estrada, “Quantifying network heterogeneity,” *Physical Review E - Statistical Physics, Plasmas, Fluids, and Related Interdisciplinary Topics*, vol. 82, no. 6, Article ID 066102, 2010.

[14] E. Estrada, “Randić index, irregularity and complex biomolecular networks,” *Acta Chimica Slovenica*, vol. 57, no. 3, pp. 597–603, 2010.

[15] B. Furtula and I. Gutman, “A forgotten topological index,” *Journal of Mathematical Chemistry*, vol. 53, no. 4, pp. 1184–1190, 2015.

[16] F. K. Bell, "A note on the irregularity of graphs," *Linear Algebra and Its Applications*, vol. 161, pp. 45–54, 1992.
[17] A. A. Dobrynin and A. A. Kochetova, "Degree distance of a graph: a degree analog of the wiener index," *Journal of Chemical Information and Computer Sciences*, vol. 34, no. 5, pp. 1082–1086, 1994.
[18] H. Abdo, S. Brandt, and D. Dimitrov, "The total irregularity of a graph," *Discrete Mathematics & Theoretical Computer Science*, vol. 16, pp. 201–206, 2014.
[19] T. Réti and A. Ali, "Some generalizations of the total irregularity of graphs," *Scientific Publications of the State University of Novi Pazar Series A Applied Mathematics Informatics and mechanics*, vol. 11, pp. 1–9, 2019.
[20] K. Ch. Das, G. Su, and L. Xiong, "Relation between degree distance and Gutman index of graphs," *MATCH Communications in Mathematical and in Computer Chemistry*, vol. 76, pp. 221–232, 2016.
[21] R. Sharafdini and T. Réti, "On the transmission-based graph topological indices," *Kragujevac Journal of Mathematics*, vol. 44, no. 1, pp. 41–63, 2020.
[22] N. V. R. Mahadev and U. N. Peled, "Threshold graphs and related topics," in *Annals of Discrete Mathematics*Elsevier, Amsterdam, Netherlands, 2004.
[23] E. Munarini, "Characteristic, admittance and matching polynomials of an antiregular graph," *Applicable Analysis and Discrete Mathematics*, vol. 3, no. 1, pp. 157–176, 2009.
[24] T. Réti, A. Ali, and I. Gutman, "On bond-additive and atoms-pair-additive indices of graphs," *Electronic Journal of Mathematics*, vol. 2, pp. 52–61, 2021.
[25] M. O. Albertson, "The irregularity of a graph," *Ars Combinatoria*, vol. 46, pp. 2019–2225, 1997.
[26] H. Abdo, D. Dimitrov, and I. Gutman, "Graphs with maximal σ irregularity," *Discrete Applied Mathematics*, vol. 250, pp. 57–64, 2018.
[27] Z. Lin, T. Zhou, X. Wang, and L. Miao, "The general Albertson irregularity index of graphs," *AIMS Mathematics*, vol. 7, no. 1, pp. 25–38, 2022.

Hindawi
Journal of Mathematics
Volume 2022, Article ID 3635499, 8 pages
https://doi.org/10.1155/2022/3635499

Research Article

Upper Bounds of Radio Number for Triangular Snake and Double Triangular Snake Graphs

Ashraf ELrokh,[1] **Elsayed Badr**,[2] **Mohammed M. Ali Al-Shamiri**,[3,4] **and Shimaa Ramadhan**[1]

[1]*Mathematics and Computer Science Department, Faculty of Science, Menoufia University, Shibin Al Kawm, Menoufia, Egypt*
[2]*Scientific Computing Department, Faculty of Computers and Artificial Intelligence, Benha University, Benha, Egypt*
[3]*Department of Mathematics, Faculty of Science and Arts, Mahayel Assir, King Khalid University, Abha, Saudi Arabia*
[4]*Department of Mathematics and Computer, Faculty of Science, Ibb University, Ibb, Yemen*

Correspondence should be addressed to Ashraf ELrokh; ashraf.hefnawy68@yahoo.com

Received 25 January 2022; Accepted 18 April 2022; Published 16 May 2022

Academic Editor: M. T. Rahim

Copyright © 2022 Ashraf ELrokh et al. This is an open access article distributed under the Creative Commons Attribution License, which permits unrestricted use, distribution, and reproduction in any medium, provided the original work is properly cited.

A radio labeling of a simple connected graph $G = (V, E)$ is a function $h: V \longrightarrow N$ such that $|h(x) - h(y)| \geq \text{diam}(G) + 1 - d(x, y)$, where diam (G) is the diameter of graph and $d(x, y)$ is the distance between the two vertices. The radio number of G, denoted by rn (G), is the minimum span of a radio labeling for G. In this study, the upper bounds for radio number of the triangular snake and the double triangular snake graphs are introduced. The computational results indicate that the presented upper bounds are better than the results of the mathematical model provided by Badr and Moussa in 2020. On the contrary, these proposed upper bounds are better than the results of algorithms presented by Saha and Panigrahi in 2012 and 2018.

1. Introduction

The field of graph theory assumes a crucial part in different fields. One of the significant regions in graph theory is graph labeling which is used in many applications such as coding theory, x-ray crystallography, radar, astronomy, circuit design, communication network addressing, data base management, and channel assignment problem. The channel assignment problem is the problem of assigning channels (nonnegative integers) to the stations in an optimal way such as the interference is avoided. In [1], Badr and Moussa proposed a work on upper bound of radio k-chromatic number for a given graph against the other which is due to Saha and Panigrahi [2]. Badr and Moussa proposed a new mathematical model for finding the upper bound of a graph [1]. In [3], Saha and Panigrahi introduced another algorithm (with time complexity $O(n^4)$) for determining the upper bound of a graph. Ali et al. gave the upper bound for the radio number of generalized gear graph [4]. Fernandez et al. proved that the radio number of the n-gear is $4n + 2$ [5]. Yao et al. were defined as a new graph radio labeling on trees, and the properties of trees labeling were shown [6]. Smitha and Thirusangu determined the radio mean number of double triangular snake graph and alternate double triangular snake graph [7]. If $p\&q$ is prime numbers, the radio numbers of zero divisor graphs $\Gamma(Z_{P^2} \times Z_q)$ were investigated by Ahmad and Haider [8].

For more details about how to formulate a problem to a mathematical model, the reader can refer to [9–11]. On the contrary, for more details about other labeling that are related to radio labeling such as radio mean, radio mean square, and radio geometric. The reader is referred to [10, 11].

In this current work, the upper bounds for radio number of the triangular snake and the double triangular snake graphs are introduced. The computational results indicate that the presented upper bounds are better than the results of the mathematical model provided by Badr and Moussa [1].

On the contrary, these proposed upper bounds are better than the results of algorithms presented by Saha and Panigrahi [2, 3].

2. Materials and Methods

In this section, we introduce some basic definitions before we prove the theorems that determine the upper bounds' radio of the number for triangular snake and double triangular snake. On the contrary, we introduce the previous works which are related to the determining of the upper bound of radio number of a graph.

Definition 1 (see [12], diameter of graph). The diameter of G is the greatest eccentricity among all vertices of G and it is denoted by diam (G).

Definition 2 (see [13], triangular snake). A triangular snake (or Δ-snake) is a connected graph in which all blocks are triangles and the block-cut-point graph is a path.

Definition 3 (see [7], double triangular snake). A double triangular snake $D(Tn)$ is obtained from two triangular snakes with a common path.

In 2013, Algorithm 1 was introduced by Saha and Panigrahi [2] for determining the upper bound of the radio number of a given graph. Algorithm 1 has $O(n^3)$ time complexity such that n is the number of the vertices of G. In 2018, Saha and Panigrahi [2] proposed a new algorithm (Algorithm 2) for determining the upper bound of the radio number of a given graph. Algorithm 2 has $O(n^4)$ time complexity. On the contrary, in 2020, Badr and Moussa [1] proposed a novel mathematical model which finds the upper bound of the radio number of a given graph.

3. Results and Discussion

Here, we introduce two theorems which determine the upper bounds for radio number of triangular snake and double triangular snake. The presented upper bounds (by Theorems 1 and 2) are better than the results of the mathematical model provided by Badr and Moussa [1]. On the contrary, these proposed upper bounds are better than the results of algorithms presented by Saha and Panigrahi [2, 3].

Theorem 1. *Let G be a triangular snake graph $(\Delta_k - \text{snake})$ with k blocks and n vertices, where $d(x, y) \geq 1$; then, the upper bound of the radio number of $\Delta_k - \text{snake}$ is defined as follows:*

$$rn(\Delta_k - \text{snake}) \leq \begin{cases} k^2 + \dfrac{k}{2}, & \text{if } k \text{ is even}, \\ k^2 + k - \dfrac{k}{2}, & \text{if } k \text{ is odd}, \end{cases} \tag{1}$$

Proof. To prove this theorem, its suffices to give a distance labeling h of $\Delta_k - \text{snake}$.

Let $x_1, x_2, x_3, \ldots, x_n$ be a $\Delta_k - \text{snake}$ of length k, i.e., diameter of $(\Delta_k - \text{snake}) = k$.

Define a function h: $V(\Delta_k - \text{snake}) \longrightarrow N$ as the following cases. □

Case 1. k is odd:

$$h(x_i) = \begin{cases} h(x_{k+1}) = 0, & \\ h(x_{k+1-i}) = ki, & 1 \leq i \leq k, \\ h(x_{k+2+j}) = k^2 + \dfrac{k}{2} - jk, & 0 \leq j \leq k-1. \end{cases} \tag{2}$$

Now, we are in a position to prove that the function $h(x)$ is the distance labeling of $\Delta_k - \text{snake}$.

For each $(i, i+1)$,

$$\begin{aligned} |ki - k(i+1)| &\geq \text{diam} + 1 - d(x, y), \\ |ki - k(i+1)| &\geq k + 1 - d(x, y), \\ k &\geq k + 1 - d(x, y). \end{aligned} \tag{3}$$

Also, for each $(j, j+1)$,

$$\begin{aligned} \left|k^2 + \frac{k}{2} - jk - k^2 + \frac{k}{2} - (j+1)k\right| &\geq \text{diam} + 1 - d(x, y), \\ \left|k^2 + \frac{k}{2} - jk - \left(k^2 + \frac{k}{2} - jk - k\right)\right| &\geq k + 1 - d(x, y), \\ |k| &\geq k + 1 - d(x, y), \\ k &\geq k + 1 - d(x, y). \end{aligned} \tag{4}$$

Suppose that $1 \leq i \leq k$, $0 \leq j \leq k-1$.

If $i = j$,

$$\begin{aligned} \left|ki - \left(k^2 + \frac{k}{2} - jk\right)\right| &\geq k + 1 - d(x, y), \\ k^2 - 2k + \frac{k}{2} &\geq k + 1 - d(x, y), \end{aligned} \tag{5}$$

otherwise,

$$\left(k^2 - \frac{k}{2} - k\right) \geq k + 1 - d(x, y). \tag{6}$$

Case 2. k is even is similarly proved:

$$h(x_i) = \begin{cases} h(x_{k+1}) = 0, & \\ h(x_{k+1-i}) = ki, & 1 \leq i \leq k, \\ h(x_{k+2+j}) = k^2 + \dfrac{k}{2} - kj, & 0 \leq j \leq k-1. \end{cases} \tag{7}$$

We show that the function $h(x)$ is the distance labeling of $\Delta_k - \text{snake}$.

For each $(i, i+1)$,

$$\begin{aligned} |ki - k(i+1)| &\geq \text{diam} + 1 - d(x,y), \\ |ki - k(i+1)| &\geq k + 1 - d(x,y), \\ k &\geq k + 1 - d(x,y). \end{aligned} \tag{8}$$

Also, for each $(j, j+1)$,

$$\begin{aligned} \left|k^2 + \frac{k}{2} - kj - \left(k^2 + \frac{k}{2} - k(j+1)\right)\right| &\geq \text{diam} + 1 - d(x,y), \\ \left|k^2 + \frac{k}{2} - kj - \left(k^2 + \frac{k}{2} - kj - \mathrm{k}\right)\right| &\geq k + 1 - d(x,y), \\ |k| &\geq k + 1 - d(x,y), \\ k &\geq k + 1 - d(x,y). \end{aligned} \tag{9}$$

Suppose that $1 \leq i \leq k$, $0 \leq j \leq k-1$.
If $i = j$,

$$\begin{aligned} \left|ki - \left(k^2 + \frac{k}{2} - jk\right)\right| &\geq k + 1 - d(x,y), \\ k^2 - \frac{3k}{2} &\geq k + 1 - d(x,y), \end{aligned} \tag{10}$$

otherwise,

$$\left(k^2 - \frac{1}{2}k\right) \geq k + 1 - d(x,y). \tag{11}$$

Example 1. Figure 1 presents the labeling Δ_3(snake) according to Theorem 1.

Theorem 2. *Let G be a double triangular snake graph with k blocks and n vertices; then, the upper bound of the radio number of double Δ_k − snake is defined as follows:*

$$rn(\Delta_k(\text{snake}) \leq \begin{cases} 3, & \text{if } k = 1, \\ 7, & \text{if } k = 2, \\ 2k^2 - k + 3, & \text{if } k \text{ is odd}, \\ 2k^2 - k + 2, & \text{if } k \text{ is even}. \end{cases} \tag{12}$$

Proof. To prove this theorem, it suffices to give a distance labeling h of double Δ_k − snake. Notice that the diameter of double triangular snake is the same as the diameter of triangular snake graph. Let $x_1, x_2, x_3, \ldots, x_n$ be a $2\,\Delta_k$ − snake of length k, where the diameter of $2(\Delta_k - \text{snake}) = k$ and $n = 3k + 1$.

Define a function h: $V(\text{double}\Delta_k - \text{snake}) \longrightarrow N$ as the following cases:

For $k = 1$, let the sufficed labeling $h(x_1) = 0, h(x_2) = 2, h(x_3) = 5$, and $h(x_4) = 3$

For $k = 2$, let $h(x_1) = 4, h(x_2) = 2, h(x_3) = 0$, $h(x_4) = 5, h(x_5) = 3, h(x_6) = 6$, and $h(x_7) = 7$ □

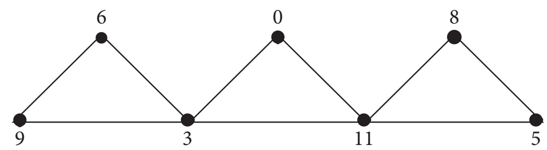

Figure 1: The radio number of Δ_3(snake).

Case 3. k is even and $k > 2$,

$$h(x_i) = \begin{cases} h(x_{k+1}) = 0, & \\ h(x_{k-i+1}) = ki, & 1 \leq i \leq k, \\ h(x_{k+i+2}) = k^2 + \dfrac{k}{2} - ki, & 0 \leq i \leq k-1, \\ (x_{2k+2+i}) = k^2 + k + 1 + (k-1)i, & 0 \leq i \leq k-1. \end{cases} \tag{13}$$

We are in a position to prove that the function $h(x_i)$ are the distance labeling of double Δ_k − snake.

For each $(i, i+1)$,

$$\begin{aligned} |ki - (k(i+1))| &\geq \text{diam} + 1 - d(x,y), \\ k &\geq k + 1 - d(x,y). \end{aligned} \tag{14}$$

For each $(i, i+1)$,

$$\begin{aligned} \left|k^2 + \frac{k}{2} - ki - \left(k^2 + \frac{k}{2} - k(i+1)\right)\right| &\geq \text{diam} + 1 - d(x,y), \\ k &\geq k + 1 - d(x,y). \end{aligned} \tag{15}$$

Also, for each $(i, i+1)$,

$$\begin{aligned} &\left|k^2 + k + 1 + (k-1)i - \left(k^2 + k + 1 + (k-1)(i+1)\right)\right| \\ &\geq \text{diam} + 1 - d(x,y), \\ &k - 1 \geq k + 1 - d(x,y). \end{aligned} \tag{16}$$

Now, suppose that $1 \leq i \leq k$ and $0 \leq j \leq k-1$:

$$\begin{aligned} \left|ki - \left(k^2 + \frac{k}{2} - kj\right)\right| &\geq \text{diam} + 1 - d(x,y), \\ k^2 + \frac{3k}{2} &\geq k + 1 - d(x,y). \end{aligned} \tag{17}$$

Suppose that $1 \leq i \leq k$ and $0 \leq j \leq k-1$:

$$\begin{aligned} \left|ki - \left(k^2 + k + 1 + (k-1)j\right)\right| &\geq \text{diam} + 1 - d(x,y), \\ k^2 - k + 2 &\geq k + 1 - d(x,y). \end{aligned} \tag{18}$$

If $i = 1$ and $j = 0$,

$$k^2 + 1 \geq k + 1 - d(x,y), \tag{19}$$

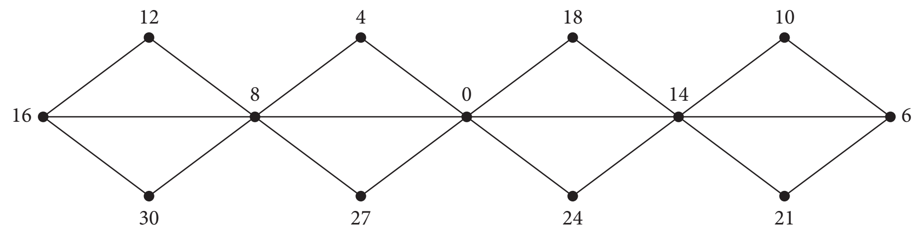

FIGURE 2: The radio number of double triangular Δ_3 (snake).

otherwise,

$$\begin{aligned} & k+1 \geq k+1-d(x,y), \\ & 1 \leq i \leq k-1 \text{ and } 0 \leq j \leq k-1, \\ & \left|k^2+\frac{k}{2}-ki-\left(k^2+k+1+(k-1)j\right)\right| \geq \text{diam}+1-d(x,y), \\ & 2k^2-\frac{5}{2}k+2 \geq k+1-d(x,y). \end{aligned} \tag{20}$$

If $i=0$ and $j=k-1$,

$$2k^2-k+2 \geq k+1-d(x,y), \tag{21}$$

otherwise,

$$k^2-\frac{k}{2}+1 \geq k+1-d(x,y). \tag{22}$$

Case 4. k is odd and $k>1$:

$$h(x_i)=\begin{cases} h(x_{k+1})=0, & \\ h(x_{k-i+1})=ki, & 1\leq i\leq k, \\ h(x_{k+i+2})=k^2+\dfrac{k+1}{2}-ki, & 0\leq i\leq k-1, \\ (x_{2k+2+i})=k^2+k+2-(k-1)i, & 0\leq i\leq k-1. \end{cases} \tag{23}$$

For each $(i,i+1)$,

$$\begin{aligned} & |ki-(k(i+1))| \geq \text{diam}+1-d(x,y), \\ & k \geq k+1-d(x,y). \end{aligned} \tag{24}$$

For each $(i,i+1)$,

$$\begin{aligned} & \left|k^2+\frac{k+1}{2}-ki-\left(k^2+\frac{k+1}{2}-k(i+1)\right)\right| \\ & \geq \text{diam}+1-d(x,y), \\ & k \geq k+1-d(x,y). \end{aligned} \tag{25}$$

Also, for each $(i,i+1)$,

$$\begin{aligned} & \left|k^2+k+2-(k-1)i-\left(k^2+k+2-(k-1)(i+1)\right)\right| \\ & \geq \text{diam}+1-d(x,y), \\ & k-1 \geq k+1-d(x,y). \end{aligned} \tag{26}$$

Now, suppose that $1\leq i\leq k$ and $0\leq j\leq k-1$:

$$\begin{aligned} & \left|ki-\left(k^2+\frac{k+1}{2}-kj\right)\right| \geq \text{diam}+1-d(x,y), \\ & k^2-\frac{3k}{2}-\frac{1}{2} \geq k+1-d(x,y), \end{aligned} \tag{27}$$

otherwise,

$$\begin{aligned} & \left|ki-\left(k^2+\frac{k+1}{2}-kj\right)\right| \geq \text{diam}+1-d(x,y), \\ & \frac{k}{2}+\frac{1}{2} \geq \text{diam}+1-d(x,y). \end{aligned} \tag{28}$$

Suppose that $1\leq i\leq k$ and $0\leq j\leq k-1$:

$$\begin{aligned} & \left|ki-\left(k^2+k+2-(k-1)j\right)\right| \geq \text{diam}+1-d(x,y), \\ & k^2-3k-1 \geq k+1-d(x,y). \end{aligned} \tag{29}$$

If $i=1$ and $j=k-1$,

$$2k-1 \geq k+1-d(x,y), \tag{30}$$

otherwise,

$$\begin{aligned} & \left|ki-\left(k^2+k+2-(k-1)j\right)\right| \geq \text{diam}+1-d(x,y), \\ & k+2 \geq k+1-d(x,y). \end{aligned} \tag{31}$$

Suppose that $0\leq i\leq k-1$ and $0\leq j\leq k-1$:

$$\begin{aligned} & \left|k^2+\frac{k+1}{2}-ki-\left(k^2+k+2-(k-1)j\right)\right| \\ & \geq \text{diam}+1-d(x,y), \\ & \frac{3}{2}k+\frac{1}{2} \geq k+1-d(x,y). \end{aligned} \tag{32}$$

If $i=0$ and $j=k-1$,

```
Input: G be an n-vertex simple connected graph, k be a positive integer, and the adjacency matrix A[n][n] of G
Output: A radio k-coloring of G.
Begin
  Compute the distance matrix D[n][n] of G using Floyed–Warshall's algorithm and the adjacency matrix A[n][n] of G.
  RadioNumber = ∞;
  for l = 1 to n do
    for i = 1 to n do
      labeling [i] = 0;
    end
    for i = 1 to n do
        for j = 1 to n do
          c[i][j] = diam + 1 − D[i][j];
        end
        c[i][j] = ∞;
    end
    for i = 2 to n do
/*find the minimum value m of the column with position p*/
        [m, p] = min [c(l, :)];
        for j = 1 to n
            c[p][j] = c[p][j] + m
            if c[p][j] < c[l][j]
              c[p][j] = c[l][j]
            end
        end
        labeling [p] = m
        l = p
    end
      /* find the max value of the labeling */
        Max_Value = max (labeling))
        if RadioNumber > Max_Value
          RadioNumber = Max_Value
        end
  end
End
```

Algorithm 1: [2] Finding a radio k-coloring of a graph.

```
Input: G be an n-vertex graph, simple connected graph, and the diameter of (diam).
Output: an upper bound of radio number of G.
Begin
  Step 1: choose a vertex u and col(u) = floor(√diam).
  Step 2: S = {u}.
  Step 3: for all v ∈ V(G) − S, compute
      temp(v) = max_{t∈s} {col(t) + max{√((D + 1 − d(u, v), 1)}}.
  Step 4: let min = min_{v∈V(G)−S} {temp(v)}.
  Step 5: choose a vertex v ∈ V(G) − S, such that temp(v) = min.
  Step 6: give col(v) = min.
  Step 7: S = S ∪ {v}
  Step 8: repeat Step 3 to Step 6 until all vertices are labeled.
  Step 9: repeat Step 1 to Step 7 for every vertex x ∈ V(G).
End
```

Algorithm 2: [3] Finding an upper bound of the radio number of a graph G.

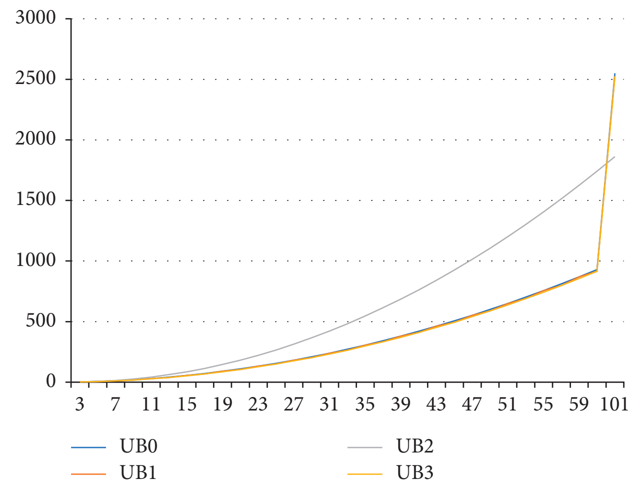

Figure 3: Comparison among UB0, Ub1, UB2, and UB3 for the radio number of triangular snake.

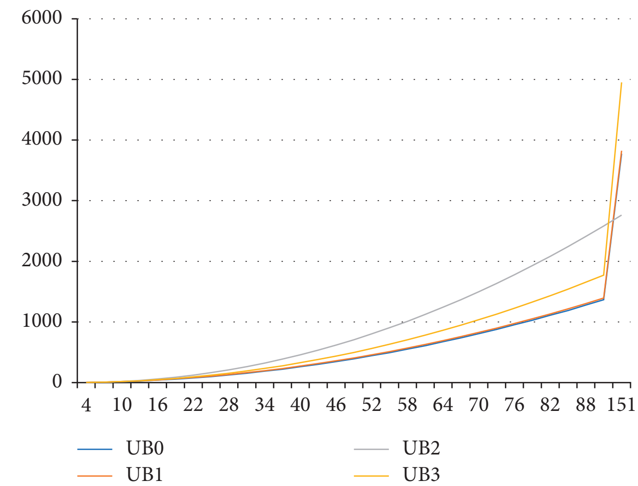

Figure 4: Comparison among UB0, Ub1, UB2, and UB3 for the radio number of double triangular snake.

Table 1: Comparison between standard radio number and the upper bound of radio number for the triangular snake graph.

k	n	UB0 [2]		UB1 [3]		UB2 [1]		UB3	
		rn	CPU time	rn	CPU time	rn	CPU time	rn	CPU time
1	3	2	0.007704	2	0.0040755	2	0.0017378	2	O(1)
2	5	6	0.004364	5	0.004255	6	0.002382	5	O(1)
3	7	12	0.00612	12	0.00555	14	0.005265	11	O(1)
4	9	20	0.024677	18	0.012055	26	0.005364	18	O(1)
5	11	30	0.051972	30	0.013155	42	0.005659	28	O(1)
6	13	42	0.230102	39	0.013621	62	0.005799	39	O(1)
7	15	56	0.307545	56	0.013755	86	0.006905	53	O(1)
8	17	72	0.308318	68	0.014298	114	0.007153	68	O(1)
9	19	90	0.468408	90	0.014749	146	0.007203	86	O(1)
10	21	110	0.751755	105	0.01493	182	0.00743	105	O(1)
11	23	132	0.924785	132	0.015201	222	0.007672	127	O(1)
12	25	156	1.219799	150	0.015988	266	0.008343	150	O(1)
13	27	182	1.674918	182	0.016105	314	0.008354	176	O(1)
14	29	210	2.689564	203	0.016197	366	0.008496	203	O(1)
15	31	240	3.224403	240	0.016201	422	0.008661	233	O(1)
16	33	272	3.567201	264	0.01711	482	0.009033	264	O(1)
17	35	306	4.447875	306	0.017625	546	0.009587	298	O(1)
18	37	342	5.561139	333	0.018556	614	0.009701	333	O(1)
19	39	380	6.933108	380	0.019099	686	0.009929	371	O(1)
20	41	420	8.345423	410	0.020327	762	0.010011	410	O(1)
21	43	462	12.868485	462	0.021287	842	0.010364	452	O(1)
22	45	506	13.787422	495	0.021983	926	0.011044	495	O(1)
23	47	552	15.946642	552	0.022126	1014	0.011472	541	O(1)
24	49	600	20.145523	588	0.029388	1106	0.011726	588	O(1)
25	51	650	22.931427	650	0.049946	1202	0.012145	638	O(1)
26	53	702	26.792638	689	0.053599	1302	0.013162	689	O(1)
27	55	756	30.007477	756	0.058895	1406	0.013417	743	O(1)
28	57	812	33.778689	798	0.060056	1514	0.013437	798	O(1)
29	59	870	39.570408	870	0.089137	1626	0.017043	856	O(1)
30	61	930	45.216577	915	0.148602	1742	0.026953	915	O(1)
50	101	2550	342.011401	2525	0.282964	1862	0.259496	2525	O(1)

Table 2: Comparison between standard radio number and for the upper bound of the radio number for the double triangular snake graph.

k	n	UB0 [2]		UB1 [3]		UB2 [1]		UB3	
		rn	CPU time	rn	CPU time	rn	CPU time	rn	CPU time
1	4	2	0.008905	3	0.013994	2	0.007179	3	O(1)
2	7	7	0.009302	8	0.014494	8	0.008093	7	O(1)
3	10	15	0.012654	17	0.015187	19	0.010171	18	O(1)
4	13	26	0.01432	29	0.016028	36	0.011224	30	O(1)
5	16	41	0.022551	44	0.026618	59	0.012734	48	O(1)
6	19	57	0.022565	62	0.031761	88	0.014698	68	O(1)
7	22	78	0.024324	83	0.097335	123	0.017663	94	O(1)
8	25	100	0.026327	107	0.099599	164	0.025045	122	O(1)
9	28	127	0.030762	134	0.168036	211	0.025465	156	O(1)
10	31	155	0.038029	164	0.217785	264	0.031522	192	O(1)
11	34	188	0.048976	197	0.312401	323	0.032649	234	O(1)
12	37	222	0.058516	233	0.476330	388	0.033239	278	O(1)
13	40	262	0.067316	272	0.648300	459	0.039245	328	O(1)
14	43	301	0.092605	314	0.831050	536	0.043670	380	O(1)
15	46	347	0.101886	359	1.087081	619	0.045682	438	O(1)
16	49	392	0.157635	407	1.389141	708	0.052569	498	O(1)
17	52	444	0.163901	458	1.740725	803	0.065006	564	O(1)
18	55	495	0.270554	512	2.151552	904	0.131148	632	O(1)
19	58	553	0.287547	569	2.625657	1011	0.156826	706	O(1)
20	61	610	0.325028	629	3.229021	1124	2.637903	782	O(1)
21	64	675	0.350093	692	3.867577	1243	2.655901	864	O(1)
22	67	737	0.355919	758	4.619990	1368	2.676703	948	O(1)
23	70	808	0.369294	827	5.625904	1499	2.698903	1038	O(1)
24	73	876	0.460056	899	6.570240	1636	3.174321	1130	O(1)
25	76	953	0.512382	974	7.552782	1779	3.321324	1228	O(1)
26	79	1027	0.553158	1052	9.093392	1928	3.592834	1328	O(1)
27	82	1110	0.625059	1133	10.404067	2083	3.720172	1434	O(1)
28	85	1190	0.740484	1217	12.811142	2244	4.019234	1542	O(1)
29	88	1280	0.77942	1304	13.942115	2411	4.892321	1656	O(1)
30	91	1365	0.974537	1394	16.356469	2584	5.109283	1772	O(1)
50	151	3775	4.497669	3824	130.59526	2763	9.981278	4952	O(1)

$$\left|k^2 + \frac{k+1}{2} - ki - \left(k^2 + k + 2 - (k-1)j\right)\right| \geq \text{diam} + 1 - d(x, y), \tag{33}$$

$$k^2 - \frac{5}{2}k - \frac{1}{2} \geq k + 1 - d(x, y),$$

otherwise,

$$k^2 - \frac{1}{2}k + \frac{3}{2} \geq k + 1 - d(x, y). \tag{34}$$

Example 2. Figure 2 presents the labeling double triangular Δ_3 (snake) according to Theorem 2.

4. Computational Study

In order to evaluate the proposed upper bounds presented by Theorems 1 and 2, we make a numerical experiment between the proposed results and the results of [1–3]. This experiment applies on two graphs (triangular snake and double triangular snake). The description of the environment is as follows: MATLAB R2016a with default options and all runs were carried out under MS Windows 7 Professional system, having Intel® Core™ i3-3217U CPU@ 1.80 GHz and 4 Gb RAM.

In Tables 1 and 2, the abbreviations Ub0, Ub1, Ub2, and Ub3 are used to denote upper bounds are due to the works of Saha and Panigrahi [2], Saha and Panigrahi [3], Badr and Moussa [1], and the proposed algorithm, respectively.

Table 1 and Figure 3 show that the proposed upper bound Ub3 overcomes the upper bound UB0 and UB2 which is due to the works of Saha and Panigrahi [2] and Badr and Moussa [1], respectively. On the contrary, the proposed upper bound Ub3 overcomes the upper bound UB1 (for k is odd only) which is due to the works of Saha and Panigrahi [2]. The upper bound (for k is even) of the UB3 and UB1 are equal.

Table 1 and Figure 4 explain that the proposed upper bounds outperform all results of UB0, UB1, and UB2 according to CPU time. On the contrary, the mathematical model UB2 [1] overcomes UB0 and UB1.

5. Conclusions

In this study, the upper bounds for the radio number of the triangular snake and the double triangular snake graphs are introduced. The computational results indicate that the presented upper bounds are better than the results of the mathematical model provided by Badr and Moussa [1]. On the contrary, these proposed upper bounds are better than the results of algorithms presented by Saha and Panigrahi [2, 3].

Data Availability

The data used to support the findings of this study are available from the corresponding author upon request.

Conflicts of Interest

The authors declare that they have no conflicts of interest.

Acknowledgments

The authors extend their appreciation to the Deanship of Scientific Research at King Khalid University for funding this work through General Research Project under Grant no. R.G.P.1/258/43.

References

[1] E. M. Badr and M. I. Moussa, "An upper bound of radio k-coloring problem and its integer linear programming model," *Wireless Networks*, vol. 26, no. 7, pp. 4955–4964, 2020.

[2] L. Saha and P. Panigrahi, "A graph radio *k*-coloring algorithm," in *Combinatorial Algorithms (IWOCA 2012): Lecure Notes in Computer Science*, S. Arumugan and W. F. Smyth, Eds., vol. 7643, Berlin, Germany, Springer, 2012.

[3] L. Saha and P. Panigrahi, "A new graph radio *k*-coloring algorithm," *Discrete Mathematics, Algorithms and Applications*, vol. 11, no. 1, p. 10, Article ID 1950005, 2019.

[4] M. Ali, M. T. Rahim, G. Ali, and M. Farooq, "An upper bound for the radio number of generalized gear graph," *Ars Combinatoria*, vol. 107, pp. 161–168, 2012.

[5] C. Fernandez, A. Flores, M. Tomova, and C. Wyels, "The radio number of gear graphs," 2008, https://arxiv.org/abs/0809.2623.

[6] M. Yao, B. Yao, J. Xie, and X. Zhang, "A new graph labelling on trees," in *Proceedings of the 2010 3rd International Conference on Biomedical Engineering and Informatics*, vol. 6, October 2010.

[7] K. M. B. Smitha and K. Thirusangu, "Radio mean labeling of triangular snake families," 2020.

[8] A. Ahmad and A. Haider, "Computing the radio labeling associated with zero divisor graph of a commutative ring," *UPB Scientific Bulletin, Series A*, vol. 81, pp. 65–72, 2019.

[9] M. S. Bazaraa, J. J. Jarvis, and H. D. Sherali, *Linear Programming and Network Flows*, Wiley, New York, NY, USA, 3rd edition, 2004.

[10] E. Badr, S. Almotairi, A. Eirokh, A. Abdel-Hay, and B. Almutairi, "An integer linear programming model for solving radio mean labeling problem," *IEEE Access*, vol. 8, pp. 162343–162349, 2020.

[11] E. Badr, S. Nada, M. Mohammed, A. Al-Shamiri, A. Abdel-hay, and A. ELrokh, "A novel mathematical model for radio mean square labeling problem," *Journal of Mathematics*, vol. 2022, Article ID 3303433, 9 pages, 2022.

[12] C. Gary and P. Zhang, *Discrete Mathematics and its Applications: Series*, K. H. Rosen, Ed., Routledge, Oxfordshire, UK, 2022.

[13] A. Rosa, "Cyclic steiner triple systems and labeling of triangular cacti," *Scientia*, vol. 5, pp. 87–95, 1967.

Hindawi
Journal of Mathematics
Volume 2022, Article ID 3785932, 9 pages
https://doi.org/10.1155/2022/3785932

Research Article

QSPR Modeling with Topological Indices of Some Potential Drug Candidates against COVID-19

Özge Çolakoğlu

Mathematics Department, Mersin University, Mersin 33343, Turkey

Correspondence should be addressed to Özge Çolakoğlu; ozgeeclkgl@gmail.com

Received 18 February 2022; Accepted 4 April 2022; Published 14 May 2022

Academic Editor: M. T. Rahim

Copyright © 2022 Özge Çolakoğlu. This is an open access article distributed under the Creative Commons Attribution License, which permits unrestricted use, distribution, and reproduction in any medium, provided the original work is properly cited.

COVID-19, which has spread all over the world and was declared as a pandemic, is a new disease caused by the coronavirus family. There is no medicine yet to prevent or end this pandemic. Even if existing drugs are used to alleviate the pandemic, this is not enough. Therefore, combinations of existing drugs and their analogs are being studied. Vaccines produced for COVID-19 may not be effective for new variants of this virus. Therefore, it is necessary to find the drugs for this disease as soon as possible. Topological indices are the numerical descriptors of a molecular structure obtained by the molecular graph. Topological indices can provide information about the physicochemical properties and biological properties of molecules in the quantitative structure-property relationship (QSPR) and quantitative structure-activity relationship (QSAR) studies. In this paper, some analogs of lopinavir, favipiravir, and ritonavir drugs that have the property of being potential drugs against COVID-19 are studied. QSPR models are studied using linear and quadratic regression analysis with topological indices for enthalpy of vaporization, flash point, molar refractivity, polarizability, surface tension, and molar volume properties of these analogs.

1. Introduction

COVID-19, which emerged in 2019, is a disease caused by severe acute respiratory syndrome coronavirus 2 (SARS-CoV-2) which is a new coronavirus. Coronavirus family refers to enveloped, positive-sense, and single-stranded RNA viruses [1]. SARS-CoV-2 is a positive single-stranded RNA virus containing proteins. COVID-19 is a respiratory disease transmitted from person to person. COVID-19 patients may present symptoms ranging from mild to severe diseases, such as fever, cough, sore throat, rhinorrhea, severe pneumonia, and septic shock [2]. With the rapid spread of this disease all over the world, the World Health Organization (WHO) declared COVID-19 as a pandemic in March 2020. The WHO reported that nearly 3 million people have died since the outbreak of the pandemic [3]. There is no medicine yet to alleviate or end this pandemic. Existing drugs are being used to alleviate the pandemic. These drugs are chloroquine, hydroxychloroquine, azithromycin, remdesivir, lopinavir, ritonavir, Arbidol, favipiravir, theaflavin, thalidomide, ribavirin, etc. [4]. Studies showed that some of these drugs are not suitable for the treatment of COVID-19 [5]. For example, FDA warns against the use of hydroxychloroquine or chloroquine for COVID-19 outside the hospital setting or a clinical trial due to the risk of heart rhythm problems [6]. Among these drugs, there are opinions that the use of remdesivir, favipiravir, and lopinavir is suitable for the treatment of COVID-19 disease [7]. Since the drugs used for HIV, SARS-CoV, and Mers-CoV do not have sufficient effect for SARS-CoV-2, many countries have focused on combinations of these drugs. In the United Kingdom, studies are being conducted on favipiravir and lopinavir/ritonavir or combination therapy [8]. In Egypt, studies are being conducted on favipiravir [9], lopinavir/ritonavir, and remdesivir combination [10], and in the United States, studies are being conducted on favipiravir, lopinavir/ritonavir [11, 12], and so on (see details in [4]).

New variants of the SARS-CoV-2 virus are emerging, and these variants are thought to be resistant to some vaccines produced for COVID-19. For this reason, it is necessary to find a drug that will prevent and end this disease as soon as possible. Drug discovery takes effort and time and is a costly process. Recently, computer-aided drug design (CADD) has been used successfully to significantly alleviate this process. This includes the prediction of electronic, drug-like, pharmacokinetic, 3D-QSAR, and physicochemical properties of target candidates.

The graph theory, which was first introduced by Euler in 1736, is a branch of discrete mathematics. It has been studied in physics, biology, computer sciences, chemistry, and so forth [13]. Chemical graph theory combines mathematical modeling of chemical phenomena with graph theory. It is focused on topological indices that are well correlated with the properties of a molecule or molecular compounds. Topological indices are widely used to predict the physicochemical and bioactivity properties of a molecule or molecular compound in the quantitative structure-property/structure-activity relationship (QSPR/QSAR) modeling [14]. The topological index is a real descriptor of the topological structure of a molecule or molecular compounds [15]. The first known topological index was the Wiener index in 1947, which was used to determine the physical properties of paraffin [16].

The molecular graph, G, is represented by unsaturated hydrocarbon skeletons of the molecule and molecular compounds. The vertices of the molecular graph correspond to non-hydrogen atoms and their set is defined by $V(G)$. The edges of molecular graph correspond to covalent bonds between the corresponding atoms and their set is defined by $E(G)$ [17]. The degree of a vertex v is defined by $d(v)$ (see [13] for basic definitions and notations on graph theory).

Omar et al. designed eight derivatives based on the core of hydroxychloroquine to use them in the treatment of COVID-19 and calculated the biological activity of designed molecules by QSAR [18]. Kirmani et al. established QSPR models with linear regression between physicochemical properties of potential antiviral drugs and some topological indices for various antiviral drugs used in the treatment of COVID-19 patients [19]. Havare obtained curvilinear regression models for boiling point of potential drugs against COVID-19 using various topological indices [20, 21]. Zhong et al. established QSPR between the ev-degree and ve-degree-based topological indices and measured the physicochemical parameters of the photochemical screened against SARS-CoV-2 [22]. Chaluvaraju and Shaikh established a multilinear regression model with the atom-bond connectivity (ABC) indices for the IC_{50} values of some drugs used in the treatment of COVID-19 [23]. Various topological indices were calculated to be used in QSPR and QSAR models of drugs used for the treatment of COVID-19 [24–27].

Rafi et al. studied analogs of lopinavir and favipiravir as potential drug candidates against COVID-19. They saw that all structurally modified analogs have been less toxic than the selected candidates and contain highly remediable properties [28].

In this paper, CID10009410, CID44271905, CID3010243, and CID271958 structures which are structural analogs of lopinavir, CID89869520 structure which is favipiravir analog, and lopinavir-d8 (CID71749833) which is ritonavir analog are considered. These structures have the property of being potential drugs against COVID-19. QSPR models are obtained by linear and quadratic regression analysis using topological indices for enthalpy of vaporization, flash point, molar refractivity, polarizability, surface tension, and molar volume properties of these structures.

2. Material and Method

Small molecules such as lopinavir and favipiravir significantly inhibit the activity of Mpro (main protease) and RdRp (viral RNA-dependent RNA polymerase) in vitro [4]. The structure of all selected compounds was downloaded from the PubChem database [29].

Lopinavir (see Figure 1) and ritonavir (see Figure 2) are inhibitors of human immunodeficiency virus-1 (HIV-1) aspartate protease. Since the previous SARS-CoV major protease has 96.1% similarity to the SARS-CoV-2 major protease, these two drugs can be used as a homologous target [30].

Favipiravir is a pyrazine carboxamide derivative with activity against RNA viruses (see Figure 2). It is an antiviral drug developed against influenza (flu virus). It was approved for the treatment of pandemic influenza emerging in Japan in 2014. It is used to treat moderate to mild COVID-19 patients. It is being studied for the treatment of COVID-19 [4, 31].

The structure of CID10009410 is a lopinavir analog and is generated by adding –F groups at the end of their two-dimensional (2D) structure [28]. CID44271905 structure which is lopinavir analog is generated by removing trimethyl-benzene fragment into the 2D structure of lopinavir [28]. CID44271958 structure is generated by adding 1,3,5-trimethyl-benzene and benzene fragments into the 2D structure of lopinavir [28]. The structure of CID3010243 is generated by removing tetrahydro-pyrimidionepropylene urea fragment and adding 2-imidazolinone fragments into lopinavir [28]. Figure 1 shows lopinavir and its analogs. CID89869520 structure which is the favipiravir analog is generated by adding –CH3 groups at the end of its 2D structure (see Figure 2) [28]. Lopinavir-d8 is a labeled selective HIV-1 protease inhibiting drug which is an analog of ritonavir, and this drug may act against COVID-19 (see Figure 2) [28].

In this study, the vertex-degree-based topological indices which are the first Zagreb index (M_1) [32], the second Zagreb index (M_2) [32], hyper-Zagreb index [33], max-min rodeg index [34], min-max rodeg index, Albertson index [35], sigma index [36], inverse symmetric deg index [37], atom-bond connectivity index [38], and inverse sum indeg index [34] are studied.

The selected bond additive and degree-based topological indices are the most studied indices and can well predict the physicochemical and bioactivity properties of chemical structures. The first and second Zagreb indices are topological indices that best predict the molar reaction and polarity of some new drugs used in cancer treatment [39]. The max-min rodeg index gives very good prediction in the linear model for enthalpy of vaporization and standard

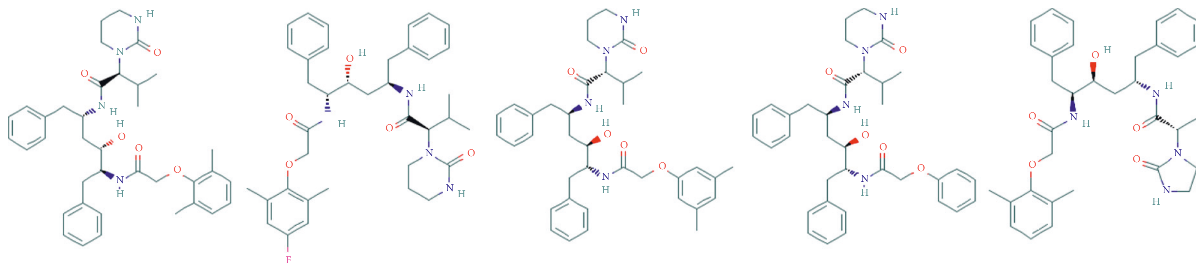

Lopinavir CID10009410 CID44271905 CID44271958 CID3010243

Figure 1: The chemical structures of lopinavir and lopinavir analogs [29].

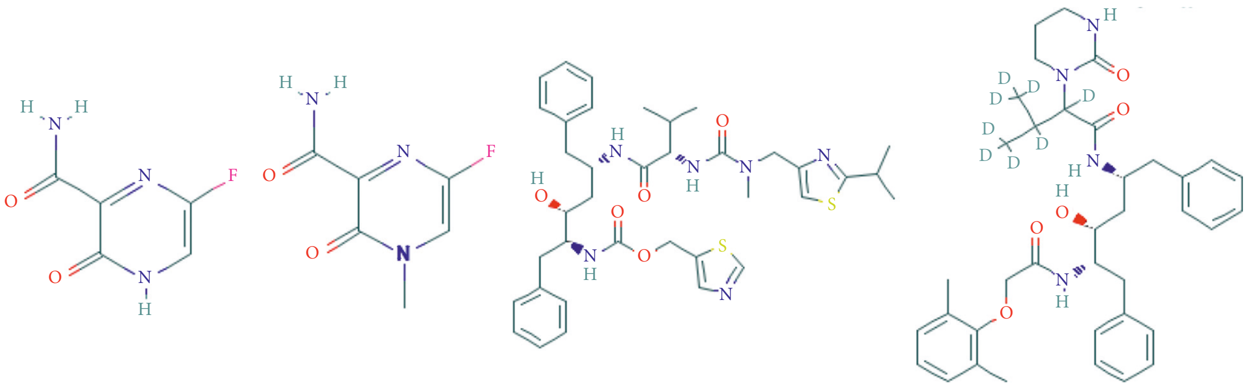

Favipiravir CID89869520 Ritonavir CID71749833

Figure 2: The chemical structures of favipiravir, ritonavir, and their analogs [29].

Table 1: Topological indices and their mathematical expressions.

Vertex-degree-based topological indices	Mathematical expressions
First Zagreb index	$M_1(G) = \sum_{uv\in E(G)}(d(u)+d(v))$
Second Zagreb index	$M_2(G) = \sum_{uv\in E(G)}(d(u)d(v))$
Hyper-Zagreb index	$HM(G) = \sum_{uv\in E(G)}(d(u)+d(v))^2$
Max-min rodeg index	$mM_{s\,de}(G) = \sum_{uv\in E(G)}\sqrt{\max\{d(u),d(v)\}/\min\{d(u),d(v)\}}$
Min-max rodeg index	$mM_{s\,de}(G) = \sum_{uv\in E(G)}\sqrt{\min\{d(u),d(v)\}/\max\{d(u),d(v)\}}$
Albertson index	$irr(G) = \sum_{uv\in E(G)}\lvert d(u)-d(v)\rvert$
Sigma index	$\sigma(G) = \sum_{uv\in E(G)}(d(u)-d(v))^2$
Inverse symmetric deg index	$IS\,DD(G) = \sum_{uv\in E(G)} d(u)d(v)/d(u)^2+d(v)^2$
Atom-bond connectivity index	$ABC(G) = \sum_{uv\in E(G)} d(u)+d(v)-2/d(u)d(v)$
Inverse sum indeg index	$ISI(G) = \sum_{uv\in E(G)} d(u)d(v)/d(u)+d(v)$

enthalpy of vaporization in the set of octane isomers and also for log water activity coefficient in the set of polychlorobiphenyles [40]. Atom-bond connectivity index has a good prediction ability when it comes to the enthalpy of formation of alkanes [38]. The first hyper-Zagreb index gives the best predictor model in the linear model for the boiling point of benzenoid hydrocarbons [41]. The inverse sum indeg index is the best predictor for the total surface area of octane isomers [34]. In addition, the ISI index is very good at predicting the vaporization enthalpy and sublimation enthalpy of monocarboxylic acids [42]. Various degree-based irregularity indices such as Albertson index and sigma index give a good prediction for physicochemical properties of octane isomers [43]. Table 1 shows the mathematical expressions of these indices.

The values of enthalpy of vaporization (E), flash point (FP), molar refractivity (MR), polarizability (P), surface tension (T), and molar volume (MV) of these potential drugs against COVID-19 are taken from ChemSpider [44]. Table 2 shows some of the physicochemical properties of potential drugs that can be used in the treatment of COVID-19.

Curvilinear regression analysis can be used to fit curves instead of straight lines. In this study, the following equations are tested:

$$\begin{aligned} Y &= a + b_1 X; n, R^2, F\,(\text{linear equation}),\\ Y &= a + b_1 X + b_2 X^2; n, R^2, F\,(\text{quadratic equation}), \end{aligned} \tag{1}$$

where Y is the response or dependent variable, a is the regression model constant, $b_i\,(i = 1, 2)$ are the coefficients for

Table 2: The physicochemical properties of potential drugs to be used in the treatment of COVID-19.

PubChem ID	Formula	E	FP	MR	P	T	MV
CID71749833	$C_{37}H_{40}D_8N_4O_5$	140.8	512.7	179,2	71	49,5	540,5
CID10009410	$C_{37}H_{47}FN_4O_5$	141,1	513,7	179,2	71	49	544,7
CID44271905	$C_{37}H_{48}N_4O_5$	140,8	512,7	179,2	71	49,5	540,5
CID3010243	$C_{36}H_{46}N_4O_5$	140	509,5	174,6	69,2	50,5	522,7
CID44271958	$C_{35}H_{44}N_4O_5$	138,9	505,1	169,5	67,2	50,9	507,9
CID89869520	$C_6H_6FN_3O_2$	63,2	185,5	41,3	16,4	72,9	110

Table 3: The values of topological indices of the molecular structures of potential drugs to be used in the treatment of COVID-19.

PubChem ID	M_1	M_2	HM	Mm_{sde}	mM_{sde}	irr	σ	ISDD	ABC	ISI
71749833	282	328	1432	74,646	46,159	60	120	24,296	24,916	63,72
10009410	236	270	1138	61,532	42,159	40	58	22,353	36,056	55,65
44271905	230	261	1100	60,250	41,214	40	56	21,976	35,321	54,3
3010243	226	259	1088	58,351	40,948	36	52	15,130	34,533	58,75
44271958	218	247	1032	55,887	40,794	32	44	19,030	33,688	52
89869520	58	66	288	16,559	9,152	14	24	4,846	8,910	13,05

the individual descriptor, X, X are independent variables, n is the number of samples used for building the regression equation, R^2 is the square of the correlation coefficient, R is the correlation coefficient, and F is the calculated value of the F-ration test. For more detailed information, see [45]. Note that when the experimental and theoretical results are close to each other, the correlation coefficient is close to 1. The observed values and model predictions must be compared to measure the predictive quality of the model (see details in [46, 47]). Therefore, it is necessary to consider the RMSE (root mean square error) metric for the predictive power of the model. It is clear that the best predictive model is the minimum error, i.e., the minimum RMSE is defined as

$$\mathrm{RMSE} = \sqrt{\frac{\sum_{i=1}^{n}\left(y_i - \hat{y}_i\right)^2}{n}}, \tag{2}$$

where y_i is the observed value of the independent variable in the test set, $\hat{y}_i$ is the predicted value of the independent variables in the test set, and n is the number of samples in the test [47]. R^2, R, F, and RMSE are considered for the goodness of fit of the model, i.e., $\max(R^2)$, max (R), $\max(F)$, and min(RMSE). The curvilinear regression analyses are obtained by using the SPSS statistical software. The independent variables in the curvilinear regression models are the values of the topological indices, which are described above, of various drugs used in the treatment of COVID-19.

3. Main Results

From Figures 1 and 2, the edge and vertex numbers of molecular graphs of chemical structures are seen. Let $E_{i,j} = \{i = d_u, j = d_v | uv \in E(G)\}$. The molecular graph of CID71749833 has 54 vertices and 57 edges. Its edges can be partitioned as $|E_{1,3}| = 6$, $|E_{1,4}| = 8$, $|E_{2,2}| = 14$, $|E_{2,3}| = 22$, $|E_{3,3}| = 2$, $|E_{3,4}| = 2$, $|E_{4,4}| = 3$. The molecular graph of CID10009410 has 47 vertices and 50 edges. Its edges can be partitioned as $|E_{1,3}| = 9$, $|E_{2,2}| = 12$, $|E_{2,3}| = 22$, $|E_{3,3}| = 7$. The molecular graph of CID44271905 has 46 vertices and 49 edges. Its edges can be partitioned as $|E_{1,3}| = 8$, $|E_{2,2}| = 12$, $|E_{2,3}| = 24$, $|E_{3,3}| = 5$. The molecular graph of CID3010243 has 45 vertices and 48 edges. Its edges can be partitioned as $|E_{1,3}| = 8$, $|E_{2,2}| = 13$, $|E_{2,3}| = 20$, $|E_{3,3}| = 7$. The molecular graph of CID44271958 has 44 vertices and 47 edges. Its edges can be partitioned as $|E_{1,3}| = 6$ $|E_{2,2}| = 16$, $|E_{2,3}| = 20$, $|E_{3,3}| = 5$. The molecular graph of CID89869520 has 12 vertices and 12 edges. Its edges can be partitioned as $|E_{1,3}| = 5$, $|E_{2,3}| = 4$, $|E_{3,3}| = 3$. The values in Table 3 are obtained from Table 1 and the above values using combinatorial computation and edge partition technique. The values of these indices were also obtained [21].

The linear and quadratic models are obtained by using the data in Table 2 and 3 with the SPSS program. Table 4 shows the correlation coefficient (R) obtained by the linear regression model between various topological indices and physicochemical properties of potential drugs against COVID-19. These physicochemical properties are the enthalpy of vaporization (E), the flash point (FP), the molar refractivity (MR), the polarizability (P), the surface tension (T), and the molar volume (MV). Among the correlation coefficients obtained for a physicochemical property, the model with max(R) is the best predictor of the regression model for that physicochemical property. Therefore, max(R) for each physicochemical property is marked in bold in Table 4.

From Table 4, the mM_{sde} index is the best estimator index for molar refraction, polarity, surface tension, and molar volume in linear regression models. The linear models obtained with these topological indices are as follows. Table 5 shows linear regression models that give the best estimate for physicochemical properties.

Table 6 shows the correlation coefficient (R) obtained by the quadratic regression model between various topological indices and physicochemical properties of potential drugs against COVID-19. max (R) for each physicochemical property is marked in bold in Table 6.

Table 4: The correlation coefficient (R) obtained by linear regression model between topological indices and physicochemical properties of various drugs used in treatment of COVID-19.

	E	FB	MR	P	T	MV
$\mathbf{M_1}$	0.960	0.960	0.965	0.966	0.964	0.966
$\mathbf{M_2}$	0.952	0.951	0.958	0.958	0.957	0.959
HM	0.934	0.934	0.941	0.942	0.940	0.942
$\mathbf{Mm_{sde}}$	0.948	0.948	0.955	0.955	0.955	0.956
$\mathbf{mM_{sde}}$	**0.991**	**0.991**	**0.992**	**0.992**	**0.991**	**0.992**
irr	0.768	0.768	0.785	0.789	0.783	0.788
σ	0.540	0.540	0.559	0.560	0.555	0.562
ISDD	0.902	0.901	0.913	0.913	0.918	0.917
ABC	0.922	0.922	0.917	0.916	0.919	0.916
ISI	0.977	0.977	0.980	0.980	0.978	0.980

Table 5: Linear regression models that give the best estimate for physicochemical properties.

$E = 44.913 + 1.514\mathrm{mM_{sde}}$	$R^2 = 0.898$	$F = 35{,}387$	SE = 11.221	RMSE = 9.161
$FB = 108.463 + 6.382\mathrm{mM_{sde}}$	$R^2 = 0.898$	$F = 35{,}242$	SE = 47.409	RMSE = 38.709
$MR = 7.814 + 2.677\mathrm{mM_{sde}}$	$R^2 = 0.913$	$F = 41.906$	SE = 18.239	RMSE = 14.891
$P = 3.148 + 1.060\mathrm{mM_{sde}}$	$R^2 = 0.913$	$F = 41.798$	SE = 7.231	RMSE = 5.904
$T = 78.578 - 0.456\mathrm{mM_{sde}}$	$R^2 = 0.910$	$F = 40.444$	SE = 3.161	RMSE = 2.580
$\mathrm{MV} = 4.834 + 8.365\mathrm{mM_{sde}}$	$R^2 = 0.914$	$F = 42.607$	SE = 56.514	RMSE = 46.143

Table 6: The correlation coefficient (R) obtained by quadratic regression model between topological indices and physicochemical properties of various drugs used in treatment of COVID-19.

	E	FB	MR	P	T	MV
$\mathbf{M_1}$	**1**	**1**	0.999	0.999	**0.999**	**0.999**
$\mathbf{M_2}$	**1**	**1**	0.999	0.999	**0.999**	**0.999**
HM	**1**	**1**	0.999	0.999	**0.999**	**0.999**
$\mathbf{Mm_{sde}}$	**1**	**1**	**1**	**1**	**0.999**	**0.999**
$\mathbf{mM_{sde}}$	**1**	**1**	0.998	0.998	0.998	0.998
irr	0.990	0.989	0.994	0.994	0.994	0.995
σ	0.962	0.962	0.973	0.972	0.973	0.975
ISDD	0.994	0.994	0.992	0.992	0.994	0.992
ABC	0.998	0.998	0.994	0.994	0.993	0.992
ISI	**1**	**1**	0.998	0.998	0.998	0.998

Table 7: The quadratic regression models that give the best estimate for the enthalpy of vaporization (E).

Regression models	R^2	F	SE	RMSE
$\mathbf{E} = 10.610 + 1.022\mathbf{M_1} - 0.002\mathbf{M_1^2}$	**1**	**100473.208**	**0.157**	**0.111**
$E = 11.244 + 0.886M_2 - 0.001M_2^2$	1	30536.699	0.285	0.201
$E = 9.401 + 0.211\mathrm{HM} - (8.320E + 5)\mathrm{HM}^2$	1	11702.730	0.460	0.325
$E = 18.477 + 5.438\mathrm{mM_{sde}} - 0.060\mathrm{mM_{sde}}^2$	1	3994.438	0.788	0.557
$E = 2.903 + 4.154\mathrm{Mm_{sde}} - 0.031\mathrm{Mm_{sde}}^2$	1	23347.231	0.326	0.230
$E = 13.056 + 4.318\mathrm{ISI} - 0.036\mathrm{ISI}^2$	1	3667.709	0.822	0.581

Table 8: The quadratic regression models that give the best estimate for the flashpoint.

Regression models	R^2	F	SE	RMSE
$\mathbf{FB} = -36.499 + 4.314\mathbf{M_1} - 0.008\mathbf{M_1^2}$,	**1**	**109749.28**	**0.634**	**0.448**
$\mathrm{FB} = -33.789 + 3.741M_2 - 0.006M_2^2$,	1	25599.895	1.312	0.928
$\mathrm{FB} = -41.520 + 0.890\mathrm{HM} - 0.000\mathrm{HM}^2$	1	9442.841	2.161	1.527
$\mathrm{FB} = -3.511 + 22.989\mathrm{mM_{sde}} - 0.255\mathrm{mM_{sde}}^2$	1	4653.265	3.078	2.176
$\mathrm{FB} = -69.004 + 17.537\mathrm{Mm_{sde}} - 0.131\mathrm{Mm_{sde}}^2$	1	16434.89	1.638	1.158
$\mathrm{FB} = -26.202 + 18.231\mathrm{ISI} - 0.154\mathrm{ISI}^2$,	1	4051.916	3.298	2.332

Table 9: The quadratic regression models that give the best estimation for the molar refractivity (MR), the polarizability (P), and the surface tension (T).

Regression models	R^2	F	SE	RMSE
$\mathbf{MR} = -60.153 + 6.950\mathbf{Mm_{sde}} - 0.050\mathbf{Mm_{sde}}^2$	**0.999**	**1743.03**	**2.092**	**1.479**
$\mathbf{P} = -23.805 + 2.754\mathbf{Mm_{sde}} - 0.020\mathbf{Mm_{sde}}^2$	**0.999**	**1819.3**	***0.811***	**0.573**
$T = 88.026 - 0.292M_1 + 0.001M_1^2$	0.998	637.521	0.589	0.416
$T = 87.825 - 0.255M_2 + 0.000M_2^2$	0.998	667.918	0.576	0.407
$T = 88.573 - 0.061HM + (2.360E - 5)HM^2$	0.998	862.918	0.518	0.366
$\mathbf{T} = 90.313 - 1.193\mathbf{Mm_{sde}} + 0.009\mathbf{Mm_{sde}}^2$	**0.998**	**956.122**	**0.482**	**0.340**

Table 10: The quadratic regression models that give the best estimate for the molar volume.

Regression models	R^2	F	SE	RMSE
$\mathrm{MV} = -163.089 + 5.271M_1 - 0.010M_1^2$	0.997	592.767	11.191	7.913
$\mathrm{MV} = -161.643 + 4.605M_2 - 0.007M_2^2$	0.998	633.566	10.826	7.654
$\mathrm{MV} - 173.989 + 1.107\mathrm{HM} + 0.000\mathrm{HM}^2$	0.998	808.010	9.589	6.780
$\mathbf{MV} = -204.851 + 21.546\mathbf{Mm_{sde}} - 0.154\mathbf{Mm_{sde}}^2$	**0.998**	**946.143**	**8.862**	**6.266**

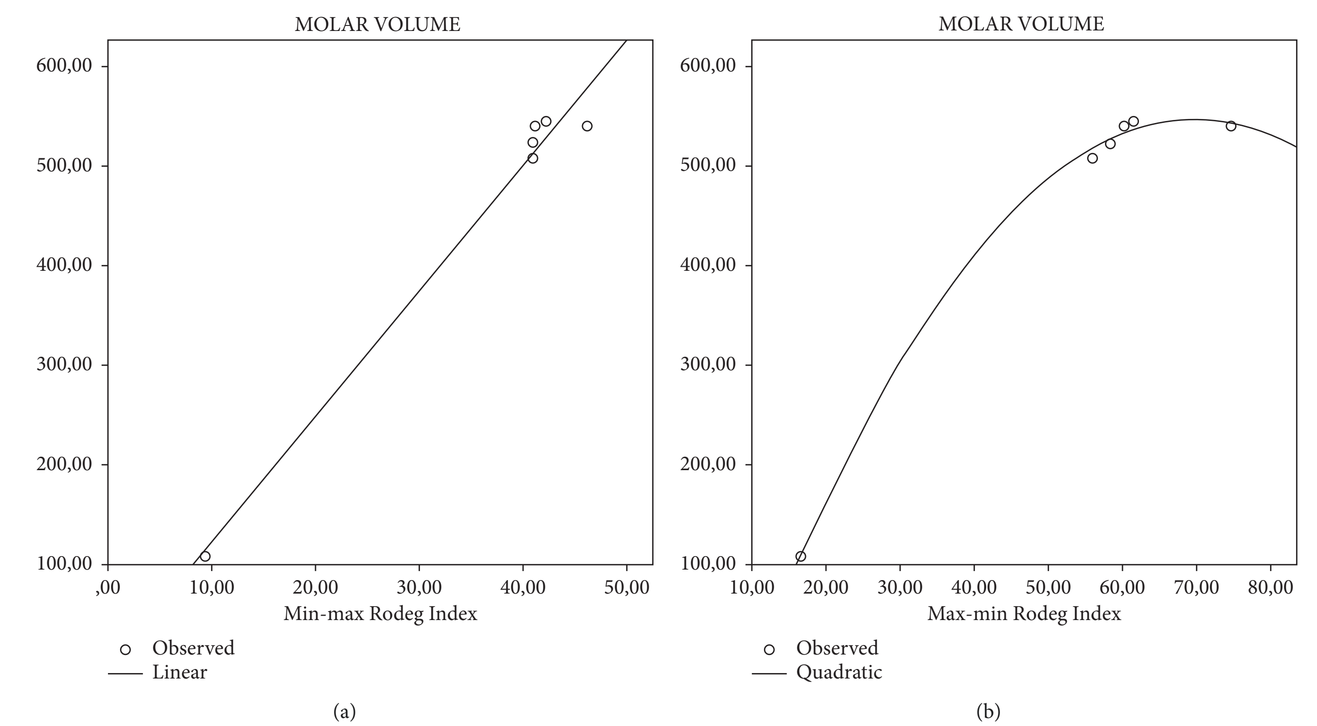

Figure 3: The plots of the linear and quadratic regression equations of the molar volume with the min-max rodeg index and the max-min rodeg index, respectively.

The regression models of the best predictive indices are given below for molar refraction, polarity, surface tension, and molar volume in quadratic regression models from Table 6. Table 7 shows quadratic regression models that give the best estimate for the enthalpy of vaporization.

From the above equations, M_1 is the best predictor index for the enthalpy of vaporization in quadratic regression models from min(RMSE), max(R^2), and max(F). Table 8 shows quadratic regression models that give the best estimate for the flash point (FP). The model that predicts the best is marked in bold (Table 8).

From the above equations, M_1 is the best predictor index for the flash point in quadratic regression models from min(RMSE), max(R^2), and max(F) (Table 8). Table 9 shows quadratic regression models that give the best estimate for the molar refractivity (MR), the polarizability (P), and the surface tension (T).

From the above equations, Mm_{sde} is the best predictor index for the polarizability, the surface tension, and the molar refractivity (MR) in quadratic regression models from min(RMSE), max(R^2), and max(F) (Table 9). Table 10 shows quadratic regression models that give the best estimate for the molar volume.

From the above equations, Mm_{sde} is the best predictor index for the molar volume in quadratic regression models from min(RMSE), max(R^2), and max(F) (Table 10).

Figure 3 shows plots of the linear and quadratic regression equations of the molar volume with the min-max rodeg index and the max-min rodeg index, respectively.

4. Conclusions

New variants may be emerging that are resistant to some vaccines produced for COVID-19. Therefore, it is necessary to produce medicine as soon as possible against COVID-19. There is no medicine yet to alleviate or end this pandemic. Existing drugs are being used to alleviate the pandemic. This study's aim is to obtain information about the topology of some chemical structures with minimum cost and minimum time with topological indices.

Four structural analogs of lopinavir, one structural analog of favipiravir, and one structural analog of ritonavir are studied. Rafi et al. [28] conducted a QSAR study for some properties of these analogs and found that their drug properties were higher and stressed that there could be potential drugs against COVID-19. In this study, QSPR modeling for some physicochemical properties of these structures is performed using the topological indices of the molecular graphs of these structures. These types of modeling are done by linear and quadratic regression analysis. Models were studied with 6 descriptors and 10 topological indices.

QSPR modeling shows that the best predictive topological index is the min-max rodeg index for enthalpy of vaporization, flash point, molar refractivity, polarizability, surface tension, and molar volume in linear regression. Also, in quadratic regression models, the best predictive topological indices are the first Zagreb index for enthalpy of vaporization and flash point and the max-min rodeg index for molar refractivity, polarizability, surface tension, and molar volume. Correlation coefficients obtained in QSPR modeling are very close to 1 and 1 in some models. The experimental and theoretical results of the models obtained are very close to each other. The predictive strength is tested for these degree-based topological indices by using some physicochemical properties of these structures. Moreover, models that are the best predictive among linear and quadratic regression models are quadratic models. The results of this study will shed light on new drug discoveries, most importantly in the treatment of COVID-19, chemistry, and pharmacy science.

The physicochemical properties of a drug are important for its use. The study is based on the idea that these drugs, which are tried and thought for the treatment of COVID-19, are used together and/or their analogs are used. By using the results of the study, if a single drug is obtained from these drugs, information about that drug can be obtained without experimenting. Thus, it can provide information about the properties of drugs that are similar to these structures or that will be obtained from the combination of these structures, saving time and money without experimenting.

Data Availability

No data were used to support this study.

Conflicts of Interest

The author declares that there are no conflicts of interest.

References

[1] G. W. Ejuh, C. Fonkem, Y. Tadjouteu Assatse et al., "Study of the structural, chemical descriptors and optoelectronic properties of the drugs hydroxychloroquine and azithromycin," *Heliyon*, vol. 6, no. 8, Article ID e04647, 2020.

[2] B. Nutho, P. Mahalapbutr, K. Hengphasatporn et al., "Why are lopinavir and ritonavir effective against the newly emerged coronavirus 2019? Atomistic insights into the inhibitory mechanisms," *Biochemistry*, vol. 59, no. 18, pp. 1769–1779, 2020.

[3] World Health Organization, "Coronavirus disease (COVID-19) pandemic," 2020, https://www.who.int/director-general/speeches/detail/who-director-general-s-opening-remarks-at-the-media-briefing-on-COVID-19---11-march-2020.

[4] E. Janik, M. Niemcewicz, M. Podogrocki, J. Saluk-Bijak, and M. Bijak, "Existing drugs considered as promising in COVID-19 therapy," *International Journal of Molecular Sciences*, vol. 22, no. 11, p. 5434, 2021.

[5] A. B. Cavalcanti, F. G. Zampieri, R. G. Rosa et al., "Hydroxychloroquine with or without azithromycin in mild-to-moderate COVID-19," *The New England Journal of Medicine*, vol. 383, pp. 2041–2052, 2020.

[6] The U.S. Food and Drug Administration, "FDA cautions against use of hydroxychloroquine or chloroquine for COVID-19 outside of the hospital setting or a clinical trial due to risk of heart rhythm problems," 2021, https://www.fda.gov/drugs/drug-safety-and-availability/fda-cautions-against-use-hydroxychloroquine-or-chloroquineCOVID-19-outside-hospital-setting-or.

[7] Z. Jin, J.-Y. Liu, R. Feng, L. Ji, Z.-L. Jin, and H.-B. Li, "Drug treatment of coronavirus disease 2019 (COVID-19) in China," *European Journal of Pharmacology*, vol. 883, Article ID 173326, 2020.

[8] ClinicalTrials.gov, "FLARE: favipiravir +/− lopinavir: a rct of early antivirals. nct04499677," 2021, https://clinicaltrials.gov/ct2/show/NCT04499677?term=NCT04499677&draw=2&rank=1.

[9] ClinicalTrials.gov, "Efficacy and safety of favipiravir in management of covid-19. nct04349241," 2021, https://clinicaltrials.gov/ct2/show/NCT04349241?term=NCT04349241&draw=2&rank=1.

[10] ClinicalTrials.gov, "Comparative therapeutic efficacy and safety of remdesivir versus lopinavir/ritonavir and remdesivir combination in COVID-19 patients," 2021, https://clinicaltrials.gov/ct2/show/NCT04738045?term=Lopinavir%2FRitonavir&cond=Covid19&draw=7&rank=2.

[11] ClinicalTrials.gov, "Favipiravir for patients with mild to moderate disease from novel coronavirus (COVID-19)," 2021, https://clinicaltrials.gov/ct2/show/NCT04600895?term=NCT04600895&draw=2&rank=1.

[12] ClinicalTrials.gov, "Trial of early therapies during non-hospitalized outpatient window," 2021, https://clinicaltrials.gov/ct2/show/NCT04372628?term=Lopinavir%2FRitonavir&cond=Covid19&draw=2.

[13] G. Chartrand and L. Lesniak, *Graphs and Digraphs*, CRS Press, Boca Raton, FL, USA, 2005.

[14] J. Devillers and A. T. Balaban, *Topological Indices and Related Descriptors in QSAR and QSPAR*, CRC Press, Boca Raton, FL, USA, 2000.

[15] I. Gutman, "A property of the simple topological index," *MATCH Communications in Mathematical and in Computer Chemistry*, vol. 25, pp. 131–140, 1990.

[16] H. Wiener, "Structural determination of paraffin boiling points," *Journal of the American Chemical Society*, vol. 69, no. 1, pp. 17–20, 1947.

[17] E. Estrada and D. Bonchev, *Chemical Graph Theory*, Chapman and Hall/CRC, New York, NY, USA, 2013.

[18] R. M. K. Omar, A. M. Najar, E. Bobtaina, and A. F. Elsheikh, "Pryazolylpyridine and triazolylpyridine derivative of hydroxychloroquine as potential therapeutic against COVID-19: theoretical evaluation," *Journal of Drug Delivery and Therapeutics*, vol. 10, pp. 181–186, 2020.

[19] S. A. K. Kirmani, P. Ali, and F. Azam, "Topological indices and QSPR/QSAR analysis of some antiviral drugs being investigated for the treatment of COVID-19 patients," *International Journal of Quantum Chemistry*, vol. 121, no. 9, Article ID e26594, 2020.

[20] Ö. Ç. Havare, "Quantitative structure analysis of some molecules in drugs used in the treatment of COVID-19 with topological indices," *Polycyclic Aromatic Compounds*, pp. 1–12. In press, 2021.

[21] Ö. Ç Havare, "On the boiling point of potential drug candidates against SARS-CoV-2 by curvilinear regression modeling," in *Proceedings of the 6th International Conference on Combinatories, Cryptograpy, Computer Science and Computing*, pp. 503–511, Tehran, Iran, November 2021.

[22] J.-F. Zhong, A. Rauf, M. Naeem, J. Rahman, and A. Aslam, "Quantitative structure-property relationships (QSPR) of valency based topological indices with COVID-19 drugs and application," *Arabian Journal of Chemistry*, vol. 14, no. 7, Article ID 103240, 2021.

[23] B. Chaluvaraju and A. B. Shaikh, "Different versions of atom-bond connectivity indices of some molecular structures: applied for the treatment and prevention of COVID-19," *Polycyclic Aromatic Compounds*, pp. 1–15. In press, 2021.

[24] J. B. Liu, M. Arockiaraj, M. Arulperumjothi, and S. Prabhu, "Distance based and bond additive topological indices of certain repurposed antiviral drug compounds tested for treating COVID-19," *International Journal of Quantum Chemistry*, vol. 121, Article ID e26617, 2021.

[25] H. Ahmed, A. Alwardi, R. S. Morgan, and D. Soner Nandappa, "γ–Domination topological indices and φP–Polynomial of some chemical structures applied for the treatment of COVID-19 patients," *Biointerface Research in Applied Chemistry*, vol. 11, no. 5, pp. 13290–13302, 2021.

[26] A. Saleh, G. B. Sophia Shalini, and B. V. Dhananjayamurthy, "Tre reducnd neighborhotd topologicil indices and RNp–polynomial for tte treatment of COVID-19," *Biointerface Research in Applied Chemistry*, vol. 11, no. 4, pp. 11817–11832, 2021.

[27] J. Wei, M. Cancan, A. U. Rehman et al., "On topologicil indices rf remdesivcr compouud used tn treatment cf corova virus (COVID 19)," *Polycyclic Aromatic Compounds*, pp. 1–19, 2021.

[28] M. O. Rafi, Md. Oliullah, G. Bhattacharje et al., "Combination of QSAR, molecular docking, molecular dynamic simulation and MM-PBSA: analogues of lopinavir and favipiravir as potential drug candidates against COVID-19," *Journal of Biomolecular Structure and Dynamics*, vol. 40, no. 8, pp. 3711–3730, 2020.

[29] PubChem, "On opcn chemistdy database at the national institutes of health (NIH)," 2021, https://pubchem.ncbi.nlm.nih.gov/.

[30] G. Bolcato, M. Bissaro, M. Pavan, M. Sturlese, and S. Moro, "Targeting the coronavirus SARS-CoV-2: computational insights into the mechanism of action of the protease inhibitors lopinavir, ritonavir and nelfinavir," *Scientific Reports*, vol. 10, Article ID 20927, 2020.

[31] K. Shiraki and T. Daikoku, "Favipiravir, an anti-influenza drug against life-threatening RNA virus infections," *Pharmacology and Therapeutics*, vol. 209, Article ID 107512, 2020.

[32] I. Gutman, B. Ruscic, N. Trinajstic, and C. F. WilsonJr., "Graph theory and molecular orbitals. XII. Acyclic polyenes," *The Journal of Chemical Physics*, vol. 62, no. 9, pp. 3399–3405, 1975.

[33] G. H. Shirdel, H. Rezapour, and A. M. Sayadi, "The hyper––zagreb index of graph operations," *Iranian Journal of Mathematical Chemistry*, vol. 4, pp. 213–220, 2013.

[34] D. Vukiccevi´c and M. Gasparov, "Bond additive modeling 1. Adriatic indices," *Crica Chemica Actata.*vol. 83, pp. 243–260, 2010.

[35] M. O. Albertson, "The irregularity of a graph," *Ars Combinatoria*, vol. 46, pp. 219–225, 1997.

[36] I. Gutman, M. Togan, A. Yurttas, A. S. Cevik, and I. N. Cangul, "Inverpe problem fsr sigia index," *MATCH Communications in Mathematical and in Computer Chemistry*, vol. 79, pp. 491–508, 2018.

[37] M. Ghorbani, S. Zangi, and N. Amraei, "New results on symmetric division deg index," *Journal of Applied Mathematics and Computing*, vol. 65, pp. 161–176, 2021.

[38] E. Estrada, L. Torres, L. Rodríguez, and I. Gutman, "An atom-bond connectivity index: modelling the enthalpy of formation of alkanes," *Indian Journal of Chemistry*, vol. 37, pp. 849–855, 1998.

[39] Ö. Ç. Havare, "Topological indices and QSPR modeling of some novel drugs used in the cancer treatment," *International Journal of Quantum Chemistry*, vol. 121, no. 24, Article ID e26813, 2021.

[40] D. Vukicevic, "Boad additime modeling 2. Mathematicpl properties mf max-mrn rodig index," *Crica Chemica Actata.*vol. 83, no. 3, pp. 261–273, 2010.

[41] G. V. Rajasekharaiah and U. P. Murthy, "Hyper-Zagreb indices of graphs and its applications," *Journal of Algebra Combinatorics Discrete Structures and Applications*, vol. 8, no. 1, pp. 9–22, 2020.

[42] Ö. Çolakoğlu Havare, "Determination of some thermodynamic properties of monocarboxylic acids using multiple linear regression," *BEU Journal of Science*, vol. 8, no. 2, pp. 466–471, 2019.

[43] T. Reti, R. Sharafdini, A. Dr´egelyi-Kiss, and H. Haghbin, "Graph irregularity indices used as molecular descriptors in QSPR studies," *MATCH Communications in Mathematical and in Computer Chemistry*, vol. 79, pp. 509–524, 2018.

[44] Chemspider, "Search asd shace chemistry," 2021, http://www.chemspider.com/AboutUs.aspx.

[45] J. C. Dearden, *Advances in QSAR Modeling*, Springer International Publishing, Cham, Switzerland, 2017.

[46] L. Wang, P. Xing, C. Wang, X. Zhou, Z. Dai, and L. Bai, "Maximil informaticn coefficient asd suppovt vectrr regressibn basnd nonlinefr featuse selection and QSmR modeling tn toxicity af alcohcl compounds to tadpoles of rana temporaria," *Journal of the Brazilian Chemical Society*, vol. 30, no. 2, pp. 279–285, 2019.
[47] V. Consonni, D. Ballabio, and R. Todeschini, "Comments on tde definition of the p2 parameter for QSvR validation," *Journal of Chemical Information and Modeling*, vol. 49, no. 7, pp. 1669–1678, 2009.

Hindawi
Journal of Mathematics
Volume 2022, Article ID 2635564, 8 pages
https://doi.org/10.1155/2022/2635564

Research Article

Assignment Computations Based on $C_{\mathbf{exp}}$ Average in Various Ladder Graphs

A.Rajesh Kannan,[1] **P. Manivannan**,[1] **K. Loganathan**,[2,3] **K. Prabu**,[4] **and Sonam Gyeltshen**[5]

[1]*Department of Mathematics, Mepco Schlenk Engineering College, Sivakasi 626005, Tamil Nadu, India*
[2]*Department of Mathematics and Statistics, Manipal University Jaipur, Jaipur 303007, Rajasthan, India*
[3]*Research and Development Wing, Live4Research, Tiruppur 638 106, Tamil Nadu, India*
[4]*Kongu Engineering College, Perundurai, Erode 638060, Tamil Nadu, India*
[5]*Department of Humanities and Management Jigme Namgyel Engineering College, Royal University of Bhutan, Dewathang, Bhutan*

Correspondence should be addressed to K. Loganathan; loganathankaruppusamy304@gmail.com and Sonam Gyeltshen; sonamgyeltshen@jnec.edu.bt

Received 20 February 2022; Revised 29 March 2022; Accepted 7 April 2022; Published 11 May 2022

Academic Editor: M. T. Rahim

Copyright © 2022 A.Rajesh Kannan et al. This is an open access article distributed under the Creative Commons Attribution License, which permits unrestricted use, distribution, and reproduction in any medium, provided the original work is properly cited.

This study introduces the $C_{\exp}$ average assignments and investigates its properties using various ladder graphs. The ladder graphs can be found in every communication networks. Ladder networks are increasingly being used in everyday life for monitoring and environmental applications such as domestic, military, surveillance, industrial, medical applications, and traffic management. These datasets are afflicted by the average representation of the graph structure. It aids in the visualisation and comprehension of data analysis. The $C_{\exp}$ labeling is used in sensor networks, adhoc networks, and other applications. It also efficiently creates a communication network after using noise reduction methods to remove salt and pepper noise.

1. Introduction

A graph labeling is the assignment of labels, conventionally indicated by integers, to edges and/or vertices of a graph in the mathematical domain of graph theory. The concept of labeling may be applied to many areas of graph theory, for example, in automata theory and formal language theory. We use [1–5] for notations and nomenclature. We recommend [6] for a thorough examination of graph labeling. Let P_n be a path on n nodes denoted by $u_{1,\mu}$, where $1 \leq \mu \leq n$, and with $n-1$ lines denoted by $e_{1,\delta}$, where $1 \leq \delta \leq n-1$, where e_μ is the line joining the vertices $u_{1,\mu}$ and $u_{1,\mu+1}$. On each edge e_δ, erect a ladder with $n-(\mu-1)$ steps including the edge e_μ, for $\mu = 1, 2, 3, \ldots, n-1$. The resulting graph is called the one-sided step graph, and it is denoted by ST_n. Let G_1 and G_2 be any two graphs with p_1 and p_2 vertices, respectively. Then, $G_1 \times G_2$ is the Cartesian product of two graphs. A ladder graph L_n is the graph $P_2 \times P_n$. The graph $G^\circ S_m$ is obtained from G by attaching m pendant vertices to each vertex of G. The triangular ladder TL_n, for $n \geq 2$, is a graph obtained from two paths by $u_1, u_2, \ldots u_n$ and $v_1, v_2, \ldots v_n$ by adding the edges $u_\mu v_\mu$, $1 \leq \mu \leq n$ and $u_\mu v_{\mu+1}$, $1 \leq \mu \leq n-1$. The slanting ladder SL_n is a graph obtained from two paths $u_1, u_2, \ldots u_n$ and $v_1, v_2, \ldots v_n$ by joining each v_μ, with $u_{\mu+1}, 1 \leq \mu \leq n-1$. The graph D_n^* having the vertices $\{a_{\mu,\delta}\colon 1 \leq \mu \leq n, \delta = 1, 2, 3, 4\}$ and its edge set is $\{a_{\mu,1}a_{\mu+1,1}, a_{\mu,3}a_{\mu+1,3}\colon 1 \leq \mu \leq n-1\} \cup \{a_{\mu,1}a_{\mu,2}, a_{\mu,2}a_{\mu,3}, a_{\mu,3}\ a_{\mu,4}, a_{\mu,4}a_{\mu,1}\colon 1 \leq \mu \leq n\}$.

2. Literature Survey

In [7], the authors talked about the F-root square mean labeling for line graph of the path, cycle, star, $P_n \circ S_1, P_n \circ S_2$, $[P_n; S_1]$, $S(P_n \circ S_1)$, ladder, slanting ladder, the crown graph $C_n \circ S_1$, and the arbitrary subdivision of S_3. The authors in [8] discussed $(1,1,0)$ F-face mean labeling some planar graphs and, in [9], face labelings of type $(1,1,1)$ for generalized prism.

Alanazi et al. explained the classical meanness of the graphs, the one-sided step graph ST_n, double-sided step graph $2ST_{2n}$, planar grid $P_m \times P_n$, ladder graph L_n, graph $L_n \circ S_m$ for $m \leq 2$, triangular ladder graph TL_n, graph $TL_n \circ S_m$ for $m \leq 2$, graph $SL_n \circ S_m$ for $m \leq 2$, slanting ladder graph SL_n, graph $SL_n \circ S_m$ for $m \leq 2$, graph D_n^*, diamond ladder graph Dl_n, and latitude ladder graph LL_n in [10–12]. Dafik slamin et al. highlighted the super (a, d)-edge-antimagic total properties of triangular book and diamond ladder graphs in [13]. Moussa and Badr discussed the odd gracefulness of few ladder graphs and proved that ladder and subdivision of ladder graphs with pendent edges are odd graceful in [14]. In [15], the authors emphasized the significance of exponential mean labeling of graphs, and they examined the exponential mean labeling of some graphs obtained from duplicating operations. Inspired by such tremendous works of researchers in the region of graph assignments in [16–25], we defined $C_{\exp}$ average assignment of graphs. A $C_{\exp}$ average of two integers is not always an integer. Consequently, $C_{\exp}$ average assignment must be an integer; we may get ceiling function by considering the integral part. In this study, our conversation and attempt is to examine the various assignment techniques on $C_{\exp}$ average assignment for few ladder graphs.

3. Methodology

A function Ψ is known as an $C_{\exp}$ average assignment of G if $\Psi\colon V(G) \longrightarrow N - \{q+2, q+3, \ldots, \infty\}$ is one to one and the instigated bijective function $\Psi^*\colon E(G) \longrightarrow N - \{1, q+2, q+3, \ldots, \infty\}$ characterized by

$$\Psi^*(uv) = \left\lceil \frac{1}{e}\left(\frac{X(v)}{X(u)}\right)^{1/Y} \right\rceil, \tag{1}$$

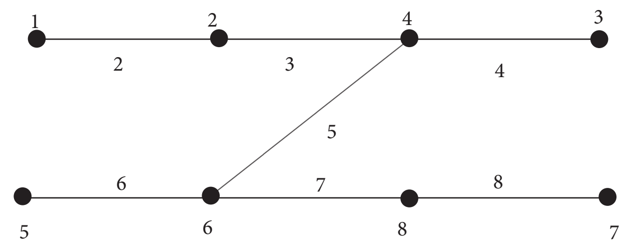

Figure 1: An $C_{\exp}$ average assignment of the graph, $SL_2 \circ S_1$.

where $X(w) = \Psi(w)^{\Psi(w)}$, $Y = \Psi(v) - \Psi(u)$, q is the number of edges, and N is the set of all natural numbers. A graph that concedes an $C_{\exp}$ average assignment is known as a $C_{\exp}$ average assignment graph.

Figure 1 shows the $C_{\exp}$ average assignment of the graph $SL_2 \circ S_1$.

4. Main Results

Theorem 1. *The one-sided step graph ST_n is an $C_{\exp}$ average assignment graph, for $n \geq 2$.*

Proof. Make the vertex assignment $\Psi\colon V(ST_n) \longrightarrow N - \{n^2+n, n^2+n+1, \ldots, \infty\}$, $\Psi(u_{1,\mu}) = n^2 - 1 + \mu$, for $2 \leq \mu \leq n$, and $\Psi(u_{\lambda,\mu}) = (1+n-\lambda)^2 + \mu - 1$, for $2 \leq \lambda \leq n$ and $1 \leq \mu \leq n+2-\lambda$.

Consequently, the instigated edge assignment Ψ^* is acquired as follows:

$$\begin{aligned}
&\Psi^*(u_{\lambda,\mu}u_{\lambda+1,\mu}) = -2n\lambda + n - \lambda + \lambda^2 + n^2 + \mu, \text{ for } n-1 \geq \lambda \geq 1 \text{ and } 1 - \lambda + n \geq \mu \geq 1,\\
&\Psi^*(u_{1,\mu}u_{1,\mu+1}) = n^2 + \mu, \text{ for } 1 \leq \mu \leq n-1, \text{ and}\\
&\Psi^*(u_{\lambda,\mu}u_{\lambda,\mu+1}) = (1+n-\lambda)^2 + \mu, \text{ for } 2 \leq \lambda \leq n \text{ and } 1 \leq \mu \leq n+1-\lambda.
\end{aligned} \tag{2}$$

As a result, for $n \geq 2$, Ψ is an $C_{\exp}$ average assignment and the one-sided step graph ST_n is an $C_{\exp}$ average assignment graph. □

Theorem 2. *The graph $P_m \times P_n$ is an $C_{\exp}$ average assignment graph, for $m \leq 4$ and $n \geq 2$.*

Proof

Case (i): $m = 2$.

Make the vertex assignment, $\Psi\colon V(P_2 \times P_n) \longrightarrow N - \{3n, 3n+1, \ldots, \infty\}$.

$\Psi(v_{\lambda\mu}) = \lambda - 3 + 3\mu$, for $1 \leq \lambda \leq 2$ and $1 \leq \mu \leq n$.

Consequently, the instigated edge assignment Ψ^* is acquired as follows.

$\Psi^*(v_{\lambda\mu} \quad v_{\lambda(\mu+1)}) = \lambda - 1 + 3\mu$, for $1 \leq \lambda \leq 2$ and $1 \leq \mu \leq n-1$.

$\Psi^*(v_{1\mu}v_{2\mu}) = -13\mu$, for $1 \leq \mu \leq n$.

Case (ii): $m = 3$.

Make the vertex assignment, $\Psi\colon V(P_3 \times P_n) \longrightarrow N - \{5n-1, 5n+1, \ldots, \infty\}$.

$\Psi(v_{\lambda\mu}) = \lambda - 5 + 5\mu$, for $1 \leq \lambda \leq 3$ and $2 \leq \mu \leq n$.

$$\Psi(v_{\lambda 1}) = \begin{cases} \lambda, & 1 \leq \lambda \leq 2,\\ 4, & \lambda = 3. \end{cases}$$

Consequently, the instigated edge assignment Ψ^* is acquired as follows:

$\Psi^*(v_{\lambda\mu}v_{\lambda(\mu+1)}) = \lambda - 2 + 5\mu$, for $1 \leq \lambda \leq 3$ and $2 \leq \mu \leq n-1$

$\Psi^*(v_{\lambda\mu}v_{(\lambda+1)\mu}) = \lambda - 4 + 5\mu$, for $1 \leq \lambda \leq 2$ and $2 \leq \mu \leq n$

$\Psi^*(v_{\lambda 1}v_{\lambda 2}) = \lambda + 3$, for $1 \leq \lambda \leq 3$,

$\Psi^*(v_{\lambda 1}v_{(\lambda+1)1}) = 1 + \lambda$, for $1 \leq \lambda \leq 2$,

Case (iii): $m = 4$ and $n \geq 3$.

Make the vertex assignment:

$\Psi\colon V(P_4 \times P_n) \longrightarrow N - \{7n-2, 7n-1, \ldots, \infty\}$

$\Psi(v_{\lambda\mu}) = \lambda - 7 + 7\mu$, for $1 \le \lambda \le 4$ and $3 \le \mu \le n$

$\Psi(v_{\lambda 2}) = \lambda + 7$, for $1 \le \lambda \le 4$

$$\Psi(v_{\lambda 1}) = \begin{cases} \lambda, & 1 \le \lambda \le 2 \\ \lambda + 1, & 3 \le \lambda \le 4 \end{cases}$$

Consequently, the instigated edge assignment Ψ^* is acquired as follows:

$$\begin{aligned}
&\Psi^*\left(v_{\lambda\mu} v_{(\lambda+1)\mu}\right) = \lambda - 6 + 7\mu, \text{ for } 1 \le \lambda \le 3 \text{ and } 3 \le \mu \le n, \\
&\Psi^*\left(v_{\lambda 2} v_{(\lambda+1)2}\right) = 8 + \lambda, \text{ for } 1 \le \lambda \le 3, \\
&\Psi^*\left(v_{\lambda 1} v_{(\lambda+1)1}\right) = \begin{cases} \lambda + 1, & 1 \le \lambda \le 2, \\ 5, & \lambda = 3, \end{cases} \\
&\Psi^*\left(v_{\lambda\mu} v_{\lambda(\mu+1)}\right) = \lambda - 3 + 7\mu \text{ for } 2 \le \lambda \le 4 \text{ and } 1 \le \mu \le n-1, \text{ and} \\
&\Psi^*\left(v_{1\mu} v_{1(\mu+1)}\right) = \begin{cases} 8\mu - 4, & 1 \le \mu \le 2, \\ 7\mu - 2, & 3 \le \mu \le n-1. \end{cases}
\end{aligned} \tag{3}$$

As a result, Ψ is an $C_{\exp}$ average assignment and the graph $P_m \times P_n$ is an $C_{\exp}$ average assignment graph, for $m \le 4$. □

Corollary 1. *Every Ladder graph $L_n = P_2 \times P_n$ is an $C_{\exp}$ average assignment graph.*

Theorem 3. *The graph $L_n \circ S_m$ is an $C_{\exp}$ average assignment graph, for $n \ge 2$ and $m \le 2$.*

Proof

Case (i): $m = 1$.

Make the vertex assignment: $\Psi\colon V(L_n \circ S_1) \longrightarrow N - \{5n, 5n+1, \ldots, \infty\}$,

$$\begin{aligned}
\Psi\left(x_1^{(\lambda)}\right) &= \begin{cases} 2, & \lambda = 1, \\ -1 + 5\lambda, & 2 \le \lambda \le n, \end{cases} \\
\Psi\left(u_1^{(\lambda)}\right) &= -4 + 5\lambda, \text{ for } 1 \le \lambda \le n, \\
\Psi(v_\lambda) &= \begin{cases} 4, & \lambda = 1, \\ -2 + 5\lambda, & 2 \le \lambda \le n \text{ and,} \end{cases} \\
\Psi(u_\lambda) &= \begin{cases} 3, & \lambda = 1, \\ -3 + 5\lambda, & 2 \le \lambda \le n. \end{cases}
\end{aligned} \tag{4}$$

Consequently, the instigated edge assignment Ψ^* is acquired as follows:

$$\begin{aligned}
\Psi^*\left(v_\lambda x_1^{(\lambda)}\right) &= \begin{cases} 3, & \lambda = 1, \\ -1 + 5\lambda, & 2 \le \lambda \le n. \end{cases} \\
\Psi^*\left(u_\lambda w_1^{(\lambda)}\right) &= 5\lambda - 3, \text{ for } 1 \le \lambda \le n, \\
\Psi^*(u_\lambda v_\lambda) &= \begin{cases} 4, & \lambda = 1, \\ -2 + 5\lambda, & 2 \le \lambda \le n, \end{cases} \\
\Psi^*(v_\lambda v_{\lambda+1}) &= 1 + 5\lambda, \text{ for } 1 \le \lambda \le n-1 \text{ and} \\
\Psi^*(u_\lambda u_{\lambda+1}) &= 5\lambda, \text{ for } 1 \le \lambda \le n-1.
\end{aligned} \tag{5}$$

Case (ii): $m = 2$.

Make the vertex assignment: $\Psi\colon V(L_n \circ S_2) \longrightarrow N - \{7n, 7n+1, \ldots, \infty\}$,

$$\begin{aligned}
\Psi\left(x_2^{(\lambda)}\right) &= \begin{cases} 8, & \lambda = 1, \\ -5 + 7\lambda, & 2 \le \lambda \le n, \lambda = 2k, k \in \mathbb{N}, \\ -2 + 7\lambda, & 2 \le \lambda \le n, \lambda = 2k+1, k \in \mathbb{N}, \end{cases} \\
\Psi\left(x_1^{(\lambda)}\right) &= \begin{cases} 2\lambda + 3, & 1 \le \lambda \le 2, \\ -6 + 7\lambda, & 3 \le \lambda \le n, \lambda = 2k+2, k \in \mathbb{N}, \\ -3 + 7\lambda, & 2 \le \lambda \le n, \lambda = 2k+1 \ k \in \mathbb{N}, \end{cases} \\
\Psi\left(w_2^{(\lambda)}\right) &= \begin{cases} 2, & \lambda = 1, \\ -1 + 7\lambda, & 2 \le \lambda \le n, \lambda = 2k, k \in \mathbb{N}, \\ -4 + 7\lambda, & 2 \le \lambda \le n, \lambda = 2k+1, k \in \mathbb{N}, \end{cases} \\
\Psi\left(w_1^{(\lambda)}\right) &= \begin{cases} 1, & \lambda = 1, \\ -3 + 7\lambda, & 2 \le \lambda \le n, \lambda = 2k, k \in \mathbb{N}, \\ -6 + 7\lambda, & 2 \le \lambda \le n, \lambda = 2k+1, k \in \mathbb{N}, \end{cases} \\
\Psi(v_\lambda) &= \begin{cases} 4, & \lambda = 1, \\ -4 + 7\lambda, & 2 \le \lambda \le n, \lambda = 2k, k \in \mathbb{N}, \\ -1 + 7\lambda, & 2 \le \lambda \le n, \lambda = 2k+1, k \in \mathbb{N}, \end{cases} \\
\Psi(u_\lambda) &= \begin{cases} 3, & \lambda = 1, \\ -2 + 7\lambda, & 2 \le \lambda \le n, \lambda = 2k, k \in \mathbb{N}, \\ -5 + 7\lambda, & 2 \le \lambda \le n, \lambda = 2k+1, k \in \mathbb{N}. \end{cases}
\end{aligned} \tag{6}$$

Consequently, the instigated edge assignment Ψ^* is acquired as follows:

$$\begin{aligned}
\Psi^*\left(v_\lambda x_2^{(\lambda)}\right) &= \begin{cases} 7\lambda - 4, & 2 \le \lambda \le n, \lambda = 2k, k \in \mathbb{N}, \\ -1 + 7\lambda, & 1 \le \lambda \le n, \lambda = 2k+1, k \in \mathbb{N}, \end{cases} \\
\Psi^*\left(v_\lambda x_1^{(\lambda)}\right) &= \begin{cases} 7\lambda - 5, & 1 \le \lambda \le n, \lambda = 2k, k \in \mathbb{N}, \\ -2 + 7\lambda, & 4 \le \lambda \le n, \lambda = 2k+1, k \in \mathbb{N}, \end{cases} \\
\Psi^*\left(u_\lambda w_2^{(\lambda)}\right) &= \begin{cases} 7\lambda - 1, & 1 \le \lambda \le n, \lambda = 2k, k \in \mathbb{N}, \\ -4 + 7\lambda, & 1 \le \lambda \le n, \lambda = 2k+1, k \in \mathbb{N}, \end{cases} \\
\Psi^*\left(u_\lambda w_1^{(\lambda)}\right) &= \begin{cases} 2, & \lambda = 1, \\ -2 + 7\lambda, & 2 \le \lambda \le n, \lambda = 2k, k \in \mathbb{N}, \\ -5 + 7\lambda, & 1 \le \lambda \le n, \lambda = 2k+1, k \in \mathbb{N}, \end{cases} \\
\Psi^*(u_\lambda v_\lambda) &= 7\lambda - 3, \text{ for } 1 \le \lambda \le n, \\
\Psi^*(v_\lambda v_{\lambda+1}) &= 7\lambda + 1, \text{ for } 1 \le \lambda \le n-1, \text{ and} \\
\Psi^*(u_\lambda u_{\lambda+1}) &= \begin{cases} 8, & \lambda = 1, \\ 7\lambda, & 2 \le \lambda \le n-1. \end{cases}
\end{aligned} \tag{7}$$

As a result, Ψ is an $C_{\exp}$ average assignment and the graph $L_n \circ S_m$ is an $C_{\exp}$ average assignment graph, for $n \ge 2$ and $m \le 2$. □

Theorem 4. *The triangular ladder graph TL_n is an $C_{\exp}$ average assignment graph, for $n \geq 2$.*

Proof. Make the vertex assignment; $\Psi: V(TL_n) \longrightarrow N - \{4n-1, 4n+1, \ldots, \infty\}$,

$$\begin{aligned}
\Psi(v_\lambda) &= \begin{cases} 4\lambda - 1, & 1 \leq \lambda \leq n-1, \\ 4n-2, & \lambda = n, \text{ and,} \end{cases} \\
\Psi(u_\lambda) &= 4\lambda - 3, \text{ for } 1 \leq \lambda \leq n.
\end{aligned} \tag{8}$$

Consequently, the instigated edge assignment Ψ^* is acquired as follows:

$$\begin{aligned}
\Psi^*(v_\lambda u_{\lambda+1}) &= 4\lambda, \text{ for } 1 \leq \lambda \leq n-1, \\
\Psi^*(u_\lambda v_{\lambda+1}) &= 1 + 4\lambda, \text{ for } 1 \leq \lambda \leq n-1, \\
\Psi^*(u_\lambda v_\lambda) &= -2 + 4\lambda, \text{ for } 1 \leq \lambda \leq n, \text{ and} \\
\Psi^*(u_\lambda u_{\lambda+1}) &= -1 + 4\lambda, \text{ for } 1 \leq \lambda \leq n-1.
\end{aligned} \tag{9}$$

As a result, Ψ is an $C_{\exp}$ average assignment and the triangular ladder graph TL_n is an $C_{\exp}$ average assignment graph, for $n \geq 2$. □

Theorem 5. *The graph $TL_n \circ S_m$ is an $C_{\exp}$ average assignment graph, for $n \geq 2$ and $m \leq 2$.*

Proof

Case (i): $m = 1$.

Make the vertex assignment; $\Psi: V(TL_n \circ S_1) \longrightarrow \mathrm{N} - \{6n-1, 6n, \ldots, \infty\}$,

$$\begin{aligned}
\Psi(x_1^{(\lambda)}) &= \begin{cases} 3, & \lambda = 1, \\ -3 + 6\lambda, & 2 \leq \lambda \leq n, \end{cases} \\
\Psi(u_1^{(\lambda)}) &= \begin{cases} -6 + 7\lambda, & 1 \leq \lambda \leq 2, \\ -5 + 6\lambda, & 3 \leq \lambda \leq n, \end{cases} \\
\Psi(v_\lambda) &= 6\lambda - 2, \text{ for } 1 \leq \lambda \leq n, \text{ and} \\
\Psi(u_\lambda) &= \begin{cases} -3 + 5\lambda, & 1 \leq \lambda \leq 2, \\ -4 + 6\lambda, & 3 \leq \lambda \leq n. \end{cases}
\end{aligned} \tag{10}$$

Consequently, the instigated edge assignment Ψ^* is acquired as follows:

$$\begin{aligned}
\Psi^*(v_\lambda x_1^{(\lambda)}) &= \begin{cases} 3, & \lambda = 1, \\ -2 + 6\lambda, & 2 \leq \lambda \leq n. \end{cases} \\
\Psi^*(u_\lambda w_1^{(\lambda)}) &= -4 + 6i, \text{ for } 1 \leq \lambda \leq n \text{ and} \\
\Psi^*(u_\lambda v_\lambda) &= \begin{cases} 4, & \lambda = 1, \\ -3 + 6\lambda, & 2 \leq \lambda \leq n, \end{cases} \\
\Psi^*(v_\lambda u_{\lambda+1}) &= 6\lambda, \text{ for } 1 \leq \lambda \leq n-1, \\
\Psi^*(v_\lambda v_{\lambda+1}) &= 1 + 6\lambda, \text{ for } 1 \leq \lambda \leq n-1, \text{ and} \\
\Psi^*(u_\lambda u_{\lambda+1}) &= -1 + 6\lambda, \text{ for } 1 \leq \lambda \leq n-1.
\end{aligned} \tag{11}$$

Case (ii): $m = 2$.

Make the vertex assignment; $\Psi: V(TL_n \circ S_2) \longrightarrow \mathrm{N} - \{8n-1, 8n, \ldots, \infty\}$,

$$\begin{aligned}
\Psi(x_2^{(\lambda)}) &= \begin{cases} 9, & \lambda = 1, \\ -6 + 8\lambda, & 2 \leq \lambda \leq n, \end{cases} \\
\Psi(x_1^{(\lambda)}) &= \begin{cases} 4, & \lambda = 1, \\ -7 + 8\lambda, & 2 \leq \lambda \leq n, \end{cases} \\
\Psi(w_2^{(\lambda)}) &= \begin{cases} 3, & \lambda = 1, \\ -2 + 8\lambda, & 2 \leq \lambda \leq n, \end{cases} \\
\Psi(w_1^{(\lambda)}) &= \begin{cases} 1, & \lambda = 1, \\ -4 + 8\lambda, & 2 \leq \lambda \leq n, \end{cases} \\
\Psi(v_\lambda) &= \begin{cases} 6, & \lambda = 1, \\ -5 + 8\lambda, & 2 \leq \lambda \leq n, \text{ and} \end{cases} \\
\Psi(u_\lambda) &= \begin{cases} 2, & \lambda = 1, \\ -3 + 8\lambda, & 2 \leq \lambda \leq n. \end{cases}
\end{aligned} \tag{12}$$

Consequently, the instigated edge assignment Ψ^* is acquired as follows:

$$\begin{aligned}
\Psi^*(v_\lambda x_2^{(\lambda)}) &= \begin{cases} 8, & \lambda = 1, \\ -5 + 8\lambda, & 2 \leq \lambda \leq n, \end{cases} \\
\Psi^*(v_\lambda x_1^{(\lambda)}) &= \begin{cases} 5, & \lambda = 1, \\ -6 + 8\lambda, & 2 \leq \lambda \leq n \end{cases} \\
\Psi^*(u_\lambda w_2^{(\lambda)}) &= \begin{cases} 3, & \lambda = 1, \\ -2 + 8\lambda, & 2 \leq \lambda \leq n, \end{cases} \\
\Psi^*(u_\lambda w_1^{(\lambda)}) &= \begin{cases} 2, & \lambda = 1, \\ -3 + 8\lambda, & 2 \leq \lambda \leq n, \end{cases} \\
\Psi^*(v_\lambda u_{\lambda+1}) &= \begin{cases} 6, & \lambda = 1, \\ 8\lambda, & 2 \leq \lambda \leq n-1, \end{cases} \\
\Psi^*(u_\lambda v_\lambda) &= 8\lambda - 4, \text{ for } 1 \leq \lambda \leq n, \\
\Psi^*(v_\lambda v_{\lambda+1}) &= \begin{cases} 9, & \lambda = 1, \\ -1 + 8\lambda, & 2 \leq \lambda \leq n-1, \text{ and} \end{cases} \\
\Psi^*(u_\lambda u_{\lambda+1}) &= \begin{cases} 7, & \lambda = 1, \\ 1 + 8\lambda, & 2 \leq \lambda \leq n-1. \end{cases}
\end{aligned} \tag{13}$$

As a result, Ψ is an $C_{\exp}$ average assignment and the graph $TL_n \circ S_m$ is an $C_{\exp}$ average assignment graph, for $n \geq 2$ and $m \leq 2$. □

Theorem 6. *The slanting ladder graph SL_n is an $C_{\exp}$ average assignment graph, for $n \geq 2$.*

Proof. Make the vertex assignment; $\Psi: V(SL_n) \longrightarrow N - \{3n-1, 3n, \ldots, \infty\}$,

$$\begin{aligned}
\Psi(v_n) &= 3n - 2, \\
\Psi(v_\lambda) &= 3\lambda, \text{ for } 1 \leq \lambda \leq n-1, \\
\Psi(u_\lambda) &= 3\lambda - 4, \text{ for } 2 \leq \lambda \leq n, \quad \text{and} \\
\Psi(u_1) &= 1.
\end{aligned} \tag{14}$$

Consequently, the instigated edge assignment Ψ^* is acquired as follows:

$$\begin{aligned}
&\Psi^*(v_\lambda u_{\lambda+1}) = 3\lambda, \text{ for } 1 \le \lambda \le n-1,\\
&\Psi^*(v_{n-1}v_n) = -2+3n,\\
&\Psi^*(v_\lambda v_{\lambda+1}) = 3\lambda+2, \text{ for } 1 \le \lambda \le n-2, \text{ and}\\
&\Psi^*(u_\lambda u_{\lambda+1}) = \begin{cases} 2, & \lambda = 1,\\ 3\lambda-2, & 2 \le \lambda \le n-1. \end{cases}
\end{aligned} \tag{15}$$

As a result, Ψ is an $C_{\exp}$ average assignment and the graph SL_n is an $C_{\exp}$ average assignment graph. □

Theorem 7. *The graph $SL_n \circ S_m$ is an $C_{\exp}$ average assignment graph, for $n \ge 2$ and $m \le 2$.*

Proof

Case *i*: $m = 1$ and $n \ge 3$.

Make the vertex assignment, $\Psi: V(SL_n \circ S_1) \longrightarrow N - \{5n-1, 5n, \ldots, \infty\}$.

$$\begin{aligned}
&\Psi\left(x_1^{(\lambda)}\right) = \begin{cases} 7, & \lambda = 1,\\ 1+5\lambda, & 2 \le \lambda \le n-1,\\ -3+5n, & \lambda = n, \end{cases}\\
&\Psi\left(w_1^{(\lambda)}\right) = \begin{cases} 3\lambda-2, & 1 \le \lambda \le 2,\\ -7+5\lambda, & 3 \le \lambda \le n, \end{cases}\\
&\Psi(v_\lambda) = \begin{cases} 6, & \lambda = 1,\\ 5\lambda, & 2 \le \lambda \le n-1,\\ 5n-2, & \lambda = n, \text{ and} \end{cases}\\
&\Psi(u_\lambda) = \begin{cases} 1+\lambda, & 1 \le \lambda \le 2,\\ -6+5\lambda, & 3 \le \lambda \le n. \end{cases}
\end{aligned} \tag{16}$$

Consequently, the instigated edge assignment Ψ^* is acquired as follows:

$$\begin{aligned}
&\Psi^*\left(v_\lambda x_1^{(\lambda)}\right) = \begin{cases} 7, & \lambda = 1,\\ 1+5\lambda, & 2 \le \lambda \le n-1,\\ -2+5n, & \lambda = n, \end{cases}\\
&\Psi^*\left(u_\lambda w_1^{(\lambda)}\right) = \begin{cases} 2, & \lambda = 1,\\ -6+5\lambda, & 2 \le \lambda \le n, \end{cases}\\
&\Psi^*(v_\lambda u_{\lambda+1}) = 5\lambda, \text{ for } 1 \le \lambda \le n-1,\\
&\Psi^*(v_\lambda v_{\lambda+1}) = \begin{cases} 5\lambda+3, & 1 \le \lambda \le n-2,\\ -3+5n, & \lambda = n-1, \end{cases}\\
&\Psi^*(u_\lambda u_{\lambda+1}) = \begin{cases} 3\lambda, & 1 \le \lambda \le 2,\\ 5\lambda-3, & 3 \le \lambda \le n-1. \end{cases}
\end{aligned} \tag{17}$$

Case (ii): $m = 2$ and $n \ge 3$.

Make the vertex assignment; $\Psi: V(SL_n \circ S_2) \longrightarrow N - \{7n-1, 7n, \ldots, \infty\}$,

$$\begin{aligned}
&\Psi\left(x_2^{(\lambda)}\right) = \begin{cases} 11, & \lambda = 1,\\ 1+7\lambda, & 2 \le \lambda \le n-3, \lambda = 2k, k \in \mathbb{N},\\ -2+7\lambda, & 2 \le \lambda \le n-3, \lambda = 2k+1, k \in \mathbb{N},\\ -9+7n, & \lambda = n-2, n = 2k, k \in \mathbb{N},\\ -16+7n, & \lambda = n-2, n = 2k+1, k \in \mathbb{N},\\ -6+7n, & \lambda = n-1, \text{ and}\\ -2+7n, & \lambda = n, \end{cases}\\
&\Psi\left(x_1^{(\lambda)}\right) = \begin{cases} 9, & \lambda = 1,\\ 7\lambda, & 2 \le \lambda \le n-3, \lambda = 2k, k \in \mathbb{N},\\ -3+7\lambda, & 2 \le \lambda \le n-3, \lambda = 2k+1, k \in \mathbb{N},\\ -12+7n, & \lambda = n-2, n = 2k, k \in \mathbb{N},\\ -17+7n, & \lambda = n-2, n = 2k+1, k \in \mathbb{N},\\ -8+7n, & \lambda = n-1, n = 2k, k \in \mathbb{N},\\ -7+7n, & \lambda = n-1, n = 2k+1, k \in \mathbb{N},\\ -4+7n, & \lambda = n, \end{cases}\\
&\Psi\left(w_{(2)}^{(\lambda)}\right) = \begin{cases} 7\lambda-5, & 1 \le \lambda \le 2,\\ -5+7\lambda, & 3 \le \lambda \le n-1, \lambda = 2k+2, k \in \mathbb{N},\\ -8+7\lambda, & 3 \le \lambda \le n-1, \lambda = 2k+1, k \in \mathbb{N},\\ -7+7n, & \lambda = n, n = 2k, k \in \mathbb{N},\\ -8+7n, & \lambda = n, n = 2k+1, k \in \mathbb{N}, \end{cases}\\
&\Psi\left(w_1^{(\lambda)}\right) = \begin{cases} 1, & \lambda = 1,\\ -5+5\lambda, & 2 \le \lambda \le 3,\\ -7+7\lambda, & 4 \le \lambda \le n-1, \lambda = 2k+2, k \in \mathbb{N},\\ -10+7\lambda, & 4 \le \lambda \le n-1, \lambda = 2k+3, k \in \mathbb{N},\\ -11+7n, & \lambda = n \text{ and } \lambda = n-1,\\ -10+7n, & \lambda = n \text{ and } \lambda = n, \end{cases}\\
&\Psi(v_\lambda) = \begin{cases} 8, & \lambda = 1,\\ 2+7\lambda, & 2 \le \lambda \le n-3, \lambda = 2k, \quad k \in \mathbb{N},\\ -1+7\lambda, & 2 \le \lambda \le n-3, \lambda = 2k+1, \quad k \in \mathbb{N},\\ -13+7n, & \lambda = n-2, n = 2k, \quad k \in \mathbb{N},\\ -15+7n, & \lambda = n-2, n = 2k+1, \quad k \in \mathbb{N},\\ -5+7n, & \lambda = n-1,\\ -3+7n, & \lambda = n, \end{cases}\\
&\Psi(u_\lambda) = \begin{cases} \lambda+2, & 1 \le \lambda \le 2,\\ -6+7\lambda, & 3 \le \lambda \le n-1, n = 2k+2, \quad k \in \mathbb{N},\\ -9+7\lambda, & 3 \le \lambda \le n-1, n = 2k+1, \quad k \in \mathbb{N},\\ -10+7n, & \lambda = n, \quad k \in \mathbb{N},\\ -9+7n, & \lambda = n, n = 2k+1, \quad k \in \mathbb{N}. \end{cases}
\end{aligned} \tag{18}$$

Consequently, the instigated edge assignment Ψ^* is acquired as follows:

$$\Psi^*\left(v_\lambda x_2^{(\lambda)}\right) = \begin{cases} 10, & \lambda = 1, \\ 2 + 7\lambda, & 2 \leq \lambda \leq n-3, \lambda = 2k, \quad k \in \mathbb{N}, \\ -1 + 7\lambda, & 2 \leq \lambda \leq n-3, \lambda = 2k+1, \quad k \in \mathbb{N}, \\ -11 + 7n, & \lambda = n-2, n = 2k, \quad k \in \mathbb{N}, \\ -15 + 7n, & \lambda = n-2, n = 2k+1, \quad k \in \mathbb{N}, \\ -5 + 7\lambda, & \lambda = n-1, \\ -2 + 7n, & \lambda = n, \end{cases}$$
$$\Psi^*\left(v_\lambda x_2^{(\lambda)}\right) = \begin{cases} 10, & \lambda = 1, \\ 2 + 7\lambda, & 2 \leq \lambda \leq n-3, \lambda = 2k, \quad k \in \mathbb{N}, \\ -1 + 7\lambda, & 2 \leq \lambda \leq n-3, \lambda = 2k+1, \quad k \in \mathbb{N}, \\ -11 + 7n, & \lambda = n-2, n = 2k, \quad k \in \mathbb{N}, \\ -15 + 7n, & \lambda = n-2, n = 2k+1, \quad k \in \mathbb{N}, \\ -5 + 7\lambda, & \lambda = n-1, \\ -2 + 7n, & \lambda = n, \end{cases}$$
$$\Psi^*\left(v_\lambda x_1^{(\lambda)}\right) = \begin{cases} 9, & \lambda = 1, \\ 1 + 7\lambda, & 2 \leq \lambda \leq n-3, \lambda = 2k, \quad k \in \mathbb{N}, \\ -2 + 7\lambda, & 2 \leq \lambda \leq n-3, \lambda = 2k+1, \quad k \in \mathbb{N}, \\ -12 + 7n, & \lambda = n-2, n = 2k, \quad k \in \mathbb{N}, \\ -16 + 7n, & \lambda = n-2, n = 2k+1, \quad k \in \mathbb{N}, \\ -6 + 7n, & \lambda = n-1, \\ -6 + 7n, & \lambda = n, \end{cases}$$
$$\Psi^*\left(u_\lambda w_2^{(\lambda)}\right) = \begin{cases} 4\lambda - 1, & 1 \leq \lambda \leq 2, \\ -5 + 7\lambda, & 3 \leq \lambda \leq n-1, \lambda = 2k+2, \quad k \in \mathbb{N}, \\ -8 + 7\lambda, & 3 \leq \lambda \leq n-1, \lambda = 2k+1, \quad k \in \mathbb{N}, \\ -8 + 7n, & \lambda = n, \end{cases} \tag{19}$$
$$\Psi^*\left(u_\lambda w_1^{(\lambda)}\right) = \begin{cases} 2, & \lambda = 1, \\ -7 + 6\lambda, & 2 \leq \lambda \leq 3, \\ -6 + 7\lambda, & 4 \leq \lambda \leq n-1, \lambda = 2k+2, \quad k \in \mathbb{N}, \\ -9 + 7\lambda, & 4 \leq \lambda \leq n-1, \lambda = 2k+3, \quad k \in \mathbb{N}, \\ -10 + 7n, & \lambda = n, n = 2k, \quad k \in \mathbb{N}, \\ -9 + 7n, & \lambda = n, n = 2k, \quad k \in \mathbb{N}, \end{cases}$$
$$\Psi^*\left(v_\lambda v_{\lambda+1}\right) = \begin{cases} 12, & \lambda = 1, \\ 7\lambda + 4, & 2 \leq \lambda \leq n-3, \\ 7n - 9, & \lambda = n-2, n = 2k, \quad k \in \mathbb{N}, \\ 7n - 10, & \lambda = n-2, n = 2k+1, \quad k \in \mathbb{N}, \\ 7n - 4, & \lambda = n-1, \end{cases}$$
$$\Psi^*\left(v_\lambda u_{\lambda+1}\right) = \begin{cases} 6, & \lambda = 1, \\ 7\lambda, & 2 \leq \lambda \leq n-1, \end{cases}$$
$$\Psi^*\left(u_\lambda u_{\lambda+1}\right) = \begin{cases} 4\lambda, & 1 \leq \lambda \leq 2, \\ 7\lambda - 4, & 3 \leq \lambda \leq n-2, \\ 7n - 13, & \lambda = n-1, n = 2k, \quad k \in \mathbb{N}, \\ 7n - 11, & \lambda = n-1, n = 2k, \quad k \in \mathbb{N}. \end{cases}$$

Case (iii): $m = 1, 2$ and $n = 2$. An $C_{\exp}$ average assignment of the graphs $SL_2 \circ S_1$ and $SL_2 \circ S_2$ are shown in Figures 1 and 2.

As a result, Ψ is an $C_{\exp}$ average assignment and the graph $SL_n \circ S_m$ is an $C_{\exp}$ average assignment graph, for $n \geq 2$ and $m \leq 2$. □

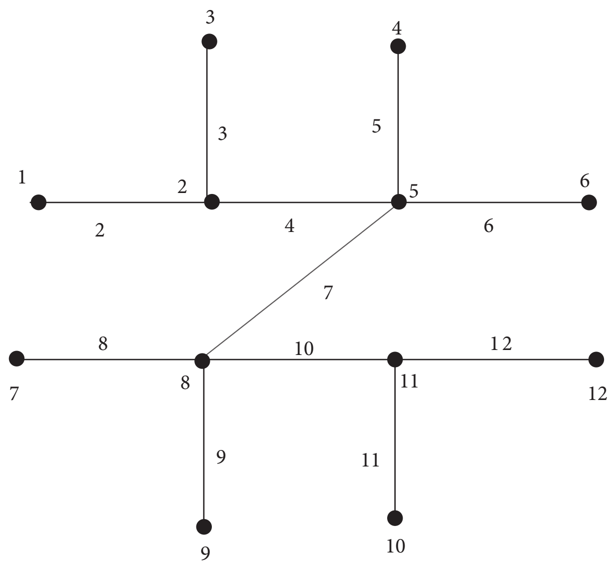

FIGURE 2: An $C_{\exp}$ average assignment of the graph $SL_2 \circ S_2$.

Theorem 8. *The graph D_n^* is an $C_{\exp}$ average assignment graph, for $n \geq 2$.*

Proof. Make the vertex assignment; $\Psi: V(D_n^*) \longrightarrow N - \{6n, 6n+1, \ldots, \infty\}$,

$$\begin{aligned}\Psi(a_{\lambda,4}) &= -1 + 6\lambda, \text{ for } 1 \leq \lambda \leq n,\\ \Psi(a_{\lambda,3}) &= -3 + 6\lambda, \text{ for } 1 \leq \lambda \leq n,\\ \Psi(a_{\lambda,2}) &= -5 + 6\lambda, \text{ for } 1 \leq \lambda \leq n, \text{ and}\\ \Psi(a_{\lambda,1}) &= -2 + 6\lambda, \text{ for } 1 \leq \lambda \leq n.\end{aligned} \tag{20}$$

Consequently, the instigated edge assignment Ψ^* is acquired as follows:

$$\begin{aligned}\Psi^*(a_{\lambda,4}a_{\lambda,1}) &= -1 + 6\lambda, \text{ for } 1 \leq \lambda \leq n,\\ \Psi^*(a_{\lambda,3}a_{\lambda,4}) &= -2 + 6\lambda, \text{ for } 1 \leq \lambda \leq n,\\ \Psi^*(a_{\lambda,2}a_{\lambda,3}) &= -4 + 6\lambda, \text{ for } 1 \leq \lambda \leq n,\\ \Psi^*(a_{\lambda,1}a_{\lambda,2}) &= -3 + 6\lambda, \text{ for } 1 \leq \lambda \leq n,\\ \Psi^*(a_{\lambda,3}a_{\lambda+1,3}) &= 6\lambda, \text{ for } 1 \leq \lambda \leq n-1, \quad \text{and}\\ \Psi^*(a_{\lambda,1}a_{\lambda+1,1}) &= 1 + 6\lambda, \text{ for } 1 \leq \lambda \leq n-1.\end{aligned} \tag{21}$$

As a result, Ψ is an $C_{\exp}$ average assignment and the graph D_n^* is an $C_{\exp}$ average assignment graph, for $n \geq 2$. □

Theorem 9. *The diamond ladder graph Dl_n is an $C_{\exp}$ average assignment graph, for $n \geq 1$.*

Proof. Make the vertex assignment; $\Psi: V(Dl_n) \longrightarrow N - \{8n-1, 8n, \ldots, \infty\}$,

$$\Psi(z_\lambda) = \begin{cases} 1, & \lambda = 1,\\ -2 + 4\lambda - \left(\dfrac{(-1)^{\lambda+1} + 1}{2}\right), & 2 \leq \lambda \leq 2n \text{ and } \lambda \textit{ is } \text{even},\\ -2 + 4\lambda - \left(\dfrac{(-1)^{\lambda+1} + 1}{2}\right), & 3 \leq \lambda \leq 2n \text{ and } \lambda \textit{ is } \text{odd},\end{cases}$$

$$\begin{aligned}\Psi(y_\lambda) &= -3 + 8\lambda, \text{ for } 1 \leq \lambda \leq n, \quad \text{and}\\ \Psi(x_\lambda) &= -5 + 8\lambda, \text{ for } 1 \leq \lambda \leq n.\end{aligned} \tag{22}$$

Consequently, the instigated edge assignment Ψ^* is acquired as follows:

$$\begin{aligned}\Psi^*(y_\lambda z_{2\lambda}) &= -2 + 8\lambda, \text{ for } 1 \leq \lambda \leq n,\\ \Psi^*(y_\lambda z_{2\lambda-1}) &= -5 + 8\lambda, \text{ for } 1 \leq \lambda \leq n, \text{ and}\\ \Psi^*(x_\lambda z_{2\lambda}) &= -3 + 8\lambda, \text{ for } 1 \leq \lambda \leq n,\\ \Psi^*(x_\lambda z_{2\lambda-1}) &= -6 + 8\lambda, \text{ for } 1 \leq \lambda \leq n,\\ \Psi^*(z_{2\lambda} z_{2\lambda+1}) &= 8\lambda, \text{ for } 1 \leq \lambda \leq n-1,\\ \Psi^*(x_\lambda y_\lambda) &= -4 + 8\lambda, \text{ for } 1 \leq \lambda \leq n,\\ \Psi^*(y_\lambda y_{\lambda+1}) &= 1 + 8\lambda, \text{ for } 1 \leq \lambda \leq n-1, \text{ and}\\ \Psi^*(x_\lambda x_{\lambda+1}) &= -1 + 8\lambda, \text{ for } 1 \leq \lambda \leq n-1.\end{aligned} \tag{23}$$

As a result, Ψ is an $C_{\exp}$ average assignment and the diamond ladder graph Dl_n is an $C_{\exp}$ average assignment graph, for $n \geq 1$. □

Theorem 10. *The latitude graph is an $C_{\exp}$ average assignment graph.*

Proof. Make the vertex assignment; $\Psi: V(G) \longrightarrow N - \{3n/2 + 1, 3n/2 + 2, \ldots, \infty\}$,

$$\Psi(u_\lambda) = \begin{cases} -2 + 3\lambda, & 1 \leq \lambda \leq \dfrac{n}{2},\\ -1 + 3\lambda 1, & \lambda = \dfrac{n}{2},\\ \dfrac{3n}{2}, & \lambda = \dfrac{n}{2} + 1,\\ 3 + 3n - 3\lambda, & \dfrac{n}{2} + 2 \leq \lambda \leq n-1,\\ 3, & \lambda = n.\end{cases} \tag{24}$$

Consequently, the instigated edge assignment Ψ^* is acquired as follows:

$$\Psi^*\left(u_\lambda u_{n+2-\lambda}\right) = -2 + 3\lambda, \text{ for } 2 \le \lambda \le \frac{n}{2},$$

$$\Psi^*\left(u_n u_1\right) = 2, \text{ and}$$

$$\Psi^*\left(u_\lambda u_{\lambda+1}\right) = \begin{cases} 3\lambda, & 1 \le \lambda \le \frac{n}{2}, \\ -1 + \frac{3n}{2}, & \lambda = \frac{n}{2} + 1, \\ 2 + 3n - 3\lambda, & \frac{n}{2} + 2 \le \lambda \le n - 1. \end{cases} \quad (25)$$

As a result, Ψ is an $C_{\exp}$ average assignment and the latitude graph is an $C_{\exp}$ average assignment graph. □

5. Conclusion

The significant properties on $C_{\exp}$ average assignment of several ladder networks are discovered in this work. Analysis of the $C_{\exp}$ average assignment of other networks can be discussed further.

Data Availability

No data were used in this study.

Conflicts of Interest

The authors declare that they have no conflicts of interest.

References

[1] J. Gross and J. Yellen, *Graph Theory and its Applications*, CRC Press, London, UK, 1999.
[2] F. Harary, *Graph Theory*, Narosa Publishing House Reading, New Delhi, India, 1988.
[3] G. Chartrand, L. Lesniak, and P. Zhang, *Graphs and Digraphs*, Taylor & Francis Group, Boca Raton, New York, USA, 6th edition, 2016.
[4] F. Buckley and F. Harary, *Distance in Graphs*, Addison-Wesley Reading, 1990.
[5] G. S. Bloom and S. W. Golomb, "Numbered complete graphs, unusual rulers, and assorted applications," *Lecture Notes in Mathematics*, vol. 642, pp. 53–65, 1978.
[6] J. A. Gallian, "A dynamic survey of graph labeling," *Electronic Journal of Combinatorics*, vol. 24, p. #DS6, 2021.
[7] S. Arockiaraj, A. Durai Baskar, and A. Rajesh, "Kannan, F-root square mean labeling of line graph of some graphs," *Utilitas Mathematica*, vol. 112, pp. 11–32, 2019.
[8] A. Meena Kumari and S. Arockiaraj, "On (1,1,0)- F-Face magic mean labeling of some graphs," *Utilitas Mathematica*, vol. 103, pp. 139–159, 2017.
[9] S. I. Butt, M. Numan, I. A. Shah, and S. Ali, "Face labelings of type (1,1,1) for generalized prism," *Ars Combinatoria*, vol. 137, pp. 41–52, 2018.
[10] A. M. Alanazi, G. Muhiuddin, A. R. Kannan, and V. Govindan, "New perspectives on classical meanness of some ladder graphs," *Journal of Mathematics*, vol. 2021, pp. 1–14, 2021.
[11] G. Muhiuddin, A. M. Alanazi, A. R. Kannan, and V. Govindan, "Preservation of the classical meanness property of some graphs based on line graph operation," *Journal of Mathematics*, vol. 2021, pp. 1–10, 2021.
[12] H. U. Afzal, M. Javaid, A. M. Alanazi, and M. G. Alshehri, "Computing edge weights of symmetric classes of networks," *Mathematical Problems in Engineering*, vol. 2021, Article ID 5562544, 22 pages, 2021.
[13] S. Dafik, R. Fitriana Eka, and L. Sya' Diyah, *Super Antimagicness of Triangular Book and Diamond Ladder Graphs*, Indoms-UGM Yogyakarta, Indonesia, 2013.
[14] M. I. Moussa and E. M. Badr, "Ladder and subdivision of ladder graphs with pendent edges are odd graceful," *International Journal on Applications of Graph Theory in Wireless Ad hoc Networks and Sensor Networks*, vol. 8, no. 1, pp. 1–8, 2016.
[15] A. Rajesh Kannan, P. Manivannan, and A. Durai Baskar, "Exponential mean labeling of some graphs obtained from duplicating operations," *Journal of Physics: Conference Series*, vol. 1597, no. 1, Article ID 012028, 2020.
[16] G. V. Ghodasara and I. I. Jadav, "New grid related cordial graphs," *International Journal Applied Mathematics*.vol. 28, no. 2, pp. 1244–1248, 2013.
[17] Y. Kurniawati and I. H. Agustin, "On the super edge local antimagic total labeling of related ladder graph," *Journal de Physique: Conf. Ser.*vol. 1465, no. 1, Article ID 012027, 2020.
[18] L. Ratnasari and Y. Susanti, "Total edge irregularity strength of ladder-related graphs," *Asian-European Journal of Mathematics*, vol. 13, no. 4, Article ID 2050072, 2020.
[19] A. Ahmed and M. G. Ruxandra, "Radio labeling of some ladder related graphs," *Mathematical Reports*, vol. 19, no. 69, pp. 107–119, 2017.
[20] R. Mohamed, "Zeen El Deen, Edge graceful labeling for some cyclic related graphs," *Advances in Mathematical Physics*, vol. 2020, pp. 1–8, 2020.
[21] L. Ratnasari and Y. Susanti, "Total edge irregularity strength of ladder-related graphs," *Asian-European Journal of Mathematics*, vol. 13, no. 4, Article ID 2050072, 2020.
[22] A. A. Elsonbaty and S. N. Daoud, "Edge even graceful labeling of cylinder grid graph," *Symmetry*, vol. 11, no. 4, pp. 584–630, 2019.
[23] P. Deb and N. B. Limaye, "On elegant labelings of triangular snakes," *Journal of Combinatorics, Information and System Sciences*, vol. 25, pp. 163–172, 2000.
[24] N. Diefenderfer, D. C. Ernst, M. G. Hastings et al., "Prime vertex labelings of several families of graphs," *Involve, a Journal of Mathematics*, vol. 9, no. 4, pp. 667–688, 2016.
[25] A. Elsonbaty and S. N. Daoud, "Edge even graceful labeling of some path and cycle related graphs," *Ars Combinatoria*, vol. 30, pp. 79–96, 2017.

Hindawi
Journal of Mathematics
Volume 2022, Article ID 9129386, 9 pages
https://doi.org/10.1155/2022/9129386

Research Article

Novel Concepts in Vague Graphs with Application in Hospital's Management System

Xiaolong Shi,[1] Saeed Kosari ,[1] N. Mehdipoor,[2] A.A. Talebi,[2] and G. Muhiuddin [3]

[1] *Institute of Computing Science and Technology, Guangzhou University, Guangzhou 510006, China*
[2] *Department of Mathematics University of Mazandaran, Babolsar, Iran*
[3] *Department of Mathematics, University of Tabuk, Tabuk 71491, Saudi Arabia*

Correspondence should be addressed to Saeed Kosari; saeedkosari38@gzhu.edu.cn

Received 24 February 2022; Revised 18 March 2022; Accepted 29 March 2022; Published 9 May 2022

Academic Editor: M. T. Rahim

Copyright © 2022 Xiaolong Shi et al. This is an open access article distributed under the Creative Commons Attribution License, which permits unrestricted use, distribution, and reproduction in any medium, provided the original work is properly cited.

Many problems of practical interest can be modeled and solved by using vague graph (VG) algorithms. Vague graphs, belonging to the fuzzy graphs (FGs) family, have good capabilities when faced with problems that cannot be expressed by FGs. Hence, in this paper, we introduce the notion of (η, γ)- HMs of VGs and classify homomorphisms (HMs), weak isomorphisms (WIs), and coweak isomorphisms (CWIs) of VGs by (η, γ)- HMs. Hospitals are very important organizations whose existence is directly related to the general health of the community. Hence, since the management in each ward of the hospital is very important, we have tried to determine the most effective person in a hospital based on the performance of its staff.

1. Introduction

Graphs, from ancient times to the present day, have played a very important role in various fields, including computer science and social networks, so that with the help of the vertices and edges of a graph, the relationships between objects and elements in a social group can be easily introduced. But there are some phenomena in our lives that have a wide range of complexities that make it impossible for us to express certainty. These complexities and ambiguities were reduced with the introduction of FSs by Zadeh [1]. Since then, the theory of FSs has become a vigorous area of research in different disciplines including logic, topology, algebra, analysis, information theory, artificial intelligence, operations research, and neural networks and planning [2–6]. The FS focuses on the membership degree of an object in a particular set. But membership alone could not solve the complexities in different cases, so the need for a degree of membership was felt. To solve this problem, Gau and Buehrer [7] introduced false-membership degrees and defined a VS as the sum of degrees not greater than 1. The first definition of FGs was proposed by Kafmann [8] in 1993, from Zade's fuzzy relations [9, 10]. But Rosenfeld [11] introduced another elaborated definition including fuzzy vertex and fuzzy edges and several fuzzy analogs of graph theoretic concepts such as paths, cycles, and connectedness. Ramakrishna [12] introduced the concept of VGs and studied some of their properties. Akram et al. [13–16] defined the vague hypergraphs, Cayley-VGs, and regularity in vague intersection graphs and vague line graphs. Rashmanlou et al. [17] investigated categorical properties in intuitionistic fuzzy graphs. Bhattacharya [18] gave some remarks on FGs, and some operations of FGs were introduced by Mordeson and Peng [19]. The concepts of weak isomorphism, coweak isomorphism, and isomorphism between FGs were introduced by Bhutani in [2]. Khan et al. [20] studied vague relations. Talebi [21, 22] investigated Cayley-FGs and some results in bipolar fuzzy graphs. Borzooei [23] introduced domination in VGs. Ghorai and Pal studied some isomorphic properties of m-polar FGs [24]. Jiang et al. [25] defined vertex covering in cubic graphs. Krishna et al. [26] presented a new concept in cubic graphs. Rao et al. [27–29] investigated dominating set, equitable dominating set, and isolated vertex in VGs. Hoseini et al. [30] given maximal product of graphs under vague environment. Jan et al. [31] introduced some root-level modifications in interval-valued fuzzy graphs. Amanathulla et al. [32] defined new concepts of paths and interval graphs. Muhiuddin et al. [33, 34] presented the reinforcement number of a graph and new results in cubic graphs.

A VG is a generalized structure of an FG that provides more exactness, adaptability, and compatibility to a system when matched with systems run on FGs. Also, a VG is able to concentrate on determining the uncertainty coupled with the inconsistent and indeterminate information of any real-world problems, where FGs may not lead to adequate results. VGs have a wide range of applications in the field of psychological sciences as well as in the identification of individuals based on oncological behaviors. Thus, in this paper, we studied level graphs of VGs and investigated HMs, WIs, and CWIs of VGs by HMs of level graphs. Likewise, we characterized some VGs by their level graphs.

2. Preliminaries

In this section, we review some concepts of graph theory and VGs.

Definition 1. Let V be a finite nonempty set. A graph $G = (V, E)$ on V consist of a vertex set V and an edge set E, where an edge is an unordered pair of distinct nodes of G. We will use pq rather than $\{p, q\}$ to denote an edge. If pq is an edge, then we say that p and q are neighbor. A graph is called complete graph if each pair of nodes are neighbor.

Definition 2. Let $G_1 = (V_1, E_1)$ and $G_2 = (V_2, E_2)$ be graphs. A mapping $h\colon V_1 \longrightarrow V_2$ is a homomorphism from G_1 to G_2 if $h(p)$ and $h(q)$ are neighbor whenever p and q are neighbor.

Definition 3. Two graphs G_1 and G_2 are isomorphic if there is a bijective mapping $\varphi\colon V_1 \longrightarrow V_2$ so that p and q are neighbor in G_1 if and only if $\varphi(p)$ and $\varphi(q)$ are neighbor in G_2, φ is named isomorphism from G_1 to G_2. An isomorphism from a graph G to itself is named an automorphism of G. The set of all automorphisms of G forms a group, which is named the automorphism group of G and shown by $\mathrm{Aut}(G)$.

Definition 4. A VS A is a pair (t_A, f_A) on set X where t_A and f_A are taken as real valued functions which can be defined on $V \longrightarrow [0,1]$ so that $t_A(p) + f_A(p) \leq 1$, $\forall p \in X$.

Definition 5. Let $A, B \in VS(V)$. We say that A is contained in B and write $A \subseteq B$, if for any $p \in V$,

$$\begin{aligned} t_A(p) &\leq t_B(p), \\ f_A(p) &\geq f_B(p). \end{aligned} \tag{1}$$

Let $K_* = \{(\eta, \gamma) | \eta, \gamma \in [0,1], \eta + \gamma \leq 1\}$. For any $(\eta_1, \gamma_1), (\eta_2, \gamma_2) \in L_*$, the orders $\leq$ and $<$ on K_* are defined as

$$\begin{aligned} &(\eta_1, \gamma_1) \leq (\eta_2, \gamma_2) \Leftrightarrow \eta_1 \leq \eta_2, \\ &\quad \gamma_1 \geq \alpha_2, \\ &(\eta_1, \gamma_1) < (\eta_2, \gamma_2) \Leftrightarrow (\eta_1, \gamma_1) \leq (\eta_2, \gamma_2), \\ &\quad \eta_1 < \eta_2, \\ &\quad \text{or } \gamma_1 > \gamma_2. \end{aligned} \tag{2}$$

It is easy to see that, $(K_*, \leq)$ constitutes a complete lattice with maximum element $(1, 0)$ and minimum element $(0, 1)$.

Definition 6. Let $A \in VS(V)$. For each $(\eta, \gamma) \in K_*$, we define $A_{(\eta,\gamma)} = \{p \in V\colon t_A(p) \geq \eta, f_A(p) \leq \gamma\}$.

Then, $A_{(\eta,\gamma)}$ is named (η, γ)-level set of A. The set $\{p | p \in V, t_A(p) > 0 \text{ or } f_A(p) < 1\}$ is called the support A and is denoted by A^*.

Let V be a finite nonempty set. Denote by $\widetilde{V}^2$ the set of all 2-element subsets of V. A graph on V is a pair (V, E) where $E \subseteq \widetilde{V}^2$, V and E are named vertex set and edge set, respectively.

Definition 7. Let V be a finite nonempty set, $A \in VS(V)$ and $B \in VFS(\widetilde{V}^2)$. The triple $X = (V, A, B)$ is named a VG on V, if for each $(p, q) \in \widetilde{V}^2$,

$$\begin{aligned} t_B(p,q) &\leq t_A(p) \wedge t_A(q), \\ f_B(p,q) &\geq f_A(p) \vee f_A(q). \end{aligned} \tag{3}$$

If $X = (V, A, B)$ is a VG, then, it is easy to see that $X^* = (A^*, B^*)$ is a graph and it is called underlying graph of X. The set of all VG on V is denoted by $VG(V)$. For given $X = (V, A, B) \in VG(V)$, in this study suppose that $A^* = V$.

Definition 8. Let $X_1 = (V_1, A_1, B_1)$ and $X_2 = (V_2, A_2, B_2)$ be two VGs. Then,

(1) A mapping $\varphi\colon V_1 \longrightarrow V_2$ is a homomorphism from X_1 to X_2, if

(i) $t_{A_1}(p) \leq t_{A_2}(\varphi(p))$, $f_{A_1}(p) \geq f_{A_2}(\varphi(p))$, for all $p \in V_1$

(ii) $t_{B_1}(pq) \leq t_{B_2}(\varphi(p)\varphi(q))$, $f_{B_1}(pq) \geq f_{B_2}(\varphi(p)\varphi(q))$, for all $pq \in \widetilde{V}^2$

(2) A mapping $\varphi\colon V_1 \longrightarrow V_2$ is a weak isomorphism from X_1 to X_2, if φ is a BH from X_1 to X_2 and $t_{A_1}(p) = t_{A_2}(\varphi(p))$, $f_{A_1}(p) = f_{A_2}(\varphi(p))$, for all $p \in V_1$.

(3) A mapping $\varphi\colon V_1 \longrightarrow V_2$ is a coweak isomorphism from X_1 to X_2, if φ is a BH from X_1 to X_2 and $t_{B_1}(pq) = t_{B_2}(\varphi(p)\varphi(q))$, $f_{B_1}(pq) = f_{B_2}(\varphi(p)\varphi(q))$, for all $pq \in \widetilde{V}^2$.

(4) An isomorphism from X_1 to X_2 is a bijective mapping $\varphi\colon V_1 \longrightarrow V_2$ so that

(i) $t_{A_1}(p) = t_{A_2}(\varphi(p))$, $f_{A_1}(p) = f_{A_2}(\varphi(p))$, for all $p \in V_1$

(ii) $t_{B_1}(pq) = t_{B_2}(\varphi(p)\varphi(q))$, $f_{B_1}(pq) = f_{B_2}(\varphi(p)\varphi(q))$, for all $pq \in \widetilde{V}^2$

Definition 9. VG $X = (V, A, B)$ is called strong vague graph (SVG) if $t_B(pq) = t_A(p) \wedge t_A(q)$, $f_B(pq) = f_A(p) \vee f_A(q)$, for all $pq \in \widetilde{V}^2$, $(t_B(pq), f_B(pq)) \neq (0, 1)$ and is called complete vague graph (CVG), if $t_B(pq) = t_A(p) \wedge t_A(q)$, $f_B(pq) = f_A(p) \vee f_A(q)$, for all $pq \in \widetilde{V}^2$. A CVG $X = (V, A, B)$ with n nodes is denoted by $K_{n,A}$.

Definition 10. Suppose that $X = (V, A, B)$ and $Y = (V, A', B')$ be two VGs. Then, X is VSG of Y, if $A \subseteq A\prime$ and $B \subseteq B\prime$.

Definition 11. Let $X = (V, A, B)$ be VG and $W \subseteq V$. Then, the VG $Y = (W, A', B')$ so that $t_{A\prime}(p) = t_A(p)$, $f_{A\prime}(p) = f_A(p)$, for all $p \in W$, $t_{B\prime}(pq) = t_B(pq)$, $f_{B\prime}(pq) = f_B(pq)$, for all $pq \in \widetilde{W}^2$, is named the induced VSG by W and shown by $X[W]$.

Definition 12. A family $\Gamma = \{\lambda_1, \lambda_2, \ldots, \lambda_k\}$ of VSs on V is named a k-coloring of VG $X = (V, A, B)$ if

(i) $\vee \Gamma = A$.

(ii) $\lambda_i \wedge \lambda_j = 0$ for $1 \leq i, j \leq k$.

(iii) For each strong edge pq of X, $\min\{\lambda_i(p), \lambda_i(q)\} = 0$ for $1 \leq i \leq k$. We say that a graph is k-colorable if it can be colored with k colors.

All the basic notations are shown in Table 1.

Table 1: Some basic notations.

Notation	Meaning
FG	Fuzzy graph
VS	Vague set
FS	Fuzzy set
VG	Vague graph
CVG	Complete vague graph
SVG	Strong vague graph
BM	Bijective mapping
HM	Homomorphism
WI	Weak isomorphism
IH	Injective homomorphism
CWI	Coweak isomorphism
BH	Bijective homomorphism
SG	Subgraph
IV	Isolated vertex
CG	Complete graph
VSG	Vague subgraph

3. Homomorphisms and Isomorphisms of Vague Graphs

In this section, we discuss the homomorphism and isomorphism of VGs by the homomorphism of level graphs in VGs.

Theorem 1. *Let V be a finite nonempty set, $A \in VS(V)$ and $B \in VS(\widetilde{V}^2)$. Then, $X = (V, A, B) \in VFG(V)$ if and only if $X_{(\eta,\gamma)} = (A_{(\eta,\gamma)}, B_{(\eta,\gamma)})$ is a graph for all $(\eta, \gamma) \in L_*$, $A_{(\eta,\gamma)} \neq \varnothing$.*

Proof. Let $X = (V, A, B)$ be VG. For each $(\eta, \gamma) \in L_*$, $A_{(\eta,\gamma)} \neq \varnothing$, assume that $pq \in B_{(\eta,\gamma)}$. Then, $t_B(pq) \geq \eta$ and $f_B(pq) \leq \gamma$. Because X is VG,

$$\begin{aligned} \lambda &\leq t_B(pq) \leq t_A(p) \wedge t_A(q), \\ \gamma &\geq f_B(pq) \geq f_A(p) \vee f_A(q). \end{aligned} \tag{4}$$

It follows that $p, q \in A_{(\eta,\gamma)}$. Therefore, $(A_{(\eta,\gamma)}, B_{(\eta,\gamma)})$ is a graph.

Conversely, let $X_{(\eta,\gamma)} = (A_{(\eta,\gamma)}, B_{(\eta,\gamma)})$ is a graph, $\forall (\eta, \gamma) \in L_*$, $A_{(\eta,\gamma)} \neq \varnothing$. For each $pq \in \widetilde{V}^2$, let $t_B(pq) = \eta$, $f_B(pq) = \gamma$. Then, $pq \in B_{(\eta,\gamma)}$. Hence, $p, q \in A_{(\eta,\gamma)}$. Thus, $t_A(p) \geq \eta, t_A(q) \geq \eta, f_A(p) \leq \gamma$, and, $f_A(q) \leq \alpha$,. This implies that $t_A(p) \wedge t_A(q) \geq \eta = t_B(pq)$ and $f_A(p) \vee f_A(q) \leq \gamma = f_B(pq)$. Therefore, $X = (V, A, B)$ is VG. □

Definition 13. Let $X = (V, A, B)$ and $Y = (W, A\prime, B\prime)$ be two VGs, $h: V \longrightarrow W$ a mapping. For any $(\eta, \gamma) \in L_*$, $A_{(\eta,\gamma)} \neq \varnothing$, if h is a homomorphism from $X_{(\eta,\gamma)} = (A_{(\eta,\gamma)}, B_{(\eta,\gamma)})$ to $Y_{(\eta,\gamma)} = (A'_{(\eta,\gamma)}, B'_{(\eta,\gamma)})$, then, h is called (η, γ)– homomorphism mapping from X to Y.

Theorem 2. *Let $X = (V, A, B)$ and $Y = (W, A\prime, B\prime)$ be two VGs. Then, $h: X \longrightarrow Y$ is a homomorphism from X to Y if and only if h is (η, γ)- homomorphism from X to Y.*

Proof. Assume that $h: X \longrightarrow Y$ is a homomorphism from X to Y. Let, $A_{(\eta,\gamma)} \neq \varnothing$, $(\eta, \gamma) \in L_*$. If $p \in A_{(\eta,\gamma)}$, then

$$\begin{aligned} t_{A\prime}(h(p)) &\geq t_A(p) \geq \eta, \\ f_{A\prime}(h(p)) &\leq f_A(p) \leq \gamma. \end{aligned} \tag{5}$$

Hence, $h(p) \in A'_{(\eta,\gamma)}$ implying h is a mapping from $A_{(\eta,\gamma)}$ to $A'_{(\eta,\gamma)}$. For $p, q \in A_{(\eta,\gamma)}$, let $pq \in B_{(\eta,\gamma)}$. Then,

$$\begin{aligned} t_B(pq) &\geq \eta, \\ f_B(pq) &\leq \gamma. \end{aligned} \tag{6}$$

Hence,

$$\begin{aligned} t_{B\prime}(h(p)h(q)) &\geq t_B(pq) \geq \eta, \\ f_{B\prime}(h(p)h(q)) &\leq f_B(pq) \leq \gamma, \end{aligned} \tag{7}$$

which implies $h(p)h(q) \in B'_{(\eta,\gamma)}$. Therefore, h is a homomorphism from $X_{(\eta,\gamma)}$ to $Y_{(\eta,\gamma)}$.

Conversely, let $h: V \longrightarrow W$ be a (η, γ)- homomorphism from X to Y. For arbitrary element $p \in X$, let $t_A(p) = c$, $f_A(p) = d$. Then, $p \in A_{(c,d)}$, hence, $h(p) \in A'_{(c,d)}$, because h is a homomorphism from $(A_{(c,d)}, B_{(c,d)})$ to $(A'_{(c,d)}, B'_{(c,d)})$. It follows that

$$\begin{aligned} t_{A\prime}(h(p)) &\geq c, \\ f_{A\prime}(h(p)) &\leq d, \end{aligned} \tag{8}$$

that is,

$$\begin{aligned} &t_{A_{\prime}}(h(p)) \geq t_A(p),\\ &f_{A_{\prime}}(h(p)) \leq f_A(x). \end{aligned} \tag{9}$$

Now for arbitraries $p, q \in V$, let $t_B(pq) = e$, $f_B(pq) = t$. Then,

$$\begin{aligned} e &= t_B(pq) \leq t_A(p) \wedge t_A(q),\\ t &= f_B(pq) \geq f_A p \vee f_A(q). \end{aligned} \tag{10}$$

Hence, $p, q \in A_{(e,t)}$ and $pq \in B_{(e,t)}$. Because h is a homomorphism from $X_{(e,t)} = (A_{(e,t)}, B_{(e,t)})$ to $Y_{(e,t)} = (A_{(e,t)}', B_{(e,t)}')$, we conclude that $h(p), h(q) \in A_{(e,t)}'$ and $h(p)g(q) \in B_{(e,t)}'$. Therefore,

$$\begin{aligned} &t_{B_{\prime}}(h(p)h(q)) \geq e = t_B(pq),\\ &f_{B_{\prime}}(h(p)h(q)) \leq t = f_B(pq). \end{aligned} \tag{11}$$

□

Theorem 3. *Let $X = (V, A, B)$ and $Y = (W, A', B')$ be two VGs. Then, $h\colon V \longrightarrow W$ is a WI from X to Y if and only if h is a bijective (η, γ)- homomorphism from X to Y and*

$$\begin{aligned} &t_A(p) = t_{A'}(h(p)),\\ &f_A(p) = f_{A'}(h(p)),\\ &\text{for all } p \in V. \end{aligned} \tag{12}$$

Proof. Let h be a WI from X to Y. From the definition of homomorphism h is a bijective homomorphism from X to Y. By Theorem 2 h is a bijective (η, γ)- homomorphism from X to Y and also by the definition of WI we have

$$\begin{aligned} &t_A(p) = t_{A'}(h(p)),\\ &f_A(p) = f_{A'}(h(p)),\\ &\text{for all } p \in V. \end{aligned} \tag{13}$$

Conversely, from hypothesis, $h\colon A_{(0,1)} = V \longrightarrow A_{(0,1)}' = W$ is a bijective mapping and

$$\begin{aligned} &t_A(p) = t_{A'}(h(p)),\\ &f_A(p) = f_{A'}(h(p)),\\ &\text{for all } p \in V. \end{aligned} \tag{14}$$

For $p, q \in V$, let $t_B(pq) = e$, $f_B(pq) = t$. Then,

$$\begin{aligned} e &= t_B(pq) \leq t_A(p) \wedge t_A(q),\\ t &= f_B(pq) \geq f_A(p) \vee f_A(q), \end{aligned} \tag{15}$$

which implies $p, q \in A_{(e,t)}$ and $pq \in B_{(e,t)}$. Because h is a homomorphism from $(A_{(e,t)}, B_{(e,t)})$ to $(A_{(e,t)}', B_{(e,t)}')$, we have $h(p), h(q) \in A_{(e,t)}'$ and $h(p)h(q) \in B_{(e,t)}'$. Hence,

$$\begin{aligned} &t_{B'}(h(p)h(q)) \geq e = t_B(pq),\\ &f_{B'}(h(p)h(q)) \leq t = f_B(pq), \end{aligned} \tag{16}$$

which complete the proof. □

Theorem 4. *Let $X = (V, A, B)$ and $Y = (W, A', B')$ be two VGs. Then, $h\colon V \longrightarrow W$ is a CWI from X to Y if and only if h is a bijective (η, γ)- homomorphism from X to Y and*

$$\begin{aligned} &t_B(pq) = t_{B'}(h(p)h(q)),\\ &f_B(pq) = f_{B'}(h(p)h(q)),\\ &\text{for all } pq \in \widetilde{V}^2. \end{aligned} \tag{17}$$

Proof. Let $h\colon V \longrightarrow W$ be a CWI from X to Y. Then, h is a bijective homomorphism from X to Y. By Theorem 2 h is a bijective (η, γ)- homomorphism from X to Y. Also by the definition of CWI

$$\begin{aligned} &t_B(pq) = t_{B'}(h(p)h(q)),\\ &f_B(pq) = f_{B'}(h(p)h(q)),\\ &\text{for all } pq \in \widetilde{V}^2. \end{aligned} \tag{18}$$

Conversely, from hypothesis, we know that $h\colon A_{(0,1)} = V \longrightarrow A_{(0,1)}' = W$ is a bijective mapping and

$$\begin{aligned} &t_B(pq) = t_{B'}(h(p)h(q)),\\ &f_B(pq) = f_{B'}(h(p)h(q)). \end{aligned} \tag{19}$$

For arbitrary element $p \in V$, suppose that $t_A(p) = c$, $f_A(p) = d$. Then, we have $p \in A_{(c,d)}$. Now because h is a homomorphism from $(A_{(c,d)}, B_{(c,d)})$ to $(A_{(c,d)}', B_{(c,d)}')$, $h(p) \in A_{(c,d)}'$. Thus, $t_{A_{\prime}}(h(p)) \geq c = t_A(p)$, $f_{A_{\prime}}(h(p)) \leq d = f_A(p)$, which implies h is a CWI from X to Y. □

Corollary 1. *Let $X = (V, A, B) \in VG(V)$, $Y = (W, A', B') \in VG(W)$. If $h\colon V \longrightarrow W$ is a CWI from X to Y, then, h is an IH from $X_{(\eta,\gamma)}$ to $Y_{(\eta,\gamma)}$, $\forall (\eta, \gamma) \in K_*$, $A_{(\eta,\gamma)} \neq \varnothing$.*

From the following example, we conclude that the converse of Corollary 1 do not need to be true.

Example 1. Let $X = (V, A, B)$ and $Y = (W, A', B')$ be two VGs, as shown in Figure 1. Consider the mapping $h\colon V \longrightarrow W$, defined by $h(v_i) = w_i$, $1 \leq i \leq 5$. In view of the (η, γ)- level graphs of X and Y in Figure 1, if $A_{(\eta,\gamma)} \neq \varnothing$ then, h is an IH from $X_{(\eta,\gamma)}$ to $Y_{(\eta,\gamma)}$, but h is not a CWI.

Theorem 5. *Let $X = (V, A, B) \in VG(V)$, $Y = (W, A', B') \in VG(W)$, and $h\colon V \longrightarrow W$ be a mapping. For each $(\eta, \gamma) \in K_*$, $A_{(\eta,\gamma)} \neq \varnothing$, if h is an isomorphism from $X_{(\eta,\gamma)}$ to a SG of $Y_{(\eta,\gamma)}$, then, h is a CWI from X to an induced VSG of Y.*

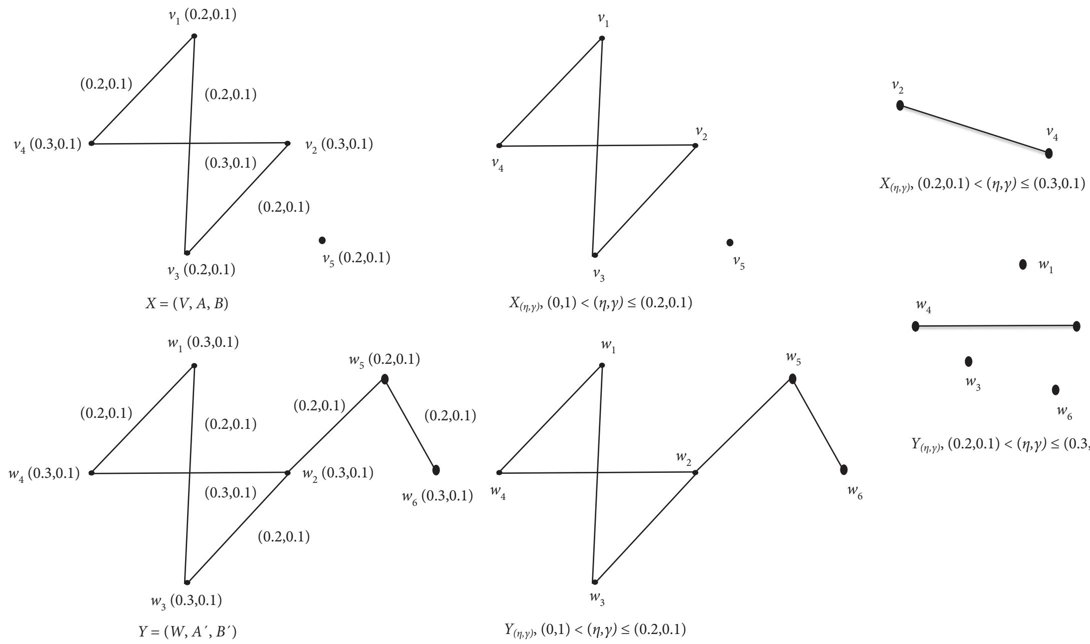

Figure 1: VGs X, Y and the mapping h: $V_i \longrightarrow W_i$ which is not a CWI.

Proof. The mapping h is an isomorphism from $X_{(0,1)} = (V, B_{(0,1)})$ to a SG $Y_{(0,1)} = (W, B_{(0,1)}')$, so h: $V \longrightarrow W$ is an IM. For arbitrary $p \in V$, suppose that $t_A(p) = \eta$, $f_A(p) = \gamma$. Then, $p \in A_{(\eta,\gamma)}$, and so $h(p) \in A_{(\eta,\gamma)}'$. Hence, $t_{A'}(h(p)) \ge \eta = t_A(p)$ and $f_{A'}(h(p)) \le \gamma = f_A(p)$. For $p, q \in V$, let $t_B(pq) = \eta$ and $f_B(pq) = \gamma$. Then, $\eta \le t_A(p)$, $\eta \le t_A(q)$, $\gamma \ge f_A(p)$, $\gamma \ge f_A(q)$ and $pq \in B_{(\eta,\gamma)}$. Hence, $p, q \in A_{(\eta,\gamma)}$ and $pq \in B_{(\eta,\gamma)}$. Since h isomorphism from $X_{(\eta,\gamma)}$ to $Y_{(\eta,\gamma)}$, we get $h(p), h(q) \in A_{(\eta,\gamma)}'$ and $h(p)h(q) \in B_{(\eta,\gamma)}'$. Therefore,

$$\begin{aligned} t_{B'}(h(p)h(q)) &\ge \eta = t_B(pq), \\ f_{B'}(h(p)h(q)) &\le \gamma = f_B(pq). \end{aligned} \tag{20}$$

Now, let $t_{B'}(h(p)h(q)) = k$, $f_{B'}(h(p)h(q)) = s$. Then, $h(p)h(q) \in A_{(k,s)}'$. Because h is injective and an isomorphism from $X_{(k,s)}$ to a SG of $Y_{(k,s)}$, we have $p, q \in A_{(k,s)}$ and $pq \in B_{(k,s)}$. Therefore,

$$\begin{aligned} t_B(pq) &\ge k = t_{B'}(h(p)h(q)), \\ f_B(pq) &\le s = f_{B'}(h(p)h(q)). \end{aligned} \tag{21}$$

Now by (20) and (21), we conclude that

$$\begin{aligned} t_{B'}(h(p)h(q)) &= t_B(pq), \\ f_{B'}(h(p)h(q)) &= f_B(pq). \end{aligned} \tag{22}$$

□

Corollary 2. *Let $X = (V, A, B)$ and $Y = (W, A', B')$ be two VGs with $|V| = |W|$, and h: $V <display> W$ a mapping. For $(\eta, \gamma) \in KL_*$, $A_{(\eta,\gamma)} \neq \varnothing$, if h is an isomorphism from $X_{(\eta,\gamma)}$ to a SG of $Y_{(\eta,\gamma)}$, then, h is a CWI from X to Y.*

Theorem 6. *Let $X = (V, A, B)$ and $Y = (W, A', B')$ be two VGs, h: $V \longrightarrow W$ be a bijective mapping. If for each $(\eta, \gamma) \in K_*$, h is an isomorphism from $X_{(\eta,\gamma)}$ to $Y_{(\eta,\gamma)}$, then, h is an isomorphism from X to Y.*

Proof. From hypothesis, h^{-1}: $W \longrightarrow V$ is a bijective mapping and an isomorphism from $Y_{(\eta,\gamma)}$ to $X_{(\eta,\gamma)}$. By Theorem 5 h is a CWI from X to Y and h^{-1} is a CWI from Y to X. Therefore, h is an isomorphism from X to Y. □

Corollary 3. *Let $X = (V, A, B)$ be VG and h: $V \longrightarrow V$ a bijective mapping. Then, h is an automorphism of X if and only if $h_{|A_{(\eta,\gamma)}}$ is an automorphism of $X_{(\eta,\gamma)}$, from an $(\eta, \gamma) \in K_*$, $A_{(\eta,\gamma)} \neq \varnothing$.*

Theorem 7. *Let $X = (V, A, B)$ be VG. Then, X is a CVG if and only if $X_{(\eta,\gamma)} = (A_{(\eta,\gamma)}, B_{(\eta,\gamma)})$ is a CG for $(\eta, \gamma) \in K_*$.*

Proof. If $X = (V, A, B)$ is a CVG and for $(\eta, \gamma) \in K_*$, $A_{(\eta,\gamma)} \neq \varnothing$, $p, q \in A_{(\eta,\gamma)}$, then, $t_A(p) \ge \eta$, $t_A(q) \ge \eta$, $f_A(p) \le \gamma$, $f_A(q) \le \gamma$, and so

$$\begin{aligned} t_B(pq) &= t_A(p) \wedge t_A(q) \ge \eta, \\ f_B(pq) &= f_A(p) \vee f_A(q) \le \gamma. \end{aligned} \tag{23}$$

Hence, $pq \in B_{(\eta,\gamma)}$. It follows that $X_{(\eta,\gamma)}$ is a CG. Conversely, suppose that $X = (V, A, B)$ is not a CVG. Then, there are $p, q \in V$ so that $t_B(pq) < t_A(p) \wedge t_A(q)$ or $f_B(pq) > f_A(p) \vee f_A(q)$. Let $t_B(pq) < t_A(p) \wedge t_A(q)$, and $t_A(p) \wedge t_A(q) = \eta$, for $\eta \in (0, 1]$. Then, $t_A(p) \ge \eta$ and $t_A(q) \ge \eta$. Hence, $x, y \in A_{(\eta,\gamma)}$, for a $\gamma \in [0, 1]$, but

$pq \notin B_{(\eta,\gamma)}$. This implies that $X_{(\eta,\gamma)}$ is not a CG. For the case $f_B(pq) > f_A(p) \vee f_A(q)$, it follows similarly. □

Theorem 8. *Let $X = (V, A, B) \in VG(V)$. Then, $X_{(\eta,\gamma)}$ has not IV, for each $(\eta,\gamma) \in K_*$, $A_{(\eta,\gamma)} \neq \emptyset$ if and only if for each $p \in V$, $\exists q \in V$ so that $t_B(pq) = t_A(p)$, $f_B(pq) = f_A(p)$.*

Proof. Suppose that for each $(\eta,\gamma) \in K_*$, $A_{(\eta,\gamma)} \neq \emptyset$, graph $X_{(\eta,\gamma)}$ has not IV and there is a node $p \in V$ so that for each $q \in V$, $t_B(pq) < t_A(p)$ or $f_B(pq) > f_A(p)$. Let $t_B(pq) < t_A(p)$ and $t_A(p) = \eta$, $fA(p) = \gamma$, for $(\eta,\gamma) \in K_*$. Then, $p \in A_{(\eta,\gamma)}$ and for each $q \in V, q \neq p$, $pqinB_{(\eta,\gamma)}$. Therefore, p is an IV in the graph $X_{(\eta,\gamma)} = (A_{(\eta,\gamma)}, B_{(\eta,\gamma)})$, which is a contradiction.

Now suppose that for $(\eta,\gamma) \in K_*$, $A_{(\eta,\gamma)} \neq \emptyset$, node $p \in A_{(\eta,\gamma)}$ is an IV in $X_{(\eta,\gamma)}$. If $qinA_{(\eta,\gamma)}$, then, $t_B(pq) \leq t_A(q) < \eta \leq t_A(p)$ or $f_B(pq) \geq f_A(q) > \gamma \geq f_A(q)$, and if $q \in A_{(\eta,\gamma)}$, it is trivial that $pginB_{(\eta,\gamma)}$, hence, $t_B(pq) < \eta \leq t_A(p)$ or $f_B(pq) > \gamma \geq f_A(p)$. Therefore, for each $q \in V$, $t_B(pq) \neq t_A(p)$, $f_B(pq) \neq f_A(p)$.

Here, we describe the relationship between coloring graph and homomorphism of graph. □

Theorem 9. *A VG $X = (V, A, B)$ is r-colorable $\Leftrightarrow$ there exists a homomorphism from X to the K_{r,A_I}.*

Proof. Assume that X be r-colorable with r colors labeled $\Gamma = \{\lambda_1, \lambda_2, \ldots, \lambda_r\}$. Let $V_i = \{v \in V | \lambda_i(v) \neq 0\}$. We define CVG $K_{r,A'}$ with vertices set $\{1, 2, \ldots, r\}$, so that the degree of membership vertex i is $t_{A'}(i) = \max\{t_A(v) \mid v \in V_i\}$ and the degree of non-membership vertex i is $f_{A'}(i) = \min\{f_A(v) | v \in V_i\}$. Now the mapping $h: X \longrightarrow K_{r,A'}$ defined by $h(v) = i$ is a graph homomorphism, because

$$\begin{aligned} t_A(v) &\leq \max\{t_A(w) | w \in V_i\} = t_{A'}(i) = t_{A'}(h(v)),\\ f_A(v) &\geq \min\{f_A(w) | w \in V_i\} = f_{A'}(i) = f_{A'}(h(v)). \end{aligned} \tag{24}$$

According to the definition of CVG, for $u \in V_i$ and $v \in V_j$ we have

$$\begin{aligned} t_B(uv) &\leq t_A(u) \wedge t_A(v) \leq t_{A'}(i) \wedge t_{A_I}(j) = t_{A'}(h(u)) \wedge t_{A'}(h(v)),\\ f_B(uv) &\geq f_A(u) \vee t_A(v) \leq t_{A'}(i) \vee t_{A'}(j) = t_{A'}(h(u)) \vee t_{A'}(h(v)). \end{aligned} \tag{25}$$

Then, $t_B(uv) \leq t_{B_I}(h(u)h(v))$, $f_B(uv) \geq f_{B'}(h(u)h(v))$, for all $uv \in \widetilde{V}^2$.

Conversely, let $g: X \longrightarrow K_{r,A'}$ be a homomorphism. For a given $k \in V(K_{r,A_I})$, define the set $h^{-1}(k) \subseteq V$ to be

$$h^{-1}(k) = \{x \in V | h(x) = k\}. \tag{26}$$

If $v \in h^{-1}(k)$, let $\lambda_k(v) = (t_{\lambda_k}(v), f_{\lambda_k}(v)) = (t_A(v), f_A(v))$, otherwise $\lambda_k(v) = 0$. Therefore, the VG X is r-colorable with coloring set $\{\lambda_1, \lambda_2, \ldots, \lambda_r\}$. □

4. Application

Nowadays, the issue of coloring is very important in the theory of fuzzy graphs because it has many applications in controlling intercity traffic, coloring geographical maps, as well as finding areas with high population density. Therefore, in this section, we have tried to present an application of the coloring of vertices in a VG.

Example 2. Let $X = (V, A_1, B_1)$ be a VG (See Figure 2). We modeled a FG by considering countries A, B, C, D as vertices of graph. The membership and nonmembership value of the vertices are the good and bad activity of a country with respect technology so that are $(t_{A_1}(A), f_{A_1}(A)) = (0.1, 0.2)$, $(t_{A_1}(B), f_{A_1}(B)) = (0.4, 0.5)$, $(t_{A_1}(C), f_{A_1}(C)) = (0.2, 0.5)$, $(t_{A_1}(D), f_{A_1}(D)) = (0.2, 0.8)$, respectively. There is an edge if they share a boundary. Let AB, BC, AC, $C\,D$, and $B\,D$ are edges of graph X. The membership and nonmembership value of the edges are the political relationship in a good and bad attitude such that $(t_{B_1}(AB), f_{B_1}(AB)) = (0.1, 0.5)$, $(t_{B_1}(BC), f_{B_1}(BC)) = (0.2, 0.8)$, $(t_{B_1}(AC), f_{B_1}(AC)) = (0.1, 0.5)$, $(t_{B_1}(C\,D), f_{B_1}(C\,D)) = (0.2, 0.8)$, $(t_{B_1}(B\,D), f_{B_1}(B\,D)) = (0.2, 0.8)$, respectively. We now want to see how many days we will need to hold a conference between these countries. Let S be a set of countries; $S = \{A, B, C, D\}$ and $P = \{AB\ BC\ AC\ C\,D\ B\,D\}$ Suppose that $S(p)$ be countries have boundary for $p \in P$. Now, form FG G with vertices set P, where $a, b \in P$ are neighbor if and only if $S(a) \cap S(b) \neq \emptyset$. For instance, $S(AB) = \{A, B\}$ and $S(BC) = \{C, B\}$. So $S(AB) \cap S(BC) = \{B\} \neq \emptyset$ and hence AB, BC are neighbor. By Theorem 9 there is a homomorphism from G to complete graph with $n = 3$. Then, 3 days are required to hold a conference between these countries, $\{\{AB, C\,D\}, \{BC\}, \{AC, B\,D\}\}$. The colored graph of the example 2 is shown in Figure 3.

In the next example, we want to identify the most effective employee of a hospital with the help of a vague influence digraph.

Example 3. Hospitals are very important organizations whose existence is directly related to the general health of the community. Researchers in each country examine factors that contribute to the success of strategic planning to improve the management status of these health organizations. The lives and health of many people are in the hands of health systems. From the safe delivery of a healthy baby to the respectful care of an elderly person, the health department has a vital and ongoing responsibility to individuals throughout their lives. The health industry has undergone many political, social, economic,

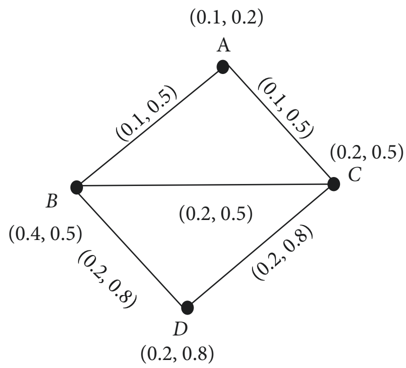

FIGURE 2: Vague graph $X = (V, A_1, B_1)$.

TABLE 2: Names of employees in a hospital and their services.

Name	Services
Taheri	Head of audiovisual department
Ameri	Environment health expert
Talebi	Head of radiology department
Taleshi	Network expert
Najafi	Medical equipment expert
Kamali	Medical records archive expert
Badri	Head of hospital

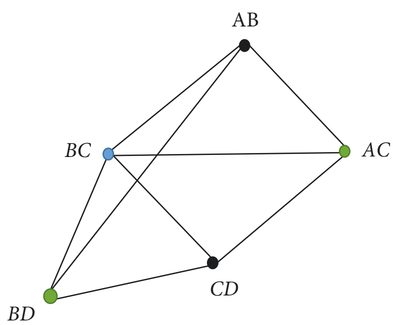

FIGURE 3: The colored graph of the example 2.

TABLE 3: The level of staff capability.

	Taheri	Ameri	Talebi	Taleshi	Najafi	Kamali	Badri
t_A	0.4	0.5	0.6	0.7	0.9	0.9	0.8
f_A	0.4	0.3	0.3	0.2	0.1	0.1	0.2

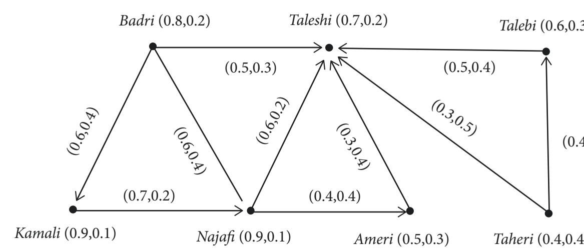

FIGURE 4: Vague influence digraph.

environmental, and technological changes since the early 1980s. These changes have created challenges for managers of healthcare organizations, especially hospitals that cannot be managed with operational plans. Thus, hospital managers have resorted to strategic planning since the 1980s to achieve excellence. Since the management in each ward of the hospital is very important, so in this section, we have tried to determine the most effective person in a hospital based on the performance of its staff. Therefore, we consider the vertices of the VIG as the heads of each ward of the hospital, and the edges of the graph as the degree of interaction and influence of each other. For this hospital, the set of staff is $F = \{\text{Taheri, Ameri, Talebi, Taleshi, Najafi, Kamali, Badri}\}$.

(i) Ameri has been working with Taleshi for 14 years and values his views on issues.

(ii) Taheri has been responsible for audiovisual affairs for a long time, and not only Ameri, but also Taleshi, are very satisfied with Taheri's performance.

(iii) In a hospital, the preservation of medical records is a very important task. Kamali is the most suitable person for this responsibility.

(iv) Talebi and Kamali have a long history of conflict.

(v) Talebi has an important role in the radiology department of the laboratory.

Given the abovementioned, we consider this a VIG. The vertices represent each of the hospital staff. Note that each staff member has the desired ability as well as shortcomings in the performance of their duties. Therefore, we use of VS to express the weight of the vertices. The true membership indicates the efficiency of the employee and the false membership shows the lack of management and shortcomings of each staff. But the edges describe the level of relationships and friendships between employees such that the true membership shows a friendly relationship between both employees and the false membership shows the degree of conflict between the two officials. Names of employees and levels of staff capability are shown in Tables 2 and 3. The adjacency matrix corresponding to Figure 4 is shown in Table 4.

Figure 4 shows that Najafi has 90% of the power needed to do the hospital work as the medical equipment expert, but does not have the 10% knowledge needed to be the boss. The directional edge of Taleshi–Ameri shows that there is 30% friendship among these two employees, and unfortunately, they have 40% conflict. Clearly, Badri has dominion over both Kamali and Najafi, and his dominance over both is 60%. It is clear that Badri is the most influential employee of the hospital because he controls both the head of the medical equipment and the medical records archive expert, who have 90% of the power in the hospital.

Table 4: Adjacency matrix corresponding to Figure 4.

	Taheri	Ameri	Talebi	Taleshi	Najafi	Kamali	Badri
Taheri	$(0,0)$	$(0,0)$	$(0.4,0.5)$	$(0.3,0.5)$	$(0,0)$	$(0,0)$	$(0,0)$
Ameri	$(0,0)$	$(0,0)$	$(0,0)$	$(0.3,0.4)$	$(0,0)$	$(0,0)$	$(0,0)$
Talebi	$(0,0)$	$(0,0)$	$(0,0)$	$(0.5,0.4)$	$(0,0)$	$(0,0)$	$(0,0)$
Taleshi	$(0,0)$	$(0,0)$	$(0,0)$	$(0,0)$	$(0,0)$	$(0,0)$	$(0,0)$
Najafi	$(0,0)$	$(0.4,0.4)$	$(0,0)$	$(0.6,0.2)$	$(0,0)$	$(0,0)$	$(0,0)$
Kamali	$(0,0)$	$(0,0)$	$(0,0)$	$(0,0)$	$(0.7,0.2)$	$(0,0)$	$(0,0)$
Badri	$(0,0)$	$(0,0)$	$(0,0)$	$(0.5,0.3)$	$(0.6,0.4)$	$(0.6,0.4)$	$(0,0)$

5. Conclusion

VGs have a wide range of applications in the field of psychological sciences as well as the identification of individuals based on oncological behaviors. With the help of VGs, the most efficient person in an organization can be identified according to the important factors that can be useful for an institution. Hence, in this paper, we introduced the notion of (η,γ)- homomorphism of VGs and classify HMs, WIs, and CWIs of VGs by (η,γ)- homomorphisms. We also investigated the level graphs of VGs to characterize some VGs. Finally, we presented two applications of VGs in coloring problem and also finding effective person in a hospital. In our future work, we will introduce new concepts of connectivity in VGs and investigate some of their properties. Also, we will study the new results of connected perfect dominating set, regular perfect dominating set, and independent perfect dominating set on VGs.

Data Availability

No data were used to support this study.

Conflicts of Interest

The authors declare that they have no conflicts of interest.

Acknowledgments

This work was supported by the National Key R&D Program of China (Grant 2019YFA0706402) and the National Natural Science Foundation of China under Grant 62172302, 62072129, and 61876047.

References

[1] L. A. Zadeh, "Fuzzy sets," *Information and Control*, vol. 8, no. 3, pp. 338–353, 1965.

[2] K. R. Bhutani, "On automorphisms of fuzzy graphs," *Pattern Recognition Letters*, vol. 9, no. 3, pp. 159–162, 1989.

[3] G. J. Klir and Bo Yuan, *Fuzzy Sets and Fuzzy Logic: Theory and Application*, Prentice Hall, Hoboken, NJ, USA, 1997.

[4] B. Kosko, *Fuzzy Things: The New Science of Fuzzy Logic*, Hyperion, New York, NY, USA, 1993.

[5] F. A. Lootsma, *Fuzzy Logic for Planning and Decision Making*, Kluwer, Alphen aan den Rijn, Netherlands, 1997.

[6] J. N. Mordeson and P. S. Nair, *Fuzzy Graph and Fuzzy Hypergraphs*, PhysicaVerlag, Heidebeg, Germany, 2nd edition, 2000.

[7] W.-L. Gau and D. J. Buehrer, "Vague sets," *IEEE Transactions on Systems, Man, and Cybernetics*, vol. 23, no. 2, pp. 610–614, 1993.

[8] A. Kauffman, *Introduction a la Theories des Sous-Emsembles 503 ous*, Masson et Cie, Echallens, Switzerland, 1973.

[9] L. A. Zadeh, "Similarity relations and fuzzy orderings," *Information Sciences*, vol. 3, no. 2, pp. 177–200, 1971.

[10] L. A. Zadeh, "Is there a need for fuzzy logic?" *Information Sciences*, vol. 178, no. 13, pp. 2751–2779, 2008.

[11] A. Rosenfeld, "Fuzzy sets and their applications to cognitive and decision processes," in *Fuzzy Sets and Their Applications*, L. A. Zadeh, K. S. Fu, and M. Shimura, Eds., Academic Press, Cambridge, MA, USA, pp. 77–95, 1975.

[12] N. Ramakrishna, "Vague graphs," *International Jounal of Computational Cognition*, vol. 7, pp. 51–58, 2009.

[13] M. Akram, A. N. Gani, and A. B. Saeid, "Vague hypergraphs," *Journal of Intelligent and Fuzzy Systems*, vol. 26, no. 2, pp. 647–653, 2014.

[14] M. Akram, S. Samanta, and M. Pal, "Cayley vague graphs," *Journal of Fuzzy Mathematics*, vol. 25, no. 2, pp. 1–14, 2017.

[15] M. Akram, F. Feng, S. Sarwar, and Y. B. Jun, "Certain types of vague graphs," *UPB Scientific Bulletin Series A: Applied Mathematica and Physics*, vol. 76, no. 1, pp. 141–154, 2014.

[16] M. Akram, W. A. Dudek, and M. Murtaza Yousaf, "Regularity in vague intersection graphs and vague line graphs," *Abstract and Applied Analysis*, vol. 2014, Article ID 525389, 10 pages, 2014.

[17] H. Rashmanlou, S. Samanta, M. Pal, and R. A. Borzooei, "Intuitionistic fuzzy graphs with categorical properties," *Fuzzy Information and Engineering*, vol. 7, no. 3, pp. 317–334, 2015.

[18] P. Bhattacharya, "Some remarks on fuzzy graphs," *Pattern Recognition Letters*, vol. 6, no. 5, pp. 297–302, 1987.

[19] J. N. Mordeson and P. Chang-Shyh, "Operations on fuzzy graphs," *Information Sciences*, vol. 79, pp. 159–170, 1994.

[20] H. Khan, M. Ahmad, and R. Biswas, "Vague relations," *International Journal of Computational Cognition*, vol. 5, no. 1, 2007.

[21] A. A. Talebi, "Cayley fuzzy graphs on the fuzzy group," *Computational and Applied Mathematics*, vol. 37, 2018.

[22] A. A. Talebi and W. A. Dudek, "Operations on level graphs of bipolar fuzzy graphs," *Bulletin Academiel De Stiinte A Republic Moldova Mathematica*, vol. 2, no. 81, pp. 107–124, 2016.

[23] R. Borzooei and H. Rashmanlou, "Domination in vague graphs and its applications," *Journal of Intelligent and Fuzzy Systems*, vol. 29, no. 5, pp. 1933–1940, 2015.

[24] G. Ghorai and M. Pal, "Some isomorphic properties of m-polar fuzzy graphs with applications," *SpringerPlus*, vol. 5, no. 1, pp. 2104–2125, 2016.

[25] H. Jiang, A. A. Talebi, Z. Shao, S. H. Sadati, and H. Rashmanlou, "New concepts of vertex covering in cubic

graphs with its applications," *Mathematics*, vol. 10, no. 3, p. 307, 2022.

[26] K. K. Krishna, Y. Talebi, H. Rashmanlou, A. A. Talebi, and F. Mofidnakhaei, "New concept of cubic graph with application," *Journal of Multiple Valued Logic and Soft Computing*, vol. 33, pp. 135–154, 2019.

[27] Y. Rao, S. Kosari, and Z. Shao, "Certain properties of vague graphs with a novel application," *Mathematics*, vol. 8, no. 10, p. 1647, 2020.

[28] Y. Rao, S. Kosari, Z. Shao, R. Cai, and L. Xinyue, "A study on domination in vague incidence graph and its application in medical sciences," *Symmetry*, vol. 12, no. 11, p. 1885, 2020.

[29] Y. Rao, S. Kosari, Z. Shao, X. Qiang, M. Akhoundi, and X. Zhang, "Equitable domination in vague graphs with application in medical sciences," *Frontiers in Physics*, vol. 9, Article ID 635642, 2021.

[30] B. Sheikh Hoseini, M. Akram, M. Sheikh Hosseini, H. Rashmanlou, and R. A. Borzooei, "Maximal product of graphs under vague environment," *Mathematical and Computational Applications*, vol. 25, no. 1, p. 10, 2020.

[31] N. Jan, K. Ullah, T. Mahmood et al., "Some root level modifications in interval valued fuzzy graphs and their generalizations including neutrosophic graphs," *Mathematics*, vol. 7, no. 1, p. 72, 2019.

[32] S. K. Amanathulla, G. Muhiuddin, D. Al-Kadi, and M. Pal, "Distance two surjective labelling of paths and interval graphs," *Discrete Dynamics in Nature and Society*, vol. 2021, Article ID 9958077, 9 pages, 2021.

[33] G. Muhiuddin, N. Sridharan, D. Al-Kadi, S. Amutha, and M. E. Elnair, "Reinforcement number of a graph with respect to half-domination," *Journal of Mathematics*, vol. 2021, Article ID 6689816, 7 pages, 2021.

[34] G. Muhiuddin, M. Mohseni Takallo, Y. B. Jun, and R. A. Borzooei, "Cubic graphs and their application to a traffic flow problem," *International Journal of Computational Intelligence Systems*, vol. 13, no. 1, pp. 1265–1280, 2020.

Hindawi
Journal of Mathematics
Volume 2022, Article ID 5094929, 11 pages
https://doi.org/10.1155/2022/5094929

Research Article

First General Zagreb Co-Index of Graphs under Operations

Muhammad Javaid [1], Muhammad Ibraheem [1], Ebenezer Bonyah [2], Uzma Ahmad [3], and Shaohui Wang [4]

[1] *Department of Mathematics, School of Science, University of Management and Technology, Lahore 54770, Pakistan*
[2] *Department of Mathematics Education, Akenten Appiah-Menka University of Skills Training and Entrepreneurial Development, Kumasi 00233, Ghana*
[3] *Department of Mathematics, University of the Punjab, Lahore, Pakistan*
[4] *Department of Mathematics, Louisiana College, Pineville, LA 71359, USA*

Correspondence should be addressed to Ebenezer Bonyah; ebbonya@gmail.com

Received 15 November 2021; Accepted 6 April 2022; Published 9 May 2022

Academic Editor: Ali Jaballah

Copyright © 2022 Muhammad Javaid et al. This is an open access article distributed under the Creative Commons Attribution License, which permits unrestricted use, distribution, and reproduction in any medium, provided the original work is properly cited.

Topological indices are graph-theoretic parameters which are widely used in the subject of chemistry and computer science to predict the various chemical and structural properties of the graphs respectively. Let G be a graph; then, by performing subdivision-related operations S, Q, R, and T on G, the four new graphs $S(G)$ (subdivision graph), $Q(G)$ (edge-semitotal), $R(G)$ (vertex-semitotal), and $T(G)$ (total graph) are obtained, respectively. Furthermore, for two simple connected graphs G and H, we define F-sum graphs (denoted by $G_{+F}H$) which are obtained by Cartesian product of $F(G)$ and H, where $F \in \{S, R, Q, T\}$. In this study, we determine first general Zagreb co-index of graphs under operations in the form of Zagreb indices and co-indices of their basic graphs.

1. Introduction

Graph theory has given different valuable tools in which likely the best tool is known as topological index (TI) that is used to predict structural and chemical properties of graphs such as connectivity, solubility, freezing point, boiling point, critical temperature, and molecular mass, see [1]. The medical behaviors and drugs' particles of the different compounds are discussed with the help of various TIs in the pharmaceutical industries, see[2]. In addition, for the study of molecules, the quantitative structures' activity relationships (QSAR) and quantitative structures' property relationships (QSPR) are very useful techniques which are mostly performed with the help of TIs [3].

There are three basic types of TIs depending on the parameters of degree, distance, and polynomial. According to recent review [4], the degree-based TIs are mostly studied. First of all, Wiener calculated the boiling point of paraffin with the help of a degree-based TI, see [5]. Gutman and Trinajsti introduced Zagreb indices and used them to compute the different structure-based characteristics of the molecular graphs [6].

Later on, Shenggui and Huiling characterized the graphs for the first general Zagreb index [7]. Bedratyuk and Savenko calculated the ordinary generating function and linear recurrence relation for the sequence of the general first Zagreb index [8].

Recently, Ashrafi et al. defined Zagreb co-index and computed it for graphs which are formed using various operations, see [9, 10]. Kinkar et al. computed the first Zagreb co-indices of trees under different conditions, see [11]. Mansour and Song established relationship between Zagreb indices and co-indices of graphs [12]. Huaa and Zhang computed sharp bounds on the first Zagreb co-index in terms of Wiener, eccentric distance sum, eccentric connectivity, and degree distance indices [13]. Gutman et al. calculated relations between the Zagreb indices and co-indices of a graph G and of its complement $\overline{G}$ [14, 15].

In graph theory, the operations (union, intersection, complement, product, and subdivision) play an important role to develop new structure of graphs. Yan et al. computed the Wiener index for new graphs using five different operations L, S, Q, R, and T on a graph G such as line graph $L(G)$, subdivided graph $S(G)$, line superposition graph $Q(G)$, triangle parallel graph $R(G)$, and total graph $T(G)$, respectively, see [16]. After that, Eliasi and Taeri computed Wiener indices of newly defined F-sum graphs represented as $(G_{1+F}G_2)$, where $F \in \{S, R, Q, T\}$ [17]. Furthermore, Deng et al. calculated Zagreb indices [18], Ibraheem et al. [19] forgot co-index, Liu et al. obtained first general Zagreb (FGZ) index [20], and Javaid et al. [21] computed the bounds of first Zagreb co-index; furthermore, they also studied the connection-based Zagreb index and co-index [22] of these graphs.

In this study, we computed FGZ co-index of graphs under operations such as $\overline{M}_1(G_{+S}H)$, $\overline{M}_1(G_{+R}H)$, $\overline{M}_1(G_{+Q}H)$, and $\overline{M}_1(G_{+T}H)$. The reset of the study is settled as follows. Section 2 contains preliminaries. In Section 3, the main results of our work are discussed, and Section 4 has the conclusion of work.

2. Preliminaries

Let G be a simple and connected graph with vertex and edge set denoted by $V(G)$ and $E(G)$, respectively. The degree of vertex any vertex v in G is the number of edges incident on it and denoted by d(v). Let G be a graph; then, its complement is defined as $|V(\overline{G})| = |V(G)|$ and $uv \notin \overline{G}$ iff $uv \in G$ denoted as $\overline{G}$. Gutman and Trinajsti introduced the first and second Zagreb indices as [6]

$$\begin{aligned} M_1(G) &= \sum_{p_1p_2 \in E(G)} [d_G(p_1) + d_G(p_2)], \\ M_2(G) &= \sum_{p_1p_2 \in E(G)} [d_G(p_1) d_G(p_2)]. \end{aligned} \tag{1}$$

Ashrafi êt al. defined first Zagreb co-index $\overline{M}_1(G)$ as follows, see [10]:

$$\overline{M}_1(G) = \sum_{y_1y_2 \notin E(G)} [d_G(y_1) + d_G(y_2)]. \tag{2}$$

Let G be a graph; then, $S(G)$ is obtained by adding one vertex in every edge of G.

(i) $R(G)$ is obtained from $S(G)$ by inserting an edge between the vertices that are adjacent in G

(ii) $Q(G)$ is obtained from $S(G)$ by inserting an edge between new vertices that adjacent edges of G

(iii) Apply both $R(G)$ and $Q(G)$ on $S(G)$; then, $T(G)$ is obtained

Suppose two connected graphs G and H; then, their $F-$sum graph is represented by $G_{+F}H$ having vertex set $|V(G_{+F}H)| = V(G) \cup E(G) \times V(H)$ and (y_1, y_2) (z_1, z_2) $\in E(G_{+F}H)$ iff $y_1 = z_1 \in V(G)$ and $y_2 \backsim z_2 \in H$ $y_2 = z_2$ $\in V(H)$ and $y_1 \backsim z_1 \in F(G)$, where $F \in \{S, R, Q, T\}$.

For details, see Figure 1 and 2.

3. Main Results

This section contains results about FGZ co-index of graphs under operations.

Theorem 1. *Let $G_{+S}H$ be S-sum graph; then, its first general Zagreb co-index is given as*

$$\begin{aligned} \overline{M}_1^{\gamma}(G_{+S}H) = {} & 2^{\theta}\left(n_2^2 e_1^2 - n_2 e_1\right) + +2^{\theta} e_1 [2n_1(e_2 + \overline{e_2}) + n_2(n_1 - 2)] \\ & + \sum_{i=0}^{\theta} \binom{\theta}{i} \Big[M_1^{\theta-i}(G)\overline{M_1}^{i+1}(H) + M_1^{\gamma-i}(G) M_1^i(H) + M_1^{i+1}(H)\left(M_1^{\gamma-i}(G) + \overline{M_1}^{\gamma-i}(G)\right) + \overline{M_1}^{i+1}(H) \\ & \left(M_1^{\gamma-i}(G) + \overline{M_1}^{\gamma-i}(G)\right) + M_1^i(H)\left(\overline{M_1}^{\theta-i}(G) + M_1^{\gamma-i}(G)\right) + M_1^{\gamma-i}(G)\overline{M_1}^{i}(H) + \overline{M_1}^{\gamma-i}(G)\left(M_1^i(H) + \overline{M_1}^{i}(H)\right) \Big], \end{aligned} \tag{3}$$

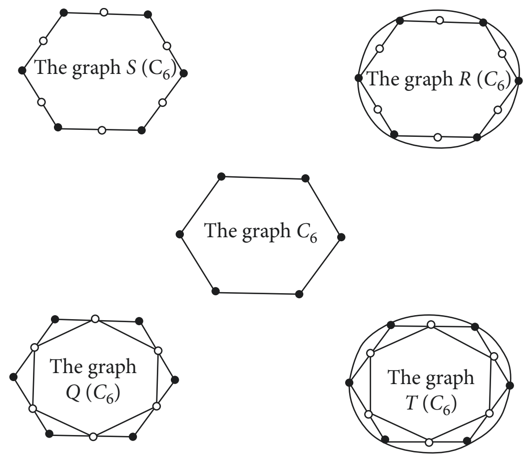

FIGURE 1: Subdivision of C_5.

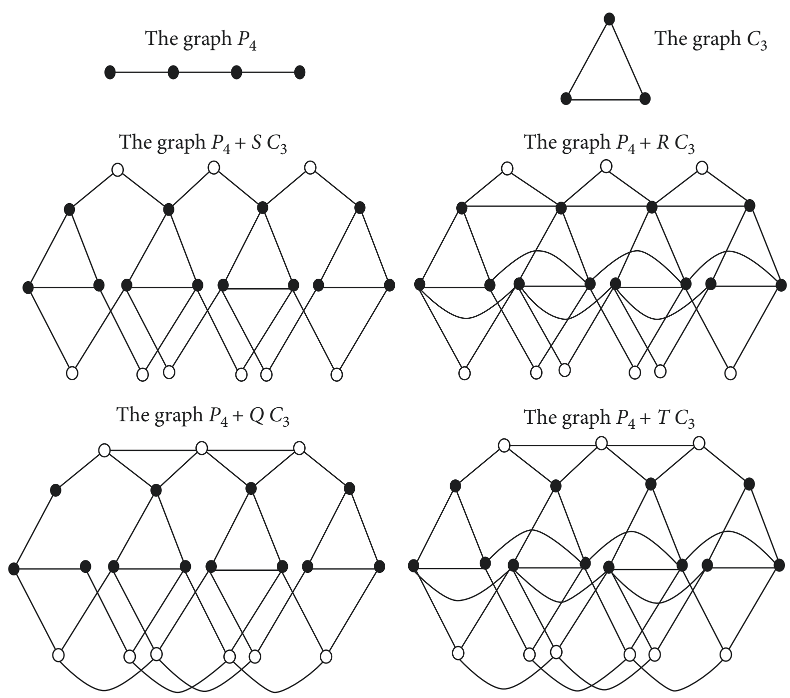

FIGURE 2: F-sum graphs for P_5 and P_6.

where $\theta = \gamma - 1$.

Proof. Using equation (2), we have

$$\overline{M}(G_{+S}H) = \sum_{(y_1,y_2)(z_1,z_2)\notin EG_{+S}H} [d(y_1,z_1) + d(y_2,z_2)],$$

$$\begin{aligned}\overline{M}_1^{\gamma}(G_{+S}H) &= \sum_{z_1,z_2\in H}\Bigg[\sum_{y_1,y_2\in V(S(G)-G)}\left[d^{\theta}_{G_{+S}H}(y_1,z_1) + d^{\theta}_{G_{+S}H}(y_2,z_2)\right] + \sum_{y_1,y_2\in V_G}\left[d^{\theta}_{G_{+S}H}(y_1,z_1) + d^{\theta}_{G_{+S}H}(y_2,z_2)\right]\\ &\quad + \sum_{y_1,y_2\in V(S(G))y_1\in V(G)y_2\in V(S(G)-G)}\left[d^{\theta}_{G_{+S}H}(y_1,z_1) + d^{\theta}_{G_{+S}H}(y_2,z_2)\right]\Bigg]\\ &= \sum A + \sum B + \sum C,\end{aligned}$$

$$\sum A = \sum_{y_1,y_2\in V(S(G)-G)}\sum_{z_1,z_2\in V_{G_2}}\left[d^{\theta}_{G_{+S}H}(y_1,z_1)+d^{\theta}_{G_{+S}H}(y_2,z_2)\right],$$

$$\sum A = 2^{\theta}\left(n_2^2e_1^2-n_2e_1\right),$$

$$\sum B = \sum B_1+\sum B_2+\sum B_3+\sum B_4+\sum B_5+\sum B_6,$$

$$\begin{aligned}\sum B_1 &= \sum_{y\in V(G)}\sum_{z_1z_2\notin E(H)}\left[d^{\theta}_{G_{+S}H}(y,z_1)+d^{\theta}_{G_{+S}H}(y,z_2)\right]\\ &= \sum_{y\in V(G)}\sum_{z_1z_2\notin E(H)}\sum_{i=0}^{\theta}\binom{\theta}{i}\left[d_G^{\theta-i}(y)d_H^i(z_1)+d_G^{\theta-i}(y)d_H^i(z_2)\right]\\ &= \sum_{y\in V(G)}\sum_{z_1z_2\notin E(H)}\sum_{i=0}^{\theta}\binom{\theta}{i}d_G^{\theta-i}(y)\left[d_H^i(z_1)+d_H^i(z_2)\right],\end{aligned}$$

$$\begin{aligned}\sum B_2 &= \sum_{y_1y_2\in E(G)}\sum_{z\in V(H)}\left[d^{\theta}_{G_{+S}H}(y_1,z)+d^{\theta}_{G_{+S}H}(y_2,z)\right]\\ &= \sum_{y_1y_2\in E(G)}\sum_{z\in V(H)}\sum_{i=0}^{\theta}\binom{\theta}{i}\left[d_G^{\theta-i}(y_1)d_H^i(z)+d_G^{\theta-i}(y_2)d_H^i(z)\right]\\ &= \sum_{y_1,y_2\in V_G}\sum_{z\in H}\sum_{i=0}^{\theta}\binom{\theta}{i}d_H^i(z)\left[d_G^{\theta-i}(y_1)d_G^{\theta-i}(y_2)\right],\end{aligned}$$

$$\begin{aligned}\sum B_3 &= \sum_{y_1y_2\in E(G)}\sum_{z_1z_2\in E(H)}\left[d^{\theta}_{G_{+S}H}(y_1,z_1)+d^{\theta}_{G_{+S}H}(y_2,z_2)\right]\\ &= \sum_{y_1y_2\in E(G)}\sum_{z_1z_2\in E(H)}\sum_{i=0}^{\theta}\binom{\theta}{i}\left[d_G^{\theta-i}(y_1)d_H^i(z_1)+d_G^{\theta-i}(y_2)d_H^i(z_2)\right],\end{aligned}$$

$$\begin{aligned}\sum B_4 &= \sum_{y_1y_2\notin E(G)}\sum_{z_1z_2\in E(H)}\left[d^{\theta}_{G_{+S}H}(y_1,z_1)+d^{\theta}_{G_{+S}H}(y_2,z_2)\right]\\ &= \sum_{y_1y_2\notin E(G)}\sum_{z_1z_2\in E(H)}\sum_{i=0}^{\theta}\binom{\theta}{i}\left[d_G^{\theta-i}(y_1)d_H^i(z_1)+d_G^{\theta-i}(y_2)d_H^i(z_2)\right],\end{aligned}$$

$$\begin{aligned}\sum B_5 &= \sum_{y_1y_2\in E(G)}\sum_{z_1z_2\notin E(H)}\left[d^{\theta}_{G_{+S}H}(y_1,z_1)+d^{\theta}_{G_{+S}H}(y_2,z_2)\right]\\ &= \sum_{y_1y_2\in E(G)}\sum_{z_1z_2\notin E(H)}\sum_{i=0}^{\theta}\binom{\theta}{i}\left[d_G^{\theta-i}(y_1)d_H^i(z_1)+d_G^{\theta-i}(y_2)d_H^i(z_2)\right],\end{aligned}$$

$$\begin{aligned}\sum B_6 &= \sum_{y_1y_2\notin E(G)}\sum_{z_1z_2\notin E(H)}\left[d^{\theta}_{G_{+S}H}(y_1,z_1)+d^{\theta}_{G_{+S}H}(y_2,z_2)\right]\\ &= \sum_{y_1y_2\notin E(G)}\sum_{z_1z_2\notin E(H)}\sum_{i=0}^{\theta}\binom{\theta}{i}\left[d_G^{\theta-i}(y_1)d_H^i(z_1)+d_G^{\theta-i}(y_2)d_H^i(z_2)\right],\end{aligned}$$

$$\begin{aligned}
\sum B &= \sum_{i=0}^{\theta}\binom{\theta}{i}\Big[M_1^{\theta-i}(G)\overline{M_1}^{i+1}(H) + M_1^{\gamma-i}(G)M_1^{i}(H)\\
&\quad + M_1^{i+1}(H)\big(M_1^{\gamma-i}(G) + \overline{M_1}^{\gamma-i}(G)\big) + \overline{M_1}^{i+1}(H)\big(M_1^{\gamma-i}(G) + \overline{M_1}^{\gamma-i}(G)\big)\Big],\\
\sum C &= \sum C_1 + \sum C_2 + \sum C_3 + \sum C_4 + \sum C_5,\\
\sum C_1 &= \sum_{y_1y_2\notin E(S(G)y_1\in V(G)y_2\in V(S(G)-G)}\ \sum_{z\in H}\left[d^{\theta}_{G_{+S}H}(y_1,z) + d^{\theta}_{G_{+S}H}(y_2,z)\right]\\
&= \sum_{y_1y_2\notin E(S(G)y_1\in V(G)y_2\in V(S(G)-G)}\ \sum_{z\in H}\sum_{i=0}^{\theta}\binom{\theta}{i}\left[d_G^{\theta-i}(y_1)d_H^{i}(z) + 2^{\theta}\right]\\
&= \sum_{i=0}^{\theta}\binom{\theta}{i}\overline{M_1}^{\theta-i}(G)M_1^{i}(H) + 2^{\theta}n_2e_1(n_1-2),\\
\sum C_2 &= \sum_{y_1y_2\in E(S(G)y_1\in V(G)y_2\in V(S(G)-G)}\ \sum_{z_1z_2\in E(H)}\left[d^{\theta}_{G_{+S}H}(y_1,z_1) + d^{\theta}_{G_{+S}H}(y_2,z_2)\right]\\
&= \sum_{y_1y_2\in E(S(G)y_1\in V(G)y_2\in V(S(G)-G)}\ \sum_{z_1z_2\in E(H)}\sum_{i=0}^{\theta}\binom{\theta}{i}\left[d_G^{\theta-i}(y_1)d_H^{i}(z_1) + 2^{\theta}\right],\\
\sum C_3 &= \sum_{y_1y_2\in E(S(G)y_1\in V(G)y_2\in V(S(G)-G)}\ \sum_{z_1z_2\notin E(H)}\left[d^{\theta}_{G_{+S}H}(y_1,z_1) + d^{\theta}_{G_{+S}H}(y_2,z_2)\right]\\
&= \sum_{y_1y_2\in E(S(G)y_1\in V(G)y_2\in V(S(G)-G)}\ \sum_{z_1z_2\notin E(H)}\sum_{i=0}^{\theta}\binom{\theta}{i}\left[d_G^{\theta-i}(y_1)d_H^{i}(z_1) + 2^{\theta}\right],\\
\sum C_4 &= \sum_{y_1y_2\notin E(S(G)y_1\in V(G)y_2\in V(S(G)-G)}\ \sum_{z_1z_2\in E(H)}\left[d^{\theta}_{G_{+S}H}(y_1,z_1) + d^{\theta}_{G_{+S}H}(y_2,z_2)\right]\\
&= \sum_{y_1y_2\notin E(S(G)y_1\in V(G)y_2\in V(S(G)-G)}\ \sum_{z_1z_2\in E(H)}\sum_{i=0}^{\theta}\binom{\theta}{i}\left[d_G^{\theta-i}(y_1)d_H^{i}(z_1) + 2^{\theta}\right],\\
\sum C_5 &= \sum_{y_1y_2\notin E(S(G)y_1\in V(G)y_2\in V(S(G)-G)}\ \sum_{z_1z_2\notin E(H)}\left[d^{\theta}_{G_{+S}H}(y_1,z_1) + d^{\theta}_{G_{+S}H}(y_2,z_2)\right]\\
&= \sum_{y_1y_2\notin E(S(G)y_1\in V(G)y_2\in V(S(G)-G)}\ \sum_{z_1z_2\notin E(H)}\sum_{i=0}^{\theta}\binom{\theta}{i}\left[d_G^{\theta-i}(y_1)d_H^{i}(z_1) + 2^{\theta}\right],\\
\sum C &= \sum_{i=0}^{\theta}\binom{\theta}{i}\Big[M_1^{i}(H)\big(\overline{M_1}^{\theta-i}(G) + M_1^{\gamma-i}(G)\big) + M_1^{\gamma-i}(G)\overline{M_1}^{i}(H) + \overline{M_1}^{\gamma-i}(G)\big(M_1^{i}(H) + \overline{M_1}^{i}(H)\big)\Big]\\
&\quad + 2^{\theta+1}e_1n_1(e_2 + \overline{e_2}).
\end{aligned} \tag{4}$$

We arrived at desired result by putting the values in equation (4). □

Theorem 2. *Let $G_{+R}H$ be R-sum graph; then, its first general Zagreb co-index is given as*

$$\overline{M}_1^{\gamma}(G_{+R}H) = 2^{\theta}\left(n_2^2e_1^2 - n_2e_1\right) + 2^{\theta}e_1\left[2n_1\left(e_2 + \overline{e_2}\right) + n_2\left(n_1 - 2\right)\right]2\sum_{i=0}^{\theta}\binom{\theta}{i}$$
$$\left[M_1^{\theta-i}(G)\overline{M_1}^{i+1}(H) + \left(M_1^{\gamma-i}(G) + \overline{M_1}^{\gamma-i}(G)\right) + \overline{M_1}^{i+1}(H)\left(M_1{}^{\gamma-i}(G) + \overline{M_1}^{\gamma-i}(G)\right)\right] \tag{5}$$
$$+ \overline{M_1}^{\theta-i}(G)M_1^i(H) + M_1^{\gamma-i}(G)\left(M_1^i(H) + \overline{M_1}^i(H)\right) + \overline{M_1}^{\gamma-i}(G)\left(M_1^i(H) + \overline{M_1}^i(H)\right),$$

where $\gamma = \theta - 1$.

Proof. Using equation (2), we have

$$\overline{M}^{\gamma}G_{+R}H = \sum_{(y_1,y_2)\,(z_1,z_2)\notin EG_{+R}H}\left[d^{\theta}(y_1,z_1) + d^{\theta}(y_2,z_2)\right],$$
$$\overline{M}_1^{\gamma}(G_{+R}H) = \sum_{z_1,z_2\in H}\left[\sum_{y_1,y_2\in(V(R(G)-G)}\left[d^{\theta}_{G_{+R}H}(y_1,z_1) + d^{\theta}_{G_{+R}H}(y_2,z_2)\right] + \sum_{y_1,y_2\in V_G}\left[d^{\theta}_{G_{+R}H}(y_1,z_1) + d^{\theta}_{G_{+R}H}(y_2,z_2)\right]\right. \tag{6}$$
$$\left. + \sum_{y_1,y_2\in V(R(G_1))y_1\in V(G_1)y_2\in V(R(G)-G)}\left[d^{\theta}_{G_{+R}H}(y_1,z_1) + d^{\theta}_{G_{+R}H}(y_2,z_2)\right]\right]$$
$$= \sum A + \sum B + \sum C.$$

Using equation 4, we directly have

$$\sum A = 2^{\theta}\left(n_2^2e_1^2 - n_2e_1\right),$$
$$\sum B = \sum B_1 + \sum B_2 + \sum B_3 + \sum B_4 + \sum B_5,$$
$$\sum B_1 = \sum_{y\in V(G)}\sum_{z_1z_2\notin E(H)}\left[d^{\theta}_{G_{+R}H}(y,z_1) + d^{\theta}_{G_{+R}H}(y,z_2)\right]$$
$$= \sum_{y\in V(G)}\sum_{z_1z_2\notin E(H)}\sum_{i=0}^{\theta}\binom{\theta}{i}\left[2d_G^{\theta-i}(y)d_H^i(z_1) + 2d_G^{\theta-i}(y)d_H^i(z_2)\right]$$
$$= 2\sum_{y\in V(G)}\sum_{z_1z_2\notin E(H)}\sum_{i=0}^{\theta}\binom{\theta}{i}d_G^{\theta-i}(y)\left[d_H^i(z_1) + d_H^i(z_2)\right] = 2\sum_{i=0}^{\theta}\binom{\theta}{i}M_1^{\theta-i}(G)\overline{M_1}^{i+1}(H),$$
$$\sum B_2 = \sum_{y_1y_2\in E(G)}\sum_{z_1z_2\in E(H)}\left[d^{\theta}_{G_{+R}H}(y_1,z_1) + d^{\theta}_{G_{+R}H}(y_2,z_2)\right]$$
$$= \sum_{y_1y_2\in E(G)}\sum_{z_1z_2\in E(H)}\sum_{i=0}^{\theta}\binom{\theta}{i}\left[2d_G^{\theta-i}(y_1)d_H^i(z_1) + 2d_G^{\theta-i}(y_2)d_H^i(z_2)\right] = 2\sum_{i=0}^{\theta}\binom{\theta}{i}M_1^{\gamma-i}(G)M_1^{i+1}(H),$$
$$\sum B_3 = \sum_{y_1y_2\notin E(G)}\sum_{z_1z_2\in E(H)}\left[d^{\theta}_{G_{+R}H}(y_1,z_1) + d^{\theta}_{G_{+R}H}(y_2,z_2)\right]$$
$$= \sum_{y_1y_2\notin E(G)}\sum_{z_1z_2\in E(H)}\sum_{i=0}^{\theta}\binom{\theta}{i}\left[2d_G^{\theta-i}(y_1)d_H^i(z_1) + 2d_G^{\theta-i}(y_2)d_H^i(z_2)\right] = 2\sum_{i=0}^{\theta}\binom{\theta}{i}\overline{M_1}^{\gamma-i}(G)M_1^{i+1}(H),$$
$$\sum B_4 = \sum_{y_1y_2\in E(G)}\sum_{z_1z_2\notin E(H)}\left[d^{\theta}_{G_{+R}H}(y_1,z_1) + d^{\theta}_{G_{+R}H}(y_2,z_2)\right]$$
$$= \sum_{y_1y_2\in E(G)}\sum_{z_1z_2\notin E(H)}\sum_{i=0}^{\theta}\binom{\theta}{i}\left[2d_G^{\theta-i}(y_1)d_H^i(z_1) + 2d_G^{\theta-i}(y_2)d_H^i(z_2)\right] = 2\sum_{i=0}^{\theta}\binom{\theta}{i}M_1^{\gamma-i}(G)\overline{M_1}^{i+1}(H),$$

$$\begin{aligned}
\sum B_5 &= \sum_{y_1y_2\notin E(G)}\sum_{z_1z_2\notin E(H)}\left[d^{\theta}_{G_{+R}H}(y_1,z_1)+d^{\theta}_{G_{+R}H}(y_2,z_2)\right]\\
&= \sum_{y_1y_2\notin E(G)}\sum_{z_1z_2\notin E(H)}\sum_{i=0}^{\theta}\binom{\theta}{i}\left[2d_G^{\theta-i}(y_1)d_H^{i}(z_1)+2d_G^{\theta-i}(y_2)d_H^{i}(z_2)\right]=2\sum_{i=0}^{\theta}\binom{\theta}{i}\overline{M_1}^{\gamma-i}(G)\overline{M_1}^{i+1}(H),\\
\sum B &= 2\sum_{i=0}^{\theta}\binom{\theta}{i}\left[M_1^{\theta-i}(G)\overline{M_1}^{i+1}(H)+\left(M_1^{\gamma-i}(G)+\overline{M_1}^{\gamma-i}(G)\right)+\overline{M_1}^{i+1}(H)\left(M_1^{\gamma-i}(G)+\overline{M_1}^{\gamma-i}(G)\right)\right],\\
\sum C &= \sum C_1+\sum C_2+\sum C_3+\sum C_4+\sum C_5,\\
\sum C_1 &= \sum_{y_1y_2\notin E\left(R(G)y_1\in V(G)y_2\in V(R(G)-G)\right.}\sum_{z\in H}\left[d^{\theta}_{G_{+R}H}(y_1,z)+d^{\theta}_{G_{+R}H}(y_2,z)\right]\\
&= \sum_{y_1y_2\notin E\left(R(G)y_1\in V(G)y_2\in V(R(G)-G)\right.}\sum_{z\in H}\sum_{i=0}^{\theta}\binom{\theta}{i}\left[2d_G^{\theta-i}(y_1)d_H^{i}(z)+2^{\theta}\right]\\
&= 2\sum_{i=0}^{\theta}\binom{\theta}{i}\overline{M_1}^{\theta-i}(G)M_1^{i}(H)+2^{\theta}n_2e_1(n_1-2),\\
\sum C_2 &= \sum_{y_1y_2\in E\left(R(G)y_1\in V(G)y_2\in V(R(G)-G)\right.}\sum_{z_1z_2\in E(H)}\left[d^{\theta}_{G_{+R}H}(y_1,z_1)+d^{\theta}_{G_{+R}H}(y_2,z_2)\right]\\
&= \sum_{y_1y_2\in E\left(R(G)y_1\in V(G)y_2\in V(R(G)-G)\right.}\sum_{z_1z_2\in E(H)}\sum_{i=0}^{\theta}\binom{\theta}{i}\left[2d_G^{\theta-i}(y_1)d_H^{i}(z_1)+2^{\theta}\right]\\
\sum C_3 &= \sum_{y_1y_2\in E\left(R(G)y_1\in V(G)y_2\in V(R(G)-G)\right.}\sum_{z_1z_2\notin E(H)}\left[d^{\theta}_{G_{+R}H}(y_1,z_1)+d^{\theta}_{G_{+R}H}(y_2,z_2)\right]\\
&= \sum_{y_1y_2\in E\left(R(G)y_1\in V(G)y_2\in V(R(G)-G)\right.}\sum_{z_1z_2\notin E(H)}\sum_{i=0}^{\theta}\binom{\theta}{i}\left[2d_G^{\theta-i}(y_1)d_H^{i}(z_1)+2^{\theta}\right]\\
\sum C_4 &= \sum_{y_1y_2\notin E\left(R(G)y_1\in V(G)y_2\in V(R(G)-G)\right.}\sum_{z_1z_2\in E(H)}\left[d^{\theta}_{G_{+R}H}(y_1,z_1)+d^{\theta}_{G_{+R}H}(y_2,z_2)\right]\\
&= \sum_{y_1y_2\notin E\left(R(G)y_1\in V(G)y_2\in V(R(G)-G)\right.}\sum_{z_1z_2\in E(H)}\sum_{i=0}^{\theta}\binom{\theta}{i}\left[2d_G^{\theta-i}(y_1)d_H^{i}(z_1)+2^{\theta}\right]\\
\sum C_5 &= \sum_{y_1y_2\notin E\left(R(G)y_1\in V(G)y_2\in V(R(G)-G)\right.}\sum_{z_1z_2\notin E(H)}\left[d^{\theta}_{G_{+R}H}(y_1,z_1)+d^{\theta}_{G_{+R}H}(y_2,z_2)\right]\\
&= \sum_{y_1y_2\notin ER(G)y_1\in V(G)y_2\in V(R(G)-G)}\sum_{z_1z_2\notin E(H)}\sum_{i=0}^{\theta}\binom{\theta}{i}\left[2d_G^{\theta-i}(y_1)d_H^{i}(z_1)+2^{\theta}\right]\\
\sum C &= 2\sum_{i=0}^{\theta}\binom{\theta}{i}\left[\overline{M_1}^{\theta-i}(G)M_1^{i}(H)+M_1^{\gamma-i}(G)\left(M_1^{i}(H)+\overline{M_1}^{i}(H)\right)+\overline{M_1}^{\gamma-i}(G)\left(M_1^{i}(H)+\overline{M_1}^{i}(H)\right)\right]\\
&\quad+2^{\theta}e_1\left[2n_1\left(e_2+\overline{e_2}\right)+n_2\left(n_1-2\right)\right].
\end{aligned}\tag{7}$$

We arrived at desired result by putting the values in equation (6). □

Theorem 3. *Let* $G_{+Q}H$ *be Q-sum graph; then, its first general Zagreb co-index is given as*

$$\begin{aligned}\overline{M}_1^{\gamma}\left(G_{+Q}H\right) = &+4^{\theta}n_2e_1\left(n_1-2\right)+4e_1\left(n_1+2\right)\left(e_2+\overline{e_2}\right)\\&\cdot\sum_{i=0}^{\theta}\binom{\theta}{i}\Big[M_1^{\theta-i}(G)\overline{M_1}^{i+1}(H)+M_1^{\gamma-i}(G)M_1^{i}(H)+M_1^{i+1}(H)\left(M_1^{\gamma-i}(G)+\overline{M_1}^{\gamma-i}(G)\right)\\&+\overline{M_1}^{i+1}(H)\left(M_1^{\gamma-i}(G)+\overline{M_1}^{\gamma-i}(G)\right)+M_1^{i}(H)\left(\overline{M_1}^{\theta-i}(G)+M_1^{\gamma-i}(G)\right)\\&+M_1^{\gamma-i}(G)\overline{M_1}^{i}(H)+\overline{M_1}^{\gamma-i}(G)\left(M_1^{i}(H)+\overline{M_1}^{i}(H)\right)\Big]+\alpha_1,\end{aligned} \tag{8}$$

where $\gamma=\theta-1$.

Proof. Using equation (2), we have

$$\begin{aligned}\overline{M}^{\gamma}\left(G_{+Q}H\right) &= \sum_{\left(y_1,y_2\right)\left(z_1,z_2\right)\notin E\left(G_{+Q}H\right.}\left[d^{\theta}\left(y_1,z_1\right)+d^{\theta}\left(y_2,z_2\right)\right],\\ \overline{M}_1^{\gamma}\left(G_{+Q}H\right) &= \sum_{z_1,z_2\in H}\Bigg[\sum_{y_1,y_2\in(V(Q(G)-G)}\left[d^{\theta}_{G_{+S}H}\left(y_1,z_1\right)+d^{\theta}_{G_{+Q}H}\left(y_2,z_2\right)\right]+\sum_{y_1,y_2\in V_G}\left[d^{\theta}_{G_{+Q}H}\left(y_1,z_1\right)+d^{\theta}_{G_{+Q}H}\left(y_2,z_2\right)\right]\\&\quad+\sum_{y_1,y_2\in V(S(G))y_1\in V(G)y_2\in V(Q(G)-G)}\left[d^{\theta}_{G_{+Q}H}\left(y_1,z_1\right)+d^{\theta}_{G_{+Q}H}\left(y_2,z_2\right)\right]\Bigg]\\&=\sum A+\sum B+\sum C,\\ \sum A &= \sum_{y_1,y_2\in V(Q(G)-G)}\sum_{z_1,z_2\in V_{G_2}}\left[d^{\theta}_{G_{+Q}H}\left(y_1,z_1\right)+d^{\theta}_{G_{+Q}H}\left(y_2,z_2\right)\right]=\alpha_1.\end{aligned} \tag{9}$$

Using equation 4, we directly have

$$\begin{aligned}\sum B &= \sum_{i=0}^{\theta}\binom{\theta}{i}\Big[M_1^{\theta-i}(G)\overline{M_1}^{i+1}(H)+M_1^{\gamma-i}(G)M_1^{i}(H)+M_1^{i+1}(H)\left(M_1^{\gamma-i}(G)+\overline{M_1}^{\gamma-i}(G)\right)\\&\quad+\overline{M_1}^{i+1}(H)\left(M_1^{\gamma-i}(G)+\overline{M_1}^{\gamma-i}(G)\right)\Big],\\ \sum C &= \sum C_1+\sum C_2+\sum C_3+\sum C_4+\sum C_5,\\ \sum C_1 &= \sum_{y_1y_2\notin E(Q(G)y_1\in V(G)y_2\in V(Q(G)-G)}\sum_{z\in H}\left[d^{\theta}_{G_{+Q}H}\left(y_1,z\right)+d^{\theta}_{G_{+Q}H}\left(y_2,z\right)\right]\\&= \sum_{y_1y_2\notin E(Q(G)y_1\in V(G)y_2\in V(Q(G)-G)}\sum_{z\in H}\sum_{i=0}^{\theta}\binom{\theta}{i}\left[d_G^{\theta-i}\left(y_1\right)d_H^{i}(z)+4^{\theta}\right]\\&= \sum_{i=0}^{\theta}\binom{\theta}{i}\overline{M_1}^{\theta-i}(G)M_1^{i}(H)+4^{\theta}n_2e_1\left(n_1-2\right),\\ \sum C_2 &= \sum_{y_1y_2\in E(Q(G)y_1\in V(G)y_2\in V(Q(G)-G)}\sum_{z_1z_2\in E(H)}\left[d^{\theta}_{G_{+Q}H}\left(y_1,z_1\right)+d^{\theta}_{G_{+Q}H}\left(y_2,z_2\right)\right]\\&= \sum_{y_1y_2\in E(Q(G)y_1\in V(G)y_2\in V(Q(G)-G)}\sum_{z_1z_2\in E(H)}\sum_{i=0}^{\theta}\binom{\theta}{i}\left[d_G^{\theta-i}\left(y_1\right)d_H^{i}\left(z_1\right)+2^{\theta}\right]=\sum_{i=0}^{\theta}\binom{\theta}{i}M_1^{\gamma-i}(G)M_1^{i}(H)+4^{\theta+2}e_1e_2,\end{aligned}$$

$$\sum C_3 = \sum_{y_1y_2\in E(Q(G)y_1\in V(G)y_2\in V(Q(G)-G)}\ \sum_{z_1z_2\notin E(H)}\left[d^{\theta}_{G_{+Q}H}(y_1,z_1)+d^{\theta}_{G_{+Q}H}(y_2,z_2)\right]$$
$$= \sum_{y_1y_2\in E(Q(G)y_1\in V(G)y_2\in V(Q(G)-G)}\ \sum_{z_1z_2\notin E(H)}\sum_{i=0}^{\theta}\binom{\theta}{i}\left[d^{\theta-i}_{G}(y_1)d^{i}_{H}(z_1)+2^{\theta}\right]=\sum_{i=0}^{\theta}\binom{\theta}{i}M_1^{\gamma-i}(G)\overline{M_1}^{i}(H)+4^{\theta+2}e_1\overline{e_2},$$
$$\sum C_4 = \sum_{y_1y_2\notin E(Q(G)y_1\in V(G)y_2\in V(Q(G)-G)}\ \sum_{z_1z_2\in E(H)}\left[d^{\theta}_{G_{+Q}H}(y_1,z_1)+d^{\theta}_{G_{+Q}H}(y_2,z_2)\right]$$
$$= \sum_{y_1y_2\notin E(Q(G)y_1\in V(G)y_2\in V(Q(G)-G)}\ \sum_{z_1z_2\in E(H)}\sum_{i=0}^{\theta}\binom{\theta}{i}\left[d^{\theta-i}_{G}(y_1)d^{i}_{H}(z_1)+4^{\theta}\right]=\sum_{i=0}^{\theta}\binom{\theta}{i}\overline{M_1}^{\gamma-i}(G)M_1^{i}(H)+4^{\theta+1}e_1e_2(n_1-2),$$
$$\sum C_5 = \sum_{y_1y_2\notin E(Q(G)y_1\in V(G)y_2\in V(Q(G)-G)}\ \sum_{z_1z_2\notin E(H)}\left[d^{\theta}_{G_{+Q}H}(y_1,z_1)+d^{\theta}_{G_{+Q}H}(y_2,z_2)\right]$$
$$= \sum_{y_1y_2\notin E(Q(G)y_1\in V(G)y_2\in V(Q(G)-G)}\ \sum_{z_1z_2\notin E(H)}\sum_{i=0}^{\theta}\binom{\theta}{i}\left[d^{\theta-i}_{G}(y_1)d^{i}_{H}(z_1)+4^{\theta}\right]=\sum_{i=0}^{\theta}\binom{\theta}{i}\overline{M_1}^{\gamma-i}(G)\overline{M_1}^{i}(H)+4^{\theta+1}e_1\overline{e_2}(n_1-2),$$
$$\sum C = \sum_{i=0}^{\theta}\binom{\theta}{i}\left[M_1^{i}(H)\left(\overline{M_1}^{\theta-i}(G)+M_1^{\gamma-i}(G)\right)+M_1^{\gamma-i}(G)\overline{M_1}^{i}(H)+\overline{M_1}^{\gamma-i}(G)\left(M_1^{i}(H)+\overline{M_1}^{i}(H)\right)\right]$$
$$+4^{\theta}\left[n_2e_1(n_1-2)+4e_1(n_1+2)(e_2+\overline{e_2})\right]. \tag{10}$$

We arrived at desired result by putting the values in equation (9). ☐

Theorem 4. *Let $G_{+T}H$ be T-sum graph; then, its first general Zagreb co-index is given as*

$$\overline{M}_1^{\gamma}(G_{+T}H)=4^{\theta}\left(n_2^2e_1^2-n_2e_1\right)+2\sum_{i=0}^{\theta}\binom{\theta}{i}\Big[M_1^{\theta-i}(G)\overline{M_1}^{i+1}(H)+\left(M_1^{\gamma-i}(G)+\overline{M_1}^{\gamma-i}(G)\right)$$
$$+\overline{M_1}^{i+1}(H)\left(M_1^{\gamma-i}(G)+\overline{M_1}^{\gamma-i}(G)\right)\overline{M_1}^{\theta-i}(G)M_1^{i}(H)+M_1^{\gamma-i}(G)\left(M_1^{i}(H)+\overline{M_1}^{i}(H)\right)$$
$$+\overline{M_1}^{\gamma-i}(G)\left(M_1^{i}(H)+\overline{M_1}^{i}(H)\right)\Big]+4^{\theta}\left[n_2e_1(n_1-2)+4e_1(n_1+2)(e_2+\overline{e_2})\right], \tag{11}$$

where $\gamma=\theta-1$.

Proof. Using equation (2), we have

$$\overline{M}_1^{\gamma}(G_{+T}H)=\sum_{(y_1,y_2)(z_1,z_2)\notin E(G_{+T}H}\left[d^{\theta}(y_1,z_1)+d^{\theta}(y_2,z_2)\right],$$
$$\overline{M}_1^{\gamma}(G_{+T}H)=\sum_{z_1,z_2\in H}\Bigg[\sum_{y_1,y_2\in(V(T(G)-V(G))}\left[d^{\theta}_{G_{+S}H}(y_1,z_1)+d^{\theta}_{G_{+T}H}(y_2,z_2)\right]+\sum_{y_1,y_2\in V_G}\left[d^{\theta}_{G_{+T}H}(y_1,z_1)+d^{\theta}_{G_{+T}H}(y_2,z_2)\right]$$
$$+\sum_{y_1,y_2\in V(S(G))y_1\in V(G)y_2\in V(T(G)-G)}\left[d^{\theta}_{G_{+T}H}(y_1,z_1)+d^{\theta}_{G_{+T}H}(y_2,z_2)\right]\Bigg]$$
$$=\sum A+\sum B+\sum C. \tag{12}$$

Using equation 9, we directly have

$$\sum A = 4^{\theta}\left(n_2^2 e_1^2 - n_2 e_1\right). \tag{13}$$

The value $\sum A$ and $\sum B$ are by equations (7) and (9) asfollows:

$$\begin{aligned}
\sum C &= \sum C_1 + \sum C_2 + \sum C_3 + \sum C_4 + \sum C_5,\\
\sum C_1 &= \sum_{y_1 y_2 \notin E(T(G) y_1 \in V(G) y_2 \in V(T(G)-G)} \sum_{z \in H} \left[d^{\theta}_{G_{+T}H}(y_1, z) + d^{\theta}_{G_{+T}H}(y_2, z)\right]\\
&= \sum_{y_1 y_2 \notin E(T(G) y_1 \in V(G) y_2 \in V(T(G)-G)} \sum_{z \in H} \sum_{i=0}^{\theta} \binom{\theta}{i} \left[2 d_G^{\theta-i}(y_1) d_H^i(z) + 4^{\theta}\right]\\
&= 2 \sum_{i=0}^{\theta} \binom{\theta}{i} \overline{M_1}^{\theta-i}(G) M_1^i(H) + 4^{\theta} n_2 e_1 (n_1 - 2),\\
\sum C_2 &= \sum_{y_1 y_2 \in E(T(G) y_1 \in V(G) y_2 \in V(T(G)-G)} \sum_{z_1 z_2 \in E(H)} \left[d^{\theta}_{G_{+T}H}(y_1, z_1) + d^{\theta}_{G_{+T}H}(y_2, z_2)\right]\\
&= \sum_{y_1 y_2 \in E(T(G) y_1 \in V(G) y_2 \in V(T(G)-G)} \sum_{z_1 z_2 \in E(H)} \sum_{i=0}^{\theta} \binom{\theta}{i} \left[2 d_G^{\theta-i}(y_1) d_H^i(z_1) + 4^{\theta}\right],\\
\sum C_3 &= \sum_{y_1 y_2 \in E(T(G) y_1 \in V(G) y_2 \in V(T(G)-G)} \sum_{z_1 z_2 \notin E(H)} \left[d^{\theta}_{G_{+T}H}(y_1, z_1) + d^{\theta}_{G_{+T}H}(y_2, z_2)\right]\\
&= \sum_{y_1 y_2 \in E(T(G) y_1 \in V(G) y_2 \in V(T(G)-G)} \sum_{z_1 z_2 \notin E(H)} \sum_{i=0}^{\theta} \binom{\theta}{i} \left[2 d_G^{\theta-i}(y_1) d_H^i(z_1) + 4^{\theta}\right]\\
&= 2 \sum_{i=0}^{\theta} \binom{\theta}{i} M_1^{\gamma-i}(G) \overline{M_1}^i(H) + 4^{\theta+2} e_1 \overline{e_2},\\
\sum C_4 &= \sum_{y_1 y_2 \notin E(T(G) y_1 \in V(G) y_2 \in V(T(G)-G)} \sum_{z_1 z_2 \in E(H)} \left[d^{\theta}_{G_{+T}H}(y_1, z_1) + d^{\theta}_{G_{+T}H}(y_2, z_2)\right]\\
&= \sum_{y_1 y_2 \notin E(T(G) y_1 \in V(G) y_2 \in V(T(G)-G)} \sum_{z_1 z_2 \in E(H)} \sum_{i=0}^{\theta} \binom{\theta}{i} \left[2 d_G^{\theta-i}(y_1) d_H^i(z_1) + 4^{\theta}\right]\\
&= 2 \sum_{i=0}^{\theta} \binom{\theta}{i} \overline{M_1}^{\gamma-i}(G) M_1^i(H) + 4^{\theta+1} e_1 e_2 (n_1 - 2),\\
\sum C_5 &= \sum_{y_1 y_2 \notin E(T(G) y_1 \in V(G) y_2 \in V(T(G)-G)} \sum_{z_1 z_2 \notin E(H)} \left[d^{\theta}_{G_{+T}H}(y_1, z_1) + d^{\theta}_{G_{+T}H}(y_2, z_2)\right]\\
&= \sum_{y_1 y_2 \notin E(T(G) y_1 \in V(G) y_2 \in V(T(G)-G)} \sum_{z_1 z_2 \notin E(H)} \sum_{i=0}^{\theta} \binom{\theta}{i} \left[2 d_G^{\theta-i}(y_1) d_H^i(z_1) + 4^{\theta}\right]\\
&= 2 \sum_{i=0}^{\theta} \binom{\theta}{i} \overline{M_1}^{\gamma-i}(G) \overline{M_1}^i(H) + 4^{\theta+1} e_1 \overline{e_2} (n_1 - 2).
\end{aligned} \tag{14}$$

By substituting the values of $\sum A$, $\sum b$, and $\sum C$ in equation (12), we obtained required proof. □

4. Conclusion

The study of the basic or factor graphs is an interesting problem in the theory of graphs where the original graphs becomes complex. In this study, we have computed FGZ co-index of graphs under operations such as $\overline{M}_1(G_{+S}H)$, $\overline{M}_1(G_{+R}H)$, $\overline{M}_1(G_{+Q}H)$, and $\overline{M}_1(G_{+T}H)$ in the terms of indices and co-indices of their basic or factor graphs.

Data Availability

The data used to support the findings of the study are included within article. However, for more details of the data can be obtained from the corresponding author.

Conflicts of Interest

The authors declare no conflicts of interest.

Authors' Contributions

Muhammad Javaid and Uzma Ahmad contributed to the discussion of the problem, validation of results, final reading, and supervision; Muhammad Ibraheem contributed to the source of the problem, the collection of material, analyzing and computing the results, and initial drafting of the study; Ebenezer Bonyah and Shaohui Wang contributed to the discussion of the problem, the methodology, and the proofreading of the final draft.

References

[1] G. Rücker and C. Rücker, "On topological indices, boiling points, and cycloalkanes," *Journal of Chemical Information and Computer Sciences*, vol. 39, no. 5, pp. 788–802, 1999.

[2] H. González-Diaz, S. Vilar, L. Santana, and E. Uriarte, "Medicinal chemistry and bioinformatics - current trends in drugs discovery with networks topological indices," *Current Topics in Medicinal Chemistry*, vol. 7, no. 10, pp. 1015–1029, 2007.

[3] A. R. Matamala and E. Estrada, "Generalised topological indices: optimisation methodology and physico-chemical interpretation," *Chemical Physics Letters*, vol. 410, pp. 343–347, 2005.

[4] K. Xu, M. Liu, K. C. Das, I. Gutman, and B. Furtula, "A survey on graphs extremal with respect to distance-based topological indices," *Match Communications in.Mathematical and in Computer Chemistry*, vol. 71, no. 3, pp. 461–508, 2014.

[5] H. Wiener, "Structural determination of paraffin boiling points," *Journal of the American Chemical Society*, vol. 69, no. 1, pp. 17–20, 1947.

[6] I. Gutman and N. Trinajstić, "Graph theory and molecular orbitals. Total φ-electron energy of alternant hydrocarbons," *Chemical Physics Letters*, vol. 17, no. 4, pp. 535–538, 1972.

[7] S. Zhang and H. Zhang, "Unicyclic graphs with the first three smallest and largest first general Zagreb index," *Match Communications in.Mathematical and in Computer Chemistry*, vol. 55, no. 20, pp. 427–438, 2006.

[8] L. Bedratyuk and O. Savenko, "The star sequence and the general first zagreb index," *Match Communications in.Mathematical and in Computer Chemistry*, vol. 72, 2017.

[9] A. R. Ashrafi, T. Došlić, and A. Hamzeh, "The Zagreb coindices of graph operations," *Discrete Applied Mathematics*, vol. 158, no. 15, pp. 1571–1578, 2010.

[10] A. R. Ashrafi, T. Došlic, and A. Hamzeh, "Extremal graphs with respect to the Zagreb coindices," *Match Communications in Mathematical and in Computer Chemistry*, vol. 65, no. 1, pp. 85–92, 2011.

[11] K. C. Das, N. Akgunes, M. Togan, A. Yurttas, I. N. Cangul, and A. S. Cevik, "On the first Zagreb index and multiplicative Zagreb coindices of graphs," *"Analele Universitatii""Ovidius""Constanta - Seria Matematica"*, vol. 24, no. 1, pp. 153–176, 2016.

[12] T. Mansour and C. Song, "The a and (a, b) analogs of zagreb indices and coindices of graphs," *International Journal of Combinatorics*, vol. 2012, Article ID 909285, 10 pages, 2012.

[13] H. Hua and S. Zhang, "Relations between Zagreb coindices and some distance-based topological indices," *Match Communications in Mathematical and in Computer Chemistry*, vol. 68, no. 1, pp. 199–208, 2012.

[14] I. Gutman, B. Furtula, Z. K. Vukicevic, and G. Popivoda, "On Zagreb indices and coindices," *Match Communications in.Mathematical and in Computer Chemistry*, vol. 74, no. 1, pp. 5–16, 2015.

[15] I. Gutman, "On coindices of graphs and their complements," *Applied Mathematics and Computation*, vol. 305, pp. 161–165, 2017.

[16] W. Yan, B.-Y. Yang, and Y.-N. Yeh, "The behavior of wiener indices and polynomials of graphs under five graph decorations," *Applied Mathematics Letters*, vol. 20, no. 3, pp. 290–295, 2007.

[17] M. Eliasi and B. Taeri, "Four new sums of graphs and their wiener indices," *Discrete Applied Mathematics*, vol. 157, no. 4, pp. 794–803, 2009.

[18] D. Sarala, H. Deng, C. Natarajan, and S. K. Ayyaswamy, "F index of graphs based on four new operations related to the strong product," *AKCE International Journal of Graphs and Combinatorics*, vol. 14, pp. 1–13. In press, 2018.

[19] M. Ibraheem, M. M. Aljohani, M. Javaid, and A. M. Alanazi, "Forgotten coindex for the derived sum graphs under cartesian product," *Journal of Chemistry*, vol. 202113 pages, Article ID 3235068, 2021.

[20] J. B. Liu, S. Javed, M. Javaid, and K. Shabbir, "Computing first general zagreb index of operations on graphs," *IEEE Access*, vol. 7, pp. 47494–47502, 2017.

[21] M. Javaid, M. Ibraheem, U. Ahmad, and J. B. Liu, "Sharp bounds of first Zagreb coindex for-sum graphs," *Journal of Mathematics*, vol. 202119 pages, Article ID 9984412, 2021.

[22] M. Javaid, U. Ali, and J. B. Liu, "Computing analysis for first zagreb connection index and coindex of resultant graphs," *Mathematical Problems in Engineering*, vol. 202119 pages, Article ID 6019517, 2021.

Hindawi
Journal of Mathematics
Volume 2022, Article ID 8521810, 9 pages
https://doi.org/10.1155/2022/8521810

Research Article

Cordial and Total Cordial Labeling of Corona Product of Paths and Second Order of Lemniscate Graphs

Ashraf ELrokh[1] **Mohammed M. Ali Al-Shamiri**[2,3] **Shokry Nada**[1] **and Atef Abd El-hay**[1,4]

[1]*Mathematics and Computer Science Department, Faculty of Science Menoufia University, Menoufia, Egypt*
[2]*Department of Mathematics, Faculty of Science and Arts, Muhayl Asser King Khalid University, Abha, Saudi Arabia*
[3]*Department of Mathematics and Computer, Faculty of Science, Ibb University, Ibb, Yemen*
[4]*Faculty of Computer and Artificial Intelligence, Modern University for Technology and Information, Cairo, Egypt*

Correspondence should be addressed to Atef Abd El-hay; atef_1992@yahoo.com

Received 19 October 2021; Revised 7 February 2022; Accepted 23 March 2022; Published 5 May 2022

Academic Editor: M. T. Rahim

Copyright © 2022 Ashraf ELrokh et al. This is an open access article distributed under the Creative Commons Attribution License, which permits unrestricted use, distribution, and reproduction in any medium, provided the original work is properly cited.

A simple graph is called cordial if it admits 0-1 labeling that satisfies certain conditions. The second order of lemniscate graph is a graph of two second order of circles that have one vertex in common. In this paper, we introduce some new results on cordial labeling, total cordial, and present necessary and sufficient conditions of cordial and total cordial for corona product of paths and second order of lemniscate graphs.

1. Introduction

Labelling methods are used for a wide range of applications in different subjects including coding theory, computer science, and communication networks. Graph labeling is an assignment of positive integers on vertices or edges or both of them which fulfilled certain conditions. Hundreds of research studies have been working with different types of labeling graphs [1–11], and a reference for this purpose is the survey written by Gallian [7]. All graphs considered, in this theme, are finite, simple, and undirected. The original concept of cordial graphs is due to Cahit [2]. He proved the following: each tree is cordial; a complete graph K_n is cordial if and only if $n \leq 3$ and a complete bipartite graph $K_{n,m}$ is cordial for all positive integers n and m [3]. Let $G = (V, E)$ be a graph, and let $f\colon V \longrightarrow \{0, 1\}$ be a labeling of its vertices, and let the induced edge labeling $f^* E \longrightarrow \{0, 1\}$ be given by $f^*(uv) = (f(u) + f(v))(\mathrm{mod} 2)$, where $e = uv (\in E)$ and $u, v \in V$. Let v_0 and v_1 be the numbers of vertices that are labeled by 0 and 1, respectively, and let e_0 and e_1 be the corresponding numbers of edges. Such a labeling is called cordial if both $|v_0 - v_1| \leq 1$ and $|e_0 - e_1| \leq 1$ hold. A graph is called cordial if it admits a cordial labeling. As an extension of the cordial labeling, we define a total cordial labeling of a graph G with vertex set and edge set as an cordial labeling such that number of vertices and edges labeled with 0 and the number of vertices and edges labeled with 1 differ by at most 1, i.e., $|(v_0 + e_0) - (e_1 + v_1)| \leq 1$. A graph with a total cordial labeling is called a total cordial graph. If the vertices of the graph are assigned values subject to certain conditions, it is known as graph labeling. Following three are the common features of any graph labeling problem: (1) a set of numbers from which vertex labels are assigned; (2) a rule that assigns a value to each edge; and (3) a condition that these values must satisfy.

A path with n vertices and $n - 1$ edges is denoted by P_n, and a cycle with n vertices and n edges is denoted by C_n [12]. The second power of a lemniscate graph is defined as the union of two second power of cycles where both have a common vertex; it is denoted by $L^2_{n,m} \equiv C^2_n \sharp C^2_m$ [13]. Obviously, $L^2_{n,m}$ has $n + m - 1$ vertices and $2n + 2m - 4$ edges. The corona product $G_1 \odot G_2$ of two graphs G_i (with n_i vertices and m_i edges), $i = 1, 2$, is the graph obtained by taking one copy of G_1 and n_1 copies of G_2 and then joining the i^{th} vertex of G_1 with an edge to every vertex in the i^{th} copy of G_2. It is easy to show that $G_1 \odot G_2$ has $n_1 (1 + n_2)$ vertices and $m_1 + n_1m_2 + n_1n_2$ edges [7, 14–18]. In this paper, we study the cordial and total cordial of the corona product $P_k \odot L^2_{n,m}$ of paths and second power of lemniscate graphs and show that this is cordial and total cordial for all positive integers k, n, m. The rest of the paper is organized as follows. In Section 1, brief summary of definitions that are useful for the present investigations is presented. Terminologies and notations are introduced in Section 2. The main result is presented in Section 3. Finally, the conclusion of this paper is introduced.

2. Terminology and Notation

Given a path or a cycle with $4r$ vertices, let L_{4r} denote the labeling 0011... 0011 (repeated r-times) and let $L^{'}_{4r}$ denote the labeling 1100... 1100 (repeated r times). The labeling 1001 1001... 1001 (repeated r times) and 0110... 0110 (repeated r times) is denoted by S_{4r} and $S^{'}_{4r}$. Let M_{2r} denote the labeling 0101 . . . 01, zero-one repeated r–times if r is even and 0101...010 if r is odd. Sometimes, we modify labeling by adding symbols at one end or the other (or both). If G and H are two graphs, where G has n vertices, the labeling of the corona $G \odot H$ is often denoted by $[A\colon B_1, B_2, B_3, \ldots, B_n]$, where A is the labeling of the n vertices of G, and B_i, $1 \le i \le n$, is the labeling of the vertices of the copy of H that is connected to the i^{th} vertex of G. For a given labeling of the corona $G \odot H$, we denote v_i and e_i $(i = 0, 1)$ to represent the numbers of vertices and edges, respectively, labeled by i. Let us denote x_i and a_i to be the numbers of vertices and edges labeled by i for the graph G. Also, we let y_i and b_i be those for H, which are connected to the vertices labeled 0 of G. Likewise, let $y^{'}_i$ and $b^{'}_i$ be those for H, which are connected to the vertices labeled 1 of G. It is easily to verify that $v_0 = x_0 + x_0y_0 + x_1y^{'}_0$, $v_1 = x_1 + x_0y_1 + x_1y^{'}_1$, $e_0 = a_0 + x_0b_0 + x_1b^{'}_0 + x_0y_1 + x_1y^{'}_0$, and $e_1 = a_1 + x_0b_1 + x_1b^{'}_1 + x_0y_0 + x_1y^{'}_1$. Thus, $v_0 - v_1 = (x_0 - x_1) + x_0(y_0 - y_1) + x_1(y^{'}_0 - y^{'}_1)$ and $e_0 - e_1 = (a_0 - a_1) + x_0(b_0 - b_1) + x_1(b^{'}_0 - b^{'}_1) + x_0(y_0 - y_1) - x_1(y^{'}_0 - y^{'}_1)$. In particular, if we have only one labeling for all copies of H, i.e., $y_i = y^{'}_i$ and $b_i = b^{'}_i$, then $v_0 = x_0 + ny_0$, $v_1 = x_1 + ny_1$, $e_0 = a_0 + nb_0 + x_0y_1 + x_1y_0$, and $e_1 = a_1 + nb_1 + x_0y_0 + x_1y_1$. Thus, $v_0 - v_1 = (x_0 - x_1) + n(y_0 - y_1)$ and $e_0 - e_1 = (a_0 - a_1) + n(b_0 - b_1) + (x_1 - x_0)(y_0 - y_1)$, where n is the order of G. Figure 1 illustrates the condition cordial and total cordial labeling of $P_3 \odot L_{3,7}$.

3. Results and Discussion

In this section, we show that the corona product of paths and second power of lemniscate graphs, $P_k \odot L^2_{n,m}$, is cordial and also total cordial for all $k \ge 1$, $n, m \ge 3$.

Throughout our proofs, the way of labeling $L^2_{n,m}$ starts always from a vertex that next the common vertex and go further opposite to this common vertex. Before considering the general form of the final result, let us first prove it in the following specific case. Our main theorem is as follows.

Theorem 1. *The corona product of paths and second power of lemniscate graphs, $P_k \odot L^2_{n,m}$, is cordial and also total cordial for all $k \ge 1$, $n, m \ge 3$.*

In order to prove this theorem, we will introduce a number of lemmas as follows.

Lemma 1. *$P_k \odot L^2_{3,m}$ is cordial and total cordial for all $k \ge 1$ and $m \ge 3$.*

Proof

Case 1. When $m \ge 3$ and $k = 2r$, $r \ge 1$, one can choose the labeling $[M_{2r}; 00100, 11011, \ldots, (r - \text{times})]$ for $P_{2r} \odot L^2_{3,3}$. Therefore, $x_0 = x_1 = r, a_0 = 0, a_1 = 2r - 1$, $y_0 = 4, y_1 = 1, b_0 = 2, b_1 = 4, y^{'}_0 = 1, y^{'}_1 = 4, b^{'}_0 = 2$, and $b^{'}_1 = 4$. Hence, $|v_0 - v_1| = 0$, $|e_0 - e_1| = 1$ and $|(v_0 + e_0) - (e_1 + v_1)| = 1$. Thus, $P_{2r} \odot L^2_{3,3}$, $r \ge 1$, is cordial and total cordial.

Case 2. When $m \ge 3$ and $k = 2r + 1$, $r \ge 0$, one can choose the labeling $[M_{2r+1}; 00100, 11011, 00100, 11011, \ldots, (\text{r} - \text{times}), 11100]$ for $P_{2r+1} \odot L^2_{3,3}$. Therefore, $x_0 = r + 1, x_1 = r, a_0 = 0, a_1 = 2r, y_0 = 4, y_1 = 1, b_0 = 2, b_1 = 4, y^{'}_0 = 1, y^{'}_1 = 4, b^{'}_0 = 2, b^{'}_1 = 4, y^{*}_0 = 2, y^{*}_1 = 3, b^{*}_0 = 4$, and $b^{*}_1 = 2$, where y^{*}_i and b^{*}_i are the numbers of vertices and edges labeled i in $L^2_{3,3}$ that are connected to the last zero in P_{4r+3}. Consequently, it is easy to show that $|v_0 - v_1| = 0$, $|e_0 - e_1| = 1$, and $|(v_0 + e_0) - (e_1 + v_1)| = 1$. Thus, $P_{2r+1} \odot L^2_{3,3}$, $r \ge 0$, is cordial and total cordial.

Case 3. When $m \equiv 0 (\text{mod} 4)$ and $k \equiv 0 (\text{mod} 4)$, that means, $k = 4r, r \ge 1$ and $m = 4t$, $t > 1$, then the labeling $[L_{4r}; 0_31_3M_{4t-4}, 0_31_3M_{4t-4}, 01L_4M^{'}_{4t-4}, 01L_4M^{'}_{4t-4}, \ldots, (r - \text{times})]$ for $P_{4r} \odot L^2_{3,4t}$ can be applied. Therefore, $x_0 = x_1 = 2r, a_0 = 2r, a_1 = 2r - 1, y_0 = y_1 = 2t + 1, b_0 = 4t + 1, b_1 = 4t, y^{'}_0 = y^{'}_1 = 2t + 1, b^{'}_0 = 4t$, and $b^{'}_1 = 4t + 1$. So, $|v_0 - v_1| = 0$, $|e_0 - e_1| = 1$, and $|(v_0 + e_0) - (e_1 + v_1)| = 1$. For the case $P_{4r} \odot L^2_{3,4}$, the labeling $[L_{4r}; 0_31_3, 0_31_3, 01L_4, 01L_4, \ldots, (r - \text{times})]$ is sufficient and thus $P_{4r} \odot L^2_{3,4t}$ is cordial and also total cordial.

Case 4. When $m \equiv 0 (\text{mod} 4)$ and $k \equiv 1 (\text{mod} 4)$ that means$k = 4r + 1, r \ge 0$ and $m = 4t$, $t > 1$, then the labeling $[L_{4r}0; 0_31_3M_{4t-4}, 0_31_3M_{4t-4}, 01L_4M^{'}_{4t-4}, 01L_4M^{'}_{4t-4}, \ldots, (r - \text{times}), 0_3L_3M_{4t-4}]$ for $P_{4r+1} \odot L^2_{3,4t}$ is considered. Therefore, $x_0 = 2r + 1, x_1 = 2r, a_0 = a_1 = 2r, y_0 = y_1 = 2t + 1, b_0 = 4t + 1, b_1 = 4t, y^{'}_0 = y^{'}_1 = 2t + 1, b^{'}_0 = 4t$, and $b^{'}_1 = 4t + 1$. Hence, $|v_0 - v_1| = 1$, $|e_0 - e_1| = 1$, and $|(v_0 + e_0) - (e_1 + v_1)| = 0$. For the case $P_{4r+1} \odot L^2_{3,4}$, the labeling $[L_{4r}0; 0_31_3, 0_31_3, 01L_4, 01L_4, \ldots, (r - \text{times}), 1_30_3]$ is sufficient and thus $P_{4r+1} \odot L^2_{3,4t}$ is cordial and total cordial.

Case 5. When $m \equiv 0 (\text{mod} 4)$ and $k \equiv 2 (\text{mod} 4)$ that means $k = 4r + 2, r \ge 0$, and $m = 4t$, $t > 1$, then the labeling $[L_{4r}10; 0_31_3M_{4t-4}, 0_31_3M_{4t-4}, 01L_4M^{'}_{4t-4}, 01L_4M^{'}_{4t-4}, \ldots, (r - \text{times}), 01L_4M^{'}_{4t-4}, 0_31_3M_{4t-4}]$ for $P_{4r+2} \odot L^2_{3,4t}$ is applied. Therefore, $x_0 = x_1 = 2r + 1, a_0 = 2r + 1, a_1 = 2r, y_0 = y_1 = 2t + 1, b_0 = 4t + 1, b_1 = 4t$, $y^{'}_0 = y^{'}_1 = 2t + 1, b^{'}_0 = 4t$, and $b^{'}_1 = 4t + 1$. So, $|v_0 - v_1| = 0$, $|e_0 - e_1| = 1$, and $|(v_0 + e_0) - (e_1 + v_1)| = 1$. For the case $P_{4r+2} \odot L^2_{3,4}$, the labeling $[L_{4r}10; 0_31_3, 0_31_3, 01L_4, 01L_4, \ldots, (r - \text{times}), 01L_4, 0_31_3]$ is sufficient and thus $P_{4r+2} \odot L^2_{3,4t}$ is cordial and total cordial.

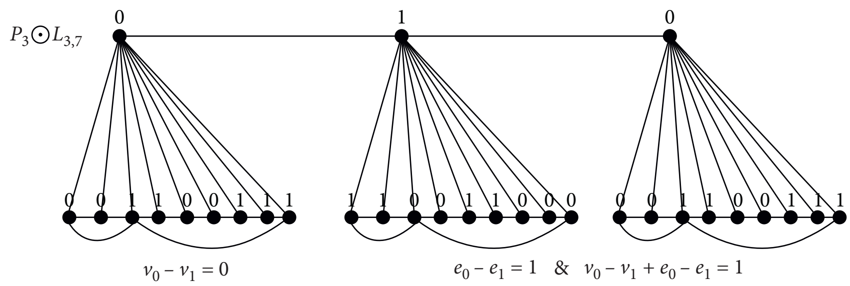

Figure 1: Cordial and total cordial labeling of $P_3 \odot L_{3,7}$.

Case 6. When $m \equiv 0 (\text{mod} 4)$ and $k \equiv 3 (\text{mod} 4)$ that means $k = 4r + 3, r \geq 0$ and $m = 4t$, $t > 1$, then one can select the labeling $[L_{4r}001; 0_3 1_3 M_{4t-4}, 0_3 1_3\ M_{4t-4}, 01L_4 M'_{4t-4}, 01L_4 M'_{4t-4}, \ldots, (r-\text{times}), 0_3 1_3 M_{4t-4}, 0_3 1_3 M_{4t-4}, 01L_4 M'_{4t-4}]$ for $P_{4r+3} \odot L^2_{3,4t}$.

Therefore, $x_0 = 2r + 2, x_1 = 2r + 1, a_0 = a_1 = 2r + 1, y_0 = y_1 = 2t + 1, b_0 = 4t + 1, b_1 = 4t, y'_0 = y'_1 = 2t + 1, b'_0 = 4t$, and $b'_1 = 4t + 1$. Hence, one can easily show that $|v_0 - v_1| = 1$, $|e_0 - e_1| = 1$ and $|(v_0 + e_0) - (e_1 + v_1)| = 0$. For the case $P_{4r+3} \odot L^2_{3,4}$, the labeling $[L_{4r}001; 0_3 1_3, 0_3 1_3, 01L_4, 01L_4 \ldots, (r-\text{times})]$ is sufficient and thus $P_{4r+3} \odot L^2_{3,4t}$ is cordial and total cordial.

Case 7. When $m \equiv 1 (\text{mod} 4)$ and $k \equiv 0 (\text{mod} 4)$ that means $k = 4r, r \geq 1$ and $m = 4t + 1$, $t > 1$, then one can choose the labeling $[L_{4r}; 101L'_4 0M'_{4t-6}0, 101\ L'_4 0M'_{4t-6}0, 010L_4 1M_{4t-6}1, 010L_4 1M_{4t-6}1, \ldots, (r-\text{times})]$ for $P_{4r} \odot L^2_{3,4t+1}$. Therefore, $x_0 = x_1 = 2r, a_0 = 2r, a_1 = 2r - 1, y_0 = 2t + 1, y_1 = 2t + 2, b_0 = 4t + 2, b_1 = 4t + 1, y'_0 = 2t + 2, y'_1 = 2t + 1, b'_0 = 4t + 2$, and $b'_1 = 4t + 1$. Hence, one can easily show that $|v_0 - v_1| = 0, |e_0 - e_1| = 1$ and $|(v_0 + e_0) - (e_1 + v_1)| = 1$. For the special case $P_{4r} \odot L^2_{3,5}$, the labeling $[L_{4r}; 01L'_4 0, 01L'_4 0, 10L_4 1, 10L_4 1, \ldots, (r-\text{times})]$ is sufficient and thus $P_{4r} \odot L^2_{3,4t+1}$ is cordial and total cordial.

Case 8. When $m \equiv 1 (\text{mod} 4)$ and $k \equiv 1 (\text{mod} 4)$ that means $k = 4r + 1, r \geq 0$ and $m = 4t + 1$, $t > 1$, then one can select the labeling $[L_{4r}0; 101L'_4 0M'_{4t-6}0, 101L'_4 0 M'_{4t-6}0, 010L_4 1M_{4t-6}1, 010L_4 1M_{4t-6}1, \ldots, (r-\text{times}), 101L'_4 1M'_{4t-6}1]$ for $P_{4r+1} \odot L^2_{3,4t+1}$. Therefore, $x_0 = 2r + 1, x_1 = 2r, a_0 = a_1 = 2r, y_0 = 2t + 1, y_1 = 2t + 2, b_0 = 4t + 2, b_1 = 4t + 1, y'_0 = 2t + 2, y'_1 = 2t + 1, b'_0 = 4t + 2$, and $b'_1 = 4t + 1$. So, $|v_0 - v_1| = 0$, $|e_0 - e_1| = 0$ and $|(v_0 + e_0) - (e_1 + v_1)| = 0$. For the special case $P_{4r+1} \odot L^2_{3,5}$, the labeling $[L'_{4r}0; 01L'_4 0, 01 L'_4 0, 10L_4 1, 10L_4 1, \ldots, (r-\text{times}), 10L_4 1]$ is sufficient and thus $P_{4r+1} \odot L^2_{3,4t+1}$ is cordial and total cordial.

Case 9. When $m \equiv 1 (\text{mod} 4)$ and $k \equiv 2 (\text{mod} 4)$ that means $k = 4r + 2, r \geq 0$ and $m = 4t + 1$, $t > 1$, then the labeling $[L_{4r}10; 101L'_4 0M'_{4t-6}0, 101\ L'_4 0M'_{4t-6}\ 0, 010\ L_4 1M_{4t-6}1, 010L_4 1M_{4t-6}1, \ldots, (r-\text{times}), 010\ L_4 1 M_{4t-6}0, 101L'_4 0M'_{4t-6}1]$ for $P_{4r+2} \odot L^2_{3,4t+1}$ can be applied. Therefore, $x_0 = 2r + 1, x_1 = 2r + 1, a_0 = 2r + 1, a_1 = 2r, y_0 = 2t + 1, y_1 = 2t + 2, b_0 = 4t + 2, b_1 = 4t + 1, y'_0 = 2t + 2, y'_1 = 2t + 1, b'_0 = 4t + 2$, and $b'_1 = 4t + 1$. Hence, $|v_0 - v_1| = 0$, $|e_0 - e_1| = 1$ and $|(v_0 + e_0) - (e_1 + v_1)| = 1$. For the special case $P_{4r+2} \odot L^2_{3,5}$, the labeling $[L_{4r}10; 01L'_4 0, 01L'_4 0, 10L_4 1, 10L_4 1, \ldots, (r-\text{times}), 10L_4 1, 01L'_4 0]$ is sufficient and thus $P_{4r+2} \odot L^2_{3,4t+1}$ is cordial and also total cordial.

Case 10. When $m \equiv 1 (\text{mod} 4)$ and $k \equiv 3 (\text{mod} 4)$ that means $k = 4r + 3, r \geq 0$ and $m = 4t + 1$, $t > 1$, then take the labeling $[L_{4r}0_2 1; 101L'_4 0M'_{4t-6}0, 101\ L'_4 0M'_{4t-6}\ 0, 010L_4\ 1M_{4t-6}1, 010L_4 1M_{4t-6}1, \ldots, (r-\text{times}), 101L'_4 0M'_{4t-6}1, 101L'_4 0M'_{4t-6}1, , 010L_4 1M_{4t-6}0]$ for $P_{4r+3} L^2_{3,4t+1}$. Therefore, $x_0 = 2r + 2, x_1 = 2r + 1, a_0 = a_1 = 2r + 1, y_0 = 2t + 1, y_1 = 2t + 2, b_0 = 4t + 2, b_1 = 4t + 1, y'_0 = 2t + 2, y'_1 = 2t + 1, b'_0 = 4t + 2$, and $b'_1 = 4t + 1$. Hence, $|v_0 - v_1| = 0$, $|e_0 - e_1| = 0$, and $|(v_0 + e_0) - (e_1 + v_1)| = 0$. For the special case $P_{4r+3} \odot L^2_{3,5}$, the labeling $[L_{4r}0_2 1; 01L'_4 0, 01L'_4 0, 10\ L_4 1, 10L_4 1, \ldots, (r-\text{times}), 01L'_4 0, 10L_4 1, 10L_4 1]$ is sufficient and thus $P_{4r+3} \odot L^2_{3,4t+1}$ is cordial and total cordial.

Case 11. When $m \equiv 2 (\text{mod} 4)$ and k even that means $m = 4t + 2$, $t > 1$, and $k = 2r, r \geq 1$, then by taking the labeling $[M_{2r}; 0_2 1L'_4 0M'_{4t-4}, 1_2 0\ L_4 1M_{4t-4}, \ldots, (r-\text{times})]$ for $P_{2r} \odot L^2_{3,4t+2}$, therefore $x_0 = x_1 = r, a_0 = 0, a_1 = 2r - 1$, $y_0 = 2t + 3, y_1 = 2t + 1, b_0 = 4t + 2, b_1 = 4t + 3, y'_0 = 2t + 1, y'_1 = 2t + 3, b'_0 = 4t + 2$, and $b'_1 = 4t + 3$. Hence, $|v_0 - v_1| = 0$, $|e_0 - e_1| = 1$ and $|(v_0 + e_0) - (e_1 + v_1)| = 1$. For the case $P_{2r} \odot L^2_{3,6}$, the labeling $[M_{2r}; 0_2 L'_4 01, 1_2 L_4 10, \ldots, (r-\text{times})]$ is sufficient and thus $P_{2r} \odot L^2_{3,6}$ is cordial and total cordial.

*Case 12.*When $m \equiv 2 (\text{mod} 4)$ and k odd that means $m = 4t + 2, t > 1$, and $k = 2r + 1, r \geq 1$, then the labeling $[M_{2r+1}; 0_2 1L'_4 0M'_{4t-4}, 1_2 0L_4 1M_{4t-4}, \ldots, (r-\text{times}), 010\ L_4 1M_{4t-4}]$ for $P_{2r+1} \odot L^2_{3,4t+2}$ is considered. Therefore, $x_0 = r + 1, x_1 = r, a_0 = 0, a_1 = 2r, y_0 = 2t + 3, y_1 = 2t + 1, b_0 = 4t + 2, b_1 = 4t + 3, y'_0 = 2t + 1, y'_1 = 2t + 3, b'_0 = 4t + 2$ and $b'_1 = 4t + 3$. So, $|v_0 - v_1| = 1$, $|e_0 - e_1| = 1$, and $|(v_0 + e_0) - (e_1 + v_1)| = 0$. For the case $P_{2r+1} \odot L^2_{3,6}$, the labeling $[M_{2r+1}; 0_2 L'_4 01, 1_2 L_4 10, \ldots, (r-\text{times}), 01L_4 10]$ is sufficient and thus $P_{2r+1} \odot L^2_{3,6}$ is cordial and total cordial.

Case 13. When $m \equiv 3 (\text{mod} 4)$ and $k \equiv 0 (\text{mod} 4)$ that means $m = 4t + 3$, $t \geq 1$, and $k = 4r, r \geq 1$, then the labeling $[L_{4r}; 0_2 M'_{4t+3}, 0_2 M'_{4t+3}, 1_2 M_{4t+3}, 1_2 M_{4t+3}, \ldots, (r-\text{times})]$ for $P_{4r} \odot L^2_{3,4t+3}$ can be applied. Therefore, $x_0 = x_1 = 2r, a_0 = 2r,\quad a_1 = 2r - 1, y_0 = 2t + 3, y$

$_1 = 2t+2, b_0 = 4t+3, b_1 = 4t+4, y_0' = 2t+2, y_1' = 2t+3, b_0{}' = 4t+3$, and $b_1' = 4t+4$. Hence, $|v_0 - v_1| = 0$, $|e_0 - e_1| = 1$, and $|(v_0+e_0) - (e_1+v_1)| = 1$. Thus, $P_{4r} \odot L^2_{3,4t+3}$ is cordial and total cordial.

Case 14. When $m \equiv 3 (\mathrm{mod} 4)$ and $k \equiv 1 (\mathrm{mod} 4)$ that means $m = 4t+3, t \geq 1$, and $k = 4r+1, r \geq 0$, then one can select the labeling $[L_{4r}^{'}0; 1_2M_{4t+3}, 1_2M_{4t+3}, 0_2M_{4t+3}^{'}, 0_2M_{4t+3}^{'}, \ldots, (r-\text{times}), 1_2M_{4t+3}]$ for $P_{4r+1} \odot L^2_{3,4t+3}$. Therefore, $x_0 = 2r+1, x_1 = 2r, a_0 = 2r+1, a_1 = 2r-1, y_0 = 2t+3, y_1 = 2t+2, b_0 = 4t+3, b_1 = 4t+4, y_0' = 2t+2, y_1' = 2t+3, b_0' = 4t+3, b_1' = 4t+4, y_0^* = 2t+2, y_1^* = 2t+3, b_0^* = 4t+3$, and $b_1^* = 4t+4$. So, $|v_0 - v_1| = 0$, $|e_0 - e_1| = 0$, and $|(v_0+e_0) - (e_1+v_1)| = 0$. Thus, $P_{4r+1} \odot L^2_{3,4t+3}$ is cordial and total cordial.

Case 15. When $m \equiv 3 (\mathrm{mod} 4)$ and $k \equiv 2 (\mathrm{mod} 4)$ that means $m = 4t+3, t > 1$, and $k = 4r+2, r \geq 0$, then one can take the labeling $[L_{4r}10; 0_31_3M_{4t-4}, 0_31_3M_{4t-4}, 01L_4M_{4t-4}^{'}, 01L_4M_{4t-4}^{'}, \ldots, (r-\text{times}), 01L_4M_{4t-4}^{'}, 0_31_3 M4t-4]$ for $P_{4r+2} \odot L^2_{3,4t}$. Therefore, $x_0 = x_1 = 2r+1, a_0 = 2r+1, a_1 = 2r, y_0 = 2t+3, y_1 = 2t+2, b_0 = 4t+3, b_1 = 4t+4, y_0' = 2t+2, y_1' = 2t+3, b_0' = 4t+3$, and $b_1' = 4t+4$. Hence, $|v_0 - v_1| = 0$, $|e_0 - e_1| = 1$, and $|(v_0+e_0) - (e_1+v_1)| = 1$. Thus, $P_{4r+2} \odot L^2_{3,4t+3}$ is cordial and total cordial.

Case 16. When $m \equiv 3 (\mathrm{mod} 4)$ and $k \equiv 3 (\mathrm{mod} 4)$ that means$m = 4t+3, t \geq 1$, and $k = 4r+1, r \geq 0$, then one can choose the labeling $[L_{4r}100; 0_2M_{4t+3}^{'}, 0_2M_{4t+3}^{'}, 1_2M_{4t+3}, 1_2M_{4t+3}, \ldots, (r-\text{times}), 1_2 M_{4t+3}, 0_2M_{4t+3}^{'}, 1_2M_{4t+3}]$ for $P_{4r+3} \odot L^2_{3,4t+3}$.

Therefore, $x_0 = 2r+2, x_1 = 2r+1, a_0 = 2r+2, a_1 = 2r, y_0 = 2t+3, y_1 = 2t+2, b_0 = 4t+3, b_1 = 4t+4, y_0' = 2t+2, y_1' = 2t+3, b_0' = 4t+3, b_1' = 4t+4, y_0^* = 2t+2, y_1^* = 2t+3, b_0^* = 4t+3$, and $b_1^* = 4t+4$. Hence, $|v_0 - v_1| = 0$, $|e_0 - e_1| = 0$, and $|(v_0+e_0) - (e_1+v_1)| = 0$. Thus, $P_{4r+3} \odot L^2_{3,4t+3}$ is cordial and total cordial. □

Lemma 2. *$P_k \odot L^2_{n,m}$ is cordial and total cordial for all $k \geq 1$ and $m > 6$.*

Proof. Let $k = 4r + i^{'}$ ($i^{'} = 0,1,2,3$ and $r \geq 1$) or $k = 2r + j^{'}$ ($j^{'} = 0,1$ and $r \geq 1$), $n = 4s + i$ and $m = 4t + j$ ($i, j = 1,2,3$ and $s, t \geq 2$), then we may use the labeling $A_{i^{'}}$ or $A_{j^{'}}$ for P_k as given in Table 1. For a given value of j with $1 \leq i, j \leq 3$, we may use one of the labeling in the set $\{B_{ij}, B_{ij}^{'}\}$ for $L_{n,m}$, where B_{ij} and $B_{ij}^{'}$ are the labeling of $L^2_{n,m}$ which are connected to the vertices labeled 0 in P_k, while B_{ij} and $B_{ij}^{'}$ are the labeling of P_m which are connected to the vertices labeled 1 in P_k as given in Table 2. Using Table 3 and the formulas $v_0 - v_1 = (x_0 - x_1) + x_0.(y_0 - y_1) + x_1.(y_0' - y_1')$, $e_0 - e_1 = (a_0 - a_1) + x_0.(b_0 - b_1) + x_1.(b_0' - b_1') + x_0.(y_0 - y_1) - x_1.(y_0' - y_1')$, and $(v_0 + e_0) - (e_1 + v_1) = (x_0 - x_1) + 2x_0. (y_0 - y_1) + (a_0 - a_1) + x_0.(b_0 - b_1) + x_1.(b_0' - b_1')$, we can compute the values shown in the last two columns of Table 3. We see that $P_k \odot L^2_{n.m}$ is isomorphic to $P_k \odot L^2_{m,n}$. Since all of these values are 1 or 0, the lemma follows. □

Lemma 3. *$P_k \odot L^2_{4,m}$ is cordial and total cordial for all $k \geq 1$ and $m > 3$.*

Proof

Case 1. When $m \equiv 0 (\mathrm{mod} 4)$ and $k = r, r \geq 1$ that means $m = 4t, t > 1$, and $k = r, r \geq 1$. Then, take the labeling $[1_r; 100L_4M_{4t-4}^{'}, \ldots, (r-\textit{times})]$ for $P_r \odot L^2_{4,4t}$. Therefore, $x_0 = 0, x_1 = r, a_0 = r-1, a_1 = 0, y_0' = 2t+2, y_1' = 2t+1, b_0' = 4t+2$, and $b_1' = 4t+2$. Hence, $|v_0 - v_1| = 0$, $|e_0 - e_1| = 1$, and $|(v_0+e_0) - (e_1+v_1)| = 1$. For the case $P_r \odot L^2_{4,4}$, the labeling $[1_r; 0_31_30, \ldots, (r-\textit{times})]$ is sufficient and thus $P_r \odot L^2_{4,4t}$, $r \geq 1$, is cordial and total cordial.

Case 2. When $m \equiv 1 (\mathrm{mod} 4)$ and $k \equiv 0 (\mathrm{mod} 4)$ that means $m = 4t+1, t > 1$, and $k = 4r, r \geq 1$, then the labeling $[S_{4r}; 10_3L_41M_{4t-6}1, 10_3L_41M_{4t-6}1, 10_3L_4 1M_{4t-6}1, 10_3L_41M_{4t-6}1, \ldots, (r-\textit{times})]$ for $P_{4r} \odot L^2_{4,4t+1}$ is applied. Therefore, $x_0 = x_1 = 2r, a_0 = 2r-1, a_1 = 2r, y_0 = 2t+2, y_1 = 2t+2, b_0 = b_1 = 4t+3, y_0' = 2t+2, y_1' = 2t+2, b_0' = 4t+3$, and $b_1' = 4t+3$. So, $|v_0 - v_1| = 0$, $|e_0 - e_1| = 1$, and $|(v_0+e_0) - (e_1+v_1)| = 1$. For the case $P_{4r} \odot L^2_{4,5}$, the labeling $[S_{4r}; 10_2L_41, 10_2L_41, 10_2L_41, 10_2L_41, \ldots, (r-\textit{times})]$ is sufficient and thus $P_{4r} \odot L^2_{4,4t+1}$ is cordial and total cordial.

Case 3. When $m \equiv 1 (\mathrm{mod} 4)$ and $k \equiv 1 (\mathrm{mod} 4)$ that means $m = 4t+1, t > 1$, and $k = 4r+1, r \geq 0$, then one can select the labeling $[S_{4r}0; 10_3L_41M_{4t-6}1, 10_3L_41M_{4t-6}1, 10_3L_41M_{4t-6}1, 10_3L_41M_{4t-6}1, \ldots, (r-\textit{times}), 10_3L_41M_{4t-6}1]$ for $P_{4r+1} \odot L^2_{4,4t+1}$. Therefore, $x_0 = 2r+1, x_1 = 2r, a_0 = a_1 = 2r, y_0 = 2t+2, y_1 = 2t+2, b_0 = b_1 = 4t+3, y_0' = 2t+2, y_1' = 2t+2, b_0' = 4t+3$, and $b_1' = 4t+3$. So, $|v_0 - v_1| = 1$. $|e_0 - e_1| = 0$, and $|(v_0+e_0) - (e_1+v_1)| = 1$. For the case $P_{4r+1} \odot L^2_{4,5}$, the labeling $[S_{4r}0; 10_2L_41, 10_2L_41, 10_2L_41, 10_2L_41, \ldots, (r-\textit{times}), 10_2L_41]$ is sufficient and thus $P_{4r+1} \odot L^2_{4,4t+1}$ is cordial and total cordial.

Case 4. When $m \equiv 1 (\mathrm{mod} 4)$ and $k \equiv 2 (\mathrm{mod} 4)$ that means $m = 4t+1, t > 1$, and $k = 4r+2, r \geq 0$, then the labeling $[S_{4r}01; 10_3L_41M_{4t-6}1, 10_3L_41M_{4t-6}1, 10_3L_41M_{4t-6}1, 10_3L_41M_{4t-6}1, \ldots, (r-\textit{times}), 10_3L_4 1M_{4t-6}1, 10_3L_41M_{4t-6}1]$ for $P_{4r+2} \odot L^2_{4,4t+1}$ is applied. Therefore, $x_0 = x_1 = 2r+1, a_0 = 2r, a_1 = 2r+1, y_0 = 2t+2, y_1 = 2t+2, b_0 = b_1 = 4t+3, y_0' = 2t+2, y_1' = 2t+2, b_0' = 4t+3$, and $b_1' = 4t+3$. Hence, $|v_0 - v_1| = 0$, $|e_0 - e_1| = 1$, and $|(v_0+e_0) - (e_1+v_1)| = 1$. For the case $P_{4r+2} \odot L^2_{4,5}$, the labeling $[S_{4r}01; 10_2L_41, 10_2L_41, 10_2L_41, 10_2L_41, \ldots, (r-\textit{times}), 10_2 L_41, 10_2L_41]$ is sufficient and thus $P_{4r+2} \odot L^2_{4,4t+1}$ is cordial and total cordial.

Case 5. When $m \equiv 1 (\mathrm{mod} 4)$ and $k \equiv 3 (\mathrm{mod} 4)$ that means and $m = 4t+1, t > 1$, and $k = 4r+3, r \geq 0$, then one can take the labeling $[S_{4r}001; 10_3L_41 M_{4t-6}1, 10_3L_41M_{4t-6}1, 10_3 L_41M_{4t-6}1, 10_3L_41 M_{4t-6}1, \ldots, (r-\textit{times}), 10_3L_41M_{4t-6}1, 10_3L_41M_{4t-6}1, 10_3L_41M_{4t-6}1]$ for $P_{4r+3} \odot L^2_{4,4t+1}$. Therefore, $x_0 = 2r+2, x_1 = 2r+1, a_0 = a_1 = 2r+1, y_0 = 2t+2, y_1 =$

Table 1: Labelling of P_k.

$K = 4r + i'$, $i' = 0, 1, 2, 3$	Labelling of P_k	x_0	x_1	a_0	a_1
$i' = 0$	$A_0 = L_{4r}$	$2r$	$2r$	$2r$	$2r - 1$
$i' = 1$	$A_1 = L_{4r}0$	$2r + 1$	$2r$	$2r$	$2r$
$i' = 2$	$A_2 = L_{4r}10$	$2r + 1$	$2r + 1$	$2r + 1$	$2r$
$i' = 3$	$A_3 = L_{4r}001$	$2r + 2$	$2r + 1$	$2r + 1$	$2r + 1$
$k = 2r + j'$, $i' = 0, 1$					
$i' = 0$	$A_4 = M_{2r}$	r	r	0	$2r - 1$
$i' = 1$	$A_5 = M_{2r+1}$	$r + 1$	r	0	$2r$

Table 2: Labelling of $L^2_{n,m}$.

$n = 4s + i$, $m = 4t + j$, $i, j = 0, 1, 2, 3$	Labelling of $L^2_{n,m}$	y_0	y_1	y_0	y_1
$i = 0$ $j = 0$	$B_{00} = L'_4$ $M_{4s-5}L'_4L'_{4t-4}$	$2s + 2t$ $+1$	$2s + 2t$ -1	$4s + 4t$ $+2$	$4s + 4t$ $+2$
$i = 0$ $j = 0$	$B'_{00} = L_4$ $M'_{4s-5}L_4M'_{4t-4}$	$2s + 2t$ -1	$2s + 2t$ $+1$	$4s + 4t$ $+2$	$4s + 4t$ $+2$
$i = 0$ $j = 1$	$B_{01} = L_4M'_{4s-5}$ $M'_{4t-6}1L'_40$	$2s + 2t$	$2s + 2t$	$4s + 4t$ -1	$4s + 4t$ -1
$i = 0$ $j = 2$	$B_{02} = L'_4M_{4s-5}$ $1L'_40M'_{4t-4}$	$2s + 2t$ $+1$	$2s + 2t$	$4s + 4t$	$4s + 4t$
$i = 0$ $j = 2$	$B'_{02} = L_4M'_{4s-5}$ $0L_41M_{4t-4}$	$2s + 2t$	$2s + 2t$ $+1$	$4s + 4t$	$4s + 4t$
$i = 0$ $j = 3$	$B_{03} = L_4$ $M'_{4s-5}M_{4t+3}$	$2s + 2t$ $+1$	$2s + 2t$ $+1$	$4s + 2t$ $+2$	$4s + 4t$ $+2$
$i = 1$ $j = 1$	$B_{11} = 1L'_40M'_{4s-6}$ $0_2M_{4t-6}0L_41$	$2s + 2t$ $+1$	$2s + 2t$	$4s + 4t$	$4s + 4t$
$i = 1$ $j = 1$	$B'_{11} = 0L_41M_{4s-6}$ $1_2M'_{4t-6}1L'_40$	$2s + 2t$	$2s + 2t$ $+1$	$4s + 4t$	$4s + 4t$
$i = 1$ $j = 2$	$B_{12} = 0L_41M_{4s-6}$ $M'_{4t-6}1L'_40$	$2s + 2t$ $+1$	$2s + 2t$ $+1$	$4s + 4t$ $+1$	$4s + 4t$ $+1$
$i = 1$ $j = 3$	$B_{13} = 1L'_40$ $M'_{4s-6}M_{4t+3}$	$2s + 2t$ $+2$	$2s + 2t$ $+1$	$4s + 4t$ $+2$	$4s + 4t$ $+2$
$i = 1$ $j = 3$	$B'_{13} = 0L_41$ $M_{4s-6}M'_{4t+3}$	$2s + 2t$ $+1$	$2s + 2t$ $+2$	$4s + 4t$ $+2$	$4s + 4t$ $+2$
$i = 2$ $j = 2$	$B_{22} = M_{4s-4}0L_41$ $L'_40M'_{4t-4}$	$2s + 2t$ $+2$	$2s + 2t$ $+1$	$4s + 4t$ $+2$	$4s + 4t$ $+2$
$i = 2$ $j = 2$	$B'_{22} = M'_{4s-4}1L'_40$ L_41M_{4t-4}	$2s + 2t$ $+1$	$2s + 2t$ $+2$	$4s + 4t$ $+2$	$4s + 4t$ $+2$
$i = 2$ $j = 3$	$B_{23} = 0L_41$ $M_{4s-5}M'_{4t+3}$	$2s + 2t$ $+2$	$2s + 2t$ $+2$	$4s + 4t$ $+3$	$4s + 4t$ $+3$
$i = 3$ $j = 3$	$B_{33} = M_{4s+2}$ M_{4t+3}	$2s + 2t$ $+2$	$2s + 2t$ $+3$	$4s + 4t$ $+3$	$4s + 4t$ $+3$
$i = 3$ $j = 3$	$B'_{33} = M_{4s+2}$ M_{4t+3}	$2s + 2t$ $+3$	$2s + 2t$ $+2$	$4s + 4t$ $+3$	$4s + 4t$ $+3$

$2t + 2$, $b_0 = b_1 = 4t + 3$, $y'_0 = 2t + 2$, $y'_1 = 2t + 2$, $b'_0 = 4t + 3$, and $b'_1 = 4t + 3$. So, $|v_0 - v_1| = 1$, $|e_0 - e_1| = 0$, and $|(v_0 + e_0) - (e_1 + v_1)| = 1$. For the case $P_{4r+3} \odot L^2_{4,5}$, the labeling $[S_{4r}01; 10_2L_41, 10_2L_41, 10_2L_41, 10_2L_41, \ldots, (r - times), 10_2L_41, 10_2L_41, 10_2L_41]$ is sufficient and thus $P_{4r+3} \odot L^2_{4,4t+1}$ is cordial and total cordial.

Case 6. When $m \equiv 2(\mathrm{mod}4)$ and k is even that means $m = 4t + 2$, $t > 1$, and $k = 2r$, $r \geq 1$. Then, one can

Table 3: Labelling of $P_k \odot L^2_{n,m}$.

i'/j'	ij	P_k	$L^2_{n,m}$	$\lvert v_0 - v_1 \rvert$	$\lvert e_0 - e_1 \rvert$	$\lvert (v_0 + e_0) - (e_1 + v_1) \rvert$
0	00	A_4	B_{00}, B'_{00}	0	1	1
1	00	A_5	$B_{00}, B'_{00}, .., B_{00}, B'_{00}, B'_{00}$	0	1	1
0	01	A_0	$B_{01}, B_{01}, B_{01}, B_{01}$	0	1	1
1	01	A_1	$B_{01}, B_{01}, B_{01}, B_{01}, \ldots, B_{01}$	1	0	1
2	01	A_2	$B_{01}, B_{01}, B_{01}, B_{01}, \ldots, B_{01}, B_{01}$	0	1	1
3	01	A_3	$B_{01}, B_{01}, B_{01} B_{01}, \ldots, B_{01}, B_{01}, B_{01}$	1	0	1
0	02	A_4	B_{02}, B'_{02}	0	1	1
1	02	A_5	$B_{02}, B'_{02}, .., B_{02}, B'_{02}, B'_{02}$	0	1	1
0	01	A_0	$B_{03}, B_{03}, B_{03}, B_{03}$	0	1	1
1	01	A_1	$B_{03}, B_{03}, B_{03}, B_{03}, \ldots, B_{03}$	1	0	1
2	01	A_2	$B_{03}, B_{03}, B_{03}, B_{03}, \ldots, B_{03}, B_{03}$	0	1	1
3	01	A_3	$B_{03}, B_{03}, B_{03}, B_{03}, \ldots, B_{03}, B_{03}, B_{03}$	1	0	1
0	11	A_4	B_{11}, B'_{11}	0	1	1
1	11	A_5	$B_{11}, B'_{11}, .., B_{11}, B'_{11}, B'_{11}$	0	1	1
0	12	A_0	$B_{12}, B_{12}, B_{12}, B_{12}$	0	1	1
1	12	A_1	$B_{12}, B_{12}, B_{12}, B_{12}, .., B_{12}$	1	0	1
2	12	A_2	$B_{12}, B_{12}, B_{12}, B_{12}, .., B_{12}, B_{12}$	0	1	1
3	12	A_3	$B_{12}, B_{12}, B_{12}, B_{12}, .., B_{12}, B_{12}, B_{12}$	1	0	1
0	13	A_4	B_{13}, B'_{13}	0	1	1
1	13	A_5	$B_{13}, B'_{13}, .., B_{13}, B'_{13}, B'_{13}$	0	1	1
0	22	A_4	B_{22}, B'_{22}	0	1	1
1	22	A_5	$B_{22}, B'_{22}, .., B_{22}, B'_{22}, B'_{22}$	0	1	1
0	23	A_0	$B_{23}, B_{23}, B_{23}, B_{23}$	0	1	1
1	23	A_1	$B_{23}, B_{23}, B_{23}, B_{23}, .., B_{23}$	1	0	1
2	23	A_2	$B_{23}, B_{23}, B_{23}, B_{23}, .., B_{23}, B_{23}$	0	1	1
3	23	A_3	$B_{23}, B_{23}, B_{23}, B_{23}, .., B_{23}, B_{23}, B_{23}$	1	0	1
0	33	A_4	B_{33}, B'_{33}	0	1	1
1	33	A_5	$B_{33}, B'_{33}, .., B_{33}, B'_{33}, B'_{33}$	0	1	1

choose the labeling $[M_{2r}; 10_3 L_4 1 M_{4t-4}, 01_3 L'_4 0 M'_{4t-4}, \ldots, (r-times)]$ for $P_{2r} \odot L^2_{4,4t+2}$. Therefore, $x_0 = x_1 = r, a_0 = 0, a_1 = 2r-1$, $y_0 = 2t+3$, $y_1 = 2t+2, b_0 = b_1 = 4t+3, y'_0 = 2t+2, y'_1 = 2t+3$, and $b'_0 = b'_1 = 4t+4$. Hence, one can easily show that $|v_0 - v_1| = 0$. $|e_0 - e_1| = 1$ and $|(v_0 + e_0) - (e_1 + v_1)| = 1$. For the special case $P_{2r} \odot L^2_{4,6}$, the labeling $[M_{2r}; 10_2 L_4 01, 01_2 L'_4 10, \ldots, (r-times)]$ is sufficient, and thus $P_{2r} \odot L^2_{4,4t+2}$, $r \geq 1$, is cordial and total cordial.

Case 7. When $m \equiv 2 (\mathrm{mod} 4)$ and k is odd that means $m = 4t+2$, $t > 1$, and $k = 2r+1$ where $r \geq 0$, then one can choose the labeling $[M_{2r+1}; 10_3 L_4 1 M_{4t-4}, 01_3 L'_4 0 M'_{4t-4}, \ldots, (r-times), 01_3 L'_4 0 M'_{4t-4}]$ for $P_{2r+1} \odot L^2_{4,4t+2}$. Therefore, $x_0 = r+1, x_1 = r, a_0 = 0, a_1 = 2r$, $y_0 = 2t+3$, $y_1 = 2t+2, b_0 = b_1 = 4t+3, y'_0 = 2t+2, y'_1 = 2t+3, b'_0 = b'_1 = 4t+4, y^*_0 = 2t+2, y^*_1 = 2t+3$, and $b^*_0 = b^*_1 = 4t+3$, where y^*_i and b^*_i are the numbers of vertices and edges labeled i in $L^2_{4,4t+2}$ that are connected to the last zero in P_{4r+3}. Consequently, it is easy to show that $|v_0 - v_1| = 0$, $|e_0 - e_1| = 1$ and $|(v_0 + e_0) - (e_1 + v_1)| = 1$. For the special case $P_{2r+1} \odot L^2_{4,6}$, the labeling $[M_{2r}; 10_2 L_4 01, 01_2 L'_4 10, \ldots, (r-times), 01_2 L'_4 10]$ is sufficient and thus $P_{2r+1} \odot L^2_{4,4t+2}$, $r \geq 0$, is cordial and total cordial.

Case 8. When $m \equiv 3 (\mathrm{mod} 4)$ and $k \equiv 0 (\mathrm{mod} 4)$ that means $m = 4t+3$, $t > 1$, and $k = 4r, r \geq 1$, then one can choose the labeling $[L_{4r}; 10_3 M_{4t} 11, 10_3 M_{4t} 11, 10_3 M_{4t} 11, 10_3 M_{4t} 11, \ldots, (r-times)]$ for $P_{4r} \odot L^2_{4,4t+3}$. Therefore, $x_0 = x_1 = 2r, a_0 = 2r-1, a_1 = 2r, y_0 = y_1 = 2t+3, b_0 = b_1 = 4t+5, y'_0 = y'_1 = 2t+3$, and $b'_0 = b'_1 = 4t+5$. Hence, one can easily show that $|v_0 - v_1| = 0$, $|e_0 - e_1| = 1$, and $|(v_0 + e_0) - (e_1 + v_1)| = 1$. Thus, $P_{4r} \odot L^2_{4,4t+3}$ is cordial and total cordial.

Case 9. When $m \equiv 3 (\mathrm{mod} 4)$ and $k \equiv 1 (\mathrm{mod} 4)$ that means $m = 4t+3$, $t > 1$, and $k = 4r+1, r \geq 0$. Then, the labeling $[L_{4r} 0; 10_3 M_{4t} 11, 10_3 M_{4t} 11, 10_3 M_{4t} 11, 10_3 M_{4t} 11, \ldots, (r-times), 10_3 M_{4t} 11]$ for $P_{4r+1} \odot L^2_{4,4t+3}$ is considered. Therefore, $x_0 = 2r+1, x_1 = 2r, a_0 = a_1 = 2r, y_0 = y_1 = 2t+3, b_0 = b_1 = 4t+5, y'_0 = y'_1 = 2t+3$, and $b'_0 = b'_1 = 4t+5$. So, $|v_0 - v_1| = 1$, $|e_0 - e_1| = 0$, and $|(v_0 + e_0) - (e_1 + v_1)| = 1$. Thus, $P_{4r+1} \odot L^2_{4,4t+3}$ is cordial and total cordial.

Case 10. When $m \equiv 3 (\mathrm{mod} 4)$ and $k \equiv 2 (\mathrm{mod} 4)$ that means $m = 4t+3$, $t > 1$, and $k = 4r+2, r \geq 0$, then one can select the labeling $[L_{4r} 01; 10_3 M_{4t} 11, 10_3 M_{4t} 11, 10_3 M_{4t} 11, 10_3 M_{4t} 11, \ldots, (r-times), 10_3 M_{4t} 11, 10_3 M_{4t} 11]$ for $P_{4r+2} \odot L^2_{4,4t+3}$. Therefore, $x_0 = x_1 = 2r+1, a_0 = 2r, a_1 = 2r+1, y_0 = y_1 = 2t+3, b_0 = b_1 = 4t+5$, $y'_0 = y'_1 = 2t+3$, and $b'_0 = b'_1 = 4t+5$. Hence, $|v_0 - v_1| = 0$, $|e_0 - e_1| = 1$, and $|(v_0 + e_0) - (e_1 + v_1)| = 1$. Thus, $P_{4r+2} \odot L^2_{4,4t+3}$ is cordial and total cordial.

Case 11. When $m \equiv 3 (\mathrm{mod} 4)$ and $k \equiv 3 (\mathrm{mod} 4)$ that means $m = 4t+3$, $t > 1$, and $k = 4r+3, r \geq 0$, then one can take the labeling $[L_{4r} 001; 10_3 M_{4t} 11, 10_3 M_{4t} 11, 10_3 M_{4t} 11, 10_3 M_{4t} 11, \ldots, (r-times)$,

$10_3M_{4t}11, 10_3M_{4t}11, 10_3M_{4t}11]$ for $P_{4r+3} \odot L^2_{4,4t+1}$. Therefore, $x_0 = 2r+2, x_1 = 2r+1, a_0 = a_1 = 2r+1$, $y_0 = y_1 = 2t+3$, $b_0 = b_1 = 4t+5, y'_0 = y'_1 = 2t+3$, and $b'_0 = b'_1 = 4t+5$. Hence, $|v_0 - v_1| = 1$, $|e_0 - e_1| = 0$, and $|(v_0+e_0) - (e_1+v_1)| = 1$. Thus, $P_{4r+3} \odot L^2_{4,4t+3}$ is cordial and also total cordial; by this, the lemma was proved. □

Lemma 4. *$P_k \odot L^2_{5,m}$ is cordial and also total cordial for all $k \geq 1$ and $m \geq 3$.*

Proof

Case 1. When $m \equiv 0 \pmod 4$ that means $m = 4t$, $t \geq 1$, since $P_k \odot L^2_{5,4}$ isomorphic to $P_k \odot L^2_{4,5}$, by Lemma 3, $P_k \odot L^2_{4,5}$ is cordial and total cordial and then $P_k \odot L^2_{5,4}$ is cordial and total cordial. Also, since $P_k \odot L^2_{5,4t}$, $t \geq 1$ isomorphic to $P_k \odot L^2_{4t,5}$, by Lemma 3, $P_k \odot L^2_{4t,5}$ is cordial and total cordial and then $P_k \odot L^2_{5,4t}$ is cordial and total cordial.

Case 2. When $m \equiv 1 \pmod 4$ and k is even that means $m = 4t+1, t \geq 1$, and $k = 2r, r \geq 1$, then one can take the labeling $[M_{2r}; L'_4 1 L'_4 0 M'_{4t-6} 0, L_4 0 L_4 1 M_{4t-6} 1, \ldots, (r - times)]$ for $P_{2r} \odot L^2_{5,4t+1}$. Therefore, $x_0 = r, x_1 = r, a_0 = 0, a_1 = 2r-1, y_0 = 2t+3, y_1 = 2t+2, b_0 = b_1 = 4t+4, y'_0 = 2t+2, y'_1 = 2t+3$, and $b'_0 = b'_1 = 4t+4$. So, $|v_0 - v_1| = 0$, $|e_0 - e_1| = 1$, and $|(v_0+e_0) - (e_1+v_1)| = 1$. For the special case $P_{2r} \odot L^2_{5,5}$, the labeling $[M_{2r}; L_4 L'_4 0, L'_4 L_4 1, \ldots, (r - times)]$ is sufficient and thus $P_{2r} \odot L^2_{5,4t+1}$, $r \geq 1$, is cordial and total cordial.

*Case 3.*When $m \equiv 1 \pmod 4$ and k is odd that means $m = 4t+1, t \geq 1$, and $k = 2r+1, r \geq 1$, then the labeling $[M_{2r+1}; L'_4 1 L'_4 0 M'_{4t-6} 0, L_4 0 L_4 1 M_{4t-6} 1, \ldots, (r - times), L_4 0 L_4 1 M_{4t-6} 1]$ for $P_{2r+1} \odot L^2_{5,4t+1}$ can be applied. Therefore, $x_0 = r+1, x_1 = r, a_0 = 0, a_1 = 2r, y_0 = 2t+3, y_1 = 2t+2, b_0 = b_1 = 4t+4, y'_0 = 2t+2, y'_1 = 2t+3 b'_0 = b'_1 = 4t+4, y^*_0 = 2t+2, y^*_1 = 2t+3$, and $b^*_0 = b^*_1 = 4t+4$, where y^*_i and b^*_i are the numbers of vertices and edges labeled i in $L_{5,4t+1}$ that are connected to the last zero in P_{2r+1}. Consequently, it is easy to show that $|v_0 - v_1| = 0$, $|e_0 - e_1| = 1$, and $|(v_0+e_0) - (e_1+v_1)| = 1$. For the special case $P_{2r+1} \odot L^2_{5,5}$, the labeling $[M_{2r+1}; L_4 L'_4 0, L'_4 L_4 1, \ldots, (r - times), L'_4 L_4 1]$ is sufficient and thus $P_{2r+1} \odot L^2_{5,4t+1}$, $r \geq 1$, is cordial and total cordial.

Case 4. When $m \equiv 2 \pmod 4$ and $k \equiv 0 \pmod 4$ that means $m = 4t+2, t \geq 1$, and $k = 4r, r \geq 1$, then one can choose the labeling $[L_{4r}; L_4 0 L_4 1 M'_{4t-4}, L_4 0 L_4 1 M'_{4t-4}, L_4 0 L_4 1 M'_{4t-4}, L_4 0 L_4 1 M'_{4t-4}, \ldots, (r - time)]$ for $P_{4r} \odot L^2_{5,4t+2}$. Therefore, $x_0 = x_1 = 2r, a_0 = 2r, a_1 = 2r-1, y_0 = y_1 = 2t+3, b_0 = b_1 = 4t+5, y'_0 = y'_1 = 2t+3$, and $b'_0 = b'_1 = 4t+5$. Consequently, it is easy to show that $|v_0 - v_1| = 0$, $|e_0 - e_1| = 1$, and $|(v_0+e_0) - (e_1+v_1)| = 1$. For the special case $P_{4r} \odot L^2_{5,6}$, the labeling $[L_4 r; L'_4 L_4 10, L'_4 L_4 10, L'_4 L_4 10, L'_4 L_4 10, \ldots, (r - time)]$ is sufficient and thus $P_{4r} \odot L^2_{5,4t+2}$ is cordial and total cordial.

Case 5. When $m \equiv 2 \pmod 4$ and $k \equiv 1 \pmod 4$ that means $m = 4t+2, t \geq 1$, and $k = 4r+1, r \geq 0$, then one can take the labeling $[L_{4r} 0; L_4 0 L_4 1 M'_{4t-4}, L_4 0 L_4 1 M'_{4t-4}, L_4 0 L_4 1 M'_{4t-4}, L_4 0 L_4 1 M'_{4t-4}, \ldots, (r - time), L_4 0 L_4 1 M'_{4t-4}]$ for $P_{4r+1} \odot L^2_{5,4t+2}$. Therefore, $x_0 = 2r+1, x_1 = 2r, a_0 = a_1 = 2r, y_0 = y_1 = 2t+3, b_0 = b_1 = 4t+5, y'_0 = y'_1 = 2t+3$, and $b'_0 = b'_1 = 4t+5$. So, $|v_0 - v_1| = 1$, $|e_0 - e_1| = 0$, and $|(v_0+e_0) - (e_1+v_1)| = 1$. For the special case $P_{4r+1} \odot L^2_{5,6}$, the labeling $[L_4 r0; L'_4 L_4 10, L'_4 L_4 10, L'_4 L_4 10, L'_4 L_4 10, \ldots, (r - time), L'_4 L_4 10]$ is sufficient and thus $P_{4r+1} \odot L^2_{5,4t+2}$ is cordial and total cordial.

Case 6. When $m \equiv 2 \pmod 4$ and $k \equiv 2 \pmod 4$ that means $m = 4t+2, t \geq 1$, and $k = 4r+2, r \geq 0$, then one can select the labeling $[L_{4r} 10; L_4 0 L_4 1 M'_{4t-4}, L_4 0 L_4 1 M'_{4t-4}, L_4 0 L_4 1 M'_{4t-4}, L_4 0 L_4 1 M'_{4t-4}, \ldots, (r - time), L_4 0 L_4 1 M'_{4t-4}, L_4 0 L_4 1 M'_{4t-4}]$ for $P_{4r+2} \odot L^2_{5,4t+2}$. Therefore, $x_0 = x_1 = 2r+1, a_0 = 2r+1, a_1 = 2r, y_0 = y_1 = 2t+3, b_0 = b_1 = 4t+5, y'_0 = y'_1 = 2t+3$, and $b'_0 = b'_1 = 4t+5$. Hence, $|v_0 - v_1| = 0$, $|e_0 - e_1| = 1$, and $|(v_0+e_0) - (e_1+v_1)| = 1$. For the special case $P_{4r+2} \odot L^2_{5,6}$, the labeling $[L_4 r10; L'_4 L_4 10, L'_4 L_4 10, L'_4 L_4 10, L'_4 L_4 10, \ldots, (r - time), L'_4 L_4 10, L'_4 L_4 10]$ is sufficient and thus $P_{4r+2} \odot L^2_{5,4t+2}$ is cordial and total cordial.

Case 7. When $m \equiv 2 \pmod 4$ and $k \equiv 3 \pmod 4$ that means $m = 4t+2, t \geq 1$, and $k = 4r+3, r \geq 0$, then the labeling $[[L_{4r} 001; L_4 0 L_4 1 M'_{4t-4}, L_4 0 L_4 1 M'_{4t-4}, L_4 0 L_4 1 M'_{4t-4}, L_4 0 L_4 1 M'_{4t-4}, \ldots, (r - time), L_4 0 L_4 1 M'_{4t-4}, L_4 0 L_4 1 M'_{4t-4}, L_4 0 L_4 1 M'_{4t-4}]$ for $P_{4r+3} \odot L^2_{5,4t+2}$ is considered. Therefore, $x_0 = 2r+2, x_1 = 2r+1, a_0 = a_1 = 2r+1, y_0 = y_1 = 2t+3, b_0 = b_1 = 4t+5, y'_0 = y'_1 = 2t+3$, and $b'_0 = b'_1 = 4t+5$. Consequently, it is easy to show that $|v_0 - v_1| = 1$, $|e_0 - e_1| = 0$, and $|(v_0+e_0) - (e_1+v_1)| = 1$. For the special case $P_{4r+3} \odot L^2_{5,6}$, the labeling $[L_4 r001; L'_4 L_4 10, L'_4 L_4 10, L'_4 L_4 10, L'_4 L_4 10, \ldots, (r - time), L'_4 L_4 10, L'_4 L_4 10, L'_4 L_4 10]$ is sufficient and thus $P_{4r+3} \odot L^2_{5,4t+2}$ is cordial and also total cordial.

Case 8. When $m \equiv 3 \pmod 4$ and k is even that means $m = 4t+3$, $t \geq 1$, and $k = 2r$ where $r \geq 1$, then the labeling $[M_{2r}; 0_3 1 M_{4t+3}, 1_3 0 M_{4t+3} \ldots, (r - times)]$ for $P_{2r} \odot L^2_{5,4t+3}$ can be applied. Therefore, $x_0 = r, x_1 = r, a_0 = 0, a_1 = 2r-1, y_0 = 2t+4, y_1 = 2t+3, b_0 = b_1 = 4t+6, y'_0 = 2t+3, y'_1 = 2t+4$, and $b'_0 = b'_1 = 4t+6$. Consequently, it is easy to show that $|v_0 - v_1| = 0$, $|e_0 - e_1| = 1$, and $|(v_0+e_0) - (e_1+v_1)| = 1$. Thus, $P_{2r} \odot L^2_{5,4t+3}$, $r \geq 1$, is cordial and total cordial.

Case 9. When $m \equiv 3 \pmod 4$ and k is odd that means $m = 4t+3$, $t \geq 1$, and $k = 2r+1$ where $r \geq 0$, then one can take the labeling $[M_{2r+1}; 0_3 1 M_{4t+3}, 1_3 0 M_{4t+3}, \ldots, (r - times), 1_3 0 M_{4t+3}]$ for $P_{2r+1} \odot L^2_{5,4t+3}$. Therefore, $x_0 = r+1, x_1 = r, a_0 = 0, a_1 = 2r$, $y_0 = 2t+3, y_1 = 2t+2$, $b_0 = b_1 = 4t+4, y'_0 = 2t+2, y'_1 = 2t+3 b'_0 = b'_1 = 4t+4, y^*_0 = 2t+3, y^*_1 = 2t+4$, and $b^*_0 = b^*_1 = 4t+6$, where y^*_i and b^*_i are the numbers of vertices and edges labeled i in $L_{5,4t+3}$ that are connected to the last zero in P_{2r+1}. So, $|v_0 - v_1| = 0$, $|e_0 - e_1| = 1$, and $|(v_0 + e_0) - (e_1 + v_1)| = 1$. Thus, $P_{2r+1} \odot L^2_{5,4t+3}$, $r \geq 1$, is cordial and total cordial, and by this, the lemma was proved. □

Lemma 5. *$P_k \odot L^2_{6,m}$ is cordial and total cordial for all m, k.*

Proof

Case 1. When $m \equiv 0\,(\text{mod}4)$, since $P_k \odot L^2_{6,4}$ is isomorphic to $P_k \odot L^2_{4,6}$ and $P_k \odot L^2_{4,6}$ is cordial and total cordial, then $P_k \odot L^2_{6,4}$ cordial and total cordial. Also, since $P_k \odot L^2_{6,4t}$ is isomorphic to $P_k \odot L^2_{4t,6}$ and $P_k \odot L^2_{4t,6}$ is cordial and total cordial, then $P_k \odot L^2_{6,4t}$ is cordial and total cordial.

Case 2. When $m \equiv 1\,(\text{mod}4)$, i.e., $m = 4t + 1$, $t \geq 1$, since $P_k \odot L^2_{6,5}$ is isomorphic to $P_k \odot L^2_{5,6}$ and $P_k \odot L^2_{4,6}$ is cordial and total cordial, then $P_k \odot L^2_{5,6}$ is cordial and total cordial. Also, since $P_k \odot L^2_{6,4t+1}$ is isomorphic to $P_k \odot L^2_{4t+1,6}$ and $P_k \odot L^2_{4t+1,6}$ is cordial and total cordial, then $P_k \odot L^2_{6,4t+1}$ is cordial and total cordial.

Case 3. When $m \equiv 2\,(\text{mod}4)$ and k is even that means $m = 4t + 2, t \geq 1$, and $k = 2r, r \geq 1$, then one can choose the labeling $[M_{2r}; L_4'01L_4'0M'_{4t-4}, L_4 10 L_4 1 M_{4t-4}, \ldots, (r - times)]$ for $P_{2r} \odot L^2_{6,4t+2}$. Therefore, $x_0 = r, x_1 = r, a_0 = 0, a_1 = 2r - 1, y_0 = 2t + 4, y_1 = 2t + 3, b_0 = b_1 = 4t + 6, y_0' = 2t + 3, y_1' = 2t + 4$, and $b_0' = b_1' = 4t + 6$. Consequently, it is easy to show that $|v_0 - v_1| = 0$ and $|e_0 - e_1| = 1$. For the special case $P_{2r} \odot L^2_{6,6}$, the labeling $[M_{2r}; L_4'0L_4'01, L_4 1 L_4 10, \ldots, (r - times)]$ is sufficient and thus $P_{2r} \odot L^2_{6,4t+2}$, $r \geq 1$, is cordial and also total cordial.

Case 4. When $m \equiv 2\,(\text{mod}4)$ and k is odd that means $m = 4t + 2$, $t \geq 1$, and $k = 2r + 1$, $r \geq 0$, then one can choose the labeling $[M_{2r+1}; L_4'01L_4'0M'_{4t-4}, L_4 10 L_4 1 M_{4t-4}, \ldots, (r - times), L_4 10 L_4 1 M_{4t-4}]$ for $P_{2r+1} \odot L^2_{6,4t+2}$. Therefore, $x_0 = r + 1, x_1 = r, a_0 = 0, a_1 = 2r, y_0 = 2t + 2t + 1, y_1 = 2s + 2t$, $b_0 = b_1 = 4s + 4t, y_0 = 2t + 4, y_1 = 2t + 3, b_0 = b_1 = 4t + 6$, $y_0' = 2t + 3, y_1' = 2t + 4, b_0' = b_1' = 4t + 6, y_0^* = 2t + 3$, $y_1^* = 2t + 4$, and $b_0^* = b_1^* = 4t + 6$, where y_i^* and b_i^* are the numbers of vertices and edges labeled i in $L^2_{6,4t+2}$ that are connected to the last zero in P_{2r+1}. So, $|v_0 - v_1| = 0$, $|e_0 - e_1| = 1$, and $|(v_0 + e_0) - (e_1 + v_1)| = 1$. For the special case $P_{2r+1} \odot L^2_{6,6}$, the labeling $[M_{2r+1}; L_4'0L_4'01, L_4 1 L_4 10, \ldots, (r - times), L_4 1 L_4 10]$ is sufficient and thus $P_{2r+1} \odot L^2_{6,4t+2}$, $r \geq 1$, is cordial and total cordial.

Case 5. When $m \equiv 3\,(\text{mod}4)$ and $k \equiv 0\,(\text{mod}4)$ that means $m = 4t + 3$, $t \geq 1$, and $k = 4r$, $r \geq 1$, then the labeling $[L_{4r}; L_4 1 M_{4t+3}, L_4 1 M_{4t+3}, L_4 1 M_{4t+3}, L_4 1 M_{4t+3}, \ldots, (r - time)]$ for $P_{4r} \odot L^2_{6,4t+3}$ is applied. Therefore $x_0 = x_1 = 2r, a_0 = 2r, a_1 = 2r - 1, y_0 = y_1 = 2t + 3, b_0 = b_1 = 4t + 7, y_0' = y_1' = 2t + 4$ and $b_0' = b_1' = 4t + 7$. Consequently, it is easy to show that $|v_0 - v_1| = 0$, $|e_0 - e_1| = 1$, and $|(v_0 + e_0) - (e_1 + v_1)| = 1$. Thus, $P_{4r} \odot L^2_{6,4t+3}$ is cordial and total cordial.

Case 6. When $m \equiv 3\,(\text{mod}4)$ and $k \equiv 1\,(\text{mod}4)$ that means $m = 4t + 3, t \geq 1$, and $k = 4r + 1, r \geq 0$, then one can choose the labeling $[L_{4r}0; L_4 1 M_{4t+3}, L_4 1 M_{4t+3}, L_4 1 M_{4t+3}, L_4 1 M_{4t+3}, \ldots, (r - time), L_4 1 M_{4t+3}]$ for $P_{4r+1} \odot L^2_{6,4t+3}$. Therefore, $x_0 = 2r + 1, x_1 = 2r, a_0 = a_1 = 2r, y_0 = y_1 = 2t + 3, b_0 = b_1 = 4t + 7, y_0' = y_1' = 2t + 4$, and $b_0' = b_1' = 4t + 7$. So, $|v_0 - v_1| = 1$, $|e_0 - e_1| = 0$, and $|(v_0 + e_0) - (e_1 + v_1)| = 1$. Thus, $P_{4r+1} \odot L^2_{6,4t+3}$ is cordial and total cordial.

Case 7. When $m \equiv 3\,(\text{mod}4)$ and $k \equiv 2\,(\text{mod}4)$ that means $m = 4t + 3, t \geq 1$, and $k = 4r + 2, r \geq 0$, then one can take the labeling $[L_{4r}10; L_4 1 M_{4t+3}, L_4 1 M_{4t+3}, L_4 1 M_{4t+3}, L_4 1 M_{4t+3}, \ldots, (r - time), L_4 1 M_{4t+3}, L_4 1 M_{4t+3}]$ for $P_{4r+2} \odot L^2_{6,4t+3}$. Therefore, $x_0 = x_1 = 2r + 1, a_0 = 2r + 1, a_1 = 2r, y_0 = y_1 = 2t + 3, b_0 = b_1 = 4t + 7, y_0' = y_1' = 2t + 4$, and $b_0' = b_1' = 4t + 7$. Hence, $|v_0 - v_1| = 0$, $|e_0 - e_1| = 1$, and $|(v_0 + e_0) - (e_1 + v_1)| = 1$. Thus, $P_{4r+2} \odot L^2_{6,4t+3}$ is cordial and total cordial.

Case 8. When $m \equiv 3\,(\text{mod}4)$ and $k \equiv 3\,(\text{mod}4)$ that means $m = 4t + 3, t \geq 1$, and $k = 4r + 3, r \geq 0$, then one can select the labeling $[L_{4r}001; L_4 1 M_{4t+3}, L_4 1 M_{4t+3}, L_4 1 M_{4t+3}, L_4 1 M_{4t+3}, \ldots, (r - time), L_4 1 M_{4t+3}, L_4 1 M_{4t+3}, L_4 1 M_{4t+3}]$ for $P_{4r+3} \odot L^2_{6,4t+3}$. Therefore, $x_0 = 2r + 2, x_1 = 2r + 1, a_0 = a_1 = 2r + 1, y_0 = y_1 = 2t + 3$, $b_0 = b_1 = 4t + 7, y_0' = y_1' = 2t + 4$, and $b_0' = b_1' = 4t + 7$. Consequently, it is easy to show that $|v_0 - v_1| = 1$, $|e_0 - e_1| = 0$, and $|(v_0 + e_0) - (e_1 + v_1)| = 1$. Thus, $P_{4r+3} \odot L^2_{6,4t+3}$ is cordial and total cordial; by this, the lemma was proved, and through the proofs of these lemmas, we have completed the proof of our main theorem. □

4. Conclusions

In this paper, we test the cordial and total cordial labeling of corona product of paths and second power of lemniscate graphs. We found that $P_k \odot L^2_{n,m}$ is cordial and also total cordial for all $k \geq 1, n, m \geq 3$. In future work, we can improve this work by using the different graphs with other mathematical operations to prove the cordial and total cordial labeling.

Data Availability

The data used to support the findings of this study are available from the corresponding author upon request.

Conflicts of Interest

The authors declare that they have no conflicts of interest.

Acknowledgments

The authors extend their appreciation to the Deanship of Scientific Research at King Khalid University for funding this work through General Research Project under grant number R.G.P.1/258/43.

References

[1] R. H. Azaizeh, A. Ahmad, and G. C. Lau, “3-total edge product cordial labelings of graphs,” *Far East Journal of Mathematical Sciences*, vol. 96, no. 2, pp. 193–209, 2015.

[2] I. Cahit, “Cordial graphs: a weaker version of graceful and harmonious Graphs,” *Ars Combinatoria*, vol. 23, pp. 201–207, 1987.

[3] I. Cahit, “On cordial and 3-eqtitable labeling of graphs,” *Utiliuies Math*, vol. 37, 1990.

[4] A. T. Diab, “On cordial labeling of the second power of paths with other graphs,” *ARS Combinatoria*, vol. 97A, pp. 327–343, 2010.

[5] R. L. Graham and N. J. A. Sloane, “On additive bases and harmonious graphs,” *SIAM Journal on Discrete Mathematics*, vol. 1, pp. 382–404, 1980.

[6] S. W. Golomb, *How to Number a Graph in Graph Theory and Computing*, R. C. Read, Ed., pp. 23–37, Academic Press, New York, NY, USA, 1972.

[7] J. A. Gallian, “A dynamic survey of graph labeling,” *The electronic Journal of Combinatorics*, vol. 9, p. DS6, 2021.

[8] A. Rosa, *On Certain Valuations of the Vertices of a Graph, Theory of Graphs (Internat Symposium, Rome, July 1966), Gordon and Breach, N.Y. and Dunod Paris*, 1967.

[9] E. Badr, S. Almotairi, A. Elrokh, A. Abdel-Hay, and B. Almutairi, “An integer linear programming model for solving radio mean labeling problem,” *IEEE Access*, vol. 8, pp. 162343–162349, 2020.

[10] E. Badr, A. A. El-hay, H. Ahmed, and M. Moussa, “Polynomial, exponential and approximate algorithms for metric dimension problem,” *International Journal of Mathematical Combinatorics*, vol. 2, pp. 50–66, 2021.

[11] A. I. H. Elrokh, S. I. M. Nada, and E. M. E. S. El-Shafey, “Cordial labeling of corona product of path graph and second power of fan graph,” *Open Journal of Discrete Mathematics*, vol. 11, no. 2, p. 31, 2021.

[12] E. Badr, S. Nada, M. Mohammed, A. Al-Shamiri, A. Abdel-Hay, and A. ELrokh, “A novel mathematical model for radio mean square labeling problem,” *Journal of Mathematics*, vol. 2022, Article ID 3303433, 9 pages, 2022.

[13] S. Nada, A. ELrokh, and A. Abdel-Hay, “The cordiality of the second power of some graphs,” *Advances and Applications in Discrete Mathematics*, 2021.

[14] S. Klavzar and M. Tavakoli, “Dominated and dominator colorings over (edge) corona and hierarchical products,” *Applied Mathematics and Computation*, vol. 390, Article ID 125647, 2021.

[15] M. Tavakoli, F. Rahbarnia, and A. R. Ashrafi, “Studying the corona product of graphs under some graph invariants,” *Transactions on Combinatorics*, vol. 3, no. 3, pp. 43–49, 2014.

[16] M. M. A. Al-Shamiri, A. Elrokh, Y. El–Mashtawye, and S. E. Tallah, “The cordial labeling for the cartesian product between paths and cycles,” *International Journal of Regulation and Governance*, vol. 8, no. 3, pp. 331–341, 2020.

[17] A. Hefnawy and Y. Elmshtaye, “Cordial labeling of corona product of paths and lemniscate graphs,” *ARS Combinatoria*, vol. 149, pp. 69–82, 2020.

[18] S. Nada, A. Elrokh, E. A. Elsakhawi, and D. E. Sabra, “The corona between cycles and paths,” *Journal of the Egyptian Mathematical Society*, vol. 25, no. 2, pp. 111–118, 2017.

Hindawi
Journal of Mathematics
Volume 2022, Article ID 4789155, 5 pages
https://doi.org/10.1155/2022/4789155

Research Article

Generalized Cut Functions and n-Ary Block Codes on UP-Algebras

Ali N. A. Koam, Azeem Haider, and Moin A. Ansari

Department of Mathematics, College of Science, Jazan University, Post Box 2097 New Campus, Jazan, Saudi Arabia

Correspondence should be addressed to Moin A. Ansari; maansari@jazanu.edu.sa

Received 8 October 2021; Accepted 8 April 2022; Published 29 April 2022

Academic Editor: M. T. Rahim

Copyright © 2022 Ali N. A. Koam et al. This is an open access article distributed under the Creative Commons Attribution License, which permits unrestricted use, distribution, and reproduction in any medium, provided the original work is properly cited.

In this paper, the work is comprised of n-ary block codes for UP-algebras and their interrelated properties. n-ary block codes for a known UP-algebra is constructed and further it is shown that for each n-ary block code U, it is easy to associate a UP-algebra U in such a way that the newly constructed n-ary block codes generated by U, i.e., U_x, contain the code U as a subset. We define a UP-algebra valued function on a set say X, then we prove that for every n-ary block-code U, a generalized UP-valued cut function exists that determines U. We have also proved that the UP-algebras associated to an n-ary block code are not unique up to isomorphism.

1. Introduction

Logical algebras like BCI/BCK, BE, KU-algebras, and many others with their fuzzy, intuitionistic, and more related concepts have been interesting topics of study for researchers in recent years and have been widely considered as a strong tool for information systems and many other branches of computer sciences including fuzzy informatics with rough and soft concepts. Imai and Iseki [1] introduced BCK/BCI algebras as a generalization of the concept of set-theoretic difference and proportional calculi. BCI/BCK algebras form an important class of logical algebras. They have numerous applications to different domains of mathematics, e.g., sets theory, semigroup theory, group theory, derivational algebras, etc. As per the requirement to establish certain rational logic systems as a logical foundation for uncertain information processing, different types of logical systems are felt to be established. For this reason, researchers introduced and studied many types of logical algebras by using the concepts of BCI/BCK algebras.

A block code is related to channel coding that is one of the main types of it. Block code adds redundancy to a message so that, at the receiver end, one can easily decode the message with a minimum number of errors, where it is already provided that the information rate would not exceed the channel capacity. The task of a block code is to encode the strings that are formed by an alphabet set say $\mathscr{C}$ into code words by encoding each letter of $\mathscr{C}$ separately. As per the importance block of codes, they can be source codes used in data compression or channel codes used for detection and correction of channel errors [2]. Codes based on a family of algorithms were constructed by Lempel and Ziv [3], which are applicable for real-world problems and sequences. A detailed terminology based on codes and decoding through graphs is discussed in [4]. Ali et al. introduced the concept of n-ary block codes related to KU-algebras in [5].

Many researchers have made their studies based on block codes in the past few years considering different branches and different directions. One of them is logical algebra. Surdive et al. studied coding theory in hyper BCK-algebras [6]. Jun and Song [7] defined and studied codes based on BCK-algebras. Further Fu and Xin [8] introduced the concept of block codes in lattices.

Iampan introduced the concept of UP-algebras [9]. Iampan contributed on different aspects related to UP-algebras in [10]. Senapati et al. [11] represented UP-algebras in an intervalued intuitionistic fuzzy environment. Moin et al. [12] introduced graphs of UP-algebras and studied related results. The binary block codes associated to UP-algebras were discussed by Moin et al. [13]. Wajsberg algebras arising from binary block codes were studied by Flaut and Vasile [14].

In this paper, we have introduced and investigated generalized UP-valued cut functions and their several properties. Also, we have established n-ary block-codes for UP-algebras by using the notion of generalized UP-valued cut functions. We show that every finite UP-algebra determines a block-code.

Section 2 contains preliminaries and related definitions with some examples. Section 3 is based on the main results.

2. Preliminaries

This section is comprises with the concepts of UP-algebras, UP-subalgebras, UP-ideals, UP-valued function (cut function), and other important terminologies with examples and some related results.

Definition 1 (see [9]). A UP-algebra is a structure $(U, *, \varnothing)$ of type $(2, 0)$ with a single binary operation $*$ that satisfies the following identities: for any $x, y, z \in U$,

(UP-1): $(y * z) * [(x * y) * (x * z)] = \varnothing$

(UP-2): $\varnothing * x = x$

(UP-3): $x * \varnothing = \varnothing$

(UP-4): $x * y = y * x = \varnothing$ implies $x = y$

For a commutative UP-algebras U we have the condition for commutativity as $x * (x * y) = y * (y * x)$.

We define a partial order relation in a UP-algebra U as $y \leq x$ if and only if $x * y = \varnothing$. If $(U, *, \varnothing)$ and $(V, \circ, \varnothing)$ are two UP-algebras, then a map $f\colon U \longrightarrow V$ with the property $f(x * y) = f(x) \circ f(y)$, for all $x, y \in U$, is called a UP-algebra morphism. If f is one-one and onto map, then f is simply called isomorphism of U.

Example 1. Let $U = \{\varnothing, a, b, c\}$ be a set in which $*$ is defined by the following Cayley table

*	∅	a	b	c
∅	∅	a	b	c
a	∅	∅	∅	∅
b	∅	a	∅	c
c	∅	a	b	∅

We observe here that $U = \{\varnothing, a, b, c\}$ is a UP-algebra.

Example 2. Let $U = \{a_n | n = 1, 2, 3, \ldots, 9\}$ and define a binary operation $*$ on U as $a_i * a_j = a_k, \forall a_i, a_j, a_k \in U$ where $k = (\mathrm{lcm}(i, j)/j)$. Then $(U, *, a_1)$ is a UP-algebra. The following table represents this operation:

$*$	a_1	a_2	a_3	a_4	a_5	a_6
a_1	a_1	a_2	a_3	a_4	a_5	a_6
a_2	a_1	a_1	a_3	a_2	a_5	a_3
a_3	a_1	a_2	a_1	a_4	a_5	a_2
a_4	a_1	a_1	a_3	a_1	a_5	a_3
a_5	a_1	a_2	a_3	a_4	a_1	a_6
a_6	a_1	a_1	a_1	a_2	a_5	a_1

Lemma 1 (see [10]). *In a UP-algebra U the following properties hold for any $a, b, c \in U$:*

(UP-5) $a * a = \varnothing$

(UP-6) $a * b = \varnothing$ *and* $b * c = \varnothing \Rightarrow a * c = \varnothing$

(UP-7) $a * b = \varnothing \Rightarrow (c * a) * (c * b) = \varnothing$

(UP-8) $a * b = \varnothing \Rightarrow (b * c) * (a * c) = \varnothing$

(UP-9) $a * (b * a) = \varnothing$

(UP-10) $(b * a) * a = \varnothing \Leftrightarrow a = b * a$

(UP-11) $a * (b * b) = \varnothing$

Lemma 2. *Let $U = (A, *, \varnothing)$ be UP-algebras, then define a binary relation $\leq$ on U as follows: for all $a, b, c \in A$*

(UP-12) $a \leq a$

(UP-13) $\varnothing \leq a$

(UP-14) $b * a \leq a$

(UP-15) $a \leq b$ *and* $b \leq a \Rightarrow a = b$

(UP-16) $b \leq a$ *and* $c \leq b \Rightarrow c \leq a$

(UP-17) $b \leq a \Rightarrow c * b \leq c * a$

(UP-18) $b \leq a \Rightarrow a * c \leq b * c$

(UP-19) $(a * b) * (a * c) \leq b * c$

Definition 2 (see [9]). A nonempty subset A of a UP-algebra U is called a UP-ideal of U if it satisfies the following conditions:

(1) $\varnothing \in A$

(2) $a * (b * c) \in A$, $b \in A$ implies $a * c \in A$, for all $a, b, c \in U$

Proposition 1. *An algebra $(U, *, \varnothing)$ of type $(2, 0)$ is a UP-algebra if and only if the given conditions are satisfied:*

(1) $(c * a) * ((b * c) * (b * a)) = \varnothing$ *for all* $a, b, c \in U$

(2) $(b * \varnothing) * a = a$ *for all* $a, b \in U$

(3) For all $a, b, c \in U$ *such that* $a * b = \varnothing, b * a = \varnothing \Rightarrow a = b$

Proof. If $(U, *, \varnothing)$ is a UP-algebra. Then, (1) follows from (UP-1).

Next, (3) follows from (UP-4).

By using (UP-2) and (UP-3) we get (2) as $(b * 1) * a = 1 * a = a$.

Indirectly we consider $(U, *, \varnothing)$ satisfies given conditions, then (UP-1) and (UP-4) follows from (1) and (2), respectively. Next, replace b by a, a by 1 and c by 1 in (1) and using (3) we get, $(\varnothing * \varnothing) * [(a * \varnothing) * (a * \varnothing)] = \varnothing \Rightarrow (a * \varnothing) * (a * \varnothing) = \varnothing \Rightarrow a * \varnothing = \varnothing$ which shows (UP-3). Further, using $a * \varnothing = \varnothing$ in (2) we get, $\varnothing * a = a$ for all $a \in U$. Hence $(U, *, \varnothing)$ is a UP-algebra.

Let $(U, *, \varnothing)$ be a finite UP-algebra with n elements and $\mathfrak{U}$ be a finite nonempty set. A map $f\colon \mathfrak{U} \longrightarrow U$ is called a UP-function. Let $\mathfrak{U}_n = \{0, 1, 2, \ldots, n-1\}$ be a finite set. In the following, we will consider UP-algebra U and the set $\mathfrak{U}$, where $U = \{l_0, l_1, \ldots, l_{n-1}\}$, $\mathfrak{U} = \{u_0, u_1, \ldots, u_{m-1}\} m \leq n$. A generalized cut function of f is a map $f_{l_j}\colon \mathfrak{U} \longrightarrow \mathfrak{U}_n, l_j \in U$, such that $f_{l_j}(u_i) = u$ if and only if $l_j * f(u_i) = l_u$, for all $l_j, l_k \in U, u_i \in \mathfrak{U}$, and $i, j, u \in \{0, 1, 2, \ldots, n-1\}$.

For such each UP-function $f\colon \mathfrak{U} \longrightarrow U$, it is easy to define an n-ary block code with codewords having length m. For this purpose, we suppose that for each element $l \in U$ the generalized cut function $f_l\colon \mathfrak{U} \longrightarrow \mathfrak{U}_n$. For every such function, there will be corresponding a codeword w_r, having symbols taken from the set $\mathfrak{U}_n$. So, we get $w_l = w_0, w_1, \ldots, w_{m-1}$, with $w_i = j, j \in K_n$, if and only if $f_l(xi) = j$, that means $l * f(xi) = l_j$. We denote this new code by U_X. Hence, it is easy to associate an n-ary block code for every such UP-algebra. □

Example 3. We take the UP-algebra $U = \{1, 2, 3, 4\}$ having $\circ$ where $\circ$ is defined by the following table:

$\circ$	1	a	b	c
1	1	a	b	c
a	1	1	a	c
b	1	1	1	c
c	1	a	b	1

We can easily show that $\mathfrak{U} = \mathfrak{U}_4 = \{1, 2, 3, 4\}$. We consider the generalized cut function $f\colon \mathfrak{U} \longrightarrow U$, $f(1) = 2$, $f(2) = a, f(3) = b, f(4) = c$ and $f_l\colon \mathfrak{U}_4 \longrightarrow \mathfrak{U}_4$, $l \in U$. In this way $r = 1$, returns the codeword $w_1 = 0000$. For $l = a$, we get the codeword 1001. In fact, $f_a(1) = 2$, since $a \circ f(1) = a \circ 1 = a = f(1)$; $f_a(a) = 1$ since $a \circ f(2) = a \circ a = 1 = f(0)$; $f_a(b) = 1$ and $a \circ f(2) = a \circ b = 1 = f(1)$; $f_a(c) = 1$, also $a \circ f(4) = a \circ c = a = f(2)$.

The following result investigates about the existence of the converse part whether it is true or not.

3. Main Results

We consider a finite set $\mathfrak{U}'_n = \{1, 2, \ldots, n-1\}$ and its n-ary codewords $U = \{v_1, v_2, \ldots, v_m\}$, of length $h, h \geq n-2$, ascending ordered after lexicographic order. We consider $v_i = v_{i1} v_{i2}, \ldots, v_{ih}, v_{ij} \in \mathfrak{U}'_n, j \in \{1, 2, \ldots, h\}$, with v_{ij} descending ordered such that $v_{i_{v_{ik}}} \leq u, i \in \{1, 2, \ldots, m\}$, $u \in \{1, 2, \ldots, \min\{n-1, h\}\}$ and $v_{ij} = 1$ in the rest.

Definition 3. Let $U = \{v_1, v_2, \ldots, v_m\}$ be an n-ary code. Further we suppose that $v_i = v_{i1}, v_{i2} \ldots, v_{ih}, v_{ij} \in \mathfrak{U}'_n$. $j \in \{1, 2, \ldots, h\}, q \geq n-2$, as above. We now associate a matrix $A = (\alpha_{st})_{s,t \in \{0,1,\ldots,l-1\}}, A \in \mathscr{A}_l(\mathfrak{U}_n)$, to this code where $l = m + h + 1$. Let $l = m + h + 1$. We define $\alpha_{ss} = 0$, $\alpha_{s0} = s, \alpha_{0s} = 0, s \in \{0, 1, 2, \ldots, l-1\}$. For $1 \leq s \leq h$, let $\alpha_{st} = 1$, if $t < s$, and $\alpha_{st} = 0$, if $t \geq s$. For $s > h$, we put $\alpha_{st} = v_{it}$, for $t \in \{1, 2, \ldots, h\}$ and $\alpha_{s(h+j)} = 1$, for $h + j < s$. We suppose that $\alpha_{st} = 0$, for $t \geq s$.

Here, A is the lower triangular matrix, and it is known as the matrix associated with the n-ary block code $U = \{v_1, v_2, \ldots, v_m\}$.

Definition 4. Consider $A \in \mathscr{A}_i(\mathfrak{U}_n)$ is associated to the n-ary block code $U = \{k_1, k_2, \ldots, k_m\}$ defined on $\mathfrak{U}'_n$. Suppose that $\mathfrak{U}_l = \{0, 1, \ldots, l-1\}$ is a nonempty set. The multiplication $i \circ j = \alpha_{ij}$ is defined on $\mathfrak{U}_l$.

Theorem 1. *The set $(\mathfrak{U}_\varnothing, \circ, 0)$ is a UP-algebra.*

Proof. We see here that Proposition 1 (2), (3) are well defined. From Definition 1, we need to show that $(b * c) * ((c * a) * (c * a)) = 1$, for all $a, b, c \in \{0, 1, \ldots, l-1\}$. For the elements a, b, c we have 3 situations here that are given as follows:

Case 1: $c = 0, b \neq 0$. We get $b * a \leq a$, which implies $a * (b * a) = 0$.

Case 2: $b = 0, c \neq 0$. We need to show that $c * ((c * a) * a) = 0$. Thus for $a = 0$, it is obvious and for $c = 0$, we obtain $(0 * a) * (0 * a) = 0 * (a * a) = 0$. For $c \neq 0, a \geq l - m, c \in \{1, 2, \ldots, h\}$, we have $((a * c) * a) = w_x w_{ac} \leq c$, therefore $c * (c * a) * a = 0$. For $c \neq 0, a \geq l - m$, $c \geq h + 1$, we obtain $c * ((c * a) * a) * c = 0$. Next, if $c * a = 1$, since $1 * a \leq n - 1 < h + 1 \leq c$, in returns we get $c * ((c * a) * a) = c * (1 * a) = 0$. If $c * a = 0$, then $c * ((c * a) * a) = c * (0 * a) = c * a = 0$. For $a < l - m$, $c \leq h + 1$, we have $c * ((c * a) * a) = 0$, since $c * a = 1$, $1 * a = 1$ and $c * 1 = 0$. For $a < l - m, c > h + 1$, it results $c * ((c * a) * a) = 0$, since $c * a = 0$, it yield $c * (0 * a) = c * a = 0$.

Case 3: $c \neq 0, b \neq 0$. Here, we have to prove that $(c * a) * ((b * k) * (b * a)) = 0$. Hence, it is shown for $a = 0$. Furthermore, let $a \neq 0$. For $a \geq l - m$ and $b, c < l - m, b < k$, we get $n - 1 \geq (b * a) \geq (c * a)$, hence $((c * a) * (b * a)) = 1$. We also get $b * c = 1$, hence $(c * a) * ((c * b) * (b * a)) = 1 * 1 = 0$. For $a \geq l - m$ and $b, c < l - m, c < b$, we get $n - 1 \geq (c * a) \geq (b * a)$, then $((c * a) * (b * a)) = 0$. It results that $(c * a) * ((b * c) * (b * a)) = 0$. For $a \geq l - m$ and $b, c \geq l - m$, $b < c$, we can get that $b * a = 1$ and $c * a = 1$, so $(c * a) * (b * a) = 0$. We also obtain $b * a = 1$, $c * a = 0$, and $b * c = 1$, since $b < c$. It yield $(c * a) * ((b * k) * (b * a)) = 1 * (0 * 1) = 1 * 1 = 0$.

Or, we can have $b * a = 0, c * a = 0$,; hence $(c * a) *$

$((b*k)*(b*a))=0$. For $a \geq l-m$ and $b,k \geq l-m$, $c<b$, we can have $b*a=1$ and $c*a=1$, hence $(c*a)*(b*a)=0$. Or, we have $c*a=1$, $b*a=0$, and $b*c=0$, as a result we get zero. We also can have $b*a=0, c*a=0$,; hence the relation is 0. For $a \leq l-m$ and $c<l-m<b$, if $b*a=0$, it shows that the asked relation is 0. If $b*a=1$, then $(c*a)*((b*k)*(b*a))=0*((c*a)*1)=\beta*1$, with $\beta \geq 1$, and $c<a$.

For $a \geq l-m$ and $b<l-m<c$, we have that $b*a=1$. If $c*a=1$, we obtain 0. If $c*a=0$, hence we find $(c*a)*((b*c)*(b*a))=(b*c)*(0*1)=(b*c)*1=0$, since $b*c \geq 1$.

For $a<l-m$ and $b,c<l-m, b<c$, we have $b*a=1, c*a=1$,; therefore, we obtain the result as zero. For $a<l-m$ and $b,c<l-m, c \leq b$, we can obtain $(c*a)*((b*c)*(b*a))=1*(0*1)=0$. Or, we find $(b*a)=0$; thus, we can say that obtained result is 0. For $a<l-m$ and $b,c<l-m, b<c$, since $b<c$, it returns $b*c=1$. We can get $b*a=1, c*a=0$ and $b*c=1$, therefore $(c*a)*((b*c)*(b*a))=0*(1*1)=1*1=0$. For $a<l-m$ and $c<l-m \leq b$, we can get $(c*a)*((b*k)*(b*a))=1*(0*1)=0$. Or, if $(b*a)=0$; thus we obtain 0 and that is required. For $a<l-m$ and $b,c \geq l-m, b<c$, we have $(b*a)=0$; then, we get zero. For $a<l-m$ and $b,c \geq l-m, b>c$, it results $(b*a)=0$, hence the asked relation is 0. □

Note.

(1) We find that a UP-algebra $(\mathfrak{U}_l, *, 0)$ from Theorem 1 is extracted by using the matrix $\mathscr{A}$, which is uniquely determined by an n-ary code, say U, given as per Definition 1; thus, we can say that $(\mathfrak{U}_r, *, 0)$ is a uniquely determined algebra.

(2) By Theorem 1, we suppose that $(C_l, *, 0)$ is the resulted UP-algebra, with $\mathfrak{U}_l=\{0,1,2,\ldots,l-1\}$. If $U=\{a_0=1, a_1, a_2, \ldots a_{l-1}\}$ with multiplication "$*$" given by the relation $a_i * a_j = a_c$ if and only if $a*b=c$, for $a,b,c \in \{0,1,2,\ldots,l-1\}$, then $(U, *, 1)$ is a UP-algebra.

(3) If we suppose that $C_h=\{0,1,2,\ldots h-1\}$, the map $f\colon C_h \longrightarrow U, f(a)=a_i$, returns a code U_X, that can be associated to the above UP-algebra $(U, *, 1)$, that contains the code U as a subset.

We consider U as an n-ary block code. Then, from Theorem 1 and above Note, we can have a UP-algebra U in such a way that the obtained n-ary block code U_X contains the n-ary block code U as of its subset. Suppose that U is a binary block code with m code words of length h. By using the abovementioned notations, consider X is the associated UP-algebra and $W=\{1, w_1, \ldots, w_r\}$ is the associated n-ary block codes that contains the code U. Next consider $w_a = a_1 a_2, \ldots, a_h$ and $w_b = b_1 b_2, \ldots, b_h$ are two codewords that belong to W. Here, we define an order relation $\leq_c$ on W by the following logic $w_a \leq w_b$ if and only if $b_i \leq a_i$, for all $i \in \{1,2,\ldots,h\}$. On $U=W$, with the order relation $\leq_c$, we define the following multiplication:

(1) $a \circ 1 = 1$ and $a \circ a = 1, \forall a \in U$

(2) $b \circ a = 1$ if $a \leq_c b, \forall a,b \in U$

(3) $b \circ a = a$ if $b \leq_c a, \forall a,b \in U$

This order relations give UP-algebra structure. It is clear that $w_l \leq_c \cdots \leq_c w_1 \leq_c 1$. □

Proposition 2. *$V=\{1, w_{l-m}, w_{l-m+1}, \ldots, w_l\}$ gives an UP-algebra ideal in the U.*

Proof. Considering $V=\{1, w_{l-m}, w_{l-m+1}, \ldots, w_l\}$. We will show that $b \in V, a \in U$, and $b \circ a \in V$, implies $a \in V$. By using multiplication rule in the UP-algebra U and chosen n-ary codes, we get for $a \in U-V, b \circ a = a \in U-V$. If $a,b \in V$, then $b \circ a = a \in V$ or $b \circ a = 1 \in V$. □

Example 4. Consider $K_5=\{0,1,2,3,4\}, n=5, q=4, m=3, l=8, V=\{w_1,w_2,w_3\}$, with $w_1=3211, w_2=4221, w_3=4321$.

Entries of the matrix $\mathscr{A}$ associated with the n-ary code U, are $a_{ij}=0, \forall i \leq j$, $a_{i1}=i-1, a_{62}=3, a_{63}=2, a_{72}=4$, $a_{73}=2, a_{74}=2, a_{82}=4, a_{83}=3, a_{84}=2$ and $a_{ij}=1$ for the rest of i and j.

The corresponding UP-algebra, $(U, \circ, 1)$, where $U=\{a_0=1, a_1, a_2, a_3, a_4, a_5, a_6, a_7\}$, is shown with the following multiplication table.

$\circ$	1	a_1	a_2	a_3	a_4	a_5	a_6	a_7
1	1	a_1	a_2	a_3	a_4	a_5	a_6	a_7
a_1	1	1	a_1	a_1	a_1	a_3	a_4	a_4
a_2	1	1	1	a_1	a_1	a_2	a_2	a_3
a_3	1	1	1	1	a_1	a_1	a_2	a_2
a_4	1	1	1	1	1	a_1	a_1	a_1
a_5	1	1	1	1	1	1	a_1	a_1
a_6	1	1	1	1	1	1	1	a_1
a_7	1	1	1	1	1	1	1	1

Considering $\mathfrak{U}=\{1,2,3,4\}$. The map $f\colon \mathfrak{U} \longrightarrow U$, $f(1)=a_1, f(2)=a_2, f(3)=a_3, f(4)=a_4$ gives us the following block code $U'=\{0000, 1000, 1100, 1110, 1111, 3211, 4221, 4321\}$, that contains U as a subset.

$$0000-1000-1100-1110-1111-3211-4221-4321. \tag{1}$$

Clearly it is a noncommutative UP-algebra as $(a_6 \circ a_7) \circ a_7 = a_1 \circ a_7 = a_4$ and $(a_7 \circ a_6) \circ a_6 = 1 \circ a_6 = a_6$. This clarifies that $\mathfrak{U}$ is not an implicative UP-algebra. Also we note that it is not a positive implicative UP-algebra. Since $(a_6 \circ a_7) \circ a_6 = a_1 \circ a_6 = a_3 \neq a_6$ and $a_3 \circ (a_6 \circ a_7) = a_3 \circ a_1 = 1 \neq (a_3 \circ a_6)(a_3 \circ a_7) = a_1 \circ a_2 = a_1$.

Example 5. Consider $K_4=\{0,1,2,3\}, n=4, q=5, m=3, l=9, U=\{w_1,w_2,w_3\}$, with $w_1=21111, w_2=32111, w_3=33111$.

Entries of the matrix $\mathscr{A}$ associated with the n-ary code U, are $a_{ij} = 0 \forall, i \leq j,\ a_{i1} = i - 1, a_{72} = 2, a_{82} = 3, a_{92} = 3,\ a_{83} = 2, a_{93} = 3$ and $a_{ij} = 1$ for the rest of i and j.

The corresponding UP-algebra $(X, \circ, 1)$, where $X = \{a_0 = 1, a_1, a_2, a_3, a_4, a_5, a_6, a_7\}$ is shown with the following multiplication table.

$\circ$	1	a_1	a_2	a_3	a_4	a_5	a_6	a_7	a_8
1	1	a_1	a_2	a_3	a_4	a_5	a_6	a_7	a_8
a_1	1	1	a_1	a_1	a_1	a_1	a_2	a_3	a_3
a_2	1	1	1	a_1	a_1	a_1	a_1	a_2	a_3
a_3	1	1	1	1	a_1	a_1	a_1	a_2	a_1
a_4	1	1	1	1	1	a_1	a_1	a_1	a_1
a_5	1	1	1	1	1	1	a_1	a_1	a_1
a_6	1	1	1	1	1	1	1	a_1	a_1
a_7	1	1	1	1	1	1	1	a_1	a_1
a_8	1	1	1	1	1	1	1	1	1

Let $K = \{1, 2, 3, 4, 5\}$. Then, $f\colon K \longrightarrow X, f(1) = a_1, f(2) = a_2, f(3) = a_3, f(4) = a_4, f(5) = a_5$ returns the given block code $U' = \{00000, 10000, 11000, 11100, 11110, 21111, 32211, 33111\}$, where U is contained in it as a subset. The diagram of this generated code is given as

$$\begin{tikzcd}[column sep=small, row sep=small] & & & & & & 32211 \\ 00000 \arrow[r, dash] & 10000 \arrow[r, dash] & 11000 \arrow[r, dash] & 11100 \arrow[r, dash] & 11110 \arrow[r, dash] & 21111 \arrow[ur, dash] \arrow[dr, dash] & \\ & & & & & & 33111 \end{tikzcd}$$

Data Availability

No data were used to support this study.

Conflicts of Interest

The authors declare that they have no conflicts of interest.

References

[1] Y. Imai and K. Iski, "On axiom systems of propositional calculi. XIV," *Proceedings of the Japan Academy*, vol. 42, no. 1, pp. 19–22, 1966.

[2] S. Lin and D. J. Costello, *Error Control Coding: Fundamentals and Applications*, Prentice Hall, Hoboken, NJ, USA, 1983.

[3] J. Ziv and A. Lempel, "Compression of individual sequences via variable-rate coding," *IEEE Transactions on Information Theory*, vol. 24, no. 5, pp. 530–536, 1978.

[4] N. Wiberg, *Codes and Decoding on General Graphs*Linkping University, Linköping, Sweden, 1996.

[5] A. N. A. Koam, M. A. Ansari, and A. Haider, "Ansari and Azeem Haider, *n*-ary block codes related to KU-algebras," *Journal of Taibah University For Science*, vol. 14, no. 1, pp. 172–176, 2020.

[6] A. T. Surdive, N. Slestin, and L. Clestin, "Coding theory and hyper BCK-algebras," *Journal of Hyperstructures*, vol. 7, no. 2, pp. 82–93, 2018.

[7] Y. B. Jun and S. Z. Song, "Codes based on BCK-algebras," *Information Sciences*, vol. 181, Article ID 51025109, 2011.

[8] Y. Fu and X. L. Xin, "Lattices and block codes," *UPB Scientific Bulletin, Series A: Applied Mathematics and Physics*, vol. 79, no. 3, 2017.

[9] A. Iampan, "A new branch of the logical algebra: UP-algebras," *Journal of Algebra and Related Topics*, vol. 5, no. 1, pp. 35–54, 2017.

[10] A. Iampan, "The UP-isomorphism theorems for UP-algebras," *Discussiones Mathematicae-General Algebra and Applications*, vol. 39, no. 1, pp. 113–123, 2019.

[11] T. Senapati, G. Muhiuddin, and K. P. Shum, "Representation of UP-Algebras in intervalued-valued intuitionistic fuzzy environment," *Italian Journal of Pure and Applied Mathematics*, vol. 38, pp. 497–518, 2017.

[12] M. Ansari, A. Haidar, and A. N. A. Koam, "On a graph associated to UP-algebras," *Mathematical and Computational Applications*, vol. 23, no. 4, p. 61, 2018.

[13] M. A. Ansari, A. N. A. Koam, and A. Haider, "On binary block codes associated to UP-algebras," *Italian Journal of Pure and Applied Mathematics*, vol. 47, pp. 205–220, 2022.

[14] C. Flaut and R. Vasile, "Wajsberg algebras arising from binary block codes," 2019, https://arxiv.org/abs/1904.07169.

Hindawi
Journal of Mathematics
Volume 2022, Article ID 3248127, 11 pages
https://doi.org/10.1155/2022/3248127

Research Article

Three-Dimensional Expansion and Graphical Concept of Generalized Triangular Fuzzy Set

Yong Sik Yun

Department of Mathematics, Jeju National University, Jeju 63243, Republic of Korea

Correspondence should be addressed to Yong Sik Yun; yunys@jejunu.ac.kr

Received 2 February 2022; Accepted 2 April 2022; Published 26 April 2022

Academic Editor: M. T. Rahim

Copyright © 2022 Yong Sik Yun. This is an open access article distributed under the Creative Commons Attribution License, which permits unrestricted use, distribution, and reproduction in any medium, provided the original work is properly cited.

We have studied the extended algebraic operations between two fuzzy numbers and calculated Zadeh's max-min composition operator for two generalized triangular fuzzy sets in $\mathbb{R}^2$. And we generalized the triangular fuzzy numbers from $\mathbb{R}^2$ to $\mathbb{R}^3$. We prove that the result of the three-dimensional case is an extension of two-dimensional case and presented it in a graph. The extension is proved by showing that the result obtained by restricting the three-dimensional result to two-dimensional result is consistent with the existing two-dimensional result.

1. Introduction

Fuzzy theory has been increasingly applied to humanities including logics and sociology as well as natural sciences from engineering to medicine. In mathematics, triangular fuzzy sets have been extensively studied, which resulted in numerous fuzzy theories. In applications of the fuzzy set theories, many operators between two fuzzy sets have been defined and calculated. In particular, Zadeh's operators have been widely applied and developed [1–3]. Recently, the application expands to fuzzy control theory [4, 5] and fuzzy logic [6–8]. The theories of triangular fuzzy numbers have been extended to generalized triangular fuzzy sets that do not have the maximum value of 1. And as the number of ambiguous fuzzy variables increases, the theories have been extended to the studies of two-dimensional and three-dimensional fuzzy sets. In that respect, the study that extended Zadeh's operator theory to two or three dimensions is meaningful. We have studied the extended algebraic operations between two fuzzy numbers [9–12] and calculated Zadeh's max-min composition operator for two generalized triangular fuzzy sets in $\mathbb{R}^2$ [13–15]. In [16], we generalized the triangular fuzzy numbers from $\mathbb{R}^2$ to $\mathbb{R}^3$. By defining a parametric operator between two α-cuts with ellipsoidal values containing the interior, we defined a parametric operator for the two triangular fuzzy numbers defined in $\mathbb{R}^3$. We proved that the results for the parametric operator are the generalization of Zadeh's extended algebraic operator on $\mathbb{R}$ [9]. In addition, we calculated the parametric operators for two generalized three-dimensional triangular fuzzy sets and presented the calculation in three-dimensional graphs [17].

In this paper, we prove that the result of the three-dimensional case is an extension of two dimensions and presented it in a graph. The extension is proved by showing that the result obtained by restricting the three-dimensional result to two dimensions is consistent with the existing two-dimensional result. The graph of the fuzzy set defined in three dimensions expresses the function value by color density. When the graph is cut with a vertical plane passing through the vertex of a generalized three-dimensional triangular fuzzy set, the function value is shown through color density on the cross section of the graph. The value of the membership function defined on the cross section can be expressed in a graph of the function defined in two dimensions. We show that this graph is consistent with the three-dimensional representation of the results in two dimensions.

2. Zadeh's Max-Min Composition Operations for Generalized Triangular Fuzzy Sets on $\mathbb{R}^2$

We define α-cut and α-set of the fuzzy set A on $\mathbb{R}$ with the membership function $\mu_A(x)$.

Definition 1. An α-cut of the fuzzy number A is defined by $A_\alpha = \{x \in \mathbb{R} \mid \mu_A(x) \geq \alpha\}$ if $\alpha \in (0,1]$ and $A_0 = \mathrm{cl}\{x \in \mathbb{R} \mid \mu_A(x) > \alpha\}$, where $\mathrm{cl}(B)$ is the closure of $B \subset \mathbb{R}$. For $\alpha \in (0,1)$, the set $A^\alpha = \{x \in X \mid \mu_A(x) = \alpha\}$ is said to be the α-set of the fuzzy set A, A^0 is the boundary of $\{x \in \mathbb{R} \mid \mu_A(x) > \alpha\}$, and $A^1 = A_1$.

We define the generalized two-dimensional triangular fuzzy numbers on $\mathbb{R}^2$ as a generalization of generalized triangular fuzzy sets on $\mathbb{R}$ and the parametric operations between two generalized two-dimensional triangular fuzzy sets. For that, we have to calculate operations between α-cuts in $\mathbb{R}$. The α-cuts are intervals in $\mathbb{R}$, but in $\mathbb{R}^2$, the α-cuts are regions, which makes the existing method of calculations between α-cuts unusable. We interpret the existing method from a different perspective and apply the method to the region valued α-cuts on $\mathbb{R}^2$.

Definition 2. A fuzzy set A with a membership function:

$$\mu_A(x,y) = \begin{cases} h - \sqrt{\dfrac{(x-x_1)^2}{a^2} + \dfrac{(y-y_1)^2}{b^2}}, & b^2(x-x_1)^2 + a^2(y-y_1)^2 \leq a^2b^2h^2, \\ 0, & \text{otherwise}, \end{cases} \tag{1}$$

where $a, b > 0$ and $0 < h < 1$ is called the generalized two-dimensional triangular fuzzy set and denoted by $(a, x_1, h, b, y_1)^2$.

The intersections of $\mu_A(x,y)$ and the vertical planes $y - y_1 = k(x - x_1)$ $(k \in \mathbb{R})$ are symmetric triangular fuzzy numbers in those planes. If $a = b$, ellipses become circles. The α-cut A_α of a generalized two-dimensional triangular fuzzy number $A = (a, x_1, h, b, y_1)^2$ is an interior of ellipse in an xy-plane including the boundary

$$A_\alpha = \left\{ (x,y) \in \mathbb{R}^2 \Big| \left(\frac{x - x_1}{a(h-\alpha)}\right)^2 + \left(\frac{y - y_1}{b(h-\alpha)}\right)^2 \leq 1 \right\}. \tag{2}$$

Definition 3. A two-dimensional fuzzy number A defined on $\mathbb{R}^2$ is called convex fuzzy number if for all $\alpha \in (0,1)$, the α-cuts,

$$A_\alpha = \left\{ (x,y) \in \mathbb{R}^2 | \mu_A(x,y) \geq \alpha \right\}, \tag{3}$$

are convex subsets in $\mathbb{R}^2$.

Theorem 1 (see [9]). *Let A be a continuous convex fuzzy number defined on $\mathbb{R}^2$ and $A^\alpha = \{(x,y) \in \mathbb{R}^2 | \mu_A(x,y) = \alpha\}$ be the α-set of A. Then, for all $\alpha \in (0,1)$, there exist continuous functions $f_1^\alpha(t)$ and $f_2^\alpha(t)$ defined on $[0, 2\pi]$ such that*

$$A^\alpha = \left\{ \left(f_1^\alpha(t), f_2^\alpha(t)\right) \in \mathbb{R}^2 | 0 \leq t \leq 2\pi \right\}. \tag{4}$$

Definition 5. Let A and B be convex fuzzy sets defined on $\mathbb{R}^2$ and

$$\begin{aligned} A^\alpha &= \left\{ \left(f_1^\alpha(t), f_2^\alpha(t)\right) \in \mathbb{R}^2 | 0 \leq t \leq 2\pi \right\}, \\ B^\alpha &= \left\{ \left(g_1^\alpha(t), g_2^\alpha(t)\right) \in \mathbb{R}^2 | 0 \leq t \leq 2\pi \right\}, \end{aligned} \tag{5}$$

be the α-sets of A and B, respectively. For $\alpha \in (0,1)$, the parametric addition, parametric subtraction, parametric multiplication, and parametric division are fuzzy sets that have their α-sets as follows.

2.1. Parametric Addition $A(+)_pB$. The parametric addition is given by the following:

$$\left(A(+)_pB\right)^\alpha = \left\{ \left(f_1^\alpha(t) + g_1^\alpha(t), f_2^\alpha(t) + g_2^\alpha(t)\right) \in \mathbb{R}^2 | 0 \leq t \leq 2\pi \right\} \tag{6}$$

2.2. Parametric Subtraction $A(-)_pB$. The parametric subtraction is given by the following:

$$\left(A(-)_pB\right)^\alpha = \left\{ \left(x_\alpha(t), y_\alpha(t)\right) \in \mathbb{R}^2 | 0 \leq t \leq 2\pi \right\}, \tag{7}$$

where

$$\begin{aligned} x_\alpha(t) &= \begin{cases} f_1^\alpha(t) - g_1^\alpha(t+\pi), & \text{if } 0 \leq t \leq \pi, \\ f_1^\alpha(t) - g_1^\alpha(t-\pi), & \text{if } \pi \leq t \leq 2\pi, \end{cases} \\ y_\alpha(t) &= \begin{cases} f_2^\alpha(t) - g_2^\alpha(t+\pi), & \text{if } 0 \leq t \leq \pi, \\ f_2^\alpha(t) - g_2^\alpha(t-\pi), & \text{if } \pi \leq t \leq 2\pi. \end{cases} \end{aligned} \tag{8}$$

2.3. Parametric Multiplication $A(\cdot)_pB$. The parametric multiplication is given by the following:

$$\left(A(\cdot)_pB\right)^\alpha = \left\{ \left(f_1^\alpha(t) \cdot g_1^\alpha(t), f_2^\alpha(t) \cdot g_2^\alpha(t)\right) \in \mathbb{R}^2 | 0 \leq t \leq 2\pi \right\}. \tag{9}$$

2.4. Parametric Division $A(/)_pB$. The parametric division is given by the following:

$$\left(A(/)_pB\right)^\alpha = \left\{(x_\alpha(t), y_\alpha(t)) \in \mathbb{R}^2 | 0 \le t \le 2\pi\right\}, \tag{10}$$

where

$$\begin{aligned} x_\alpha(t) &= \frac{f_1^\alpha(t)}{g_1^\alpha(t+\pi)}, \quad (0 \le t \le \pi),\\ x_\alpha(t) &= \frac{f_1^\alpha(t)}{g_1^\alpha(t-\pi)}, \quad (\pi \le t \le 2\pi),\\ y_\alpha(t) &= \frac{f_2^\alpha(t)}{g_2^\alpha(t+\pi)}, \quad (0 \le t \le \pi),\\ y_\alpha(t) &= \frac{f_2^\alpha(t)}{g_2^\alpha(t-\pi)}, \quad (\pi \le t \le 2\pi). \end{aligned} \tag{11}$$

For $\alpha = 0$ and $\alpha = 1$, $(A(*)_pB)^0 = \lim_{\alpha\longrightarrow 0^+}(A(*)_pB)^\alpha$ and $(A(*)_pB)^1 = \lim_{\alpha\longrightarrow 1^-}(A(*)_pB)^\alpha$, where $* = +, -, \cdot, /$.

Theorem 2 (see [10]). *Let $A = (a_1, x_1, h_1, b_1, y_1)^2$ and $B = (a_2, x_2, h_2, b_2, y_2)^2$ be two generalized two-dimensional triangular fuzzy sets. If $0 < h_1 < h_2 < 1$, then we have the following:*

(1) For $0 < \alpha < h_1$, the α-set of $A(+)_pB$ is

$$\left(A(+)_pB\right)^\alpha = \left\{(x,y) \in \mathbb{R}^2 | \left(\frac{x - x_1 - x_2}{a_1(h_1-\alpha) + a_2(h_2-\alpha)}\right) + \left(\frac{y - y_1 - y_2}{b_1(h_1-\alpha) + b_2(h_2-\alpha)}\right)^2 = 1\right\}. \tag{12}$$

(2) For $0 < \alpha < h_1$, the α-set of $A(-)_pB$ is

$$\left(A(-)_pB\right)^\alpha = \left\{(x,y) \in \mathbb{R}^2 | \left(\frac{x - x_1 + x_2}{a_1(h_1-\alpha) + a_2(h_2-\alpha)}\right)^2 + \left(\frac{y - y_1 + y_2}{b_1(h_1-\alpha) + b_2(h_2-\alpha)}\right)^2 = 1\right\}. \tag{13}$$

(3) $(A(\cdot)_pB)^\alpha = \{(x_\alpha(t), y_\alpha(t)) | 0 \le t \le 2\pi\}$, where

$$\begin{aligned} x_\alpha(t) &= x_1x_2 + (x_1a_2(h_2-\alpha) + x_2a_1(h_1-\alpha))\cos t + a_1a_2(h_1-\alpha)(h_2-\alpha)\cos^2 t, \quad 0 < \alpha < h_1,\\ y_\alpha(t) &= y_1y_2 + (y_1b_2(h_2-\alpha) + y_2b_1(h_1-\alpha))\sin t + b_1b_2(h_1-\alpha)(h_2-\alpha)\sin^2 t, \quad 0 < \alpha < h_1. \end{aligned} \tag{14}$$

(4) $(A(/)_pB)^\alpha = \{(x_\alpha(t), y_\alpha(t)) | 0 \le t \le 2\pi\}$, where

$$\begin{aligned} x_\alpha(t) &= \frac{x_1 + a_1(h_1-\alpha)\cos t}{x_2 - a_2(h_2-\alpha)\cos t},\\ y_\alpha(t) &= \frac{y_1 + b_1(h_1-\alpha)\sin t}{y_2 - b_2(h_2-\alpha)\sin t},\\ &0 < \alpha < h_1. \end{aligned} \tag{15}$$

Furthermore, we have

$$\begin{aligned} \left(A(*)_pB\right)^0 &= \lim_{\alpha\longrightarrow 0^+}\left(A(*)_pB\right)^\alpha, \quad * = +, -, \cdot, /,\\ \left(A(*)_pB\right)^{h_1} &= \lim_{\alpha\longrightarrow h_1^-}\left(A(*)_pB\right)^\alpha, \quad * = +, -, \cdot, /. \end{aligned} \tag{16}$$

If $h_1 < \alpha \le h_2$, by the Zadeh's max-min principle operations, we obtain

$$\left(A(*)_pB\right)^\alpha = \varnothing, \quad * = +, -, \cdot, /. \tag{17}$$

Example 1. (see [10]). Let $A = (6, 3, (1/2), 8, 5)^2$ and $B = (4, 2, (2/3), 5, 3)^2$. Then, by Theorem 2, we have the following:

(1) For $0 < \alpha < (1/2)$, the α-set of $A(+)_pB$ is

$$\left(A(+)_pB\right)^\alpha = \left\{(x,y) \in \mathbb{R}^2 | \left(\frac{3x - 15}{17 - 30\alpha}\right)^2 + \left(\frac{3y - 24}{22 - 39\alpha}\right)^2 = 1\right\}. \tag{18}$$

(2) For $0 < \alpha < (1/2)$, the α-set of $A(-)_pB$ is

$$\left(A(-)_pB\right)^\alpha = \left\{(x,y) \in \mathbb{R}^2 | \left(\frac{3x - 3}{17 - 30\alpha}\right)^2 + \left(\frac{3y - 6}{22 - 39\alpha}\right)^2 = 1\right\}. \tag{19}$$

(3) $(A(\cdot)_p B)^\alpha = \{(x_\alpha(t), y_\alpha(t)) | 0 \le t \le 2\pi\}$, where

$$x_\alpha(t) = 6 + (14 - 24\alpha)\cos t + 4(1-2\alpha)(2-3\alpha)\cos^2 t, \quad 0 < \alpha < \frac{1}{2},$$
$$y_\alpha(t) = 15 + \left(\frac{86}{3} - 49\alpha\right)\sin t + 20(1-2\alpha)\left(\frac{2}{3} - \alpha\right)\sin^2 t, \quad 0 < \alpha < \frac{1}{2}. \tag{20}$$

(4) $(A(/)_p B)^\alpha = \{(x_\alpha(t), y_\alpha(t)) | 0 \le t \le 2\pi\}$, where

$$x_\alpha(t) = \frac{9 + 9(1-2\alpha)\cos t}{6 - 4(2-3\alpha)\cos t},$$
$$y_\alpha(t) = \frac{15 + 12(1-2\alpha)\sin t}{9 - 15(2-3\alpha)\sin t}, \tag{21}$$
$$0 < \alpha < \frac{1}{2}.$$

3. Parametric Operations for Generalized Three-Dimensional Triangular Fuzzy Sets on $\mathbb{R}^3$

We define the generalized three-dimensional triangular fuzzy sets on $\mathbb{R}^3$ as a generalization of generalized triangular fuzzy sets on $\mathbb{R}^2$. Then, we define the parametric operations between two generalized three-dimensional triangular fuzzy sets. For that, we have to calculate operations between α-sets in $\mathbb{R}^3$. The α-sets are regions in $\mathbb{R}^2$, but in $\mathbb{R}^3$, the α-sets are ellipsoids including interior, which makes the existing method of calculations between α-sets unusable. We interpret the existing method from a different perspective and apply the method to the ellipsoids including interior-valued α-sets on $\mathbb{R}^3$.

Definition 6. A fuzzy set A with a membership function $\mu_A(x, y, z)$ such that

$$\begin{cases} h - \sqrt{\dfrac{(x-x_1)^2}{a^2} + \dfrac{(y-y_1)^2}{b^2} + \dfrac{(z-z_1)^2}{c^2}}, & \text{if } b^2c^2(x-x_1)^2 + c^2a^2(y-y_1)^2 + a^2b^2(z-z_1)^2 \le a^2b^2c^2h^2, \\ 0, & \text{otherwise,} \end{cases} \tag{22}$$

where $a, b, c > 0$ and $0 < h < 1$ is called the generalized three-dimensional triangular fuzzy set and denoted by $(h, a, x_1, b, y_1, c, z_1)^3$.

Note that $\mu_A(x, y)$ is a cone in $\mathbb{R}^2$, but we cannot know the shape of $\mu_A(x, y, z)$ in $\mathbb{R}^3$. The α-cut A_α of a generalized three-dimensional triangular fuzzy number $A = (h, a, x_1, b, y_1, c, z_1)^3$ is the following set:

$$A_\alpha = \left\{ (x, y, z) \in \mathbb{R}^3 \middle| \left(\frac{x - x_1}{a(h-\alpha)}\right)^2 + \left(\frac{y - y_1}{b(h-\alpha)}\right)^2 + \left(\frac{z - z_1}{c(h-\alpha)}\right)^2 \le 1 \right\}. \tag{23}$$

Definition 7. A three-dimensional fuzzy number A defined on $\mathbb{R}^3$ is called convex fuzzy number if for all $\alpha \in (0, 1)$, the α-cuts,

$$A_\alpha = \left\{ (x, y, z) \in \mathbb{R}^3 | \mu_A(x, y, z) \ge \alpha \right\}, \tag{24}$$

are convex subsets in $\mathbb{R}^3$.

Theorem 3 (see [17]). *Let A be a continuous convex fuzzy number defined on $\mathbb{R}^3$ and $A^\alpha = \{(x, y, z) \in \mathbb{R}^3 | \mu_A(x, y, z) = \alpha\}$ be the α-set of A. Then, for all $\alpha \in (0, 1)$, there exist continuous functions $f_1^\alpha(s), f_2^\alpha(s, t)$, and $f_3^\alpha(s, t)$ $(0 \le s \le 2\pi, -(\pi/2) \le t \le (\pi/2))$ such that*

$$A^\alpha = \left\{ \left(f_1^\alpha(s), f_2^\alpha(s, t), f_3^\alpha(s, t)\right) \in \mathbb{R}^3 | 0 \le s \le 2\pi, -\frac{\pi}{2} \le t \le \frac{\pi}{2} \right\}. \tag{25}$$

Definition 8 (see [17]). Let A and B are two continuous convex fuzzy sets defined on $\mathbb{R}^3$ and

$$A^{\alpha}=\left\{\left(f_1^{\alpha}(s), f_2^{\alpha}(s,t), f_3^{\alpha}(s,t)\right)\in\mathbb{R}^3 \mid 0\le s\le 2\pi, -\frac{\pi}{2}\le t\le\frac{\pi}{2}\right\},$$
$$B^{\alpha}=\left\{\left(g_1^{\alpha}(s), g_2^{\alpha}(s,t), g_3^{\alpha}(s,t)\right)\in\mathbb{R}^3 \mid 0\le s\le 2\pi, -\frac{\pi}{2}\le t\le\frac{\pi}{2}\right\}, \tag{26}$$

be the α-set of A and B, respectively. For $\alpha \in (0,1)$, we define that the parametric addition, parametric subtraction, parametric multiplication, and parametric division of two fuzzy sets A and B are fuzzy numbers that have their α-sets as follows:

(1) Parametric addition $A(+)_pB$:

$$\left(A(+)_pB\right)^{\alpha}=\left\{\left(f_1^{\alpha}(s)+g_1^{\alpha}(s), f_2^{\alpha}(s,t)+g_2^{\alpha}(s,t), f_3^{\alpha}(s,t)+g_3^{\alpha}(s,t)\right)\in\mathbb{R}^3 \mid 0\le s\le 2\pi, -\frac{\pi}{2}\le t\le\frac{\pi}{2}\right\}. \tag{27}$$

(2) Parametric subtraction $A(-)_pB$:

$$\left(A(-)_pB\right)^{\alpha}=\left\{\left(f_1^{\alpha}(s)-g_1^{\alpha}(s+\pi), f_2^{\alpha}(s,t)-g_2^{\alpha}(s+\pi,t), f_3^{\alpha}(s,t)-g_3^{\alpha}(s+\pi,t)\right)\in\mathbb{R}^3 \mid 0\le s\le \pi, -\frac{\pi}{2}\le t\le\frac{\pi}{2},\right.$$
$$\left.\left(A(-)_pB\right)^{\alpha}=\left\{\left(f_1^{\alpha}(s)-g_1^{\alpha}(s-\pi) f_2^{\alpha}(s,t)-g_2^{\alpha}(s-\pi,t), f_3^{\alpha}(s,t)-g_3^{\alpha}(s-\pi,t)\right)\in\mathbb{R}^3 \mid \pi\le s\le 2\pi, -\frac{\pi}{2}\le t\le\frac{\pi}{2}\right\}. \tag{28}$$

(3) Parametric multiplication $A(\cdot)_pB$:

$$\left(A(\cdot)_pB\right)^{\alpha}=\left\{\left(f_1^{\alpha}(s)\cdot g_1^{\alpha}(s), f_2^{\alpha}(s,t)\cdot g_2^{\alpha}(s,t), f_3^{\alpha}(s,t)\cdot g_3^{\alpha}(s,t)\right)\in\mathbb{R}^3 \mid 0\le s\le 2\pi, -\frac{\pi}{2}\le t\le\frac{\pi}{2}\right\}. \tag{29}$$

(4) Parametric division $A(/)_pB$:

$$\left(A(/)_pB\right)^{\alpha}=\left\{\left(\frac{f_1^{\alpha}(s)}{g_1^{\alpha}(s+\pi)}, \frac{f_2^{\alpha}(s,t)}{g_2^{\alpha}(s+\pi,t)}, \frac{f_3^{\alpha}(s,t)}{g_3^{\alpha}(s+\pi,t)}\right)\in\mathbb{R}^3 \mid 0\le s\le \pi, \frac{\pi}{2}\le t\le\frac{\pi}{2}\right\},$$
$$\left(A(/)_pB\right)^{\alpha}=\left\{\left(\frac{f_1^{\alpha}(s)}{g_1^{\alpha}(s-\pi)}, \frac{f_2^{\alpha}(s,t)}{g_2^{\alpha}(s-\pi,t)}, \frac{f_3^{\alpha}(s,t)}{g_3^{\alpha}(s-\pi,t)}\right)\in\mathbb{R}^3 \mid \pi\le s\le 2\pi, -\frac{\pi}{2}\le t\le\frac{\pi}{2}\right\}. \tag{30}$$

For $\alpha = 0$ and $\alpha = 1$, $(A(*)_pB)^0 = \lim_{\alpha\longrightarrow 0^+}(A(*)_pB)^{\alpha}$ and $(A(*)_pB)^1 = \lim_{\alpha\longrightarrow 1^-}(A(*)_pB)^{\alpha}$, where $* = +, -, \cdot, /$.

Theorem 4 (see [17]). *Let $A = (h_1, a_1, x_1, b_1, y_1, c_1, z_1)^3$ and $B = (h_2, a_2, x_2, b_2, y_2, c_2, z_2)^3$ be two generalized three-dimensional triangular fuzzy sets. If $0 < h_1 < h_2 < 1$, then we have the following:*

(1) For $0 < \alpha < h_1$, the α-set of $A(+)_pB$ is

$$\left(A(+)_pB\right)^{\alpha}=\left\{(x,y,z)\in\mathbb{R}^3 \mid \left(\frac{x-x_1-x_2}{a_1(h_1-\alpha)+a_2(h_2-\alpha)}\right)^2+\left(\frac{y-y_1-y_2}{b_1(h_1-\alpha)+b_2(h_2-\alpha)}\right)^2+\left(\frac{z-z_1-z_2}{c_1(h_1-\alpha)+c_2(h_2-\alpha)}\right)^2=1\right\}. \tag{31}$$

(2) *For* $0<\alpha<h_1$, *the* α*-set of* $A(-)_pB$ *is*

$$\left(A(-)_pB\right)^\alpha=\left\{(x,y,z)\in\mathbb{R}^3\left|\left(\frac{x-x_1+x_2}{a_1(h_1-\alpha)+a_2(h_2-\alpha)}\right)^2+\left(\frac{y-y_1+y_2}{b_1(h_1-\alpha)+b_2(h_2-\alpha)}\right)^2+\left(\frac{z-z_1+z_2}{c_1(h_1-\alpha)+c_2(h_2-\alpha)}\right)^2=1\right.\right\}. \tag{32}$$

(3) *For* $0<\alpha<h_1$, $(A(\cdot)_pB)^\alpha=\{(x_\alpha(s),y_\alpha(s,t),z_\alpha(s,t))|0\le s\le 2\pi,-(\pi/2)\le t\le(\pi/2)\}$, *where*

$$\begin{aligned}x_\alpha(s)&=x_1x_2+(x_1a_2(h_2-\alpha)+x_2a_1(h_1-\alpha))\cos s+a_1a_2(h_1-\alpha)(h_2-\alpha)\cos^2 s,\\ y_\alpha(s,t)&=y_1y_2+(y_1b_2(h_2-\alpha)+y_2b_1(h_1-\alpha))\sin s\cos t+b_1b_2(h_1-\alpha)(h_2-\alpha)\sin^2 s\cos^2 t,\\ z_\alpha(s,t)&=z_1z_2+(z_1c_2(h_2-\alpha)+z_2c_1(h_1-\alpha))\sin s\sin t+c_1c_2(h_1-\alpha)(h_2-\alpha)\sin^2 s\sin^2 t.\end{aligned} \tag{33}$$

(4) *For* $0<\alpha<h_1$, $(A(/)_pB)^\alpha=\{(x_\alpha(s),y_\alpha(s,t),z_\alpha(s,t))$ $|0\le s\le 2\pi,-(\pi/2)\le t\le(\pi/2)\}$, *where*

$$\begin{aligned}x_\alpha(s)&=\frac{x_1+a_1(h_1-\alpha)\cos s}{x_2-a_2(h_2-\alpha)\cos s},\\ y_\alpha(s.t)&=\frac{y_1+b_1(h_1-\alpha)\sin s\cos t}{y_2-b_2(h_2-\alpha)\sin s\cos t},\\ z_\alpha(s.t)&=\frac{z_1+c_1(h_1-\alpha)\sin s\sin t}{z_2-c_2(h_2-\alpha)\sin s\sin t}.\end{aligned} \tag{34}$$

Furthermore, we have

$$\begin{aligned}\left(A(*)_pB\right)^0&=\lim_{\alpha\longrightarrow 0^+}\left(A(*)_pB\right)^\alpha,\quad *=+,-,\cdot,/,\\ \left(A(*)_pB\right)^{h_1}&=\lim_{\alpha\longrightarrow h_1^-}\left(A(*)_pB\right)^\alpha,\quad *=+,-,\cdot,/,\end{aligned} \tag{35}$$

If $h_1<\alpha\le h_2$, *by the Zadeh's max-min principle operations, we obtain*

$$\left(A(*)_pB\right)^\alpha=\varnothing,\quad *=+,-,\cdot,/, \tag{36}$$

4. A Generalization from $\mathbb{R}^2$ to $\mathbb{R}^3$ of Generalized Triangular Fuzzy Sets

In this section, we show that the parametric operations for two generalized triangular fuzzy sets defined on $\mathbb{R}^3$ are a generalization of parametric operations for two generalized triangular fuzzy sets defined on $\mathbb{R}^2$. For that, we have to prove that the intersections of the results on $\mathbb{R}^3$ and $z=0$ are the same as those on $\mathbb{R}^2$.

Theorem 5. *For* $*=+,-,\cdot,/$, *let* $\mu_{A(*)B}(x,y,z)$ *and* $\mu_{A(*)B}(x,y)$ *are the results in Theorem 3 and Theorem 2, respectively. Then, we have* $\mu_{A(*)B}(x,y,0)=\mu_{A(*)B}(x,y)$.

Proof. Consider $A=(h_1,a_1,x_1,b_1,y_1,0,0)^3$ and $B=(h_2,a_2,x_2,b_2,y_2,0,0)^3$, where $0<h_1<h_2<1$.

(1) For $0<\alpha<h_1$, the α-set of $\mu_{A(+)B}(x,y,0)$ is

$$\left\{(x,y)\in\mathbb{R}^2\left|\left(\frac{x-x_1-x_2}{a_1(h_1-\alpha)+a_2(h_2-\alpha)}\right)^2+\left(\frac{y-y_1-y_2}{b_1(h_1-\alpha)+b_2(h_2-\alpha)}\right)^2=1\right.\right\}. \tag{37}$$

Similarly, we can prove that the 0–set and h_1–set of $\mu_{A(+)B}(x,y,0)$ are the same as those of $\mu_{A(+)B}(x,y)$.

(2) For $0<\alpha<h_1$, the α-set of $\mu_{A(-)B}(x,y,0)$ is

$$\left\{(x,y)\in\mathbb{R}^2\left|\left(\frac{x-x_1+x_2}{a_1(h_1-\alpha)+a_2(h_2-\alpha)}\right)^2+\left(\frac{y-y_1+y_2}{b_1(h_1-\alpha)+b_2(h_2-\alpha)}\right)^2=1\right.\right\}. \tag{38}$$

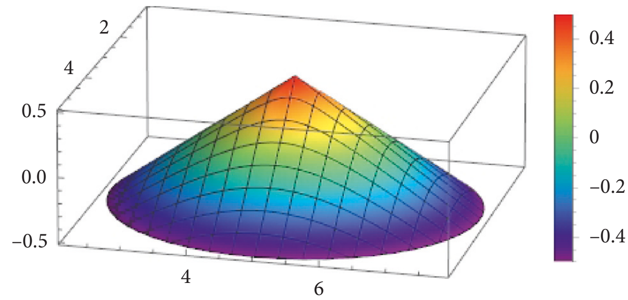

Figure 1: *A2D*.

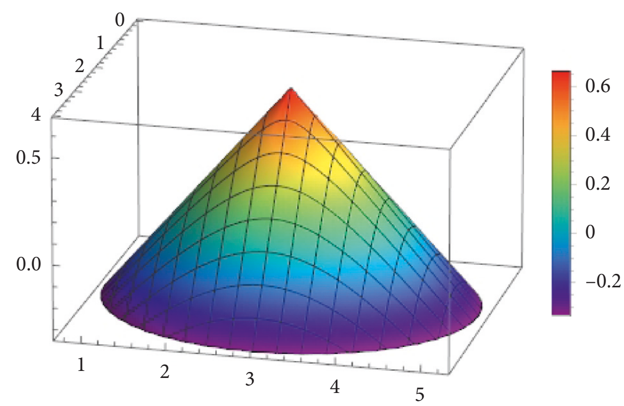

Figure 2: *B2D*.

Similarly, we can prove that the 0−set and h_1−set of $\mu_{A(-)B}(x, y, 0)$ are the same as those of $\mu_{A(-)B}(x, y)$.

(3) For $0 < \alpha < h_1$, the α-set of $\mu_{A(\cdot)B}(x, y, 0)$ is

$$S_1 = \left\{ (x_\alpha(s), y_\alpha(s,t)) \in \mathbb{R}^2 | 0 \le s \le 2\pi, -\frac{\pi}{2} \le t \le \frac{\pi}{2} \right\}, \tag{39}$$

where

$$\begin{aligned} x_\alpha(s) &= x_1x_2 + (x_1a_2(h_2-\alpha) + x_2a_1(h_1-\alpha))\cos s + a_1a_2(h_1-\alpha)(h_2-\alpha)\cos^2 s, \\ y_\alpha(s,t) &= y_1y_2 + (y_1b_2(h_2-\alpha) + y_2b_1(h_1-\alpha))\sin s\cos t + b_1b_2(h_1-\alpha)(h_2-\alpha)\sin^2 s\cos^2 t. \end{aligned} \tag{40}$$

In Theorem 2, the α-set of $\mu_{A(\cdot)B}(x, y)$ is

$$S_2 = \left\{ (x_\alpha(t), y_\alpha(t)) \in \mathbb{R}^2 | 0 \le t \le 2\pi \right\}, \tag{41}$$

where

$$\begin{aligned} x_\alpha(t) &= x_1x_2 + (x_1a_2(h_2-\alpha) + x_2a_1(h_1-\alpha))\cos t + a_1a_2(h_1-\alpha)(h_2-\alpha)\cos^2 t, \\ y_\alpha(t) &= y_1y_2 + (y_1b_2(h_2-\alpha) + y_2b_1(h_1-\alpha))\sin t + b_1b_2(h_1-\alpha)(h_2-\alpha)\sin^2 t. \end{aligned} \tag{42}$$

In three-dimensional case, the α−set becomes a convex set in $\mathbb{R}^2$. The boundary of S_1 is S_2. Clearly, $x_0(s) = x_0(t), x_{h_1}(s) = y_{h_1}(t)$, and we can prove that

$$\begin{aligned} y_0(s,t) &= y_0(t), \\ y_{h_1}(s,t) &= y_{h_1}(t). \end{aligned} \tag{43}$$

(4) For $0 < \alpha < h_1$, the α-set of $\mu_{A(/)B}(x, y, 0)$ is

$$S_3 = \left\{ (x_\alpha(s), y_\alpha(s,t)) \in \mathbb{R}^2 | 0 \le s \le 2\pi, -\frac{\pi}{2} \le t \le \frac{\pi}{2} \right\}, \tag{44}$$

where

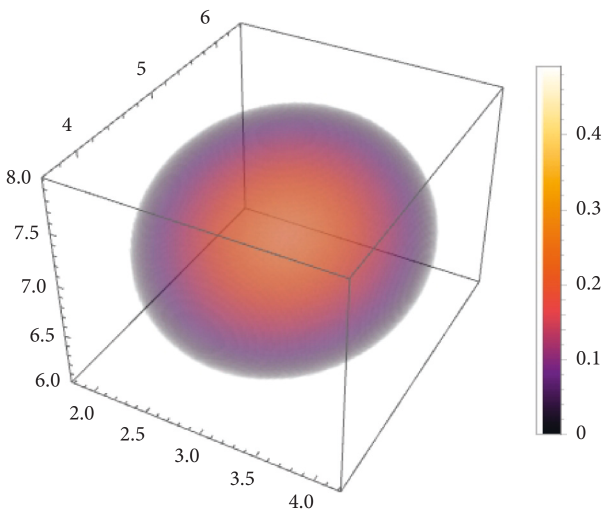

Figure 3: $A3D$.

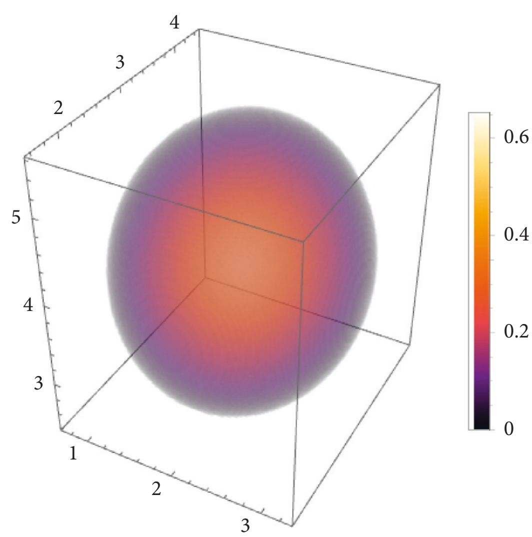

Figure 4: $B3D$.

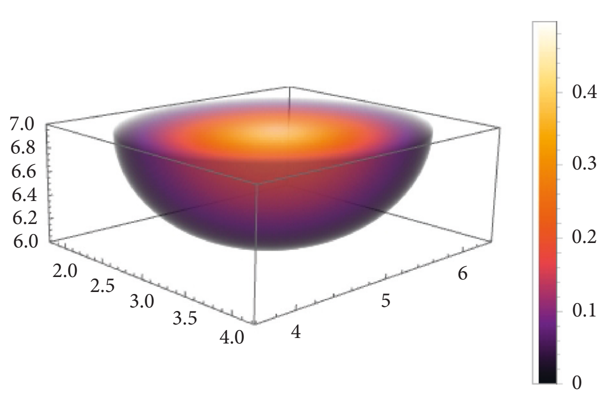

Figure 5: $A\,3D\,half - cut$.

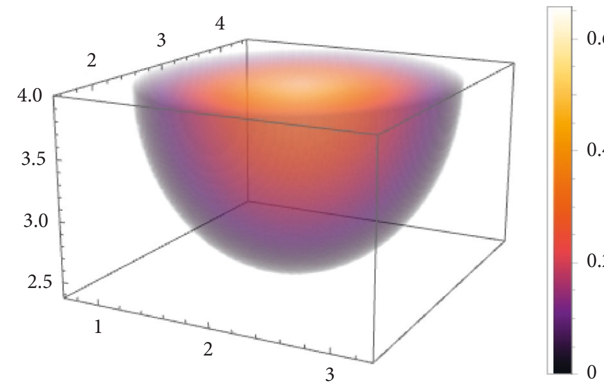

Figure 6: $B\,3D\,half - cut$.

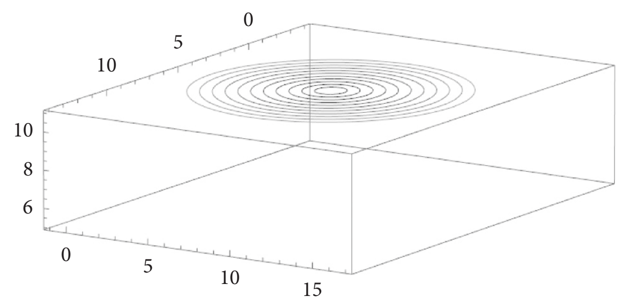

Figure 7: $A + B\,2D\,a - cut$.

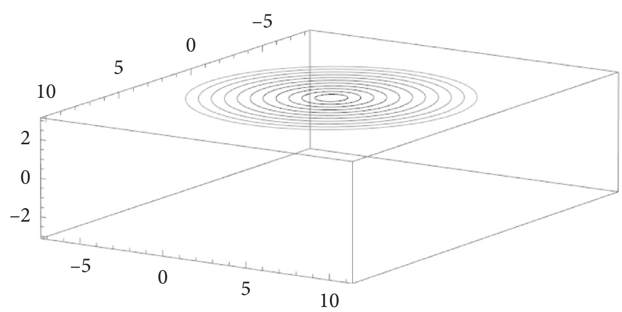

Figure 8: $A - B\,2D\,a - cut$.

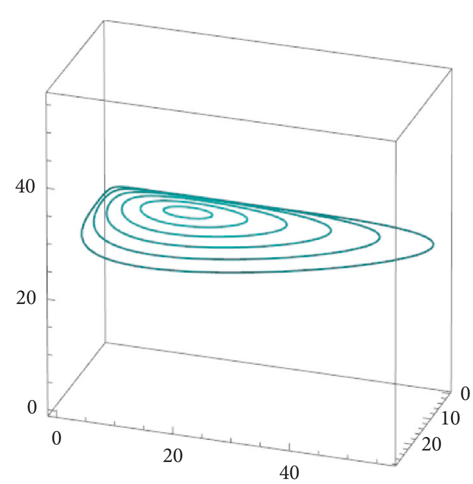

Figure 9: $AB\,2D\,a - cut$.

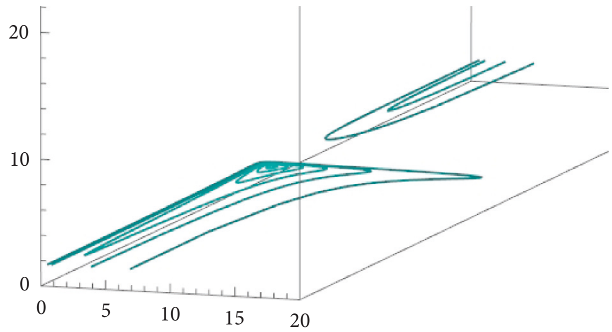

FIGURE 10: $AdB\ 2D\ a - cut$.

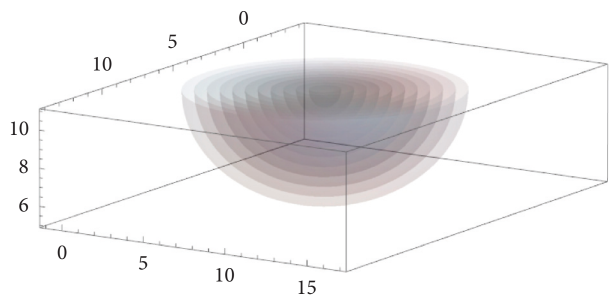

FIGURE 11: $A + B\ 3D\ half - cut$.

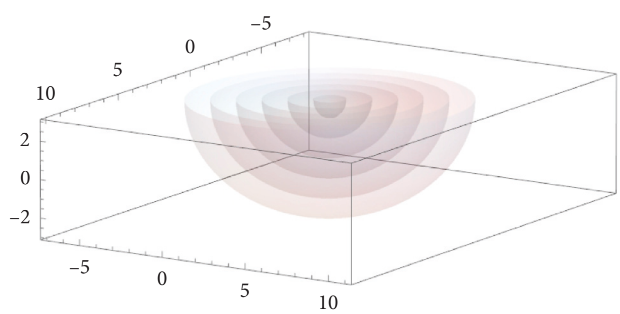

FIGURE 12: $A - B\ 3D\ half - cut$.

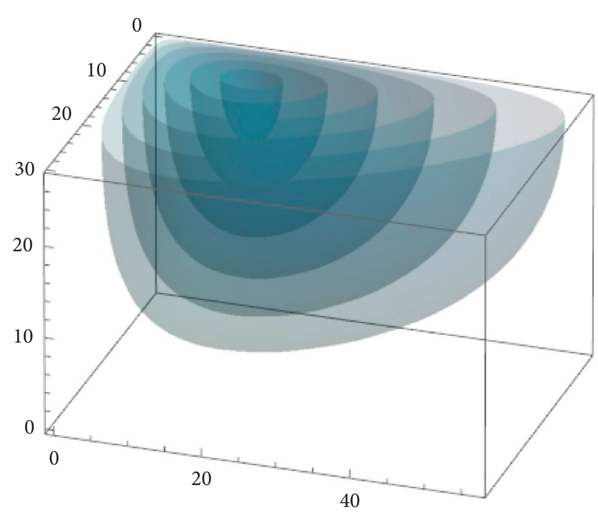

FIGURE 13: $AB\ 3D\ half - cut$.

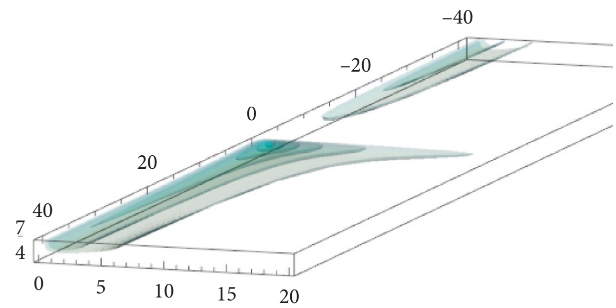

FIGURE 14: $AdB\ 3D\ half - cut$.

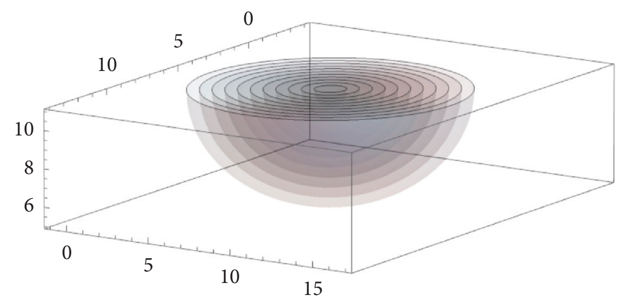

FIGURE 15: $A + B\ 2D = 3D$.

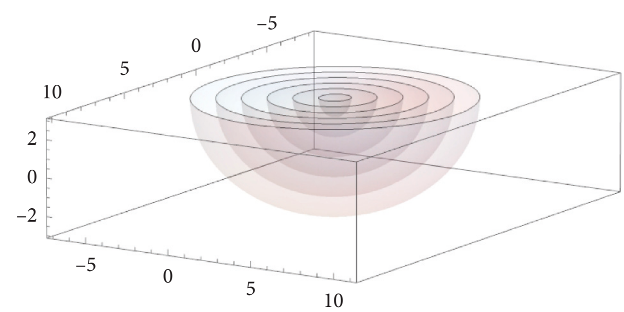

FIGURE 16: $A - B\ 2D = 3D$.

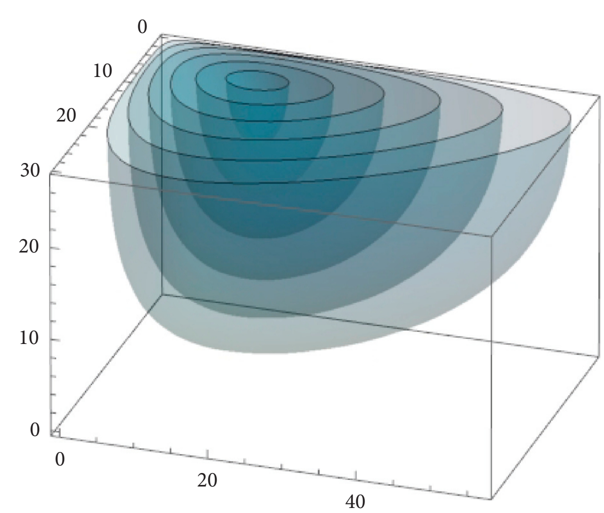

FIGURE 17: $AB\ 2D = 3D$.

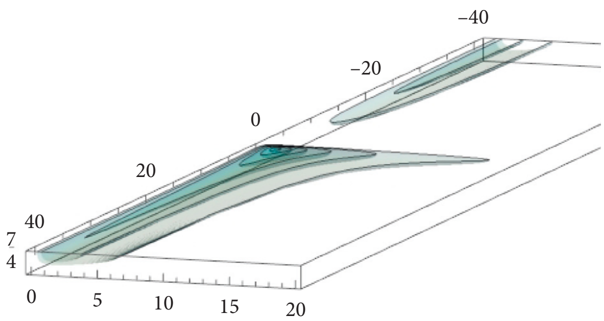

Figure 18: $AdB\,2D = 3D$.

$$x_\alpha(s) = \frac{x_1 + a_1(h_1 - \alpha)\cos s}{x_2 - a_2(h_2 - \alpha)\cos s},$$
$$y_\alpha(s.t) = \frac{y_1 + b_1(h_1 - \alpha)\sin s\cos t}{y_2 - b_2(h_2 - \alpha)\sin s\cos t}. \tag{45}$$

In Theorem 2, the α-set of $\mu_{A(/)B}(x, y)$ is

$$S_4 = \left\{(x_\alpha(t), y_\alpha(t)) \in \mathbb{R}^2 | 0 \le t \le 2\pi\right\}, \tag{46}$$

where

$$x_\alpha(t) = \frac{x_1 + a_1(h_1 - \alpha)\cos t}{x_2 - a_2(h_2 - \alpha)\cos t},$$
$$y_\alpha(t) = \frac{y_1 + b_1(h_1 - \alpha)\sin t}{y_2 - b_2(h_2 - \alpha)\sin t}. \tag{47}$$

In a three-dimensional case, the α-set becomes a convex set in $\mathbb{R}^2$. The boundary of S_3 is S_4. Clearly, $x_0(s) = x_0(t), x_{h_1}(s) = y_{h_1}(t)$, and we can prove that

$$y_0(s,t) = y_0(t),$$
$$y_{h_1}(s,t) = y_{h_1}(t). \tag{48}$$

Thus, $\mu_{A(*)B}(x, y, 0) = \mu_{A(*)B}(x, y)$. □

5. Conclusion

Extensive use of fuzzy theory in many different fields has facilitated active research on operators between fuzzy sets [18–20]. Operators of various concepts have been defined and studied, but Zadeh's operator concept is commonly studied and utilized. A correct understanding of the generalized triangular fuzzy set will be helpful in interpreting Zadeh's operators [21–24].

The conclusion of a general triangular fuzzy set in two-dimensional space is a function defined on a plane and can be expressed in a graph in three-dimensional space (Figures 1–6). Therefore, the graph in the form of an elliptical cone in two dimensions, the result of Section 2, is not difficult to understand (Figures 7–10).

However, if it is expanded to three dimensions, the domain becomes a three-dimensional set, making visual expression difficult. To help easier understanding, graphs were expressed in color density (Figures 11–14).

Each point on the cross section has a different color density, noting that each has a specific function value. In Section 4, we proved that the three-dimensional result is an extended concept of the two-dimensional result, which is indicated in graphs in Figures 15–18. When the three-dimensional result is cut with a vertical plane passing through the vertex, the cross section of the graph is two-dimensional. Function values in two-dimensional were represented in graphs with the z-axis value. Visualization of the results will lead to more application and utilization.

In Section 1, we discussed the theoretical flow and application of fuzzy sets. The study that extended Zadeh's operator theory to two or three dimensions is important in application. We have studied the extended algebraic operations between two fuzzy numbers and calculated Zadeh's max-min composition operator for two generalized triangular fuzzy sets in $\mathbb{R}^2$ and generalized the triangular fuzzy numbers from $\mathbb{R}^2$ to $\mathbb{R}^3$. The purpose of the paper is also presented.

In Section 2, we defined the generalized two-dimensional triangular fuzzy numbers on $\mathbb{R}^2$ as a generalization of generalized triangular fuzzy sets on $\mathbb{R}$ and the parametric operations between two generalized two-dimensional triangular fuzzy sets. In Theorem 2, we calculated the parametric operations between two generalized two-dimensional triangular fuzzy sets and gave an example.

In Section 3, we defined the generalized three-dimensional triangular fuzzy sets on $\mathbb{R}^3$ as a generalization of generalized triangular fuzzy sets on $\mathbb{R}^2$. Then, we defined the parametric operations between two generalized three-dimensional triangular fuzzy sets. We calculated the parametric operations between two generalized three-dimensional triangular fuzzy sets in Theorem 3.

In Section 4, we showed that the parametric operations for two generalized triangular fuzzy sets defined on $\mathbb{R}^3$ are a generalization of parametric operations for two generalized triangular fuzzy sets defined on $\mathbb{R}^2$. What has been proven is presented as an example. And the examples are expressed in various types of graphs for easier understanding.

Data Availability

No data were used to support this study.

Conflicts of Interest

The authors declare that there are no conflicts of interest regarding the publication of this article.

Acknowledgments

This research was supported by the 2022 Scientific Promotion Program funded by Jeju National University. Some of the 2D results have been published previously.

References

[1] L. A. Zadeh, "The concept of a linguistic variable and its application to approximate reasoning-I," *Information Sciences*, vol. 8, no. 3, pp. 199–249, 1975.

[2] L. A. Zadeh, "The concept of a linguistic variable and its application to approximate reasoning-II," *Information Sciences*, vol. 8, no. 4, pp. 301–357, 1975.

[3] L. A. Zadeh, "The concept of a linguistic variable and its application to approximate reasoning-III," *Information Sciences*, vol. 9, no. 1, pp. 43–80, 1975.

[4] A. M. Mustafa, Z. Gong, and M. Osman, "Fuzzy optimal control problem of several variables," *Advances in Mathematical Physics*, vol. 2019, Article ID 2182640, 12 pages, 2019.

[5] J. Ruan, X. Wang, C. Yue, G. Chen, and M. Kim, "Optimization models and algorithms for operation and control with advanced information technologies," *Scientific Programming*, vol. 2017, Article ID 4706714, 2 pages, 2017.

[6] A. M. Mustafa, Z. Gong, and M. Osman, "Fuzzy optimal control problem of several variables," *Advances in Mathematical Physics*, vol. 2019, Article ID 2182640, 12 pages, 2019.

[7] M. M. Gupta, T. Meitzler, Z. G. Hou, K. K. Garg, A. M. G. Solo, and L. A. Zadeh, "Real applications of fuzzy logic," *Advances in Fuzzy Systems*, vol. 2013, Article ID 581879, 3 pages, 2013.

[8] Z. Wenqiang, "Topic recommendation system using personalized fuzzy logic interest set," *Journal of Intelligent & Fuzzy Systems*, vol. 40, no. 2, pp. 2891–2901, 2021.

[9] J. Byun and Y. S. Yun, "Parametric operations for two fuzzy numbers," *Communications of the Korean Mathematical Society*, vol. 28, no. 3, pp. 635–642, 2013.

[10] C. I. Kim and Y. S. Yun, "Parametric operations for generalized 2-dimensional triangular fuzzy sets," *International Journal of Mathematical Analysis*, vol. 11, no. 4, pp. 189–197, 2017.

[11] H. S. Ko and Y. S. Yun, "Parametric operations between 2-dimensional triangular fuzzy number and trapezoidal fuzzy set," *Far East Journal of Mathematical Sciences*, vol. 102, no. 10, pp. 2459–2471, 2017.

[12] H. S. Ko and Y. S. Yun, "An extension of algebraic operations for 2-dimensional quadratic fuzzy number," *Far East Journal of Mathematical Sciences*, vol. 103, no. 12, pp. 2007–2015, 2018.

[13] Y. S. Yun, "Parametric operations for two 2-dimensional trapezoidal fuzzy sets," *Journal of Algebra and Applied Mathematics*, vol. 18, no. 1, pp. 27–41, 2020.

[14] Y. S. Yun, "An algebraic operations for two generalized 2-dimensional quadratic fuzzy sets," *Journal of the Chungcheong Mathematical Society*, vol. 31, no. 4, pp. 379–386, 2018.

[15] H. S. Ko, "Parametric operations for 2-dimensional fuzzy sets," PhD thesis, Department of Mathematics, Graduate School, Jeju National University, Jeju City, South Korea, 2018.

[16] Y. S. Yun, "A Zadeh′s max-min composition operator for 3-dimensional triangular fuzzy number," *Journal of Intelligent & Fuzzy Systems*, vol. 39, no. 3, pp. 3783–3793, 2020.

[17] Y. S. Yun, "Graphic representation of a dimensional expansion of triangular fuzzy number," *Journal of Mathematics*, vol. 2021, Article ID 1970553, 11 pages, 2021.

[18] M. P. A. Santim, M. C. M. Teixeira, W. A. de Souza, R. Cardim, and E. Assunção, "Design of a takagi-sugeno fuzzy regulator for a set of operation points," *Mathematical Problems in Engineering*, vol. 2012, Article ID 731298, 17 pages, 2012.

[19] S. A. M. Mohsenalhosseini and H. Mazaheri, "Approximate fixed point theorems in fuzzy norm spaces for an operator," *Advances in Fuzzy Systems*, vol. 2013, Article ID 613604, 8 pages, 2013.

[20] P. Chansangiam, "A survey on operator monotonicity, operator convexity, and operator means," *International Journal of Analysis*, vol. 2015, Article ID 649839, 8 pages, 2015.

[21] X. Zhang, W. Ma, and L. Chen, "New similarity of triangular fuzzy number and its application," *The Scientific World Journal*, vol. 2014, Article ID 215047, 7 pages, 2014.

[22] X. Cao, Z. Xing, Y. Sun, and S. Yin, "A novel dynamic multicriteria decision-making approach for low-carbon supplier selection of low-carbon buildings based on interval-valued triangular fuzzy numbers," *Advances in Civil Engineering*, vol. 2018, Article ID 7456830, 16 pages, 2018.

[23] N. Khan, N. Yaqoob, M. Shams, Y. U. Gaba, and M. Riaz, "Solution of linear and quadratic equations based on triangular linear diophantine fuzzy numbers," *Journal of Function Spaces*, vol. 2021, Article ID 8475863, 14 pages, 2021.

[24] J. Li and J. S. Chiou, "Two-dimensional fuzzy sliding mode control of a field-sensed magnetic suspension system," *Mathematical Problems in Engineering*, vol. 2014, Article ID 386796, 9 pages, 2014.

Hindawi
Journal of Mathematics
Volume 2022, Article ID 2886555, 7 pages
https://doi.org/10.1155/2022/2886555

Research Article

On Edge Irregular Reflexive Labeling for Generalized Prism

Chenxi Wang,[1] M. J. A. Khan,[2] M. Ibrahim ,[2] E. Bonyah ,[3] M. K. Siddiqui,[4] and S. Khalid[4]

[1]*Alliance Manchester Business School, The University of Manchester, Manchester, UK*
[2]*Centre for Advanced Studies in Pure and Applied Mathematics, Bahauddin Zakariya University, Multan, Pakistan*
[3]*Department of Mathematics Education, Akenten Appiah-Menka University of Skills Training and Entrepreneurial Development, Kumasi 00233, Ghana*
[4]*Department of Mathematics, Comsats University Islamabad, Lahore Campus, Lahore, Pakistan*

Correspondence should be addressed to E. Bonyah; ebonyah@aamusted.edu.gh

Received 3 January 2022; Accepted 26 January 2022; Published 7 March 2022

Academic Editor: M. T. Rahim

Copyright © 2022 Chenxi Wang et al. This is an open access article distributed under the Creative Commons Attribution License, which permits unrestricted use, distribution, and reproduction in any medium, provided the original work is properly cited.

Among the various ideas that appear while studying graph theory, which has gained much attraction especially in graph labeling, labeling of graphs gives mathematical models which value for a vast range of applications in high technology (data security, cryptography, various problems of coding theory, astronomy, data security, telecommunication networks, etc.). A graph label is a designation of graph elements, i.e., the edges and/or vertex of a group of numbers (natural numbers), and is called assignment or labeling. The vertex or edge labeling is related to their domain asset of vertices or edges. Likewise, for total labeling, we take the domain as vertices and edges both at the same time. The reflexive edge irregularity strength (res) is total labeling in which weights of edges are not the same for all edges and the weight of an edge is taken as the sum of the edge labels and the vertices associated with that edge. In the res, the vertices are labeled with nonnegative even integers while the edges are labeled with positive integers. We have to make the labels minimum, whether they are associated with vertices or edges. If such labeling exists, then it is called the res of H and is represented as $s\,\mathrm{res}(H)$. In this paper, we have computed the res for the Cartesian product of path and cycle graph which is also known as generalizing prism.

1. Introduction

Any graph H is the combination of vertices $V(H)$ along with a possibly nonempty edge set $E(H)$ of 2–element subsets of $V(H)$. In this paper, all the chosen graphs are finite, without direction, nontrivial, connected, and simple (without loops and multiedges). For details about notations, see [1, 2]. Nonnegative integers are used in this research. In 1988, Chartrand et al. [3] proposed the labeling problems in graph theory. Assign the edges positive integer to all connected simple graphs such as the graph became irregular. The irregular labeling is defined as $\psi\colon E(H) \longrightarrow \{1, 2, 3, \ldots, m\}$ and is called irregular m–labeling for graph H if all the separate nodes u and u' have distinctly weights, that is,

$$\sum_{x\in V} \psi(ux) \neq \sum_{y\in V} \psi(u'y). \tag{1}$$

Lahel, in [4], studied, in detail, for the irregularity strength. For more results, see the works of Nierhoff in [5], Dimitz et al. in [6], Amar and Togni in [7], and Gyarfas in [8].

In [9], A. Ahmad et al. defined on edge irregularity strength $(es(H))$ for any two edges u_1u_2 and $u_1'u_2'$ that the weights $w_\phi(u_1u_2)$ and $w_\phi(u_1'u_2')$ are distinct, as weight for an edge $u_1u_2 \in E(H)$ is $w_\phi(u_1u_2) = \phi(u_1) + \phi(u_2)$.

In [10], Bača et al. defined the parameter of total labeling for edge as well as vertex of graph and found the weights of an edge as sum of three integers which include the edge label and the labels of two vertices associated with that edge, and finally, every edge has distinct weight. For detailed studies on total edge irregularity strength, see [10, 11].

The concept of total edge irregularity strength has been generalized by Zhang et al. in [12] for graph will be reflexive edge irregularity strength m–labeling.

If, for any graph H, the total m–labeling defined the mapping $\psi_{e'}: E(H) \longrightarrow \{1, 2, 3 \ldots, m_{e'}\}$ and $\psi_{v'}: V(H) \longrightarrow \{0, 2, 4, \ldots, 2m_{v'}\}$, the mapping ψ is a total m–mapping of H such that $\psi(a) = \psi_v(a)$ if $a \in V(H)$ and $\psi(a) = \psi_e(a)$ if $a \in E(H)$, where $k = \max\{m_{e'}, 2m_{v'}\}$.

The total p–labeling ψ will be edge irregular reflexive p–labeling of the graph H if, for all the different edges say u_1u_2 and $u_1'u_2'$, the weights $w_\phi(u_1u_2)$ and $w_\phi(u_1'u_2')$ are not the same for every choice of edges where the weight for any edge suppose $u_1u_2 \in E(H)$ is $w_\phi(u_1u_2) = \phi(u_1) + \phi(u_1u_2) + \phi(u_2)$.

The smallest value of p for which such mapping exists is said to be res of the graph H and is represented by $\operatorname{res}(H)$. For details in reflexive edge irregularity strength, see [13–17].

For $\operatorname{res}(H)$, Nierhoff [5] proposed that for any graph $H(s,t)$ with maximum degree $\Delta(H)$ satisfies

$$\operatorname{res}(H) = \max\left\{\left\lceil \frac{|t|}{3} + r \right\rceil, \left\lfloor \frac{\Delta}{2} + 1 \right\rfloor\right\}, \tag{2}$$

where r will be 1 for $|t| \equiv 2, 3 \pmod 6$; it will be 0, otherwise.

In [12], the lemma is proven.

Lemma 1. *For all graph say H,*

$$\operatorname{res}(H) \geq \begin{cases} \left\lceil \dfrac{|t|}{3} \right\rceil + 1, & \text{if } |t| \equiv 2, 3 \pmod 6, \\ \left\lceil \dfrac{|t|}{3} \right\rceil, & \text{if } |t| \equiv 1, 4, 5 \pmod 6. \end{cases} \tag{3}$$

In the present research paper, we have investigated the res for the Cartesian product of paths and cycles.

1.1. Definition. The Cartesian product P and Q graphs is represented as $P \square Q$ and is the graph with vertices set $V(P) \times V(Q)$, with vertices (u_1, u_1') and (w_1, w_1') will be adjacent if and only if $u_1 = w_1$ and $u_1'w_1' \in E(Q)$ or $u_1' = w_1'$ and $u_1w_1 \in E(P)$.

Theorem 1. *Let P_d and C_c be path and cycle, respectively; then, for edge irregular reflexive strength of $P_d \square C_c$ with $d \geq 3$ and $c \geq 2$. We have*

$$\operatorname{res}(P_d \square C_c) = \begin{cases} \left\lceil \dfrac{(2d-1)c}{3} \right\rceil + 1, & \text{if } |(2d-1)c| \equiv 2, 3 (\mathrm{mod}6), \\ \left\lceil \dfrac{(2d-1)c}{3} \right\rceil, & \text{if } |(2d-1)c| \equiv 1, 4, 5, 6 (\mathrm{mod}6). \end{cases} \tag{4}$$

Proof. As $P_d \square C_c$ has $(2d-1)c$ edges, therefore, from Lemma 1, we obtain

$$\operatorname{res}(P_d \square C_c) \geq \begin{cases} \left\lceil \dfrac{(2d-1)c}{3} \right\rceil + 1, & \text{if } |(2d-1)c| \equiv 2, 3 (\mathrm{mod}6), \\ \left\lceil \dfrac{(2d-1)c}{3} \right\rceil, & \text{if } |(2d-1)c| \equiv 1, 4, 5, 6 (\mathrm{mod}6). \end{cases} \tag{5}$$

Next, we will show that

$$\operatorname{res}(P_d \square C_c) \leq \begin{cases} \left\lceil \dfrac{(2d-1)c}{3} \right\rceil + 1, & \text{if } |(2d-1)c| \equiv 2, 3 (\mathrm{mod}6), \\ \left\lceil \dfrac{(2d-1)c}{3} \right\rceil, & \text{if } |(2d-1)c| \equiv 1, 4, 5, 6 (\mathrm{mod}6). \end{cases} \tag{6}$$

We defined a f–labeling for this on $(P_d \square C_c)$ as follows: $\forall\, 1 \leq j \leq c$.

Let $e = x_{i,j}$, $h = x_{i+1,j}$, and $k = x_{i,j+1}$ □

Case 1. When $d \equiv 0 \pmod 3$, c is odd:

$$f(e) = \begin{cases} c(i-1), & \text{for } 1 \leq i \leq \dfrac{2d-3}{3} \ (i \text{ is odd}), \\ c(i-1) - 1, & \text{for } 2 \leq i \leq \dfrac{2d}{3} \ (i \text{ is even}), \\ k, & \text{for } \dfrac{2d+3}{3} \leq i \leq d. \end{cases} \tag{7}$$

When $c \equiv 1 \pmod 6$,

$$\begin{aligned} f((e)(k)) &= \begin{cases} j, & \text{for } 1 \leq i \leq \dfrac{2d-3}{3}, \\ j+2, & \text{for } 2 \leq i \leq \dfrac{2d}{3}, \\ \dfrac{6ci - 2(2cd - c - 1)}{3} + j, & \text{for } \dfrac{2d+3}{3} \leq i \leq d, \end{cases} \\ f((e)(h)) &= \begin{cases} j+1, & \text{for } 1 \leq i \leq \dfrac{2d-3}{3}, \\ \dfrac{c-1}{3} + 1 + j & \text{for } i = \dfrac{2d}{3}, \\ \dfrac{6ci - (4cd + c + 2)}{3} + j, & \text{for } \dfrac{2d+3}{3} \leq i \leq d-1. \end{cases} \end{aligned} \tag{8}$$

When $c \equiv 3 \pmod 6$,

$$\begin{aligned} f((e)(k)) &= \begin{cases} j, & \text{for } 1 \leq i \leq \dfrac{2d-3}{3}, \\ j+2, & \text{for } 2 \leq i \leq \dfrac{2d}{3}, \\ \dfrac{6ci - 2(2cd + 2c + 3)}{3} + j & \text{for } \dfrac{2d}{3} + 1 \leq i \leq d, \end{cases} \\ f((e)(h)) &= \begin{cases} j+1, & \text{for } 1 \leq i \leq \dfrac{2d-3}{3}, \\ \dfrac{2(c-1)}{3} + 1 + j & \text{for } i = \dfrac{2d}{3}, \\ \dfrac{6ci - 4c(d+1)}{3} + j, & \text{for } \dfrac{2d+3}{3} \leq i \leq d-1. \end{cases} \end{aligned} \tag{9}$$

When $c \equiv 5 \pmod 6$,

$$f((e)(k)) = \begin{cases} j, & \text{for } 1 \le i \le \dfrac{2d-3}{3}\ (i \text{ is odd}), \\ j+1, & \text{for } 2 \le i \le \dfrac{2d}{3}\ (i \text{ is even}), \\ \dfrac{6ci - 2(2cd + 2d - 1)}{3} + j, & \text{for } \dfrac{2d+3}{3} \le i \le d, \end{cases}$$

$$f((e)(h)) = \begin{cases} j+1, & \text{for } 1 \le i \le \dfrac{2d}{3} - 1, \\ \left(\dfrac{c-5}{3}\right) + 3 + j & \text{for } i = \dfrac{2d}{3}, \\ \dfrac{6ci - (4cd + c - 2)}{3} + j, & \text{for } \dfrac{2d}{3} + 1 \le i \le d - 1. \end{cases} \tag{10}$$

Case 2. When $d \equiv 0 \pmod 3$, c is even:

$$f(e) = \begin{cases} d(i-1), & \text{for } 1 \le i \le \dfrac{2d}{3}, \\ k, & \text{for } \dfrac{2d+3}{3} \le i \le d. \end{cases} \tag{11}$$

When $d \equiv 0 \pmod 6$,

$$f((e)(k)) = \begin{cases} j, & \text{for } 1 \le i \le \dfrac{2d}{3}, \\ (6i - 4d - 4)\dfrac{c}{3} + j, & \text{for } \dfrac{2d+3}{3} \le i \le d, \end{cases}$$

$$f((e)(h)) = \begin{cases} j, & \text{for } 1 \le i \le \dfrac{2d}{3} - 1, \\ \dfrac{c}{3} + j & \text{for } i = \dfrac{2d}{3}, \\ (6i - 4d - 1)\dfrac{c}{3} + j, & \text{for } \dfrac{2d}{3} + 1 \le i \le d - 1. \end{cases} \tag{12}$$

When $c \equiv 2 \pmod 6$,

$$f((e)(k)) = \begin{cases} j, & \text{for } 1 \le i \le \dfrac{2d}{3}, \\ \dfrac{6ci - 4(cd + c + 1)}{3} + j, & \text{for } \dfrac{2d+3}{3} \le i \le d, \end{cases}$$

$$f((e)(h)) = \begin{cases} j, & \text{for } 1 \le i \le \dfrac{2d-3}{3}, \\ \left(\dfrac{c-2}{3}\right) + j & \text{for } i = \dfrac{2d}{3}, \\ \dfrac{6ci - (4cd + c + 4)}{3} + j, & \text{for } \dfrac{2d}{3} + 1 \le i \le d - 1. \end{cases} \tag{13}$$

When $c \equiv 4 \pmod 6$,

$$f((e)(k)) = \begin{cases} j, & \text{for } 1 \le i \le \dfrac{2d}{3}, \\ \dfrac{6ci - 4(cd + c + 2)}{3} + j, & \text{for } \dfrac{2d}{3} + 1 \le i \le d, \end{cases}$$

$$f((e)(h)) = \begin{cases} j, & \text{for } 1 \le i \le \dfrac{2d}{3} - 1, \\ \dfrac{2(c-4)}{3} + j & \text{for } i = \dfrac{2d}{3}, \\ \dfrac{6ci - (4cd + c + 8)}{3} + j, & \text{for } \dfrac{2d}{3} + 1 \le i \le d - 1. \end{cases} \tag{14}$$

Case 3. When $d \equiv 1 \pmod 3$, c is even:

$$f(e) = \begin{cases} c(i-1), & \text{for } 1 \le i \le \dfrac{2d+1}{3}, \\ k, & \text{for } 2\left(\dfrac{d+2}{3}\right) \le i \le d. \end{cases} \tag{15}$$

When $d \equiv 1 \pmod 3$ and $c \equiv 0 \pmod 6$,

$$f((e)(k)) = \begin{cases} j, & \text{for } 1 \le i \le \dfrac{2d+1}{3}, \\ \dfrac{c(6i - 4d - 4)}{3} + j, & \text{for } \dfrac{2(d+2)}{3} \le i \le d, \end{cases}$$

$$f((e)(h)) = \begin{cases} j, & \text{for } 1 \le i \le 2\left(\dfrac{d-1}{3}\right), \\ \dfrac{2c}{3} + j, & \text{for } i = \dfrac{2d+1}{3}, \\ \dfrac{c(6i - 4d - 1)}{3} + j, & \text{for } \dfrac{2d+4}{3} \le i \le d - 1. \end{cases} \tag{16}$$

When $d \equiv 1 \pmod 3$ and $c \equiv 2 \pmod 6$,

$$f((e)(k)) = \begin{cases} j, & \text{for } 1 \le i \le \dfrac{2d+1}{3}, \\ \dfrac{6ci - 4(cd + c + 2)}{3} + j, & \text{for } 2\left(\dfrac{d+2}{3}\right) \le i \le d, \end{cases}$$

$$f((e)(h)) = \begin{cases} j, & \text{for } 1 \le i \le 2\left(\dfrac{d-1}{3}\right), \\ \dfrac{2(c-2)}{3} + j, & \text{for } i = \dfrac{2d+1}{3}, \\ \dfrac{6ci - (4cd + c + 8)}{3} + j, & \text{for } 2\left(\dfrac{d+2}{3}\right) \le i \le d - 1. \end{cases} \tag{17}$$

When $d \equiv 1 \pmod 3$ and $c \equiv 4 \pmod 6$,

$$f((e)(k)) = \begin{cases} j, & \text{for } 1 \le i \le \dfrac{2d+1}{3}, \\ \dfrac{6ci - 4(cd+c+1)}{3} + j & \text{for } 2\left(\dfrac{d+2}{3}\right) \le i \le d, \end{cases}$$

$$f((e)(h)) = \begin{cases} j, & \text{for } 1 \le i \le 2\left(\dfrac{d-1}{3}\right), \\ \dfrac{2(c-4)}{3} + 2 + j, & \text{for } i = \dfrac{2d+1}{3}, \\ \dfrac{6ci - (4cd+c+4)}{3} + j, & \text{for } 2\left(\dfrac{d+2}{3}\right) \le i \le d-1. \end{cases} \tag{18}$$

Case 4. When $d \equiv 1 \pmod 3$, c is odd:

$$f(e) = \begin{cases} c(i-1), & \text{for } 1 \le i \le \dfrac{2d+1}{3} \ (i \text{ is odd}). \\ c(i-1) - 1, & \text{for } 2 \le i \le \dfrac{2(d-1)}{3} \ (i \text{ is even}). \\ k, & \text{for } \dfrac{2(d+2)}{3} \le i \le d. \end{cases} \tag{19}$$

An illustration of this reflexive labeling is shown in Figures 1 and 2.

When $d \equiv 1 \pmod 3$ and $c \equiv 1 \pmod 6$,

$$f((e)(k)) = \begin{cases} j, & \text{for } 1 \le i \le \dfrac{2d+1}{3} \ (i \text{ is odd}), \\ j+2, & \text{for } 2 \le i \le \dfrac{2(n-1)}{3} \ (i \text{ is even}), \\ \dfrac{6ci - (4cd+4c-2)}{3} + j & \text{for } \dfrac{2(d+2)}{3} \le i \le d, \end{cases}$$

$$f((e)(h)) = \begin{cases} j+1, & \text{for } 1 \le i \le \dfrac{2(d-1)}{3}, \\ \dfrac{2c+1}{3} + j, & \text{for } i = \dfrac{2d+1}{3}, \\ \dfrac{6ci - (4cd+5)}{3} + j, & \text{for } \dfrac{2(n+2)}{3} \le i \le d-1. \end{cases} \tag{20}$$

When $d \equiv 1 \pmod 3$ and $c \equiv 3 \pmod 6$,

$$f((e)(k)) = \begin{cases} j, & \text{for } 1 \le i \le \dfrac{2d+1}{3} \ (i \text{ is odd}), \\ j+2, & \text{for } 2 \le i \le \dfrac{2(d-1)}{3} \ (i \text{ is even}), \\ \dfrac{c(6i-4d-4)}{3} - 2 + j & \text{for } \dfrac{2(d+2)}{3} \le i \le d, \end{cases}$$

$$f((e)(h)) = \begin{cases} j+1, & \text{for } 1 \le i \le \dfrac{2(d-1)}{3}, \\ \dfrac{2c}{3} - 1 + j, & \text{for } i = \dfrac{2d+1}{3}, \\ \dfrac{c(6i-4d-1)}{3} - 2 + j, & \text{for } \dfrac{2(d+2)}{3} \le i \le d-1. \end{cases} \tag{21}$$

When $d \equiv 1 \pmod 3$ and $c \equiv 5 \pmod 6$,

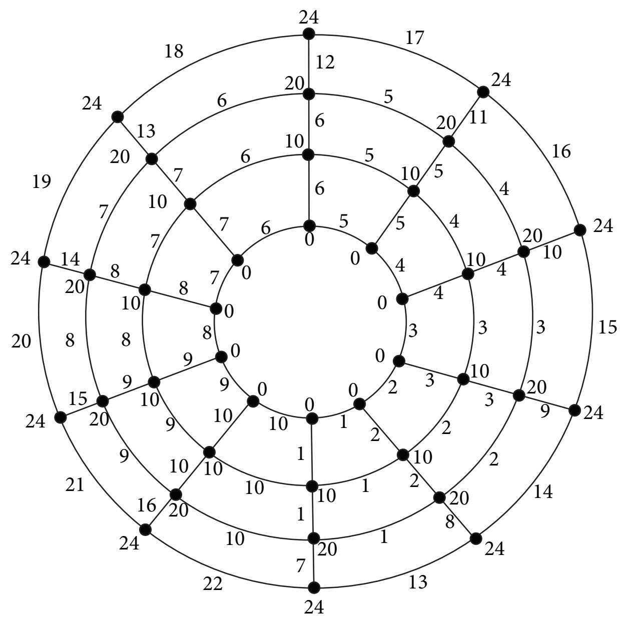

Figure 1: Twenty four labeling of $P_4\square C_{10}$.

$$
\begin{aligned}
f((e)(k)) &= \begin{cases} j, & \text{for } 1 \le i \le \dfrac{2d+1}{3} \ (i \text{ is odd}), \\[2ex] j+2, & \text{for } 1 \le i \le \dfrac{2(d-1)}{3} \ (i \text{ is even}), \\[2ex] \dfrac{6ci - 4c(d+1) - 2}{3} + j & \text{for } \dfrac{2(d+2)}{3} \le i \le d, \end{cases} \\
f((e)(h)) &= \begin{cases} j+1, & \text{for } 1 \le i \le 2\left(\dfrac{d-1}{3}\right), \\[2ex] \dfrac{2(c-5)}{3} + 3 + j, & \text{for } i = \dfrac{2d+1}{3}, \\[2ex] \dfrac{6ci - (4cd + c + 2)}{3} + j, & \text{for } \dfrac{2(d+2)}{3} \le i \le d-1. \end{cases}
\end{aligned} \tag{22}
$$

Case 5. When $d \equiv 2 \pmod 3$, c is even and $c \ge 4$:

$$
f(e) = \begin{cases} c(i-1), & \text{for } 1 \le i \le \dfrac{2d-1}{3}, \\[2ex] k, & \text{for } \dfrac{2d+2}{3} \le i \le d, \end{cases}
$$

$$
f((e)(k)) = \begin{cases} j, & \text{for } 1 \le i \le \dfrac{2d+2}{3}, \\[2ex] \dfrac{6ci - 4(cd - 2c + 3)}{3} + j & \text{for } \dfrac{2d+5}{3} + 3 \le i \le d, \end{cases}
$$

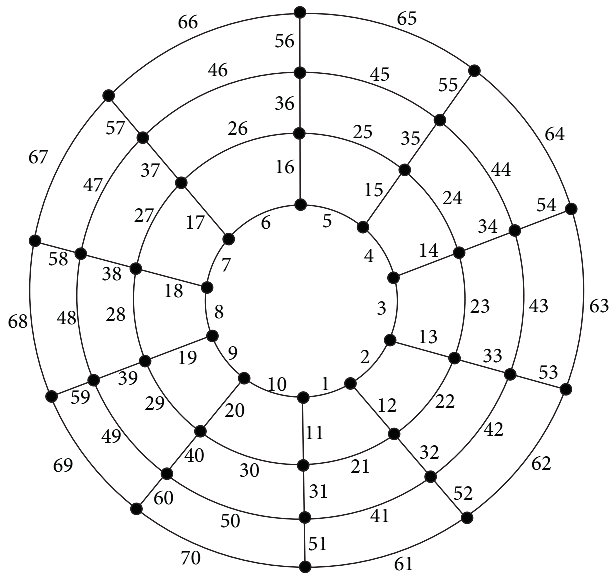

Figure 2: Edge weights of $P_4 \square C_{10}$.

$$f((e)(h)) = \begin{cases} j, & \text{for } 1 \leq i \leq \dfrac{2d-1}{3}, \\ \dfrac{6ci - 4(d-2)c - 9}{3} + j, & \text{for } \dfrac{2d+2}{3} \leq i \leq d-1. \end{cases} \quad (23)$$

Case 6. When $d \equiv 2 \,(\mathrm{mod}\, 3)$, c is odd and $c \geq 3$:

$$f(e) = \begin{cases} c(i-1), & \text{for } 1 \leq i \leq \dfrac{2d-1}{3} \; (i \text{ is odd}), \\ c(i-1)-1, & \text{for } 2 \leq i \leq \dfrac{2d+2}{3} \; (i \text{ is even}), \\ k, & \text{for } \dfrac{2d+5}{3} \leq i \leq d, \end{cases}$$

$$f((e)(k)) = \begin{cases} j, & \text{for } 1 \leq i \leq \dfrac{2d-1}{3} \; (i \text{ is odd}), \\ j+2, & \text{for } 2 \leq i \leq \dfrac{2d+2}{3} \; (i \text{ is even}), \\ \dfrac{6ci - 4(d+1)c}{3} - 2 + j & \text{for } \dfrac{2d+5}{3} \leq i \leq d, \end{cases} \quad (24)$$

$$f((e)(h)) = \begin{cases} j+1, & \text{for } 1 \leq i \leq \dfrac{2d-1}{3}, \\ (2c-2)i - \dfrac{(4d+1)(c-1)}{3} - 1 + j, & \text{for } \dfrac{2d+2}{3} \leq i \leq d-1. \end{cases}$$

Weights for reflexive edges is given as follows: for $1 \le i \le d-1\,1, \le i \le c$, weight of edge $((x_{i,j})(x_{i+1,j}))$ is $(2i-1)c+j$ and weight of the edge $((x_{i,j})(x_{i,j+1}))$ is $2c(i-1)+j$,

None of the two edges are of the same weight. So, we get the required result, for $c \ge 2$ and $d \ge 3$, which completes the proof.

2. Conclusion

In the present paper, we found the reflexive edge irregularity strength for generalized prism graph $(P_d \square C_c)$, for $d \ge 3$ and $c \ge 2$.

Data Availability

No data were used to support the findings of the study.

Conflicts of Interest

The authors declare that they have no conflicts of interest.

References

[1] S. Brandt, J. Miškuf, and D. Rautenbach, "On a conjecture about edge irregular total labelings," *Journal of Graph Theory*, vol. 57, no. 4, pp. 333–343, 2008.

[2] G. Chartrand, L. Lesniak, and P. Zhang, *Graphs and Diagraphs*, Taylor and Francis Group Boca Raton, New York, USA, 6th edition, 2016.

[3] G. Chartrand, M. S. Jacobson, J. Lehel, O. R. Oellermann, S. Ruiz, and F. Saba, "Irregular networks," *Congressus Numerantium*, vol. 64, pp. 187–192, 1988.

[4] J. Lahel, "Facts and quests on degree irregular assignment," in *Graph Theory, Combinatorics and Applications*, pp. 765–782, Wley, New York, NY, USA, 1991.

[5] T. Nierhoff, "A tight bound on the irregularity strength of graphs," *SIAM Journal on Discrete Mathematics*, vol. 13, no. 3, pp. 313–323, 2000.

[6] J. H. Dimitz, D. K. Garnick, and A. Gyárfás, "On the irregularity strength of the $m \times n$ grid," *Journal of Graph Theory*, vol. 16, pp. 355–374, 1992.

[7] D. Amar and O. Togni, "Irregularity strength of trees," *Discrete Mathematics*, vol. 190, no. 1-3, pp. 15–38, 1998.

[8] A. Gyárfás, "The irregularity strength of $K_{m,\,m}$ is 4 for odd m," *Discrete Mathematics*, no. 71, pp. 273-274, 1998.

[9] A. Ahmad, O. B. S. Al-Mushayt, and M. Bača, "On edge irregularity strength of graphs," *Applied Mathematics and Computation*, vol. 243, pp. 607–610, 2014.

[10] M. Baca, M. Miller, and J. Ryan, "On irregular total labellings," *Discrete Mathematics*, vol. 307, no. 11-12, pp. 1378–1388, 2007.

[11] A. Ahmad, M. Bača, and M. K. Siddiqui, "On edge irregular total labeling of categorical product of two cycles," *Theory of Computing Systems*, vol. 54, no. 1, pp. 1–12, 2014.

[12] X. Zhang, M. Ibrahim, S. Bokhary, and M. Siddiqui, "Edge irregular reflexive labeling for the disjoint union of gear graphs and prism graphs," *Mathematics*, vol. 6, no. 9, pp. 142–155, 2018.

[13] I. H. Agustin, M. I. Utoyo, M. Dafik, M. Venkatachalam, and F. Surahmat, "On the construction of the reflexive vertex k-labeling of any graph with pendant vertex," *International Journal of Mathematics and Mathematical Sciences*, vol. 2020, no. 1, 8 pages, Article ID 7812812, 2020.

[14] M. Baca, M. Irfan, J. Ryan, A. Semanicov-Fenovckov, and D. Tanna, "Note on edge irregular reflexive labelings of graphs," *AKCE International Journal of Graphs and Combinatorics*, vol. 16, no. 2, pp. 145–157, 2019.

[15] M. Baca, M. Irfan, J. Ryan, A. Semanicov-Fenovckov, and D. Tanna, "On edge irregular reflexive labellings for the generalized friendship graphs," *Mathematics*, vol. 5, no. 4, pp. 67–77, 2017.

[16] M. Ibrahim, S. Majeed, and M. K. Siddiqui, "Edge irregular reflexive labeling for star and caterpillar graphs," *TWMS Journal of Applied and Engineering Mathematics*, vol. 10, no. 3, pp. 718–726, 2020.

[17] D. Tanna, J. Ryan, and A. Semabičovǎ-Feňovčkovǎ, "A reflexive edge irregular labelings of prisms and wheels," *Australasian Journal of Combinatorics*, vol. 69, pp. 394–401, 2017.

Hindawi
Journal of Mathematics
Volume 2022, Article ID 9269830, 18 pages
https://doi.org/10.1155/2022/9269830

Research Article

Computing the Normalized Laplacian Spectrum and Spanning Tree of the Strong Prism of Octagonal Network

Yasir Ahamad,[1] Umar Ali,[1] Imran Siddique ,[2] Aiyared Iampan ,[3] Walaa A. Afifi,[4,5] and Hamiden Abd-El-Wahed Khalifa[6,7]

[1]*School of Mathematical Sciences, Anhui University, Hefei, Anhui 230601, China*
[2]*Department of Mathematics, University of Management and Technology, Lahore 54770, Pakistan*
[3]*Department of Mathematics, School of Science, University of Phayao, Mae Ka, Mueang, Phayao 56000, Thailand*
[4]*Department of Mathematics, Faculty of Science, Tanta University, Tanta, Egypt*
[5]*Mathematics and Statistics Department, Faculty of Science, Taibah University, Yanbu, Saudi Arabia*
[6]*Department of Operations Research, Faculty of Graduate Studies for Statistical Research, Cairo University, Giza 12613, Egypt*
[7]*Department of Mathematics, College of Science and Ats, Qassim University, Al-Badaya 51951, Saudi Arabia*

Correspondence should be addressed to Imran Siddique; imransmsrazi@gmail.com

Received 6 November 2021; Accepted 4 February 2022; Published 25 February 2022

Academic Editor: M. T. Rahim

Copyright © 2022 Yasir Ahamad et al. This is an open access article distributed under the Creative Commons Attribution License, which permits unrestricted use, distribution, and reproduction in any medium, provided the original work is properly cited.

Spectrum analysis and computing have expanded in popularity in recent years as a critical tool for studying and describing the structural properties of molecular graphs. Let O_n^2 be the strong prism of an octagonal network O_n. In this study, using the normalized Laplacian decomposition theorem, we determine the normalized Laplacian spectrum of O_n^2 which consists of the eigenvalues of matrices $\mathscr{L}_A$ and $\mathscr{L}_S$ of order $3n+1$. As applications of the obtained results, the explicit formulae of the degree-Kirchhoff index and the number of spanning trees for O_n^2 are on the basis of the relationship between the roots and coefficients.

1. Introduction

Graphs are a convenient way to depict chemical structures, where atoms are associated with vertices, while chemical bonds are associated with edges. This manifestation carries a wealth of knowledge about the molecule's chemical characteristics. In quantitative structure-activity/property relationship (QSAR/QSPR) studies, one may see that many chemical and physical properties of molecules are closely correlated with graph-theoretical parameters known as topological indices. One such graph-theoretical parameter is the multiplicative degree-Kirchhoff index (see [1]). In statistical physics (see [2]), the enumeration of spanning trees in a graph is a crucial problem. It is interesting to note that the multiplicative degree-Kirchhoff index is closely related to the number of spanning trees in a graph. The normalized Laplacian acts as a link between them.

Let G be an n-vertex simple, undirected, and connected graph with the vertex set of $V(G)$ and an edge set of $E(G)$. For standard notation and terminology, one may refer to the recent papers (see [3, 4]). The *(combinatorial) Laplacian matrix* of graph G is specified as $L_G = D_G - A_G$, where D_G is the vertex degree diagonal matrix of order n and $A(G)$ is an *adjacency matrix* of order n.

The normalized Laplacian is defined by

$$(\mathscr{L}_G)_{ij} = \begin{cases} 1, & \text{if } i = j, \\ -\dfrac{1}{\sqrt{d_{v_i} d_{v_j}}}, & \text{if } i \neq j, v_i \sim v_j, \\ 0, & \text{otherwise.} \end{cases} \quad (1)$$

Evidently, $L(G) = D(G) - A(G)$ and $\mathscr{L}(G) = D(G)^{-1/2} L(G) D(G)^{-1/2}$. As we all know, the normalized Laplacian technique is useful for analyzing the structural features of nonregular graphs. In reality, the interaction between a graph's structural features and its eigenvalues is the focus of spectral graph theory. For more information, see recent articles [5–8] or the book [9].

Many parameters were used to characterize and describe the structural features of graphs in chemical graph theory. The Wiener index [10, 11] was a well-known distance-based index, as it is known as $W(G)=\sum_{i<j}d_{ij}$. Eventually, Gutman [12] defined the Gutman index as follows:

$$\mathrm{Gut}(G)=\sum_{i<j}d_id_jd_{ij}. \tag{2}$$

In accordance with electrical network theory, Klein and Randić [13] presented a new distance function called resistance distance that is denoted as r_{ij}. The resistance distance in electrical networks is between two arbitrary vertices i and j when every edge is replaced by a unit resistor. Klein and Ivanciuc [14] called it the Kirchhoff index, the total sum of resistance distances between each pair of vertices of G, which is $Kf(G)=\sum_{i<j}r_{ij}$. Later, the degree-Kirchhoff index was established by Chen and Zhang [1] and denoted by $Kf^*(G)=\sum_{i<j}d_id_jr_{ij}$.

Because of their practical uses in physics, chemistry, and other sciences, the Kirchhoff index and the degree-Kirchhoff index have gained a lot of attention. Klein and Lovász [15, 16] separately established that

$$Kf(G)=n\sum_{k=2}^{n}\frac{1}{\nu_k}, \tag{3}$$

where $0=\nu_1<\nu_2\leq\cdots\leq\nu_n$ are the eigenvalues of $L(G)$. According to Chen [17], the degree-Kirchhoff index is,

$$Kf^*(G)=2m\sum_{k=1}^{n}\frac{1}{\nu_k}, \tag{4}$$

where $\nu_1\leq\nu_2\leq\cdots\leq\nu_n$ are the eigenvalues of $\mathscr{L}(G)$.

Since the Kirchhoff index and multiplicative degree-Kirchhoff index have been widely used in the domains of physics, chemistry, and network science. During the previous few decades, many scientists have been working on explicit formulae for the Kirchhoff and degree-Kirchhoff indices of graphs with particular structures, such as cycles [18], complete multipartite graphs [19], generalized phenylene [20], crossed octagonal [21], hexagonal chains [22], pentagonal-quadrilateral network [23], and so on. Other research on the Kirchhoff index and the multiplicative degree-Kirchhoff index of a graph has been published (see [24–31]). In organic chemistry, polyomino systems have received a lot of attention, especially in polycyclic aromatic compounds. Tree-like octagonal networks are condensed into octagonal networks that belong to the polycyclic conjugated hydrocarbons' family. The octagonal system without any branches is known as a linear octagonal network [32]. As shown in Figure 1, a linear octagonal network could also be created from a linear polyomino network by adding additional points to the line according to specified rules.

The *strong product* between the graphs G and H is denoted by $G\boxtimes H$, where the vertex set $V(G\boxtimes H)$ is $V_G\times V_H$ and $(a,x)(b,y)$ is an edge of $G\boxtimes H$ if $a=b$ and x is adjacent to y in H or $x=y$ and a is adjacent to b in G or $xy\in E(H)$ and $ab\in E_G$. In particular, the strong product of K_2 and G is known as the strong prism of G. Recently, Li [33] and Ali [34] calculated the resistance distance-based parameters of the strong prism of unique graphs, such as strong prism of S_n and $L_n\boxtimes K_2$, respectively. Let O_n^2 be the strong prism of K_2 and O_n, denoted by $O_n^2=K_2\boxtimes O_n$, as shown in Figure 2. Obviously, $|E(O_n^2)|=34n+6$ and $|V(O_n^2)|=12n+4$.

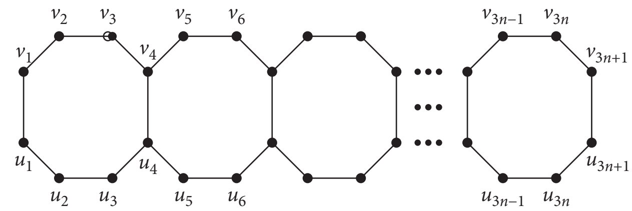

FIGURE 1: Graph O_n with labeled vertices.

In this paper, motivated by [34–36], we derive an explicit analytical expression for the multiplicative degree-Kirchhoff index and also spanning trees of O_n^2.

2. Preliminaries

In this section, we start by going over some basic notation and then introduce a suitable technique. Given the square matrix R having order n, we refer to $R[i_1,i_2,\ldots,i_k]$ as the submatrix of R that results from deleting the i_1th, i_2th, …, i_kth columns and rows. Let $\Phi(R)=\det(xI_n-R)$ be the *characteristic polynomial* of the square matrix R. The labeled vertices of O_n^2 are as depicted in Figure 2 and $V_1=\{u_1,\ldots,u_{3n+1},v_1,\ldots,v_{3n+1}\}$ and $V_2=\{u_1',\ldots,u_{3n+1}',v_1',\ldots,v_{3n+1}'\}$. The normalized Laplacian matrix $\mathscr{L}(O_n^2)$ could be represented as a block matrix below:

$$\mathscr{L}(O_n^2)=\begin{pmatrix}\mathscr{L}_{V_{11}}(O_n^2) & \mathscr{L}_{V_{12}}(O_n^2)\\ \mathscr{L}_{V_{21}}(O_n^2) & \mathscr{L}_{V_{22}}(O_n^2)\end{pmatrix}. \tag{5}$$

It is simple to verify that $\mathscr{L}_{V_{12}}(O_n^2)=\mathscr{L}_{V_{21}}(O_n^2)$ and $\mathscr{L}_{V_{11}}(O_n^2)=\mathscr{L}_{V_{22}}(O_n^2)$.

Let

$$T=\begin{pmatrix}\frac{1}{\sqrt{2}}I_{6n+2} & \frac{1}{\sqrt{2}}I_{6n+2}\\ \frac{1}{\sqrt{2}}I_{6n+2} & -\frac{1}{\sqrt{2}}I_{6n+2}\end{pmatrix}. \tag{6}$$

Then,

$$T\mathscr{L}(O_n^2)T'=\begin{pmatrix}\mathscr{L}_A(O_n^2) & 0\\ 0 & \mathscr{L}_S(O_n^2)\end{pmatrix}, \tag{7}$$

where

$$\begin{aligned}\mathscr{L}_A(O_n^2)&=\mathscr{L}_{V_{11}}+\mathscr{L}_{V_{12}},\\ \mathscr{L}_S(O_n^2)&=\mathscr{L}_{V_{11}}-\mathscr{L}_{V_{12}}.\end{aligned} \tag{8}$$

Huang et al. obtained the following lemma.

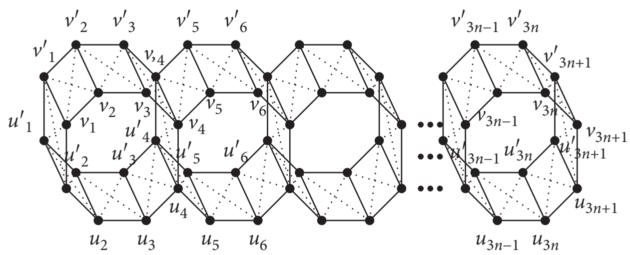

FIGURE 2: Graph O_n^2 with labeled vertices.

Lemma 1 (see [8]). *Let G be a graph and let $\mathscr{L}_A(O_n^2)$ and $\mathscr{L}_S(O_n^2)$ be as described above. Then, we have $\Phi(\mathscr{L}(O_n^2)) = \Phi(\mathscr{L}_A)\cdot\Phi(\mathscr{L}_S)$.*

Lemma 2 (see [1]). *Let $\rho_1 \le \rho_2 \le \cdots \le \rho_n$ be the eigenvalues of $\mathscr{L}(G)$; then, the degree-Kirchhoff index can also be written as $Kf^*(G) = 2m\sum_{i=2}^{n} 1/\rho_i$.*

Lemma 3 (see [17]). *Let G be n-vertex connected graph of size m; then, the spanning trees is $\tau(G) = 1/2m\prod_{i=1}^{n} d_i \prod_{k=2}^{n}\rho_k$.*

3. Main Results

In this section, we are committed to the explicit analytical solution for the multiplicative degree-Kirchhoff index, as well as the spanning tree of O_n^2. In terms of the role of normalized Laplacian $\mathscr{L}$, the following block matrices of $\mathscr{L}_{V_{11}}(O_n^2)$ and $\mathscr{L}_{V_{12}}(O_n^2)$ are obtained according to equation (8).

$$L_{V_{11}}\left(O_n^2\right) = \begin{pmatrix}
1 & -\frac{1}{5} & 0 & 0 & \cdots & 0 & 0 & -\frac{1}{5} & 0 & 0 & 0 & \cdots & 0 & 0 \\
-\frac{1}{5} & 1 & -\frac{1}{5} & 0 & \cdots & 0 & 0 & 0 & 0 & 0 & 0 & \cdots & 0 & 0 \\
0 & -\frac{1}{5} & 1 & -\frac{1}{\sqrt{35}} & \cdots & 0 & 0 & 0 & 0 & 0 & 0 & \cdots & 0 & 0 \\
0 & 0 & -\frac{1}{\sqrt{35}} & 1 & \cdots & 0 & 0 & 0 & 0 & 0 & -\frac{1}{7} & \cdots & 0 & 0 \\
\vdots & \vdots & \vdots & \vdots & \ddots & \vdots & \vdots & \vdots & \vdots & \vdots & \vdots & \ddots & \vdots & \vdots \\
0 & 0 & 0 & 0 & \cdots & 1 & -\frac{1}{5} & 0 & 0 & 0 & 0 & \cdots & 0 & 0 \\
0 & 0 & 0 & 0 & \cdots & -\frac{1}{5} & 1 & 0 & 0 & 0 & 0 & \cdots & 0 & -\frac{1}{5} \\
-\frac{1}{5} & 0 & 0 & 0 & \cdots & 0 & 0 & 1 & -\frac{1}{5} & 0 & 0 & \cdots & 0 & 0 \\
0 & 0 & 0 & 0 & \cdots & 0 & 0 & -\frac{1}{5} & 1 & -\frac{1}{5} & 0 & \cdots & 0 & 0 \\
0 & 0 & 0 & 0 & \cdots & 0 & 0 & 0 & -\frac{1}{5} & 1 & -\frac{1}{\sqrt{35}} & \cdots & 0 & 0 \\
0 & 0 & 0 & -\frac{1}{7} & \cdots & 0 & 0 & 0 & 0 & -\frac{1}{\sqrt{35}} & 1 & \cdots & 0 & 0 \\
\vdots & \vdots & \vdots & \vdots & \ddots & \vdots & \vdots & \vdots & \vdots & \vdots & \vdots & \ddots & \vdots & \vdots \\
0 & 0 & 0 & 0 & \cdots & 0 & 0 & 0 & 0 & 0 & 0 & \cdots & 1 & -\frac{1}{5} \\
0 & 0 & 0 & 0 & \cdots & 0 & -\frac{1}{5} & 0 & 0 & 0 & 0 & \cdots & -\frac{1}{5} & 1
\end{pmatrix}_{(6n+2)\times(6n+2)},$$

$$L_{V_{12}}\left(O_n^2\right) = \begin{pmatrix} -\frac{1}{5} & -\frac{1}{5} & 0 & 0 & \cdots & 0 & 0 & -\frac{1}{5} & 0 & 0 & 0 & \cdots & 0 & 0 \\ -\frac{1}{5} & -\frac{1}{5} & -\frac{1}{5} & 0 & \cdots & 0 & 0 & 0 & 0 & 0 & 0 & \cdots & 0 & 0 \\ 0 & -\frac{1}{5} & -\frac{1}{5} & -\frac{1}{\sqrt{35}} & \cdots & 0 & 0 & 0 & 0 & 0 & 0 & \cdots & 0 & 0 \\ 0 & 0 & -\frac{1}{\sqrt{35}} & -\frac{1}{7} & \cdots & 0 & 0 & 0 & 0 & 0 & -\frac{1}{7} & \cdots & 0 & 0 \\ \vdots & \vdots & \vdots & \vdots & \ddots & \vdots & \vdots & \vdots & \vdots & \vdots & \vdots & \ddots & \vdots & \vdots \\ 0 & 0 & 0 & 0 & \cdots & -\frac{1}{5} & -\frac{1}{5} & 0 & 0 & 0 & 0 & \cdots & 0 & 0 \\ 0 & 0 & 0 & 0 & \cdots & -\frac{1}{5} & -\frac{1}{5} & 0 & 0 & 0 & 0 & \cdots & 0 & -\frac{1}{5} \\ -\frac{1}{5} & 0 & 0 & 0 & \cdots & 0 & 0 & -\frac{1}{5} & -\frac{1}{5} & 0 & 0 & \cdots & 0 & 0 \\ 0 & 0 & 0 & 0 & \cdots & 0 & 0 & -\frac{1}{5} & -\frac{1}{5} & -\frac{1}{5} & 0 & \cdots & 0 & 0 \\ 0 & 0 & 0 & 0 & \cdots & 0 & 0 & 0 & -\frac{1}{5} & -\frac{1}{5} & -\frac{1}{\sqrt{35}} & \cdots & 0 & 0 \\ 0 & 0 & 0 & -\frac{1}{7} & \cdots & 0 & 0 & 0 & 0 & -\frac{1}{\sqrt{35}} & -\frac{1}{7} & \cdots & 0 & 0 \\ \vdots & \vdots & \vdots & \vdots & \ddots & \vdots & \vdots & \vdots & \vdots & \vdots & \vdots & \ddots & \vdots & \vdots \\ 0 & 0 & 0 & 0 & \cdots & 0 & 0 & 0 & 0 & 0 & 0 & \cdots & -\frac{1}{7} & -\frac{1}{5} \\ 0 & 0 & 0 & 0 & \cdots & 0 & -\frac{1}{5} & 0 & 0 & 0 & 0 & \cdots & -\frac{1}{5} & -\frac{1}{5} \end{pmatrix}_{(6n+2)\times(6n+2)}. \tag{9}$$

By equation (8), we have a matrix of order $6n+2$:

$$L_A\left(O_n^2\right)=2\begin{pmatrix}
\frac{2}{5} & -\frac{1}{5} & 0 & 0 & \cdots & 0 & 0 & -\frac{1}{5} & 0 & 0 & 0 & \cdots & 0 & 0\\
-\frac{1}{5} & \frac{2}{5} & -\frac{1}{5} & 0 & \cdots & 0 & 0 & 0 & 0 & 0 & 0 & \cdots & 0 & 0\\
0 & -\frac{1}{5} & \frac{2}{5} & -\frac{1}{\sqrt{35}} & \cdots & 0 & 0 & 0 & 0 & 0 & 0 & \cdots & 0 & 0\\
0 & 0 & -\frac{1}{\sqrt{35}} & \frac{3}{7} & \cdots & 0 & 0 & 0 & 0 & 0 & -\frac{1}{7} & \cdots & 0 & 0\\
\vdots & \vdots & \vdots & \ddots & \vdots & \vdots & \vdots & \vdots & \vdots & \vdots & \ddots & \vdots & \vdots & \vdots\\
0 & 0 & 0 & 0 & \cdots & \frac{2}{5} & -\frac{1}{5} & 0 & 0 & 0 & 0 & \cdots & 0 & 0\\
0 & 0 & 0 & 0 & \cdots & -\frac{1}{5} & \frac{2}{5} & 0 & 0 & 0 & 0 & \cdots & 0 & -\frac{1}{5}\\
-\frac{1}{5} & 0 & 0 & 0 & \cdots & 0 & 0 & \frac{2}{5} & -\frac{1}{5} & 0 & 0 & \cdots & 0 & 0\\
0 & 0 & 0 & 0 & \cdots & 0 & 0 & -\frac{1}{5} & \frac{2}{5} & -\frac{1}{5} & 0 & \cdots & 0 & 0\\
0 & 0 & 0 & 0 & \cdots & 0 & 0 & 0 & -\frac{1}{5} & \frac{2}{5} & -\frac{1}{\sqrt{35}} & \cdots & 0 & 0\\
0 & 0 & 0 & -\frac{1}{7} & \cdots & 0 & 0 & 0 & 0 & -\frac{1}{\sqrt{35}} & \frac{3}{7} & \cdots & 0 & 0\\
\vdots & \vdots & \vdots & \ddots & \vdots & \vdots & \vdots & \vdots & \vdots & \vdots & \vdots & \ddots & \vdots & \vdots\\
0 & 0 & 0 & 0 & \cdots & 0 & 0 & 0 & 0 & 0 & 0 & \cdots & \frac{2}{5} & -\frac{1}{5}\\
0 & 0 & 0 & 0 & \cdots & 0 & -\frac{1}{5} & 0 & 0 & 0 & 0 & \cdots & -\frac{1}{5} & \frac{2}{5}
\end{pmatrix}, \qquad (10)$$

and $\mathscr{L}_S(O_n^2) = \operatorname{diag}(6/5, 6/5, 6/5, 8/7, \ldots, 6/5, 6/5, 8/7, 6/5, 6/5, 8/7, \ldots, 8/7, 6/5, 6/5, 6/5)Q$, a diagonal matrix with order $6n+2$.

The normalized Laplacian spectrum of O_n^2 is constructed by the eigenvalues of $\mathscr{L}_A(O_n^2)$ and $\mathscr{L}_S(O_n^2)$, according to

Lemma 1. Given the fact that $\mathscr{L}_S(O_n^2)$ is just a diagonal matrix of order $6n+2$, it is obvious that $6/5$ with multiplicity $4n+4$ and $8/7$ with multiplicity $2n-2$ are the eigenvalues of $\mathscr{L}_S(O_n^2)$.

Let

$$A=\begin{pmatrix} \frac{2}{5} & -\frac{1}{5} & 0 & 0 & \cdots & 0 & 0 \\ -\frac{1}{5} & \frac{2}{5} & -\frac{1}{5} & 0 & \cdots & 0 & 0 \\ 0 & -\frac{1}{5} & \frac{2}{5} & -\frac{1}{\sqrt{35}} & \cdots & 0 & 0 \\ 0 & 0 & -\frac{1}{\sqrt{35}} & \frac{3}{7} & \cdots & 0 & 0 \\ \vdots & \vdots & \vdots & \vdots & \ddots & \vdots & \vdots \\ 0 & 0 & 0 & 0 & \cdots & \frac{1}{5} & -\frac{1}{5} \\ 0 & 0 & 0 & 0 & \cdots & -\frac{1}{5} & \frac{2}{5} \end{pmatrix}_{(3n+1)\times(3n+1)},$$

$$C=\begin{pmatrix} -\frac{1}{5} & 0 & 0 & 0 & \cdots & 0 & 0 \\ 0 & 0 & 0 & 0 & \cdots & 0 & 0 \\ 0 & 0 & 0 & 0 & \cdots & 0 & 0 \\ 0 & 0 & 0 & -\frac{1}{7} & \cdots & 0 & 0 \\ \vdots & \vdots & \vdots & \ddots & \vdots & \vdots & \vdots \\ 0 & 0 & 0 & 0 & \cdots & 0 & 0 \\ 0 & 0 & 0 & 0 & \cdots & 0 & -\frac{1}{5} \end{pmatrix}_{(3n+1)\times(3n+1)}. \tag{11}$$

Thus, $(1/2)\mathscr{L}_A$ could be represented by the block matrix below:

$$\frac{1}{2}\mathscr{L}_A=\begin{pmatrix} A & C \\ C & A \end{pmatrix}. \tag{12}$$

Let

$$T=\begin{pmatrix} \frac{1}{\sqrt{2}}I_{3n+1} & \frac{1}{\sqrt{2}}I_{3n+1} \\ \frac{1}{\sqrt{2}}I_{3n+1} & -\frac{1}{\sqrt{2}}I_{3n+1} \end{pmatrix}. \tag{13}$$

Then,

$$T\left(\frac{1}{2}\mathscr{L}_A\right)T'=\begin{pmatrix} A+C & 0 \\ 0 & A-C \end{pmatrix}, \tag{14}$$

where T' indicates the transposition of T. Let $P=A+C$ and $Q=A-C$. Then,

$$P=\begin{pmatrix} \frac{1}{5} & -\frac{1}{5} & 0 & 0 & \cdots & 0 & 0 & 0 \\ -\frac{1}{5} & \frac{2}{5} & -\frac{1}{5} & 0 & \cdots & 0 & 0 & 0 \\ 0 & -\frac{1}{5} & \frac{2}{5} & -\frac{1}{\sqrt{35}} & \cdots & 0 & 0 & 0 \\ 0 & 0 & -\frac{1}{\sqrt{35}} & \frac{2}{7} & \cdots & 0 & 0 & 0 \\ \vdots & \vdots & \vdots & \vdots & \ddots & \vdots & \vdots & \vdots \\ 0 & 0 & 0 & 0 & \cdots & \frac{2}{5} & -\frac{1}{5} & 0 \\ 0 & 0 & 0 & 0 & \cdots & -\frac{1}{5} & \frac{2}{5} & -\frac{1}{5} \\ 0 & 0 & 0 & 0 & \cdots & 0 & -\frac{1}{5} & \frac{1}{5} \end{pmatrix}_{(3n+1)\times(3n+1)},$$

$$Q=\begin{pmatrix} \frac{3}{5} & -\frac{1}{5} & 0 & 0 & \cdots & 0 & 0 & 0 \\ -\frac{1}{5} & \frac{2}{5} & -\frac{1}{5} & 0 & \cdots & 0 & 0 & 0 \\ 0 & -\frac{1}{5} & \frac{2}{5} & -\frac{1}{\sqrt{35}} & \cdots & 0 & 0 & 0 \\ 0 & 0 & -\frac{1}{\sqrt{35}} & \frac{4}{7} & \cdots & 0 & 0 & 0 \\ \vdots & \vdots & \vdots & \vdots & \ddots & \vdots & \vdots & \vdots \\ 0 & 0 & 0 & 0 & \cdots & \frac{2}{5} & -\frac{1}{5} & 0 \\ 0 & 0 & 0 & 0 & \cdots & -\frac{1}{5} & \frac{2}{5} & -\frac{1}{5} \\ 0 & 0 & 0 & 0 & \cdots & 0 & -\frac{1}{5} & \frac{3}{5} \end{pmatrix}_{(3n+1)\times(3n+1)}. \tag{15}$$

By Lemma 1, it is simple to verify that the eigenvalues of $(1/2)\mathscr{L}_A$ consist of those of P and Q. Suppose that the eigenvalues of P and Q are denoted by γ_i and $\xi_j\,(i,j=1,2,\ldots,3n+1)$ with $\gamma_1\le\gamma_2\le\cdots\le\gamma_{3n+1}$ and $\xi_1\le\xi_2\le\cdots\le\xi_{3n+1}$, respectively. Then, the eigenvalues of $\mathscr{L}_A$ are $2\gamma_1,2\gamma_2,\ldots,2\gamma_{3n+1}$ and $2\xi_1,2\xi_2,\ldots,2\xi_{3n+1}$.where $0=\gamma_1<\gamma_2\le\cdots\le\gamma_{3n+1}$ and $0<\xi_1\le\xi_2\le\cdots\le\xi_{3n+1}$ are eigenvalues of P and Q, respectively.

Lemma 4. *Suppose that O_n^2 is the strong product of octagonal network. Then,*

$$Kf^*\left(O_n^2\right) = 2(34n+6)\left[(4n+4)\frac{5}{6} + (2n-2)\frac{7}{8} + \frac{1}{2}\sum_{i=2}^{3n+1}\frac{1}{\gamma_i} + \frac{1}{2}\sum_{j=1}^{3n+1}\frac{1}{\xi_j}\right], \tag{16}$$

On the basis of the relation between the coefficients and roots of $\Phi(P)$ (resp. $\Phi(Q)$), the formulae of $\sum_{i=2}^{3n+1} 1/\gamma_i$ (resp. $\sum_{j=1}^{3n+1} 1/\xi_j$) are obtained in the next lemmas.

Lemma 5. *Suppose that $0=\gamma_1<\gamma_2\leq\cdots\leq\gamma_{3n+1}$ are described as above. Then,*

$$\sum_{i=2}^{3n+1}\frac{1}{\gamma_i} = \frac{1359n^3 + 1115n^2 + 434n}{14(17n+3)}. \tag{17}$$

Suppose that $\Phi(P) = x^{3n+1} + a_1x^{3n} + \cdots + a_{3n-1}x^2 + a_{3n}x = x(x^{3n} + a_1x^{3n-1} + \cdots + a_{3n-1}x + a_{3n})$. Then, $\gamma_2, \gamma_3, \ldots, \gamma_{3n+1}$ satisfy the equation below:

$$x^{3n} + a_1x^{3n-1} + \cdots + a_{3n-1}x + a_{3n} = 0, \tag{18}$$

so $1/\gamma_2, 1/\gamma_3, \ldots, 1/\gamma_{3n+1}$ satisfy the equation below:

$$a_{3n}x^{3n} + a_{3n-1}x^{3n-1} + \cdots + a_1x + 1 = 0. \tag{19}$$

Hence, by Vieta's theorem, we obtain

$$\sum_{i=2}^{3n+1}\frac{1}{\gamma_i} = \frac{(-1)^{3n-1}a_{3n-1}}{(-1)^{3n}a_{3n}}. \tag{20}$$

For the sake of convenience, consider W_i of P, which is the ith order principal submatrix generated by the first i columns and rows, $i=1,2,\ldots,3n$. Let $w_i = \det W_i$. Then,

$$\begin{aligned}
w_1 &= \frac{1}{5},\\
w_2 &= \frac{1}{25},\\
w_3 &= \frac{1}{125},\\
w_4 &= \frac{1}{875},\\
w_5 &= \frac{1}{4375},\\
w_6 &= \frac{1}{21875},
\end{aligned} \tag{21}$$

$$\begin{cases}
w_{3i} = \dfrac{2}{5}w_{3i-1} - \dfrac{1}{25}w_{3i-2}, & \text{for } 1\leq i\leq n,\\
w_{3i+1} = \dfrac{2}{7}w_{3i} - \dfrac{1}{35}w_{3i-1}, & \text{for } 1\leq i\leq n-1,\\
w_{3i+2} = \dfrac{2}{5}w_{3i+1} - \dfrac{1}{35}w_{3i}, & \text{for } 1\leq i\leq n-1.
\end{cases}$$

By explicit calculation, these general formulae can be obtained as follows:

$$\begin{cases}
w_{3i} = \dfrac{7}{5}\left(\dfrac{1}{175}\right)^i, & \text{for } 1\leq i\leq n,\\
w_{3i+1} = \dfrac{1}{5}\left(\dfrac{1}{175}\right)^i, & \text{for } 0\leq i\leq n-1,\\
w_{3i+2} = \dfrac{1}{25}\left(\dfrac{1}{175}\right)^i, & \text{for } 0\leq i\leq n-1.
\end{cases} \tag{22}$$

The structure and determinant of matrix $\mathscr{L}_A$ are preserved by a permutation similarity transformation of a square matrix, and one gets $\det U_{3n+1-i} = \det W_{3n+1-i}$. We have

$$\begin{aligned}
(-1)^{3n}a_{3n} &= \sum_{i=1}^{3n+1}\det P[i] = \sum_{i=2}^{3n}\det P[i] + 2w_{3n}\\
&= \sum_{k=1}^{n}\det P[3k] + \sum_{k=1}^{n-1}\det P[3k+1] + \sum_{k=0}^{n-1}\det P[3k+2] + 2w_{3n}\\
&= \sum_{k=1}^{n} w_{3(k-1)+2}\cdot w_{3(n-k)+1} + \sum_{k=1}^{n-1} w_{3k}\cdot w_{3(n-k)} + \sum_{k=0}^{n-1} w_{3k+1}\cdot w_{3(n-k-1)+2} + 2w_{3n}\\
&= \frac{17n+3}{625}\left(\frac{1}{175}\right)^{n-1},
\end{aligned} \tag{23}$$

as desired.

Claim 1. $(-1)^{3n-1}a_{3n-1} = 1359n^3 + 1115n^2 + 434n/8750\,(1/175)^{n-1}$.

Proof of Claim 1. Noticing that $(-1)^{3n-1}a_{3n-1}$ is equal to the sum of all principal minors of P with $3n-1$ columns and rows, we have

$$(-1)^{3n-1}a_{3n-1} = \sum_{1\le i<j}^{3n+1} \begin{vmatrix} W_{i-1} & 0 & 0 \\ 0 & Z & 0 \\ 0 & 0 & U \end{vmatrix}, \quad 1 \le i < j \le 3n+1, \tag{24}$$

where

$$Z = \begin{pmatrix} k_{i+1,i+1} & -\frac{1}{\sqrt{35}} & \cdots & 0 \\ -\frac{1}{\sqrt{35}} & k_{i+2,i+2} & \cdots & 0 \\ \vdots & \vdots & \ddots & \vdots \\ 0 & 0 & \cdots & k_{j-1,j-1} \end{pmatrix},$$

$$U = \begin{pmatrix} k_{j+1,j+1} & \cdots & 0 & 0 \\ \vdots & \ddots & \vdots & \vdots \\ 0 & \cdots & k_{3n,3n} & -\frac{1}{5} \\ 0 & \cdots & -\frac{1}{5} & k_{3n+1,3n+1} \end{pmatrix}. \tag{25}$$

Note that

$$(-1)^{3n-1}a_{3n-1} = \sum_{1\le i<j}^{3n+1} \det P[i,j] = \sum_{1\le i<j}^{3n+1} w_{i-1}\cdot w_{3n+1-j}\cdot \det Z. \tag{26}$$

□

Remark 1. If $1 \le i < i+1 = j \le 3n+1$, then Z is an empty matrix and let $\det Z = 1$. By equation (26), there are different possibilities which can be selected for i and j. Therefore, all these cases are classified as follows.

Case 1. Let $i = 3p$ and $j = 3q$, for $1 \le i < j \le 3n+1$. So, $1 \le p < q \le n$:

$$\det Z = \begin{vmatrix} \frac{2}{7} & -\frac{1}{\sqrt{35}} & 0 & 0 & \cdots & 0 & 0 \\ -\frac{1}{\sqrt{35}} & \frac{2}{5} & -\frac{1}{5} & 0 & \cdots & 0 & 0 \\ 0 & -\frac{1}{5} & \frac{2}{5} & -\frac{1}{\sqrt{35}} & \cdots & 0 & 0 \\ 0 & 0 & -\frac{1}{\sqrt{35}} & \frac{2}{7} & \cdots & 0 & 0 \\ \vdots & \vdots & \vdots & \vdots & \ddots & \vdots & \vdots \\ 0 & 0 & 0 & 0 & \cdots & \frac{2}{7} & -\frac{1}{\sqrt{35}} \\ 0 & 0 & 0 & 0 & \cdots & -\frac{1}{\sqrt{35}} & \frac{2}{5} \end{vmatrix}_{(3q-3p-1)} = (3q-3p+1)\left(\frac{1}{175}\right)^{q-p}. \tag{27}$$

Case 2. Let $i = 3p$ and $j = 3q+1$, for $1 \le i < i+1 < j \le 3n+1$. So, $1 \le p \le q \le n-1$:

$$\det Z = \begin{vmatrix} \frac{2}{7} & -\frac{1}{\sqrt{35}} & 0 & 0 & \cdots & 0 & 0 \\ -\frac{1}{\sqrt{35}} & \frac{2}{5} & -\frac{1}{5} & 0 & \cdots & 0 & 0 \\ 0 & -\frac{1}{5} & \frac{2}{5} & -\frac{1}{\sqrt{35}} & \cdots & 0 & 0 \\ 0 & 0 & -\frac{1}{\sqrt{35}} & \frac{2}{7} & \cdots & 0 & 0 \\ \vdots & \vdots & \vdots & \vdots & \ddots & \vdots & \vdots \\ 0 & 0 & 0 & 0 & \cdots & \frac{2}{5} & -\frac{1}{5} \\ 0 & 0 & 0 & 0 & \cdots & -\frac{1}{5} & \frac{2}{5} \end{vmatrix}_{(3q-3p)} = \frac{(3q-3p+2)}{7}\left(\frac{1}{175}\right)^{q-p}. \tag{28}$$

Case 3. Let $i = 3p$ and $j = 3q + 2$, for $1 \le i < j \le 3n + 1$. So, $1 \le p \le q \le n - 1$:

$$\det Z = \begin{vmatrix} \frac{2}{7} & -\frac{1}{\sqrt{35}} & 0 & 0 & \cdots & 0 & 0 \\ -\frac{1}{\sqrt{35}} & \frac{2}{5} & -\frac{1}{5} & 0 & \cdots & 0 & 0 \\ 0 & -\frac{1}{5} & \frac{2}{5} & -\frac{1}{\sqrt{35}} & \cdots & 0 & 0 \\ 0 & 0 & -\frac{1}{\sqrt{35}} & \frac{2}{7} & \cdots & 0 & 0 \\ \vdots & \vdots & \vdots & \vdots & \vdots & \vdots & \vdots \\ 0 & 0 & 0 & 0 & \cdots & \frac{2}{5} & -\frac{1}{\sqrt{35}} \\ 0 & 0 & 0 & 0 & \cdots & -\frac{1}{\sqrt{35}} & \frac{2}{7} \end{vmatrix}_{(3q-3p+1)} = \frac{(3q-3p+3)}{35}\left(\frac{1}{175}\right)^{q-p}. \tag{29}$$

Case 4. Let $i = 3p + 1$ and $j = 3q$, for $1 \le i < j \le 3n + 1$. So, $0 \le p < q \le n$:

$$\det Z = \begin{vmatrix} \frac{2}{5} & -\frac{1}{5} & 0 & 0 & \cdots & 0 & 0 \\ -\frac{1}{5} & \frac{2}{5} & -\frac{1}{\sqrt{35}} & 0 & \cdots & 0 & 0 \\ 0 & -\frac{1}{\sqrt{35}} & \frac{2}{7} & -\frac{1}{\sqrt{35}} & \cdots & 0 & 0 \\ 0 & 0 & -\frac{1}{\sqrt{35}} & \frac{2}{5} & \cdots & 0 & 0 \\ \vdots & \vdots & \vdots & \vdots & \ddots & \vdots & \vdots \\ 0 & 0 & 0 & 0 & \cdots & \frac{2}{7} & -\frac{1}{\sqrt{35}} \\ 0 & 0 & 0 & 0 & \cdots & -\frac{1}{\sqrt{35}} & \frac{2}{5} \end{vmatrix}_{(3q-3p-2)} = 35(3q-3p-1)\left(\frac{1}{175}\right)^{q-p}. \tag{30}$$

Case 5. Let $i = 3p + 1$ and $j = 3q + 1$, for $1 \leq i < j \leq 3n + 1$. So, $0 \leq p < q \leq n - 1$:

$$\det Z = \begin{vmatrix} \frac{2}{5} & -\frac{1}{5} & 0 & 0 & \cdots & 0 & 0 \\ -\frac{1}{5} & \frac{2}{5} & -\frac{1}{\sqrt{35}} & 0 & \cdots & 0 & 0 \\ 0 & -\frac{1}{\sqrt{35}} & \frac{2}{7} & -\frac{1}{\sqrt{35}} & \cdots & 0 & 0 \\ 0 & 0 & -\frac{1}{\sqrt{35}} & \frac{2}{5} & \cdots & 0 & 0 \\ \vdots & \vdots & \vdots & \vdots & \ddots & \vdots & \vdots \\ 0 & 0 & 0 & 0 & \cdots & \frac{2}{5} & -\frac{1}{5} \\ 0 & 0 & 0 & 0 & \cdots & -\frac{1}{5} & \frac{2}{5} \end{vmatrix}_{(3q-3p-1)} = 7(3q-3p)\left(\frac{1}{175}\right)^{q-p}. \tag{31}$$

Case 6. Let $i = 3p + 1$ and $j = 3q + 2$, for $1 \leq i < i + 1 < j \leq 3n + 1$. So, $0 \leq p \leq q \leq n - 1$:

$$\det Z = \begin{vmatrix} \frac{2}{5} & -\frac{1}{5} & 0 & 0 & \cdots & 0 & 0 \\ -\frac{1}{5} & \frac{2}{5} & -\frac{1}{\sqrt{35}} & 0 & \cdots & 0 & 0 \\ 0 & -\frac{1}{\sqrt{35}} & \frac{2}{7} & -\frac{1}{\sqrt{35}} & \cdots & 0 & 0 \\ 0 & 0 & -\frac{1}{\sqrt{35}} & \frac{2}{5} & \cdots & 0 & 0 \\ \vdots & \vdots & \vdots & \vdots & \ddots & \vdots & \vdots \\ 0 & 0 & 0 & 0 & \cdots & \frac{2}{5} & -\frac{1}{\sqrt{35}} \\ 0 & 0 & 0 & 0 & \cdots & -\frac{1}{\sqrt{35}} & \frac{2}{7} \end{vmatrix}_{(3q-3p)} = (3q-3p+1)\left(\frac{1}{175}\right)^{q-p}. \tag{32}$$

Case 7. Let $i = 3p+2$ and $j = 3q$, for $1 \le i < i+1 < j \le 3n+1$. So, $0 \le p < p+1 < q \le n$:

$$\det Z = \begin{vmatrix} \frac{2}{5} & -\frac{1}{\sqrt{35}} & 0 & 0 & \cdots & 0 & 0 \\ -\frac{1}{\sqrt{35}} & \frac{2}{7} & -\frac{1}{\sqrt{35}} & 0 & \cdots & 0 & 0 \\ 0 & -\frac{1}{\sqrt{35}} & \frac{2}{5} & -\frac{1}{5} & \cdots & 0 & 0 \\ 0 & 0 & -\frac{1}{5} & \frac{2}{5} & \cdots & 0 & 0 \\ \vdots & \vdots & \vdots & \vdots & \ddots & \vdots & \vdots \\ 0 & 0 & 0 & 0 & \cdots & \frac{2}{7} & -\frac{1}{\sqrt{35}} \\ 0 & 0 & 0 & 0 & \cdots & -\frac{1}{\sqrt{35}} & \frac{2}{5} \end{vmatrix}_{(3q-3p-3)} = (3q-3p+1)\left(\frac{1}{175}\right)^{q-p}. \tag{33}$$

Case 8. Let $i = 3p+2$ and $j = 3q+1$, for $1 \le i < j \le 3n+1$. So, $0 \le p < q \le n-1$:

$$\det Z = \begin{vmatrix} \frac{2}{5} & -\frac{1}{\sqrt{35}} & 0 & 0 & \cdots & 0 & 0 \\ -\frac{1}{\sqrt{35}} & \frac{2}{7} & -\frac{1}{\sqrt{35}} & 0 & \cdots & 0 & 0 \\ 0 & -\frac{1}{\sqrt{35}} & \frac{2}{5} & -\frac{1}{5} & \cdots & 0 & 0 \\ 0 & 0 & -\frac{1}{5} & \frac{2}{5} & \cdots & 0 & 0 \\ \vdots & \vdots & \vdots & \vdots & \ddots & \vdots & \vdots \\ 0 & 0 & 0 & 0 & \cdots & \frac{2}{5} & -\frac{1}{5} \\ 0 & 0 & 0 & 0 & \cdots & -\frac{1}{5} & \frac{2}{5} \end{vmatrix}_{(3q-3p-2)} = 35\,(3q-3p-1)\left(\frac{1}{175}\right)^{q-p}. \quad (34)$$

Case 9. Let $i = 3p + 2$ and $j = 3q + 2$, for $1 \le i < j \le 3n + 1$. So, $0 \le p < q \le n - 1$:

$$\det Z = \begin{vmatrix} \frac{2}{5} & -\frac{1}{\sqrt{35}} & 0 & 0 & \cdots & 0 & 0 \\ -\frac{1}{\sqrt{35}} & \frac{2}{7} & -\frac{1}{\sqrt{35}} & 0 & \cdots & 0 & 0 \\ 0 & -\frac{1}{\sqrt{35}} & \frac{2}{5} & -\frac{1}{5} & \cdots & 0 & 0 \\ 0 & 0 & -\frac{1}{5} & \frac{2}{5} & \cdots & 0 & 0 \\ \vdots & \vdots & \vdots & \vdots & \ddots & \vdots & \vdots \\ 0 & 0 & 0 & 0 & \cdots & \frac{2}{5} & -\frac{1}{\sqrt{35}} \\ 0 & 0 & 0 & 0 & \cdots & -\frac{1}{\sqrt{35}} & \frac{2}{7} \end{vmatrix}_{(3q-3p-1)} = 5\,(3q-3p)\left(\frac{1}{175}\right)^{q-p}. \quad (35)$$

Combining these results with equation (26) and Cases 1–9 yields

$$(-1)^{3n-1}a_{3n-1} = \sum_{1\le i<j\le 3n+1} w_{i-1}\cdot w_{3n+1-j}\cdot \det Z_{j-1-i} = E_1+E_2+E_3, \tag{36}$$

where

$$\begin{aligned}
E_1 &= \sum_{1\le p<q\le n}\det P[3p,3q] + \sum_{1\le p\le q\le n-1}\det P[3p,3q+1] + \sum_{1\le p\le q\le n-1}\det P[3p,3q+2] \\
&\quad + \sum_{1\le p\le n}\det P[3p,3n+1] \\
&= \frac{n(n-1)(n+2)}{250}\left(\frac{1}{175}\right)^{n-1} + \frac{n^2(n-1)}{250}\left(\frac{1}{175}\right)^{n-1} \\
&\quad + \frac{n\left(n^2-1\right)}{250}\left(\frac{1}{175}\right)^{n-1} + \frac{3n^2+n}{350}\left(\frac{1}{175}\right)^{n-1} \\
&= \frac{21n^3+15n^2-16n}{1750}\left(\frac{1}{175}\right)^{n-1}, \\
E_2 &= \sum_{1\le p<q\le n}\det P[3p+1,3q] + \sum_{1\le p<q\le n-1}\det P[3p+1,3q+1] + \sum_{1\le p\le q\le n-1}\det P[3p+1,3q+2] \\
&\quad + \sum_{1\le p\le n-1}\det P[3p+1,3n+1] + \sum_{1\le q\le n}\det P[1,3q] + \sum_{1\le q\le n-1}\det P[1,3q+1] \\
&\quad + \sum_{0\le q\le n-1}\det P[1,3q+2] + Z_{3n-1} \\
&= \frac{7n^2(n-1)}{250}\left(\frac{1}{175}\right)^{n-1} + \frac{49n(n-1)(n-2)}{1250}\left(\frac{1}{175}\right)^{n-1} + \frac{7n(n-1)^2}{250}\left(\frac{1}{175}\right)^{n-1} \\
&\quad + \frac{21n(n-1)}{250}\left(\frac{1}{175}\right)^{n-1} + \frac{n(3n+1)}{50}\left(\frac{1}{175}\right)^{n-1} + \frac{21n(n-1)}{250}\left(\frac{1}{175}\right)^{n-1} \\
&\quad + \frac{n(3n-1)}{50}\left(\frac{1}{175}\right)^{n-1} + \frac{3n}{25}\left(\frac{1}{175}\right)^{n-1} \\
&= \frac{119n^3+108n^2+73n}{1250}\left(\frac{1}{245}\right)^{n-1}, \\
E_3 &= \sum_{0\le p<q\le n}\det P[3p+2,3q] + \sum_{0\le p<q\le n-1}\det P[3p+2,3q+1] + \sum_{0\le p<q\le n-1}\det P[3p+2,3q+2] \\
&\quad + \sum_{0\le p\le n-1}\det P[3p+2,3n+1] \\
&= \frac{n(n+1)(n+3)}{8750}\left(\frac{1}{175}\right)^{n-1} + \frac{7n^2(n-1)}{250}\left(\frac{1}{175}\right)^{n-1} + \frac{n\left(n^2-1\right)}{50}\left(\frac{1}{175}\right)^{n-1} \\
&\quad + \frac{n(3n+1)}{50}\left(\frac{1}{175}\right)^{n-1} \\
&= \frac{421n^3+284n^2+3n}{8750}\left(\frac{1}{175}\right)^{n-1}.
\end{aligned} \tag{37}$$

Substituting E_1, E_2, and E_3 in Equation (36), we get Claim 2.

Also, we can get Lemma 5 by combining Claims 1 and 2.

Lemma 6. *Let* $0 < \xi_1 < \xi_2 \leq \cdots \leq \xi_{3n+1}$ *be the eigenvalues of* Q *as above. Then,*

$$\sum_{j=1}^{3n+1} \frac{1}{\xi_j} = \frac{5(\eta_1 + \eta_2)}{(45 + 13\sqrt{15})(4 + \sqrt{15})^{n-1} + (45 - 13\sqrt{15})(4 - \sqrt{15})^{n-1}}, \tag{38}$$

where
$\eta_1 = (1500 + 401\sqrt{15} + n(1605 + 397\sqrt{15}))(4 + \sqrt{15})^{n-1}$
and
$\eta_2 = (1500 - 401\sqrt{15} + n(1605 - 397\sqrt{15}))(4 - \sqrt{15})^{n-1}$.

Proof . Suppose that $\Phi(Q) = x^{3n+1} + b_1 x^{3n} + \cdots + b_{3n}x + b_{3n+1}$.

So, $1/\xi_1, 1/\xi_2, \ldots, 1/\xi_{3n+1}$ satisfy the equation below:

$$b_{3n+1}x^{3n+1} + b_{3n}x^{3n} + \cdots + b_1 x + 1 = 0. \tag{39}$$

By Vieta's theorem, we obtain

$$\begin{aligned}\sum_{j=1}^{3n+1} \frac{1}{\xi_j} &= \frac{\sum_{j=1}^{3n+1} \xi_1 \cdots \xi_{j-1}\xi_{j+1} \cdots \xi_{3n+1}}{\prod_{j=1}^{3n+1} \xi_j} \\ &= \frac{(-1)^{3n} b_{3n}}{(-1)^{3n+1} b_{3n+1}} = \frac{(-1)^{3n} b_{3n}}{\det Q}.\end{aligned} \tag{40}$$

In order to find $(-1)^{3n} b_{3n}$ and detQ in (40), consider R_i of Q, which is the ith order principal submatrix generated by the first i columns and rows, $1 \leq i \leq 3n$. Let $r_i = \det R_i$. Then, $r_1 = 3/5$, $r_2 = 1/5$, $r_3 = 7/125$, $r_4 = 23/875$, $r_5 = 39/4375$, $r_6 = 11/4375$, and

$$\begin{cases} r_{3i} = \dfrac{2}{5} r_{3i-1} - \dfrac{1}{25} r_{3i-2}, & \text{for } 1 \leq i \leq n, \\ r_{3i+1} = \dfrac{4}{7} r_{3i} - \dfrac{1}{35} r_{3i-1}, & \text{for } 1 \leq i \leq n-1, \\ r_{3i+2} = \dfrac{2}{5} r_{3i+1} - \dfrac{1}{35} r_{3i}, & \text{for } 1 \leq i \leq n-1. \end{cases} \tag{41}$$

Similar to the method used as described above, we have

$$\begin{cases} r_{3i} = \dfrac{35 + 7\sqrt{15}}{50}\left(\dfrac{4 + \sqrt{15}}{175}\right)^i + \dfrac{35 - 7\sqrt{15}}{50}\left(\dfrac{4 - \sqrt{15}}{175}\right)^i, & \text{for } 1 \leq i \leq n, \\ r_{3i+1} = \dfrac{75 + 19\sqrt{15}}{750}\left(\dfrac{4 + \sqrt{15}}{175}\right)^i + \dfrac{75 - 19\sqrt{15}}{750}\left(\dfrac{4 - \sqrt{15}}{175}\right)^i, & \text{for } 0 \leq i \leq n-1, \\ r_{3i+2} = \dfrac{45 + 11\sqrt{15}}{150}\left(\dfrac{4 + \sqrt{15}}{175}\right)^i + \dfrac{45 - 11\sqrt{15}}{150}\left(\dfrac{4 - \sqrt{15}}{175}\right)^i, & \text{for } 0 \leq i \leq n-1. \end{cases} \tag{42}$$

□

Fact 1. $\det Q = 45 + 13\sqrt{15}/9375 \quad (4 + \sqrt{15}/175)^{n-1} + 45- 13\sqrt{15}/9375(4 - \sqrt{15}/175)^{n-1}$.

Proof . Fact 1. Expanding detQ along the last row, we have

$$\begin{aligned}\det Q = \frac{3}{5}\det r_{3n} - \frac{1}{25}\det r_{3n-1} &= \frac{3}{5}\left[\frac{35 + 7\sqrt{15}}{50}\left(\frac{4 + \sqrt{15}}{175}\right)^n + \frac{35 - 7\sqrt{15}}{50}\left(\frac{4 - \sqrt{15}}{175}\right)^n\right] \\ &\quad - \frac{1}{25}\left[\frac{45 + 11\sqrt{15}}{150}\left(\frac{4 + \sqrt{15}}{175}\right)^{n-1} + \frac{45 - 11\sqrt{15}}{150}\left(\frac{4 - \sqrt{15}}{175}\right)^{n-1}\right] \\ &= \frac{45 + 13\sqrt{15}}{9375}\left(\frac{4 + \sqrt{15}}{175}\right)^{n-1} + \frac{45 - 13\sqrt{15}}{9375}\left(\frac{4 - \sqrt{15}}{175}\right)^{n-1}.\end{aligned} \tag{43}$$

□

Fact 2.

$$(-1)^{3n}b_{3n} = \frac{1500+401\sqrt{15}+n(1605+397\sqrt{15})}{1875}\left(\frac{4+\sqrt{15}}{175}\right)^{n-1} + \frac{1500-401\sqrt{15}+n(1605-397\sqrt{15})}{1875}\left(\frac{4-\sqrt{15}}{175}\right)^{n-1}. \tag{44}$$

Proof of Fact 2. Noting that $(-1)^{3n}b_{3n}$ is the summation of all principal minors of Q with $3n$ columns and rows, we have

$$\begin{aligned}(-1)^{3n}b_{3n} &= \sum_{i=1}^{3n+1}\det Q[i] = \sum_{i=1}^{3n+1}\det\begin{pmatrix} R_{i-1} & 0 \\ 0 & S_{3n+1-i}\end{pmatrix} \\ &= \sum_{i=1}^{3n+1}\det r_{i-1}\cdot \det s_{3n+1-i},\end{aligned} \tag{45}$$

where

$$S_{3n+1-i} = \begin{pmatrix} l_{i+1,i+1} & \cdots & 0 & 0 \\ \vdots & \ddots & \vdots & \vdots \\ 0 & \cdots & l_{3n,3n} & -\frac{1}{\sqrt{35}} \\ 0 & \cdots & -\frac{1}{\sqrt{35}} & l_{3n+1,3n+1}\end{pmatrix}. \tag{46}$$

The structure and determinant of matrix $\mathscr{L}_A$ are preserved by a permutation similarity transformation of a square matrix, and one gets $\det S_{3n+1-i} = \det R_{3n+1-i}$. In line with Equation (45), we have

$$\begin{aligned}(-1)^{3n}b_{3n} &= \sum_{i=1}^{3n+1}\det Q[i] = \sum_{p=1}^{n}\det Q[3p] + \sum_{p=0}^{n-1}\det Q[3p+1] + \sum_{p=0}^{n-1}\det Q[3p+2] + r_{3n} \\ &= \sum_{p=1}^{n} r_{3(p-1)+2}\cdot r_{3(n-p)+1} + \sum_{p=1}^{n-1} r_{3p}\cdot r_{3(n-p)} + \sum_{p=0}^{n-1} r_{3p+1}\cdot r_{3(n-p-1)+2} + 2r_{3n}.\end{aligned} \tag{47}$$

The following forms can also be generated by using the above equations:

$$\begin{aligned}\sum_{p=1}^{n} r_{3(p-1)+2}\cdot r_{3(n-p)+1} &= n\left[\frac{150+37\sqrt{15}}{375}\left(\frac{4+\sqrt{15}}{175}\right)^{n-1} + \frac{150-37\sqrt{15}}{375}\left(\frac{4-\sqrt{15}}{175}\right)^{n-1}\right] \\ &\quad + \frac{14\sqrt{15}}{3}\left(\frac{4+\sqrt{15}}{175}\right)^{n} - \frac{14\sqrt{15}}{3}\left(\frac{4-\sqrt{15}}{175}\right)^{n},\end{aligned} \tag{48}$$

$$\begin{aligned}\sum_{p=1}^{n-1} r_{3p}\cdot r_{3(n-p)} &= (n-1)\left[\frac{35+7\sqrt{15}}{25}\left(\frac{4+\sqrt{15}}{175}\right)^{n} + \frac{35-7\sqrt{15}}{25}\left(\frac{4-\sqrt{15}}{175}\right)^{n}\right] \\ &\quad + \frac{\sqrt{15}}{1875}\left(\frac{4+\sqrt{15}}{175}\right)^{n-1} - \frac{\sqrt{15}}{1875}\left(\frac{4-\sqrt{15}}{175}\right)^{n-1},\end{aligned} \tag{49}$$

$$\begin{aligned}\sum_{p=0}^{n-1} r_{3p+1}\cdot r_{3(n-p-1)+2} &= n\left[\frac{150+37\sqrt{15}}{375}\left(\frac{4+\sqrt{15}}{175}\right)^{n-1} + \frac{150-37\sqrt{15}}{375}\left(\frac{4-\sqrt{15}}{175}\right)^{n-1}\right] \\ &\quad + \frac{14\sqrt{15}}{3}\left(\frac{4+\sqrt{15}}{175}\right)^{n} - \frac{14\sqrt{15}}{3}\left(\frac{4-\sqrt{15}}{175}\right)^{n},\end{aligned} \tag{50}$$

$$2r_{3n} = \frac{35+7\sqrt{15}}{25}\left(\frac{4+\sqrt{15}}{175}\right)^{n} + \frac{35-7\sqrt{15}}{25}\left(\frac{4-\sqrt{15}}{175}\right)^{n}. \tag{51}$$

We can obtain the desired result of Fact 2 by substituting equations (48)–(51) into (47).

In view of (40), Facts 1 and 2 and Lemma 6 hold immediately. □

The following theorem is derived from Lemmas 4–6.

Theorem 1. *Let* $O_n^2 = K_2 \boxtimes O_n$. *Then,*

$$Kf^*(O_n^2) = \frac{4077n^3 + 10604n^2 + 4844n + 399}{21} + (34n+6)\left[\frac{(-1)^{3n}b_{3n}}{\det Q}\right], \tag{52}$$

where

$$(-1)^{3n}b_{3n} = \frac{1500 + 401\sqrt{15} + n(1605 + 397\sqrt{15})}{1875}\left(\frac{4+\sqrt{15}}{175}\right)^{n-1} + \frac{1500 - 401\sqrt{15} + n(1605 - 397\sqrt{15})}{1875}\left(\frac{4-\sqrt{15}}{175}\right)^{n-1}$$
$$\det Q = \frac{45 + 13\sqrt{15}}{9375}\left(\frac{4+\sqrt{15}}{175}\right)^{n-1} + \frac{45 - 13\sqrt{15}}{9375}\left(\frac{4-\sqrt{15}}{175}\right)^{n-1}. \tag{53}$$

The explicit formulae of the spanning trees of O_n^2 are given below.

Theorem 2. *Let* $O_n^2 = K_2 \boxtimes O_n$. *Then,*

$$\tau(O_n^2) = \frac{2^{(16n-3)} \cdot 3^{(4n+3)}}{35}\left[(45 + 13\sqrt{15})(4+\sqrt{15})^{n-1} + (45 - 13\sqrt{15})(4-\sqrt{15})^{n-1}\right]. \tag{54}$$

Proof. By Lemma 2, we have $(6/5)^{(4n+4)} \cdot (8/7)^{(2n-2)} \prod_{i=2}^{3n+1} 2\gamma_i \prod_{i=1}^{3n+1} 2\xi_i \prod_{v\in V_{O_n^2}} d_{O_n^2} = 2|E_{O_n^2}|\tau(O_n^2)$. Note that

$$\prod_{v\in V_{O_n^2}} d_{O_n^2} = 5^{8n+8} \cdot 7^{4n-4},$$
$$\left|E_{O_n^2}\right| = 34n + 6,$$
$$\prod_{i=2}^{3n+1} \gamma_i = \frac{17n+3}{625}\left(\frac{1}{175}\right)^{n-1},$$
$$\prod_{i=1}^{3n+1} \xi_i = \det Q = \frac{45 + 13\sqrt{15}}{9375}\left(\frac{4+\sqrt{15}}{175}\right)^{n-1} + \frac{45 - 13\sqrt{15}}{9375}\left(\frac{4-\sqrt{15}}{175}\right)^{n-1}. \tag{55}$$

Hence, Theorem 2 immediately follows, along with Lemma 2. □

4. Conclusion

In this study, we consider O_n^2, which is the strong prism of the octagonal network. Using the normalized Laplacian theorems, we have determined the multiplicative degree-Kirchhoff index and the spanning tree of O_n^2. New discoveries, developments, and advancements in research are still required. In the near future, we will be exploring a more complex chemistry network.

Data Availability

No data were used in this study.

Conflicts of Interest

The authors declare that they have no conflicts of interest.

Acknowledgments

The researchers would like to thank the Deanship of Scientific Research, Qassim University for funding the publication of this project.

References

[1] H. Chen and F. Zhang, "Resistance distance and the normalized Laplacian spectrum," *Discrete Applied Mathematics*, vol. 155, no. 5, pp. 654–661, 2007.
[2] Y. Liao, X. Xie, Y. Hou, and M. A. Aziz-Alaoui, "Tutte polynomials of two self-similar network models," *Journal of Statistical Physics*, vol. 174, no. 4, pp. 893–905, 2019.
[3] C. He, S. Li, W. Luo, and L. Sun, "Calculating the normalized Laplacian spectrum and the number of spanning trees of linear pentagonal chains," *Journal of Computational and Applied Mathematics*, vol. 344, pp. 381–393, 2018.
[4] J. Huang and S. Li, "On the normalised Laplacian spectrum, degree-Kirchhoff index and spanning trees of graphs," *Bulletin of the Australian Mathematical Society*, vol. 91, no. 3, pp. 353–367, 2015.
[5] H. Zhang and S. Li, "On the Laplacian spectral radius of bipartite graphs with fixed order and size," *Discrete Applied Mathematics*, vol. 229, pp. 139–147, 2017.
[6] J. B. Liu, X. F. Pan, and F. T. Hu, "The Laplacian polynomial of graphs derived from regular graphs and applications," *Ars Combinatoria*, vol. 126, pp. 289–300, 2016.
[7] Y. Peng and S. Li, "On the Kirchhoff index and the number of spanning trees of linear phenylenes," *MATCH Communications in Mathematical and in Computer Chemistry*, vol. 77, pp. 765–780, 2017.
[8] J. Huang, S. Li, and X. Li, "The normalized Laplacian, degree-Kirchhoff index and spanning trees of the linear polyomino chains," *Applied Mathematics and Computation*, vol. 289, pp. 324–334, 2016.
[9] J. A. Bondy and U. S. R. Murty, *Graph Theory with Applications*, MCMillan, London, UK, 1976.
[10] H. Wiener, "Structural determination of paraffin boiling points," *Journal of the American Chemical Society*, vol. 69, no. 1, pp. 17–20, 1947.
[11] A. A. Dobrynin, R. Entringer, and I. Gutman, "Wiener index of trees: theory and applications," *Acta Applicandae Mathematicae*, vol. 66, no. 3, pp. 211–249, 2001.
[12] I. Gutman, "Selected properties of the Schultz molecular topological index," *Journal of Chemical Information and Computer Sciences*, vol. 34, no. 5, pp. 1087–1089, 1994.
[13] D. J. Klein and M. Randić, "Resistance distance," *Journal of Mathematical Chemistry*, vol. 12, no. 1, pp. 81–95, 1993.
[14] D. J. Klein and O. Ivanciuc, "Graph cyclicity, excess conductance, and resistance deficit," *Journal of Mathematical Chemistry*, vol. 30, pp. 217–287, 2001.
[15] I. Gutman and B. Mohar, "The quasi-Wiener and the Kirchhoff indices coincide," *Journal of Chemical Information and Computer Sciences*, vol. 36, no. 5, pp. 982–985, 1996.
[16] H.-Y. Zhu, D. J. Klein, and I. Lukovits, "Extensions of the Wiener number," *Journal of Chemical Information and Computer Sciences*, vol. 36, no. 3, pp. 420–428, 1996.
[17] F. R. K. Chung, *Spectral Graph Theory*, American Mathematical Society, Providence, RI, USA, 1997.
[18] D. J. Klein, I. Lukovits, and I. Gutman, "On the definition of the hyper-Wiener index for cycle-containing structures," *Journal of Chemical Information and Computer Sciences*, vol. 35, no. 1, pp. 50–52, 1995.
[19] R. B. Bapat, M. Karimi, and J.-B. Liu, "Kirchhoff index and degree Kirchhoff index of complete multipartite graphs," *Discrete Applied Mathematics*, vol. 232, pp. 41–49, 2017.
[20] U. Ali, H. Raza, and Y. Ahmed, "On normalized Laplacians, degree-Kirchhoff index and spanning tree of generalized phenylene," *Symmetry*, vol. 13, no. 8, p. 1374, 2021.
[21] J. Zhao, J.-B. Liu, and S. Hayat, "Resistance distance-based graph invariants and the number of spanning trees of linear crossed octagonal graphs," *Journal of Applied Mathematics and Computing*, vol. 63, no. 1-2, pp. 1–27, 2020.
[22] J. Huang, S. Li, and L. Sun, "The normalized Laplacians, degree-Kirchhoff index and the spanning trees of linear hexagonal chains," *Discrete Applied Mathematics*, vol. 207, pp. 67–79, 2016.
[23] U. Ali, Y. Ahmad, S. A. Xu, and X. F. Pan, "Resistance distance-based indices and spanning trees of linear pentagonal-quadrilateral networks," *Polycyclic Aromatic Compounds*, 2021.
[24] X. Ma and H. Bian, "The normalized Laplacians, degree-Kirchhoff index and the spanning trees of cylinder phenylene chain," *Polycyclic Aromatic Compounds*, 2019.
[25] J. Palacios and J. M. Renom, "Another look at the degree-Kirchhoff index," *International Journal of Quantum Chemistry*, vol. 111, pp. 3453–3455, 2011.
[26] H. Zhang and Y. Yang, "Resistance distance and Kirchhoff index in circulant graphs," *International Journal of Quantum Chemistry*, vol. 107, no. 2, pp. 330–339, 2007.
[27] Y. Pan and J. Li, "Kirchhoff index, multiplicative degree-Kirchhoff index and spanning trees of the linear crossed hexagonal chains," *International Journal of Quantum Chemistry*, vol. 118, no. 24, Article ID e25787, 2018.
[28] S. Li, W. Wei, and S. Yu, "On normalized Laplacians, multiplicative degree-Kirchhoff indices, and spanning trees of the linear [n]phenylenes and their dicyclobutadieno derivatives," *International Journal of Quantum Chemistry*, vol. 119, no. 8, Article ID e25863, 2019.
[29] J. B. Liu, J. Chen, J. Zhao, and S. Wang, "The Laplacian spectrum, Kirchhoff index, and the number of spanning trees of the linear," *Heptagonal Networks" Complexity*, vol. 10, 2022.
[30] J.-B. Liu, J. Zhao, Z. Zhu, and J. Cao, "On the normalized laplacian and the number of spanning trees of linear heptagonal networks," *Mathematics*, vol. 7, no. 4, p. 314, 2019.
[31] T. Réti, A. Ali, and I. Gutman, "On bond-additive and atoms-pair-additive indices of graphs" Electron," *Jurnal Matematika*, vol. 2, pp. 52–61, 2021.

[32] S. Li and W. Wei, "Extremal octagonal chains with respect to the coefficients sum of the permanental polynomial," *Applied Mathematics and Computation*, vol. 328, pp. 45–57, 2018.

[33] Z. Li, Z. Xie, J. Li, and Y. Pan, "Resistance distance-based graph invariants and spanning trees of graphs derived from the strong prism of a star," *Applied Mathematics and Computation*, vol. 382, Article ID 125335, 2020.

[34] U. Ali, Y. Ahmed, S. A. Xu, and X. F. Pan, "On normalized Laplacian, degree-Kirchhoff index of the strong prism of generalized phenylenes," *Polycyclic Aromatic Compounds*, 2021.

[35] Y. G. Pan and J. P. Li, "Resistance distance-based graph invariants and spanning trees of graphs derived from the strong product of P_2 and C_n," 2019, https://arxiv.org/abs1906.04339.

[36] Y. Pan, C. Liu, and J. Li, "Kirchhoff indices and numbers of spanning trees of molecular graphs derived from linear crossed polyomino chain," *Polycyclic Aromatic Compounds*, 2020.

Hindawi
Journal of Mathematics
Volume 2022, Article ID 1670984, 9 pages
https://doi.org/10.1155/2022/1670984

Research Article

The (Multiplicative Degree-) Kirchhoff Index of Graphs Derived from the Cartesian Product of S_n and K_2

Jia-Bao Liu,[1] **Xin-Bei Peng**,[1] **Jiao-Jiao Gu**,[1] **and Wenshui Lin**[2]

[1]*School of Mathematics and Physics, Anhui Jianzhu University, Hefei 230601, China*
[2]*School of Informatics, Xiamen University, Xiamen 361005, China*

Correspondence should be addressed to Wenshui Lin; wslin@xmu.edu.cn

Received 3 November 2021; Accepted 12 January 2022; Published 17 February 2022

Academic Editor: A. Ghareeb

Copyright © 2022 Jia-Bao Liu et al. This is an open access article distributed under the Creative Commons Attribution License, which permits unrestricted use, distribution, and reproduction in any medium, provided the original work is properly cited.

It is well known that many topological indices have widespread use in lots of fields about scientific research, and the Kirchhoff index plays a major role in many different sectors over the years. Recently, Li et al. (Appl. Math. Comput. 382 (2020) 125335) proposed the problem of determining the Kirchhoff index and multiplicative degree-Kirchhoff index of graphs derived from $S_n \times K_2$, the Cartesian product of the star S_n, and the complete graph K_2. In the present study, we completely solve this problem, that is, the explicit closed-form formulae of the Kirchhoff index, multiplicative degree-Kirchhoff index, and number of spanning trees are obtained for some graphs derived from $S_n \times K_2$.

1. Introduction

In this study, we suppose that $G = (V, E)$ is a nontrivial simple and connected graph, where $V = \{v_1, v_2, \ldots, v_n\}$ and E are the vertex set and edge set of G, respectively. Let $A(G) = (a_{ij})_{n\times n}$ be the adjacency matrix, and $D(G) = \mathrm{diag}(d_1, d_2, \ldots, d_n)$ the degree matrix, where d_i is the degree of vertex v_i. Then, $L(G) = D(G) - A(G)$ is termed as the Laplacian matrix, and $\mathscr{L}(G) = D(G)^{-1/2}L(G)D(G)^{-1/2}$ the normalized Laplacian matrix of graph G. It is easily seen that

$$(\mathscr{L}(G))_{ij} = \begin{cases} 1, & \text{if } i = j; \\ -\dfrac{1}{\sqrt{d_i d_j}}, & \text{if } i \neq j \text{ and } v_i v_j \in E; \\ 0, & \text{otherwise.} \end{cases} \tag{1}$$

Let $0 = \mu_1 < \mu_2 \leq \cdots \leq \mu_n$ be the eigenvalues of $L(G)$ and $0 = \nu_1 < \nu_2 \leq \cdots \leq \nu_n$ the eigenvalues of $\mathscr{L}(G)$. The sets $Sp(L(G)) = \{\mu_1, \mu_2, \ldots, \mu_n\}$ and $Sp(\mathscr{L}(G)) = \{\nu_1, \nu_2, \ldots, \nu_n\}$ are called the Laplacian spectrum and normalized Laplacian spectrum of G, respectively.

For two vertices v_i and v_j, the distance between them written as d_{ij} is the length of the shortest path linking them. The Wiener index [1] and Gutman index [2] of G are defined as $W(G) = \sum_{i<j} d_{ij}$ and $\mathrm{Gut}(G) = \sum_{i<j} d_i d_j d_{ij}$. For these two famous topological indices, one can refer to [3–10] and the references therein.

If regard each edge in $E(G)$ as an unit resistor, then for two vertices v_i and v_j, r_{ij} is represented as the effective resistance between them [11]. In the field of chemistry, resistance distance has been studied extensively and many profound results have been obtained. One of the most famous results is the Kirchhoff index, which is used to characterize the structure of a compound. The Kirchhoff index of G is written as $Kf(G) = \sum_{i<j} r_{ij}$. It is derived from molecular diagrams and is also a form used to numerically characterize molecules. Hitherto, the Kirchhoff index has been widely applied to mathematic, chemistry, physics, and so on. Later, the following relation between $Kf(G)$ and $Sp(L(G))$ was established by Zhu et al. [12] and Gutman and Mohar [13] independently.

Lemma 1 (See [12, 13]). *Let G be a simple graph of order $n \geq 2$. Then,*

$$Kf(G) = \sum_{i=2}^{n} \frac{1}{\mu_i}. \tag{2}$$

Similarly, Chen and Zhang [14] defined the multiplicative degree-Kirchhoff index of G as $Kf^*(G) = \sum_{i<j} d_i d_j r_{ij}$. Moreover, the following relation between $Kf^*(G)$ and $Sp(\mathscr{L}(G))$ was confirmed.

Lemma 2 (See [14]). *Let G be a simple connected graph of order $n \geq 2$ and size m. Then,*

$$Kf^*(G) = 2m \sum_{i=2}^{n} \frac{1}{\nu_i}. \tag{3}$$

Nowadays, the (multiplicative degree-) Kirchhoff index has attracted a lot of attention from researchers over the few years. Furthermore, its closed-form formulae have been established depending on many kinds of graphs. For examples, the formulae of Kirchhoff index for cycles, circulant graphs, and composite graphs were obtained in [15, 16] and [17], respectively, and those of both indices for complete multipartite graphs were obtained in [18]. Besides, quite a few literature concerned the (multiplicative degree-) Kirchhoff index of polygon chains and their variants. Explicit expressions of the above index have been derived for linear polyomino chain [19], linear crossed polyomino chain [20], linear pentagonal chain [21], linear phenylenes [22, 23], cyclic phenylenes [24], Möbius phenylenes chain and cylinder phenylenes chain [25, 26], linear (n) phenylenes [27], generalized phenylenes [28, 29], linear hexagonal chain [30, 31], linear crossed hexagonal chain [32], Möbius hexagonal chain [33], periodic linear chains [34], linear octagonal chain [35], linear octagonal-quadrilateral chain [36], and linear crossed octagonal chain [37].

For two disjoint graphs G and H, the strong product of them is written as $G \otimes H$, that is, $V(G \otimes H) = V(G) \times V(H)$, and two distinct vertices (u_1, v_1) and (u_2, v_2) are contiguous. The Cartesian product of G and H, written as $G \times H$, is the graph with vertex set $V(G) \times V(H)$, and two vertices (u_1, v_1) and (u_2, v_2) are adjacent whenever $u_1 = u_2$ and $v_1 v_2 \in E(H)$ or $v_1 = v_2$ and $u_1 u_2 \in E(G)$. Figure 1 shows the graphs $S_n \otimes K_2$ and $S_n \times K_2$, where S_n and K_n denote the star and complete graph of order n, severally. Recently, Li et al. [38] determined the expressions of $Kf(S_r)$, $Kf^*(S_r)$, and $\tau(S_r)$, where S_r is a graph derived from $S_n \otimes K_2$ by randomly removing r vertical edges, and $\tau(G)$ denotes the number of spanning trees of a connected graph G. Finally, they proposed the problem of determining these three invariants for graphs derived from $S_n \times K_2$. In the present study, we completely solve this problem.

For convenience, we denote $S_n^2 = S_n \times K_2$. Then, $|V(S_n^2)| = 2n$ and $|E(S_n^2)| = 3n - 2$. Let $E' = \{ii' | i = 1, 2, \ldots, n\}$. $\mathscr{S}_{n,r}^2$ will denote the set of graphs derived from S_n^2 by discretionarily deleting r edges in E'. Obviously, the unique graph in $\mathscr{S}_{n,n}^2$ is disconnected; hence, we consider $\mathscr{S}_{n,r}^2$ for $0 \leq r \leq n-1$ only. Note also, $\mathscr{S}_{n,0}^2 = \{S_n^2\}$. In Section 2, some notations and known results are introduced, which will be applied to get our main results. In Section 3, explicit expressions of $Kf(S_n^2)$, $Kf^*(S_n^2)$, and $\tau(S_n^2)$ are obtained. Finally, $Kf(S_{n,r}^2)$ and $\tau(S_{n,r}^2)$ are determined in Section 4, where $S_{n,r}^2$ is an arbitrary graph in $\mathscr{S}_{n,r}^2$. Moreover, it is shown that $\lim_{n\longrightarrow+\infty} Kf(S_n^2)/W(S_n^2) = \lim_{n\longrightarrow+\infty} Kf(S_{n,r}^2)/W(S_{n,r}^2) = 8/15$ and $\lim_{n\longrightarrow+\infty} Kf^*(S_n^2)/\mathrm{Gut}(S_n^2) = 16/33$.

2. Preliminaries

In this section, we will introduce some basic concepts. These following celebrated definitions and fundamental lemmas can play a vital role in proving our consequences.

First, we mark the vertices of S_n^2 as in Figure 1; then, set $V_1 = \{1, 2, \ldots, n\}$ and $V_2 = \{1', 2', \ldots, n'\}$. Therefore, we have

$$\begin{aligned} L(S_n^2) &= \begin{pmatrix} L_{11}(S_n^2) & L_{12}(S_n^2) \\ L_{21}(S_n^2) & L_{22}(S_n^2) \end{pmatrix}, \\ \mathscr{L}(S_n^2) &= \begin{pmatrix} \mathscr{L}_{11}(S_n^2) & \mathscr{L}_{12}(S_n^2) \\ \mathscr{L}_{21}(S_n^2) & \mathscr{L}_{22}(S_n^2) \end{pmatrix}, \end{aligned} \tag{4}$$

where $L_{ij}(S_n^2)$ $(\mathscr{L}_{ij}(S_n^2))$ is the submatrix of $L(S_n^2)$ (respectively, $\mathscr{L}(S_n^2)$) whose rows (columns) correspond to the vertices in V_i (respectively V_j). It is easily seen that $L_{11}(S_n^2) = L_{22}(S_n^2)$, $L_{12}(S_n^2) = L_{21}(S_n^2)$, $\mathscr{L}_{11}(S_n^2) = \mathscr{L}_{22}(S_n^2)$, and $\mathscr{L}_{12}(S_n^2) = \mathscr{L}_{21}(S_n^2)$.

Let

$$T = \begin{pmatrix} \frac{1}{\sqrt{2}} I_n & \frac{1}{\sqrt{2}} I_n \\ \\ \frac{1}{\sqrt{2}} I_n & -\frac{1}{\sqrt{2}} I_n \end{pmatrix}, \tag{5}$$

and then, we have

$$\begin{aligned} TL(S_n^2)T &= \begin{pmatrix} L_A(S_n^2) & 0 \\ 0 & L_S(S_n^2) \end{pmatrix}, \\ T\mathscr{L}(S_n^2)T &= \begin{pmatrix} \mathscr{L}_A(S_n^2) & 0 \\ 0 & \mathscr{L}_S(S_n^2) \end{pmatrix}, \end{aligned} \tag{6}$$

where $L_A(S_n^2) = L_{11}(S_n^2) + L_{12}(S_n^2)$, $L_S(S_n^2) = L_{11}(S_n^2) - L_{12}(S_n^2)$, $\mathscr{L}_A(S_n^2) = \mathscr{L}_{11}(S_n^2) + \mathscr{L}_{12}(S_n^2)$, and $\mathscr{L}_S(S_n^2) = \mathscr{L}_{11}(S_n^2) - \mathscr{L}_{12}(S_n^2)$.

Based on the above arguments, by applying the technique used in [32, 39], we immediately have the following decomposition theorem, where $\Phi(B, \lambda) = |\lambda I - B|$ stands for the characteristic polynomial of B.

Lemma 3 *Let $L_A(S_n^2)$, $L_S(S_n^2)$, $\mathscr{L}_A(S_n^2)$, and $\mathscr{L}_S(S_n^2)$ be written as above. Thus, we obtain that*

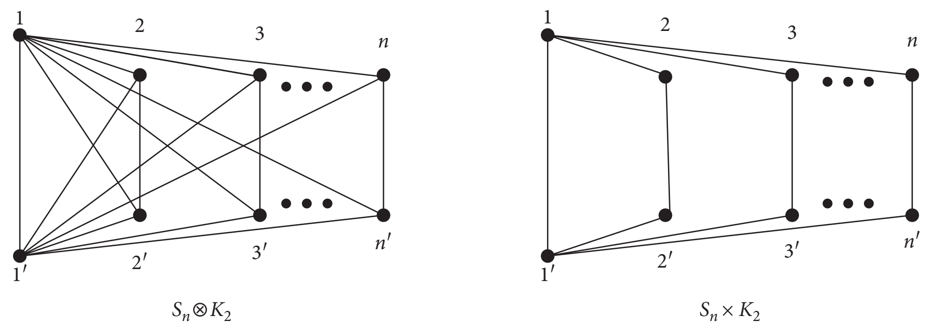

Figure 1: The graphs $S_n \otimes K_2$ and $S_n \times K_2$.

$$\begin{aligned}\Phi\left(L\left(S_n^2\right),\lambda\right) &= \Phi\left(L_A\left(S_n^2\right),\lambda\right)\Phi\left(L_S\left(S_n^2\right),\lambda\right),\\ \Phi\left(\mathscr{L}\left(S_n^2\right),\lambda\right) &= \Phi\left(\mathscr{L}_A\left(S_n^2\right),\lambda\right)\Phi\left(\mathscr{L}_S\left(S_n^2\right),\lambda\right).\end{aligned} \tag{7}$$

Lemma 4 (See [40]). *Assume that G is a connected graph with $n \geq 2$ vertices; then,*

$$\tau(G) = \frac{1}{n}\prod_{i=2}^{n}\mu_i. \tag{8}$$

3. Results for S_n^2

In this section, we will derive explicit expressions of $Kf(S_n^2)$, $Kf^*(S_n^2)$, and $\tau(S_n^2)$ as follows.

3.1. On $Kf(S_n^2)$ and $\tau(S_n^2)$. Obviously,

$$\begin{aligned}L_{11}\left(S_n^2\right) &= \begin{pmatrix} n & -1 & -1 & \dots & -1\\ -1 & 2 & 0 & \dots & 0\\ -1 & 0 & 2 & \dots & 0\\ \dots & \dots & \dots & \dots & \dots\\ -1 & 0 & 0 & \dots & 2\end{pmatrix}_{n\times n},\\ L_{12}\left(S_n^2\right) &= \begin{pmatrix} -1 & 0 & 0 & \dots & 0\\ 0 & -1 & 0 & \dots & 0\\ 0 & 0 & -1 & \dots & 0\\ \dots & \dots & \dots & \dots & \dots\\ 0 & 0 & 0 & \dots & -1\end{pmatrix}_{n\times n}.\end{aligned} \tag{9}$$

Hence,

$$L_A\left(S_n^2\right) = L_{11}\left(S_n^2\right) + L_{12}\left(S_n^2\right) = \begin{pmatrix} n-1 & -1 & -1 & \dots & -1\\ -1 & 1 & 0 & \dots & 0\\ -1 & 0 & 1 & \dots & 0\\ \dots & \dots & \dots & \dots & \dots\\ -1 & 0 & 0 & \dots & 1\end{pmatrix}_{n\times n}, \tag{10}$$

and we easily have $Sp(L_A(S_n^2)) = \{0, 1^{n-2}, n\}$, where a^k denotes the k successive a's.

Similarly, we have

$$L_S\left(S_n^2\right) = L_{11}\left(S_n^2\right) - L_{12}\left(S_n^2\right) = \begin{pmatrix} n+1 & -1 & -1 & \dots & -1\\ -1 & 3 & 0 & \dots & 0\\ -1 & 0 & 3 & \dots & 0\\ \dots & \dots & \dots & \dots & \dots\\ -1 & 0 & 0 & \dots & 3\end{pmatrix}_{n\times n}, \tag{11}$$

and get $Sp(L_S(S_n^2)) = \{2, 3^{n-2}, n+2\}$.

Hence, $Sp(L(S_n^2)) = \{0, 1^{n-2}, 2, 3^{n-2}, n, n+2\}$ from Lemma 3, and we get the following result.

Theorem 1. *Let $S_n^2 = S_n \times K_2$. Then,*

(1) $Kf(S_n^2) = 8n^3 + 3n^2 - 14n + 12/3n + 6$

(2) $\tau(S_n^2) = (n+2)\cdot 3^{n-2}$

(3) $\lim_{n\longrightarrow+\infty} Kf(S_n^2)/W(S_n^2) = 8/15$

Proof. From Lemma 1, we have

$$Kf\left(S_n^2\right) = 2n\left[(n-2) + \frac{1}{2} + \frac{n-2}{3} + \frac{1}{n} + \frac{1}{n+2}\right] = \frac{8n^3 + 3n^2 - 14n + 12}{3(n+2)}. \tag{12}$$

From Lemma 4, we immediately have

$$\tau\left(S_n^2\right) = \frac{1}{2n}\cdot 2\cdot 3^{n-2}\cdot n\cdot (n+2) = (n+2)\cdot 3^{n-2}. \tag{13}$$

Finally, we end the proof by confirming that $W(S_n^2) = 5n^2 - 8n + 4$. Let $w_i = \sum_{j\in V(S_n^2)} d_{ij}$. Obviously, $w_i = 1\cdot n + 2(n-1) = 3n - 2$ if $i = 1, 1'$, and $w_i = 1 + 1 + 2(n-1) + 3(n-2) = 5n - 6$ otherwise. Hence,

$$W\left(S_n^2\right) = \frac{1}{2}\sum_{i\in V\left(S_n^2\right)} w_i = \frac{1}{2}\left[2(3n-2) + (2n-2)(5n-6)\right] = 5n^2 - 8n + 4. \tag{14}$$

□

3.2. On $Kf^*(S_n^2)$. Consequently, we will determine $Kf^*(S_n^2)$. Obviously,

$$\mathscr{L}_{11}\left(S_n^2\right) = \begin{pmatrix} 1 & -\frac{1}{\sqrt{2n}} & -\frac{1}{\sqrt{2n}} & \cdots & -\frac{1}{\sqrt{2n}} \\ -\frac{1}{\sqrt{2n}} & 1 & 0 & \cdots & 0 \\ -\frac{1}{\sqrt{2n}} & 0 & 1 & \cdots & 0 \\ \cdots & \cdots & \cdots & \cdots & \cdots \\ -\frac{1}{\sqrt{2n}} & 0 & 0 & \cdots & 1 \end{pmatrix}_{n\times n},$$

$$\mathscr{L}_{12}\left(S_n^2\right) = \begin{pmatrix} -\frac{1}{n} & 0 & 0 & \cdots & 0 \\ 0 & -\frac{1}{2} & 0 & \cdots & 0 \\ 0 & 0 & -\frac{1}{2} & \cdots & 0 \\ \cdots & \cdots & \cdots & \cdots & \cdots \\ 0 & 0 & 0 & \cdots & -\frac{1}{2} \end{pmatrix}_{n\times n}. \tag{15}$$

Hence,

$$\mathscr{L}_A\left(S_n^2\right) = \mathscr{L}_{11}\left(S_n^2\right) + \mathscr{L}_{12}\left(S_n^2\right) = \begin{pmatrix} \frac{n-1}{n} & -\frac{1}{\sqrt{2n}} & -\frac{1}{\sqrt{2n}} & \cdots & -\frac{1}{\sqrt{2n}} \\ -\frac{1}{\sqrt{2n}} & \frac{1}{2} & 0 & \cdots & 0 \\ -\frac{1}{\sqrt{2n}} & 0 & \frac{1}{2} & \cdots & 0 \\ \cdots & \cdots & \cdots & \cdots & \cdots \\ -\frac{1}{\sqrt{2n}} & 0 & 0 & \cdots & \frac{1}{2} \end{pmatrix}_{n\times n}, \tag{16}$$

and we easily have $Sp(\mathscr{L}_A(S_n^2)) = \{0, (1/2)^{n-2}, 3n-2/2n\}$.

Similarly, we have

$$\mathscr{L}_S\left(S_n^2\right) = \mathscr{L}_{11}\left(S_n^2\right) - \mathscr{L}_{12}\left(S_n^2\right) = \begin{pmatrix} \frac{n+1}{n} & -\frac{1}{\sqrt{2n}} & -\frac{1}{\sqrt{2n}} & \cdots & -\frac{1}{\sqrt{2n}} \\ -\frac{1}{\sqrt{2n}} & \frac{3}{2} & 0 & \cdots & 0 \\ -\frac{1}{\sqrt{2n}} & 0 & \frac{3}{2} & \cdots & 0 \\ \cdots & \cdots & \cdots & \cdots & \cdots \\ -\frac{1}{\sqrt{2n}} & 0 & 0 & \cdots & \frac{3}{2} \end{pmatrix}_{n\times n}, \tag{17}$$

and get $Sp(\mathscr{L}_S(S_n^2)) = \{2, (3/2)^{n-2}, n+2/2n\}$.

Hence, $Sp(\mathscr{L}(S_n^2)) = \{0, (1/2)^{n-2}, n+2/2n, 3n-2/2n, (3/2)^{n-2}, 2\}$ from Lemma 3, and we immediately have the following result.

Theorem 2. *Let $S_n^2 = S_n \times K_2$. Then,*

(1) $Kf^*(S_n^2) = 48n^3 + 25n^2 - 180n + 116/3n + 6$

(2) $\lim_{n\longrightarrow+\infty} Kf^*(S_n^2)/Gut(S_n^2) = 16/33$

Proof. From Lemma 2, it is easily confirmed that

$$Kf^*(S_n^2) = 2(3n-2)\left[2n-4+\frac{2n}{n+2}+\frac{2n}{3n-2}+\frac{2(n-2)}{3}+\frac{1}{2}\right],$$
$$=\frac{48n^3+25n^2-180n+116}{3n+6}. \tag{18}$$

Now, let $g_i = \sum_{j\in V(S_n^2)} d_i d_j d_{ij}$. Obviously, if $i = 1, 1'$, then

$$g_i = n\cdot 2\cdot 1 + n\cdot 2\cdot 1\cdot(n-1) + n\cdot 2\cdot 2\cdot(n-1) = 7n^2-6n, \tag{19}$$

and otherwise,

$$g_i = 2\cdot n\cdot 1 + 2\cdot 2\cdot 1 + 2\cdot n\cdot 2 + 2\cdot 2\cdot 2\cdot(n-2) + 2\cdot 2\cdot 3\cdot(n-2) = 26n-36. \tag{20}$$

Hence,

$$\mathrm{Gut}(S_n^2) = \frac{1}{2}\sum_{i\in V(S_n^2)} g_i = \frac{1}{2}\left[2(7n^2-6n)+(26n-36)(2n-2)\right] = 33n^2-68n+36, \tag{21}$$

and it follows that

$$\lim_{n\longrightarrow+\infty}\frac{Kf^*(S_n^2)}{\mathrm{Gut}(S_n^2)} = \lim_{n\longrightarrow+\infty}\frac{48n^3+25n^2-180n+116}{(3n+6)(33n^2-68n+36)} = \frac{16}{33}, \tag{22}$$

which completes the proof. □

4. Results for Graphs in $\mathcal{S}_{n,r}^2$

Assume that $S_{n,r}^2$ is any graph in $\mathcal{S}_{n,r}^2$, $1\le r\le n-1$. We will carry out a computational study on $Kf(S_{n,r}^2)$ and $\tau(S_{n,r}^2)$ in this section.

We suppose that d_i is the degree of i in $S_{n,r}^2$. Therefore, $d_i = n$ or $n-1$ if $i = 1, 1'$, and $d_i = 1$ or 2 otherwise. We will compute $Sp(S_{n,r}^2)$ in the following.

Case 1. Edge $11' \notin (E_{n,r}^2)$. Then,

$$L_{11}(S_{n,r}^2) = \begin{pmatrix} n-1 & -1 & -1 & \ldots & -1 \\ -1 & d_2 & 0 & \ldots & 0 \\ -1 & 0 & d_3 & \ldots & 0 \\ \ldots & \ldots & \ldots & \ldots & \ldots \\ -1 & 0 & 0 & \ldots & d_n \end{pmatrix},$$
$$L_{12}(S_{n,r}^2) = \begin{pmatrix} 0 & 0 & 0 & \ldots & 0 \\ 0 & t_2 & 0 & \ldots & 0 \\ 0 & 0 & t_3 & \ldots & 0 \\ \ldots & \ldots & \ldots & \ldots & \ldots \\ 0 & 0 & 0 & \ldots & t_n \end{pmatrix}, \tag{23}$$

where $t_i = 0$ if $d_i = 1$ and $t_i = 1$ if $d_i = 2$, $2\le i\le n$. Hence,

$$L_A(S_{n,r}^2) = L_{11}(S_{n,r}^2) + L_{12}(S_{n,r}^2) = \begin{pmatrix} n-1 & -1 & -1 & \ldots & -1 \\ -1 & 1 & 0 & \ldots & 0 \\ -1 & 0 & 1 & \ldots & 0 \\ \ldots & \ldots & \ldots & \ldots & \ldots \\ -1 & 0 & 0 & \ldots & 1 \end{pmatrix}_{n\times n}, \tag{24}$$

and $Sp(L_A(S_{n,r}^2)) = \{0, 1^{n-2}, n\}$. On the other hand,

$$L_S(S_{n,r}^2) = L_{11}(S_{n,r}^2) - L_{12}(S_{n,r}^2) = \begin{pmatrix} n-1 & -1 & -1 & \dots & -1 \\ -1 & d_2 - t_2 & 0 & \dots & 0 \\ -1 & 0 & d_3 - t_3 & \dots & 0 \\ \dots & \dots & \dots & \dots & \dots \\ -1 & 0 & 0 & \dots & d_n - t_n \end{pmatrix}, \tag{25}$$

where $d_i - t_i = 1$ if $d_i = 1$ and $d_i - t_i = 3$ if $d_i = 2$, $2 \leq i \leq n$. We will compute $Sp(L_S(S_{n,r}^2))$ in the following cases.

Case 1.1. $r = 1$. Then, $d_i - t_i = 3$, $2 \leq i \leq n$, and we easily have

$$Sp(L_S(S_{n,r}^2)) = \left\{ 3^{n-2}, \frac{n+2+\sqrt{n^2-4n+12}}{2}, \frac{n+2-\sqrt{n^2-4n+12}}{2} \right\}. \tag{26}$$

Case 1.2. $r \geq 2$. By direct calculations, we have

$$\Phi(L_S(S_{n,r}^2), \lambda) = \left[\lambda^3 - (n+3)\lambda^2 + 3n\lambda + 2r - 2n\right](\lambda - 1)^{r-2}(\lambda - 3)^{n-r-1}. \tag{27}$$

Let $\lambda_1, \lambda_2, \lambda_3$ be the three roots of $\lambda^3 - (n+3)\lambda^2 + 3n\lambda + 2r - 2n = 0$. Then, $Sp(L_S(S_{n,r}^2)) = \{1^{r-2}, 3^{n-r-1}, \lambda_1, \lambda_2, \lambda_3\}$, and it holds that $\lambda_1\lambda_2\lambda_3 = 2n - 2r$ and

$$\frac{1}{\lambda_1} + \frac{1}{\lambda_2} + \frac{1}{\lambda_3} = \frac{\lambda_1\lambda_2 + \lambda_1\lambda_3 + \lambda_2\lambda_3}{\lambda_1\lambda_2\lambda_3} = \frac{3n}{2n-2r}, \tag{28}$$

Case 2. $11' \in (E_{n,r}^2)$. Then,

$$\begin{aligned} L_{11}(S_{n,r}^2) &= \begin{pmatrix} n & -1 & -1 & \dots & -1 \\ -1 & d_2 & 0 & \dots & 0 \\ -1 & 0 & d_3 & \dots & 0 \\ \dots & \dots & \dots & \dots & \dots \\ -1 & 0 & 0 & \dots & d_n \end{pmatrix}, \\ L_{12}(S_{n,r}^2) &= \begin{pmatrix} -1 & 0 & 0 & \dots & 0 \\ 0 & t_2 & 0 & \dots & 0 \\ 0 & 0 & t_3 & \dots & 0 \\ \dots & \dots & \dots & \dots & \dots \\ 0 & 0 & 0 & \dots & t_n \end{pmatrix}, \end{aligned} \tag{29}$$

where $t_i = 0$ if $d_i = 1$ and $t_i = -1$ if $d_i = 2$, $2 \leq i \leq n$. Hence,

$$L_A(S_{n,r}^2) = L_{11}(S_{n,r}^2) + L_{12}(S_{n,r}^2) = \begin{pmatrix} n-1 & -1 & -1 & \dots & -1 \\ -1 & 1 & 0 & \dots & 0 \\ -1 & 0 & 1 & \dots & 0 \\ \dots & \dots & \dots & \dots & \dots \\ -1 & 0 & 0 & \dots & 1 \end{pmatrix}_{n\times n}, \tag{30}$$

and $Sp(L_A(S_{n,r}^2)) = \{0, 1^{n-2}, n\}$. On the other hand,

$$L_S(S_{n,r}^2) = L_{11}(S_{n,r}^2) - L_{12}(S_{n,r}^2) = \begin{pmatrix} n+1 & -1 & -1 & \dots & -1 \\ -1 & d_2 - t_2 & 0 & \dots & 0 \\ -1 & 0 & d_3 - t_3 & \dots & 0 \\ \dots & \dots & \dots & \dots & \dots \\ -1 & 0 & 0 & \dots & d_n - t_n \end{pmatrix}, \tag{31}$$

where $d_i - t_i = 1$ if $d_i = 1$ and $d_i - t_i = 3$ if $d_i = 2$, $2 \le i \le n$. By direct calculations, we have

$$\Phi(L_S(S_{n,r}^2), \lambda) = \left[\lambda^3 - (n+5)\lambda^2 + (3n+8)\lambda + 2r - 2n - 4\right](\lambda - 1)^{r-1}(\lambda - 3)^{n-r-2}. \tag{32}$$

Let $\lambda_1, \lambda_2, \lambda_3$ be the three roots of $\lambda^3 - (n+5)\lambda^2 + (3n+8)\lambda + 2r - 2n - 4 = 0$. Then, $Sp(L_S(S_{n,r}^2)) = \{1^{r-1}, 3^{n-r-2}, \lambda_1, \lambda_2, \lambda_3\}$, and it holds that $\lambda_1\lambda_2\lambda_3 = 2n - 2r + 4$ and

$$\frac{1}{\lambda_1} + \frac{1}{\lambda_2} + \frac{1}{\lambda_3} = \frac{\lambda_1\lambda_2 + \lambda_1\lambda_3 + \lambda_2\lambda_3}{\lambda_1\lambda_2\lambda_3} = \frac{3n+8}{2n-2r+4}, \tag{33}$$

from Vieta's theorem.

Now, we are able to give the main result of this section.

Theorem 3. *If $S_{n,r}^2 \in \mathcal{S}_{n,r}^2$, $0 \le r \le n-1$, then*

(1) $Kf(S_{n,r}^2) = \{ (8n^3 - (4r+17)n^2 - (4r^2 - 26r - 6)n - 6r)/3(n-r)$, if $11' \notin E(S_{n,r}^2)$, $8n^3 - (4r-3)n^2 - (4r^2 - 30r + 14)n + 12 - 6r/3(n-r-2)$, if $11' \in E(S_{n,r}^2)$.

(2) $\tau(S_{n,r}^2) = \begin{cases} (n-r)\cdot 3^{n-r-1}, & \text{if } 11' \notin E(S_{n,r}^2), \\ (n-r+2)\cdot 3^{n-r+2}, & \text{if } 11' \in E(S_{n,r}^2), \end{cases}$

(3) $lim_{n\longrightarrow+\infty} Kf(S_{n,r}^2)/W(S_{n,r}^2) = 8/15$

Proof. If $r = 0$, then $S_{n,r}^2 \cong S_n^2$, and the conclusion holds from Theorem 1. Hence, assume $r \ge 1$. We distinguish the following two cases.

Case 1. Edge $11' \notin (E_{n,r}^2)$.

Case 1.1. $r = 1$. Then,

$$Sp(L(S_{n,r}^2)) = \left\{0, 1^{n-2}, n, 3^{n-2}, \frac{n+2-\sqrt{n^2-4n+12}}{2}, \frac{n+2+\sqrt{n^2-4n+12}}{2}\right\}. \tag{34}$$

From Lemma 1, we have

$$\begin{aligned} Kf(S_{n,r}^2) &= 2n\left[n - 2 + \frac{1}{n} + \frac{n-2}{3} + \frac{2}{n+2-\sqrt{n^2-4n+12}} + \frac{2}{n+2+\sqrt{n^2-4n+12}}\right], \\ &= \frac{8n^3 - 21n^2 + 28n - 6}{3(n-1)} \\ &= \frac{8n^3 - (4r+17)n^2 - (4r^2 - 26r - 6)n - 6r}{3(n-r)}. \end{aligned} \tag{35}$$

Then, from Lemma 2, we have

$$\begin{aligned}\tau\left(S^2_{n,r}\right) &= \frac{1}{2n}\left[n\cdot 3^{n-2}\cdot\frac{n+2-\sqrt{n^2-4n+12}}{2}\cdot\frac{n+2+\sqrt{n^2-4n+12}}{2}\right],\\ &= (n-1)\cdot 3^{n-2}\\ &= (n-r)\cdot 3^{n-r-1}.\end{aligned} \tag{36}$$

Case 1.2. $r\geq 2$. Then, $Sp(L(S^2_{n,r}))=\{0,1^{n+r-4},n,3^{n-r-1},\lambda_1,\lambda_2,\lambda_3\}$, where $\lambda_1\lambda_2\lambda_3=2n-2r$ and $1/\lambda_1+1/\lambda_2+1/\lambda_3=3n/(2n-2r)$. From Lemma 1, we have

$$\begin{aligned}Kf\left(S^2_{n,r}\right) &= 2n\left[n+r-4+\frac{1}{n}+\frac{n-r-1}{3}+\frac{3n}{2n-2r}\right],\\ &= \frac{8n^3-(4r+17)n^2-\left(4r^2-26r-6\right)n-6r}{3(n-r)}.\end{aligned} \tag{37}$$

Then, from Lemma 2, we have

$$\begin{aligned}\tau\left(S^2_{n,r}\right) &= \frac{n\cdot 3^{n-r-1}\cdot\lambda_1\cdot\lambda_2\cdot\lambda_3}{2n}=\frac{n\cdot 3^{n-r-1}\cdot(2n-2r)}{2n}\\ &= (n-r)\cdot 3^{n-r-1}.\end{aligned} \tag{38}$$

Case 2. Edge $11'\in(E^2_{n,r})$. Then, $Sp(L(S^2_{n,r}))=\{0,1^{n+r-3},n,3^{n-r-2},\lambda_1,\lambda_2,\lambda_3\}$, where $\lambda_1\lambda_2\lambda_3=2n-2r+4$ and $1/\lambda_1+1/\lambda_2+1/\lambda_3=(3n+8)/(2n-2r+4)$. From Lemma 1, we have

$$\begin{aligned}Kf\left(S^2_{n,r}\right) &= 2n\left[n+r-3+\frac{1}{n}+\frac{n-r-2}{3}+\frac{3n+8}{2n-2r+4}\right],\\ &= \frac{8n^3-(4r-3)n^2-\left(4r^2-30r+14\right)n+12-6r}{3(n-r+2)}.\end{aligned} \tag{39}$$

Then, from Lemma 2, we have

$$\tau\left(S^2_{n,r}\right)=\frac{n\cdot 3^{n-r-2}\cdot\lambda_1\cdot\lambda_2\cdot\lambda_3}{2n}=\frac{n\cdot 3^{n-r-2}\cdot(2n-2r+4)}{2n}=(n-r+2)\cdot 3^{n-r-2}. \tag{40}$$

Finally, it is straightforward to have $W(S^2_{n,r})=W(S^2_n)+r=5n^2-8n+r+4$. Hence, in both cases, it holds that

$$\lim_{n\longrightarrow+\infty}\frac{Kf\left(S^2_{n,r}\right)}{W\left(S^2_{n,r}\right)}=\frac{8}{15}. \tag{41}$$

□

Data Availability

The data used to support this study are included within the article.

Disclosure

This study is also presented in arXiv (https://arxiv.org/abs/2007.10674, cited as [41]).

Conflicts of Interest

The authors declare that they have no conflicts of interest.

Authors' Contributions

Jia-Bao Liu conceptualized the study, developed methodology, and wrote original draft. Xin-Bei Peng conceptualized the study and wrote original draft. Jiao-Jiao Gu collected resources. Wenshui Lin visualized, investigated, and conceptualized the study and collected resources.

Acknowledgments

This work was supported by the National Natural Science Foundation of China (11 771 362), Anhui Provincial Natural Science Foundation (2008085J01), and the Natural Science Fund of Education Department of Anhui Province (KJ2020A0478).

References

[1] H. Wiener, "Structural determination of paraffin boiling points," *Journal of the American Chemical Society*, vol. 69, no. 1, pp. 17–20, 1947.

[2] I. Gutman, "Selected properties of the Schultz molecular topological index," *Journal of Chemical Information and Computer Sciences*, vol. 34, no. 5, pp. 1087–1089, 1994.

[3] A. A. Dobrymin, R. Entriger, and I. Gutman, "Wiener index of trees: theory and applications," *Acta Applicandae Mathematica*, vol. 66, pp. 211–249, 2001.

[4] A. A. Dobrynin, I. Gutman, S. Klavžar, and P. Žigert, "Wiener index of hexagonal systems," *Acta Applicandae Mathematica*, vol. 72, no. 3, pp. 247–294, 2002.

[5] L. Feng, "The Gutman index of unicyclic graphs," *Discrete Mathematics, Algorithms and Applications*, vol. 04, no. 03, Article ID 1250031, 2012.
[6] J. P. Mazorodze, S. Mukwembi, and T. Vetrík, "On the Gutman index and minimum degree," *Discrete Applied Mathematics*, vol. 173, pp. 77–82, 2014.
[7] P. Paulraja and V. Sheeba Agnes, "Gutman index of product graphs," *Discrete Mathematics, Algorithms and Applications*, vol. 06, no. 04, Article ID 1450058, 2014.
[8] S. Chen, "Cacti with the smallest, second smallest, and third smallest Gutman index," *Journal of Combinatorial Optimization*, vol. 31, no. 1, pp. 327–332, 2016.
[9] S. Kavithaa and V. Kaladevi, "Gutman index and detour Gutman index of pseudo-regular graphs," *Journal of Applied Mathematics*, vol. 2017, Article ID 4180650, 2017.
[10] M. Azari, "On the Gutman index of thorn graphs," *Kragujevac Journal of Science*, vol. 40, no. 40, pp. 33–48, 2018.
[11] D. J. Klein and M. Randić, "Resistance distance," *Journal of Mathematical Chemistry*, vol. 12, no. 1, pp. 81–95, 1993.
[12] H.-Y. Zhu, D. J. Klein, and I. Lukovits, "Extensions of the wiener number," *Journal of Chemical Information and Computer Sciences*, vol. 36, no. 3, pp. 420–428, 1996.
[13] I. Gutman and B. Mohar, "The quasi-Wiener and the Kirchhoff indices coincide," *Journal of Chemical Information and Computer Sciences*, vol. 36, no. 5, pp. 982–985, 1996.
[14] H. Chen and F. Zhang, "Resistance distance and the normalized Laplacian spectrum," *Discrete Applied Mathematics*, vol. 155, no. 5, pp. 654–661, 2007.
[15] D. J. Klein, I. Lukovits, and I. Gutman, "On the definition of the hyper-wiener index for cycle-containing structures," *Journal of Chemical Information and Computer Sciences*, vol. 35, no. 1, pp. 50–52, 1995.
[16] H. Zhang and Y. Yang, "Resistance distance and Kirchhoff index in circulant graphs," *International Journal of Quantum Chemistry*, vol. 107, no. 2, pp. 330–339, 2007.
[17] H. Zhang, Y. Yang, and C. Li, "Kirchhoff index of composite graphs," *Discrete Applied Mathematics*, vol. 157, no. 13, pp. 2918–2927, 2009.
[18] R. B. Bapat, M. Karimi, and J.-B. Liu, "Kirchhoff index and degree Kirchhoff index of complete multipartite graphs," *Discrete Applied Mathematics*, vol. 232, pp. 41–49, 2017.
[19] J. Huang, S. Li, and X. Li, "The normalized Laplacian, degree-Kirchhoff index and spanning trees of the linear polyomino chains," *Applied Mathematics and Computation*, vol. 289, pp. 324–334, 2016.
[20] Y. Pan, C. Liu, and J. Li, "Kirchhoff indices and numbers of spanning trees of molecular graphs derived from linear crossed polyomino chain," *Polycyclic Aromatic Compounds*, vol. 42, no. 1, pp. 218–225, 2020.
[21] C. He, S. Li, W. Luo, and L. Sun, "Calculating the normalized Laplacian spectrum and the number of spanning trees of linear pentagonal chains," *Journal of Computational and Applied Mathematics*, vol. 344, pp. 381–393, 2018.
[22] Y. Yang, "Computing the Kirchhoff index of linear phenylenes," *Journal of Combinatorial Mathematics and Combinatorial Computing*, vol. 81, pp. 199–208, 2012.
[23] Y. Peng and S. Li, "On the Kirchhoff index and the number of spanning trees of linear phenylenes," *MATCH Commun. Math. Comput. Chem*, vol. 77, pp. 765–780, 2017.
[24] L. Ye, "On the Kirchhoff index of cyclic phenylenes," *J. Math. Study*, vol. 45, pp. 233–240, 2012.
[25] X. Geng, P. Wang, L. Lei, and S. Wang, "On the Kirchhoff indices and the number of spanning trees of Möbius phenylenes chain and cylinder phenylenes chain," *Polycyclic Aromatic Compounds*, vol. 41, no. 8, pp. 1681–1693, 2019.
[26] X. Ma and H. Bian, "The normalized Laplacians, degree-Kirchhoff index and the spanning trees of cylinder phenylene chain," *Polycyclic Aromatic Compounds*, vol. 41, no. 6, pp. 1159–1179, 2019.
[27] S. Li, W. Wei, and S. Yu, "On normalized Laplacians, multiplicative degree-Kirchhoff indices, and spanning trees of the linear [n]phenylenes and their dicyclobutadieno derivatives," *International Journal of Quantum Chemistry*, vol. 119, no. 8, Article ID e25863, 2019.
[28] C. Liu, Y. Pan, and J. Li, "On the Laplacian spectrum and Kirchhoff index of generalized phenylenes," *Polycyclic Aromatic Compounds*, vol. 41, no. 9, pp. 1892–1901, 2019.
[29] Z. Zhu and J.-B. Liu, "The normalized Laplacian, degree-Kirchhoff index and the spanning tree numbers of generalized phenylenes," *Discrete Applied Mathematics*, vol. 254, pp. 256–267, 2019.
[30] Y. Yang and H. Zhang, "Kirchhoff index of linear hexagonal chains," *International Journal of Quantum Chemistry*, vol. 108, no. 3, pp. 503–512, 2008.
[31] J. Huang, S. Li, and L. Sun, "The normalized Laplacians, degree-Kirchhoff index and the spanning trees of linear hexagonal chains," *Discrete Applied Mathematics*, vol. 207, pp. 67–79, 2016.
[32] Y. Pan and J. Li, "Kirchhoff index, multiplicative degree-Kirchhoff index and spanning trees of the linear crossed hexagonal chains," *International Journal of Quantum Chemistry*, vol. 118, no. 24, Article ID e25787, 2018.
[33] X. Ma and H. Bian, "The normalized Laplacians, degree-Kirchhoff index and the spanning trees of hexagonal Möbius graphs," *Applied Mathematics and Computation*, vol. 355, pp. 33–46, 2019.
[34] A. Carmona, A. M. Encinas, and M. Mitjana, "Kirchhoff index of periodic linear chains," *Journal of Mathematical Chemistry*, vol. 53, no. 5, pp. 1195–1206, 2015.
[35] Q. Zhu, "Kirchhoff index, degree-Kirchhoff index and spanning trees of linear octagonal chains," *The Australasian Journal of Combinatorics*, vol. 153, pp. 69–87, 2020.
[36] J. B. Liu, J. Zhao, and Z. Zhu, "On the number of spanning trees and normalized Laplacian of linear octagonal-quadrilateral networks," *International Journal of Quantum Chemistry*, vol. 119, Article ID e25971, 2019.
[37] J. Zhao, J.-B. Liu, and S. Hayat, "Resistance distance-based graph invariants and the number of spanning trees of linear crossed octagonal graphs," *Journal of Applied Mathematics and Computing*, vol. 63, no. 1-2, pp. 1–27, 2020.
[38] Z. Li, Z. Xie, J. Li, and Y. Pan, "Resistance distance-based graph invariants and spanning trees of graphs derived from the strong prism of a star," *Applied Mathematics and Computation*, vol. 382, Article ID 125335, 2020.
[39] J. Huang and S. Li, "On the normalised laplacian spectrum, degree-Kirchhoff index and spanning trees of graphs," *Bulletin of the Australian Mathematical Society*, vol. 91, no. 3, pp. 353–367, 2015.
[40] F. R. K. Chung, *Spectral Graph Theory*, American Mathematical Society Providence, RI, USA, 1997.
[41] J. B. Liu, X. B. Peng, J. J. Gu, and W. Lin, *The (Multiplicative degree-)Kirchhoff Index of Graphs Derived from the Cartesian Product of S_n and K_2*, 2020, https://arxiv.org/abs/2007.10674.

Hindawi
Journal of Mathematics
Volume 2022, Article ID 7455701, 8 pages
https://doi.org/10.1155/2022/7455701

Research Article

Extremal Trees for the Exponential of Forgotten Topological Index

Akbar Jahanbani ,[1] Murat Cancan ,[2] and Ruhollah Motamedi[1]

[1]*Department of Mathematics, Azarbaijan Shahid Madani University, Tabriz, Iran*
[2]*Faculty of Education, Van Yuzuncu Yil University, Van, Turkey*

Correspondence should be addressed to Akbar Jahanbani; akbar.jahanbani92@gmail.com

Received 16 September 2021; Revised 25 December 2021; Accepted 25 January 2022; Published 12 February 2022

Academic Editor: M. T. Rahim

Copyright © 2022 Akbar Jahanbani et al. This is an open access article distributed under the Creative Commons Attribution License, which permits unrestricted use, distribution, and reproduction in any medium, provided the original work is properly cited.

Let F be the forgotten topological index of a graph G. The exponential of the forgotten topological index is defined as $e^F(G) = \sum_{(x,y)\in S} t_{x,y}(G) e^{(x^2+y^2)}$, where $t_{x,y}(G)$ is the number of edges joining vertices of degree x and y. Let $\mathbf{T}_n$ be the set of trees with n vertices; then, in this paper, we will show that the path P_n has the minimum value for e^F over $\mathbf{T}_n$.

1. Introduction

In this paper, let $V = V(G)$ and $E(G)$ be the vertex set and edge set, respectively. Let $d_v = d_G(v)$ be the degree of a vertex v in graph G. A vertex of degree one is a pendant vertex or a leaf. A branching vertex v of a tree T is a vertex of degree $d_v \geq 3$.

Let $P = w_0 w_1, \ldots, w_{q-1} w_q$ be the path graph with length of $r(P) = q$; if $d_T(w_0) \geq 3, d_T(w_1) = \ldots = d_T(w_{q-1}) = 2$ and $d_T(w_q) = 1$, then we called P is a pendant path.

Recently, topological indices have been considered by many researchers due to their many applications in various sciences. The forgotten topological index is defined in [1] as follows:

$$F(G) = \sum_{uv\in E(G)} d_u^2 + d_v^2. \tag{1}$$

For applications of the forgotten topological index, see [2–4].

Before starting a new definition, we consider the set $S = \{(x, y) \in N \times N: 1 \leq x \leq y \leq n-1\}$, and let $t_{x,y}(G)$ be the number of edges joining vertices of degree x and y in a graph G. Therefore, the new definition will be as follows:

$$F = F(G) = \sum_{(x,y)\in S} t_{x,y}(G)\left(x^2 + y^2\right). \tag{2}$$

The exponential of the forgotten topological index F, denoted by e^F, is defined as

$$e^F = e^F(G) = \sum_{(x,y)\in S} t_{x,y}(G) e^{\left(x^2+y^2\right)}. \tag{3}$$

Recently, the exponential topological indices have attracted the attention of many researchers. In [5], the exponential Randić index is characterized. In [6], the authors have characterized the exponential atom bond connectivity and the exponential augmented Zagreb index. In [7], the problem maximal value of trees for the exponential second Zagreb index is solved. Then, in this paper, we solve the problem with finding the minimal value of e^F among trees.

2. Trees with Minimum Exponential of the Forgotten Topological Index

In this section, we will show that the path P_n has the minimal value of the exponential forgotten topological index among all trees.

Lemma 1. *Let T and T_1 be the trees in Figure 1 and A be a subtree of T. If $s \geq 3$, then $e^F(T) > e^F(T_1)$.*

Proof. By setting $k = d_T(u)$, hence, we can write

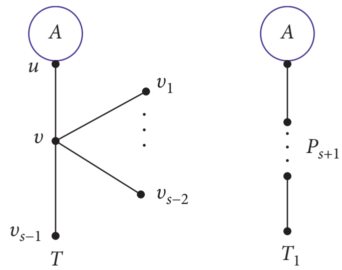

Figure 1: The trees T and T_1.

$$\begin{aligned} e^F(T)-e^F(T_1) &= \left(e^{s^2+k^2}+(s-1)e^{1+s^2}\right) \\ &\quad -\left(e^{4+k^2}+(s-2)e^8+e^5\right) \\ &= \left(e^{s^2+k^2}-e^{4+k^2}\right)+(s-2) \\ &\quad \left(e^{1+s^2}-e^8\right)+\left(e^{1+s^2}-e^5\right) \\ &\geq \left(e^{9+k^2}-e^{4+k^2}\right)+\left(e^{10}-e^8\right)+\left(e^{10}-e^5\right) \\ &> \left(e^{9+k^2}-e^{4+k^2}\right)>0. \end{aligned} \tag{4}$$

□

Lemma 2. *Let T be a tree with minimum value of e^F in $\mathbf{T}_n$ and let u be a pendant vertex T, $v \in T$. If $uv \in E(T)$, then $d_T(v)=2$.*

Proof. Suppose $d_T(v)=g$ and P be the largest path of T and contains v. Let t be an end vertex of P and o a vertex in P, where $ot \in E(T)$; hence, by applying Lemma 1, we have $d_T(o)=2$.

We continue the proof with the following two cases. □

Case 1. If $d_T(v)=g\geq 4$.

Assuming that T_1 be the tree in Figure 2 and $A_v=\sum_{i=1}^{g-1}e^{g^2+y_i^2}$, where $y_1,\ldots,y_{g-1}$ are the degrees of the adjacent vertices to v different from u. Hence, we can write

$$\begin{aligned} e^F(T)-e^F(T_1) &= A_v+e^{1+g^2}+e^5-\sum_{i=1}^{g-1}e^{(g-1)^2+y_i^2}-e^8-e^5 \\ &= \left(A_v-\sum_{i=1}^{g-1}e^{(g-1)^2+y_i^2}\right)+\left(e^{1+g^2}-e^8\right) \\ &\geq \left(A_v-\sum_{i=1}^{g-1}e^{(g-1)^2+y_i^2}\right)+\left(e^{17}-e^8\right) \\ &> \left(A_v-\sum_{i=1}^{g-1}e^{(g-1)^2+y_i^2}\right)>0. \end{aligned} \tag{5}$$

This contradicts the minimality of T.

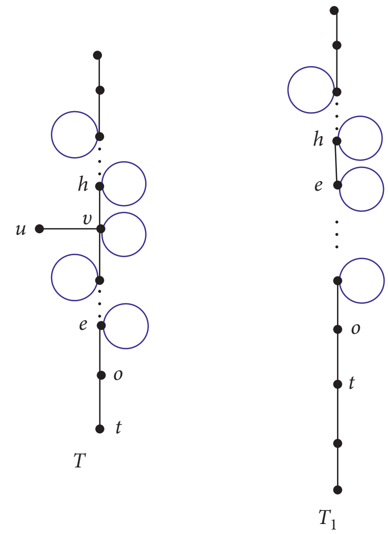

Figure 2: The trees T and T_1.

Case 2. If $d_T(v)=3$.

Suppose $h,e\in V(T)$ and $hv,ev\in E(T)$, where $h,e\neq u$, $d_T(h)=a$, and $d_T(e)=b$. By applying Lemma 1, we get $a\geq 2$ and $b\geq 2$. Let T_2 be the tree described in Figure 3. Therefore, we can write

$$\begin{aligned} e^F(T)-e^F(T_2) &= e^{9+a^2}+e^{9+b^2}+e^{10}-e^{a^2+b^2}-2e^8 \\ &= e^{9+a^2}+e^{9+b^2}-e^{a^2+b^2}+e^{10}-2e^8. \end{aligned} \tag{6}$$

Here, we show

$$f(a,b)=e^{9+a^2}+e^{9+b^2}+e^{10}>e^{a^2+b^2}+2e^8. \tag{7}$$

Since

$$f(a,2)=e^{9+a^2}+e^{13}+e^{10}>e^{a^2+4}+2e^8 \tag{8}$$

and

$$f(a,3)=e^{9+a^2}+e^{18}+e^{10}>e^{a^2+9}+2e^8, \tag{9}$$

the above inequality holds for $a\geq 2$. Therefore, for $a,b\geq 2$, we have $f(a,b)>0$. Hence, we get $e^F(T)>e^F(T_2)$. That is a contradiction; hence, we get $d_T(v)=2$.

Let v be a branching vertex of degree y of a tree T; hence, T can be viewed as the coalescence of y subtrees of T at the vertex v. We call $T_1,\ldots,T_y$ are the y branches of T at v (see Figure 4).

Definition 1 (see [5]). A branching vertex x of tree T is an outer branching vertex of T if all branches of T at x except for possibly one are paths.

Lemma 3 (see [5]). *A tree $T\in\mathbf{T}_n$ has no outer branching vertex if and only if $T\cong P_n$.*

Lemma 4. *Let $T,T_1\in\mathbf{T}_n$ be the trees in Figure 5 and R be a subtree of T, $z\geq 3$ and $x=d_T(u)\geq 2$. Then, $e^F(T)>e^F(T_1)$.*

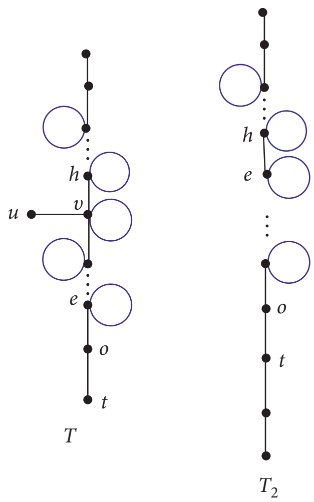

Figure 3: The trees T and T_2.

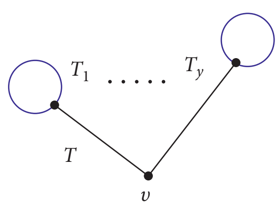

Figure 4: Branches of the tree T at v.

Proof. By direct calculation, it is not difficult to see $3 \le z \le 8$. Here, we let $z \ge 9$; therefore, we have

$$\begin{aligned} e^F(T) - e^F(T_1) &= e^{(z+1)^2+4} + (z-1)\left(e^{(z+1)^2+4} - e^{z^2+4}\right) \\ &\quad + \left(e^{(z+1)^2+x^2} - e^{z^2+x^2}\right) + \left(e^5 - 2e^8\right) \\ &> e^{(z+1)^2+4} + \left(e^5 - 2e^8\right) \ge e^{104} + \left(e^5 - 2e^8\right) > 0. \end{aligned} \tag{10}$$

□

Lemma 5. *Let $T, T_1 \in \mathbf{T}_n$ be the trees in Figure 6 and $t \ge 3$. Then, $e^F(T) > e^F(T_1)$, where $s(P_u) = -2 + \sum_{i=1}^{t} s(P_i)$.*

Proof. We describe the graph in Figure 7; let P_t be the path of length $s(P_t) = -2t + 2 + \sum_{i=1}^{t} s(P_i)$. It is not difficult to see $e^F(T) = e^F(T_3)$. Then, by repeated of Lemma 4, we get $e^F(T) > e^F(T_1)$. □

Corollary 1. *Let $T \in \mathbf{T}_n$ be a tree with a unique outer branching vertex and every pendant path has length at least 2. Then, $e^F(T) > e^F(P_n)$.*

Proof. If T has a unique outer branching vertex, hence, T has the form trees in Figure 6. Let M be the tree in Figure 8. If

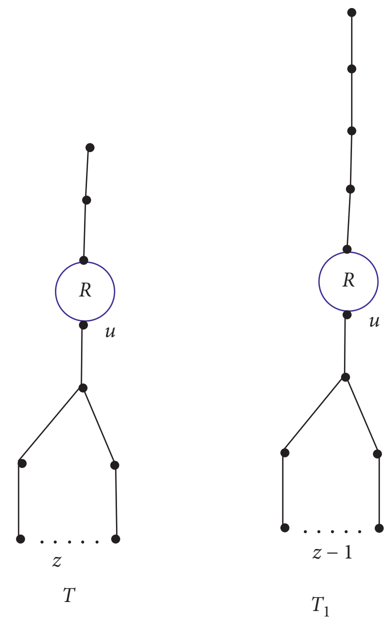

Figure 5: The trees T and T_1.

$s = 2$, then $e^F(T) = e^F(M)$. If $s \ge 3$, then by using Lemma 5, we have $e^F(T) > e^F(M)$. Hence, we can write

$$\begin{aligned} e^F(T) - e^F(P_n) &= 3e^5 + 3e^{13} + (n-7)e^8 - 2e^5 - (n-3)e^8 \\ &= e^5 + 3e^{13} - 4e^8 > 0. \end{aligned} \tag{11}$$

□

Lemma 6. *Let $T, T_1 \in \mathbf{T}_n$ be the trees in Figure 9, such that $1 \le d_T(v) \le 3$; then, $e^F(T) > e^F(T_1)$.*

Proof. By setting $x = d_T(v)$, we can write

$$\begin{aligned} e^F(T) - e^F(T_1) &= 2e^5 + 2e^{13} + e^{9+x^2} - e^5 - 3e^8 - e^{4+x^2} \\ &= e^5 + 2e^{13} - 3e^8 + \left(e^{9+x^2} - e^{4+x^2}\right) \\ &> e^5 + 2e^{13} - 3e^8 > 0. \end{aligned} \tag{12}$$

□

Lemma 7. *Let $T \in \mathbf{T}_n$ be the tree in Figure 10, $s \ge 1$ and $z \ge 0$; then, T is not minimal in $\mathbf{T}_n$.*

Proof. Set $x = d_T(u) \ge 2$, and let T_1 be tree in Figure 11. Hence, we have $e^F(T) > e^F(T_1)$ if the following conditions are hold:

(1) $s \ge 1, z \ge 2$.

(2) $s \ge 4, z \ge 0$.

It is not difficult to see that our result holds for $s + z \le 11$. Therefore, we let $z + s \ge 12$. Then,

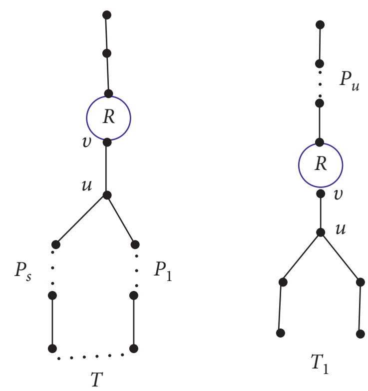

Figure 6: The trees T and T_1.

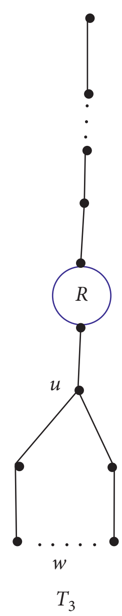

Figure 7: The tree T_3.

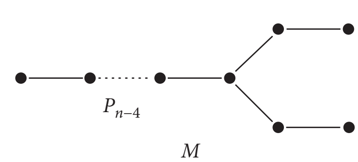

Figure 8: The tree M.

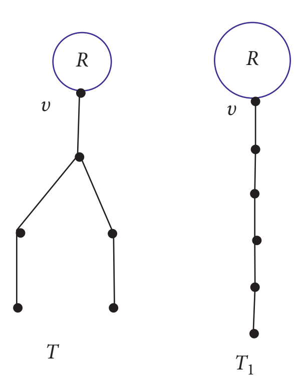

Figure 9: The trees T and T_1.

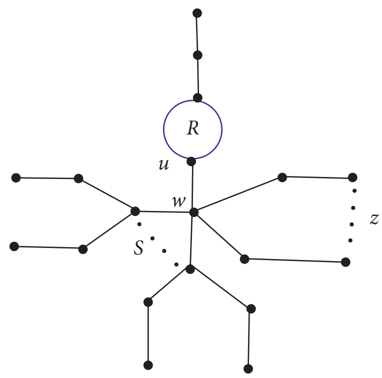

T

Figure 10: The tree T.

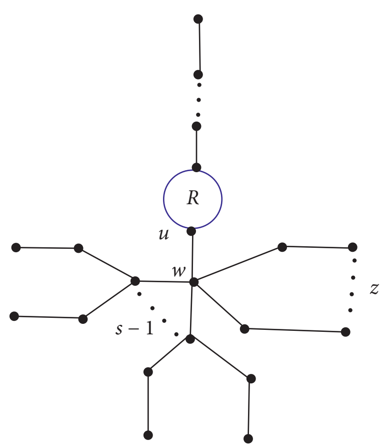

T_1

Figure 11: The tree T_1.

$$\begin{aligned} e^F(T) - e^F(T_1) &= \left(2e^5 + 2e^{13} - 5e^8\right) + (s-1) \\ &\quad \left(e^{9+(s+z+1)^2} - e^{9+(s+z)^2}\right) \\ &\quad + z\left(e^{4+(s+z+1)^2} - e^{4+(s+z)^2}\right) \\ &\quad + \left(e^{x^2+(s+z+1)^2} - e^{x^2+(s+z)^2}\right) + e^{9+(s+z+1)^2} \\ &> \left(2e^5 + 2e^{13} - 5e^8\right) > 0. \end{aligned} \tag{13}$$

To continue the proof, we must consider the following conditions:

(3) $s = 1$ and $z = 0$.

(4) $s = 1$ and $z = 1$.

(5) $s = 2$ and $z = 0$.

(6) $s = 3$ and $z = 1$.

(7) $s = 2$ and $z = 1$.

(8) $s = 3$ and $z = 0$.

Note that, in (3), (4), and (5),, we have $2 \leq d_T(w) \leq 3$; therefore, by Lemma 6, we can obtain trees with the minimum value of e^F.

Here, if (6) holds, then we consider graph T_2 in Figure 12. Hence, we can write

$$\begin{aligned} e^F(T) - e^F(T_2) &= \left(e^5 - 2e^8\right) + 3\left(e^{34} - e^{25}\right) + \left(e^{29} - e^{20}\right) \\ &\quad + \left(e^{x^2+25} - e^{x^2+16}\right) + e^{20} \\ &> \left(e^5 - 2e^8\right) + 3\left(e^{34} - e^{25}\right) + \left(e^{29} - e^{20}\right) \\ &\quad + e^{20} > \left(e^5 - 2e^8\right) + e^{20} > 0. \end{aligned} \tag{14}$$

If (7) holds, then we consider graph B in Figure 13. So, we have

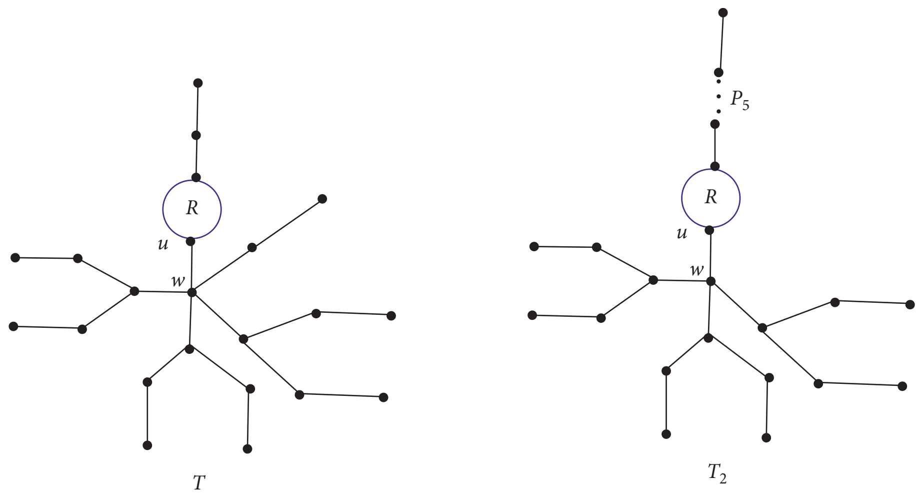

Figure 12: The trees T and T_2.

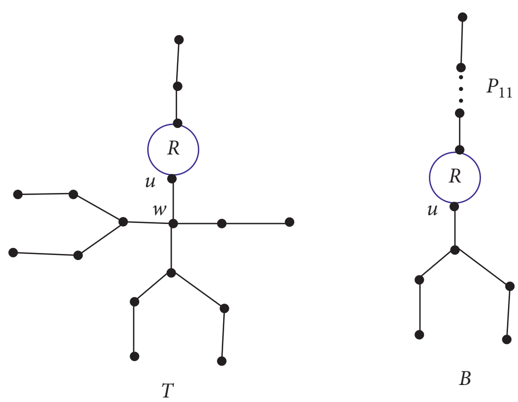

Figure 13: The trees T and B.

$$\begin{aligned} e^F(T) - e^F(B) &= 6e^5 + 4e^{13} + 2e^{25} + e^{20} + e^{x^2+16} - 3e^5 \\ &\quad - 2e^{13} - 8e^8 - e^{x^2+9} \\ &= \left(e^{x^2+16} - e^{x^2+9}\right) + 3e^5 + 2e^{13} + 2e^{25} \\ &\quad + e^{20} - 8e^8 > e^{20} - 8e^8 > 0. \end{aligned} \tag{15}$$

Finally, if (8) holds, then we consider graph C in Figure 14. Hence, we can write

$$\begin{aligned} e^F(T) - e^F(C) &= 7e^5 + 6e^{13} + 3e^{25} + e^{x^2+16} - 3e^5 - 2e^{13} \\ &\quad - 11e^8 - e^{x^2+9} \\ &= \left(e^{x^2+16} - e^{x^2+9}\right) + 4e^5 + 4e^{13} + 3e^{25} \\ &\quad - 11e^8 > 4e^5 + 4e^{13} + 3e^{25} - 11e^8 > 0. \end{aligned} \tag{16}$$

Therefore, T is not minimal in $\mathbf{T}_n$. □

Theorem 1. *Let $T \in \mathbf{T}_n$ and $T \not\equiv P_n$; then, T is not minimal for e^F.*

Proof. By using Lemma 3, we know that T has an outer branching vertex u. Using Lemmas 2, 5, and 6, we let all pendant paths of T have length at least 2 and T has the form in Figure 15, such that $d_T(v) \geq 4$, and otherwise, T is not minimal. If u is the unique outer branching vertex of T, then the result obtained by Corollary 1. Otherwise, among all outer branching vertices of T, choose u as the farthest from u. From Lemma 5, we let T is the form in Figure 16, such that $d_T(v_1) \geq 4$. Note that u_1 is the farthest outer branching vertex from u; it is clear if T_i is not a path; then, w_i is an outer branching vertex of T, and by Lemma 5, we let T_i have the form in Figure 17. Therefore, we get $e^F(T) = e^F(E)$, where E is described in Figure 18 and $s + z = q + 1$. The result follows from Lemma 7. □

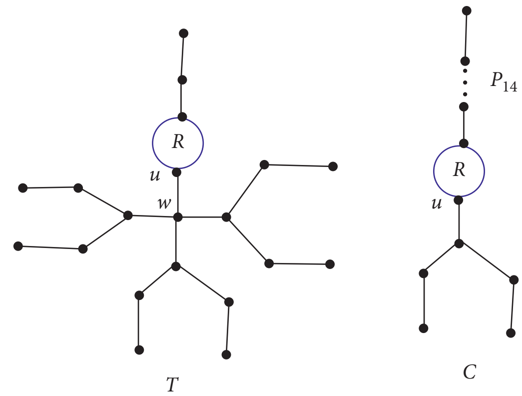

Figure 14: The trees T and C.

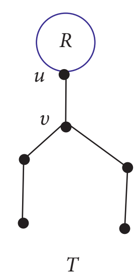

Figure 15: The tree T.

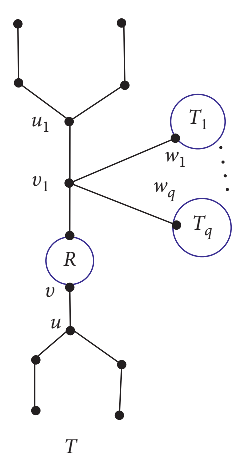

Figure 16: The tree T.

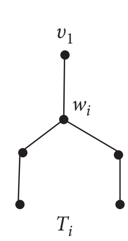

Figure 17: The tree T_i.

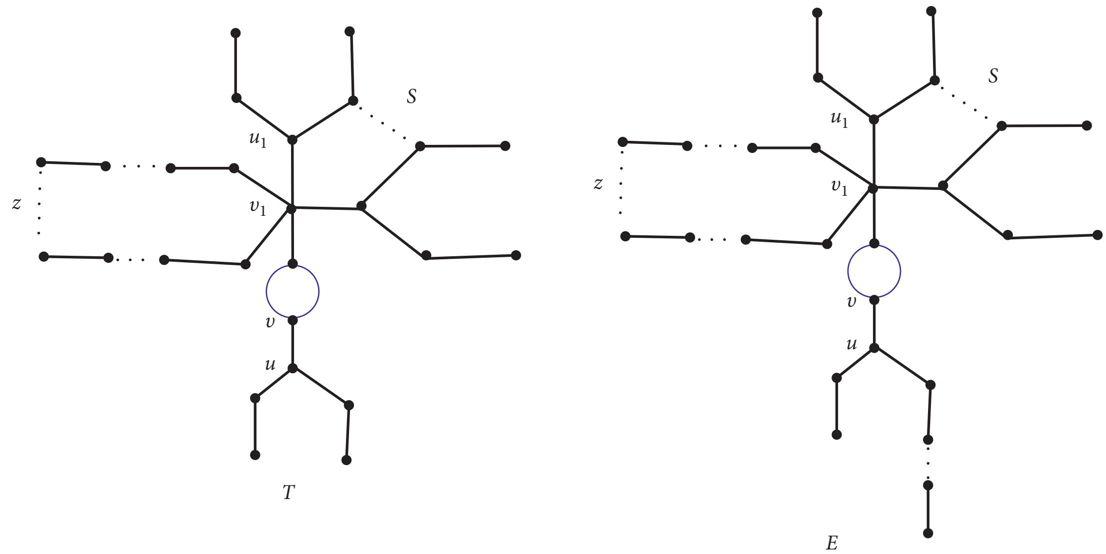

Figure 18: The tree T and E.

Data Availability

No data were used to support the findings of this study.

Conflicts of Interest

The authors declare that they have no conflicts of interest.

References

[1] B. Furtula and I. Gutman, "A forgotten topological index," *Journal of Mathematical Chemistry*, vol. 53, no. 4, pp. 1184–1190, 2015.

[2] I. Gutman and N. Trinajstić, "Graph theory and molecular orbitals: total φ-electron energy of alternant hydrocarbons," *Chemical Physics Letters*, vol. 17, no. 4, pp. 535–538, 1972.

[3] A. Jahanbani, "On the forgotten topological index of graphs, discrete mathematics," *Algorithms and Applications*, vol. 13, no. 5, Article ID 2150054, 2020.

[4] A. Jahanbani, "New bounds for degree sequence of graphs," *Computer Science Journal of Moldova*, vol. 80, pp. 188–203, 2019.

[5] R. Cruz, J. Monsalve, and J. Rada, "Trees with maximum exponential randić index," *Discrete Applied Mathematics*, vol. 283, no. 3, 2020.

[6] R. Cruz and J. Rada, "The path and the star as extremal values of vertex-degree-based topological indices among trees," *MATCH Communications in Mathematical and in Computer Chemistry*, vol. 82, pp. 715–732, 2019.

[7] M. Zeng and H. Dengy, "The maximal tree with respect to the exponential of the second zagreb index," 2020, https://arxiv.org/abs2006.08892v1.

Hindawi
Journal of Mathematics
Volume 2022, Article ID 2312206, 11 pages
https://doi.org/10.1155/2022/2312206

Research Article

A Novel Problem to Solve the Logically Labeling of Corona between Paths and Cycles

Ashraf ELrokh[1], **Mohammed M. Ali Al-Shamiri**[2,3] **and Atef Abd El-hay**[1]

[1]*Mathematics and Computer Science Department, Faculty of Science Menoufia University, Menoufia, Egypt*
[2]*Department of Mathematics, Faculty of Science and Arts, Muhayl Asser King Khalid University, Abha, Saudi Arabia*
[3]*Department of Mathematics and Computer, Faculty of Science, Ibb University, Ibb, Yemen*

Correspondence should be addressed to Ashraf ELrokh; ashraf.hefnawy68@yahoo.com

Received 25 October 2021; Accepted 17 January 2022; Published 10 February 2022

Academic Editor: M. T. Rahim

Copyright © 2022 Ashraf ELrokh et al. This is an open access article distributed under the Creative Commons Attribution License, which permits unrestricted use, distribution, and reproduction in any medium, provided the original work is properly cited.

In this study, we propose a new kind of graph labeling which we call logic labeling and investigate the logically labeling of the corona between paths P_n and cycles C_n, namely, $P_n \odot C_m$. A graph is said to be logical labeling if it has a $0-1$ labeling that satisfies certain properties. The corona $G_1 \odot G_2$ of two graphs G_1 (with n_1 vertices and m_1 edges) and G_2 (with n_2 vertices and m_2 edges) is defined as the graph formed by taking one copy of G_1 and n_1 copies of G_2 and then connecting the i^{th} vertex of G_1 with an edge to every vertex in the i^{th} copy of G_2.

1. Introduction

Graphs can be used to model a wide range of relationships and processes in physical, biological, social, and information systems. Graphs can also be used to show a wide range of real issues. The term "network" is frequently used to refer to a graph in which attributes are associated with nodes and edges, emphasising its relevance to real-world systems [1].

Graphs are used in computer science to illustrate communication networks, data administration, computational devices, and computation flow. A directed graph, for example, can represent a website's link structure, with the vertices representing web pages and the directed edges representing links from one page to another. Problems in social media, travel, biology, computer chip design, and a variety of other industries can all benefit from a similar approach. As a result, developing algorithms to manage graphs is a major topic in computer science [1, 2]. Graph rewrite systems are usually used to formalise and describe graph transformations. Graph databases, which are designed for transaction—safe, persistent storing and querying of graph—structured data, are a complement to graph transformation systems that focus on rule-based in-memory graph manipulation.

Labeling methods are used for a wide range of applications in different subjects including coding theory, computer science, and communication networks. Graph labeling is an assignment of positive integers on vertices or edges or both of them which fulfilled certain conditions. The concept of graph labeling was introduced by Rosa in 1967 [3].

The following three properties are shared by the majority of graph labeling problems:

(i) A set of numbers from which to select vertex labels

(ii) A rule that gives each edge a labeling

(iii) Some rules that these labels must meet

A Dynamic Survey of Graph Labeling by Gallian [4] is a complete survey of graph labeling. There are several contributions and various types of labeling [1, 3–15]. Graceful labeling and harmonious labeling are two of the major styles of labeling. Graceful labeling is one of the most well-known graph labeling approaches; it was independently developed by Rosa in 1966 [3] and Golomb in 1972 [5], whilst harmonious labeling was initially investigated by Graham and Sloane in 1980 [6]. Cahit proposed a third major style of labeling, cordial, in 1987 [14], which combines elements of the previous two. The cordiality of the corona between cycles C_n and paths P_n was investigated by Nada S. et al. [8]. This research focuses on graph labeling of this type. G is considered to be connected, finite, simple, and undirected throughout.

Definition 1. A binary vertex labeling of G is a mapping $f\colon V \longrightarrow \{0,1\}$ in which $f(u)$ is said to be the labeling of $u \in V$. For an edge $e = uv \in E$, where $u, v \in V$, the induced edge labeling $f^*\colon E \longrightarrow \{0,1\}$ is defined by the formula $f^*(vw) = (f(v) + f(w) + 1) \pmod 2$. Thus, for any edge e, $f^*(e) = 1$ if its two vertices have the same label and $f^*(e) = 0$ if they have different labels. Let us denote v_0 and v_1 be the numbers of vertices labeled by 0 and 1 in V, respectively, and let e_0 and e_1 be the corresponding numbers of edge in E labeled by 0 and 1, respectively.

Definition 2. If $|v_0 - v_1| \le 1$ and $|e_0 - e_1| \le 1$ hold, a binary vertex labeling f of G is said to be logical. A graph G is logical if it can be labeled logically. Gallian's survey [4] is a good starting point for further research on this topic.

Definition 3. The corona $G_1 \odot G_2$ of two graphs G_1 (with n_1 vertices and m_1 edges) and G_2 (with n_2 vertices and m_2 edges) is defined as the graph obtained by taking one copy of G_1 and n_1 copies of G_2 and then joining the i^{th} vertex of G_1 with an edge to every vertex in the i^{th} copy of G_2. According to the definition of the corona, $G_1 \odot G_2$ has $n_1 + n_1 n_2$ vertices and $m_1 + n_1 m_2 + n_1 n_2$ edges. It is clear that $G_1 \odot G_2$ is not often isomorphic to $G_2 \odot G_1$ [7, 9–12].

In this paper, we show that $P_n \odot C_m$ logical labeling if and only if $(n, m) \ne (1, 3 \pmod 4)$.

2. Terminology and Notation

P_n denotes a path having n vertices and $n-1$ edges, while C_n denotes a cycle with n vertices and n edges [9, 10]. Let M_r stand for the labeling $0101\cdots01$, zero-one repeated $r-$ times if r is even and $0101\cdots010$ if r is odd; for example, $M_6 = 010101$ and $M_5 = 01010$. The labeling $1010\cdots10$ is denoted by M_{2r}'. We sometimes change the labeling M_r or M_r' by inserting symbols at one end or the other (or both). L_{4r} denotes the labeling 0011 0011 … 0011 (repeated r-times) with $r \ge 1$ and L_{4r}' denotes the labeling 1100 1100 … 1100 (repeated r-times) with $r \ge 1$. S_{4r} represents the labeling 1001 1001 … 1001 (repeated r times) and $\overline{S}_{4r}$ represents the labeling 0110 0110… 0110 (repeated r times). In most situations, we change this by inserting symbols at one end or the other (or both), so $L_{4r}101$ represents the labeling 0011 0011 … 0011 101 (repeated r-times) when $r \ge 1$ and 101 when $r = 0$. Similarly, $1L_{4r}'$ represents the labeling 1 1100 1100 … 1100 (repeated r-times) for $r \ge 1$ and 1 when $r = 0$. Similarly, $0L_{4r}'1$ denotes 0 1100 1100 … 1100 1 when $r \ge 1$ and 01 when $r = 0$.

For the corona labeling [9], let $[L; M]$ indicate the special labeling L and M of $G \odot H$ where G is path and H is cycle. The following is an additional notation that we use. For a given labeling of the corona $G \odot H$, we choose v_i and e_i (for $i = 0, 1$) to be the numbers of labels that are i as before, we select x_i and a_i to be the amounting value for G, and we let y_i and b_i to be those for H. It is easy to verify that $v_0 = x_0 + x_0 y_0 + x_1 y_0'$, $v_1 = x_1 + x_0 y_1 + x_1 y_1'$, $e_0 = a_0 + x_0 b_0 + x_1 b_0' + x_0 y_1 + x_1 y_0'$, and $e_1 = a_1 + x_0 b_1 + x_1 b_1' + x_0 y_0 + x_1 y_1'$. Thus, $v_0 - v_1 = (x_0 - x_1) + x_0(y_0 - y_1) + x_1(y_0' - y_1')$ and $e_0 - e_1 = (a_0 - a_1) + x_0(b_0 - b_1) + x_1(b_0' - b_1') - x_0(y_0 - y_1) + x_1(y_0' - y_1')$. (1) When it comes to the proof, we only need to show that, for each specified combination of labeling, $|v_0 - v_1| \le 1$ and $|e_0 - e_1| \le 1$.

3. Results and Discussion

In this section, we show that $P_n \odot C_m$ is logical labeling if and only if $(n, m) \ne (1, 3 \pmod 4)$.

Lemma 1. *The corona $P_n \odot C_3$ is logical if and only if $n \ne 1$.*

Proof. Obviously, $P_1 \odot C_3$ isomorphic to the complete graph K_4. Since K_4 is not logical, $P_1 \odot C_3$ is not logical. Conversely, for $P_2 \odot C_3$, we choose the labeling [01: 010, 101]; hence, $v_0 - v_1 = 0$ and $e_0 - e_1 = 1$. So, $P_2 \odot C_3$ is logical, see Figure 1. For $P_3 \odot C_3$, we choose the labeling [000: 011, 111, 010]; hence, $v_0 - v_1 = 0$ and $e_0 - e_1 = 0$. So, $P_3 \odot C_3$ is logical, see Figure 2. Now, we need to study the following four cases for $n \ge 4$.

(i) Case (1) ($n \equiv 0 \pmod 4$): suppose that $n = 4r$, $r \ge 1$. We select the labeling [L_{4r}: 010, 010, 101, 101, …, (r − times)] for $P_{4r} \odot C_3$. Therefore, $x_0 = x_1 = 2r$, $a_0 = 2r - 1$, $a_1 = 2r$, $y_0 = 2$, $y_1 = 1$, $y_0' = 1$, $y_1' = 2$, $b_0 = 2$, $b_0' = 2$, $b_1 = 1$, and $b_1' = 1$. Hence, $v_0 - v_1 = (x_0 - x_1) + x_0(y_0 - y_1) + x_1(y_0' - y_1') = 0$ and $e_0 - e_1 = (a_0 - a_1) + x_0 \ (b_0 - b_1) + x_1(b_0' - b_1') - x_0(y_0 - y_1) + x_1(y_0' - y_1') = -1$. As an example, Figure 3 illustrates $P_4 \odot C_3$. Thus, $P_{4r} \odot C_3$ is logical.

(ii) Case (2) ($n \equiv 1 \pmod 4$): suppose that $n = 4r + 1$, $r \ge 1$. We select the labeling [$L_{4r}1$: 010, 010, 101, 101, …, (r − times), 010] for $P_{4r+1} \odot C_3$. Therefore, $x_0 = 2r$, $x_1 = 2r + 1$, $a_0 = 2r - 1$, and $a_1 = 2r + 1$, and for the first $4r$-vertices, $y_0 = 2$, $y_1 = 1$, $y_0' = 1$, $y_1' = 2$, $b_0 = b_0' = 2$, and $b_1 = b_1' = 1$, and for the cycle c_3 which is connected to last vertex in P_{4r+1}, we have $z_0 = 2$, $z_1 = 1$, $c_0 = 2$, and $c_1 = 1$, where z_i and c_i are the numbers of vertices and edges labeled by i in c_3 that is connected to the last vertex of P_{4r+1}. It is easy to verify that $v_0 = x_0 + x_0 y_0 + (x_1 - 1)y_0' + z_0 = 8r + 2$, $v_1 = x_1 + x_0 y_1 + (x_1 - 1)y_1' + z_1 = 8r + 2$, $e_0 = a_0 + x_0 b_0 + (x_1 - 1)b_0' + x_0 y_0 + (x_1 - 1)y_1' + c_0 + 1 = 14r + 3$, and $e_1 = a_1 + x_0 b_1 + (x_1 - 1)b_1' + x_0 y_1 + (x_1 - 1)y_0' + c_1 + 2 = 14r + 3$. It follows that $v_0 - v_1 = 0$ and $e_0 - e_1 = 0$. As an example, Figure 4 illustrates $P_5 \odot C_3$. Thus, $P_{4r+1} \odot C_3$ is logical.

(iii) Case (3) ($n \equiv 2 \pmod 4$): suppose that $n = 4r + 2$, $r \ge 1$. We choose the labeling [$L_{4r}10$: 010, 010, 101, 101, …, (r − times), 101, 010] for $P_{4r+2} \odot C_3$. Therefore, $x_0 = x_1 = 2r + 1$, $a_0 = 2r$, $a_1 = 2r + 1$, $y_0 = 2$, $y_1 = 1$, $y_0' = 1$, $y_1' = 2$, $b_0 = 2$,

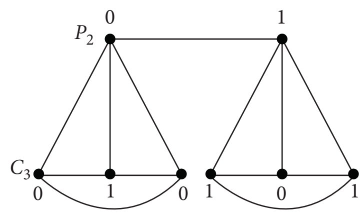

Figure 1: Logical labeling of $P_2 \odot C_3$.

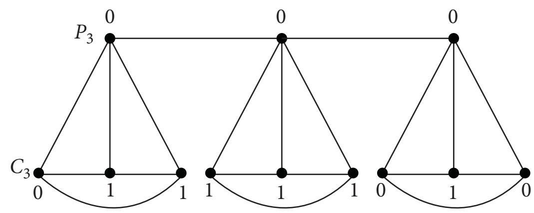

Figure 2: Logical labeling of $P_3 \odot C_3$.

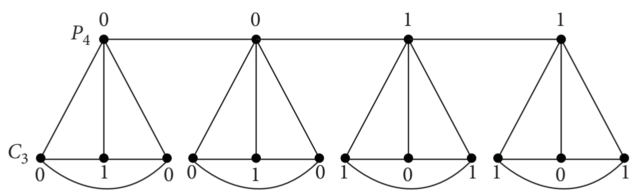

Figure 3: Logical labeling of $P_4 \odot C_3$.

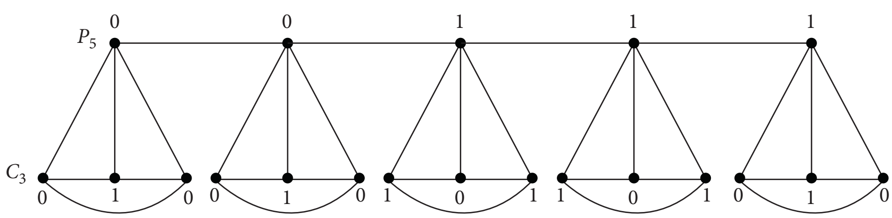

Figure 4: Logical labeling of $P_5 \odot C_3$.

$b_0' = 2$, $b_1 = 1$, and $b_1' = 1$. Hence, $v_0 - v_1 = 0$ and $e_0 - e_1 = -1$. As an example, Figure 5 illustrates $P_6 \odot C_3$. Thus, $P_{4r+2} \odot C_3$ is logical.

(iv) Case (4) ($n \equiv 3\,(\mathrm{mod}4)$): suppose that $n = 4r + 3$, $r \geq 1$. We select the labeling $[L_{4r}100\colon 010, 010, 101, 101, \ldots, (r-\text{times}), 101, 010, 101]$ for $P_{4r+3} \odot C_3$. Therefore, $x_0 = 2r + 2$, $x_1 = 2r + 1$, $a_0 = 2r + 2$, and $a_1 = 2r$, and for the first $4r$-vertices, $y_0 = 2$, $y_1 = 1$, $y_0' = 1$, $y_1' = 2$, $b_0 = b_0' = 1$, and $b_1 = b_1' = 2$, and for the cycle c_3 which is connected to last vertex of P_{4r+3}, we have $z_0 = 1$, $z_1 = 2$, $c_0 = 1$, and $c_1 = 2$, where z_i and c_i are the numbers of vertices and edges labeled by i in c_3 that is connected to the last vertex of P_{4r+3}. Similar to Case 2, we conclude that $v_0 - v_1 = 0$ and $e_0 - e_1 = 0$. As an example, Figure 6 illustrates $P_7 \odot C_3$. Hence, $P_{4r+3} \odot C_3$ is logical. Thus, the lemma is proved. □

Lemma 2. *If $m \equiv 0\,(\mathrm{mod}4)$, then the corona $P_n \odot C_m$ between paths P_n and cycles C_m is logical for all $n \geq 1$.*

Proof. Let $m = 4s$, where $s \geq 1$; then, we label the vertices of all n copies of C_{4s} as $B_0 = L_{4s}$, i.e., $y_0 = 2s$, $y_1 = 2s$, $b_0 = 2s$, and $b_1 = 2s$. Suppose that $n = 4r + i$, where $r \geq 1$ and $i = 0, 1, 2, 3$; then, for given values of i with $0 \leq i \leq 3$, we may use the labeling A_i for P_n as shown in Table 1. Using the formulas $v_0 - v_1 = (x_0 - x_1) + n(y_0 - y_1)$ and $e_0 - e_1 = (a_0 - a_1) + n(b_0 - b_1) + (x_1 - x_0)(y_0 - y_1)$ and Table 1, we can compute the values appeared in the last two columns of Table 2. Since these values are 0, −1, or 1, $P_{4r+i} \odot C_{4s}$ ($0 \leq i \leq 3$ and $r \geq 1$) is logical. As examples, Figure 7 illustrates $P_4 \odot C_4$, Figure 8 illustrates $P_9 \odot C_4$, Figure 9 illustrates $P_6 \odot C_4$, and Figure 10 illustrates $P_7 \odot C_4$. It is remaining to show that $P_n \odot C_{4s}$, $1 \leq n \leq 3$, is logical. We choose the labeling $[0\colon L_{4s}]$ for $P_1 \odot C_{4s}$. Figure 11 illustrates $P_1 \odot C_8$. So, $v_0 - v_1 = 1$ and $e_0 - e_1 = 0$, and hence, $P_1 \odot C_{4s}$

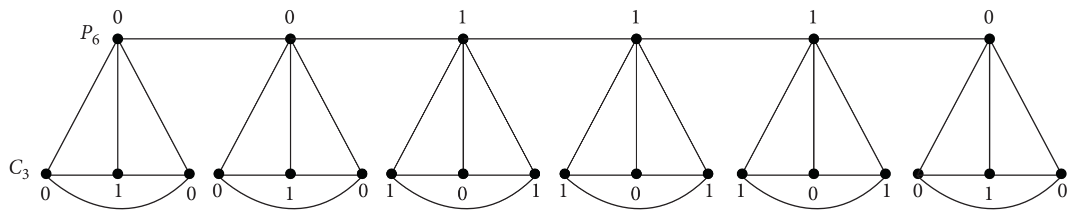

FIGURE 5: Logical labeling of $P_6 \odot C_3$.

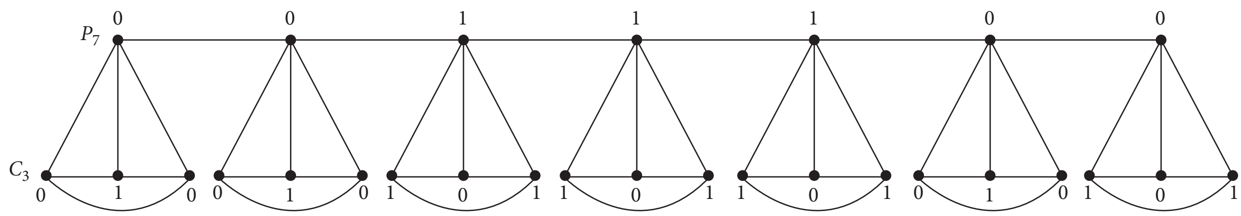

FIGURE 6: Logical labeling of $P_7 \odot C_3$.

TABLE 1: Labeling of P_n.

$n = 4r + i$, $i = 0, 1, 2, 3$	Labeling of P_n	x_0	x_1	a_0	a_1
$i = 0$	$A_0 = L_{4r}$	$2r$	$2r$	$2r - 1$	$2r$
$i = 1$	$A_1 = L_{4r}0$	$2r + 1$	$2r$	$2r$	$2r$
$i = 2$	$A_2 = L_{4r}01$	$2r + 1$	$2r + 1$	$2r + 1$	$2r$
$i = 3$	$A_3 = L_{4r}011$	$2r + 1$	$2r + 2$	$2r + 1$	$2r + 1$

TABLE 2: Combinations of labeling.

$n = 4r + i$, $i = 0, 1, 2, 3$	$m = 4s + j$, $j = 0$	P_n	C_m	$v_0 - v_1$	$e_0 - e_1$
$i = 0$	0	A_0	B_0	0	−1
$i = 1$	0	A_1	B_0	1	0
$i = 2$	0	A_2	B_0	0	1
$i = 3$	0	A_3	B_0	−1	0

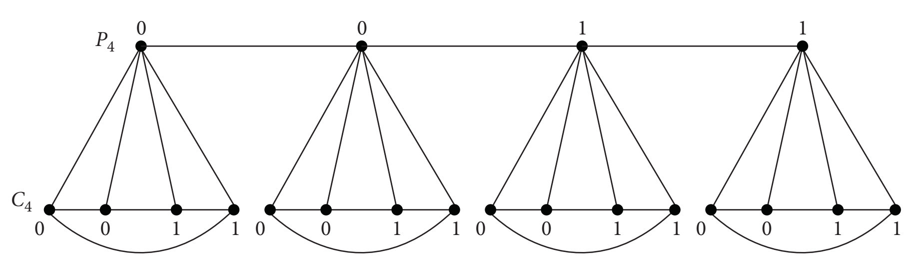

FIGURE 7: Logical labeling of $P_4 \odot C_4$.

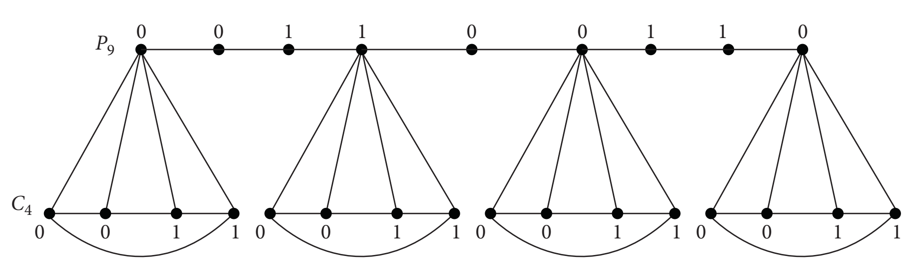

FIGURE 8: Logical labeling of $P_5 \odot C_4$.

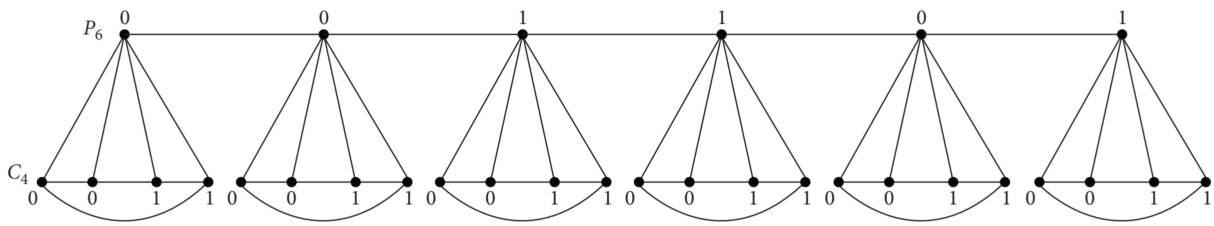

FIGURE 9: Logical labeling of $P_6 \odot C_4$.

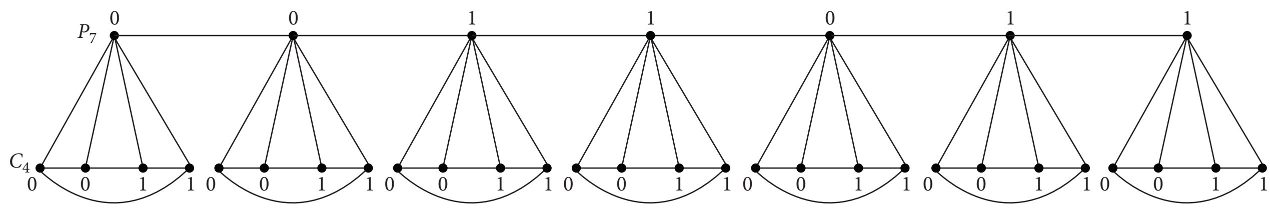

FIGURE 10: Logical labeling of $P_7 \odot C_4$.

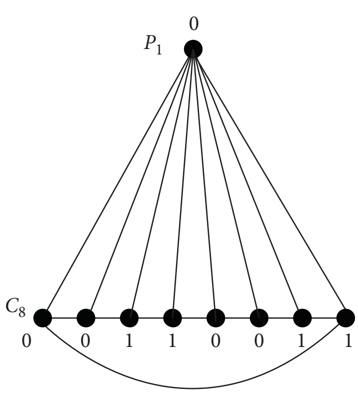

FIGURE 11: Logical labeling of $P_1 \odot C_8$.

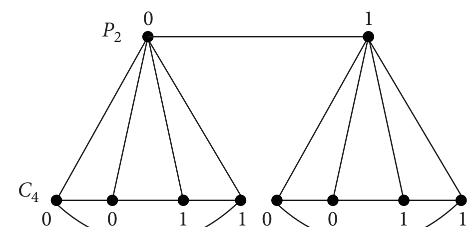

FIGURE 12: Logical labeling of $P_2 \odot C_4$.

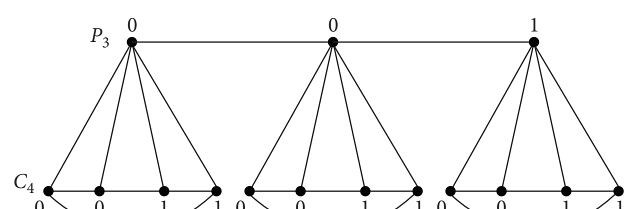

FIGURE 13: Logical labeling of $P_3 \odot C_4$.

is logical. We select the labeling [01: L_{4s}, L_{4s}] for $P_2 \odot C_{4s}$. As an example, Figure 12 illustrates $P_2 \odot C_4$. So, $v_0 - v_1 = 0$ and $e_0 - e_1 = 1$, and hence, $P_2 \odot C_{4s}$ is logical. Finally, we choose the labeling [001: L_{4s}, L_{4s}, L_{4s}] for $P_3 \odot C_{4s}$. As an example, Figure 13 illustrates $P_3 \odot C_4$. So, $v_0 - v_1 = 1$ and $e_0 - e_1 = 0$, and hence, $P_3 \odot C_{4s}$ is logical. Thus, the lemma is proved. □

Lemma 3. *If m is not congruent to* $0\,(\mathrm{mod}4)$*, then the corona S between paths P_n and cycles C_m is logical, for all $n \geq 4$ and $m \geq 4$.*

Proof. Let $n = 4r + i$ ($i = 0, 1, 2, 3$ and $r \geq 1$) and $m = 4s + j$ ($j = 1, 2, 3$ and $s \geq 1$); then, for a given value of i with $0 \leq i \leq 3$, we use the labeling A_i or A_i' for P_n, as shown in Table 3. For a given value of j with $1 \leq j \leq 3$, we used the labeling B_j or B_j' for all the n copies of C_m, where B_j is the labeling of all copies of C_m which are joined to the vertices of P_n labeled 0 in A_i or A_i' and B_j' is the labeling of all copies of C_m which are joined to the vertices of P_n labeled 1 in A_i or A_i' as given in Table 3. Figures 14–17 illustrate the examples $P_4 \odot C_5$, $P_5 \odot C_5$, $P_6 \odot C_5$, and $P_7 \odot C_5$, respectively. Using Table 3 and formulas $v_0 - v_1 = (x_0 - x_1) + x_0 (y_0 - y_1) + x_1 (y_0' - y_1')$ and $e_0 - e_1 = (a_0 - a_1) + x_0 (b_0 - b_1) + x_1 (b_0' - b_1') - x_0 (y_0 - y_1) + x_1 (y_0' - y_1')$. The numbers shown in the last two columns of Table 4 can be calculated. Because all of these numbers are either −1, 0, or 1, the lemma is proved. □

Lemma 4. *The corona $P_1 \odot C_m$ is logical for all $m \geq 3$ if and only if $m \neq 3\,(\mathrm{mod}4)$.*

Proof. If $m \equiv 3\,(\mathrm{mod}4)$, then it is easy to verify that every vertex of $P_1 \odot C_m$ has an odd degree; also, the sum of its size and order is congruent to $2\,(\mathrm{mod}4)$. Consequently, by [13], the corona $P_1 \odot C_3$ is not logical. Conversely, suppose that $m = 4s + j$, where $j = 0, 1, 2$, the following labelings are appreciated: [0: L_{4s}] for $P_1 \odot C_{4s}$, [0: $L_{4s}1$] for $P_1 \odot C_{4s+1}$, and [0: $L_{4s}11$] for $P_1 \odot C_{4s+2}$. These three cases are shown in Figures 18–20. As a result, the lemma is established. □

Table 3: Labeling of P_n and C_m.

$n = 4r + i$, $i = 0, 1, 2, 3$	Labeling of P_n	x_0	x_1	a_0	a_1
$i = 0$	$A_0 = L_{4r}$	$2r$	$2r$	$2r - 1$	$2r$
$i = 1$	$A_1 = L_{4r}0$	$2r + 1$	$2r$	$2r$	$2r$
	$A_1' = 0L_{4r}$	$2r + 1$	$2r$	$2r - 1$	$2r + 1$
$i = 2$	$A_2 = L_{4r}01$	$2r + 1$	$2r + 1$	$2r + 1$	$2r$
$i = 3$	$A_3 = L_{4r}001$	$2r + 2$	$2r + 1$	$2r + 1$	$2r + 1$
	$A_3' = L_{4r}100$	$2r + 2$	$2r + 1$	$2r$	$2r + 2$
$m = 4s + j$, $j = 1, 2, 3$	Labeling of C_m	y_0	y_1	b_0	b_1
$j = 1$	$B_1 = L_{4s}1$	$2s$	$2s + 1$	$2s$	$2s + 1$
$j = 2$	$B_2 = L_{4s}01$	$2s + 1$	$2s + 1$	$2s + 2$	$2s$
$j = 3$	$B_3 = L_{4s}011$	$2s + 1$	$2s + 2$	$2s + 2$	$2s + 1$
$m = 4s + j$, $j = 1, 2, 3$	Labeling of C_m	y_0'	y_1'	b_0'	b_1'
$j = 1$	$B_1' = L_{4s}0$	$2s + 1$	$2s$	$2s$	$2s + 1$
$j = 2$	$B_2' = L_{4s}10$	$2s + 1$	$2s + 1$	$2s$	$2s + 2$
$j = 3$	$B_3' = L_{4s}100$	$2s + 2$	$2s + 1$	$2s$	$2s + 3$

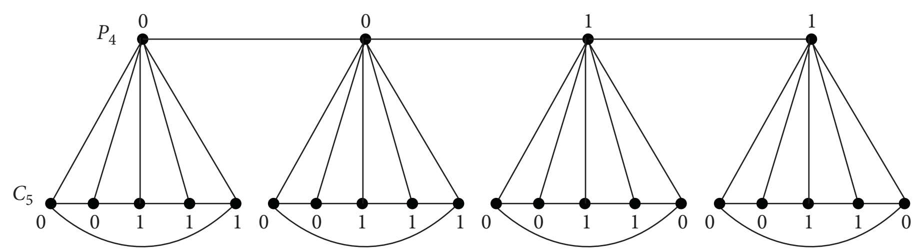

Figure 14: Logical labeling of $P_4 \odot C_5$.

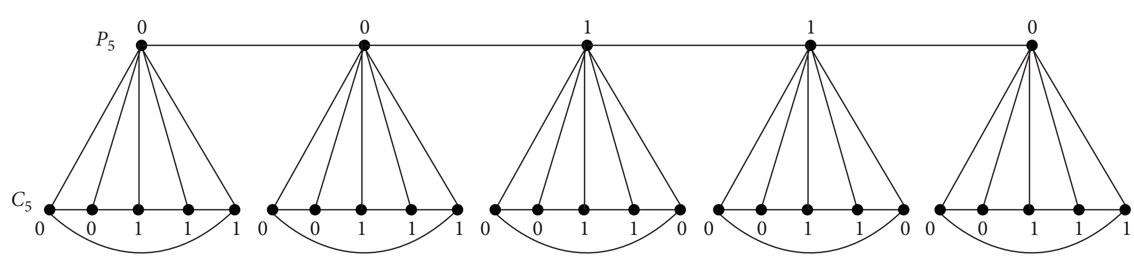

Figure 15: Logical labeling of $P_5 \odot C_5$.

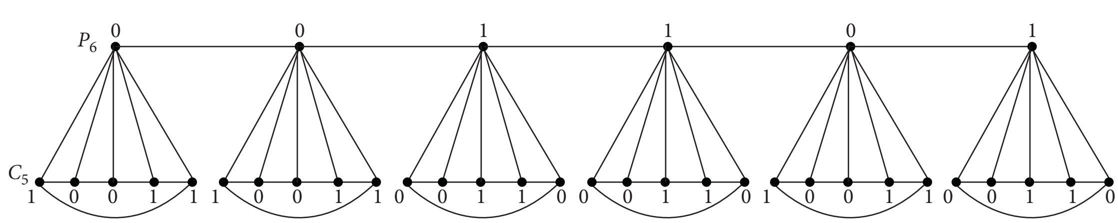

Figure 16: Logical labeling of $P_6 \odot C_5$.

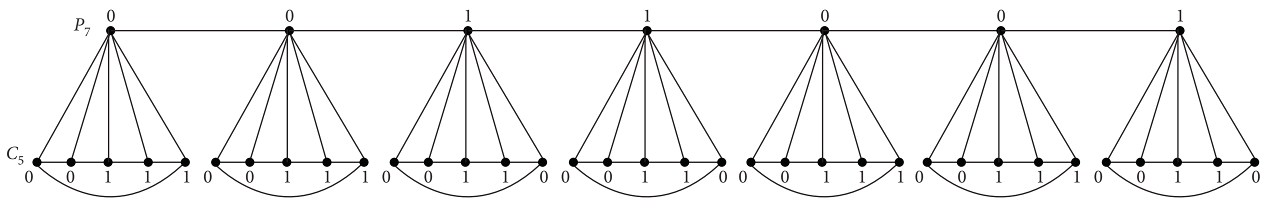

Figure 17: Logical labeling of $P_7 \odot C_5$.

Table 4: Combinations of labeling.

$n = 4r + i$, $i = 0, 1, 2, 3$	$m = 4s + j$, $j = 1, 2, 3$	P_n	C_m	$v_0 - v_1$	$e_0 - e_1$
0	1	A_0	B_1, B_1'	0	−1
0	2	A_0	B_2, B_2'	0	−1
0	3	A_0	B_3, B_3'	0	−1
1	1	A_1	B_1, B_1'	0	0
1	2	A_1'	B_2, B_2'	1	0
1	3	A_1'	B_3, B_3'	0	0
2	1	A_2	B_1, B_1'	0	1
2	2	A_2	B_2, B_2'	0	1
2	3	A_2	B_3, B_3'	0	1
3	1	A_3	B_1, B_1'	0	0
3	2	A_3'	B_2, B_2'	1	0
3	3	A_3'	B_3, B_3'	0	0

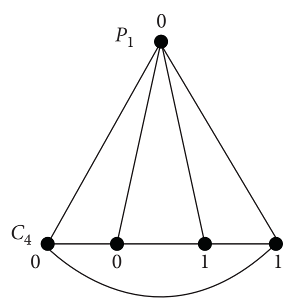

Figure 18: Logical labeling of $P_1 \odot C_4$.

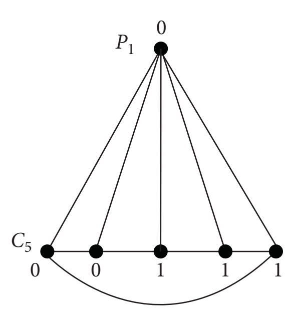

Figure 19: Logical labeling of $P_1 \odot C_5$.

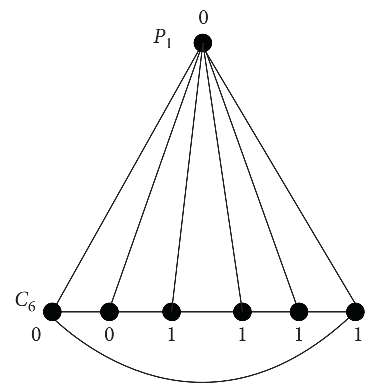

Figure 20: Logical labeling of $P_1 \odot C_6$.

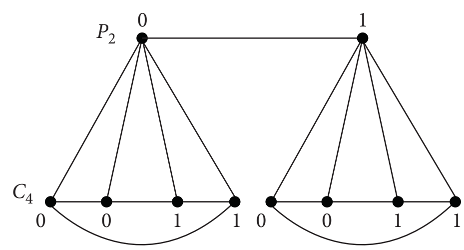

Figure 21: Logical labeling of $P_2 \odot C_4$.

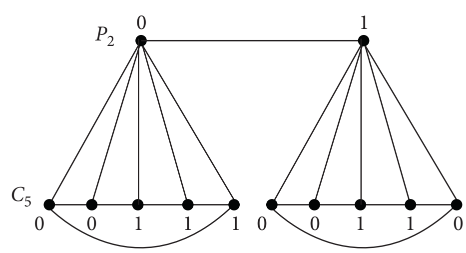

Figure 22: Logical labeling of $P_2 \odot C_5$.

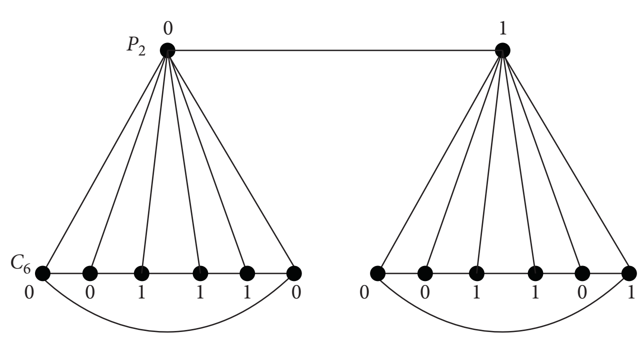

Figure 23: Logical labeling of $P_2 \odot C_6$.

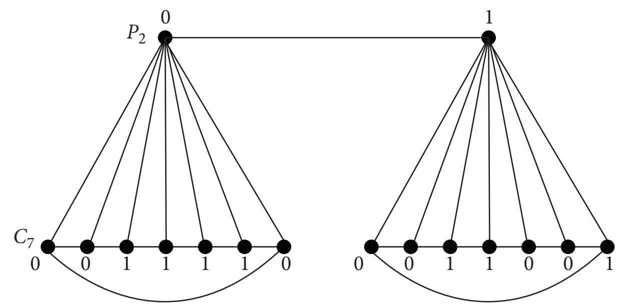

Figure 24: Logical labeling of $P_2 \odot C_7$.

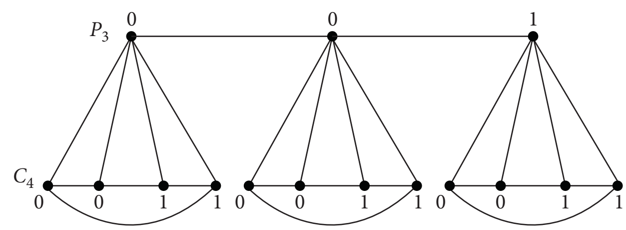

Figure 25: Logical labeling of $P_3 \odot C_4$.

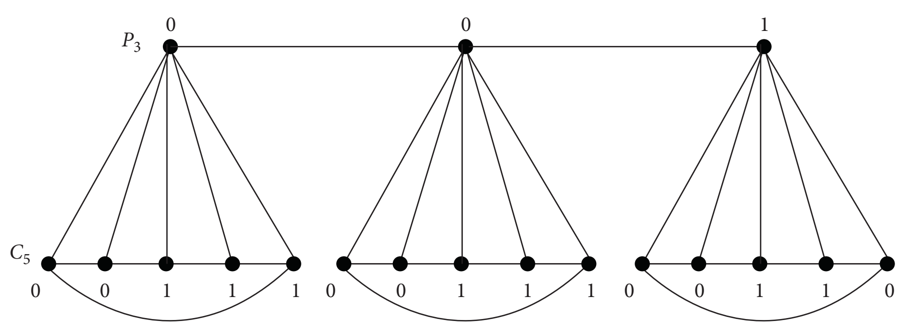

Figure 26: Logical labeling of $P_3 \odot C_5$.

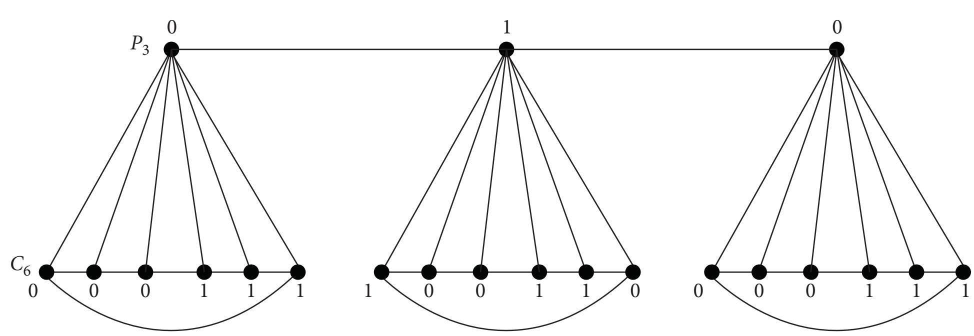

Figure 27: Logical labeling of $P_3 \odot C_6$.

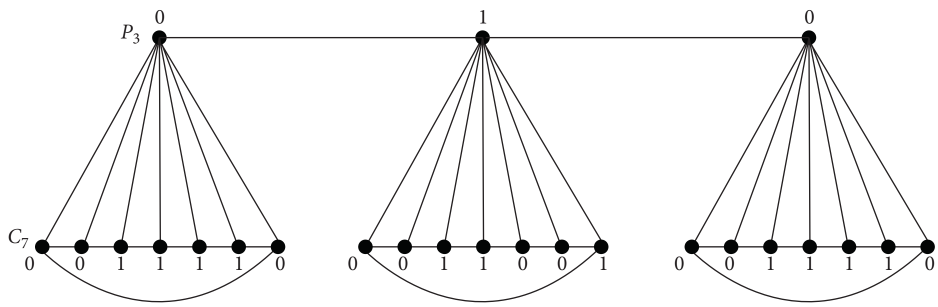

FIGURE 28: Logical labeling of $P_3 \odot C_7$.

Lemma 5. *The corona $P_n \odot C_m$, where $n = 2, 3$, are logical for all $m \geq 4$.*

Proof. We have two cases:

(i) Case (1) ($n = 2$): suppose that $m = 4s + j$, where $s \geq 1$ and $j = 0, 1, 2, 3$. The four possible subcases should be investigated for m.

  (i) Subcase (1.1) ($m = 4s$): we select the labeling $[01\colon L_{4s}, L_{4s}]$ for $P_2 \odot C_{4s}$. Therefore, $x_0 = x_1 = 1$, $a_0 = 1$, $a_1 = 0$, $y_0 = 2s$, $y_1 = 2s$, $b_0 = 2s$, $b_1 = 2s$, $y_0' = 2s$, $y_1' = 2s$, $b_0' = 2s$, and $b_1' = 2s$. As an example, Figure 21 illustrates $P_2 \odot C_4$. Hence, $v_0 - v_1 = 0$ and $e_0 - e_1 = 1$. Thus, $P_2 \odot C_{4s}$ is logical.

  (ii) Subcase (1.2) ($m = 4s + 1$): we choose the labeling $[01\colon L_{4s}1, L_{4s}0]$ for $P_2 \odot C_{4s+1}$. Therefore, $x_0 = x_1 = 1$, $a_0 = 1$, $a_1 = 0$, $y_0 = 2s$, $y_1 = 2s + 1$, $b_0 = 2s$, $b_1 = 2s + 1$, $y_0' = 2s + 1$, $y_1' = 2s$, $b_0' = 2s$, and $b_1' = 2s + 1$. As an example, Figure 22 illustrates $P_2 \odot C_5$. Hence, $v_0 - v_1 = 0$ and $e_0 - e_1 = 1$. Thus, $P_2 \odot C_{4s+1}$ is logical.

  (iii) Subcase (1.3) ($m = 4s + 2$): we select the labeling $[01\colon L_{4s}10, L_{4s}01]$ for $P_2 \odot C_{4s+2}$. Therefore, $x_0 = x_1 = 1$, $a_0 = 1$, $a_1 = 0$, $y_0 = 2s + 1$, $y_1 = 2s + 1$, $b_0 = 2s$, $b_1 = 2s + 2$, $y_0' = 2s + 1$, $y_1' = 2s + 1$, $b_0' = 2s + 1$, and $b_1' = 2s$. As an example, Figure 23 illustrates $P_2 \odot C_6$. Hence, $v_0 - v_1 = 0$ and $e_0 - e_1 = 1$. Thus, $P_2 \odot C_{4s+2}$ is logical.

  (iv) Subcase (1.4) ($m = 4s + 3$): we choose the labeling $[01\colon L_{4s}110, L_{4s}001]$ for $P_2 \odot C_{4s+3}$. Therefore, $x_0 = x_1 = 1$, $a_0 = 1$, $a_1 = 0$, $y_0 = 2s + 1$, $y_1 = 2s + 2$, $b_0 = 2s$, $b_1 = 2s + 3$, $y_0' = 2s + 2$, $y_1' = 2s + 1$, $b_0' = 2s + 2$, and $b_1' = 2s + 1$. As an example, Figure 24 illustrates $P_2 \odot C_7$. Hence, $v_0 - v_1 = 0$ and $e_0 - e_1 = 1$. Thus, $P_2 \odot C_{4s+3}$ is logical.

(ii) Case (2) ($n = 3$): suppose that $m = 4s + j$, where $s \geq 1$ and $j = 0, 1, 2, 3$. For m, we should investigate the four subcases indicated below.

  (i) Subcase (2.1) ($m = 4s$): we select the labeling $[001\colon L_{4s}, L_{4s}, L_{4s}]$ for $P_3 \odot C_{4s}$. Therefore, $x_0 = 2$, $x_1 = 1$, $a_0 = 1$, $a_1 = 1$, $y_0 = 2s$, $y_1 = 2s$, $b_0 = 2s$, $b_1 = 2s$, $y_0' = 2s$, $y_1' = 2s$, $b_0' = 2s$, and $b_1' = 2s$. As an example, Figure 25 illustrates $P_3 \odot C_4$. Hence, $v_0 - v_1 = 1$ and $e_0 - e_1 = 0$. Thus, $P_3 \odot C_{4s}$ is logical.

  (ii) Subcase (2.2) ($m = 4s + 1$): we choose the labeling $[001\colon L_{4s}1, L_{4s}1, L_{4s}0]$ for $P_3 \odot C_{4s+1}$. Therefore, $x_0 = 2$, $x_1 = 1$, $a_0 = 1$, $a_1 = 1$, $y_0 = 2s$, $y_1 = 2s + 1$, $b_0 = 2s$, $b_1 = 2s + 1$, $y_0' = 2s + 1$, $y_1' = 2s$, $b_0' = 2s$, and $b_1' = 2s + 1$. As an example, Figure 26 illustrates $P_3 \odot C_5$. Hence, $v_0 - v_1 = 0$ and $e_0 - e_1 = 0$. Thus, $P_3 \odot C_{4s+1}$ is logical.

  (iii) Subcase (2.3) ($m = 4s + 2$): we select the labeling $[010\colon 0L_{4s}1, 1L_{4s}0, 0L_{4s}1]$ for $P_3 \odot C_{4s+2}$. Therefore, $x_0 = 2$, $x_1 = 1$, $a_0 = 2$, $a_1 = 0$, $y_0 = 2s + 1$, $y_1 = 2s + 1$, $b_0 = 2s$, $b_1 = 2s + 2$, $y_0' = 2s + 1$, $y_1' = 2s + 1$, $b_0' = 2s + 2$, and $b_1' = 2s$. As an example, Figure 27 illustrates $P_3 \odot C_6$. Hence, $v_0 - v_1 = 1$ and $e_0 - e_1 = 0$. Thus, $P_3 \odot C_{4s+2}$ is logical.

  (iv) Subcase (2.4) ($m = 4s + 3$): we choose the labeling $[010\colon L_{4s}110, L_{4s}001, L_{4s}110]$ for $P_3 \odot C_{4s+3}$. Therefore, $x_0 = 2$, $x_1 = 1$, $a_0 = 2$, $a_1 = 0$, $y_0 = 2s + 1$, $y_1 = 2s + 2$, $b_0 = 2s$, $b_1 = 2s + 3$, $y_0' = 2s + 2$, $y_1' = 2s + 1$, $b_0' = 2s + 2$, and $b_1' = 2s + 1$. As an example, Figure 28 illustrates $P_3 \odot C_7$. Hence, $v_0 - v_1 = 0$ and $e_0 - e_1 = 0$. So, $P_3 \odot C_{4s+3}$ is logical. Thus, the lemma is proved.

The following theorem can be established as a result of all previous lemmas. □

Theorem 1. *The corona $P_n \odot C_m$ is logical for all $n \geq 1$ and $m \geq 3$ if and only if $(n \cdot m) \neq (1, 3 \pmod 4)$.*

4. Conclusions

In this paper, we test the logical labeling of corona product of paths and cycle graphs. We found that $P_k \odot C_m$ is logical, for all $n \geq 1$ and $m \geq 3$ if and only if $(n \cdot m) \neq (1, 3 \pmod 4)$. In future work, we can extend this work by combining the various graphs with other mathematical computations to illustrate logical labeling.

Data Availability

The data used to support the findings of this study are available from the corresponding author upon request.

Conflicts of Interest

The authors declare that they have no conflicts of interest.

Acknowledgments

The authors thank the Deanship of Scientific Research at King Khalid University for funding this research under the General Research Project (R.G.P.1/208/41) grant.

References

[1] D. Malarvizhi and V. Revathi, "A review on graphs with unique minimum dominating sets," *International Journal of Mathematics Trends and Technology*, vol. 44, no. 1, 2017.
[2] E. Badr, A. A. El-hay, H. Ahmed, and M. Moussa, "Polynomial, exponential and approximate algorithms for metric dimension problem," *International Journal of Mathematical Combinatorics*, vol. 2, pp. 50–66, 2021.
[3] A. Rosa, "On certain valuations of the vertices of a graph," *Theory of Graphs (International Symposium, Rome, July 1966)*, pp. 349–355, Gordon and Breach, New York, NY, USA and Dunod Paris, 1967.
[4] J. A. Gallian, "A dynamic survey of graph labeling," *The Electronic Journal of Combinatorics*, vol. 17, p. DS6, 2010.
[5] S. W. Golomb, *How to Number a Graph in Graph Theory and Computing*, R. C. Read, Ed., Academic Press, New York, NY, USA, pp. 23–37, 1972.
[6] R. L. Graham and N. J. A. Sloane, "On additive bases and harmonious graphs," *SIAM Journal on Algebraic and Discrete Methods*, vol. 1, no. 4, pp. 382–404, 1980.
[7] A. Hefnawy and Y. Elmshtaye, "Cordial labeling of corona product of paths and lemniscate graphs," *Ars Combinatoria*, vol. 149, pp. 69–82, 2020.
[8] S. Nada, A. Elrokh, E. A. Elsakhawi, and D. E. Sabra, "The corona between cycles and paths," *Journal of the Egyptian Mathematical Society*, vol. 25, no. 2, pp. 111–118, 2017.
[9] A. I. H. Elrokh, S. I. M. Nada, and E. M. E.-S. El-Shafey, "Cordial labeling of corona product of path graph and second power of fan graph," *Open Journal of Discrete Mathematics*, vol. 11, no. 02, pp. 31–42, 2021.
[10] S. Klavzar and M. Tavakoli, "Dominated and dominator colorings over (edge) corona and hierarchical products," *Applied Mathematics and Computation*, vol. 390, p. 125647, 2021.
[11] M. Tavakoli, F. Rahbarnia, and A. R. Ashrafi, "Studying the corona product of graphs under some graph invariants," *Transactions on Combinatorics*, vol. 3, no. 3, pp. 43–49, 2014.
[12] M. M. Ali Al-Shamiri, A. Elrokh, Y. El –Mashtawye, and S. E. Tallah, "The cordial labeling for the cartesian product between paths and cycles," *International Journal of Research-GRANTHAALAYAH*, vol. 8, no. 3, pp. 331–341, 2020.
[13] M. A. Seoud and A. Maqusoud, "On cordial and balanced labelings of graphs," *Journal of the Egyptian Mathematical Society*, vol. 7, pp. 127–135, 1999.
[14] I. Cahit, "Cordial Graphs: a weaker version of graceful and harmonious Graphs," *Ars Combinatoria*, vol. 23, pp. 201–207, 1987.
[15] E. Badr, S. Almotairi, A. Eirokh, A. Abdel-Hay, and B. Almutairi, "An integer linear programming model for solving radio mean labeling problem," *IEEE Access*, vol. 8, pp. 162343–162349, 2020.

Hindawi
Journal of Mathematics
Volume 2022, Article ID 5956802, 11 pages
https://doi.org/10.1155/2022/5956802

Research Article

Computation of Topological Indices of Double and Strong Double Graphs of Circumcoronene Series of Benzenoid (H_m)

Muhammad Shoaib Sardar,[1] **Imran Siddique**,[2] **Dalal Alrowaili**,[3] **Muhammad Asad Ali**,[1] **and Shehnaz Akhtar**[4]

[1]*School of Mathematics, Minhaj University, Lahore, Pakistan*
[2]*Department of Mathematics, University of Management and Technology, Lahore 54770, Pakistan*
[3]*Mathematics Department, College of Science, Jouf University, P. O. Box: 2014, Sakaka, Saudi Arabia*
[4]*School of Natural Science, National University of Science and Technology, Islamabad, Pakistan*

Correspondence should be addressed to Imran Siddique; imransmsrazi@gmail.com

Received 20 November 2021; Revised 21 December 2021; Accepted 3 January 2022; Published 21 January 2022

Academic Editor: M. T. Rahim

Copyright © 2022 Muhammad Shoaib Sardar et al. This is an open access article distributed under the Creative Commons Attribution License, which permits unrestricted use, distribution, and reproduction in any medium, provided the original work is properly cited.

Topological indices are very useful to assume certain physiochemical properties of the chemical compound. A molecular descriptor which changes the molecular structures into certain real numbers is said to be a topological index. In chemical graph theory, to create quantitative structure activity relationships in which properties of molecule may be linked with their chemical structures relies greatly on topological indices. The benzene molecule is a common chemical shape in chemistry, physics, and nanoscience. This molecule could be very beneficial to synthesize fragrant compounds. The circumcoronene collection of benzenoid H_m is one family that generates from benzene molecules. The purpose of this study is to calculate the topological indices of the double and strong double graphs of the circumcoronene series of benzenoids (H_m). In addition, we also present a numerical and graphical comparison of topological indices of the double and strong double graphs of the circumcoronene series of benzenoid (H_m).

1. Introduction and Preliminaries

For undetermined notations and terminologies, we refer the readers to read the book [1].

Let $\mathbb{G}(V, E)$ be a simple, finite connected graph, where the set of vertices is $V(\mathbb{G})$ and the set of edges is $E(\mathbb{G})$. For every vertex $x \in V(\mathbb{G})$, the edge connecting x and z is denoted by xz. In graph $\mathbb{G}$, the total number of edges that connects to each vertex is known as the degree of vertex. The number of connected vertices to a fixed vertex is known as neighborhood. The degree of a vertex is denoted by d_x, where $x \in V(\mathbb{G})$. Hand-shaking lemma is very productive for calculating the size of a graph $\mathbb{G}$.

Lemma 1. *If a graph $\mathbb{G}$ is having size k, then*

$$\sum_{x \in V(\mathbb{G})} \deg(x) = 2k. \tag{1}$$

In chemical graph theory, topological indices show a significant role in assisting chemists for modeling the molecular structure of chemical compounds and studying their chemical and physical characteristics. In chemistry, discovery of the drugs commonly relies on the topological descriptors. Drugs are characterized as molecular graphs, where graphs considered are simple with no multiple edges and no cycle formation. These topological descriptors provide information of a chemical compound based on the arrangement of its atoms and their bonds. A wide range of topological indices have been studied, and some of the more frequent forms of topological indices include degree-based, distance-based topological indices, and counting-related polynomials. In the topological indices, very famous and the oldest index is the Wiener index $W(G)$.

The Wiener index [2] is defined as follows:

$$W(G) = \frac{1}{2}\sum_{(x,z)} d(x,z), \tag{2}$$

where $d(x,z)$ is the distance among vertices x and z of a graph G.

A graph G's geometric arithmetic index (GA) [3] is defined as follows:

$$\mathrm{GA}(G) = \sum_{xz\in E(G)} \frac{2\sqrt{d_x d_z}}{d_x + d_z}. \tag{3}$$

A graph G' s atomic bond connectivity index (ABC) [4] is defined as follows:

$$\mathrm{ABC}(G) = \sum_{xz\in E(G)} \sqrt{\frac{d_x + d_z - 2}{d_x d_z}}. \tag{4}$$

A graph G's forgotten index (F) [5] is defined as follows:

$$F(G) = \sum_{xz\in E(G)} \left(d_x^2 + d_z^2\right). \tag{5}$$

A graph G's inverse sum indeg index (ISI) [6] is defined as follows:

$$\mathrm{ISI}(G) = \sum_{xz\in E(G)} \frac{1}{(1/d_x) + (1/d_z)}. \tag{6}$$

A graph G's general inverse sum indeg index $(\mathrm{ISI}_{(\alpha,\beta)})$ [7] is defined as follows:

$$\mathrm{ISI}_{(\alpha,\beta)}(G) = \sum_{xz\in E(G)} [d_x d_z]^{\alpha}[d_x + d_z]^{\beta}, \tag{7}$$

where α and β are the real numbers.

A graph G's first multiplicative-Zagreb (PM_1) and second multiplicative-Zagreb indices (PM_2) are defined [8] as follows:

$$\mathrm{PM}_1(G) = \prod_{xz\in E(G)} (d_x)^2, \tag{8}$$

$$\mathrm{PM}_2(G) = \prod_{xz\in E(G)} (d_x \cdot d_z). \tag{9}$$

It is also possible to write the first multiplicative-Zagreb index (PM_1) [9] for G as follows:

$$\mathrm{PM}_1(G) = \prod_{xz\in E(G)} (d_x + d_z). \tag{10}$$

Imran et al. [10–12] studied the edge Mostar index of nanostructures and chemical structures by using graph operations and also computed the eccentric connectivity polynomial of connected graphs and Mostar indices for melem chain nanostructures. For more details about topological indices, we refer the works of Xiong et al. [13], Hong et al. [14], Alaeiyan et al. [15], Ch et al. [16], and Sardar et al. [17].

Definition 1. The well-known family of the benzenoid molecular graph is circumcoronene series of benzenoid (H_m), where $(m \geq 1)$ [18]. This family of graph constructed exclusively from benzene C_6 on circumference. Certain main members of circumcoronene series of benzenoid are benzene (H_1), coronene (H_2), circumcoronene (H_3), and circumcircumcoronene (H_4) [19]. Generally, circumcoronene series of benzenoid (H_m) is shown in Figure 1.

Definition 2. In order to make a double graph $D(H_m)$ of a graph **G**, take two copies of the graph **G** and join the nodes in each copy with their neighbors in the other copy [20]. For example, the graph (H_1) and its double graph $D(H_1)$ are shown in Figure 2. In double graph of circumcoronene series of benzenoid, there are $12m^2$ vertices and $4(9m^2 - 3m)$ edges, respectively. In $D(H_m)$, we have $12m$ vertices of degree 4 and $12(m^2 - m)$ vertices of degree.

Definition 3. Consider the two copies of graph **G**, and by joining the closed neighborhoods of one graph's vertex to the vertex in an adjacent graph, one can obtain the strong double graph $\mathrm{SD}(\mathbf{G})$ of graph **G** [21]. For example, strong double graph of graph H_1 is shown in Figure 3.

This study is laid out as follows. We will examine some vertex-based topological indices of double and strong double graphs of circumcoronene series of benzenoid (H_m) in Sections 2 and 4, respectively. The comparison is given in Sections 3 and 5. In Section 6, we provide final remarks for the whole study.

2. Degree-Based Topological Indices of Double Graph of Circumcoronene Series of Benzenoid Graph (H_m)

This section contains a calculation of the degree-based indices of the double graph of circumcoronene series of benzenoid (H_m).

Theorem 1. *Let $D(H_m)$ be the double graph of circumcoronene series of benzenoid graph (H_m); then, the geometric arithmetic index of $D(H_m)$ is*

$$GA[D(H_m)] = \frac{(96m - 96)\sqrt{6}}{5} + 36m^2 - 60m + 48. \tag{11}$$

Proof. In the double graph of circumcoronene series of benzenoid, there are $12m^2$ vertices and $4(9m^2 - 3m)$ edges, respectively. There are $12m$ vertices in $D(H_m)$ of degree 4 and $12(m^2 - m)$ of degree 6.

We separate the edges of $D(H_m)$ into the edges of the type$E[d_x, d_z]$, where xz is an edge. In $D(H_m)$, we get edge of types $E_{(4,4)}$ and $E_{(4,6)}$ and $E_{(6,6)}$. A list of their edges is given in Table 1.

By using Table 1 and equation (1), the result that we obtain is

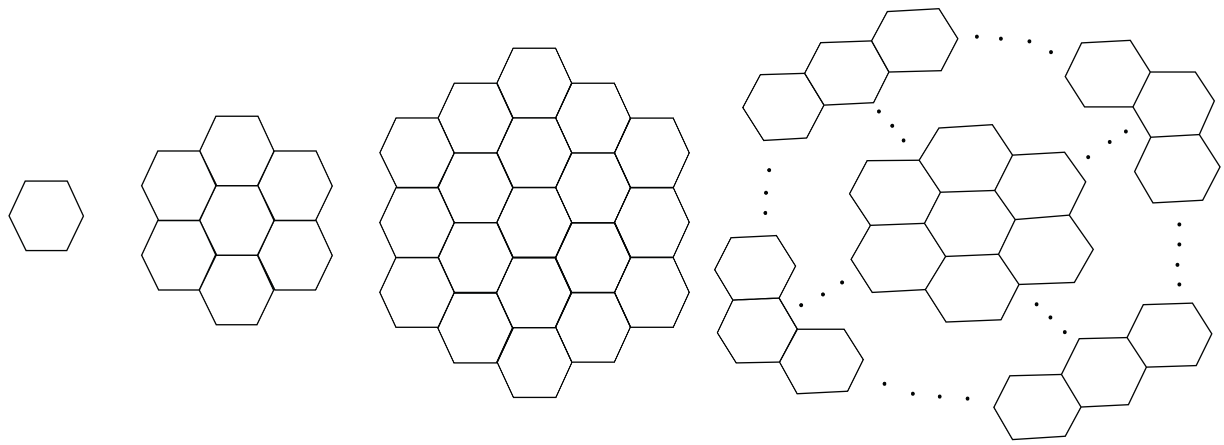

Figure 1: Circumcoronene series of benzenoid (H_1, H_2, H_3, and H_m).

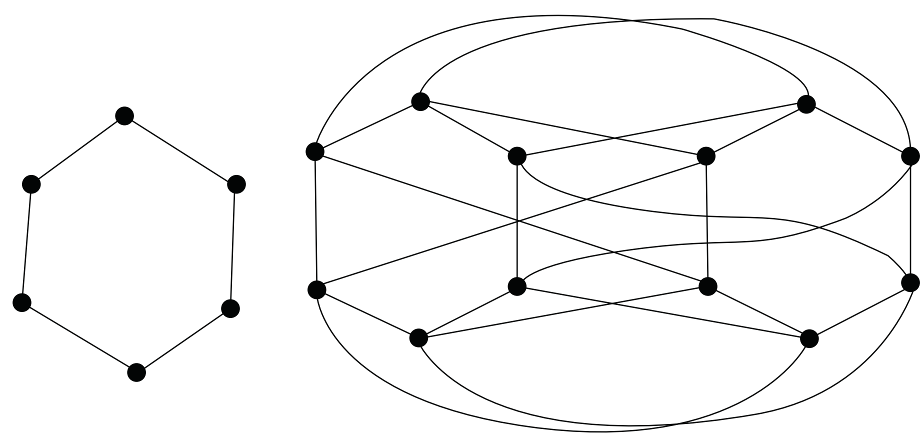

Figure 2: Circumcoronene series of benzenoid (H_1) and its double graph ($D(H_1)$).

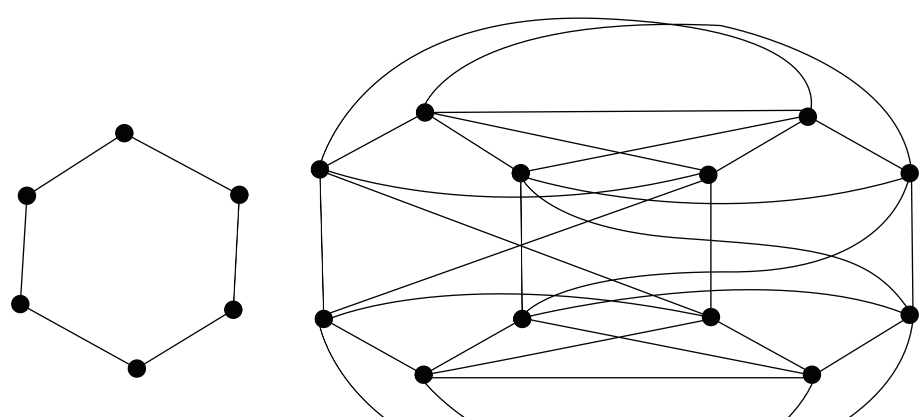

Figure 3: Circumcoronene series of benzenoid (H_1) and its strong double graph ($\mathrm{SD}(H_1)$).

Table 1: Separation of edges.

$E[d_x, d_z]$	$E_{(4,4)}$	$E_{(4,6)}$	$E_{(6,6)}$
Number of edges	24	$48(m-1)$	$36m^2 - 60m + 24$

$$\mathrm{GA}[\mathbf{G}] = \sum_{xz\in E(\mathbf{G})} \frac{2\sqrt{d_x d_z}}{d_x + d_z}.$$

$$\begin{aligned}
\mathrm{GA}[D(H_m)] &= |E_{(4,4)}| \sum_{xz\in E[D(H_m)]} \frac{2\sqrt{d_x d_z}}{d_x + d_z} + |E_{(4,6)}| \sum_{xz\in E[D(H_m)]} \frac{2\sqrt{d_x d_z}}{d_x + d_z} + |E_{(6,6)}| \sum_{xz\in E[D(H_m)]} \frac{2\sqrt{d_x d_z}}{d_x + d_z}.\\
\mathrm{GA}[D(H_m)] &= 24\left[\frac{2\sqrt{16}}{8}\right] + 48(m-1)\left[\frac{2\sqrt{24}}{10}\right] + \left(36m^2 - 60m + 24\right)\left[\frac{2\sqrt{36}}{12}\right].\\
\mathrm{GA}[D(H_m)] &= 24 + 48(m-1)\left[\frac{\sqrt{24}}{5}\right] + 36m^2 - 60m + 24.\\
\mathrm{GA}[D(H_m)] &= \frac{(96m-96)\sqrt{6}}{5} + 36m^2 - 60m + 48.
\end{aligned} \tag{12}$$

□

Theorem 2. *Let $D(H_m)$ be the double graph of circumcoronene series of the benzenoid graph (H_m); then, the ABC index of $D(H_m)$ is*

$$\begin{aligned}
\mathrm{ABC}[D(H_m)] &= \left(6\sqrt{3} + \left(6m^2 - 10m + 4\right)\sqrt{5}\right)\sqrt{2}\\
&\quad + 16\sqrt{3}(m-1).
\end{aligned} \tag{13}$$

Proof. By using Table 1 and equation (4), the result that we obtain is

$$\begin{aligned}
\mathrm{ABC}[D(H_m)] &= |E_{(4,4)}| \sum_{xz\in E[D(H_m)]} \sqrt{\frac{d_x + d_z - 2}{d_x d_z}} + |E_{(4,6)}| \sum_{xz\in E[D(H_m)]} \sqrt{\frac{d_x + d_z - 2}{d_x d_z}} + |E_{(6,6)}| \sum_{xz\in E[D(H_m)]} \sqrt{\frac{d_x + d_z - 2}{d_x d_z}}.\\
&= 24\sqrt{\frac{4+4-2}{(4)(4)}} + 48(m-1)\sqrt{\frac{4+6-2}{(4)(6)}} + \left(36m^2 - 60m + 24\right)\sqrt{\frac{6+6-2}{(6)(6)}}.\\
&= 6\sqrt{6} + 48(m-1)\sqrt{\frac{1}{3}} + \left(36m^2 - 60m + 24\right)\sqrt{\frac{5}{18}}.\\
\mathrm{ABC}[D(H_m)] &= \left(6\sqrt{3} + \left(6m^2 - 10m + 4\right)\sqrt{5}\right)\sqrt{2} + 16\sqrt{3}(m-1).
\end{aligned} \tag{14}$$

□

Theorem 3. *Let $D[H_m]$ be the double graph of circumcoronene series of benzenoid graph (H_m); then, the forgotten index of $D(H_m)$ is*

$$F[D(H_m)] = 2592m^2 - 1824m. \tag{15}$$

Proof. By using Table 1 and equation (5), the result that we obtain is

$$\begin{aligned}
F[D(H_m)] &= |E_{(4,4)}| \sum_{xz\in E[D(H_m)]} \left(d_x^2 + d_z^2\right) + |E_{(4,6)}| \sum_{xz\in E[D(H_m)]} \left(d_x^2 + d_z^2\right) + |E_{(6,6)}| \sum_{xz\in E[D(H_m)]} \left(d_x^2 + d_z^2\right).\\
&= 24\left(4^2 + 4^2\right) + 48(m-1)\left(4^2 + (6)^2\right) + \left(36m^2 - 60m + 24\right)\left(6^2 + (6)^2\right)\\
&= 768 + 2496(m-1) + \left(36m^2 - 60m + 24\right)(72).\\
F[D(H_m)] &= 2592m^2 - 1824m.
\end{aligned} \tag{16}$$

□

Theorem 4. *Let $D[H_m]$ be the double graph of circum-coronene series of the benzenoid graph (H_m); then, the inverse sum indeg index of $D(H_m)$ is*

$$\mathrm{ISI}[D(H_m)] = 108m^2 - \frac{324}{5}m + \frac{24}{5}. \quad (17)$$

Proof. By using Table 1 and equation (6), the result that we obtain is

$$\begin{aligned}\mathrm{ISI}[D(H_m)] &= |E_{(4,4)}| \sum_{xz\in E[D(H_m)]} \frac{(d_x d_z)}{(d_x + d_z)} + |E_{(4,6)}| \sum_{xz\in E[D(H_m)]} \frac{(d_x d_z)}{(d_x + d_z)} + |E_{(6,6)}| \sum_{xz\in E[D(H_m)]} \frac{(d_x d_z)}{(d_x + d_z)}\\ &= 24\left[\frac{(4)(4)}{(4+4)}\right] + 48(m-1)\left[\frac{(4)(6)}{(4+6)}\right] + \left(36m^2 - 60m + 24\right)\left[\frac{(6)(6)}{(6+6)}\right]\\ &= 48 + 48(m-1)\left[\frac{12}{5}\right] + \left(36m^2 - 60m + 24\right)[3],\\ \mathrm{ISI}[D(H_m)] &= 108m^2 - \frac{324}{5}m + \frac{24}{5}.\end{aligned} \quad (18)$$

□

Theorem 5. *Let $D[H_m]$ be the double graph of circum-coronene series of the benzenoid graph (H_m); then, the general inverse sum indeg index ($\mathrm{ISI}_{(\alpha,\beta)}$) of $D(H_m)$ is*

$$\mathrm{ISI}_{(\alpha,\beta)}[D(H_m)] = 4p[16]^{\alpha}[8]^{\beta} + 8p[16p]^{\alpha}[4(1+p)]^{\beta}. \quad (19)$$

Proof. By using Table 1 and equation (7), the result that we obtain is

$$\begin{aligned}\mathrm{ISI}_{(\alpha,\beta)}[D(H_m)] &= |E_{(4,4)}| \sum_{xz\in E[D(H_m)]} [d_x d_z]^{\alpha}[d_x + d_z]^{\beta}\\ &\quad + |E_{(4,6)}| \sum_{xz\in E[D(H_m)]} [d_x d_z]^{\alpha}[d_x + d_z]^{\beta} + |E_{(6,6)}| \sum_{xz\in E[D(H_m)]} [d_x d_z]^{\alpha}[d_x + d_z]^{\beta}\\ &= 24[(4)(4)]^{\alpha}[4+4]^{\beta} + 48(m-1)[(4)(6)]^{\alpha}[4+6]^{\beta} + \left(36m^2 - 60m + 24\right)[(6)(6)]^{\alpha}[6+6]^{\beta}\\ &= 24[16]^{\alpha}[8]^{\beta} + 48(m-1)[24]^{\alpha}[10]^{\beta} + \left(36m^2 - 60m + 24\right)[36]^{\alpha}[12]^{\beta},\end{aligned} \quad (20)$$

where α and β are the real numbers. □

Theorem 6. *Let $D[H_M]$ be the double graph of circum-coronene series of the benzenoid graph (H_m); then, the first multiplicative-Zagreb index of $D(H_m)$ is*

$$\mathrm{PM}_1[D(H_m)] = (3m-2)\left[13271040(m-1)^2\right]. \quad (21)$$

Proof. By using Table 1 and equation (10), the result that we obtain is

$$\begin{aligned}\mathrm{PM}_1[D(H_m)] &= |E_{(4,4)}| \prod_{xz\in E[D(H_m)]} (d_x + d_z) \times |E_{(4,6)}| \prod_{xz\in E[D(H_m)]} (d_x + d_z) \times |E_{(6,6)}| \prod_{xz\in E[D(H_m)]} (d_x + d_z),\\ PM_1[D(H_m)] &= 24(8) \times 48(m-1)(10) \times \left(36m^2 - 60m + 24\right)(12),\\ PM_1[D(H_m)] &= 192 \times (480m - 480) \times \left(432m^2 - 720m + 288\right),\\ PM_1[D(H_m)] &= (3m-2)\left[13271040(m-1)^2\right].\end{aligned} \quad (22)$$

□

Theorem 7. *Let $D[H_m]$ be the double graph of circumcoronene series of the benzenoid graph (H_m); then, the second multiplicative-Zagreb index of $D(H_m)$ is*

$$\mathrm{PM}_2[D(H_m)] = \left(m - \frac{2}{3}\right)\left[573308928(m-1)^2\right]. \tag{23}$$

Proof. By using Table 1 and equation (9), the result that we obtain is

$$\begin{aligned}
\mathrm{PM}_2[D(H_m)] &= \left|E_{(4,4)}\right| \prod_{xz\in E[D(H_m)]} (d_x \cdot d_z) \times \left|E_{(4,6)}\right| \prod_{xz\in E[D(H_m)]} (d_x \cdot d_z) \times \left|E_{(6,6)}\right| \prod_{xz\in E[D(H_m)]} (d_x \cdot d_z),\\
\mathrm{PM}_2[D(H_m)] &= 24(16) \times 48(m-1)(24) \times \left(36m^2 - 60m + 24\right)(36),\\
\mathrm{PM}_2[D(H_m)] &= 442368(m-1) \times \left(1296m^2 - 2160m + 864\right),\\
\mathrm{PM}_2[D(H_m)] &= \left(m - \frac{2}{3}\right)\left[573308928(m-1)^2\right].
\end{aligned} \tag{24}$$

□

3. Comparison

In this section, we present a numerical and graphical comparison of topological indices that included the first multiplicative-Zagreb index (PM_1), general inverse sum indeg index ($\mathrm{ISI}_{(\alpha,\beta)}$), atom bond connectivity index (ABC), forgotten index (F), geometric arithmetic index (GA), second multiplicative-Zagreb index (PM_2), and inverse sum indeg index (ISI) for $m = 1, 2, 3, 4, \ldots, 10$ for the double graph of circumcoronene series of the benzenoid graph $(D(H_m))$, as given in Table 2 and Figure 4.

4. Degree-Based Topological Indices of Strong Double Graphs of Circumcoronene Series of Benzenoid Graph (H_m)

This section contains a calculation of the degree-based indices of the strong double graph of circumcoronene series of benzenoid (H_m). Figure 3 shows the strong double graph of (H_1).

Theorem 8. *Let $SD(H_M)$ be the double graph of circumcoronene series of the benzenoid graph (H_m); then, the geometric arithmetic index of $SD(H_m)$ is*

$$\mathrm{GA}[\mathrm{SD}(H_m)] = (8m-8)\sqrt{35} + 42m^2 - 60m + 48. \tag{25}$$

Proof. In the strong double graph of circumcoronene series of benzenoid, there are $12m^2$ vertices and $6(7m^2 - 2m)$ edges, respectively. There are $12m$ vertices in $\mathrm{SD}(H_m)$ of degree 5 and $12m(m^2-1)$ of degree 7.

We separate the edges of $\mathrm{SD}(H_m)$ into the edges of the type$E(d_x, d_z)$, where xz is an edge. In $\mathrm{SD}(H_m)$, we get edge of types $E_{(5,5)}$ and $E_{(5,7)}$ and $E_{(7,7)}$. A list of their edges is given in Table 3.

By using Table 3 and equation (1), the result that we obtain is

$$\begin{aligned}
\mathrm{GA}[G] &= \sum_{xz\in E(G)} \frac{2\sqrt{d_x d_z}}{d_x + d_z},\\
\mathrm{GA}[\mathrm{SD}(H_m)] &= \left|E_{(5,5)}\right| \sum_{xz\in E[\mathrm{SD}(H_m)]} \frac{2\sqrt{d_x d_z}}{d_x + d_z} + \left|E_{(5,7)}\right| \sum_{xz\in E[\mathrm{SD}(H_m)]} \frac{2\sqrt{d_x d_z}}{d_x + d_z} + \left|E_{(7,7)}\right| \sum_{xz\in E[\mathrm{SD}(H_m)]} \frac{2\sqrt{d_x d_z}}{d_x + d_z},\\
\mathrm{GA}[\mathrm{SD}(H_m)] &= (6m+24)\frac{2\sqrt{25}}{10} + 48(m-1)\frac{2\sqrt{35}}{12} + \left(42m^2 - 66m + 24\right)\frac{2\sqrt{49}}{14},\\
\mathrm{GA}[\mathrm{SD}(H_m)] &= (6m+24) + 48(m-1)\left[\frac{\sqrt{35}}{6}\right] + 42m^2 - 66m + 24,\\
\mathrm{GA}[\mathrm{SD}(H_m)] &= (8m-8)\sqrt{35} + 42m^2 - 60m + 48.
\end{aligned} \tag{26}$$

□

TABLE 2: Computation of topological indices of double graph of circumcoronene series of benzenoid $(D(H_m))$.

m	$GA(D(H_m))$	$ABC(D(H_m))$	$F(D(H_m))$	$ISI(D(H_m))$	$PM_1(D(H_m))$	$PM_2(D(H_m))$
1	24	14.697	768	48	0	0
2	119.03	67.710	6720	307.20	5.3084×10^{7}	7.6441×10^{8}
3	286.06	158.67	17856	782.40	3.7159×10^{8}	5.3509×10^{9}
4	525.09	287.58	34176	1473.6	1.1944×10^{9}	1.7199×10^{10}
5	836.12	454.42	55680	2380.8	2.7604×10^{9}	3.9749×10^{10}
6	1219.2	659.24	82360	3504	5.3084×10^{9}	7.6441×10^{10}
7	1674.2	901.98	1.1424×10^{5}	4843.2	9.0774×10^{9}	1.3071×10^{11}
8	2201.2	1182.7	1.5129×10^{5}	6398.4	1.4306×10^{10}	2.0601×10^{11}
9	2800.2	1501.3	1.9353×10^{5}	8169.6	2.1234×10^{10}	3.0576×10^{11}
10	3471.3	1857.9	2.4096×10^{5}	10156.8	3.0099×10^{10}	4.3342×10^{11}

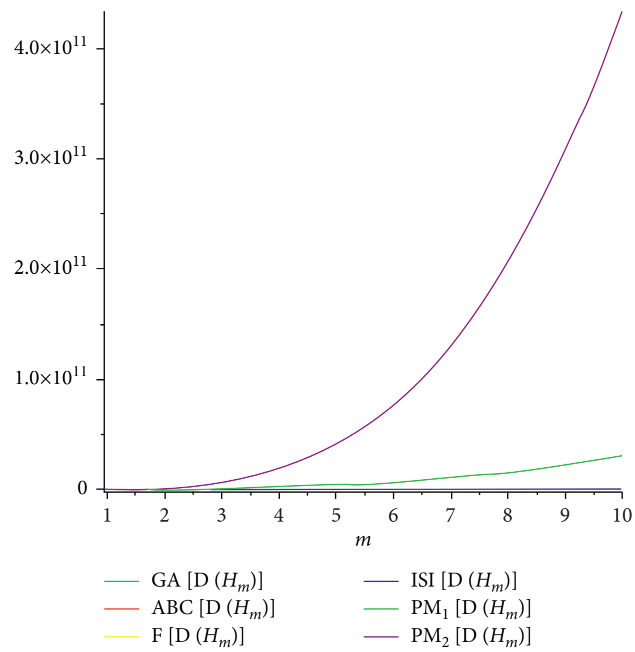

FIGURE 4: Graphical representation of topological indices of double graph of circumcoronene series of benzenoid $(\mathbf{H_m})$.

TABLE 3: Separation of edges.

$E(d_x, d_z)$	$E_{(5,5)}$	$E_{(5,7)}$	$E_{(7,7)}$
Number of edges	$6m+24$	$48(m-1)$	$42m^2-66m+24$

Theorem 9. *Let $SD(H_m)$ be the strong double graph of circumcoronene series of the benzenoid graph (H_m); then, the ABC index of $SD(H_m)$ is*

$$ABC[SD(H_m)] = \frac{((240m-240)\sqrt{7}+84m+336)\sqrt{2}}{35} + \left(12m - \frac{48}{7}\right)\sqrt{3}(m-1). \quad (27)$$

Proof. By using Table 3 and equation (4), the result that we obtain is

$$\mathrm{ABC}[\mathrm{SD}(H_m)] = |E_{(5,5)}| \sum_{xz\in E[\mathrm{SD}(H_m)]} \sqrt{\frac{d_x+d_z-2}{d_xd_z}} + |E_{(5,7)}| \sum_{xz\in E[\mathrm{SD}(H_m)]} \sqrt{\frac{d_x+d_z-2}{d_xd_z}} + |E_{(7,7)}| \sum_{xz\in E[\mathrm{SD}(H_m)]} \sqrt{\frac{d_x+d_z-2}{d_xd_z}}$$
$$= (6m+24)\sqrt{\frac{5+5-2}{(5)(5)}} + 48(m-1)\sqrt{\frac{5+7-2}{(5)(7)}} + \left(42m^2-66m+24\right)\sqrt{\frac{7+7-2}{(7)(7)}}$$
$$= (6m+24)\frac{\sqrt{8}}{5} + 48(m-1)\sqrt{\frac{2}{7}} + \left(42m^2-66m+24\right)\frac{\sqrt{12}}{7},$$
$$\mathrm{ABC}[\mathrm{SD}(H_m)] = \frac{((240m-240)\sqrt{7}+84m+336)\sqrt{2}}{35} + \left(12m-\frac{48}{7}\right)\sqrt{3}(m-1). \tag{28}$$

□

Theorem 10. *Let $SD[H_m]$ be the strong double graph of circumcoronene series of the benzenoid graph (H_m); then, the forgotten index of $SD(H_m)$ is*

$$F[\mathrm{SD}(H_m)] = 4116m^2 - 2616m. \tag{29}$$

Proof. By using Table 3 and equation (5), the result that we obtain is

$$F[\mathrm{SD}(H_m)] = |E_{(5,5)}| \sum_{xz\in E[\mathrm{SD}(H_m)]} \left(d_x^2+d_z^2\right) + |E_{(5,7)}| \sum_{xz\in E[\mathrm{SD}(H_m)]} \left(d_x^2+d_z^2\right) + |E_{(7,7)}| \sum_{xz\in E[\mathrm{SD}(H_m)]} \left(d_x^2+d_z^2\right)$$
$$= (6m+24)\left(5^2+5^2\right) + 48(m-1)\left(5^2+7^2\right) + \left(42m^2-66m+24\right)\left(7^2+7^2\right) \tag{30}$$
$$= (300m+1200) + 3552(m-1) + \left(42m^2-66m+24\right)(98),$$
$$F[\mathrm{SD}(H_m)] = 4116m^2 - 2616m.$$

□

Theorem 11. *Let $SD[H_m]$ be the strong double graph of circumcoronene series of the benzenoid graph (H_m); then, the inverse sum indeg index of $SD(H_m)$ is*

$$\mathrm{ISI}[\mathrm{SD}(H_m)] = 147m^2 - 76m + 4. \tag{31}$$

Proof. By using Table 3 and equation (6), the result that we obtain is

$$\mathrm{ISI}[\mathrm{SD}(H_m)] = |E_{(5,5)}| \sum_{xz\in E[\mathrm{SD}(H_m)]} \frac{(d_xd_z)}{(d_x+d_z)} + |E_{(5,7)}| \sum_{xz\in E[\mathrm{SD}(H_m)]} \frac{(d_xd_z)}{(d_x+d_z)}$$
$$+ |E_{(7,7)}| \sum_{xz\in E[\mathrm{SD}(H_m)]} \frac{(d_xd_z)}{(d_x+d_z)}$$
$$= (6m+24)\left[\frac{(5)(5)}{(5+5)}\right] + 48(m-1)\left[\frac{(5)(7)}{(5+7)}\right] + \left(42m^2-66m+24\right)\left[\frac{(7)(7)}{(7+7)}\right] \tag{32}$$
$$= (15m+60) + 140(m-1) + \left(42m^2-66m+24\right)\left[\frac{49}{14}\right],$$
$$\mathrm{ISI}[\mathrm{SD}(H_m)] = 147m^2 - 76m + 4.$$

□

Theorem 12. *Let $SD(H_m)$ be the strong double graph of circumcoronene series of the benzenoid graph (H_m); then, the general inverse sum indeg index ($ISI_{(\alpha,\beta)}$) of $SD(H_m)$ is*

$$\mathrm{ISI}_{(\alpha,\beta)}[\mathrm{SD}(H_m)] = (6m+24)[25]^{\alpha}[10]^{\beta} + 48(m-1)[35]^{\alpha}[12]^{\beta} + \left(42m^2-66m+24\right)[49]^{\alpha}[14]^{\beta}. \tag{33}$$

Proof. By using Table 3 and equation (7), the result that we obtain is

$$\begin{aligned}\mathrm{ISI}_{(\alpha,\beta)}[\mathrm{SD}(H_m)] &= \left|E_{(5,5)}\right| \sum_{xz\in E[\mathrm{SD}(H_m)]} [d_x d_z]^{\alpha}[d_x+d_z]^{\beta} + \left|E_{(5,7)}\right| \sum_{xz\in E[\mathrm{SD}(H_m)]} [d_x d_z]^{\alpha}[d_x+d_z]^{\beta} + \left|E_{(7,7)}\right| \\ &\quad \cdot \sum_{xz\in E[\mathrm{SD}(H_m)]} [d_x d_z]^{\alpha}[d_x+d_z]^{\beta} \\ &= (6m+24)[(5)(5)]^{\alpha}[5+5]^{\beta} + 48(m-1)[(5)(7)]^{\alpha}[5+7]^{\beta} + \left(42m^2-66m+24\right)[(7)(7)]^{\alpha}[7+7]^{\beta} \\ &= (6m+24)[25]^{\alpha}[10]^{\beta} + 48(m-1)[35]^{\alpha}[12]^{\beta} + \left(42m^2-66m+24\right)[49]^{\alpha}[14]^{\beta},\end{aligned} \tag{34}$$

where α and β are the real numbers. □

Theorem 13. *Let $SD[H_m]$ be the strong double graph of circumcoronene series of the benzenoid graph (H_m); then, the first multiplicative-Zagreb index of $SD(H_m)$ is*

$$\mathrm{PM}_1[\mathrm{SD}(H_m)] = 20321280\left(m-\frac{4}{7}\right)(m+4)(m-1)^2. \tag{35}$$

Proof. By using Table 3 and equation (10), the result that we obtain is

$$\begin{aligned}\mathrm{PM}_1[\mathrm{SD}(H_m)] &= \left|E_{(5,5)}\right| \sum_{xz\in E[\mathrm{SD}(H_m)]} (d_x+d_z) \times \left|E_{(5,7)}\right| \sum_{xz\in E[\mathrm{SD}(H_m)]} (d_x+d_z) \times \left|E_{(7,7)}\right| \sum_{xz\in E[\mathrm{SD}(H_m)]} (d_x+d_z), \\ \mathrm{PM}_1[\mathrm{SD}(H_m)] &= (6m+24)(10) \times 48(m-1)(12) \times \left(42m^2-66m+24\right)(14), \\ \mathrm{PM}_1[\mathrm{SD}(H_m)] &= (60m+240) \times (576m-576) \times \left(588m^2-924m+336\right), \\ \mathrm{PM}_1[\mathrm{SD}(H_m)] &= 20321280\left(m-\frac{4}{7}\right)(m+4)(m-1)^2.\end{aligned} \tag{36}$$

□

Theorem 14. *Let $SD[H_m]$ be the strong double graph of circumcoronene series of the benzenoid graph (H_m); then, the second multiplicative-Zagreb index of $SD(H_m)$ is*

$$\mathrm{PM}_2[\mathrm{SD}(H_m)] = 518616000\left(m-\frac{4}{7}\right)(m+4)(m-1)^2. \tag{37}$$

Table 4: Computation of topological indices of strong double graph of circumcoronene series of benzenoid $(SD(H_m))$.

m	$GA(SD(H_m))$	$ABC(SD(H_m))$	$F(SD(H_m))$	$ISI(SD(H_m))$	$PM_1(SD(H_m))$	$PM_2(SD(H_m))$
1	30	16.970	1500	75	0	0
2	143.33	75.715	11232	440	1.7418×10^{8}	4.4453×10^{9}
3	340.66	176.03	29196	1099	1.3818×10^{9}	3.5266×10^{10}
4	621.99	317.91	55392	2052	5.0165×10^{9}	1.2802×10^{11}
5	987.32	501.37	89820	3299	1.2959×10^{10}	3.3073×10^{11}
6	1436.6	726.39	132480	4840	2.7579×10^{10}	7.0384×10^{11}
7	9070.0	993.00	183372	6675	5.1732×10^{10}	1.3202×10^{12}
8	2587.3	1301.1	242496	8804	8.8763×10^{10}	2.2653×10^{12}
9	3288.6	1650.9	309852	11227	1.4250×10^{11}	3.6368×10^{12}
10	4074.0	2042.2	385440	13944	2.1728×10^{11}	5.5450×10^{12}

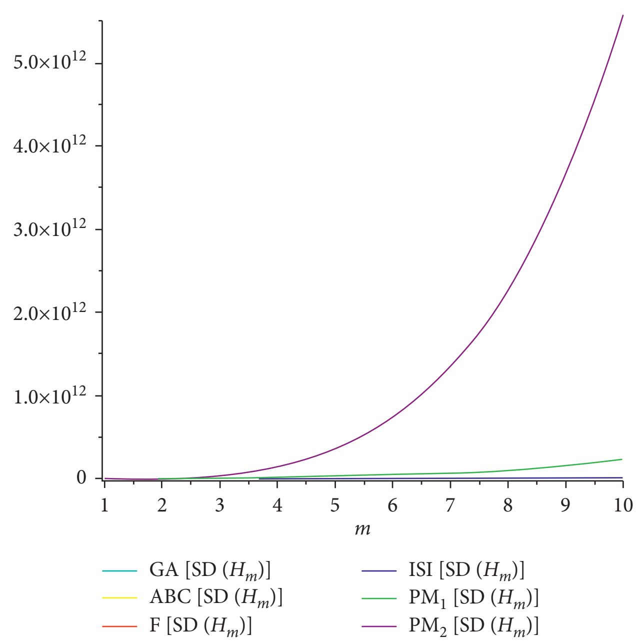

Figure 5: Graphical representation of topological indices of the strong double graph of circumcoronene series of benzenoid (H_m).

Proof. By using Table 3 and equation (9), the result that we obtain is

$$\begin{aligned}
PM_2[SD(H_m)] &= |E_{(5,5)}| \prod_{xz\in E[SD(H_m)]} (d_x\cdot d_z)\times|E_{(5,7)}| \prod_{xz\in E[SD(H_m)]} (d_x\cdot d_z)\times|E_{(7,7)}| \prod_{xz\in E[SD(H_m)]} (d_x\cdot d_z),\\
PM_2[SD(H_m)] &= (6m+24)(25)\times 48(m-1)(35)\times\left(42m^2-66m+24\right)(49),\\
PM_2[SD(H_m)] &= 252000(m+3)(m-1)\times\left(2058m^2-3234m+1176\right),\\
PM_2[SD(H_m)] &= 518616000\left(m-\frac{4}{7}\right)(m+4)(m-1)^2.
\end{aligned} \tag{38}$$

□

5. Comparison

In this section, we present a numerical and graphical comparison of topological indices that included the first multiplicative-Zagreb index (PM_1), general inverse sum indeg index ($ISI_{(\alpha,\beta)}$), atom bond connectivity index (ABC), forgotten index (F), geometric arithmetic index (GA), second multiplicative-Zagreb index (PM_2), and inverse sum indeg index (ISI) for $m = 1, 2, 3, 4, \ldots, 10$ for the strong double graph of circumcoronene series of the benzenoid graph ($SD(H_m)$), as given in Table 4 and Figure 5.

6. Conclusion

We have computed the closed formulae of topological indices such as the first multiplicative-Zagreb index (PM_1), general inverse sum indeg index ($ISI_{(\alpha,\beta)}$), atom bond connectivity index (ABC), forgotten index (F), geometric arithmetic index (GA), second multiplicative-Zagreb index (PM_2), and inverse sum indeg index (ISI) of double and strong double graphs of circumcoronene series of benzenoid H_m ($m \geq 1$). Chemical compounds can be studied by these indices in order to understand their diverse properties. The geometric structure and comparison of obtained results are shown graphically and numerically. Those results are convenient for further study as they do not include any polynomial.

Data Availability

The data used to support the findings of this study are available from the corresponding author upon request.

Conflicts of Interest

The authors declare that they have no conflicts of interest.

References

[1] R. J. Wilson, *Introduction to Graph Theory*, John Wiley & Sons, New York, NY, USA, 1986.

[2] H. Wiener, "Structural determination of paraffin boiling points," *Journal of the American Chemical Society*, vol. 69, no. 1, pp. 17–20, 1947.

[3] B. Furtula and D. Vukicevic, "Topological index based on the ratios of geometrical and arithmetical mean of end-vertex degrees of edge," *Journal of Mathematical Chemistry*, pp. 1369–1376, 2009.

[4] K. Das, I. Gutman, and B. Furtula, "On atom–bond connectivity index," *Filomat*, vol. 26, no. 4, pp. 733–738, 2012.

[5] B. Furtula and I. Gutman, "A forgotten topological index," *Journal of Mathematical Chemistry*, vol. 53, no. 4, pp. 1184–1190, 2015.

[6] K. Pattabiraman, "Inverse sum indeg index of graphs," *AKCE International Journal of Graphs and Combinatorics*, vol. 15, no. 2, pp. 155–167, 2018.

[7] P. Ali, S. A. K. Kirmani, O. Al Rugaie, and F. Azam, "Degree-based topological indices and polynomials of hyaluronic acid-curcumin conjugates," *Saudi Pharmaceutical Journal*, vol. 28, no. 9, pp. 1093–1100, 2020.

[8] R. Kazemi, "Note on the multiplicative Zagreb indices," *Discrete Applied Mathematics*, vol. 198, pp. 147–154, 2016.

[9] M. Eliasi, A. Iranmanesh, and I. Gutman, "Multiplicative versions of first zagreb index," *MATCH Communications in Mathematical Nd in Computer Chemistry*, vol. 68, no. 1, pp. 217–230, 2012.

[10] M. Imran, S. Akhter, and Z. Iqbal, "On eccentric polynomial of F-Sum of connected graphs," *Compllexity*, vol. 2020, Article ID 5061682, 9 pages, 2020.

[11] M. Imran, S. Akhter, and Z. Iqbal, "Edge mostar index of chemical structures and nanostructures using graph operations," *Iternational Journal of Quantum Chemistry*, vol. 120, no. 15, 2020.

[12] S. Akhter, M. Imran, and Z. Iqbal, "Moster indices of SiO nanostructures andmelem chain nanostructures," *International Journal of Quantum Chemistry*, vol. 121, no. 5, 2020.

[13] M. An and L. Xiong, "Some results on the inverse sum indeg index of a graph," *Information Processing Letters*, vol. 134, pp. 42–46, 2018.

[14] G. Hong, Z. Gu, M. Javid, H. M. Awais, and M. K. Siddiqui, "Degree based topological invariants of metal-organic networks," *IEEE Access*, vol. 8, pp. 68288–68300, 2020.

[15] M. Alaeiyan, M. S. Sardar, S. Zafar, and Z. Zahid, "Computation of topological indices of line graph of jahangir graph," *International Journal of Applied Mathematics*, vol. 12, 2018.

[16] D. K. Ch, M. Marjan, M. Emina, and M. Igor, "Bonds for symmetric division deg index of graphs," *Faculty of Sciences and Mathematics*, vol. 33, no. 3, pp. 638–698, 2019.

[17] M. S. Sardar, S. Zafar, and Z. Zahid, "Certain topological indices of line graph of Dutch windmill graphs," *Southeast Asian Bulletin of Mathematics*, pp. 119–129, 2020.

[18] Y. Gao, M. R. Farahani, and W. Nazeer, "On topological indices of circumcoronene series of benzenoid," *Chemmical Methdologies*, pp. 39–46, 2018.

[19] Y. Gao, M. R. Farahani, M. S. Sardar, and S. Zafar, "On the sanskruti index of circumcoronene series of benzenoid," *Applied Mathematics*, vol. 08, no. 04, pp. 520–524, 2017.

[20] M. A. Ali, M. S. Sardar, I. Siddique, and D. Alrowaili, "Vertex-based topological indices of double and strong double graph of Dutch windmill graph," *Journal of Chemistry*, vol. 2021, p. 12, 2021.

[21] T. A. Chishti, H. A. Ganie, and S. Pirzada, "Properties of strong double graphs," *Journal of Discrete Mathematical Sciences and Cryptography*, vol. 17, no. 4, pp. 311–319, 2014.

Hindawi
Journal of Mathematics
Volume 2022, Article ID 8325139, 5 pages
https://doi.org/10.1155/2022/8325139

Research Article

Some Bond Incident Degree Indices of Cactus Graphs

Akbar Ali[1] **Akhlaq Ahmad Bhatti,**[2] **Naveed Iqbal**[1] **Tariq Alraqad**[1]
Jaya Percival Mazorodze[3] **Hicham Saber,**[1] **and Abdulaziz M. Alanazi**[4]

[1]*Department of Mathematics, Faculty of Science, University of Ha'il, Ha'il, Saudi Arabia*
[2]*Department of Sciences and Humanities, National University of Computer and Emerging Sciences, Lahore Campus, B-Block, Faisal Town, Lahore, Pakistan*
[3]*Department of Mathematics, University of Zimbabwe, Harare, Zimbabwe*
[4]*School of Mathematics, University of Tabuk, Tabuk 71491, Saudi Arabia*

Correspondence should be addressed to Jaya Percival Mazorodze; mazorodzejaya@gmail.com

Received 13 October 2021; Accepted 21 December 2021; Published 21 January 2022

Academic Editor: M. T. Rahim

Copyright © 2022 Akbar Ali et al. This is an open access article distributed under the Creative Commons Attribution License, which permits unrestricted use, distribution, and reproduction in any medium, provided the original work is properly cited.

A connected graph in which no edge lies on more than one cycle is called a cactus graph (also known as Husimi tree). A bond incident degree (BID) index of a graph G is defined as $\sum_{uv\in E(G)} f(d_G(u), d_G(v))$, where $d_G(w)$ denotes the degree of a vertex w of G, $E(G)$ is the edge set of G, and f is a real-valued symmetric function. This study involves extremal results of cactus graphs concerning the following type of the BID indices: $I_{f_i}(G) = \sum_{uv\in E(G)} [f_i(d_G(u))/d_G(u) + f_i(d_G(v))/d_G(v)]$, where $i \in \{1, 2\}$, f_1 is a strictly convex function, and f_2 is a strictly concave function. More precisely, graphs attaining the minimum and maximum I_{f_i} values are studied in the class of all cactus graphs with a given number of vertices and cycles. The obtained results cover several well-known indices including the general zeroth-order Randić index, multiplicative first and second Zagreb indices, and variable sum exdeg index.

1. Introduction

All the graphs considered in this study are connected. The notation and terminology that are used in this study but not defined here can be found in some standard graph-theoretical books [6, 7].

Graph invariants of the following form are known as the bond incident degree (BID) indices [5]:

$$BID(G) = \sum_{uv\in E(G)} f(d_G(u), d_G(v)), \tag{1}$$

where $d_G(w)$ denotes the degree of a vertex $w \in V(G)$ of the graph G, $E(G)$ is the edge set of G, and f is a real-valued symmetric function. In this study, we are concerned with the following type [2] of the BID indices:

$$I_{f_i}(G) = \sum_{uv\in E(G)} \left[\frac{f_i(d_G(u))}{d_G(u)} + \frac{f_i(d_G(v))}{d_G(v)}\right] = \sum_{v\in V(G)} f_i(d_G(v)) \tag{2}$$

where $i \in \{1, 2\}$, f_1 is a strictly convex function, and f_2 is a strictly concave function.

A connected graph in which no edge lies on more than one cycle is called a cactus graph (also known as Husimi tree [9]). In the present study, we study the graphs attaining the minimum and maximum I_{f_i} values from the class of all cactus graphs with a given number of vertices and cycles. Our main results cover the general zeroth-order Randić index ${}^0R_\alpha$ [3], variable sum exdeg index SEI_a [13], multiplicative first Zagreb index Π_1 [8], multiplicative second Zagreb index Π_2 [1, 8, 10], and sum lordeg index SL [12, 14], where the aforementioned indices for a graph G are defined as follows:

$${}^0R_\alpha(G) = \sum_{v\in V(G)} [d_G(v)]^\alpha,$$

$$SEI_a(G) = \sum_{v\in V(G)} d_G(v) a^{d_G(v)},$$

$$\Pi_1(G) = \prod_{v \in V(G)} [d_G(v)]^2,$$

$$\Pi_2(G) = \prod_{uv \in E(G)} d_G(u) d_G(v) = \prod_{v \in V(G)} [d_G(v)]^{d_G(v)},$$

$$SL(G) = \sum_{v \in V(G)} d_G(v) \sqrt{\ln[d_G(v)]}$$

$$= \sum_{v \in V(G); d_G(v) \geq 2} d_G(v) \sqrt{\ln[d_G(v)]}. \tag{3}$$

A graph in which every vertex has degree less than 5 is known as a chemical graph.

Although we cannot apply our main result on the Lanzhou index [15] for finding the extremal graphs from the class of all cactus graphs, we still are able to utilize one of our main results for finding the graphs having the minimum Lanzhou index among all chemical cactus graphs, where the Lanzhou index for a graph G is defined as

$$Lz(G) = \sum_{v \in V(G)} (n - d_G(v) - 1)[d_G(v)]^2. \tag{4}$$

We end this section with the remark that the Lanzhou index is same [11] as the graph invariant ${}^0R_3$.

2. Main Results

By an n-vertex graph, we mean a graph of order n. In a graph, a set of pairwise nonadjacent edges is called a matching. The elements of a matching are known as independent edges.

Theorem 1. *The graph formed by adding r-independent edges in the n-vertex star S_n (Figure 1) uniquely attains the maximum I_{f_1} value and minimum I_{f_2} value in the class of all n-vertex cactus graphs having r cycles, where n and r are the fixed integers satisfying the inequalities $n \geq 2r + 1$, $n \geq 4$, and $r \geq 0$.*

Proof. We prove the result for the graph invariant I_{f_1}. The result regarding the other invariant can be proved in a fully analogous way. Let G be a graph having the maximum I_{f_1} value in the given class of graphs. It is enough to show that G has the maximum degree $n-1$. Contrarily, we assume that that the maximum degree of G is at most $n-2$. Let $v \in V(G)$ be a vertex of maximum degree. Then, there exists at least one neighbor, say w of v which has at least one neighbor not adjacent to v. Let $w_1, w_2, \ldots, w_k$ be those neighbors of w that are not adjacent to v. If G' is the graph formed by adding the edges $w_1v, w_2v, \ldots, w_kv$ in G and removing the edges $w_1w, w_2w, \ldots, w_kw$ from G (Figure 2), then we have

$$\begin{aligned} I_{f_1}(G) - I_{f_1}(G') = f_1(d_G(v)) - f_1(d_G(v) + k) \\ + f_1(d_G(w)) - f_1(d_G(w) - k). \end{aligned} \tag{5}$$

Note that the cactus graphs G and G' have the same number of cycles as well as order. By using Lagrange's mean

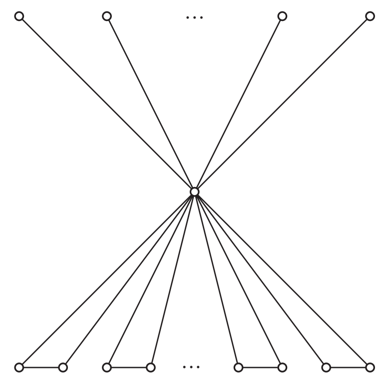

Figure 1: The extremal graph mentioned in Theorem 1.

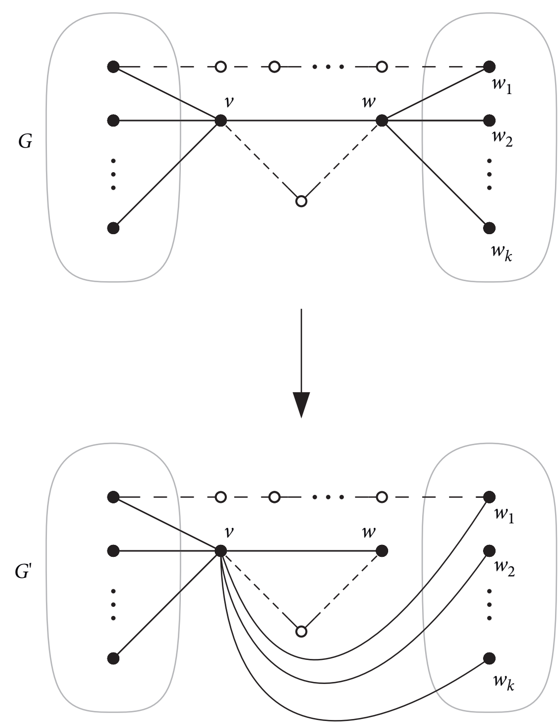

Figure 2: The graph transformation used in the proof of Theorem 1. The white vertices and doted edges may or may not exist provided that every edge lies on at most one cycle.

value theorem, we conclude that there exist real numbers a_1 and a_2, such that

$$\begin{aligned} a_1 &\in (d_G(w) - k, d_G(w)), \\ a_2 &\in (d_G(v), d_G(v) + k), \\ I_{f_1}(G) - I_{f_1}(G') &= k[f_1'(a_1) - f_1'(a_2)]. \end{aligned} \tag{6}$$

The fact $d_G(w) \leq d_G(v)$ implies that $a_1 < a_2$, which further implies that the right hand side of equation (6) is negative because f_1 is a strictly convex function. Thus, one has $I_{f_1}(G) - I_{f_1}(G') < 0$, a contradiction to the maximality of $I_{f_1}(G)$. □

Corollary 1. *In the class of all n-vertex cactus graphs having r cycles, the graph formed by adding r independent edges in the n-vertex star S_n uniquely attains the maximum general zeroth-order Randić index ${}^0R_\alpha$ for $\alpha > 1$ or $\alpha < 0$, maximum variable sum exdeg index SEI_a for $a > 1$, maximum multiplicative second Zagreb index Π_2, maximum sum lordeg index SL, minimum general zeroth-order Randić index ${}^0R_\alpha$ for $0 < \alpha < 1$, and minimum multiplicative first Zagreb index Π_1, where n and r are the fixed integers satisfying the inequalities $n \geq 2r + 1$, $n \geq 4$, and $r \geq 0$.*

Proof. We observe that a graph G attains its maximum Π_2 value or minimum Π_1 value in a class of graphs if and only if G attains its maximum $\ln \Pi_2$ value or minimum $\ln \Pi_1$ value, respectively, in the considered class of graphs. We define $\phi_1(x) = xa^x$ with $a > 1$ and $x \geq 1$; $\phi_2(x) = x^\alpha$ with $x \geq 1$ and $\alpha > 1$ or $\alpha < 0$; $\phi_3(x) = x \ln x$ with $x \geq 1$; $\phi_4(x) = x\sqrt{\ln x}$ with $x \geq 2$; $\phi_5(x) = 2 \ln x$ with $x \geq 1$; and $\phi_6(x) = x^\alpha$ with $x \geq 1$ and $0 < \alpha < 1$. It can be easily verified that for each $i \in \{1, 2, 3, 4\}$, ϕ_i is strictly convex and for each $j \in \{5, 6\}$, ϕ_j is strictly concave. Thus, the required conclusion follows from Theorem 1.

A graph of order n and size m is called an (n, m)-graph. □

Lemma 2 (see [4]). *If G attains the minimum I_{f_1} value or maximum I_{f_2} value among all connected (n, m)-graphs and $v \in V(G)$, then the minimum degree of G is at least 2, where n and m are the fixed integers satisfying the conditions $3n \geq 2m$, $n \geq 4$, and $m \geq n$.*

The next result is a direct consequence of Lemma 2.

Corollary 3. *If G is a graph attaining the minimum I_{f_1} value or maximum I_{f_2} value in the class of all n-vertex cactus graphs having r cycles, then the minimum degree of G is 2, where n and r are the fixed integers satisfying the inequalities $n \geq 2r + 1$, $n \geq 6$, and $r \geq 2$.*

Denote by $N_G(v)$ the set of neighbors of a vertex $v \in V(G)$ of a graph G.

Theorem 2. *If G is a graph attaining the minimum I_{f_1} value or maximum I_{f_2} value in the class of all n-vertex cactus graphs having r cycles and $v \in V(G)$, then the minimum degree of G is 2 and*

$$d_G(v) \leq \begin{cases} 4, & \text{if } v \text{ lies on some cycle}, \\ 3, & \text{otherwise}, \end{cases} \tag{7}$$

where n and r are the fixed integers satisfying the inequalities $n \geq 2r + 1$, $n \geq 6$, and $r \geq 2$.

Proof. We prove the result for the graph invariant I_{f_1}. The result regarding the other invariant can be proved in a fully analogous way. Let G be a graph having the minimum I_{f_1} value in the given class of graphs.

From Corollary 3, it follows that the minimum degree of G is 2. Next, we prove that

$$d_G(v) \leq \begin{cases} 4, & \text{if } v \text{ lies on some cycle}, \\ 3, & \text{otherwise}, \end{cases} \tag{8}$$

First, assume that v lies one some cycle C of G. Suppose to the contrary that $d_G(v) \geq 5$. Let $N_G(v) \backslash V(C) := \{v_1, v_2, \ldots, v_r\}$, where $V(C)$ denotes the set of vertices of the cycle C. For $i = 1, 2, \ldots, r$, denote by M_i the component of the graph $G - \{v\}$ containing the vertex v_i. It is claimed that no more than two vertices of $N_G(v) \setminus V(C)$ lie on the same component of the graph $G - \{v\}$; if v_k, v_l, and v_m lie on the same component of the graph $G - \{v\}$, then the vertices v_k, v_l, v_m, and v lie on a cycle whose each edge belongs to more than one cycle of G, which contradicts the definition of G. □

Case 1. There exists at least one i, such that the component M_i contains a unique vertex of $N_G(v) \setminus V(C)$.

Suppose, without loss of generality, that the component M_1 contains none of $v_2, v_3, \ldots, v_r$. We note that there exists at least one component M_j with $j \geq 2$, such that M_j contains at least one vertex $u \in V(G)$ satisfying $d_G(u) = 2$. Certainly, both the graphs G and $G' \cong G - \{vv_1\} + \{uv_1\}$ have the same number of cycles and vertices. On the other hand, we have

$$\begin{aligned} I_{f_1}(G) - I_{f_1}(G') &= f_1(d_G(v)) - f_1(d_G(v) - 1) \\ &\quad + f_1(d_G(u)) - f_1(d_G(u) + 1) \\ &= f_1(d_G(v)) - f_1(d_G(v) - 1) \\ &\quad - [f_1(3) - f_1(2)]. \end{aligned} \tag{9}$$

By using Lagrange's mean value theorem, we conclude that there exist real numbers a_1 and a_2, such that

$$\begin{aligned} a_1 &\in (2, 3), \\ a_2 &\in (d_G(v) - 1, d_G(v)), \\ I_{f_1}(G) - I_{f_1}(G') &= f_1'(a_2) - f_1'(a_1). \end{aligned} \tag{10}$$

The assumption $d_G(v) \geq 5$ implies that $a_1 < a_2$, which further implies that the right hand side of equation (2) is positive because f_1 is a strictly convex function. Thus, one has $I_{f_1}(G) - I_{f_1}(G') > 0$, a contradiction to the minimality of $I_{f_1}(G)$.

Case 2. For each $i \in \{1, 2, \ldots, r\}$, exactly two vertices of the set $N_G(v) \setminus V(C)$ lie on the component M_i.

Suppose, without loss of generality, that $M_1 = M_2$. It is clear that $M_1 \neq M_j$ for each $j \in \{3, \ldots, r\}$, and there exists at least one component M_j with $j \geq 3$, such that M_j contains at least one vertex $w \in V(G)$ satisfying $d_G(w) = 2$. It is obvious that both the graphs G and $G'' \cong G - \{vv_1, vv_2\} + \{wv_1, wv_2\}$ have the same number of cycles and vertices. On the other hand, we have

$$\begin{aligned} I_{f_1}(G) - I_{f_1}(G'') &= f_1(d_G(v)) - f_1(d_G(v) - 2) \\ &\quad + f_1(d_G(w)) - f_1(d_G(w) + 2) \\ &= f_1(d_G(v)) - f_1(d_G(v) - 2) \\ &\quad - [f_1(4) - f_1(2)]. \end{aligned} \tag{11}$$

By using Lagrange's mean value theorem, we conclude that there exist real numbers a_3 and a_4, such that

$$\begin{aligned} a_3 &\in (2,4),\\ a_4 &\in \left(d_G(v)-2, d_G(v)\right),\\ I_{f_1}(G)-I_{f_1}(G'') &= 2\left[f_1'(a_4)-f_1'(a_3)\right]. \end{aligned} \tag{12}$$

We note, for the present case, that the degree of v is at least 6, which implies that $a_3 < a_4$, which further implies that the right hand side of (12) is positive because f_1 is a strictly convex function. Thus, one has $I_{f_1}(G) - I_{f_1}(G'') > 0$, a contradiction to the minimality of $I_{f_1}(G)$.

Thus, $d_G(v) \le 4$ when v lies on some cycle of G.

It is still left to prove that $d_G(v) \le 3$ when v does not belong to any cycle of G. Suppose to the contrary that $d_G(v) = r \ge 4$ and that v does not belong to any cycle of G. As before, we take $N_G(v) = \{v_1, v_2, \ldots, v_r\}$, and for $i \in \{1, 2, \ldots, r\}$, we denote by M_i the component of the graph $G - v$ containing the vertex v_i. We observe that $M_i \ne M_j$ whenever $i \ne j$; if the components M_i and M_j are the same for some $i \ne j$, then the path from v_i to v_j in $G - \{v\}$ together with the path $v_i v v_j$ yields a cycle in G containing v, which is a contradiction. We note that there exists at least one component M_j with $j \ge 2$, such that M_j contains at least one vertex $x \in V(G)$ satisfying $d_G(x) = 2$. It is obvious that both the graphs G and $G''' \cong G - \{v_1 v\} + \{v_1 x\}$ have the same number of cycles and vertices. On the other hand, we have

$$\begin{aligned} I_{f_1}(G)-I_{f_1}(G'') &= f_1\left(d_G(v)\right)-f_1\left(d_G(v)-1\right)\\ &\quad+f_1\left(d_G(x)\right)-f_1\left(d_G(x)+1\right)\\ &= f_1\left(d_G(v)\right)-f_1\left(d_G(v)-1\right)\\ &\quad-\left[f_1(3)-f_1(2)\right]. \end{aligned} \tag{13}$$

By using Lagrange's mean value theorem, we conclude that there exist real numbers a_5 and a_6, such that

$$\begin{aligned} a_5 &\in (2,3),\\ a_6 &\in \left(d_G(v)-1, d_G(v)\right),\\ I_{f_1}(G)-I_{f_1}(G'') &= f_1'(a_6)-f_1'(a_5). \end{aligned} \tag{14}$$

The assumption $d_G(v) \ge 4$ implies that $a_3 < a_4$, which further implies that the right hand side of equation (4) is positive because f_1 is a strictly convex function. Thus, one has $I_{f_1}(G) - I_{f_1}(G'') > 0$, a contradiction to the minimality of $I_{f_1}(G)$. Thus, $d_G(v) \le 3$ when v does not belong to any cycle of G.

Corollary 4. *If G is a graph attaining the minimum general zeroth-order Randić index ${}^0R_\alpha$ for $\alpha > 1$ or $\alpha < 0$, minimum variable sum exdeg index SEI_a for $a > 1$, minimum multiplicative second Zagreb index Π_2, minimum sum lordeg index SL, maximum general zeroth-order Randić index ${}^0R_\alpha$ for $0 < \alpha < 1$, and maximum multiplicative first Zagreb index Π_1, in the class of all n-vertex cactus graphs having r cycles and $v \in V(G)$, then the minimum degree of G is 2 and*

$$d_G(v) \le \begin{cases} 4, & \text{if } v \text{ lies on some cycle},\\ 3, & \text{otherwise}, \end{cases} \tag{15}$$

where n and r are the fixed integers satisfying the inequalities $n \ge 2r + 1$, $n \ge 6$, and $r \ge 2$.

Proof. We observe that a graph G attains its minimum Π_2 value or maximum Π_1 value in a class of graphs if and only if G attains its minimum $\ln \Pi_2$ value or maximum $\ln \Pi_1$ value, respectively, in the considered class of graphs. We define $\phi_1(x) = xa^x$ with $a > 1$ and $x \ge 1$; $\phi_2(x) = x^\alpha$ with $x \ge 1$ and $\alpha > 1$ or $\alpha < 0$; $\phi_3(x) = x \ln x$ with $x \ge 1$; $\phi_4(x) = x\sqrt{\ln x}$ with $x \ge 2$; $\phi_5(x) = 2 \ln x$ with $x \ge 1$; and $\phi_6(x) = x^\alpha$ with $x \ge 1$ and $0 < \alpha < 1$. It can be easily verified that for each $i \in \{1, 2, 3, 4\}$, ϕ_i is strictly convex, and for each $j \in \{5, 6\}$, ϕ_j is strictly concave. Thus, the required conclusion follows from Theorem 2.

We observe that the function $\psi(x) = (n - 1 - x)x^2$ is strictly convex for $x < (n - 1)/3$. Thus, we have the next corollary regarding the Lanzhou index. □

Corollary 5. *If G is a graph attaining the minimum Lanzhou index in the class of all n-vertex chemical cactus graphs having r cycles and $v \in V(G)$, then the minimum degree of G is 2 and*

$$d_G(v) \le \begin{cases} 4, & \text{if } v \text{ lies on some cycle},\\ 3, & \text{otherwise}, \end{cases} \tag{16}$$

where n and r are the fixed integers satisfying the inequalities $n \ge 2r + 1$, $n \ge 6$, and $r \ge 2$.

Data Availability

The data used to support the findings of this study are available from the corresponding author upon request.

Conflicts of Interest

The authors declare that they have no conflicts of interest.

Acknowledgments

This research was funded by Scientific Research Deanship at University of Ha'il, Saudi Arabia, through project number RG-20 031.

References

[1] I. R. Abdolhosseinzadeh, F. Rahbarnia, and M. Tavakoli, "Some indices of edge corona of two graphs," *Applied Mathematics E-Notes*, vol. 18, pp. 13–24, 2018.
[2] A. Ali, *Some vertex-degree-based topological indices of graphs*, PhD thesis, National University of Computer and Emerging Sciences, Lahore, Pakistan, 2016.
[3] A. Ali, I. Gutman, E. Milovanović, and I. Milovanović, "Sum of powers of the degrees of graphs: extremal results and bounds," *MATCH Communications in Mathematical and in Computer Chemistry*, vol. 80, pp. 5–84, 2018.
[4] A. Ali, I. Gutman, I. Gutman, H. Saber, and A. Alanazi, "On bond incident degree indices of (n,m) -graphs," *Match*

Communications in Mathematical and in Computer Chemistry, vol. 87, no. 1, pp. 89–96, 2022.

[5] A. Ali, Z. Raza, and A. A. Bhatti, "Bond incident degree (BID) indices of polyomino chains: a unified approach," *Applied Mathematics and Computation*, vol. 287-288, pp. 28–37, 2016.

[6] J. A. Bondy and U. S. R. Murty, *Graph Theory*, Springer, London, UK, 2008.

[7] G. Chartrand, L. Lesniak, and P. Zhang, *Graphs & Digraphs*, CRC Press, Boca Raton, FL, USA, 2016.

[8] I. Gutman, "Multiplicative Zagreb indices of trees," *Bulletin of International Mathematical Virtual Institute*, vol. 1, pp. 13–19, 2011.

[9] F. Harary and G. E. Uhlenbeck, "On the number of Husimi trees: I," *Proceedings of the National Academy of Sciences*, vol. 39, no. 4, pp. 315–322, 1953.

[10] A. Iranmanesh, M. Hosseinzadeh, and I. Gutman, "On multiplicative Zagreb indices of graphs," *Iranian Journal of Mathematical Chemistry*, vol. 3, pp. 145–154, 2012.

[11] I. Milovanović, M. Matejić, and E. Milovanović, "A note on the general zeroth-order Randić coindex of graphs," *Contributions to Mathematics*, vol. 1, pp. 17–21, 2020.

[12] I. Tomescu, "Properties of connected -graphs extremal relatively to vertex degree function index for convex functions," *MATCH Communications in Mathematical and in Computer Chemistry*, vol. 85, pp. 285–294, 2021.

[13] B. Vukičević, "Bond additive modeling 4. QSPR and QSAR studies of the variable Adriatic indices," *Croatica Chemica Acta*, vol. 84, pp. 87–91, 2011.

[14] D. Vukičević and M. Gašperov, "Bond additive modeling 1. Adriatic indices," *Croatica Chemica Acta*, vol. 83, pp. 43–260, 2010.

[15] D. Vukičević, Q. Li, J. Sedlar, and T. Došlić, "Lanzhou index," *MATCH Communications in Mathematical and in Computer Chemistry*, vol. 80, pp. 863–876, 2018.

Hindawi
Journal of Mathematics
Volume 2022, Article ID 5946616, 9 pages
https://doi.org/10.1155/2022/5946616

Research Article

Energy of Certain Classes of Graphs Determined by Their Laplacian Degree Product Adjacency Spectrum

Asim Khurshid,[1] Muhammad Salman ,[1] Masood Ur Rehman ,[2] and Mohammad Tariq Rahim [3]

[1] *Department of Mathematics, The Islamia University of Bahawalpur, Bahawalpur 63100, Pakistan*
[2] *Department of Mathematics, University College of Zhob, BUITEMS, Zhob 85200, Pakistan*
[3] *Department of Mathematics, Abbottabad University of Science and Technology, Abbottabad 22010, Pakistan*

Correspondence should be addressed to Mohammad Tariq Rahim; tariq.rahim@nu.edu.pk

Received 9 October 2021; Accepted 11 December 2021; Published 10 January 2022

Academic Editor: Feng Feng

Copyright © 2022 Asim Khurshid et al. This is an open access article distributed under the Creative Commons Attribution License, which permits unrestricted use, distribution, and reproduction in any medium, provided the original work is properly cited.

In this study, we investigate the Laplacian degree product spectrum and corresponding energy of four families of graphs, namely, complete graphs, complete bipartite graphs, friendship graphs, and corona products of 3 and 4 cycles with a null graph.

1. Introduction

The graph energy was firstly introduced by Ivan Gutman in 1978 [1]. His idea was motivated by the well-known Hückel molecular orbital theory by Erich Hückel in 1930s, which permits pharmacologists to imprecise energies associated π-electron orbital of molecules called conjugated hydrocarbons [2]. The spectrum and the energy of a graph have significant applications and connections in the branches of Mathematics, such as linear algebra and combinatorial optimization fields which have lot to do with graph spectrum and energy. The combinatorial and graph theoretical approaches have strong bonding to solve real-life problems. Many results and methods from the spectral graph theory can be applied for the practicalities and evolution of matrix theory [3]. An ordered pair $\Gamma = (V, E)$, called a graph with vertex set of Γ, is denoted by V and its edge set by E. Two vertices u, v are adjacent if they make an edge in Γ, and we denote it by $u \sim v$. The number of edges incident to a vertex v of Γ is the degree of v, and it is denoted by $d(v)$ [4, 5]. The adjacency matrix of Γ, of order n denoted by $A(\Gamma)$, is a square symmetric matrix of order $n \times n$ whose ijth element can be found as [3]

$$a_{ij} = \begin{cases} 0, & \text{if } u \nsim v, \\ \text{number of edges between } u \text{ and } v, & \text{if } u \sim v. \end{cases} \tag{1}$$

For energy and spectrum of graph Γ, let $A(\Gamma)$ be the adjacency matrix, the summation of absolute values of its eigenvalues compose energy of graph and these eigenvalues related with their multiplicities forms the spectrum of graph [4], i.e.,

$$Sp(\Gamma) = \begin{pmatrix} \lambda_1 & \lambda_2 & \ldots & \lambda_n \\ n(\lambda_1) & n(\lambda_2) & \ldots & n(\lambda_n) \end{pmatrix}, \tag{2}$$

and

$$E(\Gamma) = \sum_{i=1}^{n} |\lambda_i|, \tag{3}$$

where $n(\lambda_1), n(\lambda_2), \ldots, n(\lambda_n)$ are the multiplicities of the eigenvalues $\lambda_1, \lambda_2, \ldots, \lambda_n$ of $A(\Gamma)$. In [6], the degree product adjacency matrix, for a simple connected graph Γ having n vertices say $v_1, v_2, \ldots, v_n$, is a real symmetric matrix, denoted by $DP\ A(\Gamma) = [d_{ij}]$,1 with

$$d_{ij} = \begin{cases} d(v_i)d(v_j), & \text{if } v_i \sim v_j, \\ 0, & \text{otherwise.} \end{cases} \quad (4)$$

The Laplacian degree product adjacency matrix of Γ is defined as

$$L_{DP\ A}(\Gamma) = DP\ A(\Gamma) - D(\Gamma), \quad (5)$$

where $D(\Gamma)$ is the degree matrix of Γ having diagonal entries as the degree of each vertex and all other entries are zero. The spectrum (1) and energy (2) obtained correspond to the eigenvalues of $L_{DP\ A}(\Gamma)$ and are called the Laplacian degree product adjacency spectrum and energy, $LSp_{DP\ A}(\Gamma)$ and $LE_{DP\ A}(\Gamma)$, respectively [7], as the degree sum concept was conceived earlier in [8].

2. Main Results

In this module, we study the Laplacian degree product adjacency spectrum and energy of some well-known families of graphs, such as complete graphs, complete bipartite graphs, friendship graphs, and corona products of 3 and 4 cycles with null graph. We also evaluate the correct spectrum and the energy of degree product adjacency matrix of the corona product of 4 cycle with null graphs (thorny 4-cycle ring), which was found incorrect in [6].

2.1. Complete Graphs K_x. Let $\{v_1, v_2 \ldots, v_x\}$ be the vertex set of K_x; then, the following result provides the Laplacian degree product adjacency spectrum and energy of K_x.

Theorem 1. *For $x \geq 2$, let K_x be a complete graph. Then,*

$$LSp_{DP\ A}(K_x) = \begin{pmatrix} x(x^2-3x+2) & x(1-x) \\ 1 & x-1 \end{pmatrix}, \quad (6)$$

and Laplacian degree product adjacency energy of K_x is $2(2x-3)$-times the size of K_x.

Proof. First of all note that $d(v_i) = x-1$, for each $1 \leq i \leq x$. Accordingly, we have the following Laplacian degree product adjacency matrix:

$$L_{DP\ A}(K_x) = \begin{array}{c} \\ v_1 \\ v_2 \\ v_3 \\ \cdots \\ v_x \end{array} \begin{pmatrix} v_1 & v_2 & v_3 & \cdots & v_x \\ (1-x) & (1-x)^2 & (1-x)^2 & \ldots & (1-x)^2 \\ (1-x)^2 & (1-x) & (1-x)^2 & \ldots & (1-x)^2 \\ (1-x)^2 & (1-x)^2 & (1-x) & \ldots & (1-x)^2 \\ \vdots & \vdots & \vdots & \ddots & \vdots \\ (1-x)^2 & (1-x)^2 & (1-x)^2 & \ldots & (1-x) \end{pmatrix}. \quad (7)$$

Eigenvalues of $L_{DP\ A}(K_x)$ are

$$\begin{aligned} &x(1-x), (x-1) - \text{times}, \\ &x(x^2-3x+2), 1 - \text{time}. \end{aligned} \quad (8)$$

These eigenvalues provide the required spectrum. Moreover, by (3), we have

$$\begin{aligned} LE_{DP\ A}(K_x) &= (x-1)|x(1-x)| + \left|x(x^2-3x+2)\right| \\ &= 2(2x-3)\begin{pmatrix} x \\ 2 \end{pmatrix}. \end{aligned} \quad (9)$$

Since the size of K_x is $\begin{pmatrix} x \\ 2 \end{pmatrix}$, so the result is proved. □

2.2. Complete Bipartite Graphs $K_{x,y}$. Let a complete bipartite graph $K_{x,y}$ with vertex sets $V_x(\Gamma) = \{v_1, v_2, \ldots, v_x\}$ and $V_y(\Gamma) = \{v_{x+1}, v_{x+2}, \ldots, v_y\}$ be as partitions. The order and the size of $K_{x,y}$ graph are $x+y$ and xy, respectively. Then, the Laplacian degree product adjacency spectrum and energy of $K_{x,y}$ can be obtained from the following result.

Theorem 2. *For $x, y \geq 1$, a complete bipartite graph $K_{x,y}$, then*

$$LSp_{DP\,A}\left(K_{x,y}\right)=\begin{cases}\begin{pmatrix}\dfrac{-(x+y)}{2}\pm\dfrac{1}{2}\sqrt{4y^3x^3+1} & -x & -y\\ 1 & y-1 & x-1\end{pmatrix}, & y=x+1 \text{ with } x\geq 1,\\ \begin{pmatrix}\dfrac{-(x+y)}{2}\pm\dfrac{1}{2}\sqrt{4y^3x^3+(y-x)^2} & -x & -y\\ 1 & y-1 & x-1\end{pmatrix}, & y>x\geq 1 \text{ with } y\neq x+1,\\ \begin{pmatrix}x\left(x^2-1\right) & -x\left(x^2+1\right) & -x\\ 1 & 1 & 2(x-1)\end{pmatrix}, & x=y\geq 1,\\ \begin{pmatrix}\dfrac{-(1+y)}{2}\pm\dfrac{1}{2}\sqrt{4y^3+(1-y)^2} & -1\\ 1 & y-1\end{pmatrix} & x=1 \text{ and } y\geq 1.\end{cases} \tag{10}$$

Moreover,

$$LE_{DP\,A}\left(K_{x,y}\right)=\begin{cases}2\left(x^3+x^2-x\right), & \text{whenever } x=y\geq 1,\\ 2xy, & \text{otherwise.}\end{cases} \tag{11}$$

Proof. Note that $d(v_i)=y$, for each $1\leq i\leq x$ and $d(v_j)=x$, for each $x+1\leq j\leq y$. Accordingly, the Laplacian degree product adjacency matrix of $K_{x,y}$ is

$$L_{DP\,A}\left(K_{x,y}\right)=\begin{array}{c} \\ v_1\\ v_2\\ v_3\\ \vdots\\ v_x\\ v_{x+1}\\ v_{x+2}\\ \vdots\\ v_{x+y}\end{array}\left(\begin{array}{cccccccc} v_1 & v_2 & v_3 & \vdots & v_x & v_{x+1} & v_{x+2} \cdots & v_{x+y}\\ -y & 0 & 0 & \ldots & 0 & xy & xy\ \ldots & xy\\ 0 & -y & 0 & \ldots & 0 & xy & xy\ \ldots & xy\\ 0 & 0 & -y & \ldots & 0 & xy & xy\ \ldots & xy\\ \vdots & \ldots & \ldots & \ddots & \ldots & \ldots & \ldots\ \ldots & \vdots\\ 0 & 0 & 0 & \ldots & -y & xy & xy\ \ldots & xy\\ xy & xy & xy & \ldots & xy & -x & 0\ \ldots & 0\\ xy & xy & xy & \ldots & xy & 0 & -x\ \ldots & 0\\ \vdots & \ldots & \ldots & \ddots & \ldots & \ldots & \ldots\ \ddots & \vdots\\ xy & xy & xy & \ldots & xy & 0 & 0\ \ldots & -x\end{array}\right). \tag{12}$$

Next, we have four cases to discuss.

Case I ($y=x+1$ with $x\geq 1$): eigenvalues of $L_{DP\,A}(K_{x,y})$ are

$$\begin{aligned}&\frac{-(y+x)}{2}\pm\frac{1}{2}\sqrt{4y^3x^3+1}1-\text{time},\\ &-x(y-1)-\text{times},\\ &-y(x-1)-\text{times}.\end{aligned} \tag{13}$$

The required spectrum can be obtained by these eigenvalues. Furthermore, by (3), we have

$$\begin{aligned}LE_{DP\,A}\left(K_{x,y}\right)&=\left|\frac{-(y+x)}{2}+\frac{1}{2}\sqrt{4y^3x^3+1}\right|+\left|\frac{-(y+x)}{2}-\frac{1}{2}\sqrt{4y^3x^3+1}\right|+(y-1).|-x|+(x-1).|-y|\\ &=2xy.\end{aligned} \tag{14}$$

Case II ($y \neq x+1$ with $y > x \geq 1$): we get the following eigenvalues of $L_{DP\,A}(K_{x,y})$:

$$\begin{aligned}&\frac{-(y+x)}{2} \pm \frac{1}{2}\sqrt{4x^3y^3+(y-x)^2}1-\text{time},\\&-x(y-1)-\text{times},\\&-y(x-1)-\text{times}.\end{aligned} \tag{15}$$

The required spectrum can be obtained by these eigenvalues. Moreover, by (3), we have

$$\begin{aligned}LE_{DP\,A}(K_{x,y}) &= \left|\frac{-(y+x)}{2}+\frac{1}{2}\sqrt{4x^3y^3+(y-x)^2}\right| + \left|\frac{-(y+x)}{2}-\frac{1}{2}\sqrt{4x^3y^3+(y-x)^2}\right| + (y-1).|-x| + (x-1).|-y|\\&= 2xy.\end{aligned} \tag{16}$$

Case III ($x = y \geq 1$): eigenvalues of $L_{DP\,A}(K_{x,x})$ are as follows:

$$\begin{aligned}&x(x^2-1), 1-\text{time},\\&-x(x^2+1), 1-\text{time},\\&-x, 2(x-1)-\text{times}.\end{aligned} \tag{17}$$

These eigenvalues provide the required spectrum. Furthermore, by (3), we have

$$\begin{aligned}LE_{DP\,A}(K_{x,x}) &= |x(x^2-1)| + |-x(x^2+1)| + 2(x-1).|-x|\\&= 2(x^3+x^2-x).\end{aligned} \tag{18}$$

Case IV ($x = 1$ and $y \geq 1$): we get eigenvalues of $L_{DP\,A}(K_{1,y})$ as follows:

$$\begin{aligned}&\frac{-(1+y)}{2} \pm \frac{1}{2}\sqrt{4y^3+(1-y)^2}, 1-\text{time},\\&-1, (y-1)-\text{times}.\end{aligned} \tag{19}$$

These eigenvalues provide the required spectrum. Using (3), we have the following energy of $K_{1,y}$:

$$\begin{aligned}LE_{DP\,A}(K_{1,y}) &= \left|\frac{-(1+y)}{2}+\frac{1}{2}\sqrt{4y^3+(1-y)^2}\right| + \left|\frac{-(1+y)}{2}-\frac{1}{2}\sqrt{4y^3+(1-y)^2}\right| + (y-1).|-1|\\&= 2y.\end{aligned} \tag{20}$$

It completes the proof. □

2.3. Friendship Graphs F_x. A friendship graph F_x has $2x+1$ vertices, and it can be assembled by connecting x clones of the cycle C_3 with a common vertex. Let the vertex set of ith copy of C_3 be $\{v_1^i, v_2^i, v_3^i\}$, where $1 \leq i \leq x$. Let the common vertex be $v = v_1^1 = v_1^2 = \ldots = v_1^x$. Then, the vertex set of F_x is

$$\{v\} \bigcup_{i=1}^{x} \{v_2^i, v_3^i\}. \tag{21}$$

Theorem 3. *For $x \geq 2$, let a friendship graph F_x; then,*

$$\begin{aligned}LSp_{DP\,A}(F_x) &= \begin{pmatrix} 2 & -6 & (1-x) \pm \sqrt{32x^3+(1+x)^2} \\ x-1 & x & 1 \end{pmatrix},\\LE_{DP\,A}(F_x) &= 10x-4.\end{aligned} \tag{22}$$

Proof. In F_x, $d(v) = 2x$ and $d(v_2^i) = d(v_3^i) = 2$ for $1 \leq i \leq x$. Then, the Laplacian degree product adjacency matrix is as follows:

$$L_{DP\ A}(F_x)=\begin{array}{c c} & \begin{array}{ccccccccc} v & v_2^1 & v_3^1 & v_2^2 & v_3^2 & \dots & v_2^x & v_3^x \end{array} \\ \begin{array}{c} v \\ v_2^1 \\ v_3^1 \\ v_2^2 \\ v_3^2 \\ \vdots \\ v_2^x \\ v_3^x \end{array} & \begin{pmatrix} -2x & 4x & 4x & 4x & 4x & \dots & 4x & 4x \\ 4x & -2 & 4 & 0 & 0 & \dots & 0 & 0 \\ 4x & 4 & -2 & 0 & 0 & \dots & 0 & 0 \\ 4x & 0 & 0 & -2 & 4 & \dots & 0 & 0 \\ 4x & 0 & 0 & 4 & -2 & \dots & 0 & 0 \\ \vdots & \vdots & \vdots & \vdots & \vdots & \ddots & \vdots & \vdots \\ 4x & 0 & 0 & 0 & 0 & \dots & -2 & 4 \\ 4x & 0 & 0 & 0 & 0 & \dots & 4 & -2 \end{pmatrix} \end{array}. \tag{23}$$

The eigenvalues of Laplacian degree product adjacency matrix of F_x are

$$\begin{gathered} 2,\ (x-1)-\text{times}, \\ -6,\ x-\text{times}, \\ (1-x)\pm\sqrt{32x^3+(1+x)^2},\ 1-\text{time}. \end{gathered} \tag{24}$$

The required spectrum can be obtained by these eigenvalues. These eigenvalues provide the following energy:

$$\begin{aligned} LE_{DP\ A}(F_x) &= (x-1).|2|+x.|-6|+\left|(1-x)+\sqrt{32x^3+(1+x)^2}\right|+\left|(1-x)-\sqrt{32x^3+(1+x)^2}\right| \\ &= 10x-4. \end{aligned} \tag{25}$$

□

2.4. Corona Products of 3 and 4 Cycles with Null Graphs. The corona product of graphs Γ and Ω is expressed as $\Gamma^{\circ}\Omega$. It can be made by drawing one copy of Γ and $|V(\Gamma)|$ copies of Ω and connecting the ith vertex of Γ with each vertex of ith copy of Ω [9–11]. Let Γ be an x-cycle C_x with vertices $v_1, v_2, \dots, v_x$ and Ω be a null graph N_k. Then, the vertex set of $C_x{}^{\circ}N_k$ is

$$V(C_x)\bigcup_{j=1}^{x}\left\{v_i^j;1\le i\le k\right\}, \tag{26}$$

where the set $\left\{v_i^j;1\le i\le k\right\}$ is the vertex set of jth copy of N_k in $C_x{}^{\circ}N_k$. In this portion, we evaluate the Laplacian degree product spectrum and energy of $C_x{}^{\circ}N_k$ for $x=3$ and 4.

Theorem 4. *For $k\ge 1$, let the corona product be $C_x{}^{\circ}N_k$; then,*

$$\begin{aligned} LSp_{DP\ A}(C_3{}^{\circ}N_k) &= \begin{pmatrix} \frac{1}{2}\left(\left(2k^2+7k+5\right)\pm\sqrt{4k^4+32k^3+93k^2+114k+49}\right) & -\frac{1}{2}\left(\left(k^2+5k+7\right)\mp\sqrt{k^4+14k^3+51k^2+66k+25}\right) & -1 \\ 1 & 2 & 3(k-1)) \end{pmatrix}, \\ LE_{DP\ A}(C_3{}^{\circ}N_k) &= 4\left(k^2+5k+4\right). \end{aligned} \tag{27}$$

Proof. Note that $d(v_j)=k+2$, for each $j=1,2,3$, and $d(v_i^j)=1$, for each $1\le j\le 3$ and $1\le i\le k$. For the convenience, we let $k+2=\alpha$. Then, the Laplacian degree product adjacency matrix of $C_x{}^{\circ}N_k$ is

$$\begin{array}{c} \\ v_1 \\ v_2 \\ v_3 \\ v_1^1 \\ \vdots \\ v_k^1 \\ v_1^2 \\ \vdots \\ v_k^2 \\ v_1^3 \\ \vdots \\ v_k^3 \end{array}\begin{pmatrix} v_1 & v_2 & v_3 & v_1^1 & \dots & v_k^1 & v_1^2 & \dots & v_k^2 & v_1^3 & \dots & v_k^3 \\ -\alpha & \alpha^2 & \alpha^2 & \alpha & \dots & \alpha & 0 & \dots & 0 & 0 & \dots & 0 \\ \alpha^2 & -\alpha & \alpha^2 & 0 & \dots & 0 & \alpha & \dots & \alpha & 0 & \dots & 0 \\ \alpha^2 & \alpha^2 & -\alpha & 0 & \dots & 0 & 0 & \dots & 0 & \alpha & \dots & \alpha \\ \alpha & 0 & 0 & -1 & \dots & 0 & 0 & \dots & 0 & 0 & \dots & 0 \\ \vdots & \vdots & \vdots & \vdots & \ddots & \vdots & \vdots & \dots & \vdots & \vdots & \dots & \vdots \\ \alpha & 0 & 0 & 0 & \dots & -1 & 0 & \dots & 0 & 0 & \dots & 0 \\ 0 & \alpha & 0 & 0 & \dots & 0 & -1 & \dots & 0 & 0 & \dots & 0 \\ \vdots & \vdots & \vdots & \vdots & \dots & \vdots & \vdots & \ddots & \vdots & \vdots & \dots & \vdots \\ 0 & \alpha & 0 & 0 & \dots & 0 & 0 & \dots & -1 & 0 & \dots & 0 \\ 0 & 0 & \alpha & 0 & \dots & 0 & 0 & \dots & 0 & -1 & \dots & 0 \\ \vdots & \vdots & \vdots & \vdots & \dots & \vdots & \vdots & \dots & \vdots & \vdots & \ddots & \vdots \\ 0 & 0 & \alpha & 0 & \dots & 0 & 0 & \dots & 0 & 0 & \dots & -1 \end{pmatrix} \tag{28}$$

The eigenvalues obtained from the above matrix of $C_x{}^\circ N_k$ are

$$\begin{aligned} &\frac{2k^2+7k+5}{2} \pm \sqrt{\frac{4k^4+32k^3+93k^2+114k+49}{4}}, 1-\text{times}, \\ &-\frac{k^2+5k+7}{2} \pm \frac{1}{2}\sqrt{k^4+14k^3+51k^2+66k+25}, 2-\text{times}, \\ &\quad -1, 3(k-1)-\text{times}. \end{aligned} \tag{29}$$

Then, the required spectrum can be obtained by these eigenvalues. Also, by (3), we have

$$\begin{aligned} LE_{DP\,A}(C_3{}^\circ N_k) &= \left|\frac{2k^2+7k+5}{2} + \sqrt{\frac{4k^4+32k^3+93k^2+114k+49}{4}}\right| + \left|\frac{2k^2+7k+5}{2} - \sqrt{\frac{4k^4+32k^3+93k^2+114k+49}{4}}\right| + \\ &\quad \left|-\left(\frac{k^2+5k+7}{2}\right) + \frac{1}{2}\sqrt{k^4+14k^3+51k^2+66k+25}\right| + \left|-\left(\frac{k^2+5k+7}{2}\right) - \frac{1}{2}\sqrt{k^4+14k^3+51k^2+66k+25}\right| \\ &\quad + 3(k-1)|-1| \\ &= 4\left(k^2+5k+4\right). \end{aligned} \tag{30}$$

□

Theorem 5. *For $k \geq 1$, let the corona product be $C_x{}^\circ N_k$; then, $LSp_{DP\,A}(C_x{}^\circ N_k)$ is*

$$\begin{aligned} &\begin{pmatrix} -\frac{1}{2}\left(\left(2k^2+9k+11\right) \mp \sqrt{4k^4+40k^3+133k^2+178k+81}\right) & -\frac{1}{2}\left((k+3) \mp \sqrt{4k^3+17k^2+18k+1}\right. & \frac{1}{2}\left(\left(2k^2+7k+5\right) \pm \sqrt{4k^4+32k^3+93k^2+114k+49}\right) & -1 \\ 1 & 2 & 1 & 4(k-1)) \end{pmatrix} \\ &LE_{DP\,A}(C_4{}^\circ N_k) = 4k^2+22k+18. \end{aligned} \tag{31}$$

Proof. Note that $d(v_j) = k+2$, for each $j = 1, 2, 3, 4$, and $d(v_i^j) = 1$, for each $1 \leq j \leq 4$ and $1 \leq i \leq k$. For the convenience, we let $k+2 = \alpha$. Then, the Laplacian degree product adjacency matrix of $C_4{}^\circ N_k$ is as

$$\begin{array}{cc} & \begin{array}{ccccccccccc} v_1 & v_2 & v_3 & v_4 & v_1^1 & \dots & v_k^1 & v_1^4 & \dots & v_k^4 \end{array} \\ \begin{array}{c} v_1 \\ v_2 \\ v_3 \\ v_4 \\ v_1^1 \\ \vdots \\ v_k^1 \\ v_1^4 \\ \vdots \\ v_k^4 \end{array} & \begin{pmatrix} -\alpha & \alpha^2 & 0 & \alpha^2 & \alpha & \dots & \alpha & 0 & \dots & 0 \\ \alpha^2 & -\alpha & \alpha^2 & 0 & 0 & \dots & 0 & 0 & \dots & 0 \\ 0 & \alpha^2 & -\alpha & \alpha^2 & 0 & \dots & 0 & 0 & \dots & 0 \\ \alpha^2 & 0 & \alpha^2 & -\alpha & 0 & \dots & 0 & \alpha & \dots & \alpha \\ \alpha & 0 & 0 & 0 & -1 & \dots & 0 & 0 & \dots & 0 \\ \vdots & \vdots & \vdots & \vdots & \vdots & \ddots & \vdots & \vdots & \dots & \vdots \\ \alpha & 0 & 0 & 0 & 0 & \dots & -1 & 0 & \dots & 0 \\ 0 & 0 & 0 & \alpha & 0 & \dots & 0 & -1 & \dots & 0 \\ \vdots & \vdots & \vdots & \vdots & \vdots & \dots & \vdots & \vdots & \ddots & \vdots \\ 0 & 0 & 0 & \alpha & 0 & \dots & 0 & 0 & \dots & -1 \end{pmatrix} \end{array}. \tag{32}$$

The eigenvalues of Laplacian degree product adjacency matrix of $C_4{}^{\circ}N_k$ are

$$\begin{aligned} & -\frac{2k^2+9k+11}{2} \pm \sqrt{\frac{4k^4+40k^3+133k^2+178k+81}{4}}, 1-\text{time}, \\ & -\frac{k+3}{2} \pm \sqrt{\frac{4k^3+17k^2+18k+1}{4}}, 2-\text{times}, \\ & \frac{2k^2+7k+5}{2} \pm \sqrt{\frac{4k^4+32k^3+93k^2+114k+49}{4}}, 1-\text{time}, \\ & -1 \, 4(k-1)-\text{times}. \end{aligned} \tag{33}$$

Then, the required spectrum can be obtained by these eigenvalues. Furthermore, by (3), we have

$$\begin{aligned} LE_{DP\ A}(C_4{}^{\circ}N_k) = & \left| -\frac{2k^2+9k+11}{2} + \sqrt{\frac{4k^4+40k^3+133k^2+178k+81}{4}} \right| \\ & + \left| -\frac{2k^2+9k+11}{2} - \sqrt{\frac{4k^4+40k^3+133k^2+178k+81}{4}} \right| \\ & + 2.\left| -\frac{k+3}{2} + \sqrt{\frac{4k^3+17k^2+18k+1}{4}} \right| \\ & + 2.\left| -\frac{k+3}{2} - \sqrt{\frac{4k^3+17k^2+18k+1}{4}} \right| \\ & + \left| \frac{2k^2+7k+5}{2} + \sqrt{\frac{4k^4+32k^3+93k^2+114k+49}{4}} \right| \\ & + \left| \frac{2k^2+7k+5}{2} - \sqrt{\frac{4k^4+32k^3+93k^2+114k+49}{4}} \right| \\ & + 4(k-1).|-1| \\ = & \, 2\left(2k^2+11k+9\right). \end{aligned} \tag{34}$$

□

3. Appendix

In [6], Mirajkar and Doddamani considered the corona product $C_4{}^{\circ}N_{k-2}$ for $k \geq 3$ (also called thorny cycle rings $C_{4,k}$) and investigated its energy and spectrum on the base of degree product adjacency matrix. During computations of our results on $C_4{}^{\circ}N_{k-2}$, the eigenvalues investigated in [6] were found incorrect. In this section, we provide the correct energy and spectrum of $C_4{}^{\circ}N_{k-2}$. First of all, note that the degree product adjacency matrix of $C_4{}^{\circ}N_{k-2}$ is

$$DP\ A\left(C_4{}^{\circ}N_{k-2}\right) = \begin{array}{c} \\ v_1 \\ v_2 \\ v_3 \\ v_4 \\ v_1^1 \\ v_2^1 \\ \vdots \\ v_1^4 \\ v_2^4 \end{array} \begin{pmatrix} v_1 & v_2 & v_3 & v_4 & v_1^1 & v_2^1 & \dots & v_1^4 & v_2^4 \\ 0 & k^2 & 0 & k^2 & k & k & \dots & 0 & 0 \\ k^2 & 0 & k^2 & 0 & 0 & 0 & \dots & 0 & 0 \\ 0 & k^2 & 0 & k^2 & 0 & 0 & \dots & 0 & 0 \\ k^2 & 0 & k^2 & 0 & 0 & 0 & \dots & k & k \\ k & 0 & 0 & 0 & 0 & 0 & \dots & 0 & 0 \\ k & 0 & 0 & 0 & 0 & 0 & \dots & 0 & 0 \\ \vdots & \vdots & \vdots & \vdots & \vdots & \vdots & \ddots & \vdots & \vdots \\ 0 & 0 & 0 & k & 0 & 0 & \dots & 0 & 0 \\ 0 & 0 & 0 & k & 0 & 0 & \dots & 0 & 0 \end{pmatrix} \quad (35)$$

Mirajkar and Doddamani's investigated eigenvalues are

$$\begin{aligned} & k\left(\sqrt{k^2+2} \pm k\right), 1-\text{time}, \\ & -k\left(\sqrt{k^2+2} \pm k\right), 1-\text{time}, \\ & \pm k\sqrt{2}, 2-\text{times}, \\ & 0, 4(k-3)-\text{times}. \end{aligned} \quad (36)$$

Whereas, the correct eigenvalues of $DP\ A\left(C_4{}^{\circ}N_{k-2}\right)$ are

$$\begin{aligned} & \pm k^2 + k\sqrt{k^2+k-2}, 1-\text{time}, \\ & \mp k^2 - k\sqrt{k^2+k-2}, 1-\text{time}, \\ & \pm k\sqrt{k-2}, 2-\text{times}, \\ & 0, 4(k-3)-\text{times}. \end{aligned} \quad (37)$$

Accordingly, we get the following energy and spectrum of $C_4{}^{\circ}N_{k-2}$ in the corrected form:

$$\begin{aligned} E_{DP\ A}\left(C_4{}^{\circ}N_{k-2}\right) &= \left|k^2 + k\sqrt{k^2+k-2}\right| + \left|-k^2 + k\sqrt{k^2+k-2}\right| + \left|-k^2 - k\sqrt{k^2+k-2}\right| \\ &\quad + \left|k^2 - k\sqrt{k^2+k-2}\right| + 2.\left|-k\sqrt{k-2}\right| + 2.\left|k\sqrt{k-2}\right|, \\ Sp_{DP\ A}\left(C_4{}^{\circ}N_{k-2}\right) &= \begin{pmatrix} \pm k^2 + k\sqrt{k^2+k-2} & \mp k^2 - k\sqrt{k^2+k-2} & \pm k\sqrt{k-2} & 0 \\ 1 & 1 & 2 & 4(k-3) \end{pmatrix}. \end{aligned} \quad (38)$$

4. Accomplishment Remarks

In this study, we construct the general formulas for spectrums and energies of four different families of graphs, by using Laplacian degree product adjacency matrix. We also obtained faultless and correct eigenvalues of $C_4{}^{\circ}N_{k-2}$, which were defined in [6].

Data Availability

All kinds of data and materials, used to compute the results, are provided in Section 1.

Conflicts of Interest

The authors declare no conflicts of interest.

Authors' Contributions

Asim Khurshid carried out computation and wrote the initial draft; Muhammad Salman supervised the study, administrated the project, analysed data, and developed the methodology; Masood ur Rehman: wrote and reviewed the manuscript, carried out formal analysis, and edited the study; Mohammad Tariq Rahim conceptualized the study and visualized the study.

References

[1] I. Gutman, "The energy of a graph," *Ber.Math.Stat.Sket. Forschungsz.Graz*, vol. 103, pp. 1–22, 1978.

[2] C. Woods, "My favorite application using graph eigenvalues: graph energy," 2013, http://www.math.ucsd.edu/fan/teach/262/13/262notes/Woods Midterm.pdf.

[3] D. M. Cvetković, M. Doob, and H. Sachs, *Spectra of Graphs: Theory and Applications 3rd Revised and Enlarged Edition*, Wiley, New York, USA, 1998.

[4] N. Biggs, *Algebraic Graph Theory*, Cambridge University Press, Cambridge, UK, 1993.

[5] F. Harary, *Graph Theory*, Addison - Wesely, Boston, MA, USA, 1969.

[6] K. G. Mirajkar and B. R. Doddamani, "On energy and spectrum of degree product adjacency matrix for some class of graphs," *International Journal of Applied Engineering Research*, vol. 14, no. 7, pp. 1546–1554, 2019.

[7] K. G. Mirajkar and B. R. Doddamani, "On the bounds of Laplacian energy for degree product adjacency matrix of regular graph," *Research Guru:Online Journal of Multidisciplinary Subjects*, vol. 1, no. 13, pp. 10–17, 2019.

[8] H. S. Ramane, D. S. Revankar, and J. B. Patil, "Bounds for the degree sum eigenvalues and degree sum energy of a graph," *International Journal of Pure and Applied Mathematical Sciences*, vol. 6, pp. 161–167, 2013.

[9] D. Bonchev and D. J. Klein, "On the wiener number of thorn trees, stars, rings and rods," *Croatica Chemica Acta*, vol. 75, no. 2, pp. 613–620, 2002.

[10] R. Frucht and F. Harary, "On the corona of two graphs," *Aequationes Mathematicae*, vol. 4, no. 1, p. 264, 1970.

[11] H. B. Walikar, H. S. Ramane, L. Sindagi, S. S. Shirakol, and I. Gutman, "Hosoya polynomial of thorn trees, rods, rings and trees," *Kragujevac Journal of Science*, vol. 28, pp. 47–56, 2006.

Hindawi
Journal of Mathematics
Volume 2021, Article ID 4880092, 12 pages
https://doi.org/10.1155/2021/4880092

Research Article

On Computation Degree-Based Topological Descriptors for Planar Octahedron Networks

Wang Zhen,[1] Parvez Ali,[2] Haidar Ali,[3] Ghulam Dustigeer,[4] and Jia-Bao Liu[5]

[1]*School of Computer Engineering, Anhui Wonder University of Information Engineering, Hefei 231201, China*
[2]*Department of Mechanical Engineering, College of Engineering, Qassim University, Unaizah, Saudi Arabia*
[3]*Department of Mathematics, Riphah International University, Faisalabad, Pakistan*
[4]*Department of Mathematics and Statistics, University of Agriculture, Faisalabad, Pakistan*
[5]*School of Mathematics and Physics, Anhui Jianzhu University, Hefei 230601, China*

Correspondence should be addressed to Haidar Ali; haidar3830@gmail.com

Received 18 September 2021; Accepted 9 October 2021; Published 1 November 2021

Academic Editor: Ljubisa Kocinac

Copyright © 2021 Wang Zhen et al. This is an open access article distributed under the Creative Commons Attribution License, which permits unrestricted use, distribution, and reproduction in any medium, provided the original work is properly cited.

A molecular graph is used to represent a chemical molecule in chemical graph theory, which is a branch of graph theory. A graph is considered to be linked if there is at least one link between its vertices. A topological index is a number that describes a graph's topology. Cheminformatics is a relatively young discipline that brings together the field of sciences. Cheminformatics helps in establishing QSAR and QSPR models to find the characteristics of the chemical compound. We compute the first and second modified K-Banhatti indices, harmonic K-Banhatti index, symmetric division index, augmented Zagreb index, and inverse sum index and also provide the numerical results.

1. Introduction

Graph theory provides topological indices, which are a useful tool. Cheminformatics is a contemporary academic discipline that brings together chemistry, mathematics, and information science. It investigates the connections between quantitative structure-activity relationship (QSAR) and quantitative structure-property relationship (QSPR), which are used to predict biological activities and chemical compound characteristics.

The silicate structures [1] formed from the POH network, TP network, and hex POH network [2] are discussed in this article.

The following is the procedure for making POH networks .

Step 1: consider a m-dimensional silicate network.

Step 2: connect new vertices in the centre of each triangular face to existing vertices in the adjacent triangular face.

Step 3: all of the new centre vertices in the same silicate cell must be connected.

Step 4: for the m dimension, the resultant graph is known as the planar octahedron network as shown in Figure 1. Remove all silicon vertices from the graph. The triangle prism network as shown in Figure 2 and the hex POH network as shown in Figure 3 are also possible.

Let ψ represent a graph. Then, modified first and second K-Banhatti indices [3] can be defined as

$$\mathrm{MK}_1\mathrm{B}(\psi) = \sum_{ab\in E(\psi)} \left(\frac{1}{(d_a + d_b)}\right), \tag{1}$$

$$\mathrm{MK}_2\mathrm{B}(\psi) = \sum_{ab\in E(\psi)} \left(\frac{1}{(d_a \times d_b)}\right). \tag{2}$$

Harmonic K-Banhatti index [4] of a graph ψ is defined as

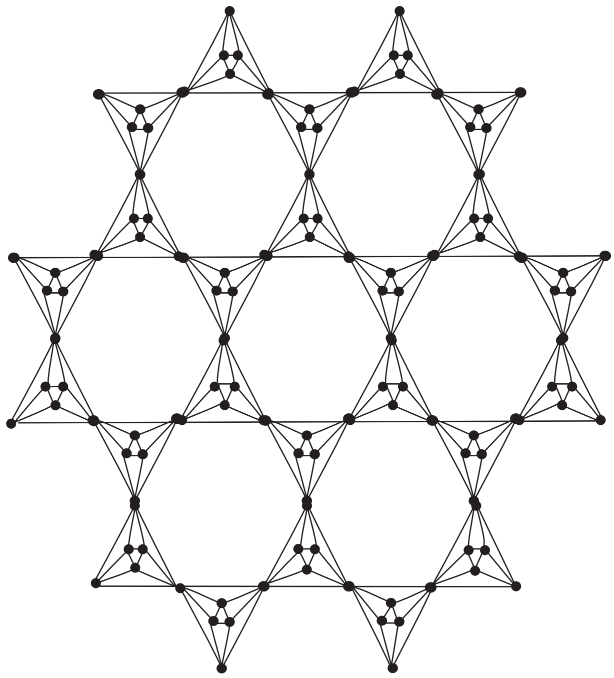

Figure 1: Planar octahedral network POH (2).

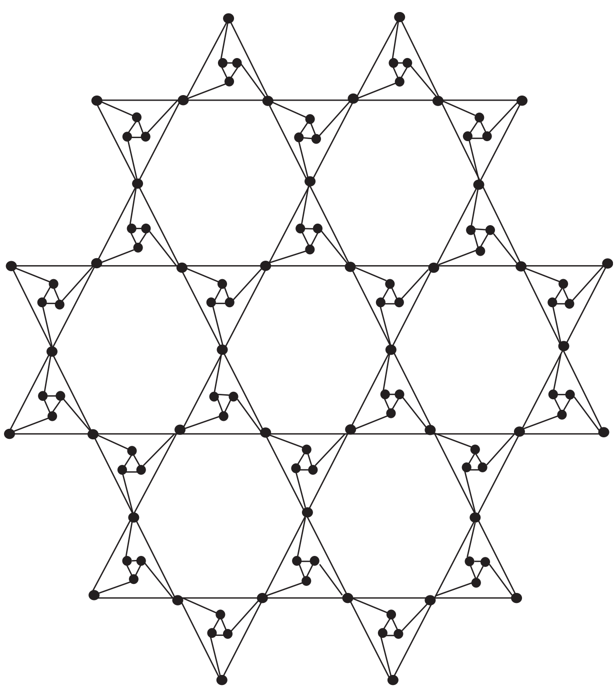

Figure 2: Triangular prism network TP (2).

$$\mathrm{HKB}(\psi) = \sum_{ab\in E(\psi)} \left(\frac{2}{(d_a + d_b)}\right). \tag{3}$$

Symmetric division index of a graph [5] is defined as

$$\mathrm{SD}(\psi) = \sum_{ab\in E(\psi)} \left(\frac{d_a}{d_b} + \frac{d_b}{d_a}\right). \tag{4}$$

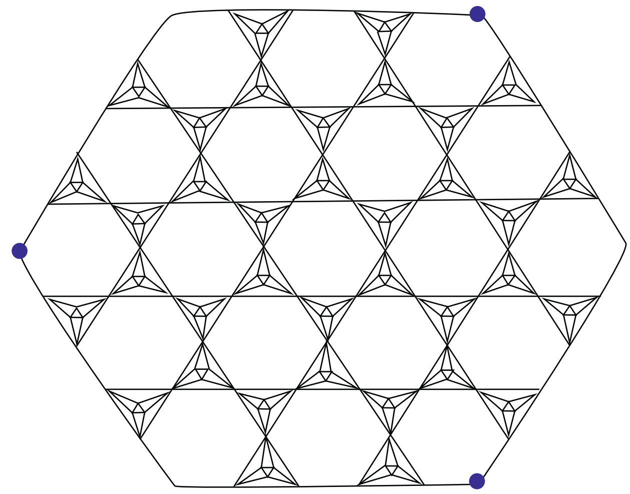

Figure 3: Hexagonal planar octahedral network HPOH (2).

Augmented Zagreb index of a graph ψ [4] is defined as

$$\mathrm{AG}(\psi) = \sum_{ab\in E(\psi)} \left(\frac{d_a \times d_b}{d_a + d_b - 2}\right)^3. \tag{5}$$

Inverse sum index of a graph ψ is defined as

$$I(\psi) = \sum_{ab\in E(\psi)} \left(\frac{d_a \times d_b}{d_a + d_b}\right). \tag{6}$$

2. Main Results

We research different indices on different kinds of planar octahedron networks. Nowadays, extensive research studies are being conducted in the field of chemical graph theory for further studying topological indices of various graphs [6–13]. For the basic notations and definitions, see [14, 15].

2.1. Results for Planar Octahedron Network POH (m). The planar octahedron network is the resulting graph for the m dimension. All silicon vertices should be removed from the scene. There are also the triangular prism network and the hex POH network. Now, we calculate several key indices for the POH network in the following theorems.

Theorem 1. *Consider the planar octahedral network POH (m); then, its first and second modified K-Banhatti indices are equal to*

$$\begin{aligned} \mathrm{MK_1B}(\psi_1) &= \frac{51}{8}m^2 + \frac{3}{4}m, \\ \mathrm{MK_2B}(\psi_1) &= \frac{81}{32}m^2 + \frac{9}{16}m. \end{aligned} \tag{7}$$

Proof. Let $\psi_1 \cong \mathrm{POH}(m)$. From equation (1), we have

$$\mathrm{MK_1B}(\psi) = \sum_{ab\in E(\psi)} \left(\frac{1}{(d_a + d_b)}\right). \tag{8}$$

Using Table 1, we have

$$\begin{aligned}\mathrm{MK_1B}(\psi_1) &= \frac{1}{4+4}\left|E_1(\mathrm{POH}(m))\right| + \frac{1}{4+8}\left|E_2(\mathrm{POH}(m))\right| + \frac{1}{8+8}\left|E_3(\mathrm{POH}(m))\right| \\ &= \frac{1}{8}\left|E_1(\mathrm{POH}(m))\right| + \frac{1}{12}\left|E_2(\mathrm{POH}(m))\right| + \frac{1}{16}\left|E_3(\mathrm{POH}(m))\right| \\ &= \frac{1}{8}\left(18m^2 + 12m\right) + \frac{1}{12}\left(36m^2 - 48m + 12\right) + \frac{1}{16}\left(18m^2 - 36m + 18\right).\end{aligned} \tag{9}$$

We get the following value after calculations:

$$\Rightarrow \mathrm{MK_1B}(\psi_1) = \frac{51}{8}m^2 + \frac{3}{4}m. \tag{10}$$

Let $\psi_1 \cong \mathrm{POH}(m)$. From equation (2), we have

$$\begin{aligned}\mathrm{MK_2B}(\psi_1) &= \frac{1}{4\times 4}\left|E_1(\mathrm{POH}(m))\right| + \frac{1}{4\times 8}\left|E_2(\mathrm{POH}(m))\right| + \frac{1}{8\times 8}\left|E_3(\mathrm{POH}(m))\right| \\ &= \frac{1}{16}\left|E_1(\mathrm{POH}(m))\right| + \frac{1}{32}\left|E_2(\mathrm{POH}(m))\right| + \frac{1}{64}\left|E_3(\mathrm{POH}(m))\right| \\ &= \frac{1}{16}\left(18m^2 + 12m\right) + \frac{1}{32}\left(36m^2 - 48m + 12\right) + \frac{1}{64}\left(18m^2 - 36m + 18\right).\end{aligned} \tag{12}$$

We get the following value after calculations:

$$\Rightarrow \mathrm{MK_2B}(\psi_1) = \frac{81}{32}m^2 + \frac{9}{16}m. \tag{13}$$

□

Theorem 2. *The harmonic K-Banhatti and symmetric division indices are equal in the POH (m) network.*

$$\begin{aligned}\mathrm{HKB}(\psi) &= \frac{51}{4}m^2 + \frac{3}{2}m, \\ \mathrm{SD}(\psi) &= 162m^2.\end{aligned} \tag{14}$$

Table 1: Edge partition.

(d_a, d_b)	Number of edges
$E_1 = (4,4)$	$18m^2 + 12m$
$E_2 = (4,8)$	$36m^2 - 48m + 12$
$E_3 = (8,8)$	$18m^2 - 36m + 18$

$$\mathrm{MK_1B}(\psi) = \sum_{ab\in E(\psi)} \left(\frac{1}{(d_a + d_b)}\right). \tag{11}$$

Using Table 1, we have

Proof. Let $\varphi_1 \cong \mathrm{POH}(m)$ network; from equation (3),

$$\mathrm{HKB}(\psi) = \sum_{ab\in E(\psi)} \frac{2}{(d_a + d_b)}. \tag{15}$$

Using Table 1, we have

$$\begin{aligned}\mathrm{HKB}(\psi_1) &= \frac{2}{4+4}\left|E_1(\mathrm{POH}(m))\right| + \frac{2}{4+8}\left|E_2(\mathrm{POH}(m))\right| + \frac{2}{8+8}\left|E_3(\mathrm{POH}(m))\right| \\ &= \frac{2}{8}\left|E_1(\mathrm{POH}(m))\right| + \frac{2}{12}\left|E_2(\mathrm{POH}(m))\right| + \frac{2}{16}\left|E_3(\mathrm{POH}(m))\right| \\ &= \frac{1}{4}\left(18m^2 + 12m\right) + \frac{1}{6}\left(36m^2 - 48m + 12\right) + \frac{1}{8}\left(18m^2 - 36m + 18\right).\end{aligned} \tag{16}$$

We get the following value after calculations:

$$\Rightarrow \mathrm{HKB}(\psi_1) = \frac{51}{4}m^2 + \frac{3}{2}m. \tag{17}$$

For the symmetric division index of a graph using equation (3),

$$\mathrm{SD}(\psi) = \sum_{ab\in E(\psi)} \left(\frac{d_a}{d_b} + \frac{d_b}{d_a}\right). \tag{18}$$

Using Table 1, we have

$$\begin{aligned}
\mathrm{SD}(\psi_1) &= \left(\frac{4}{4} + \frac{4}{4}\right)\left|E_1(\mathrm{POH}(m))\right| + \left(\frac{4}{8} + \frac{8}{4}\right)\left|E_2(\mathrm{POH}(m))\right| + \left(\frac{8}{8} + \frac{8}{8}\right)\left|E_3(\mathrm{POH}(m))\right| \\
&= 2\left|E_1(\mathrm{POH}(m))\right| + \left(\frac{1}{2} + \frac{2}{1}\right)\left|E_2(\mathrm{POH}(m))\right| + 2\left|E_3(\mathrm{POH}(m))\right| \\
&= 2\left(18m^2 + 12m\right) + \frac{5}{2}\left(36m^2 - 48m + 12\right) + 2\left(18m^2 - 36m + 18\right).
\end{aligned} \tag{19}$$

After calculations,

$$\Rightarrow \mathrm{SD}(\psi_1) = 162m^2. \tag{20}$$

□

Theorem 3. *Then, augmented Zagreb and inverse sum indices are equal to the POH network.*

$$\begin{aligned}
\mathrm{AG}(\psi_1) &= \frac{416820224}{128625}m^2 - \frac{2836480}{3087}m, \\
I(\psi_1)&204m^2 - 24m.
\end{aligned} \tag{21}$$

Proof. Let $\varphi_1 \cong \mathrm{POH}(m)$ network. For the augmented Zagreb index, using equation (5),

$$\mathrm{AG}(\psi) = \sum_{ab\in E(\psi)} \left(\frac{d_a \times d_b}{d_a + d_b - 2}\right)^3. \tag{22}$$

Using Table 1, we have

$$\begin{aligned}
\mathrm{AG}(\psi_1) &= \left(\frac{16}{6}\right)^3 \left|E_1(\mathrm{POH}(m))\right| + \left(\frac{32}{10}\right)^3 \left|E_2(\mathrm{POH}(m))\right| + \left(\frac{64}{14}\right)^3 \left|E_3(\mathrm{POH}(m))\right| \\
&= \left(\frac{16}{6}\right)^3 \left(18m^2 + 12m\right) + \left(\frac{32}{10}\right)^3 \left(36m^2 - 48m + 12\right) + \left(\frac{64}{14}\right)^3 \left(18m^2 - 36m + 18\right).
\end{aligned} \tag{23}$$

After some calculations, we get

$$\Rightarrow \mathrm{AG}(\psi_1) = \frac{416820224}{128625}m^2 - \frac{2836480}{3087}m. \tag{24}$$

For the inverse sum index and by using equation (6), we have

$$I(\psi) = \sum_{ab\in E(\psi)} \left(\frac{d_a \times d_b}{d_a + d_b}\right). \tag{25}$$

Using Table 1, we have

$$\begin{aligned}
I(\psi_1) &= \left(\frac{16}{8}\right)\left|E_1(\mathrm{POH}(m))\right| + \left(\frac{32}{12}\right)\left|E_2(\mathrm{POH}(m))\right| + \left(\frac{64}{16}\right)\left|E_3(\mathrm{POH}(m))\right| \\
&= 2\left(18m^2 + 12m\right) + \left(\frac{32}{12}\right)\left(36m^2 - 48m + 12\right) + 4\left(18m^2 - 36m + 18\right).
\end{aligned} \tag{26}$$

After calculations,

$$\Rightarrow I(\psi_1) = 204m^2 - 24m. \tag{27}$$

□

2.2. Results for Triangular Prism Network TP (m). In this part, we propose the theorem for the TP network.

Theorem 4. *The first and second modified K-Banhatti indices are equal to the TP network:*

$$\mathrm{MK_1B}(\psi_2) = \frac{13}{2}m^2 + \frac{2}{3}m,$$
$$\mathrm{MK_2B}(\psi_2) = \frac{7}{2}m^2 + \frac{2}{3}m. \tag{28}$$

Proof. Let $\psi_2 \cong \mathrm{TP}(m)$. From equation (1), we have

Table 2: Edge partition of TP network.

(d_a, d_b)	Number of edges
$E_1 = (3,3)$	$18m^2 + 6m$
$E_2 = (3,6)$	$18m^2 + 6m$
$E_3 = (6,6)$	$18m^2 - 36m + 18$

$$\mathrm{MK_1B}(\psi) = \sum_{ab\in E(\psi)} \left(\frac{1}{(d_a + d_b)}\right). \tag{29}$$

Using Table 2, we have

$$\begin{aligned}\mathrm{MK_1B}(\psi_2) &= \frac{1}{3+3}\left|E_1(\mathrm{TP}(m))\right| + \frac{1}{3+6}\left|E_2(\mathrm{TP}(m))\right| + \frac{1}{6+6}\left|E_3(\mathrm{TP}(m))\right|\\ &= \frac{1}{6}\left|E_1(\mathrm{TP}(m))\right| + \frac{1}{9}\left|E_2(\mathrm{TP}(m))\right| + \frac{1}{12}\left|E_3(\mathrm{TP}(m))\right|\\ &= \frac{1}{6}\left(18m^2 + 6m\right) + \frac{1}{9}\left(18m^2 + 6m\right) + \frac{1}{12}\left(18m^2 - 36m + 18\right).\end{aligned} \tag{30}$$

After some calculations, we get

$$\Rightarrow \mathrm{MK_1B}(\psi_2) = \frac{13}{2}m^2 + \frac{2}{3}m. \tag{31}$$

Let $\psi_2 \cong \mathrm{TP}(m)$. From equation (2), we have

$$\mathrm{MK_1B}(\psi) = \sum_{ab\in E(\psi)} \left(\frac{1}{(d_a + d_b)}\right). \tag{32}$$

Using Table 2, we have

$$\begin{aligned}\mathrm{MK_2B}(\psi_2) &= \frac{1}{3\times 3}\left|E_1(\mathrm{TP}(m))\right| + \frac{1}{3\times 6}\left|E_2(\mathrm{TP}(m))\right| + \frac{1}{6\times 6}\left|E_3(\mathrm{TP}(m))\right|\\ &= \frac{1}{9}\left|E_1(\mathrm{TP}(m))\right| + \frac{1}{18}\left|E_2(\mathrm{TP}(m))\right| + \frac{1}{36}\left|E_3(\mathrm{TP}(m))\right|\\ &= \frac{1}{9}\left(18m^2 + 6m\right) + \frac{1}{18}\left(18m^2 + 6m\right) + \frac{1}{36}\left(18m^2 - 36m + 18\right).\end{aligned} \tag{33}$$

After calculations,

$$\Rightarrow \mathrm{MK_2B}(\psi_2) = \frac{7}{2}m^2 + \frac{2}{3}m. \tag{34}$$

□

Theorem 5. *In the POH (m) network, the harmonic K-Banhatti and symmetric division indices are equal to*

$$\mathrm{HKB}(\psi_2) = 13m^2 + \frac{4}{3}m,$$
$$\mathrm{SD}(\psi_2) = 117m^2 + 3m. \tag{35}$$

Proof. Let $\varphi_2 \cong \mathrm{TP}(m)$ network, and by using equation (3), we have

$$\mathrm{HKB}(\psi) = \sum_{ab\in E(\psi)} \frac{2}{(d_a + d_b)}. \tag{36}$$

Using Table 2, we have

$$\begin{aligned}\mathrm{HKB}(\psi_2) &= \frac{2}{3+3}\left|E_1(\mathrm{TP}(m))\right| + \frac{2}{3+6}\left|E_2(\mathrm{TP}(m))\right| + \frac{2}{6+6}\left|E_3(\mathrm{TP}(m))\right| \\ &= \frac{2}{6}\left|E_1(\mathrm{TP}(m))\right| + \frac{2}{9}\left|E_2(\mathrm{TP}(m))\right| + \frac{2}{12}\left|E_3(\mathrm{TP}(m))\right| \\ &= \frac{1}{3}\left(18m^2 + 6m\right) + \frac{2}{9}\left(18m^2 + 6m\right) + \frac{1}{6}\left(18m^2 - 36m + 18\right).\end{aligned} \tag{37}$$

After calculations,

$$\Rightarrow \mathrm{HKB}(\psi_2) = 13m^2 + \frac{4}{3}m. \tag{38}$$

For the symmetric division index of a graph using equation (3), we have

$$\mathrm{SD}(\psi) = \sum_{ab\in E(\psi)} \left(\frac{d_a}{d_b} + \frac{d_b}{d_a}\right). \tag{39}$$

Using Table 2, we have

$$\begin{aligned}\mathrm{SD}(\psi_2) &= \left(\frac{3}{3} + \frac{3}{3}\right)\left|E_1(\mathrm{TP}(m))\right| + \left(\frac{3}{6} + \frac{6}{3}\right)\left|E_2(\mathrm{TP}(m))\right| + \left(\frac{6}{6} + \frac{6}{6}\right)\left|E_3(\mathrm{TP}(m))\right| \\ &= 2\left|E_1(\mathrm{TP}(m))\right| + \left(\frac{1}{2} + 2\right)\left|E_2(\mathrm{TP}(m))\right| + 2\left|E_3(\mathrm{TP}(m))\right| \\ &= 2\left(18m^2 + 6m\right) + \frac{5}{2}\left(18m^2 + 6m\right) + 2\left(18m^2 - 36m + 18\right).\end{aligned} \tag{40}$$

After some calculations, we get

$$\Rightarrow \mathrm{SD}(\psi_2) = 117m^2 + 3m. \tag{41}$$

□

Theorem 6. *The augmented Zagreb and inverse sum indices are equal to the TP network.*

$$\begin{aligned}\mathrm{AG}(\psi_2) &= \frac{1853423451}{1372000}m^2 - \frac{534408759}{1372000}m, \\ I(\psi_2) &= 204m^2 - 24m.\end{aligned} \tag{42}$$

Proof. Let $\varphi_2 \cong \mathrm{POH}(m)$ network. Using equation (5) for the augmented Zagreb index,

$$\mathrm{AG}(\psi) = \sum_{ab\in E(\psi)} \left(\frac{d_a \times d_b}{d_a + d_b - 2}\right)^3. \tag{43}$$

Using Table 2, we have

$$\begin{aligned}\mathrm{AG}(\psi_2) &= \left(\frac{9}{4}\right)^3\left|E_1(\mathrm{TP}(m))\right| + \left(\frac{18}{7}\right)^3\left|E_2(\mathrm{TP}(m))\right| + \left(\frac{36}{10}\right)^3\left|E_3(\mathrm{TP}(m))\right| \\ &= \left(\frac{9}{4}\right)^3\left(18m^2 + 6m\right) + \left(\frac{18}{7}\right)^3\left(18m^2 + 6m\right) + \left(\frac{36}{10}\right)^3\left(18m^2 - 36m + 18\right).\end{aligned} \tag{44}$$

We get the following value after calculations:

$$\Rightarrow \mathrm{AG}(\psi_2) = \frac{1853423451}{1372000}m^2 - \frac{534408759}{1372000}m. \tag{45}$$

For the inverse sum index and by using equation (6), we have

$$I(\psi) = \sum_{ab\in E(\psi)} \left(\frac{d_a \times d_b}{d_a + d_b}\right). \tag{46}$$

Using Table 2, we have

$$\begin{aligned} I(\psi_2) &= \left(\frac{9}{6}\right)\left|E_1(\mathrm{TP}(m))\right| + 2\left|E_2(\mathrm{TP}(m))\right| + 3\left|E_3(\mathrm{TP}(m))\right| \\ &= \left(\frac{9}{6}\right)\left(18m^2 + 6m\right) + 2\left(18m^2 + 6m\right) + 3\left(18m^2 - 36m + 18\right). \end{aligned} \tag{47}$$

After calculations,

$$\Rightarrow I(\psi_2) = 117m^2 - 15m. \tag{48}$$

□

2.3. Results for Hexagonal Planar Octahedron (HPOH) Network. In this part, we propose the theorem for the HPOH network.

Theorem 7. *The first and second modified K-Banhatti indices are equal to the hex POH network:*

$$\begin{aligned} \mathrm{MK_1B}(\psi_3) &= \frac{51}{8}m^2 - 4m - \frac{13}{8}, \\ \mathrm{MK_2B}(\psi_3) &= \frac{81}{32}m^2 - \frac{15}{16}m - \frac{39}{32}. \end{aligned} \tag{49}$$

Proof. Let $\psi_3 \cong \mathrm{HPOH}(m)$. From equation (1), we have

$$\mathrm{MK_1B}(\psi) = \sum_{ab\in E(\psi)} \left(\frac{1}{(d_a + d_b)}\right). \tag{50}$$

Using Table 3, we have

$$\begin{aligned} \mathrm{MK_1B}(\psi_3) &= \frac{1}{4+4}\left|E_1(\mathrm{HPOH}(m))\right| + \frac{1}{4+8}\left|E_2(\mathrm{HPOH}(m))\right| + \frac{1}{8+8}\left|E_3(\mathrm{HPOH}(m))\right| \\ &= \frac{1}{8}\left|E_1(\mathrm{HPOH}(m))\right| + \frac{1}{12}\left|E_2(\mathrm{HPOH}(m))\right| + \frac{1}{16}\left|E_3(\mathrm{HPOH}(m))\right| \\ &= \frac{1}{8}\left(18m^2 + 18m - 30\right) + \frac{1}{12}\left(36m^2 - 48m + 12\right) + \frac{1}{16}\left(18m^2 - 36m + 18\right). \end{aligned} \tag{51}$$

We get the following value after calculations:

$$\Rightarrow \mathrm{MK_1B}(\psi_3) = \frac{51}{8}m^2 - 4m - \frac{13}{8}. \tag{52}$$

Let $\psi_2 \cong \mathrm{HPOH}(m)$. From equation (2), we have

$$\mathrm{MK_1B}(\psi) = \sum_{ab\in E(\psi)} \left(\frac{1}{(d_a + d_b)}\right). \tag{53}$$

Using Table 3, we have

$$\begin{aligned} \mathrm{MK_2B}(\psi_3) &= \frac{1}{4\times 4}\left|E_1(\mathrm{HPOH}(m))\right| + \frac{1}{4\times 8}\left|E_2(\mathrm{HPOH}(m))\right| + \frac{1}{8\times 8}\left|E_3(\mathrm{HPOH}(m))\right| \\ &= \frac{1}{16}\left|E_1(\mathrm{HPOH}(m))\right| + \frac{1}{32}\left|E_2(\mathrm{HPOH}(m))\right| + \frac{1}{64}\left|E_3(\mathrm{HPOH}(m))\right| \\ &= \frac{1}{16}\left(18m^2 + 18m - 30\right) + \frac{1}{32}\left(36m^2 - 48m + 12\right) + \frac{1}{64}\left(18m^2 - 36m + 18\right). \end{aligned} \tag{54}$$

Table 3: Edge partition.

(d_a, d_b)	Number of edges
$E_1 = (4,4)$	$18m^2 + 18m - 30$
$E_2 = (4,8)$	$36m^2 - 48m + 12$
$E_3 = (8,8)$	$18m^2 - 36m + 18$

We get the following value after calculations:

$$\Rightarrow \mathrm{MK_2B}(\psi_3) = \frac{81}{32}m^2 - \frac{15}{16}m - \frac{39}{32}. \quad (55)$$

□

Theorem 8. *Then, harmonic K-Banhatti and symmetric division indices are equal to the hex POH network:*

$$\mathrm{HKB}(\psi_3) = \frac{51}{4}m^2 - 8m - \frac{13}{4},$$
$$\mathrm{SD}(\psi_3) = 162m^2 - 156m + 6. \quad (56)$$

Proof. Let $\varphi_1 \cong \mathrm{HPOH}(m)$ network, and from equation (3),

$$\mathrm{HKB}(\psi) = \sum_{ab\in E(\psi)} \frac{2}{(d_a + d_b)}. \quad (57)$$

Using Table 3, we have

$$\begin{aligned}\mathrm{HKB}(\psi_3) &= \frac{2}{4+4}\left|E_1(\mathrm{HPOH}(m))\right| + \frac{2}{4+8}\left|E_2(\mathrm{HPOH}(m))\right| + \frac{2}{8+8}\left|E_3(\mathrm{HPOH}(m))\right| \\ &= \frac{2}{8}\left|E_1(\mathrm{HPOH}(m))\right| + \frac{2}{12}\left|E_2(\mathrm{HPOH}(m))\right| + \frac{2}{16}\left|E_3(\mathrm{HPOH}(m))\right| \\ &= \frac{1}{4}\left(18m^2 + 18m - 30\right) + \frac{1}{6}\left(36m^2 - 48m + 12\right) + \frac{1}{8}\left(18m^2 - 36m + 18\right).\end{aligned} \quad (58)$$

We get the following value after calculations:

$$\Rightarrow \mathrm{HKB}(\psi_3) = \frac{51}{4}m^2 - 8m - \frac{13}{4}. \quad (59)$$

For the symmetric division index of a graph using equation (3), we have

$$\mathrm{SD}(\psi) = \sum_{ab\in E(\psi)} \left(\frac{d_a}{d_b} + \frac{d_b}{d_a}\right). \quad (60)$$

Using Table 3, we have

$$\begin{aligned}\mathrm{SD}(\psi_3) &= \left(\frac{4}{4} + \frac{4}{4}\right)\left|E_1(\mathrm{HPOH}(m))\right| + \left(\frac{4}{8} + \frac{8}{4}\right)\left|E_2(\mathrm{HPOH}(m))\right| + \left(\frac{8}{8} + \frac{8}{8}\right)\left|E_3(\mathrm{HPOH}(m))\right| \\ &= 2\left|E_1(\mathrm{HPOH}(m))\right| + \left(\frac{1}{2} + \frac{2}{1}\right)\left|E_2(\mathrm{HPOH}(m))\right| + 2\left|E_3(\mathrm{HPOH}(m))\right| \\ &= 2\left(18m^2 + 18m - 30\right) + \frac{5}{2}\left(36m^2 - 48m + 12\right) + 2\left(18m^2 - 36m + 18\right).\end{aligned} \quad (61)$$

After calculations,

$$\Rightarrow \mathrm{SD}(\psi_3) = 162m^2 - 156m + 6. \quad (62)$$

□

Theorem 9. *The augmented Zagreb and inverse sum indices are equal to the hex POH network:*

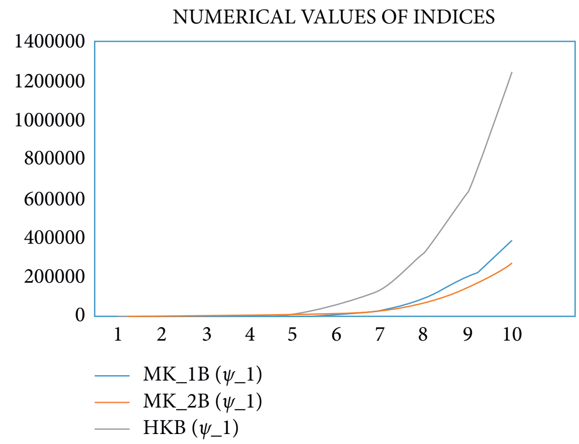

Figure 4: For POH 1.

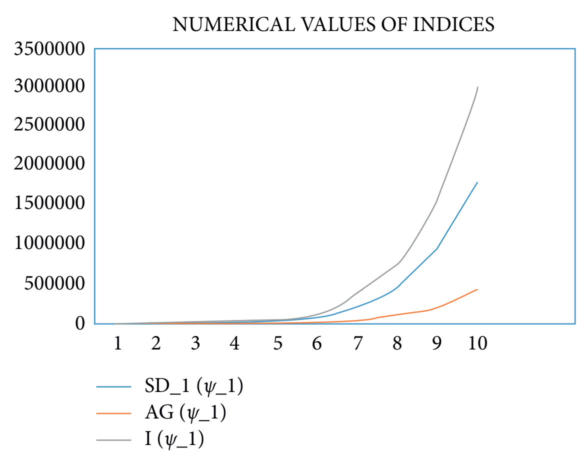

Figure 5: For POH 2.

$$\mathrm{AG}(\psi_3) = \frac{416820224}{128625}m^2 - \frac{600773632}{128625}m + \frac{595764224}{385875},$$
$$I(\psi_3) = 204m^2 - 236m + 44. \tag{63}$$

Proof. Let $\varphi_1 \cong \mathrm{HPOH}(m)$ network. Using equation (5) for the augmented Zagreb index,

$$\mathrm{AG}(\psi) = \sum_{ab\in E(\psi)} \left(\frac{d_a \times d_b}{d_a + d_b - 2}\right)^3. \tag{64}$$

Using Table 3, we have

$$\begin{aligned}\mathrm{AG}(\psi_3) &= \left(\frac{16}{6}\right)^3 |E_1(\mathrm{HPOH}(m))| + \left(\frac{32}{10}\right)^3 |E_2(\mathrm{HPOH}(m))| + \left(\frac{64}{14}\right)^3 |E_3(\mathrm{HPOH}(m))| \\ &= \left(\frac{16}{6}\right)^3 \left(18m^2 + 18m - 30\right) + \left(\frac{32}{10}\right)^3 \left(36m^2 - 48m + 12\right) + \left(\frac{64}{14}\right)^3 \left(18m^2 - 36m + 18\right).\end{aligned} \tag{65}$$

We get the following value after calculations:

$$\Rightarrow \mathrm{AG}(\psi_3) = \frac{416820224}{128625}m^2 - \frac{600773632}{128625}m + \frac{595764224}{385875}. \tag{66}$$

For the inverse sum index and by using equation (6), we have

$$I(\psi) = \sum_{ab\in E(\psi)} \left(\frac{d_a \times d_b}{d_a + d_b}\right). \tag{67}$$

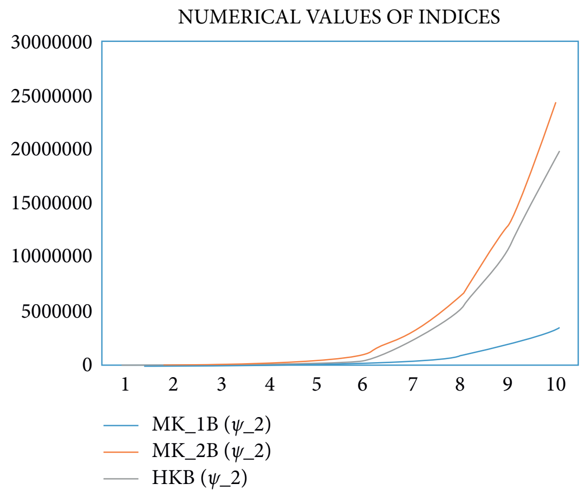

Figure 6: For TP 1.

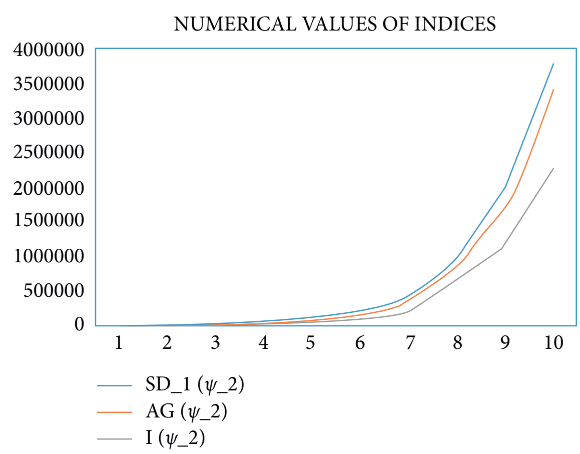

Figure 7: For TP 2.

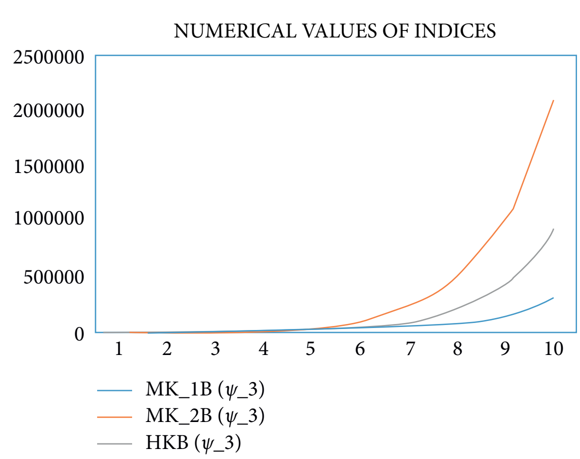

Figure 8: For hex POH 1.

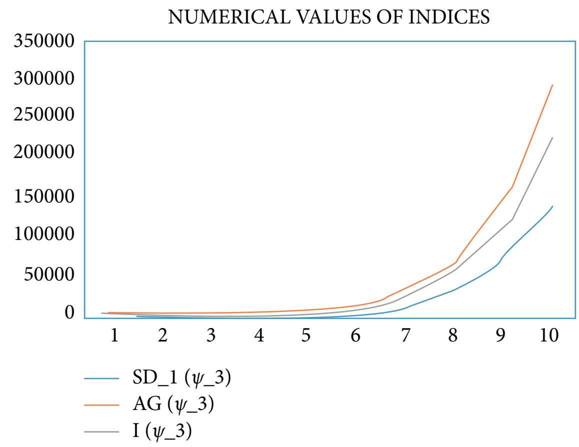

FIGURE 9: For hex POH 2.

Using Table 3, we have

$$\begin{aligned} I(\psi_3) &= \left(\frac{16}{8}\right)\left|E_1(\mathrm{HPOH}(m))\right| + \left(\frac{32}{12}\right)\left|E_2(\mathrm{HPOH}(m))\right| + \left(\frac{64}{16}\right)\left|E_3(\mathrm{HPOH}(m))\right| \\ &= 2\left(18m^2 + 18m - 30\right) + \left(\frac{32}{12}\right)\left(36m^2 - 48m + 12\right) + 4\left(18m^2 - 36m + 18\right). \end{aligned} \tag{68}$$

After calculations,

$$\Rightarrow I(\psi_3) = 204m^2 - 236m + 44. \tag{69}$$

□

3. Comparison of Indices through Graphs

The comparison of the first and second K-Banhatti, harmonic K-Banhatti, symmetric division, augmented Zagreb, and inverse sum indices for the POH network, TP network, and HPOH network is conducted for different values. The comparison graphs are shown in Figures 4–9 .

4. Conclusion

In this paper, first and the second K-Banhatti, harmonic K-Banhatti, symmetric division, augmented Zagreb, and inverse sum indices have been computed for the planar octahedron networks. From a chemical standpoint, these findings might be useful for computer scientists and chemists, who come across these networks. Additional multiplicative degree-based indices should be computed soon.

Data Availability

No data were used to support this study.

Conflicts of Interest

The authors declare that they have no conflicts of interest.

Authors' Contributions

Wang Zhen was responsible for software Parvez Ali contributed in collection of data. Haidar Ali contributed to original draft preparation. Ghulam Dustigeer was responsible for methodology. Jia-Bao Liu reviewed and edited the manuscript.

Acknowledgments

This research was supported by the Anhui Province University Discipline (Professional) Top Talent Academic Funding Project (grant no. gxbjZD2021091).

References

[1] P. D. Manuel and I. Rajasingh, "Minimum metric dimension of silicate networks," *Ars Combinatoria*, vol. 98, pp. 501–510, 2011.

[2] F. S. Raj and A. George, "Network embedding on planar octahedron networks," in *Proceedings of the 2015 IEEE International Conference on Electrical, Computer and Communication Technologies (ICECCT)*, pp. 1–6, Coimbatore, India, March 2015.

[3] I. Gutman, B. Rusić, N. Trinajstić, and C. F. Wilcox Jr, "Graph theory and molecular orbitals. XII. Acyclic polyenes," *The Journal of Chemical Physics*, vol. 62, no. 9, pp. 3399–3405, 1975.

[4] V. R. Kulli, "Multiplicative hyper-Zagreb indices and coindices of graphs: computing these indices of some nanostructures," *International Research Journal of Pure Algebra*, vol. 6, no. 7, pp. 342–347, 2016.

[5] J. B. Liu, Z. Jing, M. Jie, and C. Jinde, "The hosoya index of graphs formed by a fractal graph," *Fractals*, vol. 27, no. 8, Article ID 1950135, 2019.

[6] S. Akhtar and M. Imran, "On molecular topological properties of benzenoid structures," *Canadian Journal of Chemistry*, vol. 94, pp. 687–698, 2016.

[7] A. Q. Baig, M. Naeem, and W. Gao, "Revan and hyper-revan indices of octahedral and icosahedral networks," *Applied Mathematics and Nonlinear Sciences*, vol. 3, no. 1, pp. 33–40, 2018.

[8] W. Gao, A. Q. Baig, W. Khalid, and M. R. Farahani, "Molecular description of copper (II) oxide," *Macedonian Journal of Chemistry and Chemical Engineering*, vol. 36, pp. 93–99, 2017.

[9] M. Hu, H. Ali, M. A. Binyamin, B. Ali, J. B. Liu, and C. Fan, "On distance-based topological descriptors of chemical interconnection networks," *Journal of Mathematics*, vol. 2021, Article ID 5520619, 10 pages, 2021.

[10] F. Simonraj and A. George, "Embedding of poly honeycomb networks and the metric dimension of star of david network," *International Journal on Applications of Graph Theory In wireless Ad Hoc Networks And sensor Networks*, vol. 4, no. 4, pp. 11–28, 2012.

[11] G. H. Shirdel, H. Rezapour, and A. M. Sayadi, "The hyper Zagreb index of graph operations," *Iranian Journal of Mathematical Chemistry*, vol. 4, pp. 213–220, 2013.

[12] K. M. Smith, "On neighbourhood degree sequences of complex networks," *Scientific Reports*, vol. 9, no. 1, p. 8340, 2019.

[13] H. Wiener, "Structural determination of paraffin boiling points," *Journal of the American Chemical Society*, vol. 69, no. 1, pp. 17–20, 1947.

[14] M. V. Diudea, I. Gutman, and J. Lorentz, *Molecular Topology*, Babes-Bolyai University, Cluj-Napoca, Romania, 2001.

[15] N. Trinajstić, *Chemical Graph Theory*, CRC Press, Boca Raton, FL, USA, 1983.